Volume 22 · Issue 3
June 2025

Asian Journal of WATER, ENVIRONMENT AND POLLUTION

ISSN: 0972-9860 (Print)
ISSN: 1875-8568 (Online)

ACCSCIENCE PUBLISHING

WSSET
World Society of Sustainable Energy Technologies

Asian Journal of Water, Environment and Pollution

Print ISSN: 0972-9860
Online ISSN: 1875-8568

Asian Journal of Water, Environment and Pollution is an international, peer-reviewed, academic Open Access journal. It aims to publish high-quality, original research and practical solutions across a wide range of topics that address global environmental challenges. These include water availability and pollution management, global warming and climate adaptation, solid and liquid waste management, mining impacts and environmental degradation, renewable energy integration, energy access and sustainability, and policy analysis focused on social equity. The journal also covers infrastructure development, transnational water body pollution, energy storage and conversion, low-carbon and zero-energy buildings, and sustainable transport systems.

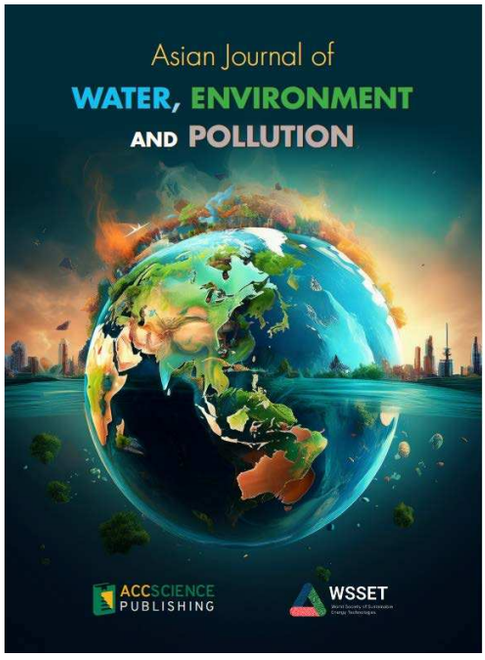

About the Publisher

AccScience Publishing is a publishing company based in Singapore. We publish a range of high-quality, open-access, peer-reviewed journals and books from a broad spectrum of disciplines.

Contact Us

Managing Editor
ajwep.office@accscience.sg

AccScience Publishing
9 Raffles Place, Republic Plaza 1 #06-00 Singapore 048619.

Volume 22 • Issue 3 • June 2025
ISSN 0972-9860 (print) ISSN 1875-8568 (online)

Asian Journal of Water, Environment and Pollution

Editor-in-Chief
Chengyun Zhou
Hunan University, Changsha, China

ACCSCIENCE PUBLISHING
Access Science Without Barriers

Full issue copyright © 2025 AccScience Publishing
All rights reserved. Without permission in writing from the publisher, this full issue publication in its entirety may not be reproduced or transmitted for commercial purposes in any form or by any means, electronic or mechanical, including photocopying, recording, or any information storage and retrieval system. Permissions may be sought from ajwep.office@accscience.sg.

Article copyright © Respective Author(s)
See articles for copyright year. All articles in this full issue publication are open-access. There are no restrictions in the distribution and reproduction of individual articles, provided the original work is properly cited. However, permission to reuse copyrighted materials of an article for commercial purposes is applicable if the article is licensed under Creative Commons Attribution-NonCommercial License. Check the specific license before reusing.

ASIAN JOURNAL OF WATER, ENVIRONMENT AND POLLUTION

ISSN: 0972-9860 (print)
ISSN: 1875-8568 (online)

Editorial and Production Credits

Publisher: AccScience Publishing
Managing Editor: Irene Zhao
Production Editor: Samyuktha Balakrishnan
Article Layout and Typeset: Sinjore Technologies (India)

For all advertising queries, contact ajwep.office@accscience.sg.

Supplementary file

Supplementary files of articles can be obtained at https://accscience.com/journal/AJWEP/22/3.

Disclaimer

AccScience Publishing is not liable to the statements, perspectives, and opinions contained in the publications. The appearance of advertisements in the journal shall not be construed as a warranty, endorsement, or approval of the products or services advertised and/or the safety thereof. AccScience Publishing disclaims responsibility for any injury to persons or property resulting from any ideas or products referred to in the publications or advertisements. AccScience Publishing remains neutral with regard to jurisdictional claims in published maps and institutional affiliations.

Asian Journal of Water, Environment and Pollution

Editorial Board

Editor-in-Chief

Chengyun Zhou, *China*

Executive Editor

Upaka Rathnayake, *Ireland*

Associate Editors

Ziwei Chen, *UK*
Maocai Shen, *China*
Wenjun Wang, *China*

*Editorial Board Members**

Mardiana Idayu Ahmad, *Malaysia*
Khalil Ahmad, *Pakistan*
Awais Ahmad, *Pakistan*
Abdeltif Amrane, *France*
Amit Awasthi, *India*
Rohit B. Meshram, *India*
Abubakr Bahaj, *UK*
Rangan Banerjee, *India*
Michele Bottarelli, *Italy*
Laura Bulgariu, *Romania*
Salvatore Carlucci, *Cyprus*
Constantinos Cartalis, *Greece*
Wei-Hsin Chen, Taiwan
Yulong Ding, *UK*
Muhammad Ehsan, *Mexico*
Daniele Fattorini, *Italy*
Francesco Fiorito, *Australia*
Gagné François, *Canada*
Yang Gao, *China*
Vladimir I. Golik, *Russia*
Qiulai He, *China*
Md. Emran Hossain, *USA*
Jie Ji, *China*
Nadeem Ahmad Khan, *India*
Ali Kilicarslan, *Turkey*
Roman V. Klyuev, *Russia*
Chee Kong YAP, *Malaysia*
Katarzyna Kubiak-Wójcicka, *Poland*
Angui Li, *China*
Qiang Li, *China*
Qingchao Li, *China*
Tapas Mallick, *UK*
Edward Ng, *China*
Armando Oliveira, *Portugal*
Mohammad Oves, *Saudi Arabia*
Maulin P Shah, *India*
Ashok Pandey, *India*
Pradhan Parth Sarthi, *India*
Gang Pei, *China*
Richard Powell, *UK*
Ram Prasad, *India*
Namal Rathnayake, *Japan*
K. Srinivas Reddy, *India*
Prakash Sarangi, *India*
Li Shao, *UK*
Binbin Shao, *China*
Jichao Sun, *China*
Kwok Wai Tham, *Singapore*
Chi-Hwa Wang, *Singapore*
Ruzhu Wang, *China*
Liu Wen, *China*
Yuying Yan, *UK*
Hongxing Yang, *China*
Yi Yang, *China*
Weiming Zhang, *China*
Lizhi Zhang, *China*
Xudong Zhao, *UK*
Tianshou Zhao, *China*
Maiyong Zhu, *China*
Yingxin Zhu, *China*
Muhammad Zubair, *Pakistan*
Walter Timo de Vries, *Germany*

Youth Editorial Board Member

Mingming Ge, *China*

*Editorial Board Members as of June 26, 2025

ACCSCIENCE PUBLISHING

Volume 22 | Issue 3 | June 2025 | Page 1 – 220 |

Asian Journal of Water, Environment and Pollution

https://accscience.com/journal/AJWEP

CONTENTS

REVIEW ARTICLES

1 **Redefining plastic terminology: The urgent need for standardised definitions in science and policy**
Austine Ofondu Chinomso Iroegbu, Moipone Linda Teffo, Emmanuel Rotimi Sadiku

15 **Nano-biofertilizers: A promising technology for sustainable soil fertility, soil health, and environmental protection**
Hayyawi W. A. Al-Juthery, Rand A. H. G. Al-Taee, Ali S. Alhasan, Diaa F. Hassan, Nisreen A. A. Al-Jassani, Raid Shaalan Jarallah

ORIGINAL RESEARCH ARTICLES

32 **SpillNet: A modified convolutional neural network model for oil spill detection**
Tokula I. Umaha, Felix Ale, Ikpaya D. Ikpaya, John A. Momoh, Steve A. Adeshina, Ilesanmi A. Daniyan, Adeyinka P. Adedigba

46 **Variation in phytochemical and functional traits of Suaeda monoica across three sites in Jeddah, Saudi Arabia**
Ameina S. Almoshadak

63 **Exploring municipal solid waste management practices and public perceptions in north coastal Andhra Pradesh, India**
Nakka Lakshmi Srikanth, Neyyila Saibabu, Neyyala Chaitanya

73 **Comparative environmental impact assessment of traditional and eco-friendly denim trousers manufacturing: A cradle-to-grave life cycle assessment**
Kazi Rezwan Hossain, Mohammad Faizur Rahman

88 **Environmental applications of molecular graph learning: Graph neural network based prediction of partition coefficients**
Pravinkumar M. Sonsare, Roshni Khedgaonkar, Kavita Singh, Pratik Agrawal

104 **Digital and precision farming, emissions trade-offs, and food crop yields in Pakistan**
Agha Amad Nabi, Muhammad Khalid Anser, Muhammad Asif, Khalid Zaman

119 **Assessing long-term groundwater level trends in Karakalpakstan using non-parametric statistical methods**
Mehdi Fuladipanah, Kenjabek Rozumbetov, Namal Rathnayake, Valery Erkudov, Mirzohid Koriyev, Upaka Rathna

134 **Projected trends in extreme heat in Senegal from 2020 to 2080**
Moussa Sow, Demba Gaye

153 **Sources of environmental law: National legislation of Ukraine and international legal documents**
Yuliia Leheza, Anatolii Kuzmenko, Oleksandr Pashchenko, Valeriya Tulyantseva, Yevhen Leheza

164 **Sustainable wastewater management and risk assessment in Maghnia**
Chachoua Mounira

185 **Determining optimal cultivation parameters for a portable hydroponic system using the nutrient film technique**
Kateryna Vasylkovska, Mykola Kovalov, Oleksii Vasylkovskyi, Daria Michailova

198 **The effects of urbanization on air pollution and public health in Vietnam: An empirical analysis**
Duy Hung Bui, Xuan-Hoa Nghiem

211 **User perspectives on sustainable innovation in the construction industry**
Jozef Švajlenka, Terézia Pošiváková, Hermawan Hermawan

Asian Journal of Water, Environment and Pollution. Vol. 22, No. 3 (2025), pp. 1-14.
doi: 10.36922/AJWEP025200158

REVIEW ARTICLE

Redefining plastic terminology: The urgent need for standardised definitions in science and policy

Austine Ofondu Chinomso Iroegbu*, Moipone Linda Teffo, and Emmanuel Rotimi Sadiku

Department of Chemical, Metallurgical and Materials Engineering, Institute for Nano-Engineering Research, Tshwane University of Technology, Pretoria, Gauteng, South Africa

***Corresponding author:** Austine Ofondu Iroegbu (aoiroegbu@gmail.com)

Received: May 17, 2025; Revised: May 27, 2025; Accepted: May 28, 2025; Published online: June 20, 2025

Abstract: Plastic pollution is a pervasive global threat, yet efforts to mitigate it are hindered by inconsistent terminology across scientific, industrial, and policy domains. Key terms, such as "polymer," "plastic," and "macromolecule" are often used interchangeably despite distinct meanings. This semantic confusion undermines research integrity, muddles regulatory frameworks, and impedes effective environmental management. Without universally accepted definitions or a clear classification system, data comparability, policy implementation, and interdisciplinary collaboration are significantly compromised. This study systematically examines the scope and impact of terminological inconsistencies in plastics discourse. We conducted a structured review of recent (2020 – 2025) peer-reviewed literature spanning polymer science and environmental policy to assess how definitional ambiguity affects research outcomes and decision-making. The findings reveal that ambiguous usage of fundamental terms has led to misinterpretations in scientific studies, inconsistent policy decisions, and fragmented mitigation strategies. In response, we propose a standardization framework guided by the International Union of Pure and Applied Chemistry principles, delineating clear criteria to distinguish polymers, plastics, and macromolecules. We recommend embedding these standardized definitions across academic publications, industry standards, and environmental policies to improve communication, ensure regulatory clarity, and support sustainable management practices. By establishing a coherent global terminology for plastics, this work underscores an urgent call for collective action. Standardizing the language of plastics will not only enhance data comparability and strengthen international policy initiatives, but also ensure that scientists, policymakers, and industry leaders can collaboratively craft effective, evidence-based solutions to plastic pollution.

Keywords: Plastics; Polymers; Environmental policy; Terminology standardization; Sustainability

1. Introduction

Plastic pollution has emerged as one of the most critical environmental challenges of the 21st century, with far-reaching consequences for ecosystems, biodiversity, and human health.[1-3] The extensive production and widespread use of synthetic polymers have intensified concerns over their persistence in the environment, leading to severe ecological and socio-economic impacts.[2,3] However, the effectiveness of research and policy interventions aimed at mitigating plastic pollution is often undermined by inconsistent terminology in

scientific, industrial, and regulatory discourse. For example, the interchangeable use of terms, such as "plastics," "polymers," and "macromolecules" has contributed to ambiguity in understanding the scope of plastic pollution, its classification, and the implications for policy formulation.[4-8] This is critical because we live in a language-driven world where the usage of words and their symbolic representations shapes thoughts, influences interpretations, and ultimately defines approaches to conventional issues.[1,9] Therefore, in scientific discourse, precise definitions play a crucial role in shaping policies, guiding societal perceptions, and determining responses to environmental challenges.[1] It is unarguable that establishing clear, accurate, and well-founded definitions that authentically reflect the subject matter is essential for effective communication and informed decision-making.

The advent of synthetic polymer production has ushered in a pervasive environmental challenge in the form of plastic pollution.[2,3,10-12] This issue has garnered increasing attention over the decades, as evidenced by the vast literature that varies in scope, scientific rigor, and tone.[2,13-20] For example, a search in Google Scholar using the term "plastic pollution" yields an enormous collection of literature on this subject. Given this significant volume of reports, vital questions emerge. For instance, "Why has the scientific discourse on plastic pollution persisted over the years?" "Are we addressing polymer or plastic pollution?" "Are there comprehensive solutions to address this challenge?" This paper critically examines the persistent issue of terminological inconsistencies in plastic pollution discourse. By systematically reviewing the literature from 2020 to 2025, we assess the extent to which terminology variations influence scientific research and policy frameworks. Unlike previous reviews that primarily discuss plastic pollution from an environmental or technological perspective, this study highlights the definitional challenges that hinder effective communication and problem-solving in the field.

To address this challenge, we propose a standardization framework aligned with the International Union of Pure and Applied Chemistry (IUPAC) principles. This framework provides clear distinctions between plastics, polymers, and macromolecules, thereby ensuring greater precision in academic research, industrial applications, and policy-making. The study advocates the integration of standardized terminology into the scientific literature, environmental policies, and industrial regulations to enhance clarity, improve data harmonization, and support evidence-based decision-making.

Furthermore, this work challenges present perceptions and misconceptions surrounding plastic pollution, urging researchers and policymakers to adopt contextually appropriate definitions that reflect the material properties, environmental impacts, and regulatory requirements. By refining the language used in plastic pollution discourse, this study seeks to promote a more accurate, informed, and unified approach to addressing one of the most pressing environmental issues of our time.

2. Methodology

To systematically assess the inconsistencies in polymer-related terminology and propose a standardization framework, this study employed a structured literature review. The methodology was designed to ensure a rigorous, transparent, and reproducible analysis of the definitions and classifications of plastics, polymers, and macromolecules within scientific, industrial, and policy contexts.

A comprehensive review of peer-reviewed literature was conducted by searching databases, such as Scopus, Web of Science, and ScienceDirect, focusing on publications from 2020 to 2025 to capture recent advancements and policy discussions. Selection criteria prioritized studies that directly addressed terminological inconsistencies, environmental implications of misclassification, and the role of standardized definitions in regulatory frameworks. Key data points were extracted to identify patterns of inconsistencies, assess their impact on scientific discourse and policy, and evaluate existing classification models. The findings informed the development of a standardization framework aligned with the IUPAC principles, ensuring scientific accuracy and practical applicability. A summary of the methodological approach is presented in Table 1.

3. Terminology ambiguity of plastic

Macromolecules are fundamental to life and technology. From DNA and proteins to advanced synthetic materials, they underpin biological structures and industrial innovations alike.[5,21-28] The evolution of polymer science has enabled the development of countless materials with tailored properties, propelling progress across multiple domains.[5,29] Despite their centrality, the terms "macromolecule" and "polymer" are frequently used interchangeably in the literature, often without clarification, leading to scientific ambiguity. While common, this conflation deviates

Table 1. Overview of a structured methodology for terminology standardization in plastic pollution discourse

Component	Description
Research approach	Structured literature review
Objective	To analyze terminological inconsistencies in polymer science and plastic pollution discourse and propose a standardization framework
Data sources	Scopus, Web of Science, and ScienceDirect
Timeframe of literature	2020 – 2025 (to ensure relevance and alignment with recent scientific and policy developments)
Selection criteria	- Peer-reviewed articles, reports, and policy papers related to plastic pollution and polymer terminology - Publications address definitional inconsistencies and their impact on scientific discourse and policymaking.
Data extraction	- Identification of commonly used definitions for plastics, polymers, and macromolecules - Analysis of inconsistencies in terminology usage across disciplines - Assessment of policy implications and recommendations.
Framework development	- Alignment with International Union of Pure and Applied Chemistry principles for standardization - Classification of plastics based on composition, function, and environmental impact - Proposal of terminology standardization model for academic, industrial, and policy applications.
Expected contribution	- Improved clarity and consistency in polymer science terminology - Enhanced communication between researchers, policymakers, and industry stakeholders - A foundation for more effective regulatory and environmental management strategies.

from precision. As Hartmann *et al.*[4] noted, the lack of internationally harmonized definitions contributes to terminological confusion across research, legislation, and public discourse. Similarly, the report of Zhu and Wang.[30] highlights the inconsistent usage of "polymer," "plastic," and "material" when discussing biodegradable alternatives. As summarized in Table 2, even reports in reputable journals employ these terms synonymously, often without differentiating between raw resins, compounded products, and processed articles.

According to Figge *et al.,*[33] a valid definition must include a definiendum (the term being defined) and a definiens (its conceptual boundaries). Good definitions are inclusive yet specific and free of counterexamples. Existing definitions of macromolecule (i.e., large molecules composed of repeating chemical units) and polymer (i.e., composed of macromolecules) do not always meet this standard. For instance, proteins, such as hemoglobin and nucleic acids, such as DNA are classified as macromolecules, despite lacking strictly repeating monomeric sequences.[34-37] In contrast, materials, such as polythene and polystyrene are composed of chemically identical repeating units (e.g., ethylene or styrene), meeting the formal criterion for polymers.[5,21,29] Hence, while all polymers are composed of macromolecules, not all macromolecules are polymers.[21,29] This distinction is illustrated in Figure 1: A macromolecule resembles a single strand of noodle, whereas a polymer is the entire bowl composed of multiple strands of noodles.

In essence, macromolecules can exist independently, but polymers cannot exist without comprising multiple macromolecules. A polymer's bulk properties depend on the collective characteristics of its constituent macromolecules, such as molecular weight distribution, chain length, and polydispersity index.[38-41] Unlike small molecules with discrete melting points, polymers exhibit continuous properties, such as melting or glass transition ranges, because of variations among chains.[21,22,29,42] Further complicating matter is polymer memory, the phenomenon whereby the history of processing conditions (e.g., thermal or mechanical) can influence future behavior through residual stresses or orientation effects.[42-44] This means even polymers of identical chemical composition can behave differently based on processing, aging, and external stimuli.[39,43,44] Such variability defies one-size-fits-all modeling and reinforces that no two polymers are ever truly identical, even if synthesized from the same monomers.

Ambiguous terminology undermines scientific rigor and complicates environmental regulation, materials classification, and policy development.[31,32,45] Establishing clear distinctions between macromolecules and polymers is essential for academic precision

Table 2. Examples of interchangeable use of "polymer," "macromolecule," and "plastic" across scientific journals

Journal	Type	Title	Impact factor (2024)	Usage of terms	References
Macromolecules	Peer-reviewed	Plastic pollution: A material problem?	5.1	Refers to "plastics (generally used as a synonym for polymers)"	31
Nature Reviews Materials	Peer-reviewed	Reducing environmental plastic pollution by designing polymer materials for managed end-of-life	79.8	Describes plastics as "a ubiquitous class of synthetic polymer materials"	32
ACS Omega	Peer-reviewed	Plastic pollution: A perspective on matters arising	4.1	States that "plastics are polymeric systems (i.e., macromolecules)"	3

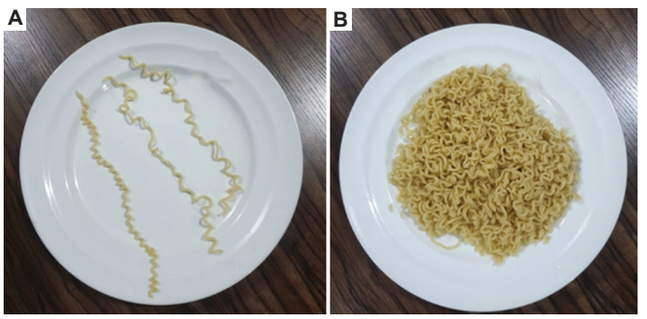

Figure 1. Basic illustration of macromolecules and polymers. (A) Macromolecules; (B) Polymers. Image produced by First Author

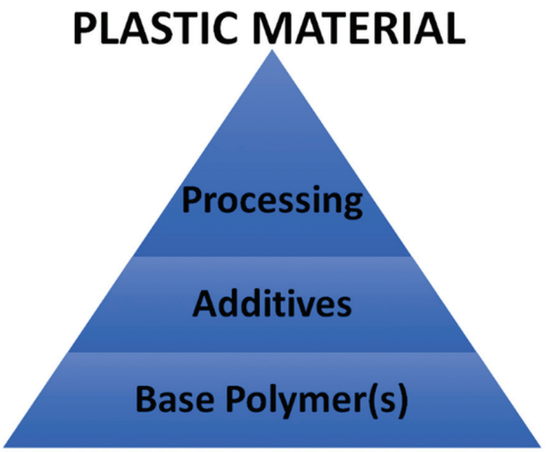

Figure 2. Representation of a plastic material. Image produced by the authors. Created with MS PowerPoint and https://pixlr.com/express/; 2025; Austine Ofondu Chinomso Iroegbu

and harmonizing industrial standards and regulatory language.[4] As such, we strongly advocate for alignment with IUPAC definitions, which promote consistency across sectors and disciplines. Doing so will facilitate more effective stakeholder collaboration, enhance plastic pollution diagnostics, and support innovation in sustainable materials development.

4. Distinction between polymers and plastics

Plastics represent one of the most transformative innovations in science and technology. However, for clarity in this discourse, we define plastics as synthetic or semi-synthetic composite materials composed primarily of polymers and additives, engineered for specific end-use applications. As illustrated in Figure 2, plastics are not merely polymers; they are functional materials tailored through compounding and physicochemical modification.

Plastics include thermoplastics, materials that can be melted and reshaped, and thermosets, which irreversibly harden upon curing. A pure polymer resin without additives or structural modification is not plastic.[41,43,44] Instead, plastics comprise formulated systems, where the polymer serves as the matrix and is integrated with additives, such as plasticizers, stabilizers, fillers, or colorants.[41,43,46] These additives impart critical properties, such as flexibility, durability, or ultraviolet (UV) resistance, enabling applications ranging from packaging films and fibers to foams, laminates, and molded components. Semi-synthetic materials, such as rayon and cellulose acetate, derived from natural polymers, are classified as plastics due to their engineered modification.[41,43,46] Similarly, elastomers like styrene-butadiene rubber become plastics when compounded, cast, and vulcanized into end products, such as automotive tires.[41,43,46-48] In contrast, in their

raw form, unprocessed styrene or butadiene polymers remain polymers, not plastics. The same logic applies to materials, such as polyurethane, used in mattresses and footwear: Only when processed with additives and cured do they qualify as plastics.[49-51] Once plastics are cured through heat, UV exposure, or ambient conditions, reprocessing becomes impractical as they transition into composites.[52]

Furthermore, coatings and paints (e.g., on vehicles, ships, and buildings) are classified as plastics due to their polymer-based formulations (e.g., alkyds, acrylics, epoxies, and polyvinylidene fluorides) and the inclusion of additives. These materials undergo crosslinking and adhere to substrates, contributing to plastic pollution in terrestrial, atmospheric, and aquatic environments.[2,41,43,46,53] Similarly, textiles, wigs, synthetic eyelashes, footwear, and similar consumer products, often formulated from polymer-based fibers with functional additives, are effectively plastics.[3]

Despite their widespread utility and contributions to modern life,[3] plastics are now at the center of environmental concern due to their persistent pollution and complex degradation behaviour.[2,3,54] An accessible analogy can be drawn from cake baking (Figure 3): Flour serves as the base (analogous to polymers), while ingredients, such as eggs, fat, and sugar (additives) determine the structure, texture, and taste.[55,56] Similarly, polymers are the base material in plastics, and additives define performance, form, and application.[41,57,58] The intricacy of cake chemistry reflects the multifactorial nature of plastic formulation: Different combinations

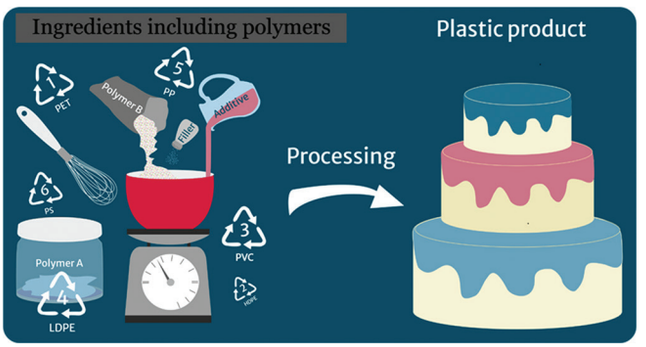

Figure 3. Cake illustration correlating the complex nature of plastics

Abbreviations: HDPE: High-density polyethylene; LDPE: Low-density polyethylene; PET: Polyethylene terephthalate; PP: Polypropylene; PS: Polystyrene; PVC: Polyvinyl chloride. Image produced by the authors. Created with https://pixlr.com/express/ and MS PowerPoint; 2025; Austine Ofondu Chinomso Iroegbu

of polymers, additives, and processing methods result in vastly different materials and environmental behaviors.[41,41,52,59-64]

This understanding positions plastics as engineered composites, not simply as polymers. Recognizing this complexity is essential for advancing accurate classifications, improving pollution diagnostics, and developing targeted mitigation strategies.

In conclusion, the continued misuse and oversimplification of the term "plastic" undermine sustainable solutions. Existing definitions often fail to reflect the scientific complexity of modern plastic materials, either by being too narrow to capture emerging formulations or too broad to be practically applicable. Addressing this ambiguity is essential for refining scientific discourse, guiding environmental policy, and supporting more effective communication and innovation in sustainability research.

5. Real-world repercussions of terminology inconsistency: Complexity in plastic pollution classification

Inconsistent terminology surrounding polymers, macromolecules, and plastics presents substantial environmental, regulatory, and ethical challenges. Plastics, which are engineered polymer-based materials, are integral to modern society, with applications ranging from electronics and electrical insulation to medical devices, such as syringes and catheters. However, their widespread use is paralleled by their pervasive environmental footprint, including macro-, micro-, and nano-plastics that pose a growing threat to global ecosystems and sustainability efforts.[3,65-68] Since 1950, plastic production has exceeded seven billion metric tons,[3] spurring movements to ban single-use plastics, promote bio-based alternatives, and accelerate circular economy strategies.[69-75]

Plastic pollution encompasses the intentional or unintentional release of plastic debris, often laden with additives, into ecosystems, where it interacts with environmental components to cause harm.[2,3] However, quantifying this pollution remains difficult. For instance, textile fibers, both synthetic (e.g., polyester, nylon) and natural (e.g., cotton, silk), release countless microfibers during wearing and washing, yet the environmental impact of these emissions remains largely unmeasured due to the absence of comprehensive data on clothing production.[3,76,77] In addition, the export of unwanted garments and electronics, often labeled as second-hand

goods, from developed to developing nations perpetuates environmental degradation and ethical inequities.[3,78,79]

Biodegradable polymers also present challenges when converted into plastics. For example, cellulose, though naturally biodegradable, becomes a persistent pollutant when processed into products, such as cigarette filters.[80-82] One discarded filter can contaminate up to 1,000 L of water due to leached toxins, such as pesticides, heavy metals, and organic pollutants. Similarly, tires, which comprise diverse and confidential chemical formulations, contribute 5 – 10% of marine plastic pollution, excluding terrestrial pollution, where accumulation may be even greater.[83-92] The tire industries' lack of compositional transparency and technological heterogeneity poses significant challenges for regulation and pollution mitigation.[3,85-87]

Electronic waste (e-waste), including discarded computers, phones, and televisions, is a significant source of plastic pollution.[93-95] It's dynamic and poorly characterized composition increases its environmental risk. Projections estimate that by 2030, global e-waste will exceed 70 million metric tons, excluding the growing reliance on plastics in solar panels, electric vehicles, and robotic systems.[96-99]

The emergence of bioplastics, such as polylactic acid (PLA), reflects the drive toward more sustainable materials. PLA, derived from renewable resources, is used in packaging, electronics, and medical applications.[93,94,100] However, despite its bio-based origin, PLA remains plastic and contributes to pollution if it does not fully degrade in natural environments.[93,101-104] Its biodegradation is often conditional, requiring specific composting conditions, and may not result in complete mineralization.[3,105,106] Moreover, the environmental promise of biopolymers is frequently compromised by their need for performance-enhancing additives that may not be biodegradable.[30,107,108]

The terms "green" and "biodegradable plastics" are thus misleading. Truly sustainable materials must demonstrate full environmental compatibility, meaning that all components, polymers, additives, and by-products are inherently and rapidly biodegradable under natural conditions.[1,3,93,109] In addition, they should exhibit biocompatibility, ensuring they are non-toxic to living organisms.[1,3,93,109] Unfortunately, present bioplastics often fall short of these criteria. Their performance is influenced by numerous variables, including polymer structure, environmental pH, temperature, and the nature of degradation by-products.[1,3,107,110,111]

In summary, inconsistent definitions of "plastic," "polymer," and "macromolecule" obscure our understanding of pollution sources, hinder effective policy, and perpetuate misconceptions, such as the infallibility of biodegradable alternatives. Until universally accepted definitions are adopted, efforts to address plastic pollution will remain fragmented and less effective.

6. Implications of poorly defined terminology

The distinction between polymers and plastics is fundamental in environmental policies, yet ambiguities in their classification have led to inconsistent regulations that hinder effective strategies for mitigating plastic pollution. Policies often treat all plastics as the same, leading to overly broad or inaccurate bans and restrictions that fail to differentiate or identify the challenge.[112] For example, expanded polystyrene (styrofoam) was included in the latest European Union ban on single-use plastic. While styrofoam is a polymeric material, it does not meet the criteria for plastics for the following reasons: No additives or chemical modifications. Unlike plastics, styrofoam is made from pure polystyrene expanded with gas (e.g., pentane, carbon dioxide [CO2]). It does not contain plasticizers, stabilizers, or other chemical modifications that alter its base polymer properties. Styrofoam is created by expanding polystyrene beads, trapping air pockets within them. Distinct from plastics, which undergo chemical processing or additive incorporation. Thus, Styrofoam should be classified separately from traditional plastics in scientific discourse, environmental policy, and material science. Regulatory frameworks should recognize this distinction to ensure more precise classification and waste management strategies.

In another example, the United States Environmental Protection Agency (US EPA) clarifications on biodegradability, compostability, and bio-based plastics reveal several inconsistencies and gaps in the present regulatory framework, material classification, and environmental strategies.[113] For example, the EPA defines plastic as biodegradable if it fully decomposes within 1 year after disposal.[113] However, this does not ensure that the degradation process is environmentally benign, only that the material disappears from sight. The rate of degradation is prioritized over the nature of degradation, meaning that if a plastic breaks down into microplastics within a year, it can still be considered biodegradable. Biodegradability should not be defined based on time alone; it should ensure complete, harmless degradation in natural environments. If a material leaves harmful residues, persistent microplastics, or toxic

compounds, it should not be classified as biodegradable, regardless of how quickly it disappears. Closing the material loop should be the standard, ensuring that materials are purposefully designed to degrade into non-toxic, bioresorbable components that benefit the ecosystems.[113]

The EPA allows the plastic to be labeled as biodegradable, even if it requires industrial composting, incineration, or landfill conditions for degradation. Many biodegradable plastics, such as PLA, require high-temperature industrial composting facilities, but these facilities are not widely available. If these materials end up in landfills or marine environments, they persist as conventional plastics, even though they are marked as biodegradable. Biodegradable material should not require special environmental conditions; it should break down naturally where it is disposed of (e.g., soil, water, and marine ecosystems).[113] If plastic only degrades under industrial conditions but persists in oceans and soil, it should be classified as compostable but not biodegradable. Environmental adaptability must be a key criterion; biodegradable plastics should degrade effectively under diverse real-world conditions without human intervention.

The EPA's vague biodegradability definitions create loopholes for deception and allow marketers to market materials as environmentally friendly when they still cause long-term environmental harm. For example, some oxo-degradable plastics are labeled biodegradable because they break down into smaller fragments, but these fragments persist as microplastics in soil and marine environments.[113] EPA's definition does not distinguish between complete biodegradation and fragmentation, allowing misleading claims that mask ongoing plastic pollution.[113] We argue that biodegradability should require complete mineralization, meaning that plastics should fully degrade into natural compounds (CO_2, water, and biomass) without persistent residues. If a material fragments into microplastics instead of fully degrading, it should not be classified as biodegradable.

The EPA only defines biodegradability based on decomposition but ignores the environmental effects of the breakdown process. Plastics that degrade into acidic byproducts, heavy metals, or toxic residues are still considered biodegradable under the EPA's criteria. There is no requirement for the degradation process to be neutral or beneficial to the environment. Biodegradable plastics should have a net-zero or positive environmental impact, meaning their degradation does not harm ecosystems and ideally enriches them. If plastic breakdown byproducts cause soil contamination, water pollution, or harm to marine life, it should not be labeled biodegradable. Materials should be bioresorbable, ensuring they reintegrate into nature without disrupting ecosystems.

The US EPA does not mandate eco-design, meaning manufacturers are not required to design plastics with a sustainable end-of-life strategy. Many so-called biodegradable plastics are still made using fossil fuels, contain harmful additives, or require high-energy processing. If a plastic's production process contributes to environmental degradation, it should not be classified as biodegradable. Biodegradable plastics should be intentionally designed from the start with sustainability in mind. This means removing harmful additives, using bioresorbable materials, and ensuring complete reintegration into the environment. Closing the material loop should be a regulatory requirement, ensuring that materials are biodegradable and contribute to long-term sustainability. Eco-design should encompass responsible sourcing, energy-efficient production, and non-toxic degradation. Inconsistencies in definitions and terminologies result in policies that promote a one-size-fits-all approach.

7. Implications and recommendations

Despite significant advancements in understanding plastic pollution, a definitive conclusion regarding the toxicity of plastic particles remains elusive due to the complexity of individual plastic materials. However, their ubiquitous environmental presence poses substantial risks to critical Earth systems, biodiversity, and ecosystem services. Addressing these concerns requires the continuous refinement of toxicological testing methods and the development of novel approaches to assess the long-term environmental and health impacts of plastic debris across different size categories. Given the complexity of plastic weathering, which involves continuous degradation and multiple simultaneous processes, an interdisciplinary approach is required to bridge research gaps and improve hazard assessments beyond conventional toxicological studies.

One critical yet underexplored aspect of plastic toxicity assessments is the role of plastic-associated chemicals, including additives, residual monomers, and degradation by-products. These compounds significantly contribute to the hazardous nature of plastics but remain poorly characterized due to their diverse chemical compositions and the need for advanced analytical techniques. Present plastic leachate

Table 3. Proposed standardization framework for plastics and polymers

Component	Description
Definition standardization	Establish universally accepted definitions for "plastics," "polymers," and "macromolecules" based on International Union of Pure and Applied Chemistry guidelines to prevent ambiguity and misinterpretations.
Material classification	Develop a classification system distinguishing plastics by composition (e.g., fossil-based, bio-based), processing methods (e.g., thermoplastics, thermosets), and degradation potential (e.g., biodegradable, non-biodegradable).
Terminology consistency	Ensure consistency in terminology across scientific disciplines, industry, and policy frameworks to prevent confusion in environmental assessments, product labeling, and regulatory documents.
Regulatory alignment	Align definitions and classifications with international regulatory standards (e.g., American Standards Testing and Materials and International Standard Organization) to harmonize global policy efforts and facilitate international trade.
Scientific and industrial integration	Integrate standardized definitions into industrial manufacturing standards, scientific research methodologies, and sustainability frameworks to improve cross-sector collaboration.
Environmental impact assessment	Incorporate life cycle assessments into plastic material classification to evaluate long-term sustainability, recyclability, and ecological footprint.
Education and public awareness	Develop educational programs and public awareness campaigns to ensure all stakeholders (scientists, policymakers, industry leaders, and consumers) understand and adopt standardized definitions.
Technological innovations	Encourage research into sustainable plastic alternatives, including enhanced biodegradable plastics, bio-based polymers, and closed-loop recycling technologies for a more sustainable future.
Implementation and policy recommendations	Propose policies that enforce standardized definitions in product labeling, waste management regulations, and international trade agreements to ensure global compliance and drive effective plastic pollution mitigation.

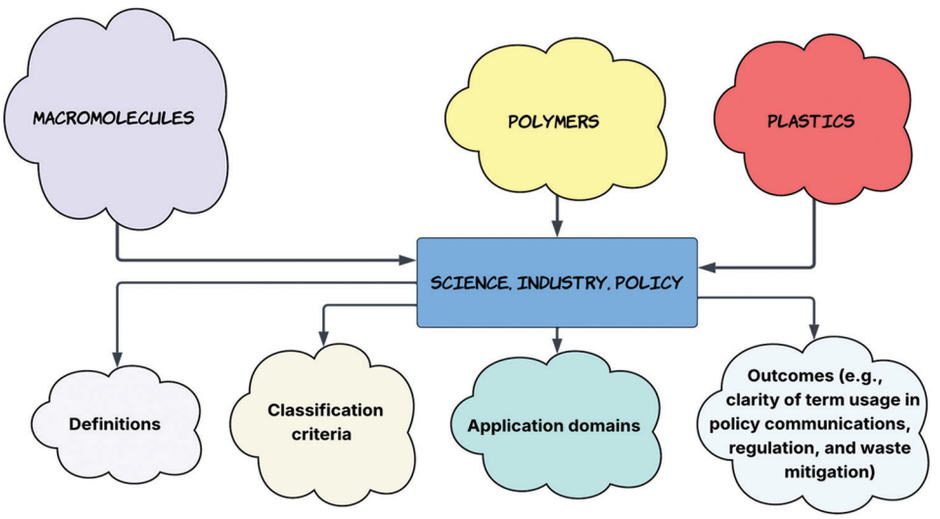

Figure 4. Visual synthesis of proposed terminology standardization framework. Image produced by the authors. Created with https://lucid.app/documents/#/home?folder_id=recent; 2025; Austine Ofondu Chinomso Iroegbu

toxicity assessments lack standardized protocols, leading to inconsistencies in reported hazard levels. In addition, many hydrophobic plastic-associated chemicals present challenges in aqueous toxicity testing due to their limited solubility, further complicating risk evaluations.

Table 4. Overview of plastic-related terminological inconsistencies across major regulatory bodies and standard organizations

Regulatory body/region	Present definition/term	Inconsistency	Implication
European Union Directive 2019/904	Plastic=polymer-based material	Omits additive requirement	Overbroad bans, e.g., on pure expanded polystyrene
United States Environmental Protection Agency	Biodegradable=breaks down in <1 year	Allows microplastic fragmentation	Mislabeling harmful materials as "eco-friendly"
International Union of Pure and Applied Chemistry	Polymer versus macromolecule versus plastic	Precise distinction	Not widely adopted in policy or industry
American Society for Testing and Materials/ISO	Varies by committee (e.g., D883, ISO 472)	Lack of harmonization	Conflicts in international trade and labeling

International Organization for Standardization

To effectively address these challenges and promote a harmonized understanding of plastic-related terminology, we propose a standardized framework that aligns with global scientific, industrial, and regulatory standards (Table 3 and Figure 4). This framework ensures that definitions and classifications are universally understood, preventing misinterpretations and facilitating more effective policymaking.

8. Conclusion

As illustrated in the summary Table 4, clear and precise terminology is far more than a semantic detail and is foundational for effective environmental science, policy, and management. Yet today, ambiguity in defining basic terms, such as "plastic" and "polymer" has fostered misaligned policies, inefficient resource allocation, and inconsistent mitigation efforts.

As plastic pollution escalates worldwide, the need to reassess how we define and classify plastics becomes increasingly urgent. For example, as research reveals new long-term health and ecological impacts of plastic debris, outdated definitions often fail to capture the full scope of these risks, resulting in regulations that lag behind scientific reality. Moreover, plastics are highly complex materials, frequently composites of multiple polymers, additives, and degradation byproducts, and simplistic definitions cannot account for this complexity. Such oversimplification hampers our ability to accurately assess environmental risks and devise targeted management strategies.

At the global level, a harmonized lexicon for plastics is essential to coordinate international efforts and enforce environmental agreements. Without alignment in terminology, countries maintain inconsistent plastic waste classifications, recycling practices, and regulatory standards, undermining progress in combating plastic pollution.

Meanwhile, rapid innovation in material science, from novel biodegradable polymers to advanced composite plastics, demands that definitions and regulations keep pace with these advances. Meeting this challenge requires systemic change. We must overhaul how plastics are defined and categorized across scientific discourse and legal frameworks by grounding definitions in robust scientific consensus (such as IUPAC guidelines) and adopting them universally. This shift should extend beyond academia and government: Standardized language about plastics must permeate industry practices, educational curricula, and public discourse, ensuring a common understanding among all stakeholders.

By embracing clear, standardized definitions of plastics and plastic pollution, the global community can establish a shared foundation for action. A common language will facilitate more effective waste management and recycling initiatives, while also ensuring more coherent regulations worldwide. Ultimately, addressing terminological ambiguity is not just an academic exercise but a catalyst for stronger global stewardship. Embracing a common language empowers science-based policies, unifies international efforts, and bolsters our capacity to preserve environmental and human health for future generations.

Acknowledgments

None.

Funding

None.

Conflict of interest

The authors declare they have no competing interests.

Author contributions

Conceptualization: Austine Ofondu Iroegbu
Writing – original draft: Austine Ofondu Iroegbu
Writing – review & editing: All authors

Availability of data

Not applicable.

References

1. Holdgate MW. *A Perspective of Environmental Pollution*. 1st ed. Cambridge: University Press; 1979.
2. Iroegbu AOC, Sadiku RE, Ray SS, Hamam Y. Plastics in municipal drinking water and wastewater treatment plant effluents: Challenges and opportunities for South Africa-a review. *Environ Sci Pollut Res*. 2020;27(12):12953-12966. doi: 10.1007/s11356-020-08194-5
3. Iroegbu AOC, Ray SS, Mbarane V, Bordado JC, Sardinha JP. Plastic pollution: A perspective on matters arising: Challenges and opportunities. *ACS Omega*. 2021;6(30):19343-19355. doi: 10.1021/acsomega.1c02760
4. Hartmann NB, Hüffer T, Thompson RC, *et al*. Are we speaking the same language? recommendations for a definition and categorization framework for plastic debris. *Environ Sci Technol*. 2019;53(3):1039-1047. doi: 10.1021/acs.est.8b05297
5. Billmeyer FW. *Textbook of Polymer Science*. 3rd ed. Germany: Wiley-VCH; 1962.
6. IUPAC. Polymer. In: *The IUPAC Compendium of Chemical Terminology*. United States: International Union of Pure and Applied Chemistry (IUPAC); 2014. doi: 10.1351/goldbook.P04735
7. IUPAC. Macromolecule (polymer molecule). In: *The IUPAC Compendium of Chemical Terminology*. United States: International Union of Pure and Applied Chemistry (IUPAC); 2014. doi: 10.1351/goldbook.M03667
8. Wright SL, Kelly FJ. Plastic and human health: A micro issue? *Environ Sci Technol*. 2017;51(12):6634-6647. doi: 10.1021/acs.est.7b00423
9. Ogden CK, Richards IA. *The Meaning of Meaning - A Study of the Influence of Language Upon Thought And of the Science of Symbolism*. 1st ed. California: A Harvest Book, Harcourt, Brace and World, Inc.; 1923.
10. Rothman R, Ryan AJ. The history and future of plastics. In: Alice A. Horthon, editors. *Plastic Pollution in the Global Ocean*. Vol 1. Singapore: World Scientific; 2023. p. 21-46. doi: 10.1142/9789811259111_0002
11. De Falco F, Di Pace E, Avella M, Cocca M. Impact of plastics on marine environments: From macro- to microplastic pollution. In: *Sustainability of Polymeric Materials*. Berlin: De Gruyter; 2020. p. 23-38. doi: 10.1515/9783110590586-002
12. Hoff GP. Nylon as a textile fiber. *Ind Eng Chem*. 1940;32(12):1560-1564.
13. Carpenter EJ, Anderson SJ, Harvey GR, Miklas HP, Peck BB. Polystyrene spherules in coastal waters. *Science.* 1972;178(4062):749-750. doi: 10.1126/science.178.4062.749
14. Carpenter EJ, Smith KL Jr. Plastics on the sargasso sea surface. *Science.* 1972;175(4027):1240-1241. doi: 10.1126/science.175.4027.1240
15. National Academy of Sciences. *Assessing Potential Ocean Pollutants*. United States: US National Academy of Sciences; 1975.
16. Nakashima E, Isobe A, Kako S, Itai T, Takahashi S, Guo X. The potential of oceanic transport and onshore leaching of additive-derived lead by marine macro-plastic debris. *Mar Pollut Bull*. 2016;107(1):333-339. doi: 10.1016/j.marpolbul.2016.03.038
17. Reynolds C, Ryan PG. Micro-plastic ingestion by waterbirds from contaminated wetlands in South Africa. *Mar Pollut Bull*. 2018;126:330-333. doi: 10.1016/j.marpolbul.2017.11.021
18. Beaumont NJ, Aanesen M, Austen MC, *et al*. Global ecological, social and economic impacts of marine plastic. *Mar Pollut Bull*. 2019;142:189-195. doi: 10.1016/j.marpolbul.2019.03.022
19. Briassoulis D. Agricultural plastics as a potential threat to food security, health, and environment through soil pollution by microplastics: Problem definition. *Sci Total Environ*. 2023;892:164533. doi: 10.1016/j.scitotenv.2023.164533
20. Rothstein SI. Plastic particle pollution of the surface of the atlantic ocean: Evidence from a Seabird. *Condor*. 1973;75(3):344-345. doi: 10.2307/1366176
21. Charles E, Carraher JR. *Carraher's Polymer Chemistry*. 10th ed. Francis: Taylor and Francis Group, LLC; 2018.
22. Charles E, Carraher JR. *Giant Molecules: Essential Materials for Everyday Living and Problem Solving*. 2nd ed. Hoboken, New Jersey: John Wiley and Sons, Inc.; 2003.
23. Alexander Y, Grosberg A, Khokhlov AR. *Giant Molecules: Here, There, and Everywhere*. 2nd ed. Singapore: World Scientific Publishing Co. Pvt Ltd.; 2011.
24. Fan LZ, He H, Nan CW. Tailoring inorganic-polymer composites for the mass production of solid-State batteries. *Nat Rev Mater.* 2021;6(11):1003-1019.

doi: 10.1038/s41578-021-00320-0
25. Valino AD, Dizon JRC, Espera AH, Chen Q, Messman J, Advincula RC. Advances in 3D printing of thermoplastic polymer composites and nanocomposites. *Prog Polym Sci*. 2019;98:101162. doi: 10.1016/J.PROGPOLYMSCI.2019.101162
26. Zhao HY, Yu MY, Liu J, Li X, Min P, Yu ZZ. Efficient preconstruction of three-dimensional graphene networks for thermally conductive polymer composites. *Nanomicro Lett.* 2022;14(1):129. doi: 10.1007/S40820-022-00878-6
27. Wang S, Luo Z, Liang J, *et al*. Polymer nanocomposite dielectrics: Understanding the matrix/particle interface. *ACS Nano.* 2022;16(9):13612-13656. doi: 10.1021/ACSNANO.2C07404
28. Dong J, Hu R, Niu Y, *et al*. Enhancing high-temperature capacitor performance of polymer nanocomposites by adjusting the energy level structure in the micro-/meso-scopic interface region. *Nano Energy*. 2022;99:107314. doi: 10.1016/J.NANOEN.2022.107314
29. Koltzenburg S, Maskos M, Nuyken O. *Polymer Chemistry*. Berlin, Germany: Springer Berlin Heidelberg; 2023. p. 14197.
30. Zhu J, Wang C. Biodegradable plastics: Green hope or greenwashing? *Mar Pollut Bull*. 2020;161:111774. doi: 10.1016/j.marpolbul.2020.111774
31. Millican JM, Agarwal S. Plastic pollution: A material problem? *Macromolecules*. 2021;54(10):4455-4469. doi: 10.1021/acs.macromol.0c02814
32. Law KL, Narayan R. Reducing environmental plastic pollution by designing polymer materials for managed end-of-life. *Nat Rev Mater*. 2021;7(2):104-116. doi: 10.1038/s41578-021-00382-0
33. Figge F, Thorpe AS, Gutberlet M. Definitions of the circular economy: Circularity matters. *Ecol Econ*. 2023;208:107823. doi: 10.1016/j.ecolecon.2023.107823
34. Yu J, Yu DW, Checkla DM, Freedberg IM, Bertolino AP. Human hair keratins. *J Invest Dermatol*. 1993;101(1):S56-S59. doi: 10.1016/0022-202X(93)90501-8
35. Branden C, Tooze J. *Introduction to Protein Structure*. 2nd ed. NY, USA: Garland Science, Taylor and Francis Group, LLC; 1999.
36. Ward WS. Deoxyribonucleic acid loop domain tertiary structure in mammalian spermatozoa. *Biol Reprod*. 1993;48(6):1193-1201. doi: 10.1095/biolreprod48.6.1193
37. Saenger W. *Principles of Nucleic Acid Structure*. New York: Springer; 1984. doi: 10.1007/978-1-4612-5190-3
38. Riseman J, Kirkwood JG. The intrinsic viscosity, translational and rotatory diffusion constants of rod-like macromolecules in solution. *J Chem Phys*. 1950;18(4):512-516. doi: 10.1063/1.1747672
39. Khanna YP, Reimschuessel AC, Banerjie A, Altman C. Memory effects in polymers. II. Processing history vs. Crystallization rate of nylon 6-observation of phenomenon and product behavior. *Polym Eng Sci*. 1988;28(24):1600-1606. doi: 10.1002/pen.760282405
40. Graessley WW. Entangled linear, branched and network polymer systems - molecular theories. In: *Synthesis and Degradation Rheology and Extrusion*. Vol 47. Germany: Springer-Verlag; 1982. p. 67-117. doi: 10.1007/BFb0038532
41. Kohlgrüber K, Bierdel M, Rust H. *Plastics Compounding and Polymer Processing - Fundamentals, Machines, Equipment, Application Technology*. Germany: Carl Hanser Verlag, München; 2021.
42. Reiter G. The memorizing capacity of polymers. *J Chem Phys*. 2020;152(15):150901. doi: 10.1063/1.5139621
43. Tadmor Z, Gogos CG. *Principles of Polymer Processing*. 2nd ed. Hoboken, NJ, USA: John Wiley and Sons, Inc.; 2006.
44. Saldívar-Guerra E, Vivaldo-Lima E, editors. *Handbook of Polymer Synthesis, Characterization, and Processing*. United States: Wiley; 2013. doi: 10.1002/9781118480793
45. Desidery L, Lanotte M. Polymers and plastics: Types, properties, and manufacturing. In: *Plastic Waste for Sustainable Asphalt Roads*. Amsterdam: Elsevier; 2022. p. 3-28. doi: 10.1016/B978-0-323-85789-5.00001-0
46. Seiffert S. *Physical Chemistry of Polymers - A Conceptual Introduction*. Berlin, Germany: Walter De Gruyter GmbH; 2020.
47. Akiba M, Hashim AS. Vulcanization and crosslinking in elastomers. *Prog Polym Sci*. 1997;22(3):475-521. doi: 10.1016/S0079-6700(96)00015-9
48. Rajesh Babu R, Shibulal GS, Chandra AK, Naskar K. Compounding and vulcanization. In: Visakh P, Thomas S, Chandra A, Mathew A, editors. *Advances in Elastomers I: Advanced Structured Materials*. Vol 11. Berlin: Springer Nature; 2013. p. 83-135. doi: 10.1007/978-3-642-20925-3_4
49. Ge C, Wang S, Zheng W, Zhai W. Preparation of microcellular thermoplastic polyurethane (TPU) foam and its tensile property. *Polym Eng Sci*. 2018;58:E158-E166. doi: 10.1002/PEN.24813
50. Datta J, Kasprzyk P. Thermoplastic polyurethanes derived from petrochemical or renewable resources: A comprehensive review. *Polym Eng Sci*. 2018;58:E14-E35. doi: 10.1002/PEN.24633
51. Johnson L, Samms J. Thermoplastic polyurethane technologies for the textile industry. *J Coated Fabr*. 1997;27(1):48-62.

doi: 10.1177/152808379702700106
52. Dodiuk H, editor. *Handbook of Thermoset Plastics*. 4th ed. Amsterdam: William Andrew - Elsevier; 2022.
53. Tamburri MN, Soon ZY, Scianni C, *et al*. Understanding the potential release of microplastics from coatings used on commercial ships. *Front Mar Sci*. 2022;9:1074654. doi: 10.3389/fmars.2022.1074654
54. Iroegbu AOC, Ray SS. Bamboos: From bioresource to sustainable materials and chemicals. *Sustain (Switzerland)*. 2021;13(21):12200. doi: 10.3390/su132112200
55. Wilderjans E, Luyts A, Brijs K, Delcour JA. Ingredient functionality in batter type cake making. *Trends Food Sci Technol*. 2013;30(1):6-15. doi: 10.1016/j.tifs.2013.01.001
56. Bennion EB, Bamford GST. In: Bent AJ, editor. *The Technology of Cake Making*. Germany, US: Springer; 1997. doi: 10.1007/978-1-4757-6690-5
57. Matthews FL, Rawlings RD. *Composite Materials: Engineering and Science*. Delhi: WoodHead Publishing; 1999.
58. Brendan R. *Tire Engineering - An Introduction*. 1st ed. United States: CRC Press; 2021.
59. Grossman RF, Lutz JT Jr., editors. *Polymer Modifiers and Additives*. United States: CRC Press; 2000. doi: 10.1201/9781482273755
60. Mascia L, Xanthos M. An overview of additives and modifiers for polymer blends: Facts, deductions, and uncertainties. *Adv Polym Technol*. 1992;11(4):237-248. doi: 10.1002/adv.1992.060110402
61. Iroegbu AOC, Ray SS. Recent developments and future perspectives of biorenewable nanocomposites for advanced applications. *Nanotechnol Rev*. 2022;11(1):1696-1721. doi: 10.1515/ntrev-2022-0105
62. Evans MS. *Tyre Compounding for Improved Performance*. United Kingdom: ISmithers Rapra Publishing; 2001.
63. Bart JCJ. Polymer additive analysis at the limits. *Polym Degrad Stab*. 2003;82(2):197-205. doi: 10.1016/S0141-3910(03)00196-4
64. Chanda M, Roy SK. *Plastics Technology Handbook, Third Edition*. 4th ed. United States: CRC Press; 2006. doi: 10.1201/9781420006360
65. Science Museum. *The Age of Plastic: From Parkesine to Pollution*. Science Museum; 2019. Available from: https://www.sciencemuseum.org.uk/objects/and/stories/chemistry/age/plastic/parkesine-pollution [Last accessed on 2023 Nov 17].
66. Azzarello MY, Van-Vleet E. Marine birds and plastic pollution. *Mar Ecol Prog Ser*. 1987;37:295-303. doi: 10.3354/meps037295
67. MacLeod M, Arp HPH, Tekman MB, Jahnke A. The global threat from plastic pollution. *Science*. 2021;373(6550):61-65. doi: 10.1126/science.abg5433
68. Windsor FM, Durance I, Horton AA, Thompson RC, Tyler CR, Ormerod SJ. A catchment-scale perspective of plastic pollution. *Glob Chang Biol*. 2019;25(4):1207-1221. doi: 10.1111/gcb.14572
69. Han WB, Lee JH, Shin JW, Hwang SW. Advanced materials and systems for biodegradable, transient electronics. *Adv Mater*. 2020;32(51):2002211. doi: 10.1002/adma.202002211
70. Rujnić-Sokele M, Pilipović A. Challenges and opportunities of biodegradable plastics: A mini review. *Waste Manag Res*. 2017;35(2):132-140. doi: 10.1177/0734242X16683272
71. Greenpeace Africa. *Greenpeace Africa commends Uganda for the Ban on Plastic Bags*. GreenPeace; 2018. Available from: https://www.greenpeace.org/archive-africa/en/press-centre-hub/greenpeace-africa-commends-uganda-for-the-ban-on-plastic-bags [Last accessed on 2018 Nov 19].
72. Cornejo-D'Ottone M, Molina V, Pavez J, Silva N. Greenhouse gas cycling by the plastisphere: The sleeper issue of plastic pollution. *Chemosphere*. 2020;246:125709. doi: 10.1016/j.chemosphere.2019.125709
73. Shen M, Huang W, Chen M, Song B, Zeng G, Zhang Y. (Micro)plastic crisis: Un-ignorable contribution to global greenhouse gas emissions and climate change. *J Clean Prod*. 2020;254:120138. doi: 10.1016/j.jclepro.2020.120138
74. Moustafa H, Youssef AM, Darwish NA, Abou-Kandil AI. Eco-friendly polymer composites for green packaging: Future vision and challenges. *Compos Part B Eng*. 2019;172:16-25. doi: 10.1016/j.compositesb.2019.05.048
75. Circle Economy. *The Circularity Gap Report 2021*. World Economic Forum; 2021. Available from: https://www.circularity-gap.world/2022#download-the-report [Last accessed on 2022 Mar 08].
76. O'Brien S, Okoffo ED, O'Brien JW, *et al*. Airborne emissions of microplastic fibres from domestic laundry dryers. *Sci Total Environ*. 2020;747:141175. doi: 10.1016/j.scitotenv.2020.141175
77. Hernandez E, Nowack B, Mitrano DM. Polyester textiles as a source of microplastics from households: A mechanistic study to understand microfiber release during washing. *Environ Sci Technol*. 2017;51(12):7036-7046. doi: 10.1021/acs.est.7b01750
78. The Guardian News and Media. '*It's the Industry's Dirty Secret': Why Fashion's Oversupply Problem is an Environmental Disaster*. *Fashion Industry*. Available from: https://www.theguardian.com/fashion/2024/jan/18/its/the/industrys/dirty/secret/why/fashions-oversupply-problem-is-an-environmental-disaster [Last accessed on 2024 Apr 06].

79. Gündoğdu S, editor. *Plastic Waste Trade*. Switzerland: Springer Nature; 2024. doi: 10.1007/978-3-031-51358-9
80. Green DS, Almroth BC, Altman R, *et al*. Time to kick the butt of the most common litter item in the world: Ban cigarette filters. *Sci Total Environ*. 2023;865:161256. doi: 10.1016/j.scitotenv.2022.161256
81. Belzagui F, Buscio V, Gutiérrez-Bouzán C, Vilaseca M. Cigarette butts as a microfiber source with a microplastic level of concern. *Sci Total Environ*. 2021;762:144165. doi: 10.1016/j.scitotenv.2020.144165
82. Novotny TE, Lum K, Smith E, Wang V, Barnes R. Cigarettes butts and the case for an environmental policy on hazardous cigarette waste. *Int J Environ Res Public Health*. 2009;6(5):1691-1705. doi: 10.3390/ijerph6051691
83. Stanton T, Johnson M, Nathanail P, MacNaughtan W, Gomes RL. Freshwater and airborne textile fibre populations are dominated by 'natural', not microplastic, fibres. *Sci Total Environ*. 2019;666:377-389. doi: 10.1016/j.scitotenv.2019.02.278
84. Sillanpää M, Sainio P. Release of polyester and cotton fibers from textiles in machine washings. *Environ Sci Pollut Res Int*. 2017;24(23):19313-19321. doi: 10.1007/s11356-017-9621-1
85. Luo Z, Zhou X, Su Y, *et al*. Environmental occurrence, fate, impact, and potential solution of tire microplastics: Similarities and differences with tire wear particles. *Sci Total Environ*. 2021;795:148902. doi: 10.1016/j.scitotenv.2021.148902
86. Rauert C, Vardy S, Daniell B, Charlton N, Thomas KV. Tyre additive chemicals, tyre road wear particles and high production polymers in surface water at 5 urban centres in Queensland, Australia. *Sci Total Environ*. 2022;852:158468. doi: 10.1016/j.scitotenv.2022.158468
87. Goßmann I, Herzke D, Held A, *et al*. Occurrence and backtracking of microplastic mass loads including tire wear particles in northern Atlantic air. *Nat Commun*. 2023;14(1):3707. doi: 10.1038/s41467-023-39340-5
88. Malizia A, Monmany-Garzia AC. Terrestrial ecologists should stop ignoring plastic pollution in the anthropocene time. *Sci Total Environ*. 2019;668:1025-1029. doi: 10.1016/j.scitotenv.2019.03.044
89. De Souza Machado AA, Kloas W, Zarfl C, Hempel S, Rillig MC. Microplastics as an emerging threat to terrestrial ecosystems. *Glob Chang Biol*. 2018;24(4): 1405-1416. doi: 10.1111/gcb.14020
90. Kole PJ, Löhr AJ, Van Belleghem FG, Ragas AM. Wear and tear of tyres: A stealthy source of microplastics in the environment. *Int J Environ Res Public Health*. 2017;14(10):1265. doi: 10.3390/ijerph14101265
91. Knight LJ, Parker-Jurd FNF, Al-Sid-Cheikh M, Thompson RC. Tyre wear particles: An abundant yet widely unreported microplastic? *Environ Sci Pollut Res*. 2020;27(15):18345-18354. doi: 10.1007/s11356-020-08187-4
92. Andersson-Sköld Y, Johanesson M, Gustafsson M, *et al*. *Microplastics from Tyre and Road Wear - A Literature Review*. Swedish National Road and Transport Research Institute; 2020. Available from: https://www.vti.se [Last accessed on 2021 Mar 23].
93. Iroegbu AO, Ray SS. Lignin and keratin-based materials in transient devices and disposables: Recent advances toward materials and environmental sustainability. *ACS Omega*. 2022;7(13):10854-10863. doi: 10.1021/acsomega.1c07372
94. Iroegbu AOC, Ray SS. Nanocellulosics in transient technology. *ACS Omega*. 2022;7(51):47547-47566. doi: 10.1021/acsomega.2c05848
95. Chandrasekaran SR, Avasarala S, Murali D, Rajagopalan N, Sharma BK. Materials and energy recovery from e-waste plastics. *ACS Sustain Chem Eng*. 2018;6(4):4594-4602. doi: 10.1021/acssuschemeng.7b03282
96. Tian Y, Chen C, Sagoe-Crentsil K, Zhang J, Duan W. Intelligent robotic systems for structural health monitoring: Applications and future trends. *Autom Constr*. 2022;139:104273. doi: 10.1016/j.autcon.2022.104273
97. Onat NC, Kucukvar M. A systematic review on sustainability assessment of electric vehicles: Knowledge gaps and future perspectives. *Environ Impact Assess Rev*. 2022;97:106867. doi: 10.1016/j.eiar.2022.106867
98. Daniela-Abigail HL, Tariq R, El Mekaoui A, *et al*. Does recycling solar panels make this renewable resource sustainable? Evidence supported by environmental, economic, and social dimensions. *Sustain Cities Soc*. 2022;77:103539. doi: 10.1016/j.scs.2021.103539
99. Sodhi M, Banaszek L, Magee C, Rivero-Hudec M. Economic lifetimes of solar panels. *Procedia CIRP*. 2022;105:782-787. doi: 10.1016/j.procir.2022.02.130
100. Ghosh K, Jones BH. Roadmap to biodegradable plastics-current State and research needs. *ACS Sustain Chem Eng*. 2021;9(18):6170-6187. doi: 10.1021/acssuschemeng.1c00801
101. Innocenti FD. Biodegradability and compostability. In: Chiellini E, Solaro R, editors. *Biodegradable Polymers and Plastics*. 1st ed., Vol. 1. United States: Springer; 2003. p. 33-45. doi: 10.1007/978-1-4419-9240-6_2
102. Emadian SM, Onay TT, Demirel B. Biodegradation of bioplastics in natural environments. *Waste Manag*. 2017;59:526-536. doi: 10.1016/j.wasman.2016.10.006

103. Chinaglia S, Tosin M, Degli-Innocenti F. Biodegradation rate of biodegradable plastics at molecular level. *Polym Degrad Stab*. 2018;147:237-244. doi: 10.1016/j.polymdegradstab.2017.12.011
104. Jeon O, Bouhadir KH, Mansour JM, Alsberg E. Photocrosslinked alginate hydrogels with tunable biodegradation rates and mechanical properties. *Biomaterials*. 2009;30(14):2724-2734. doi: 10.1016/j.biomaterials.2009.01.034
105. Li R, Tao J, Huang D, *et al*. Investigating the effects of biodegradable microplastics and copper ions on probiotic (*Bacillus amyloliquefaciens*): Toxicity and application. *J Hazard Mater*. 2023;443:130081. doi: 10.1016/j.jhazmat.2022.130081
106. Ali W, Ali H, Gillani S, Zinck P, Souissi S. Polylactic acid synthesis, biodegradability, conversion to microplastics and toxicity: A review. *Environ Chem Lett*. 2023;21(3):1761-1786. doi: 10.1007/s10311-023-01564-8
107. Gerngross TU, Slater SC. How green are green plastics? *Sci Am*. 2000;283(2):36-41. doi: 10.1038/scientificamerican0800-36
108. Gulizia AM, Patel K, Philippa B, Motti CA, Van Herwerden L, Vamvounis G. Understanding plasticiser leaching from polystyrene microplastics. *Sci Total Environ*. 2023;857:159099. doi: 10.1016/j.scitotenv.2022.159099
109. Albertsson AC, Hakkarainen M. Designed to degrade. *Science*. 2017;358(6365):872-873. doi: 10.1126/science.aap8115
110. Sun B, Hu Y, Cheng H, Tao S. Releases of brominated flame retardants (BFRs) from microplastics in aqueous medium: Kinetics and molecular-size dependence of diffusion. *Water Res*. 2019;151:215-225. doi: 10.1016/j.watres.2018.12.017
111. Bandow N, Will V, Wachtendorf V, Simon FG. Contaminant release from aged microplastic. *Environ Chem*. 2017;14(6):394. doi: 10.1071/EN17064
112. Environment ECDG for. *Turning the Tide on Single-Use Plastics*. European: Publications Office of the European Union; 2021. doi: 10.2779/800074
113. US-EPA. *Frequently Asked Questions about Plastic Recycling and Composting*. National Strategy; 2024. Available from: https://www.epa.gov/trash/free/waters/frequently/asked/questions/about/plastic/recycling/and/composting#biodegradable [Last accessed on 2025 Feb 03].

Asian Journal of Water, Environment and Pollution. Vol. 22, No. 3 (2025), pp. 15-31.
doi: 10.36922/AJWEP025160123

REVIEW ARTICLE

Nano-biofertilizers: A promising technology for sustainable soil fertility, soil health, and environmental protection

Hayyawi W. A. Al-Juthery[1], Rand A. H. G. Al-Taee[2], Ali S. Alhasan[1], Diaa F. Hassan[3]*, Nisreen A. A. Al-Jassani[4], and Raid Shaalan Jarallah[1]

[1]Department of Soil and Water Resources, College of Agriculture, University of Al-Qadisiyah, Al Diwaniyah, Qadisiyyah, Iraq
[2]Department of Soil and Water Resources, College of Agriculture and Forestry, University of Mosul, Mosul, Nineveh, Iraq
[3]Department of Civil Engineering, College of Engineering, Al-Qasim Green University, Al-Qasim, Babylon, Iraq
[4]Department of Soil and Water Resources, College of Education for Girls, University of Kufa, Kufa, Najaf, Iraq
***Corresponding author:** Diaa F. Hassan (diaafliah@wrec.uoqasim.edu.iq)

Received: April 19, 2025; 1st revised: May 13, 2025; 2nd revised: May 26, 2025; Accepted: May 28, 2025; Published online: June 24, 2025

Abstract: The rapidly increasing global demand for food security urgently calls for agricultural technologies that can boost productivity without contributing to environmental degradation. A group of fertilizers that combines nanotechnology with beneficial microorganisms – known as nano-biofertilizers – has shown tremendous potential to enhance plant growth, increase yields, and improve soil health. Controlled nutrient release, enhanced microbial activities, and improved nutrient-use efficiency are key benefits of these new fertilizers, collectively leading to higher crop productivity with reduced environmental impact. These advantages contribute to sustainable agriculture by reducing the use of chemical fertilizers, surface soil degradation, nutrient leaching, and greenhouse gas emissions. Recent research findings have also highlighted their role in increasing plant resilience to abiotic stress factors, enhancing soil microbial diversity, and supporting ecological balance. This paper presents a comprehensive analysis of the multifaceted roles of nano-biofertilizers in modern agriculture, focusing on their contributions to plant physiology, soil health, environmental sustainability, and long-term agricultural productivity. Through empirical integration, we argue that nano-biofertilizers could be a transformative tool in advancing sustainable farming and achieving global environmental conservation goals.

Keywords: Fertilizer innovation; Microbial bioinoculant; Plant growth and yield; Soil health and sustainability; Plant-microbe interaction; Nutrient efficiency; Microbial activity

1. Introduction

As a recent development, the integration of nanotechnology with biofertilizers is being practiced to promote soil health and environmental sustainability. Nanobiofertilizers combine the advantages of biological fertilizers with advanced delivery mechanisms enabled by nanomaterials. As a result, they can increase nutrient efficiency, reduce the environmental impact associated with nutrient losses, and address potential environmental risks.

Chemical fertilizers have marked a breakthrough in traditional farming practices; however, their use

typically leads to nutrient leaching, soil degradation, and water pollution. On the contrary, nano-biofertilizers release nutrients gradually and more efficiently deliver the specific nutrients that plants need. This approach allows for reduced fertilizer application, thereby significantly decreasing potential environmental harm. Garg *et al.*[1] support the view that nano-biofertilizers enhance nutrient availability, resulting in improved plant growth and yield. The inclusion of beneficial microbes in nano-biofertilizers likely contributes to soil health, as these organisms are involved in nutrient solubilization, nitrogen fixation, and suppression of soil-borne pathogens. According to Sambangi *et al.,*[2] the application of nano-biofertilizers containing plant growth-promoting rhizobacteria improves microbial activity and soil fertility.

Another main benefit of the nano-biofertilizer is environmental protection. They help reduce greenhouse gas emissions and water pollution caused by nutrient runoff, as they lower the dependency on chemical fertilizers. Nanophosphorus fertilizers, for instance, enhance plant growth with minimal environmental harm, as the applied doses are not excessive, an effect demonstrated by Miranda-Villagómez *et al.*[3] Separately, Madlala and Khanyile[4] indicated that the physical properties of nanoparticles, such as size, shape, and crystallinity, significantly influence the efficiency of nutrient utilization by plants. The study also confirmed that agglomeration and nanoscale loss could reduce the effectiveness of nanofertilizers, highlighting the importance of standardizing preparation and analysis methods to ensure reproducibility.

In summary, nano-biofertilizers represent a forward-looking approach to sustainable agriculture. They enhance nutrient efficiency uptake, support soil microbial health, and are environmentally friendly, positioning them as a vital component of future farming practices.

2. The concept of nano-biofertilizers: A scientific perspective

The ever-increasing demand for sustainable agriculture worldwide has initiated a new trend: Nano-biofertilizers, which combine nanotechnology with biofertilization to improve soil fertility, enhance crop productivity, optimize nutrient use, and minimize environmental harm. Conventional fertilizers have been widely used for decades, but their overuse has led to soil degradation, water pollution, and loss of biodiversity.[5,6] In the context of nutrient management, the concept of nano-biofertilizers has emerged. These involve the combination of microbial inoculants with nanoparticles to improve nutrient uptake, stimulate microbial activity, and maintain healthy, living soils.[7]

2.1. Defining nano-biofertilizers

Nano-biofertilizers represent a new generation of fertilizers that include:

(i) Nanoparticles: Serve as nutrient carriers, enhancing bioavailability and enabling controlled nutrient release.

(ii) Biofertilizers: These are microbial substances containing beneficial microorganisms such as *Rhizobium*, *Azotobacter*, *Mycorrhizae*, and phosphate-solubilizing bacteria, which play crucial roles in biological nitrogen fixation, phosphorus solubilization, and plant growth promotion.[8]

2.2. Mechanisms of action

Nano-biofertilizers function through multiple mechanisms, including nutrient delivery, soil retention, and plant uptake, which collectively make them superior to conventional fertilizers.[9]

(i) Controlled nutrient release: Nanoparticles, particularly in nanofertilizers, enable a slow and controlled release of nutrients, thereby reducing leaching losses and enhancing nutrient-use efficiency.[10] A critical aspect is the improvement of nitrogen and phosphorus use efficiency, as both nutrients are commonly lost through volatilization and runoff.[11]

(ii) Enhanced microbial activity: Nano-biofertilizers can improve the viability and effectiveness of beneficial soil microorganisms. For example, nano-silica and nano-chitosan support microbial safety and promote the growth of probiotic bacteria.[12] Enzyme activity in soil, which contributes to enhanced nutrient bioavailability, is also improved by nano-zinc biofertilizers.[13]

(iii) Improved plant nutrient uptake: Nanoparticles promote better root penetration and improved mobility of nutrients in the soil, leading to more efficient uptake of essential elements by plants.[14] Studies have shown that nano-biofertilizers increase root biomass and chlorophyll content, two effects directly linked to enhanced crop yield.[15]

2.3. Types of nano-biofertilizers

Table 1 presents the development of nano-biofertilizers targeting different nutrient deficiencies and soil conditions.

2.4. Advantages of nano-biofertilizers

Table 2 summarizes the various environmental and agricultural benefits of nano-biofertilizers compared to their conventional counterparts.

3. The role of nano-biofertilizers in soil fertility and health

Soil fertility is a crucial factor influencing soil health and its capacity to support productivity. It has been recognized that while conventional fertilizers have been widely applied to improve soil fertility, over-reliance on them often results in soil compaction, which can contribute to nutrient leaching and environmental pollution.[20,21] Nano-biofertilizers, which combine nanotechnology with biofertilizers, have therefore been proposed as an environmentally friendly alternative that stimulates microbial activity and enhances overall soil health.

3.1. Nano-biofertilizers and mechanisms in soil fertility

The use of nanoparticle-based formulations combined with biofertilizers to enhance nutrient availability and microbial activity in soil is referred to as nano-biofertilizers. Nanoparticles serve as carriers for nutrients and beneficial organisms, improving their stability and efficacy.[22,23] For example,[24] observed increased nitrogen availability in soil through slow-release techniques, which consequently decreased dependency on chemical fertilizers. Nano-biofertilizers also stimulate soil enzyme activity, a primary factor in nutrient cycling. Specifically, urease and phosphatase activities in the soil increased after nanobiofertilizer application, making nitrogen and phosphorus more available.[25,26] Such improvements in nutrient efficiency directly contribute to increased agricultural output and soil fertility.

3.2. Impact on soil microbial communities

Microbial populations are key determinants of soil health due to their diversity and functional roles. Nano-biofertilizers elevate populations of beneficial bacteria such as *Rhizobium*, which fixes nitrogen, and *Pseudomonas*, which solubilizes phosphates.[27,28] The use of nano-biofertilizers has been shown to improve microbial biomass and enzymatic activities critical for the decomposition of organic matter and nutrient recycling.[29] In addition, nanoparticles such as nano-silica and nano-zinc have been reported to suppress pathogenic microbes while promoting the growth of beneficial ones. This dual effect supports soil health and reduces the incidence of soil-borne diseases.[30,31]

3.3. Sustainability and environmental benefits

Conventional fertilizers, in addition to supplying nutrients, often cause nutrient runoff, leading to eutrophication. On the contrary, nano-biofertilizers enhance nutrient use efficiency, reducing nutrient losses to the environment. Their slow-release properties ensure that nutrients are supplied to plants over an extended period, reducing the frequency of applications and minimizing environmental contamination. Nano-biofertilizers also promote microbial decomposition of plant residues and organic fertilizers, thereby increasing soil organic matter content. This, in turn, improves soil

Table 1. Types and main functions of nano-biofertilizers with key references

Type	Main function	References
Nano-nitrogen biofertilizers	Enhance biological nitrogen fixation and minimize Nitrogen losses	10
Nano-phosphate solubilizing bacteria	Increase phosphorus solubilization and availability	9
Nano-potassium biofertilizers	Improve potassium uptake and soil cation exchange capacity	16
Nano-zinc biofertilizers	Boost enzyme activity and micronutrient absorption	15
Nano-silica biofertilizers	Increase plant resistance to drought and pathogens	17

Table 2. Environmental and agronomic benefits of nano-biofertilizers compared to traditional fertilizers

Benefit	Description	References
Higher nutrient efficiency	Reduces nutrient losses and improves plant uptake	5
Enhanced microbial function	Promotes soil biodiversity and nitrogen fixation	18
Reduction in chemical fertilizers	Decreases synthetic fertilizer dependency	12
Eco-friendly and sustainable	Limits soil pollution and groundwater contamination	19

structure, enabling better water retention to support root growth and facilitating the gaseous exchange necessary for healthy crop development.[32,33]

A quantitative representation of the role of nanobiofertilizers in sustaining soil fertility is shown in Figure 1. The chart illustrates six key functional contributions: (i) "Improved nutrient absorption" (20%) highlights the enhanced efficiency of nutrient uptake due to nanoscale delivery systems; (ii) "Enhanced microbial activity" (18%) refers to the stimulation of beneficial soil microorganisms facilitated by nano-encapsulated inoculants; (iii) "Soil structure enhancement" (17%) includes improved soil porosity and aggregation resulting from increased microbial exudates; (iv) "Long-term soil sustainability" (15%) reflects the cumulative effect of balanced nutrient release and ecological compatibility; (v) "Reduction in chemical fertilizers" (15%) demonstrates how nano-formulations reduce the need for synthetic inputs; and (vi) "Increase in organic matter" (15%) indicates the build-up of carbon and organic residues due to microbial and plant-soil interactions. These interconnected roles reinforce the multifunctional benefits of nano-biofertilizers in improving soil health over time.

4. The role of nano-biofertilizers in plant growth and yield

Over the years, nano-biofertilizers have attracted mounting attention as a sustainable approach to stimulate plant growth and improve agricultural output. This is due to the synergistic effects of nanotechnology and biological fertilizers, which enhance nutrient availability and strengthen plant growth and soil health while minimizing pollution from fertilizer applications.[34] In this paper, the critical role of nano-biofertilizers in enhancing crop productivity, their mechanisms of action, and their advantages over conventional fertilizers are discussed.

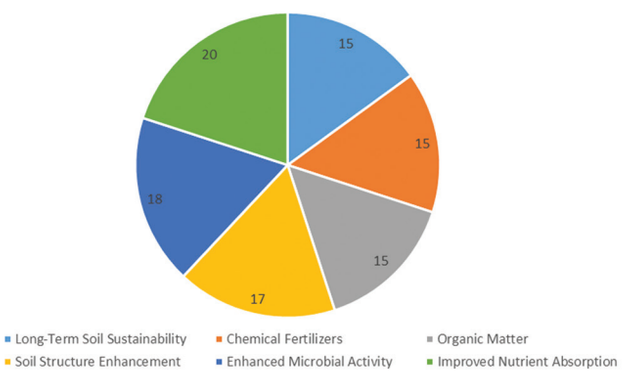

Figure 1. The role of nano-biofertilizers in sustaining soil fertility

4.1. Mechanisms of action of nano-biofertilizers

The primary functions of nano-biofertilizers are improving nutrient use efficiency in crops, inducing beneficial microbial activity, and enhancing soil structure. Simply put, these fertilizers are engineered to deliver nutrients to plants in controlled and targeted manners at the nanoscale.[35,36] Due to their small size, nanoparticles have a large surface area that allows close contact with roots for more effective nutrient uptake by plants.[37] In addition, biofertilizers contain beneficial microorganisms, such as nitrogen-fixing bacteria and phosphate-solubilizing fungi, which enhance nutrient availability and absorption.[38,39]

One of the most important mechanisms through which nano-biofertilizers act is by releasing essential nutrients from otherwise inaccessible forms. For example, nano-encapsulated nitrogen fertilizers reduce nitrogen losses due to leaching and volatilization, ensuring a steady supply of nitrogen to crops. Similarly, nano-phosphorus fertilizers increase phosphorus solubilization and uptake, promoting proper root growth and higher crop yields.

4.2. Advantages of nano-biofertilizers over conventional fertilizers

Conventional fertilizers have a significant drawback compared to nano-biofertilizers: They are often highly inefficient in nutrient delivery and can be detrimental to the environment, as well as less effective in helping plants cope with stress conditions. Conventional fertilizers frequently leach nutrients, causing pollution of both soil and water. In contrast, nano-biofertilizers release nutrients in a controlled manner, thereby reducing environmental degradation caused by nutrient wastage.[40,41] Moreover, the microbial components of biofertilizers improve soil organic matter and soil fertility, providing long-term benefits for sustainable agriculture.[42,43]

Another major advantage of nano-biofertilizers is their potential to increase plant tolerance to abiotic stresses such as drought, salinity, and metal toxicity. Studies have shown that plants treated with nano-biofertilizers exhibit improved drought tolerance linked to increased activity of antioxidant enzymes.[18] This effect is particularly important given the increasing impacts of climate change on agriculture.

Various studies have also demonstrated that nano-biofertilizers significantly enhance crop yield and productivity. For example, Meena *et al.*[44] showed that applying nano-biofertilizers to wheat increased grain yield by 20 – 30% compared to traditional fertilizers. Similar trials conducted on maize and rice reported higher biomass, increased chlorophyll content, and greater grain yields following nano-biofertilizer application.[45,46] These findings clearly indicate that nano-biofertilizers can play a major role in improving food security through sustainable agricultural practices.

Nano-biofertilizers combine nanoparticles with biological agents, including plant growth-promoting bacteria, which have been widely observed to stimulate plant growth and productivity (Table 3).

These studies indicate the potential for enhancing certain plant parameters and yields by combining biofertilizers with nanoparticles. However, in practice, the effectiveness of nano-biofertilizers may vary under the same conditions in which conventional fertilizers often fail. Therefore, further organized research is imperative to test formulations and application methods, with the aim of optimizing their performance across different agroecological zones.

4.3. Comparison: Nano-biofertilizers versus conventional biofertilizers (yield and soil health)

The integration of nanotechnology with biofertilizers aims to overcome some limitations of traditional biofertilizers. In terms of crop yield under field conditions, nano-biofertilizers demonstrate a clear advantage. Conventional biofertilizers (microbial inoculants) can improve yields by enhancing nutrient availability and soil biological activity. However, their effects are often gradual and variable, as they rely on living organisms whose performance may be inconsistent due to environmental stress or poor survival in the soil. In contrast, nano-biofertilizers typically exhibit faster and stronger impacts on crop growth, as nano-carriers provide immediate and efficient nutrient delivery in addition to microbial benefits. For example, field trials have reported that applying nutrients in nano form (like nanourea) can achieve yields comparable to or even higher than those achieved with standard fertilizer rates, despite using smaller quantities.[50] In one study, foliar application of nano-urea allowed a 25% reduction in conventional urea usage with no yield loss in wheat and rice. Another experiment on soybeans showed a ~20% higher seed yield when using nano-hydroxyapatite (a nano-phosphorus fertilizer) compared to traditional phosphate fertilizer.[51] These results suggest nano-enhanced biofertilizers can outperform traditional biofertilizers in terms of immediate yield gains, owing to the controlled nutrient release and targeted uptake. However, recent evidence also cautions that nanofertilizers are not a complete substitute for bulk fertilizers in all cases. Adequate macronutrient supply is still required, and nano-formulations are most effective as supplements to optimize efficiency rather than as replacements.

When considering long-term soil health, nano-biofertilizers offer additional advantages beyond conventional formulations. Conventional biofertilizers are well-known for their contribution to long-term soil health. They help build organic matter, improve soil structure, and increase microbial diversity. Their effects on soil fertility are cumulative over multiple growing seasons through mechanisms such as nitrogen fixation or phosphorus solubilization, and they are valued for being eco-friendly. Nano-biofertilizers aim to combine these long-term soil benefits with more immediate nutrient delivery. As they incorporate beneficial microbes and/or organic compounds, they continue to support soil biological health in much the same way as traditional biofertilizers. In addition, nano-carriers can protect microbes from environmental stress and ensure

Table 3. Summary of different types of nano-biofertilizers and their observed effects

Nano-biofertilizer composition	Observed effects on plants	References
Mesoporous silica nanoparticles with Bacillus sp. CP4 and AHP3	Enhanced plant growth and nutrient uptake	47
Zinc oxide nanoparticles with *Bacillus* sp. CP4 and AHP3	Improved plant growth and nutrient absorption	47
Copper oxide nanoparticles with *Bacillus* sp. CP4 and AHP3	Increased plant growth metrics and nutrient uptake	47
Silicon dioxide nano-fertilizers	Increased nitrogen and phosphorus content in plants; decreased sodium content; improved plant growth and yield	48
Nano-biofertilizer capsules	Enhanced plant growth physiology and yield	49

more effective delivery to the rhizosphere. Some studies have reported that nano-biofertilizer application leads to higher soil enzyme activities and microbial biomass compared to conventional treatments, indicating a stimulated soil microbiome alongside crop growth promotion. Over multiple growing seasons, this may translate into improved soil structure and nutrient cycling. However, definitive long-term field studies are still limited. One concern is the potential for negative effects on soil properties from the accumulation of nanoparticles (e.g., heavy metal buildup or pH shifts). So far, short- and medium-term field data are promising, showing maintained or improved soil fertility and no adverse effects on soil biota, but ongoing monitoring is necessary. Farmer adoption of nano-biofertilizers may ultimately depend on their consistent field performance across varied environments. While traditional biofertilizers can fail under suboptimal field conditions such as drought or poor soils, nano-biofertilizers have demonstrated greater resilience by continuing to release nutrients and support microbial activity even under stress. For instance, polymer-encapsulated biofertilizer nanoparticles can stabilize microbes against heat and desiccation, delivering better results than free microbial inoculants. This suggests that nano-based formulations may provide more reliable long-term benefits in heterogeneous field environments. Overall, nano-biofertilizers appear to match or exceed conventional biofertilizers in enhancing crop yields while also sustaining soil health. They combine the slow-building advantages of biofertilization with the rapid nutrient availability offered by nanotechnology. Nevertheless, agronomists emphasize the need for more multi-season trials to assess long-term impacts on soil quality indicators such as organic carbon content and microbial diversity. Such data will be critical in establishing whether nano-biofertilizers can sustain or even improve long-term soil health compared to traditional biofertilizers.

5. Nano-biofertilizer manufacturing technologies

Nano-biofertilizers can be manufactured using several methods, as outlined in Table 4, which integrate nanotechnology with biological agents for nutrient delivery, thereby supporting sustainable agriculture.

5.1. Encapsulation with nanomaterials

Encapsulation is one of the most widely used manufacturing techniques for nano-biofertilizers. In this approach, microbial inoculants or nutrient formulations are enclosed within nano-sized carriers, often made from biopolymers such as chitosan, alginate, or starch. This method improves the stability and viability of microbial strains and allows for the gradual release of nutrients into the rhizosphere.

A practical example is the use of chitosan–alginate nanocapsules embedded with nitrogen-phosphorus-potassium nutrients and plant growth-promoting rhizobacteria, which have been successfully employed in field trials. The inclusion of humic acid as a cross-linker produced porous capsules with extended nutrient availability and improved root colonization. These nanocapsules can be applied as soil granules, seed coatings, or foliar sprays. Uniform-sized beads can be produced using a sodium alginate–calcium chloride

Table 4. Summary of common nano-biofertilizer manufacturing methods, along with references to relevant studies

Manufacturing method	Description	References
Encapsulation with nanomaterials	Biofertilizers are encapsulated within nanomaterial coatings, such as chitosan and alginate crosslinked with humic acid, to improve stability and controlled nutrient release	49
Green synthesis using microorganisms	Microorganisms such as bacteria, fungi, and algae are used to biosynthesize nanoparticles, which are then combined with biofertilizers. This eco-friendly approach leverages the natural reducing agents produced by these organisms	52
Chemical methods (e.g., sol –gel, hydrothermal)	Chemical techniques such as sol-gel and hydrothermal methods are employed to synthesize nanoparticles, which are then integrated with biofertilizers. These methods allow for precise control over particle size and composition	53
Top-down and bottom-up approaches	Top-down approaches involve breaking down bulk materials into nanoparticles, while bottom-up approaches assemble nanoparticles from atomic or molecular components. Both methods are used to create nano-biofertilizers with desired properties	1

cross-linking process, which ensures ease of handling and consistent field performance.[54-56]

5.2. Biological (green) synthesis

Green synthesis utilizes the natural biochemical pathways of living organisms – bacteria, fungi, algae, or plants – to reduce metal salts into nanoparticles. This bottom-up approach is eco-friendly, avoids the use of hazardous chemicals, and aligns with organic farming practices. Certain microbes, such as filamentous fungi or actinobacteria, can precipitate nanoparticles like zinc oxide (ZnO), iron oxide, or selenium through enzymatic activity. For example, extracts from *Chlorella vulgaris* have been used to synthesize iron oxide nanoparticles, which possess antifungal and plant-growth-promoting properties. In addition, *Aspergillus* species have been employed to produce nano-phosphate fertilizers, which have shown promising results in maize cultivation. Some key advantages of this method are its biocompatibility, low energy requirements, and sustainability. However, some challenges remain, including low productivity, variable particle size, and difficulty in large-scale standardization.[57]

5.3. Chemical synthesis methods

Chemical techniques such as sol-gel, hydrothermal synthesis, and co-precipitation are widely used in the production of nanofertilizers. These methods allow for precise control over particle size and purity. For instance, nano-hydroxyapatite, which is synthesized through hydrothermal methods, has demonstrated improved phosphorus availability and 20%–30% higher yields in soybean and wheat when compared to conventional phosphate fertilizers.

Another example is nano-urea, which has been commercialized by the Indian Farmers Fertilizer Cooperative (IFFCO) and is produced through industrial encapsulation and reverse osmosis. The main benefits include uniformity, effectiveness, and adaptability. However, there are some limitations associated with this method, such as high production costs, chemical residues, and the need for advanced equipment.[58]

5.4. Top-down versus bottom-up nanofabrication

In top-down fabrication, bulk materials are broken down into nanoparticles through physical methods such as ball milling or grinding. For example, rock phosphate has been milled into nanophosphate particles and combined with microbial solubilizers to improve nutrient availability in calcareous soils. Bottom-up approaches, as discussed above, assemble particles from atoms or molecules using biological or chemical processes.

In summary, Top-down fabrication is simple but energy-intensive and more challenging when it comes to controlling particle size, whereas bottom-up is more precise and controllable but may require complex inputs.[59]

5.5. Economic and scalability considerations

Each synthesis method varies in cost, efficiency, and scalability. Encapsulation and biosynthesis are eco-friendly but slower and less uniform. Chemical synthesis is effective and precise but costly and infrastructure-intensive. Top-down methods are straightforward but may not yield optimal nanostructures.

For large-scale farming, low-cost biological or precipitation methods may be best, whereas, for high-value crops, more expensive encapsulated fertilizers may be justified.

Overall, each method plays a specific role: Encapsulation combines slow-release with microbial protection; green synthesis is sustainable and chemical-free; chemical synthesis offers high precision; and hybrid methods strike a balance between cost and efficiency.[60]

Despite the diversity of methods used to manufacture nano-biofertilizers, there is significant variation in economic efficiency and industrial scalability. For example, chemical methods such as pyrolysis or co-precipitation are effective in producing homogeneous particles with high precision, but they are expensive and require complex technical infrastructure. In contrast, biosynthesis using microorganisms or plant extracts represents a lower-cost and more environmentally friendly alternative, but it still faces challenges in standardizing the physical properties of the produced particles. Therefore, evaluating the effectiveness of these technologies is not limited to release efficiency or stability. Economic factors, such as raw material and energy costs, and the potential for commercial scalability to meet the requirements of large-scale agriculture, must also be considered.

These methods highlight the diverse approaches in the production of nano-biofertilizers, with each beneficial microorganism and technology used for nutrient nanoparticle loading playing a unique role in enhancing nutrient delivery and promoting sustainable agricultural practices.

6. The role of nano-biofertilizers in sustaining soil fertility

Soil fertility quite plays an important role in determining agricultural productivity as well as the sustainability of ecosystems. Conventional chemical

fertilizers have a long history of providing essential nutrients to crops; however, their overuse has led to soil degradation, disruptions to microbial activity, and environmental pollution. In contrast, nano-biofertilizers offer a sustainable alternative by maximizing nutrient efficiency and promoting microbial activity, ultimately enhancing soil health. These advanced fertilizers combine nanotechnology and biofertilization approaches to optimize nutrient delivery and ensure ecological sustainability.[17]

6.1. Nanotechnology innovations in nano-biofertilizers for improved nutrient use efficiency

The high surface area of nano-phosphorus helps control and reduces leaching and volatilization losses of the applied phosphorus source.[15] The slow and steady release of essential nutrients like nitrogen, phosphorus, and potassium improves plant uptake efficiency while minimizing environmental contamination.[11] For example, nitrogen nano-capacitated fertilizers can deliver nitrogen slowly and in a targeted manner, reducing nitrogen losses commonly associated with conventional mineral fertilizers.[10] Reducing the frequency of source material application can lead to significant cost savings by minimizing resource wastage, a common issue with traditional fertilizer use. This enhances resource efficiency and is considered an attractive investment factor, as optimal resource use is one of the most important determinants of successful and sustainable agricultural investment.[61]

6.2. Healthy soil microbiome

Nano-biofertilizers also play a crucial role in promoting a healthy soil microbiome. Conventional chemical fertilizers often harm beneficial microorganisms in the soil, leading to soil degradation and nutrient imbalances. Gold nanoparticles doped with essential elements such as zinc, iron, and silica have been shown to enhance microbial growth, enzyme activities, and nitrogen fixation.[7] Microbial strains such as *Azotobacter* spp., *Rhizobium* spp., and *Bacillus* spp. are commonly included in nano-biofertilizers to promote healthy soils and support plant growth.[18] These strains contribute to the soil by:

(i) Biological nitrogen fixation, which reduces reliance on synthetic nitrogen sources.
(ii) Phosphate solubilization, which increases the availability of phosphorus to plants.
(iii) Supporting the plant in initiating and developing roots, enhancing nutrient uptake.

In addition, studies have shown that nano-biofertilizers improve microbial diversity, leading to better soil aggregation and more efficient decomposition of organic matter, both of which are key indicators of sustainable soil fertility.[9]

6.3. Improvement of soil structure and organic matter

Nano-biofertilizers may also indirectly improve soil structure, porosity, and aggregation. Increased porosity and aggregation result in reduced soil compaction and enhanced root-zone aeration. This, in turn, contributes to higher organic matter content by stimulating microbial-driven carbon and nitrogen cycling. Nano-based amendments can help sustain long-term fertility by reducing soil erosion, improving water-holding capacity, and enhancing the stability of organic matter. For instance, nano-clay and biochar-enhanced biofertilizers have reduced erosion while improving water retention and organic matter stability, leading to greater long-term fertility sustainability.[62]

6.4. Reduction in chemical fertilizer dependency

A key objective of sustainable agriculture is to reduce dependency on synthetic fertilizers. This goal is increasingly being achieved through the use of nano-biofertilizers due to the following factors:

(i) Enhanced nutrient retention and the requirement for lower application rates of fertilizers.[19]
(ii) Reduced environmental pollution due to decreased nitrate leaching and greenhouse gas emissions, thereby minimizing ecological harm.[63]
(iii) Improved resistance of plants to abiotic stresses[64] such as drought and salinity, though not necessarily heavy metal toxicity.

For example, nano-zinc biofertilizers have been shown to mitigate zinc toxicity – commonly observed with conventional zinc sulfate fertilizers – while simultaneously promoting plant growth.[15] Another example is nano-silica biofertilizers, which enhance resistance to disease and drought in crops by strengthening plant cell walls and improving water retention, as reported by Lateef *et al.*[65]

6.5. Long-term soil fertility and sustainability

Nano-biofertilizers have the potential to sustain long-term soil fertility through several mechanisms:

(i) Maintaining soil pH at an equilibrium level by gradually releasing nutrients into the soil solution.
(ii) Reducing salinization, thereby preventing the rapid buildup of chemical residues.

(iii) Enhancing carbon sequestration, which contributes to mitigating the impacts of climate change.[19]

Nano-biofertilizers help conserve soil biodiversity, promoting the sustainable management of soil fertility. They support the development of a balanced soil ecosystem and ensure that soils remain productive and viable as a resource for future generations.

7. Role of nano-biofertilizers in environmental protection and sustainability

Agricultural productivity and sustainability are becoming increasingly important in light of rising global food demand and growing environmental degradation. While conventional chemical fertilizers have been effective in boosting crop productivity, they pose significant environmental risks, including land degradation, water pollution, and greenhouse gas emissions.[66] In response, nano-biofertilizers have emerged as sustainable alternatives that enhance plant growth while minimizing ecological harm.[67] This section discusses the role of nano-biofertilizers in promoting environmental protection and long-term sustainability.

7.1. Integration with precision agriculture: Remote sensing and artificial intelligence (AI)

The integration of nano-biofertilizers with precision agriculture technologies – such as remote sensing, drones, and AI—represents a forward-looking approach to sustainable farming. Remote sensing tools (e.g., satellites, drones, and field sensors) can detect spatial variations in nutrient deficiencies, allowing targeted application of nano-biofertilizers only where needed. This minimizes waste and maximizes efficiency. For example, Normalized Difference Vegetation Index maps generated by drones can guide site-specific applications via smart sprayers, reducing both input cost and environmental impact. Additionally, sensors based on the Internet of Things and AI systems can optimize nutrient application timing and dosage by predicting crop nutrient demands or stress conditions. Nanosensors embedded in the soil can monitor nitrate levels in real time, transmitting data to AI models that trigger precise foliar applications. Because nano-formulations are typically in liquid or fine particle form, they are well-suited for modern variable-rate applicators and drone-based spraying systems. Countries such as India have already piloted drone-based nano-urea applications with promising outcomes. This integration supports the "4R" nutrient stewardship strategy (right source, right rate, right time, and right place), thereby enhancing productivity and resource-use efficiency. As such, nano-biofertilizers are well-aligned with the evolving framework of data-driven, smart agriculture.[68,69]

7.2. Balanced perspective: Agronomic benefits versus environmental risks

Nano-biofertilizers offer clear agronomic benefits, but a balanced analysis must also acknowledge their potential drawbacks. On the benefits side, nano-biofertilizers can significantly improve nutrient use efficiency and crop productivity. Studies indicate that nano-formulations can increase plant nutrient uptake and yields by up to 30% compared to conventional fertilizers.[70] For example, controlled nano-nutrient delivery has been shown to boost chlorophyll content and root growth, translating into higher biomass and grain yield.[71] These fertilizers also enhance stress tolerance (e.g., drought and salinity) and stimulate beneficial soil microbes, contributing to long-term soil fertility. In summary, nano-biofertilizers can maintain high yields with smaller doses, potentially reducing nutrient leaching and environmental pollution.

On the limitations and environmental risks side, it is important to recognize that engineered nanoparticles may pose ecological challenges. Unlike conventional fertilizers, which typically dissolve or biodegrade, some nanoparticles are persistent and may accumulate in soil with repeated applications.[70] Persistent nanoparticles could affect soil health and ecosystem dynamics if they accumulate faster than they degrade. For instance, excessive or improper use of nano-fertilizers can result in nanoparticle pollution, which may adversely impact plant growth and soil biota. Moreover, research shows that nano-fertilizer applications can alter the composition of soil microbial communities, with both beneficial and deleterious effects.[72] Certain nanoparticles (e.g., ZnO, copper [II] oxide) at high concentrations have been found to reduce microbial diversity and activity.[73] A recent meta-analysis reported that nanomaterials reduced soil microbial biomass by ~14% on average and slightly decreased microbial diversity, highlighting this concern. Disruption of beneficial microbes (such as nitrogen-fixers or decomposers) could negatively affect nutrient cycling and soil health. Nanoparticles may also harm non-target organisms (e.g., earthworms and insects) and can enter water bodies through surface runoff. Laboratory studies have noted phytotoxic effects at high nanoparticle doses, including inhibited seed germination and chlorosis in plants exposed to certain metal oxide nanoparticles. Given these uncertainties, researchers emphasize the need for thorough, long-term

environmental assessments of nano-biofertilizers.[1] Overall, while nano-biofertilizers have the potential to reduce the environmental footprint of agriculture by lowering fertilizer requirements, a cautious approach is warranted. Potential risks—such as nanoparticle accumulation, impacts on the soil microbiome, and unknown long-term ecosystem effects—should be transparently acknowledged. This balanced perspective ensures that the review does not appear overly optimistic and aligns with current calls in the literature for comprehensive risk–benefit analyses of nanotechnology in agriculture.[70]

7.3. Environmental benefits of nano-biofertilizers

Nano-biofertilizers combine nanotechnology with bio-based nutrient sources to improve nutrient use efficiency while reducing environmental degradation. The release nutrients more slowly than conventional fertilizers, minimizing leaching into water bodies and reducing soil contamination.[74] The use of nanocarrier-encapsulated essential nutrients improves bioavailability, allowing for lower application rates while maintaining high crop yields.[75] In addition, nano-biofertilizers stimulate microbial diversity and soil health by promoting beneficial microbial interactions. For example, nitrogen-fixing bacteria in bio-nanocomposites enhance nitrogen availability and reduce dependence on synthetic nitrogen, a major contributor to nitrate pollution.[76] Such biological interventions help maintain long-term soil fertility and support environmental stability.

7.4. Contribution to sustainability

The application of nanotechnology in biofertilizers aligns closely with the principles of sustainable agriculture, aiming to lower chemical inputs and maximize resource efficiency.[77] Furthermore, nano-biofertilizers help reduce the carbon footprint, as their precision application reduces the need for energy-intensive manufacturing, transportation, and excessive usage.[18]

They also support plant climate resilience by mitigating the effects of abiotic stress factors like drought and salinity. Nanoparticles such as ZnO and silica, when incorporated into biofertilizers, have been shown to improve water retention and enable plant growth under adverse conditions.[78] These features position nano-biofertilizers as a strategic tool in addressing the effects of climate change on agriculture.

8. Challenges and future perspectives

Challenges in the large-scale adoption of nano-biofertilizers include concerns regarding nanoparticle toxicity regulations and production costs.[79] Extensive research is needed to evaluate their long-term impacts on ecosystems and human health.[80] This should be a priority for governments and research institutions – to develop safe, cost-effective, and environmentally benign products that can be widely adopted. However, implementation in numerous regions remains hindered by high costs, difficulties in scaling up production, and regulatory approval hurdles.[16] Future research should focus on:

(i) The development of biodegradable nano-carriers for microbial stabilization.
(ii) The assessment of long-term impacts on soil health.
(iii) The commercialization of low-cost nano-biofertilizers for global agriculture.

There is significant potential for nano-biofertilizers to revolutionize sustainable and precise food production systems in agriculture.[19] Key regulatory challenges include the absence of clear legal frameworks governing the use of nanoparticles in agriculture, which delays their commercial adoption. Economic challenges also persist, such as high initial production costs and limited government support in many developing countries. Barriers to farmer adoption include a lack of awareness, limited technical knowledge, and concerns about potential environmental impacts. As Rai *et al.*[74] emphasized, the limited availability of long-term studies and insufficient understanding of nanoparticle behavior in the environment remain major obstacles to the widespread application of this technology in agriculture.

8.1. Regulatory frameworks and global examples

The regulatory landscape for nano-biofertilizers is still developing, with approaches varying widely across countries. Globally, no unified regulatory framework exists for nanofertilizers. This regulatory gap means that approval processes, safety evaluations, and labeling requirements for nano-enabled fertilizers are handled differently depending on jurisdiction. Several illustrative examples can be provided: (i) India – proactive regulatory inclusion: India has been one of the early adopters of nanofertilizer regulation. In 2021, the Indian government amended its fertilizer control order (FCO) to officially include "nanofertilizers" as a distinct category. Specific guidelines and quality standards were issues – for instance, the FCO now defines and sets specifications for nano urea (liquid), including permissible nutrient content and particle size. Initially, the IFFCO was authorized to commercially produce nano-urea.[81] As a result, any nano-fertilizer in India must undergo a government approval process,

demonstrating efficacy and safety before entering the market. This move has facilitated the rollout of IFFCO's nano-urea to farmers under regulatory oversight; however, the approval is provisional—the inclusion of nano-urea was initially granted for 3 years, indicating that regulators are adopting a cautious approach while gathering performance and safety data. India's example illustrates a country developing a dedicated regulatory framework for nano-fertilizers, aiming to promote innovation (particularly by encouraging reduced urea consumption) while maintaining regulatory oversight;[81] (ii) European Union (EU) – existing chemical and fertilizer laws: In the EU, nanomaterials are regulated under broader chemical and product safety regulations. The EU fertilizing products regulation 2019/1009 does not explicitly create a separate category for nanofertilizers but requires labeling if a product contains intentionally manufactured nanomaterials, according to specific size thresholds. In practice, nano-biofertilizers in the EU are assessed under existing frameworks like Registration, Evaluation, Authorization, and Restriction of Chemicals for chemical safety, and under fertilizer regulations for efficacy. While the EU provides guidance on nanomaterials in food and feed, regulatory guidance for agricultural inputs is still evolving. Products containing nanoscale ingredients must be clearly indicated to end-users in the EU, and risk assessments are conducted on a case-by-case basis. However, there is currently no distinct approval pathway for nano-fertilizers, placing them in a regulatory gray area between fertilizer laws and general nanomaterial policies. This can hamper innovation, as manufacturers may face uncertainty regarding regulatory requirements, and regulators may lack specific protocols for assessing the behavior of nanoparticles in soil. The EU's approach reflects a cautious stance, treating nano-biofertilizers within existing frameworks while emphasizing the precautionary principle;[82] (iii) United States and other regions – lack of nano-specific fertilizer rules: In the United States, fertilizers (excluding pesticides) are primarily regulated at the state level, with some oversight from federal agencies like the United States Department of Agriculture and the environmental protection agency (EPA). Currently, there are no fertilizer laws specifically targeting nanoscale products; nano-biofertilizers are regulated similarly to conventional fertilizers in terms of nutrient claims. However, any novel materials, such as nanoparticle coatings, may be subjected to environmental and safety regulations (e.g., the Toxic Substances Control Act may apply if the nanoparticles are considered new chemical substances). Although the EPA has started evaluating nanopesticides under specific guidelines, nano-fertilizers have received comparative regulatory attention. Many countries in Africa, Asia, and Latin America also lack explicit nano-specific regulations. Most rely on traditional fertilizer approval systems that do not address nanoscale issues. A recent review pointed out that many nations have yet to draft regulatory guidelines for nano-agricultural products. This absence of oversight means such products could reach markets without thorough safety evaluation. While this can accelerate innovation and market entry, it raises concerns about safety, consistency, and public trust. For instance, in countries without specific regulations, a company may sell a "nano-biofertilizer" containing engineered nanoparticles without any obligation to test or label it as such. This presents a risk of regulatory lag, where technological advancement outpaces policy development, which could lead to either environmental harm or diminished consumer confidence.[83]

8.2. Farmer awareness, training, and adoption in developing countries

Regardless of how effective nano-biofertilizers may be, their real-world impact ultimately depends on farmer adoption. In many developing countries, farmer awareness and education regarding this emerging technology remain limited. Successful implementation therefore requires targeted outreach and training at the grassroots level.

8.2.1. Current awareness gap

As nano-biofertilizers represent a relatively recent innovation, many farmers (especially smallholders) are unfamiliar with the term or may associate "nano" with something overly technical, risky, or expensive. Surveys and extension reports consistently indicate that a lack of knowledge is a major barrier to the adoption of improved agricultural inputs in developing regions. A recent analysis highlighted that economic, technological, and perceptual barriers limit farmers' willingness to adopt nano-agricultural products in the absence of adequate awareness and guidance.

8.2.2. Need for training programs

To bridge this gap, targeted training and demonstration programs are essential. Farmers must understand how nano-biofertilizers work (e.g., their slow-release properties), the correct application methods, and the benefits they offer. Improper use could lead to reduced efficacy or wastage of products. For example, it is important that farmers learn that nano-formulations

require lower dosages than conventional fertilizers and that over-application can be harmful or counterproductive. Educational programs should also address safe handling practices, compatibility with other agrochemicals, and integration into existing fertilization schedules.

Governments and agricultural extension agencies in some countries have begun implementing such initiatives. In India, for example, field demonstrations and "farmer field days" for nano-urea have been organized, allowing growers to observe yield improvements with reduced fertilizer input. This participatory approach builds trust and understanding through firsthand observation and practical experience.

8.2.3. Benefits of awareness

When farmers understand the value of nano-biofertilizers – such as reduced input costs and improved productivity – they are more likely to adopt the technology. For smallholder and resource-poor farmers, special attention must be given to affordability, appropriate packaging sizes (e.g., small sachets), and clear labeling (preferably using pictorial instructions). Training modules should cover topics such as identifying deficiency symptoms, appropriate timing and dosage, safe storage practices, and long-term benefits for soil health.

8.2.4. Challenges in developing countries

Weak extension infrastructure and skepticism toward new technologies can hinder effective outreach. Farmers may ask: "Why switch from manure or urea to something unfamiliar?" To address this, the involvement of trusted local figures – such as lead farmers, agricultural officers, or cooperatives – is vital. Furthermore, training helps prevent misuse (e.g., over-application), ensuring responsible and efficient use of nano-biofertilizers.

The successful adoption of nano-biofertilizers depends significantly on farmer education and training. Without this foundation, innovations risk remaining limited to research trials and failing to reach millions of potential beneficiaries. This section introduces a socio-economic dimension to the review, by emphasizing that technological advancement must be accompanied by effective knowledge transfer, particularly in regions where yield gaps are wide and the need for sustainable agriculture is most pressing.

8.3. Antibiotic resistance gene transfer risk from microbial components

The potential risk of antibiotic resistance gene (ARG) transfer from the microbial components of nano-biofertilizers is a significant biosafety concern. Many plant growth-promoting bacteria used in biofertilizers naturally harbor ARGs, sometimes located on mobile genetic elements such as plasmids. The large-scale application of such bacteria could introduce ARGs into the soil microbiome, where horizontal gene transfer to native microbes or even opportunistic pathogens may occur. Studies have shown that strains such as *Pseudomonas fluorescens* can carry resistance to antibiotics such as tetracycline, and repeated soil exposure may increase the abundance of resistant microbes. Although nano-components themselves do not cause resistance, nanoparticles may create stress conditions that potentially facilitate gene exchange. To mitigate this, researchers recommend rigorous screening of microbial strains using molecular diagnostics or genome sequencing to ensure they lack transferable ARGs. Regulatory agencies should consider incorporating ARG risk assessments into the biofertilizer approval process. While current guidelines often focus on pathogen exclusion, ARG monitoring remains largely unaddressed. Therefore, responsible development of nano-biofertilizers must include biosafety evaluations of microbial inputs to prevent unintended contributions to antimicrobial resistance.[84,85]

9. Effect of fertilizer type and concentration on soil health

Soil is one of the most important components of the agricultural environment. It serves as the medium in which plants grow and obtain nutrients and water. With the increasing demand for agricultural production, fertilizers have become essential to replenish nutrients lost from the soil. However, the type and concentration of fertilizer used play a significant role in determining the extent to which both soil and plants benefit, as well as the broader environmental impact. Healthy soil is the foundation of productive farming. It supports plant growth, regulates water, filters pollutants, and sustains biodiversity. However, maintaining soil health is a growing concern as modern agriculture relies heavily on fertilizers. While fertilizers help boost crop yields, their type and concentration can significantly influence soil vitality over time.

The impact of fertilizer type and concentration on soil health cannot be overlooked. Although fertilizers are intended to enhance agricultural productivity, their unplanned or excessive use can negatively affect both the environment and long-term soil fertility. Striking a balance in fertilizer application and choosing appropriate

types are keys to maintaining healthy and productive soil for future generations. Understanding the impact of fertilizer type and concentration on soil health is critical to achieving sustainable agriculture. While fertilizers contribute to increased productivity, their indiscriminate use can lead to soil degradation and environmental pollution. Therefore, adopting sustainable agricultural practices that balance productivity with the preservation of soil and environmental health is essential.

Organic fertilizers differ significantly from chemical fertilizers in their impact on soil health. Organic fertilizers, such as compost and manure, improve soil structure and increase its organic matter content, improving aeration as well as the soil's ability to retain moisture and nutrients. These fertilizers also enhance soil biological activity by creating a favorable environment for the growth of beneficial microorganisms that contribute to soil health and fertility. Although their effects are slower to manifest, they are long-lasting, sustainable, and environmentally friendly. In contrast, chemical fertilizers provide nutrients rapidly, accelerating plant growth and increasing yields in the short term. However, excessive use can negatively impact soil health in the long term. Overuse of chemical fertilizers leads to salt accumulation, degradation of soil structure, reduced microbial diversity, and an increased risk of groundwater contamination. Therefore, a balanced use of both fertilizer types, based on the specific needs of soil and plants, is recommended to ensure high productivity while preserving soil health and sustainability. Nutrient inputs such as chemical fertilizers and animal manure have positively influenced soil health characteristics. Fertilizers may enhance soil organic matter when applied appropriately. However, further research is needed to better understand the impact of these inputs on soil health and carbon storage.[86] A study by Pahalvi *et al.*[87] emphasizes the importance of maintaining soil health to ensure sustainable ecosystems and agricultural productivity. It highlights that the physical, chemical, and biological properties of soil are affected by the excessive use of chemical fertilizers. While these fertilizers contribute to increased crop yields, they also reduce microbial activity, degrade soil quality, and pollute the environment. The study concludes that continued reliance on chemical fertilizers threatens soil biodiversity and negatively impacts its long-term health.

Researchers[88,89] have also noted that soil is an essential natural resource for plant growth, and its health is significantly affected by human interventions such as tillage, irrigation, and fertilization. Nitrogen, a key nutrient in fertilization, influences soil organic matter, microbial populations, and acidity. Studies have shown that applying nitrogen at optimal rates promotes plant growth and increases organic matter without compromising soil health.[18] However, excessive nitrogen application can lead to organic matter loss and increased acidity, which negatively impacts soil microorganisms. As such, balanced nutrient management and the incorporation of organic fertilizers are recommended to maintain and improve soil health.[90]

10. Conclusion

Nano-biofertilizers have demonstrated significant potential in enhancing soil fertility by improving nutrient absorption, boosting microbial activity, and reducing dependence on chemical fertilizers. While current findings affirm their positive role in sustainable agriculture, further research is essential to evaluate their long-term impacts under various soil and crop conditions. Future studies should also assess their cost-effectiveness, environmental safety, and compatibility with traditional fertilization practices to fully harness their potential.

Nano-biofertilizers are thus considered a promising innovation in sustainable agriculture. They enhance microbial activity, improve soil structure, reduce the need for chemical inputs, and support long-term sustainability. With continued research into environmentally friendly, relatively inexpensive, and efficient nano-biofertilizer formulations, this technology could revolutionize agricultural practices worldwide, contributing to the production of healthier and more secure food systems. Nano-biofertilizers have the potential to improve nutrient efficiency, enhance soil health, and minimize environmental pollution. Although challenges remain, further research and supportive policies can accelerate their integration into diverse and mainstream agricultural practices, paving the way for a greener and more sustainable future.

Acknowledgments

None.

Funding

None.

Conflict of interest

The authors declare that they have no competing interests.

Author contributions

Conceptualization: All authors
Formal analysis: All authors
Investigation: Hayyawi W. A. Al-Juthery, Rand A. H. G. Al-Taee, Ali S. Alhasan
Methodology: Hayyawi W. A. Al-Juthery, Rand A. H. G. Al-Taee, Diaa F. Hassan,
Writing – original draft: Hayyawi W. A. Al-Juthery, Rand A. H. G. Al-Taee, Ali S. Alhasan
Writing – review & editing: All authors

Availability of data

Not applicable.

References

1. Garg D, Sridhar K, Stephen Inbaraj B, Chawla P, Tripathi M, Sharma M. Nano-biofertilizer formulations for agriculture: A systematic review on recent advances and prospective applications. *Bioengineering (Basel)*. 2023;10(9):1010. doi: 10.3390/bioengineering10091010
2. Sambangi P, Gopalakrishnan S, Pebam M, Rengan AK. Nano-biofertilizers on soil health, chemistry, and microbial community: Benefits and risks. *Proc Indian Natl Sci Acad*. 2022;88(3):357-368. doi: 10.1007/s43538-022-00094-1
3. Miranda-Villagómez E, Trejo-Téllez LI, Gómez-Merino FC, Sandoval-Villa M, Sánchez-García P, Aguilar-Méndez MÁ. Nanophosphorus fertilizer stimulates growth and photosynthetic activity and improves P status in rice. *J Nanomater*. 2019;2019(1):5368027. doi: 10.1155/2019/5368027
4. Madlala NC, Khanyile N. Examining the correlation between the inorganic nano-fertilizer physical properties and their impact on crop performance and nutrient uptake efficiency. *Nanomaterials (Basel)*. 2024;14(8):1263. doi: 10.3390/nano14151263
5. Liu R, Lal R. Nano-enhanced fertilizers for improved crop productivity and soil sustainability. *Crit Rev Plant Sci*. 2021;40(1):1-24.
6. Badiri ZK, Al-Juthery HW. Effect of spraying some bio and nano stimulants fortified with potassium on some qualitative traits and active substances in rice grain. *AIP Conf Proc*. 2024;3079(1):020013. doi: 10.1063/5.0202277
7. Mishra S, Tripathi DK, Singh VP. Microbial synergy with nano-biofertilizers in sustainable agriculture. *Plant Soil Sci Rev*. 2020;52(1):89-104.
8. Singh S, Prasad R. Nano-biofertilizers: A sustainable approach for soil fertility. *Agric Adv*. 2020;9(2):178-198.
9. Kumar R, Ghosh D, Sharma S. Microbial interactions in nano-biofertilizer treated soils. *Soil Biol Rep.* 2021;89:219-232.
10. Subramanian KS, Rahale CS. Nano-encapsulated nitrogen fertilizers for sustainable crop production. *J Agric Sci*. 2015;42(1):45-58.
11. Parikh SJ, Mukherjee S. Advances in nano-fertilizers for soil nutrient management. *Annu Rev Plant Biol*. 2020;71(1):405-432.
12. Mukherjee S, Singh R. Advances in nano-biofertilizers for enhanced soil microbial activity. *Microbiol Today*. 2021;28(2):212-226.
13. Mishra S, Tripathi DK, Singh VP. Synergistic effects of nanoparticles and biofertilizers. *Environ Sci Biotechnol*. 2017;31(4):405-417.
14. Liu X, Feng Z, Chen L. Nano-fertilizers and their potential in precision agriculture. *Adv Soil Res*. 2019;35(2):198-213.
15. Ditta A, Arshad M, Ibrahim M. Zinc oxide nano-biofertilizers and their effect on soil fertility. *J Agron Soil Sci*. 2018;65(3):423-437.
16. Raliya R, Tarafdar JC, Biswas P. Nano-P biofertilizers for sustainable agriculture. *Soil Biol Rep.* 2013;52(2):119-132.
17. Shang J, Wang D, Xiang H. Impact of nano-silica biofertilizers on soil organic matter and microbial activity. *Environ Sci J*. 2014;45(2):112-125.
18. Singh B, Choudhary R, Verma N. Nano-biofertilizers and their role in mitigating climate change impacts. *Clim Resil Agric J.* 2022;17(3):112-130.
19. Verma A, Srivastava R, Gupta R. Carbon sequestration and soil sustainability with nano-fertilizers. *Soil Environ Res*. 2022;12(3):98-114.
20. Chen H, Liu L, Zhang Z. *Advances in Nano-Biofertilizers for Sustainable Agriculture*. Vol. 12. London: Springer Nature; 2020. p. 45-60.
21. Al-Juthery HW, Lahmoud NR, Alhasan AS, Al-Jassani NA, Houria A. Nano-fertilizers as a novel technique for maximum yield in wheat biofortification (article review). *IOP Conf Ser Earth Environ Sci.* 2022;1060(1):012043. doi: 10.1088/1755-1315/1060/1/012043
22. Rai S, Verma A, Choudhary P. Nano-biofertilizers and their role in sustainable farming. J *Nano Agric*. 2021;10(2):55-72.
23. Drebee HA, Abdul Razak NA, Mohsen AA. Maize production forecasting in Iraq: A Box-Jenkins approach for the period of 2022-2026. *IOP Conf Ser Earth Environ Sci.* 2023;1259(1):012128. doi: 10.1088/1755-1315/1259/1/012128
24. Sharma T, Singh B. Advancing soil fertility using nano-biofertilizers. *Nat Rev Soil Sci*. 2022;5(4):301-320.
25. Hussain S, Ahmad N, Khan R. Impact of nano-biofertilizers on enzymatic activities in soil. *Soil Biol*

Biochem. 2021;32(1):88-101.
26. Jafaar AA, Mohammed RJ, Hassan DF. Effect of phosphorus fertilizer and irrigation level on desert soil management and potato yield. *Int J Agric Stat Sci*. 2022;18(2):1-11.
27. Patel M, Joshi R, Shah S. Enhancing soil health through bio-nanotechnology. *Sustain Agric Rev*. 2020;15(1):210-225.
28. Hamid MQ. Mycorrhiza and *Trichoderma* fungi role in improving soil physical properties planted with maize (*Zea mays* L.). *SABRAO J Breed Genet*. 2025;57(1):260-269.
doi: 10.54910/sabrao2025.57.1.25
29. Kumar V, Yadav P, Thakur R. Microbial interactions in soil: Role of nano-biofertilizers. *Agric Microbiol J*. 2023;29(3):120-135.
30. Ghosh S, Mukherjee A. Effect of nano-biofertilizers on soil microbiota and plant health. *J Agric Sci*. 2021;18(4):233-245.
31. Al-Juthery HW, Yousif SAA, Lahmod NR, Alhasan AS, Tiamooz SH, Musa RF. Response wheat to spray some of synthetic nano fertilizers. *IOP Conf Ser Earth Environ Sci*. 2022;1060:012030.
32. Singh R, Kumar P, Gupta A. Soil organic matter improvement using nano-biofertilizers. In*t J Soil Sci*. 2021;14(3):189-203.
33. Hundi HK, Hamid MQ, Noori AA. Role of ochrobactrum bacteria and organic matter in plant growth and the content of N, P, and K under soil salinity stress. J *Environ Earth Sci*. 2025;7(5):130-139.
doi: 10.30564/jees.v7i5.8777
34. Singh J, Rathore A, Gupta R. Nano-biofertilizers: An eco-friendly solution for sustainable agriculture. *Int J Agric Innov*. 2020;12(3):178-195.
35. Rai M, Ribeiro C, Mattoso L, Duran N. Nanotechnology applications in agriculture: An emerging trend. *Nanosci Agric*. 2021;14(5):269-288.
36. Akol AM, Nassif N, Jaddoa KA, Radhi K, Hassan DF. Effect of irrigation methods, tillage systems and seeding rate on water consumption, biological yield and harvest index of wheat (*Triticum aestivum* L.). *Int J Agric Stat Sci*. 2021;17(3):230-242.
37. Sharma R, Kumar S, Bhardwaj D. Nanoparticles and their role in plant growth promotion. *J Plant Physiol Growth*. 2019;11(4):299-314.
38. Kumar P, Sharma S, Singh N. Biofertilizers and their role in sustainable agriculture. *Curr Adv Agric Sci*. 2020;8(4):311-328.
39. Akol AM, Hassan DF, Mohammed RJ, *et al*. Optimizing wheat yield and water use efficiency using AquaCrop model calibration and validation in various irrigation and tillage systems under climate change. *Soil Sci Ann*. 2024;75(3):1-12.
doi: 10.37501/soilsa/195823
40. Mukherjee A, Ghosh A, Saha B. Environmental benefits of nano-biofertilizers in modern agriculture. *Agric Sci Technol Rev*. 2022;20(1):85-102.
41. Drebee HA, Razak NAA, Shaybth RT. Understanding the causes of the decline in the iraqi agricultural sector's contribution to the GDP. *IOP Conf Ser Earth Environ Sci*. 2022;1060(1):012146.
doi: 10.1088/1755-1315/1060/1/012146
42. Patra JK, Mishra RR, Thatoi H. Microbial biofertilizers and their role in soil fertility management. *Microb Biotechnol Adv*. 2020;6(2):198-210.
43. Salman EE, Akol AM, Abdel Hamza JS, Naje AS. Implementation of the AquaCrop model for forecasting the effects of climate change on water consumption and potato yield under various irrigation techniques. *Nat Environ Pollut Technol*. 2024;23(2):1201-1207.
doi: 10.46488/NEPT.2024.v23i02.056
44. Meena H, Prasad R, Yadav S. Application of nano-biofertilizers in wheat for enhancing productivity. *J Crop Improv*. 2020;15(2):145-167.
45. Rajput VD, Minkina T, Fedorenko A. Nano-fertilizers for sustainable agriculture: An overview of recent developments. *J Agric Nanotechnol*. 2021;7(1):33-57.
doi: 10.3390/nano12010173
46. Hassan DF, Ati AS, Neima AS. Calibration and evaluation of aquacrop for maize (*Zea mays* L.) under different irrigation and cultivation methods. *J Ecol Eng*. 2021;22(10):192-204.
47. Karunakaran A, Fathima Y, Singh P, Beniwal R, Singh J, Ramakrishna W. Next-generation biofertilizers: nanoparticle-coated plant growth-promoting bacteria biofertilizers for enhancing nutrient uptake and wheat growth. *Agriculture*. 2024;14(4):517.
doi: 10.3390/agriculture14040517
48. Singh RR, Saurabh S, Prakash V, *et al*. Enhancing sustainability in agriculture with nanofertilizers. *SN Appl Sci*. 2024;6(1):267.
doi: 10.1007/s42452-024-06267-5
49. González M, Jodeh S, Alkowni R. Nano bio fertilizer capsules for sustainable agriculture. *Sci Rep*. 2024;14:62973.
doi: 10.1038/s41598-024-62973-5
50. Maaz TM, Dobermann A, Lyons SE, Thomson AM. Review of research and innovation on novel fertilizers for crop nutrition. *NPJ Sustain Agric*. 2025;3:25.
doi: 10.1038/s44264-025-00066-0
51. Liu R, Lal R. Synthetic apatite nanoparticles as a phosphorus fertilizer for soybean (Glycine max). *Sci Rep*. 2014;4(1):5686.
doi: 10.1038/srep05686
52. Yadav AN, Kour D, Yadav N. Nano-biofertilizers for agricultural sustainability. *J Appl Biol Biotechnol*. 2023;11(5):1-4.
doi: 10.7324/JABB.2023.16266
53. Patel C, Singh J, Karunakaran A, Ramakrishna W. Evolution of nano-biofertilizer as a green technology for

agriculture. *Agriculture*. 2023;13(10):1865.
doi: 10.3390/agriculture13101865

54. Verma R, Pathak D, Rajput VD. Nanocarrier-based encapsulated fertilizers: Recent advances and field application prospects. *Environ Technol Innov*. 2023;30:103093.
doi: 10.1016/j.eti.2022.103093
55. Isabel JB, Balamurugan A, Devi PR, Periyasamy S. Chitosan-encapsulated microbial biofertilizer: A breakthrough for enhanced tomato crop productivity. *Int J Biol Macromol*. 2024;260:129462.
doi: 10.1016/j.ijbiomac.2024.12946
56. Ingle PU, Shende SS, Shingote PR, *et al*. Chitosan nanoparticles (ChNPs): A versatile growth promoter in modern agricultural production. *Heliyon*. 2022;8(11):e11893.
doi: 10.1016/j.heliyon.2022.e11893
57. Psathas P, Zindrou A, Papachristodoulou C, Boukos N, Deligiannakis Y. Tandem control of la-doping and CuO-heterojunction on $SrTiO_3$ perovskite by double-nozzle flame spray pyrolysis: Selective H2 vs. CH4 photocatalytic production from H_2O/CH_3OH. *Nanomaterials*. 2023;13(3):482.
doi: 10.3390/nano13030482
58. Kottegoda N, Sandaruwan C, Priyadarshana G, et al. Urea-hydroxyapatite nanohybrids for slow release of nitrogen. *ACS Nano.* 2017;11(2):1214-1221.
doi: 10.1021/acsnano.6b07781
59. Yin N, Yang P, Liu S, Pan S, Zhang Z. AI for tribology: Present and future. *Friction*. 2024;12(6):1060-1097.
doi: 10.1007/s40544-024-0879-2
60. Kalhapure R, Patil A. Economic feasibility of nano-biofertilizer production: A comparative assessment of synthesis methods. *Curr Res Environ Sustain*. 2022;4:100147.
doi: 10.1016/j.crsust.2022.100147
61. Drebee HA, Razak NAA, Brisam AA. What are the determinants of investment in the Iraqi agricultural sector? *IOP Conf Ser Earth Environ Sci.* 2021;735(1):012038.
doi: 10.1088/1755-1315/735/1/012038
62. Hamid MQ. Response of physical properties of sandy soil treated with different levels of natural soil conditioners zeolite and perlite. *Sarhad J Agric*. 2025;41(2):591-599.
doi: 10.17582/journal.sja/2025/41.2.591.599
63. Ghormade V, Deshpande MV, Paknikar KM. Perspectives for nano-biotechnology enabled protection and nutrition of plants. *Biotechnol Adv*. 2011;29(6):792-803.
doi: 10.1016/j.biotechadv.2011.06.007
64. Jatav RS, Singh N, Tiwari P. Nano-biofertilizers for sustainable agriculture and soil resilience. *Front Plant Sci*. 2023;14:112-134.
65. Lateef A, Nazir R, Javed S. Silica nanoparticles as plant growth enhancers. *Plant Biotechnol Rep.* 2021;15(4):456-472.
66. Adisa IO, Reddy DHK, Arslan Z. Nanotechnology in fertilizer development: Current trends and future perspectives. *Environ Sci Pollut Res*. 2020;27(11):12459-12476.
67. Shang Y, Yang S, Wang Y. Nanocarriers for controlled fertilizer release: Advances and applications. *Adv Mater Sustain Agric*. 2021;39(1):25-38.
68. Romanovski V, Zhang Z, Akbarisehat A. Nanobiosensors for precision farming and sustainable agriculture. In: *Agricultural Sustainability through Nanotechnology*. USA: CRC Press; 2025. p. 156-174.
69. Upadhyay PK, Dey A, Singh VK, *et al*. Conjoint application of nano-urea with conventional fertilizers: An energy efficient and environmentally robust approach for sustainable crop production. *Plos one*. 2023;18(7):e0284009.
doi: 10.1371/journal.pone.0284009
70. Atanda SA, Shaibu RO, Agunbiade FO. Nanoparticles in agriculture: Balancing food security and environmental sustainability. *Discov Agric*. 2025;3(1):26.
doi: 10.1007/s44279-025-00159-x
71. Arora PK, Tripathi S, Omar RA, *et al*. Next-generation fertilizers: The impact of bionanofertilizers on sustainable agriculture. *Microb Cell Fact*. 2024;23:254.
doi: 10.1186/s12934-024-02528-5
72. Upadhyay PK, Dey A, Singh VK, *et al*. Changes in microbial community structure and yield responses with the use of nano-fertilizers of nitrogen and zinc in wheat-maize system. *Sci Rep.* 2024;14:1100.
doi: 10.1038/s41598-023-48951-3
73. Chen S, Teng Y, Luo Y, Kuramae E, Ren W. Threats to the soil microbiome from nanomaterials: A global meta and machine-learning analysis. *Soil Biol Biochem*. 2024;188:109248.
doi: 10.1016/j.soilbio.2023.109248
74. Rai M, Acharya R, Singh P. Nanotechnology-based biofertilizers for sustainable agriculture. *J Nanosci Nanotechnol*. 2022;22(6):4512-4524.
75. Usman K, Ahmed A, Alam M. Precision agriculture and nanotechnology: The future of farming. *Precision Agric Rev*. 2023;28(5):189-205.
76. Sarkar A, Rakshit A. Bio-nanocomposites in sustainable agriculture. *Environ Sci Adv.* 2020;4(2):56-72.
77. Bhagat S, Kumar R, Sharma S. Sustainable agriculture through nano-biofertilizers: A review. *J Agric Environ Res*. 2021;45(2):78-89.
78. Khan S, Malik A, Hussain M. Role of nanotechnology in plant stress tolerance: An overview. *J Plant Sci Technol*. 2021;12(4):234-248.
79. Mishra V, Tripathi RD, Srivastava S. Environmental and safety concerns of nano-fertilizers: A critical review. *Environ Nanotechnol Monit Manage.* 2023;18(3):100481.
80. Verma R, Gupta S, Mehta D. Policy and regulatory challenges in nano-agriculture. *J Agric Policy Sustain*. 2022;13(1):45-63.
81. Sakhno Y, Miletto I, Paul G, Jaisi DP. A novel route

to enhance the dissolution of apatite: Structural incorporation of hydrogen phosphate. *NanoImpact*. 2022;28:100422.
doi: 10.1016/j.impact.2022.100422

82. Singh D, Gurjar BR. Nanotechnology for agricultural applications: Facts, issues, knowledge gaps, and challenges in environmental risk assessment. *J Environ Manag*. 2022;322:116033.
doi: 10.1016/j.jenvman.2022.116033
83. Noguera-Oviedo K, Aga DS. Nanofertilizers and U.S. Regulations: What we know and what we don't. *Nano Today*. 2020;35:100950.
doi: 10.1016/j.nantod.2020.100950
84. Wang K, Yin D, Sun Z, Wang Z, You S. Distribution, horizontal transfer and influencing factors of antibiotic resistance genes and antimicrobial mechanism of compost tea. J Hazard Mater. 2022;438:129395.
doi: 10.1016/j.jhazmat.2022.129395
85. Sharma P, Pal N, Kumawat M, *et al*. Antibiotic and non-antibiotic determinants of antimicrobial resistance: Insights from water ecosystems. *ACS EST Water*. 2024;4(11):4671-4689.
doi: 10.1021/acsestwater.4c00305
86. Howe JA, McDonald MD, Burke J, *et al*. Influence of fertilizer and manure inputs on soil health: A review. *Soil Security*. 2024;16(3):100155.
doi: 10.1016/j.soisec.2024.100155
87. Pahalvi HN, Rafiya L, Rashid S, Nisar B, Kamili AN. Chemical fertilizers and their impact on soil health. In: Dar GH, Bhat RA, Mehmood MA, Hakeem KR, editors. *Microbiota and Biofertilizers*. Vol. 2. Cham: Springer; 2021.
doi: 10.1007/978-3-030-61010-4_1
88. Kumar Meena A, Rupesh T, Siddartha Naik B, *et al*. Impact of nitrogen fertilizers on soil health. *Int J Curr Microbiol Appl Sci*. 2020;11:993-1008.
89. Hassan DF, Ati AS, Naima AS. Evaluation of the performance of the aquacrop model under different irrigation and cultivation methods and their effect on water consumption. *Iraqi J Agric Sci.* 2023;54(2):478-490.
90. Mohammed RJ, Suliman AA. Land suitability assessment for wheat production using analytical hierarchy process and parametric method in babylon province. *J Ecol Eng*. 2023;24(7):75-87.

ACCSCIENCE PUBLISHING

Asian Journal of Water, Environment and Pollution. Vol. 22, No. 3 (2025), pp. 32-45.
doi: 10.36922/ajwep.8282

ORIGINAL RESEARCH ARTICLE

SpillNet: A modified convolutional neural network model for oil spill detection

Tokula I. Umaha[1,2], Felix Ale[1,2], Ikpaya D. Ikpaya[1,2], John A. Momoh[1,2], Steve A. Adeshina[3], Ilesanmi A. Daniyan[4]*, and Adeyinka P. Adedigba[5]

[1]Department of Systems Engineering, School of Engineering, African University of Science and Technology, Garki, Abuja, Nigeria

[2]National Space Research and Development Agency, Institute of Space Science and Engineering, Abuja Obasanjo Space Centre, Abuja, Nigeria

[3]Department of Electrical and Electronics Engineering, Faculty of Engineering, Nile University of Nigeria, Abuja, Nigeria

[4]Department of Mechatronics Engineering, College of Engineering, Bells University of Technology, Ota, Ogun, Nigeria

[5]Department of Mechatronics Engineering, Faculty of Engineering and Technology, Federal University of Technology, Minna, Niger, Nigeria

***Corresponding author:** Ilesanmi A. Daniyan (iadaniyan@bellsuniversity.edu.ng)

Received: December 29, 2024; Revised: February 10, 2025; Accepted: February 21, 2025; Published Online: March 6, 2025

Abstract: Rapid and accurate detection of oil spills is crucial for initiating timely response measures to mitigate environmental impacts. This study proposes an oil spill detection method based on a modified convolutional neural network, termed "SpillNet." The architecture integrates multiple depthwise separable convolutional layers, batch normalization, and residual connections to enhance feature extraction and learning capabilities. The dataset consists of synthetic aperture radar images obtained from Sentinel-1 satellites, part of the European Space Agency's Copernicus program. Model training was conducted on an NVIDIA Tesla T4 GPU available on Google Colab, with up to 12GB of random access memory. Programming was carried out in the Python environment using Python 3.7, and all required libraries were installed through pip. The results indicate that the proposed model achieves an accuracy of 0.946947, a mean Intersection over Union of 0.58124, and a mean specificity of 0.944469. These results demonstrate that the proposed model outperforms existing models in the oil spill segmentation task. This study contributes to advancing automated oil spill detection by offering a reliable and efficient solution for early oil spill detection and environmental monitoring.

Keywords: Batch normalization; Convolutional neural network; Model; Oil spill; Programming; Synthetic aperture radar

1. Introduction

Oil spills pose a significant threat to marine and coastal environments, causing long-lasting damage to ecosystems, wildlife, and human health. If not controlled, they can result in environmental pollution that devastates marine life. Major sources of oil spills include oil tanker accidents, damaged ships or pipelines, illegal bunkering, and the indiscriminate disposal of oil into water bodies, among others.[1] Rapid and accurate detection of oil spills is crucial for initiating timely response measures to mitigate their impact, protect marine life, and ensure a clean and safe environment. Over the years, methods, such as aerial photography

and the use of pressure sensors mounted on pipelines have been conventionally employed for oil spill detection. However, these methods are often ineffective and time-consuming. The evolution of remote sensing techniques, particularly synthetic aperture radar (SAR) imagery, as an oil spill detection and monitoring tool for large ocean areas, has proven to be effective due to its ability to penetrate cloud cover and operate both day and night.[1] SAR uses a microwave sensor that records the backscattering signals at different frequencies to form a two-dimensional image. This method is unaffected by environmental conditions, such as cloudy weather or the absence of sunlight, and it is cost-effective, covering larger areas. However, there is a risk of misclassification in this approach, which may affect the accuracy of oil spill detection due to the resemblance of captured oil spill spots to other areas with similar features.

In recent years, advancements in machine learning (ML), particularly convolutional neural networks (CNNs), have revolutionized image analysis tasks.[2-4] ML approaches can autonomously extract high-level features from SAR images and classify them with minimal error. CNNs, which are often used for studying and classifying large datasets, have proven effective in oil spill detection. Their high accuracy and precision make them particularly suitable for classification tasks, especially when dealing with datasets that contain similar features. The extraction of high-level image features by CNNs makes it possible to classify images accurately. The ability of CNNs to automatically learn features from raw data makes them ideal for complex image recognition tasks.[5] While several state-of-the-art models have been developed for oil spill detection, they often face challenges in generalizing to diverse SAR image conditions and varying spill characteristics.[6,7]

This study aims to address these challenges by designing and implementing a novel CNN-based algorithm termed "SpillNet," specifically tailored for oil spill detection in SAR images. The "SpillNet" model is a modified form of the conventional CNN and training algorithm that incorporates features such as depthwise separable convolutional layers (DSCL), batch normalization (BN), and residual connections (RC), which improve the training process and ensure robust detection and classification of oil spills. The proposed algorithm leverages the unique characteristics of SAR data and the robust feature extraction capabilities of CNNs to enhance detection accuracy. Furthermore, the study evaluates the model's performance on both seen and unseen SAR images to assess its generalization capabilities.

To validate the efficacy of the proposed algorithm, its performance is compared against existing state-of-the-art models using a comprehensive set of evaluation metrics. The results demonstrate significant improvements in detection accuracy, showcasing the potential of this novel CNN approach in enhancing oil spill monitoring efforts.

By advancing the accuracy and efficiency of oil spill detection, this research contributes to the broader goals of environmental protection and disaster management. The study has applications in the oil and gas industry, where it can assist with environmental protection and oil spill management. It is also useful for making predictions to prevent oil spills and enhancing early detection for more effective responses.

This paper is structured as follows: Section 1 provides a general overview of oil spills and background on the state-of-the-art technologies used to mitigate their impact. Section 2 presents the literature review, covering both traditional and non-traditional approaches to oil spill detection, their limitations, and the challenges they face while also identifying the research gaps and the novelty of this study. Section 3 details the methodology employed, while Section 4 reports and discusses the results obtained. The study concludes with a discussion of the limitations, recommendations, and directions for future research.

2. Literature review

2.1. Traditional approaches to oil spill detection

Historically, oil spill detection has been performed using optical and SAR images.[8,9] While optical sensors are useful, they are limited by cloud cover and lighting conditions.[10] On the other hand, SAR can operate in all weather conditions and at any time of day or night,[11] making it a preferred choice for monitoring marine environments. Techniques, such as thresholding,[12] segmentation,[13] and texture analysis[9] have been employed to identify oil spills in SAR images. However, these methods often require significant human intervention and are prone to false positives from look-alikes, such as low-wind areas, sea ice, and natural surfactants.

2.2. ML and CNNs

ML has introduced automation to oil spill detection, reducing the reliance on human experts. Early ML approaches employed shallow models such as support vector machines and random forests, which showed promise but were limited in handling complex image features. The introduction of deep learning, particularly

CNNs, has dramatically improved the performance of image classification tasks, including oil spill detection.[14] CNNs are a class of deep learning models designed to process grid-like data, such as images. They are composed of multiple layers, including convolutional layers, pooling layers, and fully connected layers. CNNs automatically learn hierarchical features from input images, making them highly effective for complex pattern recognition. Typically, ML models identify and classify dark spots or regions in SAR images that indicate areas covered by oil on the sea surface, due to the scattering of the SAR signal from the oil. These dark spots or regions could either be oil spills or look-alikes.[13-16] The accuracy of the developed model in differentiating oil spills from look-alikes depends on how well the model is trained for identification and classification tasks. The three main steps involved in oil spill detection and classification include: (i) training the dataset and identifying the dark spots, (ii) extracting features from these dark spots, and (iii) training a classifier using the extracted features.

Once trained, the model can be used to classify selected dark spots.

2.3. Applications of CNNs in oil spill detection

Several studies have demonstrated the efficacy of CNNs in detecting oil spills from satellite imagery. Fingas and Brown[15] provided a comprehensive review of oil spill remote sensing techniques, emphasizing the potential of CNNs.

More recent work by Mahmoudi Ghara *et al.*[8] introduced a novel CNN architecture specifically designed for oil spill detection, incorporating attention mechanisms to focus on relevant parts of the image. Their approach significantly reduced false positives, particularly in complex environments with numerous look-alikes.[8] Similarly, Zhan *et al.*[17] applied transfer learning to leverage pre-trained CNNs, achieving state-of-the-art results with limited labeled data.

Table 1 presents some of the ML approaches that have been implemented for detecting and classifying oil spills with high accuracy.

2.4. Challenges and limitations of CNNs in oil spill detection

Despite the success of CNNs, several challenges remain. One major issue in oil spill detection is the scarcity of labeled training data, which is essential for training deep learning models. Annotating large datasets is expensive and time-consuming. Although data augmentation and synthetic data generation have been proposed as solutions, these techniques still have limitations.[28]

Another challenge is the high computational cost associated with training CNNs.[29] Advanced models require significant computational resources, which may not be readily available in all research settings. In addition, while CNNs excel at detecting oil spills in homogeneous environments, their performance can degrade in heterogeneous or noisy conditions.

2.5. Identified research gaps

Existing research has demonstrated some automated techniques for oil spill detection. For instance, Daniyan *et al.*[30] developed a test rig comprising four flow lines, each equipped with pressure sensors and gauges. The system relies on a microcontroller as the main controller, with pressure transducers for monitoring and detecting pressure drops below a threshold. However, the potential of ML approaches and their data computational abilities were not explored. Daniyan *et al.*[31] also reported the development of an inline inspection robot for detecting issues such as cracks and corrosion in pipelines to prevent oil spills. Despite the reported advances, several gaps in research remain, particularly in utilizing CNNs for oil spill detection. One limitation of the study is the reliance on prototype development without validation against real datasets and empirical results. In addition, the integration of CNNs with other ML approaches, such as recurrent neural networks for temporal analysis, could enhance detection accuracy over time. Moreover, the development of lightweight CNN models capable of running on less powerful hardware would make this technology more accessible.

The novelty of this study lies in the development and implementation of a unique CNN-based algorithm termed "SpillNet," specifically designed for oil spill detection in SAR images. The proposed algorithm leverages the unique characteristics of SAR data and the robust feature extraction capabilities of CNNs to improve detection accuracy. The architecture integrates multiple DSCL, BN, and RC to enhance feature extraction and learning capabilities. The DSCL enables the model to learn the relationships between complex patterns, such as distinguishing oil spills from their look-alikes, with lower computational complexity compared to standard convolutions. This reduces time and costs, making the process more efficient. Moreover, the model breaks down the convolution operations into individual channel and spatial (pointwise) information, reducing the parameters needed to train the datasets. This

Table 1. Existing machine learning models for oil spill detection and their outcomes

References	Method	Outcome
Zhan *et al*.[17]	Combination of CNNs with the DBSCAN clustering algorithm	The proposed model achieves an oil spill class pixel accuracy of 89.21%
Zhang *et al*.[18]	An improved mask R-CNN model using a combination of convolutional and pooling layers to extract features, followed by fully connected layers for classification	The model achieved a high accuracy of 91.5% in detecting oil spills in SAR images
Ma *et al*.[19]	Deep convolutional neural network	The improved DeepLabv3+model, using ResNet-101 as the backbone network and GN as the normalization layer, achieved superior performance with high precision (98.92%) and an inference time of 0.19 s
Yekeen *et al*.[20]	Convolutional neural network (Mask R-CNN) model employing computer vision instance segmentation for oil spill detection and classification	The proposed model achieved an accuracy of 98.3%
Feinauer *et al*.[21]	Enhanced CNN model based on GoogleNet and VGG16 combined with transfer learning	The GoogleNet transfer learning model achieved an improved outcome with 97.5% training accuracy, 95.6% validation accuracy, and a training loss of 0.0894
Mahmoud *et al*.[22]	A novel deep learning model based on the Dual Attention Model with enhanced conventional UNet segmentation network	The proposed model achieved an overall accuracy of 94.2%, outperforming the traditional UNet
Ahmed *et al*.[23]	Segmentation network model implemented in conditional generative adversarial network	The proposed model achieved oil spill segmentation with an average accuracy of 99.04%, an Intersection over the Union index of 96.59%, and a precision of 85.24%
Huang *et al*.[24]	Faster R-CNN	The model achieved precision and recall metrics of 89.23% and 89.14%, respectively
Basit *et al*.[25]	UNet convolutional neural network model	The mean intersection over union value for all the classes was 75.70%
Abba *et al*.[26]	Three deep-learning algorithms for satellite image classification: ResNet50, VGG19, and InceptionV4	InceptionV4 outperformed other algorithms with a classification accuracy of 97% for cloudy, desert, green areas, and water, followed by VGG19 at 96% accuracy, and ResNet50 at 93%
Dehghani-Dehcheshmeh *et al*.[27]	Combination of different loss functions on CNN networks and hybrid models of DeepLabV3+, FC-DenseNet, and U-Net networks based on vision transformers	The F1-scores for the individual DeepLabV3+, FC-DenseNet, and U-Net network models were 75.08%, 73.94%, and 60.85%, respectively, while the integrated model of CNN and ViT produced the best F1-score of 78.48%

Abbreviations: CNNs: Convolutional neural networks; DBSCAN: Density-based spatial clustering of applications with noise; GN: Group normalization; R-CNN: Region-based convolutional neural network; SAR: Synthetic aperture radar; ViT: Vision Transformer.

approach reduces the probability of overfitting, thereby improving the model's robustness and generalization ability. Furthermore, BN normalizes the input across layers to prevent internal variations, which facilitates convergence, accelerates the learning rate, and improves the model's generalization. Given the complexity of the oil dataset and the possibility of look-alikes, it is crucial to use an algorithm that is less sensitive to the effects of initial weights and prevents fluctuations during training. Thus, the introduction of BN acts as both a

regularizer and stabilizer during the training process, allowing for a faster and more stable rate of learning while reducing dependence on weight initialization. In addition, the RCs ensure effective training of the deep networks by providing shortcut paths for gradient flow. This prevents gradients from becoming too small as they propagate back through the network. The special feature of the modified CNN model, "SpillNet," is its ability to analyze SAR images and automatically identify and classify oil spills and look-alikes. It is sensitive to important surface characteristics of the ground or water, such as texture, color differences, and patterns, allowing it to accurately locate oil spills and distinguish them from other look-alikes. This reduces the likelihood of false positives and demonstrates the model's robust predictive and classification capabilities.

3. Methodology

This section describes the SAR image dataset used, as well as the data augmentation techniques employed to enhance the dataset and the pre-processing steps for preparing the data for CNN. The procedural steps for the development and implementation of the proposed SpillNet model are presented in Figure 1. These steps are divided into three major phases: (i) data collection (which is further divided into the pre-processing and data storage phases), (ii) model development and implementation (which includes algorithm modification and training, along with the selection of training resources), and (iii) the output and performance evaluation phase. In the model development and implementation phase, the images were loaded into the deep learning environment, and multiple convolution layers were applied with filters to extract important features from the images. BN was first applied to ensure a good distribution of the dataset, followed by the use of the Rectified Linear Unit (ReLU) activation functions to introduce non-linearity and detect initial features. Pooling layers were also applied to downsample feature maps, which were then flattened into a one-dimensional array. Dense layers were used for classification, with the model classifying the images into oil spill and non-oil spill (including the look-alikes) categories. The final

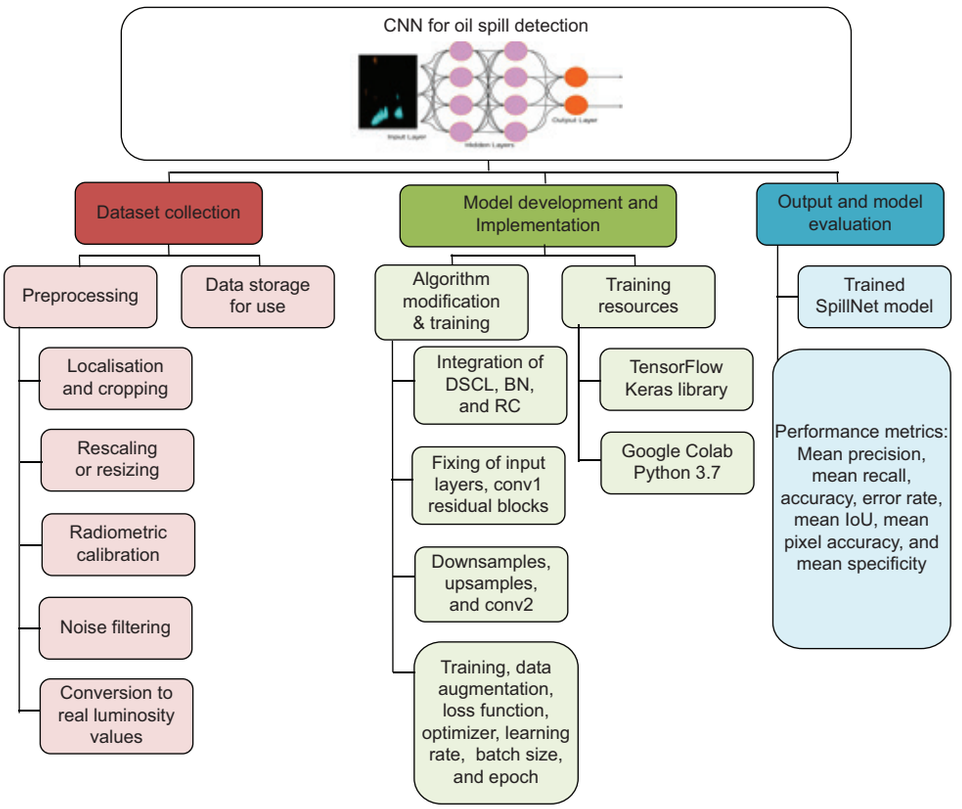

Figure 1. Procedural steps for the development and implementation of the proposed SpillNet model Abbreviations: BN: Batch normalization; conv1: Initial convolution layer; conv2: Final convolution layer; CNN: Convolutional neural network; DSCL: Depthwise separable convolutional layers; IoU: Intersection over Union; RC: Residual connections.

phase involved output generation and performance evaluation. Detailed explanations of the steps are provided in Sections 3.1-3.5.

3.1. Data collection and pre-processing

The data for this study, as detailed by Krestenitis *et al.*,[32] consists of SAR images obtained from the Sentinel-1 satellites, part of the European Space Agency's Copernicus program. These satellites are equipped with a C-band SAR system, providing wide coverage with a pixel spacing of 10 × 10 m, and operate effectively under various weather and illumination conditions. The dataset includes 1,112 SAR images, each annotated with ground truth masks confirming the presence of oil spills, which were verified through records from the European Maritime Safety Agency.[32]

To address the challenge of class imbalance and enhance the model's generalization capabilities, various data augmentation techniques were applied. These techniques include random resizing, horizontal and vertical flipping, and random cropping of the images. This augmentation process helps create a more robust training dataset by introducing variability in the input images, simulating different scales and orientations of oil spills.

The pre-processing pipeline, as implemented by Krestenitis *et al.*,[32] involves several steps to ensure the SAR images are in a suitable format for the CNN model:

(i) Localization and cropping: Each confirmed oil spill was localized according to the European Maritime Safety Agency records, and relevant regions were cropped from the raw SAR images
(ii) Rescaling: The cropped images were rescaled to a resolution of 1250 × 650 pixels to standardize the input size
(iii) Radiometric calibration: This step was applied to project the images into a common plane and correct any variations in sensor readings
(iv) Speckle noise filtering: A 7 × 7 median filter was used to reduce speckle noise, which is common in SAR images
(v) Conversion to real luminosity values: A linear transformation was applied to convert the images from decibel scale to real luminosity values, ensuring consistent brightness levels across the dataset.[32]

3.2. Modification of the CNN architecture and algorithm design

The proposed modified CNN architecture, termed SpillNet, is specifically designed for efficient and accurate oil spill detection in SAR images. This architecture integrates multiple DSCL, BN, and RC to enhance feature extraction, learning, and classification capabilities.

The modifications were implemented by adjusting several architectural components of the CNN model, including convolutional layers, residual blocks, filter sizes, data augmentation techniques (such as random resizing, horizontal/vertical flipping, and cropping), regularization methods, and hyperparameter tuning. By introducing data augmentation, the size of the training dataset was increased, allowing the model to learn across a broad range of input parameters, thus fostering robust classification. The modified CNN model comprised an initial and final convolution layer, with upsampling and downsampling layers in between. The purpose of multiple CNN layers was to allow the network to learn complex data, promoting effective feature extraction, learning, training, and classification capabilities. The different filter sizes employed at each layer allowed the model to capture and extract features at various scales and layers. For instance, small filters capture fine features, while large filters capture more significant features, enabling the model to identify relationships between the images for improved classification.

Depthwise separable convolutions significantly reduce the number of parameters and the computational burden without compromising performance.[33] RC, introduced by He *et al.*,[34] facilitates the training of very deep networks by providing shortcut paths for gradient flow. This helps prevent the gradients from becoming too small as they propagate back through the network.[34] Downsampling reduces the spatial dimensions, allowing the network to capture coarse features and reduce computational complexity, while upsampling restores the original resolution, refining the extracted features for accurate reconstruction.[35]

The architecture components included the following:

(i) Input layer: Accepted SAR images with a specified shape of 224 × 224 × 3
(ii) Initial convolution layer (conv1): A 128-filter 7 × 7 convolutional layer with padding, followed by BN and ReLU activation to detect initial features
(iii) Residual blocks: Four residual blocks, each containing two separable convolutional layers with 128 filters and 3 × 3 kernels, followed by BN and ReLU activation after each convolution. The block's input was added to its output to maintain gradient flow
(iv) Downsample layers: Downsample 1: A 256-filter 3 × 3 convolution with stride 2, followed by BN and

ReLU activation and two additional residual blocks with 256 filters. Downsample 2: A 512-filter 3 × 3 convolution with stride 2, followed by BN and ReLU activation

(v) Upsample Layers: Upsample 1: Upsampling by a factor of two, followed by a 256-filter separable convolution, BN, and ReLU activation. Upsample 2: Upsampling by a factor of two, followed by a 128-filter separable convolution, BN, and ReLU activation

(vi) Final convolution layer (conv2): A 1×1 convolution with the number of filters equal to the number of classes (five), followed by a softmax activation to produce the final output segmentation map.

The training process and parameter settings involved the following:

(i) Data augmentation: Techniques such as random resizing, horizontal/vertical flipping, and cropping were applied to enhance the training dataset.

(ii) Loss function: Categorical cross-entropy was used as the loss function, as expressed by Equation I:

$$L\left(y,\hat{y}\right)=-\sum_{i=1}^{N}y_i\log\left(\widehat{y_1}\right) \quad \text{(I)}$$

where y represents the ground truth label, $\hat{y}$ is the predicted probability, and N is the number of classes.

(iii) Optimizer: The Adam optimizer was selected for its efficiency and adaptability in handling sparse gradients.

(iv) Learning rate: The learning rate was set to 1×10^{-4}, with potential adjustments based on model convergence during training.

(v) Batch size: A batch size of eight was used to balance memory constraints and training efficiency.

(vi) Epochs: The model was trained for 100 epochs, with early stopping if the validation accuracy did not improve for 20 consecutive epochs.

(vii) Callbacks: Various callbacks were employed, including EarlyStopping, ReduceLROnPlateau, ModelCheckpoint, CSVLogger, and TensorBoard, to monitor and adjust the training process.

(viii) Training steps: The number of steps per epoch was calculated based on the size of the training and validation datasets, ensuring all data were utilized.

3.3. Implementation tools and frameworks

The development and training of the proposed model were carried out using the TensorFlow framework and Keras library. For data pre-processing, NumPy and Pandasa were used due to their efficiency in handling large datasets for numerical computations and data manipulation and analysis. Matplotlib was employed for data visualization, while OpenCV was used for image manipulation. TensorBoard was used to monitor training metrics in real-time. In addition, the development and training processes were carried out on Google Colab, a free cloud-based environment by Google for executing Python code.

3.4. Computational resources

The model was trained on an NVIDIA Tesla T4 GPU available on Google Colab, with up to 12 GB of random access memory. The Python environment was set up with Python 3.7, and all required libraries were installed through pip. Google Drive was used for storing datasets, checkpoints, and logs, ensuring seamless access and management of training data. Figure 2 presents the residual block, while Figure 3A and B illustrate the architecture of the proposed SpillNet model.

3.5. Algorithm for the training process

Input: SAR images I and ground truth annotations G, batch size $B = 8$, epochs $E = 100$, learning rate $\alpha = 1 \times 10^{-4}$, seed S.

1. Load data: I and G into memory.
2. Initialize parameters:
   $S \leftarrow$ random seed value
   $B \leftarrow 8$
   $E \leftarrow 100$
   $\alpha \leftarrow 1 \times 10^{-4}$
3. Split data: (I_{train}, G_{train}), $(I_{val}, G_{val}) \leftarrow$ split I and G into training and validation sets.
4. For each epoch e from 1 to E:
   Shuffle (I_{train}, G_{train}) using seed S
   Set steps_per_epoch $\leftarrow [len\ (I_{train}/B)]$
   Set validation_steps $\leftarrow [len\ (I_{val}/B)]$
   For each mini-batch b from 1 to steps_per_epoch:
   $(I_b, G_b) \leftarrow$ Get a mini-batch of size B from (I_{train}, G_{train})
   Data augmentation: $I_b \leftarrow$ Apply random resizing, flipping and cropping to I
   Preprocessing: $I_b \leftarrow$ Normalize and resize I_b to 224 × 224 pixels
   Forward pass: $\leftarrow$ SpillNet (I_b)
   Compute loss: $L \leftarrow$ Categorical Cross-Entropy Loss $(G_b,)$
   Backpropagation and update weights: Update SpillNet weights using
   Adam optimizer and learning rate α.

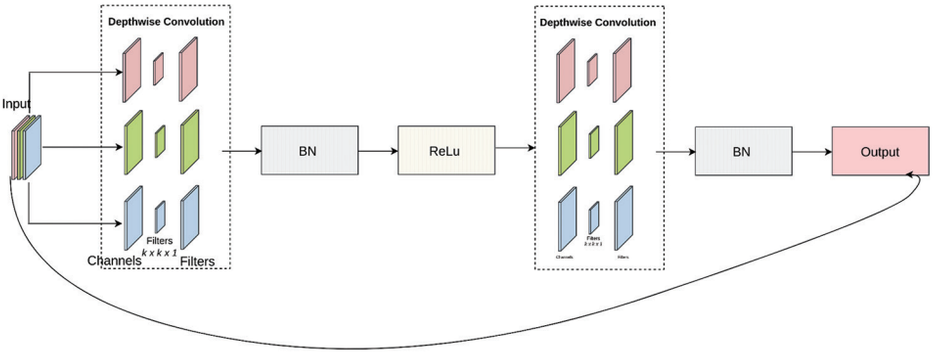

Figure 2. Residual block
Abbreviations: BN: Batch normalization; ReLu: Rectified Linear Unit.

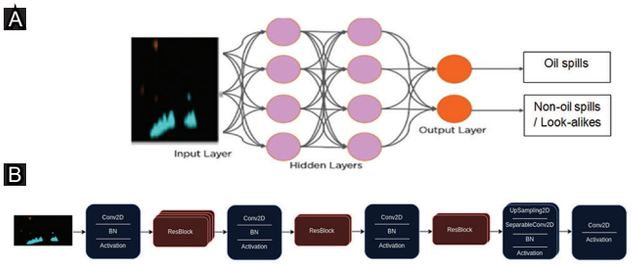

Figure 3. The architecture of the proposed SpillNet model. (A) Network diagram of the proposed SpillNet model showing the input, hidden, and output layers. (B) Block diagram of the proposed SpillNet model
Abbreviations: BN: Batch normalization; Conv2D: Final convolution layer; ResBlock: Residual Block.

5. Validation: Evaluate SpillNet on (I_{val}, G_{val})
   Monitor validation accuracy and loss. Adjust learning rate if performance plateaus.
6. Model checkpoint: Save the best model based on validation accuracy.

Repeat steps 2 – 6 until convergence or reaching E epochs.

Output: Trained SpillNet model.

The primary difference between the SpillNet model and the conventional CNN models lies in the architecture. Multiple DSCL, BN, and RC were integrated into SpillNet to enhance feature extraction, learning, and classification capabilities, unlike traditional CNN models. DSCL splits the convolutional layers into multiple layers, enabling the model to learn complex relationships, such as distinguishing oil spills and look-alike features, with reduced computational complexity compared to standard convolutions. This modification makes the model more time- and cost-efficient. Furthermore, the BN in SpillNet was positioned before the ReLU activation function to ensure a well-distributed dataset and prevent variance issues that could hinder training. RC enhanced the model's feature extraction and learning capabilities, ensuring smoother training of deep networks.

4. Results and discussion

The performance of the developed SpillNet model was evaluated on the dataset. In addition, SpillNet's performance was compared to existing deep learning CNN segmentation models, including UNet, LinkNet, Feature Pyramid Network (FPN), and Pyramid Scene Parsing Network (PSPNet). The evaluation results are presented and thoroughly analyzed in this section.

4.1. Model validation assessment

Table 2 presents the detection and segmentation results of various models, including Spillnet, LinkNet, FPN, PSPNet, and Unet. The table compares their performance based on metrics such as mean precision, mean recall, accuracy, error rate, mean IoU, mean pixel accuracy, and mean specificity. The results demonstrate that SpillNet significantly outperforms the other models across most of these metrics.

In this study, seven performance indicators were employed to evaluate the performance of various models employed for detecting oil spills. These indicators include: mean precision, mean recall, accuracy, error rate, mean IoU, mean pixel accuracy, and mean specificity. Mean precision is a measure of the accuracy of positive predictions, while mean recall reflects the completeness of positive predictions. High values for both precision and recall are generally desirable when evaluating the performance of ML algorithms, though there may be a trade-off between the two. Accuracy indicates the performance of the CNN model in making

predictions based on the data used, while error rate represents incorrect predictions or detections. Mean IoU is a performance metric used to evaluate the algorithm's accuracy in making correct detections, while mean pixel accuracy is a segmentation metric that indicates the percentage of pixels correctly classified in the image. This is the ratio of correctly classified pixels to the total number of pixels in the image. Mean specificity represents the ability of the proposed model to correctly predict true negatives for each available category.

The results obtained indicate the performance of the CNN model in making predictions based on the data used.

From Table 3, it can be observed that the proposed SpillNet model achieved the highest mean precision of 0.623542, accuracy of 0.946947, mean IoU of 0.58124, mean pixel accuracy of 0.598060, and mean specificity of 0.944469, with the least error rate of 0.061053. This demonstrates the superior performance of the Spillnet model. Although the PSPNet achieved the highest mean recall of 0.587413 compared to SpillNet's mean recall of 0.571559, overall, Spillnet outperformed the other models. For example, the proposed mean IoU (0.581241) was notably higher than those of FPN (0.473193), PSPNet (0.508106), and UNet (0.481241). This indicates that the proposed model is better at capturing the boundaries of an oil spill. Furthermore, the proposed model showed the lowest error rate of 0.061053, reinforcing its robustness in segmentation tasks. These performance metrics for SpillNet were superior to those of existing deep-learning CNN segmentation models, as shown in Table 3, including UNet, LinkNet, FPN, and PSPNet. These findings confirm that the proposed model outperforms

Table 2. Validation results

Model	Mean precision	Mean recall	Accuracy	Error rate	Mean IoU	Mean pixel accuracy	Mean specificity
LinkNet	0.587804	0.548060	0.919029	0.081971	0.469090	0.546060	0.922446
FPN	0.552293	0.566916	0.909360	0.090640	0.473193	0.566916	0.923545
PSPNet	0.608340	0.587413	0.924690	0.075310	0.508106	0.587413	0.936614
UNet	0.613542	0.541559	0.936947	0.063053	0.481241	0.541559	0.924469
SpillNet	0.623542	0.571559	0.946947	0.061053	0.581241	0.598060	0.944469

Abbreviations: FPN: Feature Pyramid Network; IoU: Intersection over Union; PSPNet: Pyramid Scene Parsing Network.

Table 3. Comparative analysis of the developed model and existing convolutional neural network models used for oil spill detection

References	Proposed technique	Accuracy/precision (%)
Present study	Integration of multiple depthwise separable convolutional layers, batch normalization, and residual connections	94.70
Das *et al*.[45]	CNN with ReLU and sigmoid activation function, binary cross-entropy, and Adam optimizer	99.06
Guo *et al*.[46]	CNN with sigmoid activation function	91.33
Hidalgo *et al*.[47]	CNN with ReLU* and softmax activation function, and stochastic gradient descent	96.64
Cantorna *et al*.[48]	CNN with ReLU and binary cross-entropy	98.30
Zeng and Wang[49]	CNN with ReLU and softmax cross-entropy, and Adam optimizer	94.01
Song *et al*.[50]	Integrated CNN and support vector machine with ReLU and softmax activation function, and cross-entropy	99.19
Kang *et al*.[51]	CNN and transformer models	91.00
Liu *et al*.[38]	Multi-source knowledge graph reasoning approach	27.81
Hamza *et al*.[52]	Conventional CNN with standard convolutions	94.30
Mahmoud *et al*.[22]	Enhanced conventional CNN UNet segmentation model with integrated dual attention model	94.20

Abbreviations: CNN: Convolutional neural network; ReLu: Rectified Linear Unit.

the existing models in oil spill classification and segmentation tasks.

Figures 4 and 5 display a comparative analysis of the accuracy of the different models employed in this study, highlighting the superior performance of SpillNet.

Figure 6 shows the predicted areas of oil spills using the SpillNet model. Using the proposed CNN SpillNet model, the dark spots were identified, segmented, and classified. This model outperformed other CNN models employed due to its effective dark spot segmentation, which enhanced the feature extraction process, resulting in a high accuracy of SpillNet for dark spot classification. The model segmented the SAR images into super-pixel patches and performed classification based on the extracted features. Areas with deep dark spots were identified as oil spill regions, while areas with light dark spots were classified as look-alike areas. The developed SpillNet CNN model was able to differentiate between

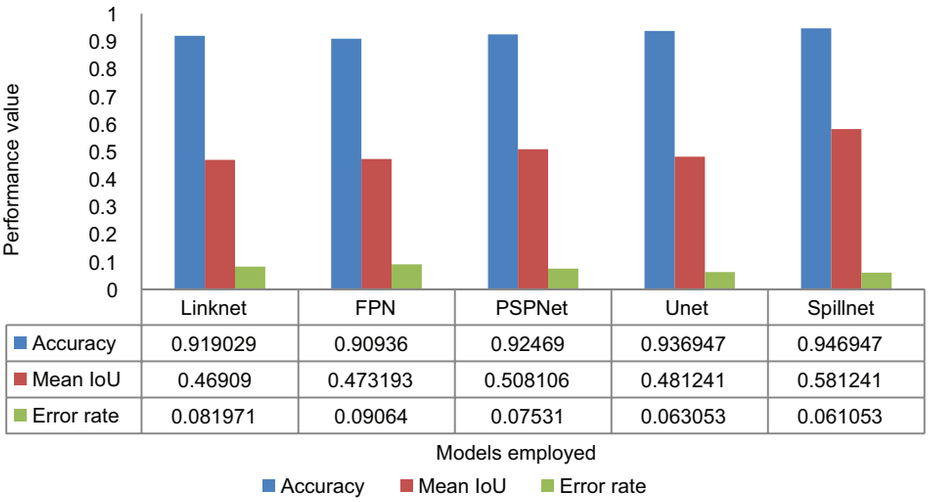

	Linknet	FPN	PSPNet	Unet	Spillnet
Accuracy	0.919029	0.90936	0.92469	0.936947	0.946947
Mean IoU	0.46909	0.473193	0.508106	0.481241	0.581241
Error rate	0.081971	0.09064	0.07531	0.063053	0.061053

Figure 4. Comparative analysis of the accuracy, mean Intersection over Union, and error rates of the different models
Abbreviations: FPN: Feature Pyramid Network; PSPNet: Pyramid Scene Parsing Network.

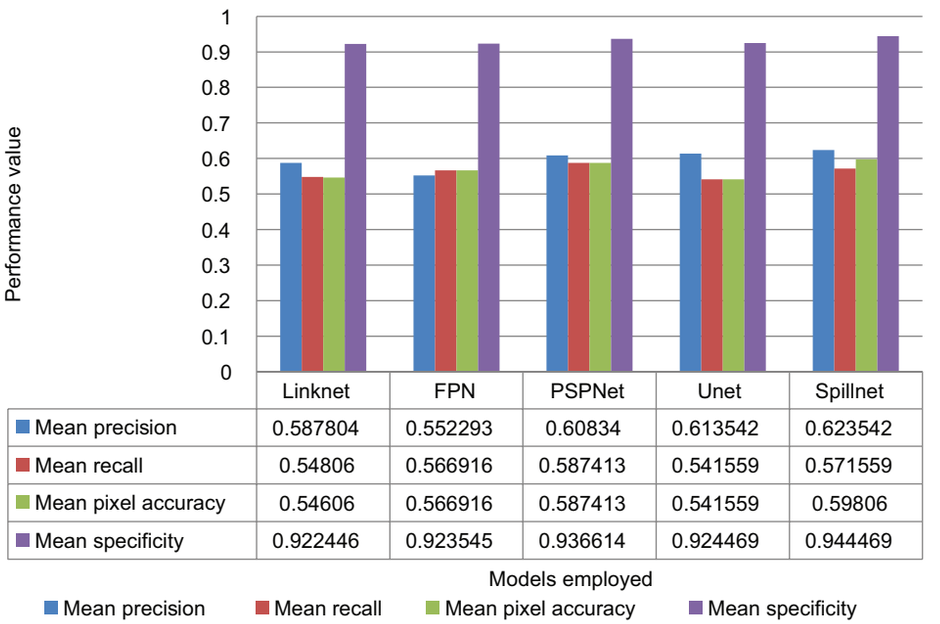

	Linknet	FPN	PSPNet	Unet	Spillnet
Mean precision	0.587804	0.552293	0.60834	0.613542	0.623542
Mean recall	0.54806	0.566916	0.587413	0.541559	0.571559
Mean pixel accuracy	0.54606	0.566916	0.587413	0.541559	0.59806
Mean specificity	0.922446	0.923545	0.936614	0.924469	0.944469

Figure 5. Comparative analysis of the mean performance metrics of the different models
Abbreviations: FPN: Feature Pyramid Network; PSPNet: Pyramid Scene Parsing Network.

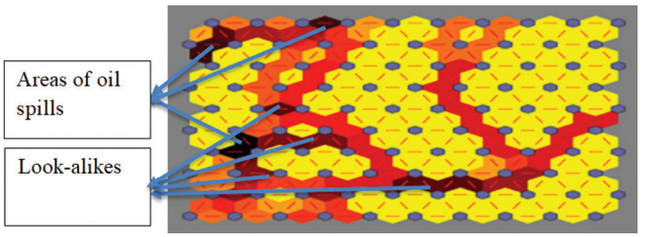

Figure 6. Identified areas of oil spills using the convolutional neural network SpillNet model

oil spill areas and look-alike regions, achieving a high accuracy of 0.946947. The appearance of oil spills can vary across different locations depending on factors such as wind speed, water conditions, nature of the spill, and lighting. Furthermore, SAR images can be affected by noise and other forms of interference, which may increase false positives and affect the accuracy of classification. Hence, the ability of the proposed SpillNet model to distinguish between actual areas of oil spills and their look-alikes represents an improvement over existing studies. Mera *et al.*[36] indicated light dark spots may result from low wind speeds rather than oil spills. Najouri *et al.*[37] stated that there is a higher probability of obtaining look-alikes when sea wind speeds are too high or low, and they recommended a wind speed range of 2.08 – 8.33 m/s for accurate oil spill detection. Thus, to improve the accuracy of predictions, Liu *et al.*[38] suggested incorporating auxiliary datasets, such as the wind speed and direction data, to improve the model's predictive capabilities.

4.2. Discussion

With an accuracy of 0.946947, the evaluation results demonstrated that the proposed model outperforms the existing models in the oil spill segmentation task.

The effectiveness of the proposed model in segmenting oil spill regions was evident from its mean IoU and Dice coefficient. By striking a satisfactory balance between precision and recall, the proposed model effectively identified true positives while minimizing false positives. This balance is important for oil spill detection, as both false alarms and missed detections can have significant impacts. With a high accuracy of 0.946947, the model proved to be a robust tool for oil spill detection, capable of correctly classifying the majority of pixels in SAR images. The architectural design of the proposed model, which included separable convolutional layers and RC, enabled efficient training and faster convergence. The model's efficiency was advantageous for oil spill detection applications, especially in cases where computational resources are limited. The model performed well on the validation dataset, indicating that it can generalize effectively on unseen data and can be used in real-world oil spill applications. Nevertheless, there are limitations. While the proposed model's mean IoU was competitive, it was slightly lower than that of the FPN model. This finding suggests that the proposed model may not always achieve maximum overlap between its predictions and the ground truth segments.

The results obtained by Zhan *et al.*,[17] who combined the CNNs with the density-based spatial clustering of applications with a noise clustering algorithm, achieved a pixel accuracy of 89.21%, which is higher than the one obtained for the SpillNet model proposed in this study (0.598060). However, the SpillNet model showed greater overall accuracy than the model proposed by Zhan *et al.*[17] The algorithm developed by Vyas *et al.*[12] for oil spill detection first analyzed the SAR images and assigned probabilities to the dark spots to identify an oil spill or a resemblance. The results obtained by Bui *et al.*,[39] using a combination of deep learning model and data augmentation technique based on the generative adversarial network model, showed a mean Intersection over Union of 72.49%, with a 2.56% increase in the mean Intersection over Union after applying data augmentation. These results indicate the feasibility of using ML approaches for oil spill detection. The predictive model developed by Ukpaka *et al.*[40] for pipe leakage and insulation failure detection in natural gas transmission pipelines achieved an accuracy of 92.2%.

Ukenedo *et al.*[41] suggested the implementation of a Health, Safety, and Environmental management system policy in the oil and gas industry to effectively mitigate unsafe conditions such as crude oil spills. Khaira *et al.*[42] recommended the use of Internet of Things-based online condition monitoring tools to promote early fault detection and enhance the reliability of industrial systems, equipment, and infrastructure, such as oil pipelines. Similarly, Waghmare *et al.*[43] suggested employing failure mode effects analysis for failure detection and classification to achieve high reliability in industrial systems and equipment.

The automation of oil spill detection using artificial intelligence, as demonstrated in this study, is a proactive step toward environmental protection. For example, Promise *et al.*[44] highlighted that operations in the upstream, midstream, and downstream oil sectors in Nigeria are a major cause of environmental pollution, which poses significant threats to the environment, aquatic life, plant life, and soil nutrients.

Table 2 presents a comparative analysis of the developed model with existing CNN models employed for oil spill detection. The results of the comparative analysis showed that the proposed model (integrating multiple DSCL, BN, and RC) aligns well with the outcomes of existing studies, with some improvements. This indicates that the proposed model can train on oil spill datasets and accurately detect oil spills using SAR image analysis. The proposed model can also autonomously differentiate between oil spills and look-alike regions with similar features.

Table 3 presents a further comparative analysis of the developed model with existing CNN models used for oil spill detection, demonstrating that the proposed SpillNet model offers improvements over some existing CNN models deployed for similar applications.

5. Conclusions, recommendations, and future works

This study developed and evaluated a novel CNN model for oil spill detection using SAR images. Specifically, an integrated multiple DSCL, BN, and RC were proposed to enhance feature extraction and learning capabilities. The dataset employed consisted of SAR images obtained from the Sentinel-1 satellites, part of the European Space Agency's Copernicus program, and the model was trained on an NVIDIA Tesla T4 GPU available on Google Colab, with programming done in the Python 3.7 environment. The proposed algorithm leveraged the unique characteristics of SAR data and the robust feature extraction capabilities of CNNs to enhance detection accuracy. The SpillNet model achieved a mean precision of 0.623542, mean recall of 0.571559, accuracy of 0.946947, mean IoU of 0.58124, mean pixel accuracy of 0.598060, and mean specificity of 0.944469, with a negligible error rate of 0.061053. These results outperform those obtained by existing deep-learning CNN segmentation models, including UNet, LinkNet, FPN, and PSPNet. This demonstrates that the proposed model surpasses other models in the oil spill classification and segmentation tasks. Furthermore, the model effectively differentiated between actual oil spill areas and their look-alikes, thereby improving detection accuracy. This indicates that the proposed model is both robust and efficient, making it a valuable tool for oil spill detection in real-world applications. By maintaining a balance between precision and recall, the model minimized false alarms and missed detections. Thus, the developed "SpillNet" model is recommended for implementation in the detection of oil spills using SAR images, and it offers a time- and cost-effective approach to oil spill management. This study contributes to advancing automated oil spill detection by offering a reliable and efficient solution for early oil spill detection and environmental monitoring in general. However, there is a need for larger, more diverse annotated datasets to further improve the model's robustness. Future work should focus on enhancing segmentation precision and processing speed to optimize the model for real-world applications.

Acknowledgments

None.

Funding

None.

Conflict of interest

The authors declare no conflicts of interest.

Author contributions

Conceptualization: All authors
Investigation: All authors
Methodology: All authors
Writing-original draft: All authors
Writing-review & editing: All authors

Availability of data

The data supporting the findings of this study are available from the corresponding author upon reasonable request.

References

1. Del Frate F, Petrocchi A, Lichtenegger J, Calabresi G. Neural networks for oil spill detection using ERS-SAR data. *IEEE Trans Geosci Remote Sens.* 2000;38(5):2282-2287. doi: 10.1109/36.868885
2. Hou L, Samaras D, Kurç T, Gao Y, Davis J, Saltz J. Patch-based Convolutional Neural Network for whole Slide Tissue Image Classification. In: *2016 IEEE Conference Computer Vision Pattern Recognition CVPR*; 2016. doi: 10.1109/cvpr.2016.266
3. Iqbal J, Vogt M, Bajorath J. Activity landscape image analysis using convolutional neural networks. *J Cheminform*. 2020;12(1):34.

doi: 10.1186/s13321-020-00436-5
4. Wang J, Zeng X, Shan D, Zhou Q, Peng H. Image target recognition based on improved convolutional neural network. *Math Probl Eng.* 2022;2022:2213295. doi: 10.1155/2022/2213295
5. *[Citation Report] Neuromorphic Processing at Tera-OP/s Speeds with Soliton Crystal Microcombs.* Available from: https://scite.ai/reports/neuromorphic-processing-at-tera-op-s-speeds-G3mRdKWE?showReferences=true [Last accessed on 2024 Jun 13].
6. Topouzelis K. Oil Spill Detection by SAR Images: Dark formation detection, feature extraction and classification algorithms. *Sensors*. 2008;8(10):6642-6659. doi: 10.3390/s8106642
7. Schvartzman I, Havivi S, Maman S, Rotman SR, Blumberg DG. Large oil spill classification using sar images based on spatial histogram. *Int Arch Photogramm Remote Sens Spatial Inform Sci.* 2016;XLI-B8:1183-1186. doi: 10.5194/isprs-archives-XLI-B8-1183-2016
8. Mahmoudi Ghara F, Shokouhi SB, Akbarizadeh G. A new technique for segmentation of the oil spills from synthetic-aperture radar images using convolutional neural network. *IEEE J Sel Top Appl Earth Obs Remote Sens.* 2022;15:8834-8844. doi: 10.1109/JSTARS.2022.3213768
9. Chen Y, Wang Z. Marine Oil spill detection from SAR images based on attention u-net model using polarimetric and wind speed information. *Int J Environ Res Public Health*. 2022;19(19):19. doi: 10.3390/ijerph191912315
10. Kumar A, Roy AH, Andreadis KM, He X, Butler C. A multi-sensor approach to characterize winter water-level drawdown patterns in lakes. *Remote Sens.* 2024;16(6):947. doi: 10.3390/rs16060947.
11. Pham-Duc B, Prigent C, Aires F. Surface water monitoring within cambodia and the vietnamese mekong delta over a year, with Sentinel-1 SAR observations. *Water*. 2017;9(6):366. doi: 10.3390/w9060366
12. Vyas G, Bhan A, Gupta D. Detection of oil Spills using Feature Extraction and Threshold Based Segmentation Techniques. In: *2015 2nd International Conference on Signal Processing and Integrated Networks (SPIN)*; 2015. p. 579-583. doi: 10.1109/SPIN.2015.7095433
13. Liu P, Li Y, Liu B, Chen P, Xu J. Semi-automatic oil spill detection on X-Band marine radar images using texture analysis, machine learning, and adaptive thresholding. *Remote Sens.* 2019;11(7):756. doi: 10.3390/rs11070756
14. Temitope Yekeen S, Balogun AL. Advances in remote sensing technology, machine learning and deep learning for marine oil spill detection, prediction and vulnerability assessment. *Remote Sens.* 2020;12(20):756. doi: 10.3390/rs12203416
15. Fingas MF, Brown CE. Review of oil spill remote sensing. *Spill Sci Technol Bull.* 1997;4(4):199-208. doi: 10.1016/S1353-2561(98)00023-1
16. Zhang C, Harrison PA, Pan X, Li H, Sargent I, Atkinson PM. Scale Sequence Joint Deep Learning (SS-JDL) for land use and land cover classification. *Remote Sens Environ.* 2020;237:111593. doi: 10.1016/j.rse.2019.111593
17. Zhan C, Bai K, Tu B, Zhang W. Offshore Oil spill detection based on CNN, DBSCAN, and hyperspectral imaging. *Sensors*. 2024;24(2):411. doi: 10.3390/s24020411
18. Zhang J, Ai B, Shangand H, Li B. Oil detection in SAR Images Based on Improved Mask R-CNN Model. In: Proceeding SPIE 12815. *Internaational Conference on Remote Sensing, Mapping and Geograhic Systems*; 2023. doi: 10.1117/12.3010303
19. Ma X, Xu J, Wu P, Kong P. Oil spill detection based on deep convolutional neural networks using polarimetric scattering information from Sentinel-1 SAR images. *IEEE Trans Geosci Remote Sens*. 2022;60:4204713.
20. Yekeen ST, Balogun AL, Wan Yusof KB. A novel deep learning instance segmentation model for automated marine oil spill detection. *ISPRS J Photogramm Remote Sens.* 2020;167:190-200.
21. Feinauer DM, Latif G, Alenazy AM, Tayem N, Alghazo J, Alzubaidi L. Oil Spill Identification Using Deep Convolutional Neural Networks. In: Proceedings - 2022 14th IEEE International Conference on Computational Intelligence and Communication Networks, CICN 2022. Institute of Electrical and Electronics Engineers; 2022. p. 240-245. doi: 10.1109/CICN56167.2022.10008373
22. Mahmoud AS, Mohamed SA, El-Khoriby RA, AbdelSalam HM, El-Khodary IA. Oil spill identification based on dual attention unet model using synthetic aperture radar images. *J Indian Soc Remote Sens.* 2023;51:121-133. doi: 10.1007/s12524-022-01624-6
23. Ahmed S, ElGharbawi T, Salah M, El-Mewafi M. Deep neural network for oil spill detection using Sentinel-1 data: Application to Egyptian coastal regions. *Geomatics Nat Hazards Risk*. 2022;14(1):76-94.
24. Huang X, Zhang B, Perrie W, Lu Y, Wang C. A novel deep learning method for marine oil spill detection from satellite synthetic aperture radar imagery. *Mar Pollut Bull*. 2022;179:113666.
25. Basit A, Siddique MA, Sarfraz MS. Deep Learning Based Oil Spill Classification Using UNET Convolutional Neural Network. In: 2021 IEEE International Geoscience and Remote Sensing Symposium IGARSS, Brussels, Belgium; 2021. p. 3491-3494. doi: 10.1109/IGARSS47720.2021.9553646
26. Abba AS, Mustaffa NH, Hashim SZM, Alwee R. Oil

spill classification based on satellite image using deep learning techniques. *Baghdad Sci.J.* 2024;21(2(SI):0684.
27. Dehghani-Dehcheshmeh S, Akhoondzadeh M, Homayouni S. Oil spills detection from SAR Earth observations based on a hybrid CNN transformer networks. *Mar Pollut Bull.* 2023;190:114834.
28. Kalyan KS. A survey of GPT-3 family large language models including ChatGPT and GPT-4. *Rochester, NY*: Cornell University, New York; 2023. doi: 10.2139/ssrn.4593895
29. Urolagin S, Nayak J, Acharya UR. Gabor CNN based intelligent system for visual sentiment analysis of social media data on cloud environment. *IEEE Access*. 2022;10:132455-132471. doi: 10.1109/ACCESS.2022.3228263
30. Daniyan IA, Dahunsi OA, Oguntuase OB, Daniyan OL, Mpofu K. Development of a prototype test rig for leak detection in pipelines. *Procedia CIRP.* 2019;80:524-529. doi: 10.1016/j.procir.2019.01.016
31. Daniyan IA, Balogun V, Ererughurie OK, Daniyan OL, Oladapo BI. Development of an inline inspection robot for the detection of pipeline defects. *J Facilities Manag.* 2022;20(2):193-217. doi: 10.1108/JFM-01-2021-0010
32. Krestenitis M, Orfanidis G, Ioannidis K, Avgerinakis K, Vrochidis S, Kompatsiaris I. Oil spill identification from satellite images using deep neural networks. *Remote Sens.* 2019;11(15):1762. doi: 10.3390/rs11151762
33. Chollet F. Xception: Deep Learning with Depthwise Separable Convolutions, *2017 IEEE Conference on Computer Vision and Pattern Recognition (CVPR)*, Honolulu, HI, USA, 2017, pp. 1800-1807. doi: 10.1109/CVPR.2017.195
34. He K, Zhang X, Ren S, Sun J. Deep Residual Learning for Image Recognition, *2016 IEEE Conference on Computer Vision and Pattern Recognition (CVPR)*, Las Vegas, NV, USA, 2016, pp. 770-778. doi: 10.1109/CVPR.2016.90
35. Mustafa A, Kim H, Hilton A. MSFD: Multi-Scale segmentation-based feature detection for wide-baseline scene reconstruction. *IEEE Trans Image Process.* 2019;28(3):1118-1132. doi: 10.1109/TIP.2018.2872906
36. Mera D, Bolon-Canedo V, Cotos JM, Alonso-Betanzos A. On the use of feature selection to improve the detection of sea oil spill in SAR images. *Comput Geosci.* 2017;100:166-178.
37. Najouri Z, Rianzanoff S, Defontaines B, Xavier JP. A statistical approach to preprocess and enhance c-band SAR images in order to detect automatically marine oi slicks. *IEEE Trans Geosci Remote Sens.* 2018;56:2554-2564.
38. Liu X, Zhang Y, Zhou H, *et al*. Multi-source knowledge graph reasoning for ocean oil spill detection from satellite SAR images. *Int J Appl Earth Observ Geoinform.* 2023;116:103153.
39. Bui NA, Oh Y, Lee I. Oil spill detection and classification through deep learning and tailored data augmentation. *Int J Appl Earth Observ Geoinform.* 2024;129:103845. doi: 10.1016/j.jag.2024.103845
40. Ukpaka CP, Puyate YT, Nwokide LC. Predictive model to detect insulation failure and pipe leakage in natural gas transmission pipeline using simulation software. *Indian J Eng.* 2019;16:135-166.
41. Ukenedo OG, Ukpaka CP, Nkoi B. Effects of unsafe acts and conditions on the reliability of equipment installation in oil and gas servicing unit: A Case Study. *Indian J Eng*. 2022;19(51):294-309.
42. Khaira A, Dwivedi RK, Srivastava S. A state of the art review of online condition monitoring tools using ndt as principal testing technique. *Indian J Eng*. 2016;13(33):338-346.
43. Waghmare SN, Raut DN, Mahajan SK, Bhamare SS. Improving reliability for SMES in India by using faults classification. *Indian J Eng.* 2016;13(33):354-361.
44. Promise NU, Ukpaka CP, Puyate YT. Biokinetics of crude oil remediation using Dogoyaro (*Azadirachta indica*) Stem. *Indian J Eng.* 2020;17(47):250-260.
45. Das K, Janardhana P, Narayana H. Application of CNN based image classification technique for oil spill detection. *Indian J Geo Mar Sci.* 2023;52(1):5-14.
46. Guo H, Wu D, An J. Discrimination of oil slicks and look-alikes in polarimetric SAR images using CNN. *Sensors*. 2017;17(8):1837. doi: 10.3390/s17081837
47. Hidalgo MN, Gallego AJ, Gil P, Pertusa A. Two-stage convolutional neural network for ship and spill detection using SLAR images. *IEEE Trans Geosci Remote Sens*. 2018;56(9):5217-5230. doi: 10.1109/TGRS. 2018.2812619
48. Cantorna D, Dafonte C, Iglesias A, Arcay B. Oil spill segmentation in SAR images using convolutional neural networks. A comparative analysis with clustering and logistic regression algorithms. *Appl Soft Comput.* 2019;84:105716. doi: 10.1016/j.asoc.2019.105716
49. Zeng K, Wang Y. A deep convolutional neural network for oil spill detection from spaceborne SAR images. *Remote Sens.* 2020;12(6):1015. doi: 10.3390/rs12061015
50. Song D, Zhen Z, Wang B, *et al*. A novel marine oil spillage identification scheme based on convolution neural network feature extraction from fully polarimetric SAR imagery. *IEEE Access*. 2020;8:59801-59820. doi: 10.1109/ACCESS.2020.2979219
51. Kang J, Yang C, Yi J, Lee Y. Detection of marine oil spill from planetscope images using CNN and transformer models. J Mar Sci Eng. 2024;12:2095.
52. Hamza MS, Jauro SS, Ismail M. Oil spill detection using convolutional neural network. *Bima J Sci Technol.* 2023;7(4):15-30.

ACCSCIENCE PUBLISHING

Asian Journal of Water, Environment and Pollution. Vol. 22, No. 3 (2025), pp. 46-62.
doi: 10.36922/ajwep.8523

ORIGINAL RESEARCH ARTICLE

Variation in phytochemical and functional traits of *Suaeda monoica* across three sites in Jeddah, Saudi Arabia

Ameina S. Almoshadak*

Department of Biological Sciences, Faculty of Science, King Abdulaziz University Jeddah, Jeddah, Saudi Arabia
***Corresponding author**: Ameina S. Almoshadak (aalmashdaq@kau.edu.sa)

Received: January 13, 2025; 1st revised: January 16, 2025; 2nd revised: February 15, 2025; 3rd revised: February 25, 2025; Accepted: February 28, 2025; Published Online: April 28, 2025

Abstract: This study explores the intricate relationship between collection sites and the physiological responses of *Suaeda monoica* in Jeddah, focusing on photosynthetic pigment levels, osmomodulatory compounds, secondary metabolites, antioxidant potential, nutrient content, and heavy metal accumulation. Site (S)1 sample exhibited the highest chlorophylls a and b contents, whereas the S3 sample showed superior carotenoid levels. Osmoregulatory compounds demonstrated significant site-specific variations, with the S3 sample displaying elevated soluble sugar levels and the S1 sample showing heightened levels of soluble proteins and free amino acids. Secondary metabolites, encompassing phenols, flavonoids, alkaloids, and terpenoids, exhibited distinct accumulation patterns in samples across sites, with phenols being the most prevalent. In addition, the site samples' antioxidant potential (1,1-diphenyl-2-picrylhydrazyl activity and total antioxidant capacity) varied significantly, with the S1 sample displaying notable antioxidant capacity. The gas chromatography-mass spectrometry analysis of *S. monoica* leaf ethanolic extracts revealed significant qualitative and quantitative variances linked to the collection sites, revealing a rich diversity of chemical classes. Site-specific phytoconstituents, such as palmitic and nonanoic acids, and unique compounds, such as 2-thiazolamine, characterized the compositions at different sites, suggesting an environmental influence on phytochemical profiles. Furthermore, nitrogen and phosphorus levels varied significantly across sites and plant organs, with the S1 sample showing elevated nitrogen content in roots and phosphorus content in leaves. Heavy metal accumulation varied markedly between soil, roots, and leaves, emphasizing the phytoremediation potential of *S. monoica*. Collectively, these results illustrated the versatility and phytoremediation potential of *S. monoica* with its growth habitat.

Keywords: *Suaeda monoica*; Halophytes; Secondary metabolites; Osmotic adjustment; Antioxidative potential; Phytochemical composition; Phytoremediation

1. Introduction

Suaeda monoica Forssk. ex J. F. Gmel. (commonly known as sea blight) is a plant species predominant in coastal salt marshes belonging to the family Amaranthaceae.[1] This plant has an intriguing morphology, demonstrates adaptation to many environments, and possesses notable ecological and economic significance. *S. monoica* has garnered interest for its possible therapeutic effects and contribution to preserving coastal ecosystems.[1,2] The morphological structure of *S. monoica* enables it to flourish in many habitats, including salty and coastal ones. The plant is characterized by its succulent nature, featuring thick, fleshy green stems and leaves. The plant exhibits a prostrate or ascending growth habit, attaining a vertical height of 10 – 50 cm. The edible leaves

display an alternate arrangement, featuring a cylindrical form and frequently containing succulent traits.[3] The flowers of *S. monoica* are small and inconspicuous, usually exhibiting a greenish or reddish coloration. Significantly, S. *monoica* is a monoecious species with male and female flowers on the same plant.[4]

S. monoica is adapted to thrive in saline and coastal habitats characterized by high salinity levels, limited freshwater availability, and tidal influences. *S. monoica* has developed mechanisms to tolerate challenging conditions through its succulent leaves and stems. This versatility enables it to thrive and prevail in regions where plant species find it challenging to survive,[5] in addition to its role in the protection of shorelines from erosion. The distribution of *S. monoica* spans across different regions of the world. It is primarily found in coastal areas of Asian countries, including Saudi Arabia, India, Pakistan, Bangladesh, and Myanmar. In addition, it is also present in certain parts of Africa, such as Tunisia, Egypt, and Sudan.[6,7]

S. monoica has been reported to have potential applications in the field of phytoremediation.[8] It can tolerate high levels of toxic heavy metals, such as chromium, lead, nickel, copper, iron, and manganese,[8-10] thereby improving soil quality for subsequent agricultural activities. In addition, *S. monoica* was used to manufacture papers in India.[11] Apart from its ecological significance, *S. monoica* also exhibits promising medicinal properties, in which various parts of the plant, including leaves, stems, and seeds, are used in traditional remedies for treating ailments such as rheumatism, inflammation, paralysis, asthma, snake bites, skin diseases, ulcers, and gastrointestinal disorders.[12] The plant extracts have shown antimicrobial, antioxidant, antitumor, anti-inflammatory, antiviral, insecticidal, hepatoprotective, and wound healing properties, highlighting their potential for the development of new pharmaceuticals.[13-15] The medicinal significance of *S. monoica* is attributed to its diverse array of naturally occurring components, including proteins, phenols, tannins, resins, terpenoids, glycosides, flavonoids, fatty acids, sterols, and alkaloids.[7,16,17]

The primary objective of this study was to compare the levels of photosynthetic pigments, soluble sugars (SSs), proteins, and various secondary metabolites, including phenols, terpenoids, flavonoids, and alkaloids, in extracts from the leaves and roots of *S. monoica* collected from three different localities in Jeddah, Saudi Arabia. In addition, the research aimed to investigate how variations in collection sites influence the photochemical composition of the leaf ethanolic extracts and to assess the phytoremediation potential of the plant parts from these locations.

2. Materials and methods

2.1. Study area

In the present study, root and leaf samples of the *S. monoica* plant and soil samples were collected from three distinct localities across Jeddah, Saudi Arabia. The collection was performed during the summer (July) of 2023. The geographical coordinates of the collection sites are depicted in the provided map (Figure 1). These sites are designated as S1 (21.384489N, 39.198132E), S2 (21.240190N, 39.1441230E), and S3 (21.4972650N, 39.2196770E) (Figure 1). The weather data of the collection sites are provided in Table 1.

2.2. Plant and soil sample collection

Soil samples (collected from a depth of 0 – 30 cm) and samples of *S. monoica* roots and leaves (at the pre-flowering stage) were procured from each study site (15 plant samples per site) during the summer of 2023 (July–August). A voucher sample of *S. monocia* at each site was deposited at the Herbarium of the College of Sciences, King Abdulaziz University. The soil samples were taken using a hand auger as the designated sampling tool, dehydrated at 105°C for 3 days, and sieved through a 22 mm sieve. The samples were stored in paper bags until further analysis. The root and leaf samples were collected manually and kept in an icebox before being transferred to the laboratory. Subsequently, the plant samples were meticulously rinsed with distilled water to remove any remaining contaminants. After cleansing, a part of the leaf samples was immediately measured for leaf photosynthetic pigments. The residual leaf and root samples were air-dried in a shaded area for 5 days and subjected to a final drying procedure in an air-drying oven at 60°C until a stable weight was attained. The dried root and leaf samples were then finely ground into a powder and sieved through a 2 mm mesh to ensure uniform particle size and the removal of any larger debris or undesirable substances. To maintain the quality and integrity of the samples, they were securely stored in paper bags until further analysis.

2.3. Soil characterization analysis

The physical and chemical characteristics of the soil samples collected from the study locations were determined following the procedures outlined in the Association of Official Analytical Chemists[18] guidelines. The analyzed soil characteristics encompassed pH

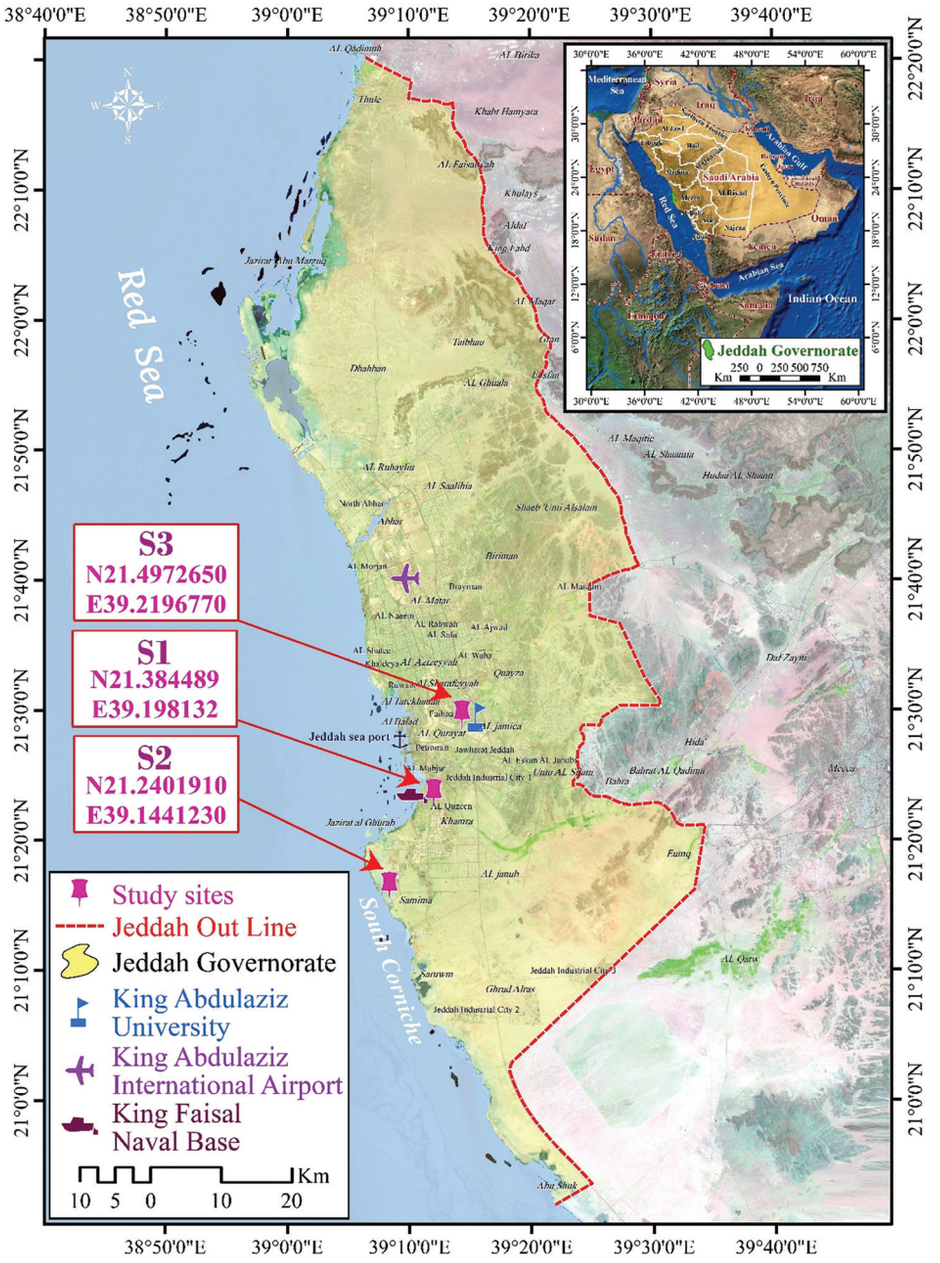

Figure 1. Satellite map of the study area. The map shows the sampling sites (S1 – S3) in Jeddah, Saudi Arabia.

Table 1. Weather data for the three collection sites in Jeddah during the summer of 2023

Site	Temperature (°C)			RH (%)	Rin (mm/month)	Eto (mm/month)
	T_{max}	T_{min}	Average			
Site 1	38.58	29.64	33.92	48.6	0.40	6.32
Site 2	38.65	29.81	33.99	48.5	0.34	5.65
Site 3	39.53	30.01	34.12	46.8	0.31	6.08

Abbreviations: Eto: Reference evapotranspiration; RH: Average relative humidity; Rin: Average precipitation; T_{max}: Maximum air temperature; T_{min}: Minimum air temperature.

levels, electrical conductivity (EC [mS/cm]), total dissolved solutes (TDS [mg/L]), organic matter (OM [%]), as well as various anions (phosphate, sulfate, nitrate, carbonate, and bicarbonate) and cations (sodium, potassium, calcium, and magnesium). The determined concentrations of anions and cations were expressed in milliequivalents per liter (meq/l), as detailed in Table 2.

2.4. Plant analyses

The leaf photosynthetic pigments were extracted using 85% cold acetone and subjected to centrifugation at 10,000 rpm for 10 min. Their optical densities were measured at 663, 644, and 452 nm. The quantification of each pigment (chlorophyll [Chl] a, Chl b, and carotenoids) was conducted following the methodologies delineated by Metzner *et al*.[19] and expressed in mg/g dry matter (DM).

The dried powdered *S. monoica* leaf and root samples were extracted in a borate buffer (pH 8.5) and filtered through a Whatman No. 1 filter paper to determine the total SS and protein content. The total content of SSs in the filtrates was quantified using the phenol-sulfuric acid method described by Dubois *et al*.[20] with glucose as a standard sugar and expressed as mg/g DM. The total soluble protein (SP) content was determined following Bradford,[21] employing bovine serum albumin as a protein standard. The absorbance at 595 nm was measured after mixing the extract or standard protein with the Coomassie brilliant blue G250 reagent, and the results were expressed in mg/g DM.

The amino acid content of *S. monoica* leaf and root samples was analyzed using the ninhydrin assay on the ethanolic extract, with glycine as a standard.[22] After the reaction mixture was boiled, cooled, and shaken well, the absorbance at 570 nm was used to calculate the amino acid content in mg/g DM.

Proline level was estimated using the method of Bates *et al*.[23] The plant materials were homogenized in 3% aqueous sulfosalicylic acid, and the supernatant from centrifugation was utilized for proline estimation. Proline concentration in mg/g DM was calculated using absorbance at 520 nm after the reaction mixture was extracted with toluene.

Total phenolic content was determined in the ethanolic extracts based on the technique outlined by Jindal and Singh.[24] After mixing the extract with Folin-Ciocalteu's reagent and sodium carbonate, the absorbance at 650 nm was used for phenols quantification (mg/g DM).

Flavonoid content was determined using the colorimetric aluminum chloride method.[25] Flavonoid quantification (mg/g DM) was performed at the absorbance of 417 nm using a quercetin calibration curve after mixing the ethanolic extract with aluminum chloride and potassium acetate.

Total alkaloid content was assessed (mg/g DM) by reacting bromocresol green with alkaloids in the ethanolic extracts,[26] using atropine as the reference alkaloid.

Table 2. Physical and chemical characteristics of the soil samples collected during July 2023 from three different localities at Jeddah

Parameters	Site 1	Site 2	Site 3	Fisher's test	*p*-value	LSD
pH	7.47±0.05^{a}	7.17±0.02^{b}	7.06±0.06^{c}	95.65	0.0000	0.076
Electrical conductivity (mS/cm)	2.93±0.10^{a}	2.73±0.07^{b}	0.53±0.02^{c}	1001.21	0.0000	0.146
Total dissolved solutes (mg/L)	4052±25.4^{a}	3623±11.7^{b}	2185±9.2^{c}	35635.7	0.0000	17.93
Organic matter (%)	1.5±0.05^{a}	0.45±0.02^{b}	1.65±0.04^{a}	69.011	0.0001	0.312
Phosphate (meq/L)	1.02±0.02^{ab}	0.79±0.01^{b}	1.08±0.08^{a}	5.616	0.0422	0.164
Sulfate (meq/L)	18.0±0.9^{b}	5.5±0.5^{c}	20.3±1.0^{a}	328.49	0.0000	1.532
Nitrate (meq/L)	1.40±0.08^{c}	2.44±0.06^{b}	3.85±0.12^{a}	201.202	0.0000	0.302
Sodium (meq/L)	13.75±0.57^{a}	12.47±0.73^{b}	5.18±0.27^{c}	555.094	0.0000	0.693
Potassium (meq/L)	0.29±0.01^{a}	0.21±0.01^{b}	0.38±0.02^{a}	9.583	0.0136	0.139
Magnesium (meq/L)	8.56±0.61^{b}	5.78±0.37^{c}	13.57±0.83^{a}	6005.78	0.0000	0.175
Calcium (meq/L)	0.37±0.00^{b}	0.28±0.00^{b}	0.67±0.01^{a}	19.801	0.0023	0.188
Carbonate (meq/L)	ND	ND	ND	-	-	-
Bicarbonate (meq/L)	1.69±0.08^{c}	3.05±0.10^{a}	1.79±0.03^{b}	1922.53	0.0000	0.059

Notes: ^{a,b,c}Different letters in the same row represent significant variations at a 5% level. Sites having different letters indicate significant differences in the parameters measured, whereas the same letters indicate no significant differences in the parameters measured.
Abbreviations: LSD: Least significant difference; meq: milliequivalents; ND: Not detected; *p*: Probability.

The total terpenoid content of *S. monoica* (mg/g DM) was estimated by reacting the extracts with chloroform, adding concentrated sulfuric acid, incubating, and measuring absorbance at 532 nm, with linalool used as a standard terpenoid.[27]

2.5. Antioxidant activity of root and shoot extracts

The electron-donating activity of *S. monoica* extracted with ethanol was determined by assessing its ability to bleach the purple color of the 1,1-diphenyl-2-picrylhydrazyl (DPPH).[28] A 0.1 mL extract sample was added to 3.9 mL of a 36 mg DPPH-methanol solution. After a 60-min dark incubation, the absorbance was measured at 515 nm relative to a blank. The decrease in the DPPH free radical was quantified as a percentage (%).

The total antioxidant capacity (TAC) of *S. monoica* ethanolic extracts was quantified using the procedure by Ahmed *et al*.[29] A mixture of 3 mL phosphomolybdate reagent, and 300 µL of the ethanolic extract or standard ascorbic acid was incubated at 95°C for 90 min. After cooling, the absorbance was recorded at 765 nm, and the TAC was expressed in µg ascorbic acid equivalent (AAE)/g DM.

2.6. Phytochemical active constituents of *S. monoica* leaf extracts using gas chromatography-mass spectrometry

To determine the phytochemical composition of the leaf extracts of *S. monoica* collected from the study sites in Jeddah, a Clarus 580/560S mass spectrometer (PerkinElmer, United States) was utilized. The chromatographic column employed for separation was an Elite-5MS with a length of 30 m length, an internal diameter of 0.25 mm, and a film thickness of 0.25 µm. The temperature program for the oven was meticulously controlled: initially set at 35°C, ramped up at a rate of 8°C/min to 150°C with a 3-min hold time, and subsequently increased at a rate of 10°C/min to reach 280°C. Inlet and transfer lines were kept at 250°C. Helium was used as the carrier gas at 1 mL/min. To inject 1 µL aliquots from diluted samples, the Autosampler AS3000 (Thermo Fisher Scientific, United States) was used in split mode with a solvent delay of 3 min. In full scan mode, a 70 eV ionization voltage was used to capture the mass spectrum from 40 to 650 m/z. Flame ionization detection identified the components after chromatographic separation. Their spectra were rigorously examined against the recognized National Institute of Standards and Technology's Mass Spectrometry 2.0 structural database compounds to determine their identities, molecular weights, and other attributes.

2.7. Mineral analysis of plant and soil samples

The root and leaf powders, alongside the soil samples collected, underwent wet digestion procedures utilizing a mixture of 65% nitric acid and 30% hydrogen peroxide (5:2 v/v). Digestion vessels were subjected to heating in a sand bath on a hot plate, reaching temperatures between 95°C and 135°C until the solutions were clear.[30] Post-cooling, the clear solutions were filtered, transferred into volumetric flasks, and diluted to their final volumes using deionized water. The concentrations of the selected heavy metal ions (aluminum [Al], cadmium [Cd], cobalt [C], chromium [Cr], copper [Cu], nickel [Ni], lead [Pb], and zinc [Zn]) within the digested samples were quantified utilizing inductively coupled plasma-optical emission spectroscopy (Polyscan 61E, Thermo Jarrell-Ash Corp., United States).

2.8. Statistical analysis

All analyses were conducted in triplicate, and the results were presented as the mean of three replicates ± the standard deviation. Statistical analysis was performed using a one-way analysis of variance to separate means, with the least significant difference *post hoc* test utilized at a significance threshold of $p \leq 0.05$. The statistical software Statistical Package for Social Sciences version 19.0 was utilized to conduct all statistical assessments of the obtained data. Using the Origin software (SPSS version 19.0), the Pearson correlation coefficients were employed to determine the level and type of the relationship between each pair of determined attributes.

3. Results and discussion

3.1. Physical and chemical soil properties of the study sites

The data in Table 2 delineates the variation in the physical and chemical properties among the three investigated soil sites where *S. monoica* was collected. Statistically, all studied parameters varied significantly ($p<0.05$) across the collection sites. The obtained data revealed that site S1 exhibited the highest pH (7.47), EC (2.93 mS/cm), and TDS (4,052 mg/L) among the sites. Conversely, the soil at site S3 demonstrated a propensity toward neutrality (pH 7.06) with lower salinity levels (EC, 0.53 mS/cm) and TDS (2,185 mg/L). Notably, OM was most abundant at site S3 (1.65%) and lowest at site S2 (0.45%).

Regarding mineral composition, site S3 surpassed the other sites in phosphate, sulfate, nitrate, potassium, magnesium, and calcium content (1.08, 20.3, 3.85, 0.38, 13.57, and 0.67 meq/L, respectively). Sodium concentration was highest at site S1 (13.75 meq/L), whereas bicarbonate levels peaked at site S2 (3.05 meq/L). Interestingly, carbonate anion was undetected across all study sites. Overall, soil analysis indicated that site S3 was the most favorable for optimal crop growth due to its physical attributes, low salinity, and abundance of essential nutrients required for plant growth and development.

3.2. Photosynthetic pigments in *S. monoica* leaves

The impact of the collection site on photosynthetic pigment levels in *S. monoica* leaves from the study sites is detailed in Table 3. Statistical analysis revealed that Chl a and carotenoids exhibited highly significant increases ($p<0.01$) in response to collection sites, whereas Chl b was significantly affected ($p<0.05$) by site. Leaves from site S1 exhibited the highest Chl a and Chl b contents (0.60 and 0.37 mg/g DM, respectively). In contrast, those from S3 showed the highest carotenoid content (0.74 mg/g DM), which was relatively close to that of carotenoids of leaves collected from S1 (0.71 mg/g DM). The findings suggest that S1 fostered optimal growth conditions for *S. monoica* due to its elevated Chl levels, reinforcing the halophytic nature of the plant, which thrives in saline environments. The results also support the hypothesis that plants of the same species exhibit diverse responses to salinity through quantitative and qualitative variations in their adaptive mechanisms.[31]

The observed differences in photosynthetic pigment levels between sites could be attributed to environmental factors and genetic variability. Environmental conditions such as salinity, nutrient availability, light intensity, and temperature can influence photosynthetic pigment biosynthesis.[32,33] Therefore, higher salinity at site S3 may have triggered the accumulation of carotenoids as a protective mechanism against oxidative stress. The relatively lower salinity at site S1 may have favored Chl synthesis. Genetic differences among *S. monoica* populations at the investigated sites could also contribute to the observed variations, as genetic diversity often underlies differential stress responses in halophytes.[44]

Previous studies have demonstrated varying Chl responses in halophytes under saline conditions, with some species showing enhanced Chl levels in correlation with salt concentration, whereas others exhibit no significant changes.[34] The increased Chl content in *S. monoica* at site S1 in response to salinity can be attributed to enhanced energy production for stress management, growth promotion, osmotic stress mitigation, oxidative damage protection, and overall performance optimization in high-salinity conditions.[32,33] Moreover, the heightened carotenoid levels at the most saline site (S3) suggest that increasing carotenoid concentrations may serve as a strategy to maintain Chl levels rather than diminishing them across varying salinity levels.[37] This aligns with the studies associating elevated carotenoid levels with increased salt tolerance in some plant species.[35,38]

3.3. Osmomodulatory compounds in *S. monoica* roots and leaves

The levels of osmomodulatory compounds, including SSs, SPs, free amino acids (FAA), and free proline (FP), in *S. monoica* roots and leaves in response to the collection sites are delineated in Table 4. Statistically, the difference in collection sites had a highly significant impact ($p<0.01$) on the levels of all osmoregulatory molecules measured in both the roots and leaves of

Table 3. Photosynthetic pigments in the leaves of *Suaeda monoica*

Site	Chlorophyll a (mg/g DM)	Chlorophyll b (mg/g DM)	Carotenoids (mg/g DM)
Site 1	0.60±0.01[a]	0.37±0.00[a]	0.71±0.02[b]
Site 2	0.50±0.00[b]	0.30±0.00[b]	0.61±0.03[c]
Site 3	0.41±0.01[c]	0.30±0.01[b]	0.74±0.02[a]
Source of variation			
Fisher's test	100.96	6.017	57.576
Probability	0.0000	0.0368	0.0001
Least significant difference	0.033	0.261	0.0339

Notes: [a,b,c]The different letters in the same column represent significant variations at a 5% level. Sites having different letters indicate significant differences in the parameters measured, whereas the same letters indicate no significant differences in the parameters measured.
Abbreviation: DM: Dry matter.

Table 4. Osmomodulatory compounds level in the root and leaf samples of *Suaeda monoica*

Organ	Soluble sugars (mg/g DM)	Soluble proteins (mg/g DM)	Free amino acids (mg/g DM)	Free proline (mg/g DM)
Root Site 1	45.45±4.85[a]	6.43±0.10[c]	10.78±2.07[b]	1.18±0.09[d]
Root Site 2	32.55±2.47[b]	6.38±0.24[c]	9.74±1.38[c]	0.97±0.11[d]
Root Site 3	49.69±0.42[a]	5.27±0.33[d]	7.74±0.92[d]	3.72±0.19[a]
Leaves Site 1	37.75±0.63[b]	14.06±0.09[a]	13.59±0.52[a]	2.65±0.04[b]
Leaves Site 2	45.26±1.85[a]	12.19±0.12[b]	6.28±1.11[e]	2.77±0.11[b]
Leaves Site 3	46.68±4.95[a]	12.24±0.35[b]	5.31±0.83[f]	2.29±0.18[c]
Source of variation				
Fisher's test	12.775	799.654	292.516	190.942
Probability	0.0002	0.0000	0.0000	0.0000
Least significant difference	5.534	0.4149	0.559	0.231

Notes: [a,b,c]The different letters in the same column represent significant variations at a 5% level. Sites having different letters indicate significant differences in the parameters measured, whereas the same letters indicate no significant differences in the parameters measured.
Abbreviation: DM: Dry matter.

S. monoica. Overall, SS exhibited the highest levels among the measured compounds in leaf and root samples across the investigated sites, with FP being documented as the least abundant osmoregulatory molecule.

The results indicated that SS levels were significantly higher in the roots and leaves of *S. monoica* from site S3 than in the other sites (49.69 and 46.68 mg/g DM, respectively). In contrast, the lowest levels were observed in the roots of site S2 and the leaves of site S1. Nevertheless, the roots and leaves of *S. monoica* collected from site S1 displayed the highest levels of SP and FAA among the sites. Specifically, SP levels were recorded at 6.43 and 14.06 mg/g DM in roots and leaves, respectively, whereas FAA levels were measured at 10.78 and 13.59 mg/g DM in roots and leaves, respectively. Roots and leaves from site S3 exhibited the lowest accumulation of FAA, with the least SP accumulation observed in the roots of *S. monoica* at site S3 and the leaves of site S2. In contrast to SP, the highest levels of FP were documented in the roots of *S. monoica* from site S3 and in the leaves collected from site S2 (3.72 and 2.77 mg/g DM, respectively). Meanwhile, the roots of *S. monoica* at site S2 and the leaves at site S3 accumulated the lowest levels of FP.

These findings revealed *S. monoica* as a resilient halophytic plant species that uses adaptation tactics to accumulate osmoregulatory chemicals to live in harsh environmental conditions. Haque *et al*.[39] revealed that *S. monoica*'s photosynthetic capacity can be boosted under specific conditions, resulting in a higher accumulation of carbon and nitrogen molecules and the ability to efficiently overcome tough settings. These findings align with the reports of Joshi *et al*.,[8] who found that *S. monoica* predominantly accumulates SS, SP, and FP as organic compounds to combat harsh environmental challenges. This implies that this species likely utilizes a variety of organic solutes concurrently for osmoregulation and osmoprotection, with the varying significance of each potentially linked, at least partially, to enhanced biosynthesis or reduced catabolism mechanisms within individual species.[40] These results are corroborated by the observation that halophytes concentrate and redistribute low molecular weight organic solutes across distinct subcellular.[38,39,42,43] In addition, osmolytes such as FP and SS have been identified as pivotal factors in osmotic adjustment in certain *Suaeda* species.[44] These osmolytes could regulate the overall metabolic pool through alterations in the expression of signaling proteins and biosynthetic enzymes related to stress-responsive genes.[45]

The variation in osmomodulatory compounds between sites likely reflects the interplay between environmental stressors and genetic adaptations. For example, the higher accumulation of SSs in site S3 samples may be a response to increased salinity, as sugars play a crucial role in osmotic adjustment and stress protection.[41] Similarly, the elevated levels of FP in site S2 samples could indicate a site-specific stress response, as proline is known to accumulate under drought and salinity stress.[48] However, without detailed data on soil composition, water availability, and genetic differences among the *S. monoica* populations at each

site, it is difficult to determine the precise mechanism of these variations. Future investigations should focus on characterizing these factors to better understand the mechanisms underlying the observed differences.

3.4. Secondary metabolites in *S. monoica* roots and leaves

The data presented in Table 5 illustrate the abundance patterns of secondary metabolites measured in the roots and leaves of *S. monoica*. Statistical analyses indicated that the variation in the concentrations of phenols, flavonoids, alkaloids, and terpenoids was highly significant ($p<0.01$), influenced by the collection site and the plant organ ($p<0.05$). Among the secondary metabolites evaluated, phenols emerged as the most abundant, whereas flavonoids were the least prevalent in both the roots and leaves across all sites examined.

Specifically, the roots of *S. monoica* growing at site S1 exhibited the highest concentrations of phenols, flavonoids, and alkaloids (8.77, 0.45, and 2.60 mg/g DM, respectively). In contrast, the roots from site S3 demonstrated the highest accumulation of terpenoids (0.836 mg/g DM). In the leaves, plants from site S1 accumulated greater amounts of phenols and alkaloids (27.81 and 3.05 mg/g DM, respectively). Meanwhile, leaves from site S3 showed higher levels of flavonoids and terpenoids (0.68 and 1.036 mg/g DM, respectively). Overall, it was observed that collection sites with elevated salinity levels (S1) corresponded with increased accumulation of secondary metabolites in both roots and leaves, likely as a physiological response enabling the plants to better withstand environmental stress.

Research has demonstrated that environmental factors may impact the synthesis of secondary compounds in plant tissues. According to Tuteja and Sopory,[46] plants modify their metabolic profile following the changing seasons and fluctuations in light conditions, carbon dioxide levels, availability of water and nutrients, and temperature. Secondary metabolites influence plant self-defense and anxiety adaptability, functioning as regulatory factors and antioxidants while exhibiting distinctive dietary and curative effects.[47] In addition, these compounds are involved in various biochemical processes, such as activating enzymes, eliminating reactive oxygen species (ROS), regulating signaling, and mitigating phototoxicity.[49]

Phenols are precursors of lignin, which is a critical stress defense mechanism, particularly in roots. They can regulate the makeup and rigidness of the cell wall in response to stressful situations.[50] Furthermore, phenolics and carotenoids defend against ultraviolet irradiation, whereas glucosinolates and alkaloids are significant feeding barriers against herbivory, and some terpenoids can function as semiotic or signaling compounds.[46,47] The preservation of the lipid phase in thylakoid membranes is a mechanism in which terpenoids and their derivatives alleviate heat stress.[53] Thus, the findings of this study corroborate the hypothesis that the roots and leaves of *S. monoica* develop considerable quantities of anti-stress secondary metabolites to survive the adverse conditions of their growing environments, especially at site S1.

Table 5. Secondary metabolites level in the root and leaf samples of *Suaeda monoica*

Organ	Phenols (mg/g DM)	Flavonoids (mg/g DM)	Alkaloids (mg/g DM)	Terpenoids (mg/g DM)
Root Site 1	8.77±0.15^{d}	0.45±0.02^{b}	2.60±0.101^{ab}	0.711±0.088^{c}
Root Site 2	6.93±0.48^{d}	0.41±0.07^{b}	1.70±0.091^{bc}	0.828±0.064^{bc}
Root Site 3	4.66±0.35^{e}	0.15±0.02^{c}	0.90±0.085^{c}	0.836±0.055^{bc}
Leaves Site 1	27.81±2.51^{a}	0.31±0.02^{bc}	3.05±0.023^{a}	0.858±0.115^{b}
Leaves Site 2	23.86±0.95^{b}	0.25±0.12^{bc}	2.40±0.112^{ab}	0.914±0.086^{ab}
Leaves Site 3	15.55±0.69^{c}	0.68±0.16^{a}	2.50±0.098^{a}	1.036±0.073^{a}
Source of variation				
Fisher's test	202.642	8.642	5.3720	5.116
Probability	0.0000	0.0103	0.0080	0 0.0096
Least significant difference	2.0598	0.216	1.249	0.1462

Notes: ^{a,b,c}The different letters in the same column represent significant variations at a 5% level. Sites having different letters indicate significant differences in the parameters measured, whereas the same letters indicate no significant differences in the parameters measured.

Abbreviation: DM: Dry matter.

The observed differences in secondary metabolite accumulation between sites may be driven by environmental factors, such as soil salinity, nutrient availability, and climatic conditions, as well as genetic variability among *S. monoica* populations. For instance, the higher accumulation of phenols and alkaloids in site S1 samples could be a response to specific stressors such as high salinity or oxidative stress, as these compounds are known to play protective roles under such conditions.[51,52,57] However, the genetic profile of these plants at each site could potentially cause significant differences in secondary metabolite composition.

3.5. Antioxidative potential of *S. monoica* roots and leaves

Table 6 presents the antioxidant potential of *S. monoica* root and leaf extracts collected from different sites in Jeddah, as determined by the DPPH radical scavenging activity and the TAC. The DPPH activity was significantly impacted by the collection site and the plant organ ($p<0.05$), whereas the TAC of the extracts was significantly affected ($p<0.01$). The root extract of *S. monoica* at site S2 and the leaf extract of site S3 exhibited the highest DPPH activity (83.09% and 87.80%, respectively). However, the TAC of the root and leaf extracts of *S. monoica* at site S1 was the most significant compared to the other sampling sites (60.79 and 82.59 μg AAE/g DM, respectively). The TAC of the root and leaf extracts at site S1 suggests that subjecting *S. monoica* to challenging conditions enhances its ability to produce antioxidant molecules as a survival mechanism in harsh conditions.

Table 6. Antioxidative potential of the root and leaf extracts of *Suaeda monoica*

Organ	DPPH activity (%)	TAC (μg AAE/g DM)
Root Site 1	80.46±4.44^{b}	60.79±0.93^{c}
Root Site 2	83.09±2.22^{ab}	53.69±0.66^{d}
Root Site 3	72.97±5.25^{c}	60.25±0.40^{c}
Leaves Site 1	82.33±4.27^{ab}	82.59±0.21^{a}
Leaves Site 2	82.54±4.20^{ab}	81.53±0.04^{a}
Leaves Site 3	87.80±0.12^{a}	72.85±1.60^{b}
Source of variation		
Fisher's test	4.813	649.595
Probability	0.0120	0.0000
Least significant difference	6.817	0.6781

Notes: ^{a,b,c}The different letters in the same column represent significant variations at a 5% level. Sites having different letters indicate significant differences in the parameters measured, whereas the same letters indicate no significant differences in the parameters measured.
Abbreviations: AAE: Ascorbic acid equivalent; DM: Dry matter; DPPH: 1,1-diphenyl-2-picrylhydrazyl; TAC: Total antioxidant capacity.

The high concentration of secondary metabolites in the roots and leaves of *S. monoica* contributes to the high antioxidant potential of their extracts, particularly at site S1. As stated by Kranner *et al*.,[54] the activation of mechanisms that protect and repair cells, such as the antioxidant defense system, occurs rapidly following cellular stress. This activation may explain the significant rise in antioxidant capacity. Boestfleisch *et al*.[55] suggested that increasing light intensities and salt levels enhance the antioxidant capacity of halophytic species. Furthermore, the higher antioxidant activity of the extracts from the roots and leaves may be attributed to the high concentration of phenols, flavonoids, and terpenoids in *S. monoica*. Given that phenolics, flavonoids, and terpenoids are potent antioxidants, the enhanced antioxidant activity of the extracts is likely due to their elevated levels.[56]

The differences in antioxidant potential between the study sites may reflect variations in environmental effectors and genetic architecture among *S. monoica* populations. The higher antioxidant capacity in the site S1 sample could be a response to elevated oxidative stress for mitigating the damaging ROS.[62] However, without detailed data on the environmental conditions and genetic profiles of the plants at each site, it is difficult to definitively attribute the differences in antioxidant potential to specific factors.

3.6. Phytochemical composition of *S. monoica* leaf extracts

The GC-MS analysis of the phytochemical constituents in the ethanolic extracts derived from *S. monoica* leaves exhibited significant qualitative and quantitative differences based on the specific collection site (Table 7). The leaf extracts exhibited a diverse array of chemical classes, encompassing sesquiterpenes, phenols, hydrocarbons, amino acids, aldehydes, amines, fatty acids, alkaloids, diterpenes, glycosides, esters, and silicate derivatives. Notably, the principal active phytoconstituents identified in *S. monoica* extract collected from site S1 included palmitic acid, tau-muurolol, nonanoic acid, and δ-amorphene (24.13%, 10.14%, 10.09%, and 9.09%, respectively). On the other hand, the predominant phytoconstituents in the plant extract collected from site S2 displayed a distinct composition, with nonanoic acid, palmitic

Table 7. Gas chromatography-mass spectrometry analysis of the phytochemical compositions of *Suaeda monoica* ethanol extract

Pk#	RT (minutes)	Compound name	Area %			Formula	Chemical class
			Site 1	Site 2	Site 3		
1	6.544	δ-Amorphene	9.09	5.61	3.00	$C_{15}H_{24}$	Sesquiterpene
2	7.159	1,1-diphenyl-4-phenylthiobut-3-en-1-ol	0.65	2.28	-	$C_{22}H_{20}OS$	Phenol
3	7.369	2-(1,3-dioxolan-2-yl) furan	3.73	8.27	5.91	$C_8H_{10}O_4$	Hydrocarbon
4	8.855	γ-aminobutyric acid	3.17	5.21	8.74	$C_4H_9NO_2$	Amino acid
5	10.671	(-)-Spathulenol	0.97	1.75	1.13	$C_{15}H_{24}O$	Sesquiterpene
6	11.301	2,6-nonadienal, 3,7-dimethyl-	4.56	7.85	-	$C_{11}H_{18}O$	Aldehyde
7	11.466	2-thiazolamine, 4-(3,4-dimethoxyphenyl)-5-methyl-	-	2.24	-	$C_{12}H_{14}N_2O_2S$	Amine
8	11.651	Nonanoic acid	10.09	25.85	16.58	$C_9H_{18}O_2$	Fatty acid
9	12.826	Quinazoline, 4-(methylthio)-2-phenyl-	4.97	2.94	0.94	$C_{17}H_{16}N_2OS$	Alkaloid
10	13.327	Amiphenazole	1.00	0.72	-	$C_9H_9N_3S$	Alkaloid
11	13.877	Cubenol	1.53	0.97	0.82	$C_{15}H_{26}O$	Sesquiterpene
12	14.262	tau-Muurolol	10.14	2.55	3.93	$C_{15}H_{26}O$	Sesquiterpene
13	16.093	4-bromo-2-thiaadamantane	3.22	1.13	0.92	$C_{17}H_{21}Br$	Hydrocarbons
14	17.063	7-Tetracyclo[6.2.1.0 (3.8) 0 (3.9)] undecanol, 4,4,11, 11-tetramethyl-	1.00	0.78	3.80	$C_{15}H_{24}O$	Sesquiterpene
15	17.623	Myristic acid	2.38	1.16	-	$C_{14}H_{28}O_2$	Fatty acid
16	17.998	1,4-naphthoquinone, 6-ethyl-2,3,5,7-tetrahydroxy-	-	2.38	4.10	$C_{12}H_{10}O_6$	Phenol
17	18.669	Phytol	3.56	4.62	4.47	$C_{20}H_{40}O$	Diterpene
18	19.684	16-octadecenal	0.80	3.28	1.78	$C_{18}H_{34}O$	Fatty aldehyde
19	21.490	Cinnamic acid, p-(trimethylsiloxy)-, methyl ester	3.39	1.89	-	$C_{13}H_{18}O_3Si$	Phenol
20	21.805	Palmitic acid	24.13	12.78	17.69	$C_{16}H_{32}O_2$	Fatty acid
21	22.010	Digitoxin	0.78	0.58	1.97	$C_{41}H_{64}O_{13}$	Glycoside
22	23.596	9,12-octadecadienoyl chloride, (Z, Z)-	2.43	-	6.95	$C_{18}H_{31}ClO$	Fatty acids
23	24.081	Arachidic acid	2.16	0.57	2.33	$C_{20}H_{40}O_2$	Fatty acid
24	25.932	Cyclobarbital	3.57	2.09	2.82	$C_{12}H_{16}N_2O_3$	Alkaloid
25	29.773	trans-4-(2-(5-nitro-2-furyl) vinyl)-2-quinolinamine	-	-	5.74	$C_{15}H_{11}N_3O_3$	Alkaloid
26	30.814	Phthalic acid, 2-ethylhexyl isohexyl ester	4.77	-	1.80	$C_{22}H_{34}O_4$	Organic acid
27	34.175	Silicic acid, diethyl bis (trimethylsilyl) ester	-	-	3.01	$C_{10}H_{28}O_4Si_3$	Silicate ester
28	37.136	1,2-Benzisothiazol-3-amine	-	-	1.25	$C_7H_6N_2S$	Alkaloid

Abbreviations: Pk#: Peak number, RT: Retention time.

acid, 2-(1,3-dioxolan-2-yl)furan, and 2,6-nonadienal, 3,7-dimethyl identified as the most abundant compounds (25.85%, 12.78%, 8.27%, and 7.85%, respectively). However, site S3 sample showed a prevalence of palmitic acid, nonanoic acid, γ-aminobutyric acid, and 9,12-octadecadienoyl chloride as the prominent compounds (17.69%, 16.58%, 8.74%, and 6.95%, respectively).

Site S2 sample was characterized by 2-thiazolamine, 4-(3,4-dimethoxyphenyl)-5-methyl as an exclusive component unique to this site. Conversely, site S3 sample was characterized by three distinct compounds

trans-4-(2-(5-nitro-2-furyl)vinyl)-2-quinolinamine, silicic acid, diethyl bis(trimethylsilyl) ester, and 1,2-benzisothiazol-3-amine. The findings also indicated the absence of 1,4-naphthoquinone, 6-ethyl-2,3,5,7-tetrahydroxy from site S1, 9,12-octadecadienoyl chloride (Z,Z) from site S2 sample, as well as the absence of 1,1-diphenyl-4-phenylthiobut-3-en-1-ol, 2,6-nonadienal, 3,7-dimethyl, amiphenazole, myristic acid, and cinnamic acid, p-(trimethylsiloxy)-, methyl ester from the plants collected from site S3. In addition, the quantities of the common compounds exhibited quantitative variations in *S. monoica* leaf extracts in response to the difference in the collection site. The observed chemical polymorphism in *S. monoica* leaf extracts might be attributed to genetic diversity and the varying ambient environmental conditions. The presence of unique compounds at specific sites (e.g., 2-thiazolamine in site S2 sample and trans-4-(2-(5-nitro-2-furyl)vinyl)-2-quinolinamine in site S3 sample) may reflect site-specific adaptations to environmental stressors.

The findings of this study underscore the pronounced variability exhibited by *S. monoica*, a variability contingent upon the specific site of collection. This observed chemical polymorphism likely arises from genetic diversity, potentially intertwined with the heterogeneous environmental conditions in Saudi Arabia, encompassing factors such as humidity levels, thermal fluctuations, and soil composition. Some species inhabit specific ecological niches that are highly sensitive to climate changes, significantly affecting their phytochemical composition.[36,58] In a study by Roy and Dutta,[3] an analysis of *S. monoica* extract unveiled a spectrum of phytochemical classes, including amines, ketones, esters, fatty acids, phytol, phenols, hydrocarbons, and heterocyclic compounds, mirroring the diversity observed in our investigation. Their findings corroborated the presence of nonanoic acid, myristic acid, phytol, cinnamic acid, and palmitic acid within the leaf extract of *S. monoica*. These compounds have been recognized for their pharmacological characteristics, encompassing antifungal, antibacterial, antitumor, antioxidant, nematocidal, antiandrogenic, and hypocholesterolemic properties.[3,53,54]

Moreover, consistent with our results, a prior investigation on the phytochemical profile of *S. monoica* growing in Saudi Arabia affirmed the prevalence of sesquiterpenes, renowned for their notable wound-healing capabilities.[16] Additional screenings of *S. monoica* extracts have unveiled a diverse array of phytochemical compounds such as glycosides, terpenoids, phenols,[17] sterols, amino acids,[59] and a spectrum of fatty acids, including myristic, pentadecanoic, palmitic, nonadecanoic, arachidic, linoleic, and linolenic acids,[61] as well as triterpenoids and sterols.[63]

3.7. Nitrogen and phosphorus levels in *S. monoica* roots and leaves and collection sites

Table 8 provides an overview of the total nitrogen and phosphorus levels in the collection sites and the roots and leaves of *S. monoica* across the three different collection sites. The nitrogen content exhibited a highly significant variation ($p<0.01$), whereas the phosphorus content showed significant variation ($p<0.05$) in response to both the plant organ and the collection site. The present investigation demonstrated that nitrogen was significantly accumulated in the roots of *S. monoica* at site S1 (15.37 mg/g DM), the leaves of site S2 (9.16 mg/g DM), and the soil of site S3 (4.81 mg/g DM) compared to the corresponding samples. The roots of site S1 possessed a higher phosphorus content (1.19 mg/g DM), whereas the leaves and soil of site S3 exhibited the highest phosphorus levels (0.79 and 0.94 mg/g DM, respectively) compared to their counterparts in this study.

As a halophyte, *S. monoica* shows remarkable adaptations to survive in extreme environments. Its nutrient acquisition techniques can be better understood

Table 8. Nitrogen and phosphorus levels in the soil, root, and leaf samples of *Suaeda monoica*

Sample	Nitrogen (mg/g DM)	Phosphorus (mg/g DM)
Soil Site 1	1.75 ± 0.27^{f}	0.88 ± 0.04^{bc}
Soil Site 2	4.30 ± 0.20^{de}	0.69 ± 0.13^{c}
Soil Site 3	4.81 ± 0.37^{d}	0.94 ± 0.10^{b}
Root Site 1	15.37 ± 1.07^{a}	1.19 ± 0.01^{a}
Root Site 2	6.52 ± 1.26^{c}	0.92 ± 0.01^{b}
Root Site 3	1.02 ± 0.13^{f}	0.86 ± 0.08^{bc}
Leaves Site 1	3.71 ± 0.26^{e}	0.82 ± 0.14^{bc}
Leaves Site 2	9.16 ± 0.53^{b}	0.92 ± 0.11^{b}
Leaves Site 3	4.43 ± 0.32^{de}	0.97 ± 0.09^{b}
Source of variation		
Fisher's test	148.993	4.269
Probability	0.0000	0.0221
Least significant difference	1.061	0.206

Note: ^{a,b,c,d,e,f}The different letters in the same column represent significant variations at a 5% level.
Abbreviation: DM: Dry matter.

by analyzing the nitrogen and phosphorus content in its roots and leaves. Phosphorus is required for energy transmission, cell division, and root development, whereas nitrogen influences protein synthesis and photosynthesis – two of the most important processes in plant growth. In *S. monoica*, nitrogen and phosphorus distribution may vary between roots and leaves based on their functions. Roots typically contain higher phosphorus concentrations, as they are vital for energy storage and uptake from the soil. Phosphorus in leaves could be lower but strategically located for efficient energy utilization. *Suaeda* species can modify their growth rhythm and adjust their capacity to absorb and utilize phosphorus to adapt to nitrogen-loaded environments.[64] Furthermore, *Suaeda* plays a crucial role in the cycling of biogenic elements, especially phosphorus, by absorbing external nitrogen from both terrestrial sources and the atmosphere, impacting the composition and activity of soil microbes.[57,58,65] This reflects the influence of environmental conditions and variations in plant nutrient uptake efficiency. The higher nitrogen content in the roots at site S1 could be caused by elevated soil nitrogen levels or enhanced nitrogen uptake efficiency under saline conditions. Thus, analyzing nitrogen and phosphorus content in *S. monoica* growth habitat, roots, and leaves can shed light on its nutrient utilization efficiency and adaptations to saline environments, offering valuable insights into its survival strategies.

3.8. Phytoremediation potential of *S. monoica* at different collection sites

The concentrations of heavy metals in the growth habitat, roots, and leaves of *S. monoica* at three different sites in Jeddah are detailed in Table 9. A highly significant ($p<0.01$) difference in the distribution of heavy metals was observed between the soil, roots, and leaves of *S. monoica* at the sites under investigation. Across all three sites, the soil samples exhibited notably higher metal concentrations, with the order of concentration being Al > Cd > Co > Pb > Ni > Cu > Cr > Zn. Specifically, soil samples from site S3 displayed higher levels of Al, Cd, Co, Cr, and Ni (28.79, 24.79, 21.83, 0.30, and 2.04 mg/g DM, respectively), whereas site S1 sample showed higher levels of Cu, Pb, and Zn (0.75, 3.12, and 0.28 mg/g DM, respectively).

The roots of plants at site S1 demonstrated a greater capacity to accumulate higher concentrations of Al, Cd, Cr, Cu, Pb, and Zn (0.67, 0.45, 0.09, 0.13, 2.15, and 5.00 mg/g DM, respectively) compared to roots at

Table 9. Accumulation of heavy metals in the soil, root, and leaf samples of *Suaeda monoica*

Sample	Aluminium (mg/g DM)	Cadmium (mg/g DM)	Cobalt (mg/g DM)	Chromium (mg/g DM)	Copper (mg/g DM)	Nickel (mg/g DM)	Lead (mg/g DM)	Zinc (mg/g DM)
Soil Site 1	15.88±0.02^{c}	11.57±0.17^{c}	13.00±1.87^{c}	0.19±0.07^{c}	0.75±0.07^{a}	1.02±0.00^{c}	3.12±0.00^{a}	0.28±0.00^{b}
Soil Site 2	17.21±0.02^{b}	16.54±0.09^{b}	18.58±2.17^{b}	0.24±0.00^{b}	0.05±0.00^{g}	1.02±0.00^{c}	1.01±0.00^{d}	0.04±0.00^{e}
Soil Site 3	28.79±0.03^{a}	24.79±0.27^{a}	21.83±1.08^{a}	0.30±0.01^{a}	0.06±0.00^{f}	2.04±0.05^{a}	1.08±0.11^{cd}	0.05±0.00^{de}
Root Site 1	0.67±0.01^{d}	0.45±0.00^{e}	1.01±0.07^{f}	0.09±0.00^{e}	0.13±0.00^{c}	0.54±0.02^{f}	2.15±0.01^{b}	5.00±0.02^{a}
Root Site 2	0.09±0.00^{f}	0.23±0.05^{f}	2.48±0.12^{d}	0.07±0.00^{f}	0.08±0.00^{e}	0.57±0.05^{ef}	1.08±0.02^{c}	0.10±0.00^{d}
Root Site 3	0.17±0.00^{ef}	0.37±0.08^{e}	1.97±0.17^{e}	0.06±0.00^{f}	0.09±0.00^{d}	0.61±0.01^{e}	0.09±0.01^{g}	0.05±0.00^{de}
Leaves Site 1	0.35±0.01^{e}	0.67±0.01^{d}	1.05±0.08^{f}	0.09±0.00^{e}	0.17±0.00^{b}	0.98±0.12^{d}	0.72±0.00^{e}	0.19±0.00^{c}
Leaves Site 2	0.16±0.00^{f}	0.62±0.00^{d}	2.47±0.24^{d}	0.07±0.00^{f}	0.09±0.00^{d}	0.42±0.02^{g}	0.61±0.00^{f}	0.07±0.00^{de}
Leaves Site 3	0.19±0.00^{ef}	0.45±0.06^{e}	1.24±0.05^{f}	0.12±0.00^{d}	0.08±0.00^{e}	1.24±0.83^{b}	0.08±0.01^{g}	0.02±0.00^{e}
Source of variation								
Fisher's test	32,756.38	65,088.23	7,888.875	785.098	7,054.767	1,424.908	3,763.301	6,743.418
Probability	0.0000	0.0000	0.0000	0.0000	0.0000	0.0000	0.0000	0.0000
Least significant difference	0.1915	0.1163	0.3034	0.0101	0.0084	0.0429	0.0514	0.0644

Notes: [a,b,c,d,e,f]The different letters in the same column represent significant variations at a 5% level. Sites having different letters indicate significant differences in the parameters measured, whereas the same letters indicate no significant differences in the parameters measured.

Abbreviation: DM: Dry matter.

other sites. Notably, the highest concentration of Co (2.48 mg/g DM) was observed in the roots at site S2, whereas the highest concentration of Ni (0.61 mg/g DM) was found in the roots at site S3. A similar pattern of metal accumulation in the roots at site S1 was also observed in the leaves of the same site, with concentrations of Al, Cd, Cu, Pb, and Zn being 0.35, 0.67, 0.17, 0.72, and 0.19 mg/g DM, respectively. Leaves at site S2 accumulated a higher concentration of Co (2.47 mg/g DM), whereas leaves at site S3 accumulated more Cr and Ni (0.12 and 1.24 mg/g DM, respectively) compared to other sites. Notably, the investigation revealed the remarkable phytoremediation potential of *S. monoica* roots for Zn, Co, and Pb and the leaves' ability to remediate a substantial amount of Co, Ni, and Cd despite their toxicity to the plant.

The observed differences in heavy metal accumulation between sites may reflect variations in soil metal concentrations, salinity, and plant metal uptake efficiency. The higher accumulation of Zn and Pb in the roots and leaves of *S. monoica* at site S1 could be a response to elevated soil metal levels or enhanced metal uptake efficiency under saline conditions. Consistent with our findings, Ibraheem et al.[5] have documented *S. monoica* as a potent phytoextraction of Cr, Co, Cu, Ni, and Zn. Similarly, Joshi *et al*.[8] have highlighted the reliable heightened capacity of *S. monoica* for Zn, Mn, Fe, Cu, Cr, and Cd compared to *Tamarix indica* and *Cressa cretica*. The plant-specific translocation mechanism likely contributes to the substantial accumulation of all metals. This conjecture aligns with the principle that the accumulation of one element by a plant typically foretells the accumulation of other metals as well.[59,60,67] A comparative analysis of our findings with earlier studies on the phytoremediation potential of halophytes reveals that *S. monoica* is deemed a moderate accumulator and holds promise for remediating heavy metal-contaminated saline soils.[68-70]

3.9. Correlation between the measured traits

Considering the assessed characteristics of *S. monoica* at the various collection sites, 188 correlation coefficients were investigated (Figure 2). Among these, 33 traits displayed highly significant values (p<0.01) with a correlation coefficient (r) ≥0.62, whereas 36 traits showed significant associations (p<0.05) with a correlation coefficient ≥0.36. Notably, the amino acid content strongly correlated with Cu (0.80), whereas the protein content showed strong associations with phenols, alkaloids, TAC, and Cd (0.94, 0.75, 0.93, and 0.80, respectively). Conversely, proline negatively

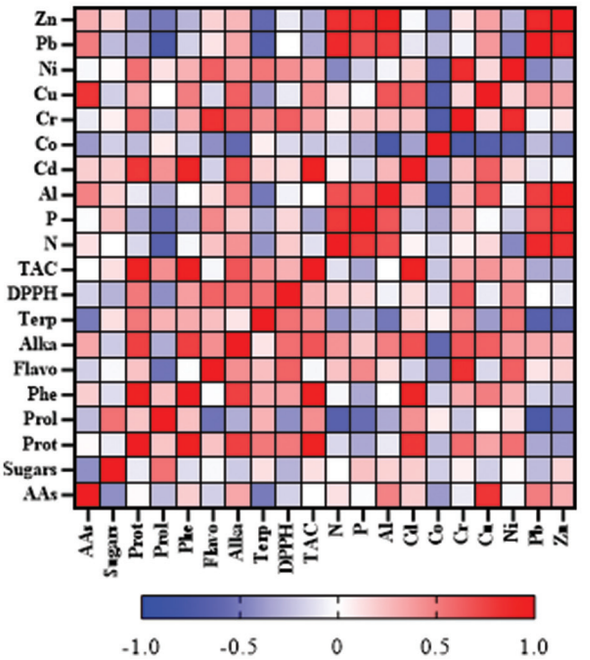

Figure 2. Pearson's correlation coefficients among the evaluated attributes in *Suaeda monoica* collected from three localities in Jeddah

Abbreviations: AAs: Amino acids; Al: Aluminium; Alka: Alkaloids; Cd: Cadmium; Co: Cobalt; Cr: Chromium; Cu: Copper; DPPH: 1,1-diphenyl-2-picrylhydrazyl; Flavo: Flavonoids; N: Nitrogen; Ni: Nickel; P: Phosphorus; Pb: Lead; Phe: Phenols; Prol: Proline; Prot: Protein; TAC: Total antioxidant capacity; Terp: Terpenoids; Zn: Zinc.

correlated with N and Pb (−0.66 and −0.75, respectively). Furthermore, the phenols content displayed positive associations with alkaloids, TAC, and Cd (0.76, 0.95, and 0.89, respectively), whereas the flavonoid content exhibited positive associations with Cr (0.83) and Ni (0.62). Similarly, the alkaloid content showed strong correlations with TAC, Cd, Cr, and Cu (0.66, 0.69, 0.65, and 0.62, respectively), whereas DPPH exhibited a correlation with Cr (0.62) and TAC was correlated with Cd (0.94). The nitrogen content in *S. monoica* linearly correlated with P, Al, Pb, and Zn contents (0.79, 0.68, 0.87, and 0.83, respectively). In addition, phosphorus content correlated with Al, Pb, and Zn (0.66, 0.70, and 0.83, respectively). Al showed positive correlations with Cu, Pb, and Zn (0.66, 0.76, and 0.92, respectively) but a negative correlation with Co (−0.75). Conversely, Co exhibited negative correlations with Cr and Cu (−0.70 and −0.66, respectively), whereas Cr positively correlated with Ni (0.85), and Pb correlated with Zn (0.88). Notably, a positive relationship was

observed between amino acids and proteins and the heavy metals Cu and Cd, whereas proline exhibited an inverse correlation with Pb. Furthermore, P positively correlated with Al, Pb, and Zn. Hence, our findings suggest that *S. monoica* can increase its amino acids, proteins, and phosphorus production in response to metal pollution. In addition, this plant may synthesize proline, an osmomodulator, depending on the intensity of metal contamination.

4. Conclusion

Physiological and biochemical responses of *S. monoica* in Jeddah are significantly affected by the collection site. The observed variations in photosynthetic pigments, osmoregulatory compounds, secondary metabolites, antioxidant capacity, nutrient content, and heavy metal accumulation show that plants can adapt and cope with stress. Furthermore, the study explained the variation in phytochemical profiles of *S. monoica* leaves across different collection sites, including compounds and chemical classes unique to each site. Differential accumulations of components at different sites suggest that the plant responds to environmental conditions differently, with implications for phytoremediation. These findings underscore the influence of environmental factors on the qualitative and quantitative composition of phytoconstituents in *S. monoica* extracts, emphasizing the need for site-specific considerations in phytochemical analyses and potential implications for phytoremediation, pharmacological applications, and ecological studies. Moreover, the study unveiled that *S. monoica* exhibits potential as a model plant for afforestation initiatives and possibly for cultivating economically valuable plants in contaminated environments. Further research into the molecular mechanisms underlying these responses could enhance our knowledge of plant-environment interactions and inform sustainable environmental management practices.

Acknowledgments

None.

Funding

None.

Conflict of interest

The author declares no conflicts of interest.

Author contributions

This is a single-authored article.

Availability of data

Data of this study are available from the corresponding author upon reasonable request.

References

1. Shakthi A, Linoj J, Suresh V, Hussein M, Selvamani M. Evaluation of antibacterial and anti-oxidant activities of *Suaeda monoica* extract for its potential application. *Cureus*. 2024;16(1):e53091. doi: 10.7759/cureus.53091
2. Rajathi F, Arumugam R, Saravanan S, Anantharaman P. Phytofabrication of gold nanoparticles assisted by leaves of *Suaeda monoica* and its free radical scavenging property. *J Photochem Photobiol B Biol*. 2014;135:75-80. doi: 10.1016/j.jphotobiol.2014.03.016
3. Roy M, Dutta TK. Evaluation of phytochemicals and bioactive properties in mangrove associate *Suaeda monoica* Forssk. ex J.F.Gmel. of Indian sundarbans. *Front. Pharmacol*., 2021;12:e584019. doi: 10.3389/fphar.2021.584019
4. Aluri JSR, Kumar R, Chappidi PR. Reproductive biology of mangrove plants *Clerodendrum inerme, Derris trifoliata, Suaeda maritima, Suaeda monoica, Suaeda nudiflora*. *Transylv Rev Syst Ecol Res*. 2016;18(3):31-68. doi: 10.1515/trser-2015-0092
5. Ibraheem F, Al-Zahrani A, Mosa A. Physiological adaptation of three wild halophytic *Suaeda* species: Salt tolerance strategies and metal accumulation capacity. *Plants* (*Basel*). 2022;11:e537. doi: 10.3390/plants11040537
6. Lakshmanan G, Rajeshkannan C, Kavitha A, Mekala B, Kamaladevi N. Preliminary screening of biologically active constituents of *Suaeda monoica* and *Sesuvium portulocastrum* from palayakayal mangrove forest of Tamilnadu. *J Pharmacogn Phytochem.* 2013;2(3):149-152.
7. Elsharabasy FS, Metwall NS, Mahmoud AH, *et al*. Phytoconstituents and hepatoprotective effect of *Suaeda monoica* Forssk and *Suaeda pruinosa* Lange. *Biomed Pharmacol J*. 2019;12:117-129. doi: 10.13005/bpj/1620
8. Joshi A, Kanthaliya B, Rajput V, Minkina T, Arora J. Assessment of phytoremediation capacity of three halophytes: *Suaeda monoica, Tamarix indica* and *Cressa critica*. *Biol Futur*. 2020;71:301-312. doi: 10.1007/s42977-020-00038-0
9. Ayyappan D, Ravindran KC. Potentiality of *Suaeda monoica* Forsk. A salt marsh halophyte on

bioaccumulation of heavy metals from tannery effluent. *Int J Mod Res Rev.* 2014;2:267-274.
10. Song H, Sun Z. Temporal variations and bioaccumulation of heavy metals in different *Suaeda salsa* marshes of the Yellow River estuary, China. *Environ Sci Pollut Res.* 2014;21:14174-14187. doi: 10.1007/s11356-014-3296-7
11. Panta S, Flowers T, Lane P, Doyle R, Haros G, Shabala S. Halophyte agriculture: Success stories. *Environ Exp Bot*. 2014;107:71-83. doi: 10.1016/j.envexpbot.2014.05.006
12. Muthazhagan K, Thirunavukkarasu P, Ramanathan T, Kannan D. Studies on phytochemical screening, antimicrobial and anti radical scavenging effect coastal salt mash plant of a *Suaeda monoica*. *Res J Phytochem*. 2014;8:102-111.
13. Hawas UW, El-Kassem LTA, Shaher FM, Al-Farawati R, Ghandourah M. Phytochemical compositions of some red sea halophyte plants with antioxidant and anticancer potentials. *Molecules*. 2022;27:e3415. doi: 10.3390/molecules27113415
14. Ravikumar S, Gnanadesigan M, Serebiah J, Inbaneson S. Hepatoprotective effect of an Indian salt marsh herb *Suaeda monoica* Forsk. Ex. Gmel against concanavalin-A induced toxicity in rats. *Life Sci Med Res*. 2010;2010:1-9.
15. Siddiqui NA, Mothana RA, Al-Said MS, *et al*. Cell proliferation activity delineated by molecular docking of four new compounds isolated from the aerial parts of *Suaeda monoica* Forssk. ex. J.F. Gmel. *Saudi Pharm J.* 2020;28:172-186. doi: 10.1016/j.jsps.2019.11.019
16. Al-Said MS, Siddiqui NA, Mukhair MA, *et al*. A novel monocyclic triterpenoid and a norsesquaterpenol from the aerial parts of *Suaeda monoica* Forssk. ex J.F. Gmel with cell proliferative potential. *Saudi Pharm J.* 2017;25:1005-1010. doi: 10.1016/j.jsps.2017.03.008
17. Lakshmanan G, Rajeshkannan C, Kavitha A, Mekala B, Kamaladevi N. Preliminary screening of biologically active constituents of *Suaeda monoica* and *Sesuvium portulacastrum* from palayakayal mangrove forest of Tamilnadu. *J Pharmacogn Phytochem*. 2013;2:149-152.
18. AOAC. Official Methods of Analysis of Association of Official Analytical Chemists. 18th ed. Washington, DC, USA: AOAC; 2010.
19. Metzner H, Rau H, Senger H, *et al*. Trace elements' uptake and antioxidant response to excess of manganese in *in vitro* cells of sensitive and tolerant wheat. *Planta*. 1965;65:186-194. doi: 10.1007/bf00384998
20. Dubois M, Gilles K, Hamilton J, Rebers P, Smith F. Colorimetric method for determination of sugars and related substances. *Anal Chem*. 1965;28:350-356. doi: 10.1021/ac60111a017
21. Bradford MM. A rapid and sensitive method for the quantitation of microgram quantities of protein utilizing the principle of protein-dye binding. *Anal Biochem*. 1976;72:248-254. doi: 10.1016/0003-2697(76)90527-3
22. Lee YYP, Takahashi T. An improved colorimetric determination of amino acids with the use of ninhydrin. *Anal Biochem*. 1966;14:71-77. doi: 10.1016/0003-2697(66)90057-1
23. Bates LS, Waldren RP, Teare ID. Rapid determination of free proline for water-stress studies. *Plant Soil*. 1973;39:205-207. doi: 10.1007/BF00018060
24. Jindal KK, Singh RN. Phenolic content in male and female *Carica papaya*: A possible physiological marker for sex identification of vegetative seedlings. *Physiol Plant.* 1975;33:104-107. doi: 10.1111/j.1399-3054.1975.tb03774.x
25. Chang CC, Yang MH, Wen HM, Chern JC. Estimation of total flavonoid content in propolis by two complementary colorimetric methods. *J Food Drug Anal*. 2002;10:178-182.
26. Shamsa F, Monsef H, Ghamooshi R, Verdian-Rizi M. Spectrophotometric determination of total alkaloids in some Iranian medicinal plants. *J Appl Hortic*. 2010;12:69-70.
27. Ghorai N, Chakraborty S, Gucchait S, Saha SK, Biswas S. Estimation of total terpenoids concentration in plant tissues using a monoterpene, linalool as standard reagent. *Protoc Exch.* 2012;5.
28. Sermakkani M, Thangapandian V. Phytochemical screening for active compounds in *Pedalium murex* L. *Recent Res Sci Technol*. 2010;2:110-114.
29. Ahmed D, Baig H, Zara S. Seasonal variation of phenolics, flavonoids, antioxidant and lipid peroxidation inhibitory activity of methanolic extract of *Melilotus indicus* and its sub-fractions in different solvents. *Int J Phytomed*. 2012;4:326-332.
30. Saad-Allah KM, Elhaak MA. Hyperaccumulation activity and metabolic responses of *Solanum nigrum* in two differentially polluted growth habitats. *J Saudi Soc Agric Sci*. 2017;16:227-235. doi: 10.1016/j.jssas.2015.08.001
31. Ltaeif HB, Sakhraoui A, González-Orenga S, *et al*. Responses to salinity in four *Plantago* species from Tunisia. *Plants*. 2021;10:e1392. doi: 10.3390/plants10071392
32. Munns R, Tester M. Mechanisms of salinity tolerance. *Annu Rev Plant Biol*. 2008;59:651-681. doi: 10.1146/annurev.arplant.59.032607.092911
33. Ashraf M, Harris PJC. Photosynthesis under stressful environments: An overview. *Photosynthetica*. 2013;51(2):163-190. doi: 10.1007/s11099-013-0021-6
34. Rangani J, Parida AK, Panda A, Kumari A. Coordinated changes in antioxidative enzymes protect the

photosynthetic machinery from salinity induced oxidative damage and confer salt tolerance in an extreme halophyte *Salvadora persica* L. *Front Plant Sci.* 2016;7:e50. doi: 10.3389/fpls.2016.00050

35. Ben Hsouna A, Michalak M, Kukula-Koch W, *et al*. Evaluation of halophyte biopotential as an unused natural resource: The case of *Lobularia maritima*. *Biomolecules*. 2022;12:e1583. doi: 10.3390/biom12111583
36. Chaudhry S, Sidhu GPS. Climate change regulated abiotic stress mechanisms in plants: A comprehensive review. *Plant Cell Rep.* 2022;41:1-31. doi: 10.1007/s00299-021-02759-5
37. Ghanem AMFM, Mohamed E, Kasem AMMA, El-Ghamery AA. Differential salt tolerance strategies in three halophytes from the same ecological habitat: Augmentation of antioxidant enzymes and compounds. *Plants*. 2021;10:e1100. doi: 10.3390/plants10061100
38. Boughalleb F, Denden M. Physiological and biochemical changes of two halophytes, *Nitraria retusa* (Forssk.) and *Atriplex halimus* (L.) under increasing salinity. *Agric J.* 2011;6:327-339. doi: 10.3923/aj.2011.327.339
39. Haque MI, Siddiqui SA, Jha B, Rathore MS. Interactive effects of abiotic stress and elevated CO_2 on physio-chemical and photosynthetic responses in *Suaeda* species. *J Plant Growth Regul.* 2022;41:2930-2948. doi: 10.1007/s00344-021-10485-1
40. Mishra A, Tanna B. Halophytes: Potential resources for salt stress tolerance genes and promoters. *Front Plant Sci*. 2017;8:e829. doi: 10.3389/fpls.2017.00829
41. Parida AK, Jha B. Salt tolerance mechanisms in mangroves: A review. *Trees*. 2010;24(2):199-217. doi: 10.1007/s00468-010-0417-x
42. Parida AK, Veerabathini SK, Kumari A, Agarwal PK. Physiological, anatomical and metabolic implications of salt tolerance in the halophyte *Salvadora persica* under hydroponic culture condition. *Front Plant Sci.* 2016;7:e351. doi: 10.3389/fpls.2016.00351
43. Rajput VD, Chen Y, Ayup M. Effects of high salinity on physiological and anatomical indices in the early stages of *Populus euphratica* growth. *Russ J Plant Physiol.* 2015;62:229-236. doi: 10.1134/S1021443715020168
44. Al-Shamsi N, Hussain MI, El-Keblawy A. Physiological responses of the xerohalophyte *Suaeda vermiculata* to salinity in its hyper-arid environment. *Flora*. 2020;273:e151705. doi: 10.1016/j.flora.2020.151705
45. Wang R, Wang X, Liu K, Zhang XJ, Zhang LY, Fan SJ. Comparative transcriptome analysis of halophyte *Zoysia macrostachya* in response to salinity stress. *Plants* (*Basel*). 2020;9:e458. doi: 10.3390/plants9040458
46. Tuteja N, Sopory SK. Chemical signaling under abiotic stress environment in plants. *Plant Signal Behav*. 2008;3:525-536. doi: 10.4161/psb.3.8.6186
47. Li Q, Song J. Analysis of widely targeted metabolites of the euhalophyte *Suaeda salsa* under saline conditions provides new insights into salt tolerance and nutritional value in halophytic species. *BMC Plant Biol*. 2019;19:388. doi: 10.1186/s12870-019-2006-5
48. Ashraf M, Foolad MR. Roles of glycine betaine and proline in improving plant abiotic stress resistance. *Environ Exp Bot.* 2007;59(2):206-216. doi: 10.1016/j.envexpbot.2005.12.006
49. Mitra R, Ghosh S, Mukherjee G, Acharya Chowdhury A. Secondary metabolites: Treasure trove for future medicine. In: Mérillon JM, Ramawat KG, editors. *Plant Specialized Metabolism for Plant Protection: Genomics and Biotechnology*. Cham: Springer Nature Switzerland; 2023. p. 1-45.
50. D'Auria JC, Gershenzon J. The secondary metabolism of *Arabidopsis thaliana*: Growing like a weed. *Curr Opin Plant Biol*. 2005;8:308-316. doi: 10.1016/j.pbi.2005.03.012
51. Arbona V, Iglesias DJ, Talón M, Gómez-Cadenas A. Plant phenotype demarcation using nontargeted LC-MS and GC-MS metabolite profiling. *J Agric Food Chem*. 2009;57:7338-7347. doi: 10.1021/jf9009137
52. Karowe DN, Grubb C. Elevated CO_2 increases constitutive phenolics and trichomes, but decreases inducibility of phenolics in *Brassica rapa* (*Brassicaceae*). *J Chem Ecol*. 2011;37:1332-1340. doi: 10.1007/s10886-011-0044-z
53. Demkura PV, Ballaré CL. UVR8 mediates UV-B-induced arabidopsis defense responses against *Botrytis cinerea* by controlling sinapate accumulation. *Mol Plant*. 2012;5:642-652. doi: 10.1093/mp/sss025
54. Kranner I, Minibayeva FV, Beckett RP, Seal CE. What is stress? Concepts, definitions and applications in seed science. *New Phytol*. 2010;188:655-673. doi: 10.1111/j.1469-8137.2010.03461.x
55. Boestfleisch C, Wagenseil NB, Buhmann AK, *et al*. Manipulating the antioxidant capacity of halophytes to increase their cultural and economic value through saline cultivation. *AoB Plants*. 2014;6:plu046. doi: 10.1093/aobpla/plu046
56. Rodrigues MJ, Soszynski A, Martins A, *et al*. Unravelling the antioxidant potential and the phenolic composition of different anatomical organs of the marine halophyte *Limonium algarvense*. *Ind Crops Prod*. 2015;77:315-322. doi: 10.1016/j.indcrop.2015.08.061

57. Ramakrishna A, Ravishankar GA. Influence of abiotic stress signals on secondary metabolites in plants. *Plant Signal Behav*. 2011;6(11):1720-1731. doi: 10.4161/psb.6.11.17613
58. Miguel MG, Duarte J, Figueiredo AC, Barroso JG, Pedro LG. *Thymus carnosus* boiss.: Effect of harvesting period, collection site and type of plant material on essential oil composition. *J Essent Oil Res.* 2005;17:422-426. doi: 10.1080/10412905.2005.9698950
59. Al-Shawi AAA, Hameed MF, Ali NH, Hussein KA. Investigations of phytoconstituents, antioxidant and anti-liver cancer activities of *Saueda monoica* Forssk extracted by microwave-assisted extraction. *Asian Pac J Cancer Prev*. 2020;21:2349-2355. doi: 10.31557/APJCP.2020.21.8.2349
60. Martelloni L, Frasconi C, Sportelli M, Fontanelli M, Raffaelli M, Peruzzi A. Flaming, glyphosate, hot foam and nonanoic acid for weed control: A comparison. *Agronomy*. 2020;10:e129. doi: 10.3390/agronomy10010129
61. Chandrasekaran M, Kannathasan K, Venkatesalu V. Antimicrobial activity of fatty acid methyl esters of some members of *Chenopodiaceae*. *Z Naturforsch C J Biosci*. 2008;63:331-336. doi: 10.1515/znc-2008-5-604
62. Gill SS, Tuteja N. Reactive oxygen species and antioxidant machinery in abiotic stress tolerance in crop plants. *Plant Physiol Biochem*. 2010;48(12):909-930. doi: 10.1016/j.plaphy.2010.08.016
63. Yezhelyev MV, Gao X, Xing Y, Al-Hajj A, Nie S, O'Regan RM. Emerging use of nanoparticles in diagnosis and treatment of breast cancer. *Lancet Oncol*. 2006;7:657-667. doi: 10.1016/S1470-2045(06)70793-8
64. Sun Z, Yu L, Hu X, Chen B. Effects of enhanced nitrogen load on variation and turnover of phosphorus in the plant-soil system of *Suaeda salsa* marsh in the Yellow River estuary, China. *J Soils Sediments*. 2023;23:2428-2443. doi: 10.1007/s11368-023-03490-2
65. Hu X, Sun Z. Effects of exogenous nitrogen import on variations of nutrient in decomposing litters of *Suaeda salsa* in coastal marsh of the Yellow River estuary, China. *Environ Sci Pollut Res*. 2021;28:33165-33180. doi: 10.1007/s11356-021-12926-6
66. Milić D, Luković J, Ninkov J, *et al*. Heavy metal content in halophytic plants from inland and maritime saline areas. *Cent Eur J Biol.* 2012;7:307-317. doi: 10.2478/s11535-012-0015-6
67. Mujeeb A, Aziz I, Ahmed MZ, Alvi SK, Shafiq S. Comparative assessment of heavy metal accumulation and bio-indication in coastal dune halophytes. *Ecotoxicol Environ Saf*. 2020;195:e110486. doi: 10.1016/j.ecoenv.2020.110486
68. Li B, Wang J, Yao L, *et al*. Halophyte *Halogeton glomeratus*, a promising candidate for phytoremediation of heavy metal-contaminated saline soils. *Plant Soil.* 2019;442:323-331. doi: 10.1007/s11104-019-04152-4
69. Lutts S, Qin P, Han RM. Salinity influences biosorption of heavy metals by the roots of the halophyte plant species *Kosteletzkya pentacarpos*. *Ecol Eng.* 2016;95:682-689. doi: 10.1016/j.ecoleng.2016.06.009
70. Kouhi SMM, Moudi M. Assessment of phytoremediation potential of native plant species naturally growing in a heavy metal-polluted saline-sodic soil. *Environ Sci Pollut Res Int*. 2020;27:10027-10038. doi: 10.1007/s11356-019-07578-6

Asian Journal of Water, Environment and Pollution. Vol. 22, No. 3 (2025), pp. 63-72.
doi: 10.36922/ajwep.8593

ORIGINAL RESEARCH ARTICLE

Exploring municipal solid waste management practices and public perceptions in north coastal Andhra Pradesh, India

Nakka Lakshmi Srikanth, Neyyila Saibabu*, and Neyyala Chaitanya
Department of Basic Science and Humanities, Aditya Institute of Technology and Management, Srikakulam, Andhra Pradesh, India
***Corresponding author:** Neyyila Saibabu (saibabuneyyilamba@adityatekkali.edu.in)

Received: January 18, 2025; Revised: March 11, 2025; Accepted: April 17, 2025; Published Online: May 5, 2025

Abstract: Municipal solid waste management (MSWM) presents a critical challenge in rapidly urbanizing regions, particularly in developing nations, where population growth and migration place increasing strain on infrastructure. This study examines MSWM practices and public perceptions in north coastal Andhra Pradesh, India, with a focus on waste collection, transportation, generation and reduction, reuse and recycling, composition, and separation. The research aims to assess the effectiveness of current MSWM strategies, identify gaps, and propose improvements based on best management practices. Through an analysis of existing regulations and levels of public engagement, this study provides insights into optimizing waste management approaches within the regulatory framework. The findings contribute to the development of sustainable waste management solutions that enhance environmental quality and urban livability. This research identifies key practices that improve waste management systems and offers recommendations for municipal bodies seeking to enhance efficiency and promote sustainability in waste reduction and resource recovery. The results underscore the importance of integrated solid waste management strategies and public participation in effectively addressing the growing challenges of urban waste management.

Keywords: Infrastructure services; Municipal solid waste management; Recycling; Sustainable cities; Urbanization; Waste reduction

1. Introduction

Material that is unneeded or unusable, a substance discarded after its initial use, or one deemed worthless, flawed, or obsolete is classified as waste.[1] However, joint goods and by-products are considered to have relatively low economic value rather than being classified as outright waste.[2] Innovations that enhance the value of waste can transform it into a resource, a general product, or a by-product, thereby reducing its negative environmental impact and promoting sustainability.[3] Waste is typically discarded when it no longer serves a purpose, yet it is only considered true waste when it cannot be reused, repurposed, or recycled.[4] To prevent environmental degradation, waste disposal is managed through curbside collection, direct landfill delivery, or specialized waste treatment facilities designed to minimize contamination, particularly of groundwater resources.[5] Waste categories include municipal solid waste (household waste/garbage), hazardous waste, and sewage, each requiring different disposal and management strategies to mitigate ecological harm.[6]

1.1. Definition of solid waste management (SWM)

SWM refers to the systematic control of waste materials from their generation to final disposal, ensuring minimal environmental and public health risks. It involves various stages, including waste collection, transportation, processing, recycling, and final disposal through landfilling or incineration.[7] The primary objective of SWM is to reduce waste-related hazards while optimizing resource efficiency and sustainability. Urbanization and population growth have significantly increased waste generation, posing serious challenges for municipal authorities, especially in developing countries.[8] SWM also encompasses strategies for waste reduction, resource recovery, and sustainable disposal methods to ensure urban cleanliness and environmental protection.[9] Inefficient waste management can lead to environmental pollution, health hazards, and burdens on infrastructure.[10] Effective SWM practices incorporate waste reduction strategies, recycling programs, and regulatory frameworks to ensure efficient resource utilization and environmental protection.[11] Regulations play a crucial role in guiding waste management policies. Countries implement legal frameworks to govern waste collection, disposal methods, and sustainability initiatives.[12] In developing regions, challenges such as inadequate infrastructure, financial constraints, and lack of public awareness hinder effective SWM.[13] However, adopting an integrated waste management approach, including community participation and technological advancements, can enhance urban livability.[14] Sustainable waste management strategies are essential for mitigating pollution, conserving resources, and supporting overall environmental and public health goals.[15]

1.2. Review of literature

Municipal SWM (MSWM) is a significant challenge in India due to rapid urbanization, industrialization, and population growth. According to the Central Pollution Control Board,[16] India generates approximately 62 million tons of municipal solid waste annually, of which only 43 million tons are collected and 12 million tons are treated. The increasing waste generation necessitates efficient waste management practices to ensure sustainability and public health. This literature review explores existing research on MSWM in India, focusing on waste management practices, regulatory frameworks, challenges, and future recommendations. Several studies have examined the various aspects of MSWM in India. Singh[17] conducted a case study in Indore, highlighting the city's successful waste segregation, collection, and disposal mechanisms. Similarly, Singh[18] emphasized the need for improvement in urban waste management through better governance and citizen participation. Sharholy *et al*.[9] reviewed MSWM in Indian cities, identifying issues such as inadequate waste collection, poor infrastructure, and the lack of scientific disposal methods. Jha *et al.*[19] analyzed SWM strategies and highlighted the necessity of integrated waste management approaches. Furthermore, Kumar *et al.*[20] provided a qualitative assessment of MSWM, emphasizing the role of policy implementation and financial investment. The Indian government has implemented various policies and regulations to improve MSWM. The Municipal Solid Waste (Management and Handling) Rules, 2000, and the subsequent SWM Rules, 2016, mandated scientific waste disposal, segregation at source, and extended producer responsibility.[21,22] The recently updated SWM Rules, 2024, seek further improvements in waste reduction and recycling. Maharashtra has taken proactive measures through the Maharashtra Non-Biodegradable Garbage Control Act, 2006, which bans plastic bags and promotes waste segregation,[23,24] providing annual reports on the compliance and enforcement of waste management policies.[25,26] A significant focus of MSWM is transitioning toward a circular economy. Mugambi and Windberg[27] emphasized resource recovery prospects, while Zaman and Lehmann[4] discussed transforming cities into "zero waste" ecosystems. Sajja and Meesala[28] analyzed waste reduction strategies in retail supply chains, highlighting sustainable waste management practices. Key challenges identified in the literature include: (i) infrastructure deficiency: limited landfill sites and inefficient waste processing facilities; (ii) public awareness: lack of segregation at source and improper disposal habits;[29] (iii) financial constraints: insufficient funds for waste collection and treatment; (iv) informal sector involvement: a significant portion of recycling is handled by informal waste pickers, as noted by Wilson *et al*.;[6] (v) technological innovations: adoption of waste-to-energy technologies;[30] and (vi) public–private partnerships: encouraging private investments in MSWM.[31]

MSWM has become a pressing issue in rapidly urbanizing regions due to increasing population density and waste generation.[32] Urban local bodies and municipal corporations are responsible for reducing and efficiently processing solid waste, yet many struggle with inadequate waste collection, transportation, and disposal systems.[33] The inefficiency of these systems often exacerbates the environmental and public health hazards associated with unregulated waste disposal.

A study conducted in Accra, Ghana, by Oteng-Ababio *et al.*[34] explored three strategies for addressing urbanization challenges: community-led SWM, storm drain widening, and retention pond construction. Among these, retention pond construction yielded both direct economic benefits, such as reduced flood damage, and indirect benefits, including fewer disruptions to transportation and commerce, accumulating a total value stream of Ghanaian Cedi 284 million. Similarly, a study by Mugambi and Windberg[27] in Naivasha, Kenya, highlighted the link between inadequate waste management and poor sanitation, revealing that 65% of urban residents lack access to basic sanitation services, while 17% lack safe drinking water. The global trend toward circular economies emphasizes waste resource recovery as a crucial component of sustainable urban development. Effective strategies, such as waste segregation at source, composting of organic waste, and conversion of non-biodegradable waste into recyclable materials, are necessary to alleviate the burden on landfills and promote sustainable urban infrastructure.[35] Studies have also highlighted the significance of waste-to-energy technologies, such as anaerobic digestion and incineration, as viable alternatives to traditional landfilling.[36,37]

These approaches align with global waste reduction policies, such as the 3Rs (Reduce, Reuse, Recycle) framework**,** promoted by international organizations like the United Nations Environment Programme.[38,39] However, challenges remain in terms of financial constraints, lack of public awareness, and inadequate enforcement of waste management policies.[40] Addressing these issues requires a multifaceted approach that integrates policy reforms, technological advancements, and behavioral change among urban populations to create resilient and sustainable waste management systems. Srikanth and Rao[41,42] provided a comparative overview of SWM practices across various Indian municipalities. The analysis indicated that while larger metropolitan areas have adopted semi-mechanized systems and public–private partnerships, smaller towns still rely heavily on manual collection and open dumping. The study emphasized the need for uniform policy enforcement, capacity-building at the local level, and integration of informal waste workers into the formal system to ensure effective waste management.

1.3. Rationale for the study

One of the fundamental functions of municipal corporations is the management and disposal of human waste, a responsibility often constrained by financial constraints. Traditional city trash management methods are not only costly but also rely on a high standard of cleanliness, which is frequently unachievable in low-income regions. Consequently, numerous municipal companies have implemented low-cost waste disposal technologies that require a minimal budget to operate. However, the operation and maintenance costs of such waste management systems are often underestimated and typically borne by the local corporation.

The chosen selected are highly significant and relevant to the current situation. Pilot studies conducted in several municipal corporations in Visakhapatnam, Vizianagaram, and Srikakulam have shown that these municipal authorities are seeking efficient MSWM solutions and are facing issues with municipal solid waste, particularly due to the rapid expansion of markets.

The primary goals of the study are to examine the current municipal waste management practices in selected municipal corporations, identify the various problems faced by corporations and stakeholders, enhance waste management practices in the sample areas, and, ultimately, provide a workable solution based on the data collected. Additionally, this study is highly pertinent to the current state of society.

1.4. Research scope

For municipal corporations, the SWM program is a crucial decision. It is necessary to consider both the economic viability of the chosen program and the limitations of the currently available disposal options. Recycling programs are gaining popularity, but their actual economic viability is still low. This is primarily due to the high costs of recycled materials, with some materials not even covering the cost of recycling. Furthermore, the pricing dynamics of the secondary product market are volatile, which hinders investment in recycling capacity.

By implementing a flexible waste management program that permits the use of landfills when recycling is not practical, this study aims to reduce uncertainty over the advantages of recycling. If recycling proves too costly, landfill strategies, which are typically less expensive than recycling, can serve as a buffer. However, the municipal corporation may have to incur higher capital expenses to maintain a more sophisticated waste management program that can restore landfills as needed.

The waste management strategies employed by selected municipal corporations in the districts of Visakhapatnam, Vizianagaram, and Srikakulam are

the focus of this study. The research is restricted to these districts. To achieve the objectives and test the hypothesis, the data gathered are thoroughly analyzed. As a result, this study examines a number of aspects of municipal waste management procedures, incorporating the views of municipal corporation employees and civilian stakeholders.

1.5. Waste hierarchy

The waste hierarchy is considered a crucial component of integrated SWM. Based on environmental principles, the hierarchy suggests treating waste differently based on its properties. Reusing or reducing waste content helps prevent certain amounts of waste. Secondary raw materials must be produced from another portion of the waste flow. The remaining waste can be recovered, while some can be composted or converted into energy (Figure 1).

However, this environmental order is often not followed in practice. Large volumes of waste are either burned in open spaces or, worse, discarded carelessly in developing nations. Due to their significant environmental impact, these practices are not included in the waste hierarchy. Consequently, these alternatives are now represented in the shaded region. Policymakers can effectively use this ranking of waste management options as a basis, although integrated SWM extends beyond the waste hierarchy. It is well recognized that hierarchies should be applied with flexibility, serving as a broad framework for long-term ecological solutions. Despite its value, the hierarchy has been harshly and frequently criticized. First, the ranking of environmental effects may be accurate for some cases, but not for others.

1.6. Objectives of the research

The present study aims to evaluate the effectiveness of MSWM practices in selected municipal corporations of north-coastal Andhra Pradesh. The research also seeks to understand stakeholder perspectives and identify opportunities for improvement. The specific objectives are as follows:

(i) To examine the various waste management practices adopted by the selected municipal corporations in north coastal Andhra Pradesh
(ii) To assess the perceptions of stakeholders regarding SWM in the municipal corporations of the study area
(iii) To evaluate the performance of municipal corporations in implementing waste management practices, in relation to stakeholder perceptions
(iv) To propose feasible and sustainable solutions for the effective implementation of SWM practices in the selected municipal corporations.

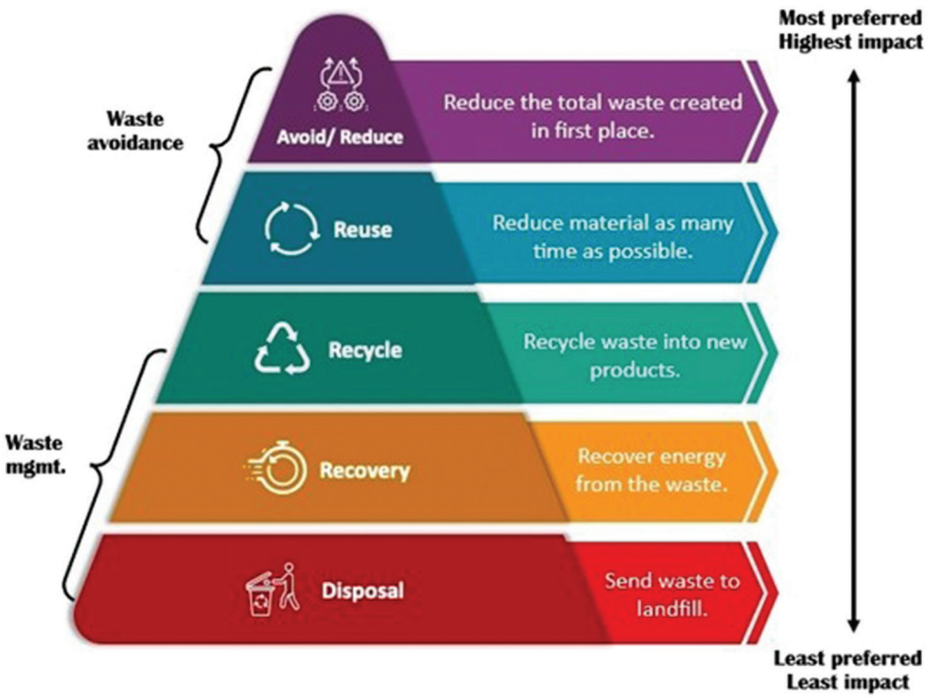

Figure 1. The waste hierarchy
Source: Authors' own illustration created using sketchbubble.com

2. Methodology

This study employed both primary and secondary data sources, applying appropriate research methods to collect the necessary information. Secondary data consisted of reports from municipal corporations and local governments, gathered from journals, websites, early thesis submissions, and related sources. Primary data were collected using standardized questionnaires administered to the general public and employees involved in waste management in the selected municipal corporations. A brief description of both primary and secondary data sources is provided below.

Primary data refers to information directly gathered by the researchers through field-based methods such as experiments, observations, surveys, and in-person interviews. Data were obtained from staff members and residents of selected municipal corporations in the districts of Srikakulam, Vizianagaram, and Visakhapatnam. Collection methods included the use of structured questionnaires, informal conversations, field observations, and other relevant fieldwork. To ensure appropriate targeting, researchers developed separate questionnaires for two respondent groups: solid waste disposal employees and the general public. An appropriate sample size was determined by the researchers, and a quota sampling technique was employed to select participants from each the general population in each municipal corporation.

In parallel, the researchers reviewed secondary data to support and contextualize the primary findings. This included data from government publications, websites, books, magazine articles, internal records, and other relevant materials. For this study, the researchers gathered secondary data from books, M. Phil. and Ph.D. theses, academic journals, numerous websites, newspapers, articles, government reports, publications, and online sources provided by government organizations.

2.1. Research hypothesis

To examine the relationship between stakeholder perceptions and various factors influencing SWM, the following research hypotheses were formulated:

H_{01}: There is no significant difference in the perceptions of the type of solid waste generated in the stakeholders' households in the selected municipal corporations.

Alternative hypothesis: There is a significant difference in the perceptions of the type of solid waste generated in the stakeholders' households in the selected municipal corporations.

H_{02}: There is no significant relationship between the education level of residents and the segregation practices of solid waste in the selected municipal corporations.

Alternative hypothesis: There is a significant relationship between the education level of residents and segregation practices of solid waste in the selected municipal corporations.

The research tool used in this study was a questionnaire administered to residents of the municipal corporation. The primary objective of this study is to evaluate the efficacy of SWM procedures and policies among different municipal corporations in north coastal Andhra Pradesh. In this context, a timeline was created by the researchers to gather insights into public perceptions and attitudes toward the application of SWM policies and strategies in the selected municipal corporation areas.

For data analysis, Excel spreadsheets and SPSS-18 were used. The full set of data was examined using statistical tests such as the F-test, Chi-square test, Spearman rank correlation, cross-tabulation, and percentage analysis.

2.2. Sampling design

The selection of municipal corporations was guided by two primary criteria: (i) accessibility for researchers to conduct fieldwork effectively, and (ii) the presence of significant waste management in the region. Based on these criteria, the municipal corporations in the districts of Visakhapatnam, Vizianagaram, and Srikakulam were selected for the study and size of the sample shown in Table 1.

3. Results

3.1. Data analysis I

H_{01}: There is no significant difference in stakeholders' perceptions regarding the type of solid waste generated in their households across the selected municipal corporations.

Table 2 displays the perceptual variations regarding the types of solid waste generated at home among different demographic groups. Among the three municipal corporations, Visakhapatnam recorded the highest mean perceptive score (12.15), while Srikakulam had the lowest (12.08), with corresponding standard deviations of 3.321 and 3.308. The computed *F*-value (0.033) and *p*-value (0.968) indicate no statistically significant difference in perceptions across the corporations. This suggests a consistent understanding of solid waste types regardless of municipal location.

Table 1. A sample of municipal corporations studied

Districts	Municipal corporation	Residents
Srikakulam	Srikakulam	200
Vizianagaram	Vizianagaram	200
Visakhapatnam	GVMC	500
Total		900

Source: Municipal Corporation profiles of Srikakulam, Vizianagaram, and Visakhapatnam (2021).
Abbreviation: GVMC: Greater Visakhapatnam Municipal Corporation.

In terms of gender, males reported a slightly higher mean score (12.18) than females (12.07), with standard deviations of 3.291 and 3.36, respectively. However, the *p*-value (0.616) and *F*-value (0.501) confirm that this difference is not statistically significant, indicating similar perceptions between male and female respondents.

Regarding marital status, unmarried respondents had a slightly higher mean score (12.27) compared to married respondents (12.09), with standard deviations

Table 2. Differences in stakeholders' perceptions of the type of solid waste generated in households

Demographic groups	Variables	*n*	Mean	Standard deviation	Standard error	*F*-value	*p*-value
Municipal corporations	Srikakulam	200	12.08	3.308	0.234	0.033	0.968
	Vizianagaram	200	12.13	3.363	0.238		
	Visakhapatnam	500	12.15	3.321	0.149		
	Total	900	12.13	3.324	0.111		
Gender	Male	450	12.18	3.291	0.155	0.501	0.616
	Female	450	12.07	3.36	0.158		
Marital status	Married	713	12.09	3.296	0.123	0.659	0.510
	Unmarried	187	12.27	3.434	0.251		
Age	Below 30 years	233	12.24	3.437	0.225	0.177	0.912
	31 – 40 years	325	12.12	3.277	0.182		
	41 – 50 years	152	12.14	3.437	0.279		
	Above 50 years	190	12.00	3.191	0.231		
	Total	900	12.13	3.324	0.111		
Educational qualification	Secondary	84	12.18	3.44	0.375	0.505	0.679
	Higher secondary	207	12.31	3.304	0.23		
	Graduation	382	11.98	3.33	0.17		
	Post-graduation and above	227	12.19	3.3	0.219		
	Total	900	12.13	3.324	0.111		
Occupation	Student	217	12.24	3.449	0.234	0.187	0.945
	Employee	253	12.11	3.134	0.197		
	Business person	220	12.06	3.247	0.219		
	Artisan	105	11.95	3.673	0.358		
	Housewife/unemployed	105	12.24	3.353	0.327		
	Total	900	12.13	3.324	0.111		
Monthly income (Indian Rupees)	Nil	261	12.27	3.258	0.202	0.365	0.873
	<10,000	107	12.16	3.484	0.337		
	10,000 – 20,000	168	12.23	3.353	0.259		
	20,000 – 30,000	146	12.02	3.358	0.278		
	30,000 – 40,000	147	11.85	3.267	0.269		
	40,000 – 50,000	71	12.10	3.373	0.4		
	Total	900	12.13	3.324	0.111		

Table 3. Relationship between the education level of residents and segregation practices in solid waste management in the selected municipal corporations, analyzed using the Chi-square test

Education level	*n*	Bins have a cover		Segregation of dry and wet waste	
		Yes	No	Yes	No
10th grade	84	13	71	41	43
12th grade	207	25	182	123	84
Graduation	382	215	167	184	198
Post-graduation	227	146	81	150	77
Total	900	399	501	498	402

Table 4. Chi-square analysis

Variable	Chi-square	*p*-value @ LOS 5%
Bins have a cover	174.44	0.00001
Segregation of dry and wet waste	21.3876	0.000087

Abbreviation: LOS: Level of significance.

of 3.434 and 3.296, respectively. The *p*-value (0.510) and *F*-value (0.659) suggest no significant difference in perceptions based on marital status.

The average score of 12.24, as reported by the age group under 30, was higher than that of other age groups, while the lowest average score of 12.00 was observed in the age group above 50. Their respective standard deviations were 3.437 and 3.191. Given the p=0.912 and the computed *F*-value of 0.177, the results suggest no statistically significant difference. This finding indicates that there are no appreciable differences in the perceived amount of solid trash produced at home across different age groups.

With respect to educational qualifications, the higher secondary group recorded the highest perception score of 12.31, while the post-graduation and above group had the lowest average score of 11.98. Their standard deviations were 3.304 and 3.33, respectively. The p=0.679 and the computed *F*-value of 0.505 suggests that the observed differences are not statistically significant. This implies that levels of education do not significantly affect perceptions of household solid waste generation.

In terms of occupation, artisans recorded the lowest average perception score of 11.95, while students and housewives/unemployed had the highest average scores of 12.24. The standard deviations were 3.449 and 3.673, respectively. The p=0.945 and the computed *F*-value of 0.187 again indicate no significant difference, suggesting that occupational categories do not meaningfully influence perceptions of household solid waste generation.

Regarding income, the lowest average score of 11.85 was recorded among families earning between Indian Rupees 30,000 and 40,000, while the highest average score of 12 was observed in families with incomes between 10,000 and 20,000. The respective standard deviations were 3.353 and 3.267. The p=0.873 and *F*-value of 0.365 suggest that income level does not significantly influence perceptions of solid waste generated.

Therefore, the null hypothesis – that there are no significant differences in stakeholders' perceptions of the type of solid waste generated in their homes across the selected municipal corporations – is accepted.

3.2. Data analysis II

H_{02}: There is no significant relationship between the education level of residents and the segregation of solid waste in the selected municipal corporations.

Table 3 displays the relationship between the education level of residents and the segregation of solid waste in the selected municipal corporations. In Table 4, a significant relationship was observed between the education level of residents and their responses regarding segregation practices in SWM, specifically, the use of bins with covers (χ^2 =174.44, p=0.00001). A significant relationship was also found between the education level of residents and the segregation of solid waste (χ^2 =21.3876, p=0.000087).

Hence, the null hypothesis is rejected (χ^2 = 21.3876, p = 0.000087). It can be concluded that there is a significant relationship between the education level of residents and the segregation practices of solid waste in the selected municipal corporations.

4. Recommendations

Based on the findings of this study, several initiatives can be made to improve the effectiveness of SWM practices in the selected municipal corporations:

(i) The government should firmly establish educational initiatives and implement a structured waste management hierarchy system within municipal corporations, which all stakeholders must adhere to at every stage of waste generation.

(ii) Public awareness should be increased regarding the proper waste composition, as many residents are not

adequately informed about solid waste treatment facilities. Every resident must be encouraged to actively participate in MSWM systems.

(iii) The Confederation of Indian Industries has recommended the implementation of Extended Producer Responsibility measures. Businesses should adopt these measures, as they also play a crucial role in the success of MSWM.

5. Conclusion

This study contributes to the understanding of the relatively low level of awareness regarding the impact of waste management on sustainable development and sound environmental practices. Developing waste management strategies from the ground up is crucial. The two main aspects of waste management, waste storage, and primary disposal, continue to pose significant challenges for researchers. The findings indicate that in the study region, sustainable collection and disposal methods, proper storage, efficient waste collection systems, and segregation of waste at the household level are essential components of effective MSWM. Techniques such as waste reduction, reuse, recycling, and composting are better adapted to address this issue, considering the types and composition of waste generated by households and businesses. These management strategies should be incorporated into a comprehensive and sustainable waste management framework. Furthermore, the monitoring process must be given careful attention. Current waste management systems should incorporate well-structured waste management initiatives and prioritize public education. Awareness programs should be specifically designed to enhance public understanding of the significance of waste management for sustainable environmental development in the region. Finally, the development of regulatory frameworks and the implementation of additional initiatives should be actively monitored and enforced by the relevant authorities.

Acknowledgments

None.

Funding

None.

Conflict of interest

The authors declare no conflicts of interest.

Author contributions

Conceptualization: Nakka Lakshmi Srikanth
Formal analysis: Nakka Lakshmi Srikanth
Investigation: Neyyila Saibabu
Methodology: Neyyila Saibabu
Writing – original draft: Nakka Lakshmi Srikanth
Writing – review & editing: Neyyala Chaitanya

Availability of data

The data supporting the findings of this study are available from the corresponding author on reasonable request.

References

1. Pongrácz E, Pohjola VJ. Re-defining waste, the concept of ownership, and the role of waste management. *Resour Conserv Recycl*. 2004;40(2):141-153. doi: 10.1016/j.resconrec.2003.12.002
2. Ayres RU, Ayres LW, editors. *A Handbook of Industrial Ecology.* United Kingdom: Edward Elgar Publishing; 2002.
3. Geyer R, Jambeck JR, Law KL. Production, use, and fate of all plastics ever made. *Sci Adv*. 2017;3(7):e1700782. doi: 10.1126/sciadv.1700782
4. Zaman AU, Lehmann S. Challenges and opportunities in transforming a city into a "zero waste city". *Challenges*. 2013;4(2):73-93. doi: 10.3390/challe2040073
5. Hoornweg D, Bhada-Tata P. *What a Waste: A Global Review of Solid Waste Management*. World Bank; 2012. Available from: https://openknowledge.worldbank.org/handle/10986/17388 [Last accessed on 2024 Sep 29].
6. Wilson DC, Velis C, Cheeseman C. Role of informal sector recycling in waste management in developing countries. *Habitat Int.* 2006;30(4):797-808. doi: 10.1016/j.habitatint.2005.09.005
7. Tchobanoglous G, Theisen H, Vigil S. *Integrated Solid Waste Management: Engineering Principles and Management Issues.* United States: McGraw-Hill; 1993.
8. Guerrero LA, Maas G, Hogland W. Solid waste management challenges for cities in developing countries. *Waste Manag*. 2013;33:220-232. doi: 10.1016/j.wasman.2012.09.008
9. Sharholy M, Ahmad K, Mahmood G, Trivedi RC. Municipal solid waste management in Indian cities-A review. *Waste Manag.* 2008;28(2):459-467. doi: 10.1016/j.wasman.2007.02.008
10. *Identification of Tourism Circuits Across India, Interim Report (Revised)-Maharashtra.* Ministry of Tourism, Government of India; 2012. Available from: https://tourism.gov.in/

writereaddata/cmspagepicture/file/marketresearch/tentavelyidentifedcircuitforvariousstates/new/mahrashtra.pdf [Last accessed on 2024 Oct 12].
11. Mehta M, Mehta D. *Performance Benchmarking of Urban Water Supply and Sanitation in Maharashtra: Data Book (2008-09)*. Ahmedabad: CEPT University; 2011. Available from: https://www.pas.org.in/portal/document/resourcesfiles/pdfs/classwisecityprofilesmaharashtra/cityprofilesclasscmaharashtra.pdf [Last accessed on 2024 Oct 14].
12. MOSPI. *Municipal Solid Waste Statistics in India*. Ministry of Statistics and Programme Implementation, Government of India; 2023.
13. IJAMTES. Review on Solid Waste Management in India. International Journal of Advanced Multidisciplinary Technical Education and Science; 2020.
14. NSWAI. *Review on Solid Waste Management Practice in India - A State of the Art.* Maharashtra; National Solid Waste Association of India; 2020.
15. IJEAT. Solid Waste Management Challenges in Visakhapatnam. International Journal of Engineering and Advanced Technology; 2019.
16. Central Pollution Control Board (CPCB). *Annual Report on Solid Waste Management in India. Ministry of Environment, Forest and Climate Change*. Government of India; 2021.
17. Singh R. Municipal solid waste management in the city of Indore: A case study. *Int J Waste Manag Sustain*. 2021;14(3):45-60.
18. Singh S. Solid waste management in urban India: Imperatives for improvement. *J Urban Plan Dev*. 2020;146(4):1-12. doi: 10.1061/(ASCE)UP.1943-5444.0000625
19. Jha AK, Singh SK, Singh GP, Gupta PK. Sustainable municipal solid waste management in low-income group of cities: A review. *Trop Ecol*. 2011;52(1):123-131.
20. Kumar S, Mondal AN, Gaikwad SA, Devotta S, Singh RN. Qualitative assessment of municipal solid waste management in Indian cities. *Environ Sci Pollut Res.* 2004;11(3):196-205. doi: 10.1065/espr2004.05.202
21. *Ministry of Environment and Forests Notification.* New Delhi; 2013. Available from: https://www.indiaenvironmentportal.org.in/files/file/municipal%20solid%20waste%20(management%20and%20handling)%20rules,%202013.pdf [Last accessed on 2024 Oct 05].
22. *Municipal Solid Waste (Management and Handling) Rule*; 2000. Available from: https://www.moef.nic.in/legis/hsm/mswmhr.html [Last accessed on 2024 Oct 16].
23. *Handbook on Scaling up Solid and Liquid Waste Management in Rural Areas, Ministry of Environment and Forests Notification*. The Gazette of India; 2013. Available from: https://www.indiaenvironmentportal.org.in [Last accessed on 2024 Oct 09].
24. *Maharashtra Non-Biodegradable Garbage (Control) Act 2006: Maharashtra Plastic Carry Bags (Manufacture and Usage) Rules 2006, Jawaharlal Nehru National Urban Renewal Mission: Twelfth Finance Commission Recommendations*. Available from: https://www.unep.or.jp/ietc/gpwm/data/t2/is_2_p_policyandregulations_pune.pdf [Last accessed on 2024 Oct 18].
25. Mehta M, Mehta D. *Performance Benchmarking of Urban Water Supply and Sanitation in Maharashtra: Data Book (2008-09)*. Ahmedabad, India: CEPT University; 2011. p. 18. Available from: https://www.pas.org.in/portal/document/resourcesfiles/pdfs/classwisecityprofilesmaharashtra/cityprofilesclasscmaharashtra.pdf [Last accessed on 2024 Oct 20].
26. Sontakke YB. *Report on Environmental Status of Kolhapur Region, Maharashtra.* Regional Officer, MPC Board, Kolhapur, Maharashtra Pollution Control Board. Available from: https://mahenvis.nic.in/Pdf/envreportkolhapur.pdf [Last accessed on 2024 Oct 22].
27. Mugambi JK, Windberg K. *Setting the Groundwork for the Circular Economy: Waste Resource Recovery Prospects.* Naivasha, Kenya. Circular Economy, Pollution, Waste and Pollution; 2020.
28. Sajja GS, Meesala MK. Analysis on waste reduction strategies for retailers among their SCM distributional partners. *J Mod Technol*. 2025;1:150-174.
29. Singh J, Thakur R, Verma P. Solid waste management challenges in Urban India. *Waste Manag.* 2023;154:12-22.
30. UN-Habitat. *World Cities Report 2020: The Value of Sustainable Urbanization. United Nations Human Settlements Programme*. Nairobi, Kenya: UN-Habitat; 2020.
31. World Bank. *What a Waste 2.0*: *A Global Snapshot of Solid Waste Management to 2050.* World Bank; 2018. Available from: https://openknowledge.worldbank.org/handle/10986/30317 [Last accessed on 2024 Oct 06].
32. Gupta S, Mohan K, Prasad R, Gupta S, Kansal A. Solid waste management in India: Options and opportunities. *Resour Conserv Recycl*. 1998;24(2):137-154. doi: 10.1016/S0921-3449(98)00033-0
33. Awasthi M, Agarwal M, Singh R. Urbanization and its impact on urban services: A case study. *J Urban Plan Dev*. 2021;147(3):04021030.
34. Oteng-Ababio M, Ablo A, Wong B. Ghana *Priorities: Cost-benefit Analysis of Urbanization Challenges in Accra, Ghana*. *International Growth Centre Working Paper Series*. Copenhagen Consensus Center; 2020.
35. Omuboye C, Nweke-Eze C. Natural gas utilization: Simulation of steam methane reforming and decarbonization by diethanolamine absorption for hydrogen production in Nigeria. *J Mod Technol*. 2024;1(2):94-105.
36. Indira Gandhi Institute of Development Research. *State of Environment Report: Maharashtra.* Mumbai: Indira Gandhi

Institute of Development Research; 2014. p. 151. Available from: https://moef.nic.in/soer/state/soereporomaharashtra.pdf [Last accessed on 2024 Nov 02].
37. Sasikumar K, Sashi Kumar K, Krishna SG. *Solid Waste Management. Eastern Economy Edition*. New Delhi: Asoke K. Ghosh, PHI Learning Private Limited; 2009. Available from: https://books.google.co.in/books/about/solid_waste_management.html [Last accessed on 2024 Nov 09].
38. United Nations Environment Programme (UNEP). *Global Waste Management Outlook*. Kenya: UNEP; 2015.
39. United Nations Environment Programme. *Solid Waste Management*. Vol. I. United Nations Environment Programme (UNEP). Available from: https://www.unep.org/ietc/portals/136/swmvol1part1chapters1to3.pdf [Last accessed on 2024 Dec 16].
40. *ENVIS Centre on Urban Municipal Solid Waste Management*; 2014. Available from: https://www.nswai.org/index.php [Last accessed on 2024 Oct 08].
41. Srikanth NL, Rao GT. A brief analysis of solid waste management practices among different municipalities in India. *ANVESAK Int J Manag*. 2021;51:103-108.
42. Srikanth NL, Rao GT. Status of municipal solid waste management practices in India. *AIMS J Manag*. 2023;8(2):418.

Asian Journal of Water, Environment and Pollution. Vol. 22, No. 3 (2025), pp. 73-87.
doi: 10.36922/ajwep.6241

ORIGINAL RESEARCH ARTICLE

Comparative environmental impact assessment of traditional and eco-friendly denim trousers manufacturing: A cradle-to-grave life cycle assessment

Kazi Rezwan Hossain and Mohammad Faizur Rahman*

Department of Textile Engineering, Faculty of Engineering, Ahsanullah University of Science and Technology, Dhaka, Bangladesh

***Corresponding author:** Mohammad Faizur Rahman (rashedtex@aust.edu)

Received: November 19, 2024; 1st revised: December 31, 2024; 2nd revised: May 8, 2025; Accepted: May 8, 2025; Published Online: May 27, 2025

Abstract: The denim sector, particularly in developing nations such as Bangladesh, is drawing increasing attention due to its significant environmental impact. Traditional denim production processes involve high water and energy consumption, synthetic chemicals, and unsustainable raw materials, all of which contribute significantly to pollution and resource depletion. While environmentally friendly substitutes are emerging, their overall environmental performance in the local setting remains underexplored. Following ISO 14040/44 standards and the ReCiPe 2016 Midpoint (H) methodology, this research intends to assess and compare the environmental impacts of traditional and eco-friendly denim manufacturing in Bangladesh through a cradle-to-grave life cycle assessment. Seven key impact categories were analyzed: climate change (greenhouse gas emissions), water consumption, terrestrial acidification, eutrophication, land use, fossil resource scarcity, and human toxicity. The functional unit was defined as 1,000 pairs of denim pants. Data were collected through field surveys, interviews, utility records, and secondary databases. Compared to the traditional model, the environmentally friendly scenario demonstrated significant reductions in environmental impacts, including a 30% reduction in climate effect, 64% reduction in water usage, 50% in acidification, 40% in eutrophication, 41% in fossil resource use, and 50% in human toxicity. Although sustainable production required 10% more land, the advantages in other categories outweighed this trade-off. Monte Carlo simulations were conducted to address uncertainty and validate the robustness of the results. This study offers a context-specific dataset for industry players considering investments in sustainable technology and highlights the clear environmental advantages of adopting greener production techniques. These insights can inform targeted policy changes and assist in the larger shift toward environmentally friendly textile manufacturing in developing countries.

Keywords: Life cycle assessment; Denim life cycle; Cradle-to-grave; Eco-friendly; Environmental impact; Environmental sustainability

1. Introduction

Environmental issues have spurred increasing reliance on life cycle assessment (LCA) as a reliable technique for estimating the environmental effects of industrial activities in recent years. Among the sectors under close examination for their environmental impact and resource load, denim production stands out, especially

in developing nations such as Bangladesh.[1,2] The literature reviewed in several studies underscores the need for environmental LCA frameworks, such as those described in the ISO 14040/44 standards, to offer standardized, transparent, and repeatable assessments.[3] These frameworks, under the cradle-to-grave approach, enable a thorough evaluation spanning the entire life cycle – from the procurement of raw materials and manufacturing process through consumption to end-of-life treatment. By defining system boundaries, assigning functional units, and choosing suitable effect categories, the ISO 14040/44 standards provide a structured foundation for environmental LCAs.[4,5] This systematic methodology ensures consistency and comparability across various studies and industrial sectors. Within denim manufacturing, the ISO standards have been exceptionally helpful in identifying environmental hotspots in both traditional and environmentally friendly production techniques.[6,7] Many studies have used these criteria to pinpoint critical phases of denim manufacture where improved chemical management, water usage, and energy consumption could result in an appreciable reduction in environmental burden.[8,9]

Typical environmentally intensive phases in traditional denim manufacturing include cotton farming, chemical-intensive dying – often with indigo – multiple wash cycles with water, and mechanical treatments. These operations are associated with excessive water and energy consumption and substantial pollution outputs.[10] On the other hand, environment-friendly denim manufacturing employs cutting-edge technologies and eco-friendly practices aimed at mitigating these detrimental effects. Innovations such as waterless dyeing methods, enzyme-based treatments, and digital finishing techniques reduce resource inputs and limit hazardous emissions. Several studies have consistently shown that these approaches significantly reduce the environmental impact of denim manufacturing.[11-13]

The cradle-to-grave scope of these assessments, capturing the total environmental impacts from raw material extraction to end-of-life disposal, is vital.[14] In the context of denim manufacturing, a cradle-to-grave strategy emphasizes that the advantages of eco-friendly production extend beyond the manufacturing stage to encompass product use and post-consumption management. For example, while environment-friendly technologies may significantly lower water and energy consumption during manufacturing, these advantages could be negated if downstream operations, such as inadequate waste management or limited recycling, are not concurrently optimized.[15] Accurately capturing the full life cycle impacts and tracking progress in production efficiency and waste management practices depends on this thorough evaluation approach.[16]

Adopting the ReCiPe 2016 Midpoint (H) life cycle impact assessment (LCIA) technique marks a major methodological breakthrough in LCA research.[17] This technique provides a systematic means of assessing environmental effects in several domains, including:

- Climate change (global warming potential): Calculates greenhouse gas (GHG) emissions throughout the life cycle, revealing how different processes contribute to global warming; it evaluates emissions that support acid deposition, compromise soil quality, and influence terrestrial ecosystems.[18,19]
- Terrestrial acidification: Assesses emissions that contribute to acid deposition, impairing soil quality, and affecting terrestrial ecosystems.[20]
- Eutrophication potential assessment: Evaluates the potential of nutrient runoff to trigger excessive algal growth in aquatic environments, thereby disrupting ecosystems.[21]
- Water use: Measures water consumption – especially important in areas facing water shortage.[22]
- Land use: Evaluates the environmental impact of land transformation, such as that required for raw materials manufacturing.[23]
- Fossil resource scarcity (FRS): Assesses the depletion of non-renewable energy resources, especially pertinent in energy-intensive operations.[24]
- Human toxicity potential (HTP): Examines the potential adverse effects on human health due to the industrial use of harmful substances.[25]

Bangladesh offers a unique case study that compares traditional and eco-friendly denim manufacturing techniques, given the prominence of denim production in its textile industry. Driven by economic needs and evolving regulatory frameworks, the sector has historically relied on traditional manufacturing techniques, resulting in substantial resource consumption and significant environmental damage.[26,27] However, recent initiatives in eco-friendly manufacturing have introduced innovative technologies and methods aimed at lowering water and energy use, minimizing chemical emissions, and promoting sustainable waste management. Nevertheless, these developments also highlight the need for further investigations to address operational, financial, and technical obstacles associated with scaling up green technologies within existing manufacturing systems.

Adopting a comprehensive, cradle-to-grave LCA approach – supported by the rigor of the ISO 14040/44

standards and the detailed impact assessments offered by the ReCiPe 2016 Midpoint (H) – provides a clear understanding of the environmental performance of denim manufacturing based on current literature.[28] This methodological integration not only facilitates comparison between eco-friendly and traditional production techniques but also helps pinpoint targeted areas for improvement.

1.1. Research gap

Although many studies have examined environmental LCAs in textile manufacturing, significant gaps remain, especially in comparing eco-friendly and traditional denim manufacturing in Bangladesh. First, despite the application of ISO 14040/44 criteria and the ReCiPe 2016 Midpoint (H) method in several studies, few have combined these frameworks in a comprehensive, cradle-to-grave evaluation encompassing all life cycle stages. Rather than providing a holistic view that connects upstream and downstream effects, current research often focuses on specific life cycle phases. This fragmentation hampers the ability to fully assess the systematic benefits of green innovations in denim production.

Second, while there is extensive LCA research in developed nations, far fewer studies focus on developing countries such as Bangladesh, where adopting eco-friendly manufacturing practices presents unique challenges. This gap is critical, as the environmental performance of eco-friendly methods can vary significantly between developed and developing contexts. In Bangladesh, where industrial practices are evolving rapidly, comparative LCAs that reflect local production conditions and resource constraints are essential. Future research should therefore prioritize context-specific investigations that go beyond merely benchmarking environmental impacts. Instead, studies should consider practical implications to better support the adoption of the LCA approach by textile manufacturers.

2. Methodology

This study followed the ISO 14040/44 guidelines and employed a cradle-to-grave LCA to compare two denim manufacturing scenarios in Bangladesh: A conventional traditional process (S1) and an eco-friendly process (S2). The ReCiPe 2016 Midpoint (H) method, implemented in openLCA (openLCA: Version-2.1, manufacturer-GreenDelta, Country-Germany), was used to evaluate seven impact categories: Climate change, water consumption, terrestrial acidification, freshwater eutrophication, land use, FRS, and human toxicity. In accordance with ISO recommendations, no normalization or weighting was applied. The research framework for this study is illustrated in Figure 1.

Key aspects of the LCA methodology – including the functional unit, system boundaries, life cycle inventory (LCI) data, and impact assessment – are described in the subsequent sections, with a focus on study-specific details.

2.1. Functional unit and system boundary

The functional unit is 1,000 pairs of denim trousers, representing a typical production batch at the factory scale. This upscaled unit captures the aggregated environmental load with mass-producing jeans and provides results relevant to industrial operations. Each pair of denim trousers is made of 100% cotton (approximately 610 g/pair, 3/1 twill, 380 g/m^2 fabric). The S1 and S2 scenarios provide equivalent functional performance – 1,000 jeans with an estimated lifetime of approximately 200 wear-and-wash cycles per garment.

The system boundary is cradle-to-grave (Figure 2), encompassing all stages from raw material extraction to end-of-life. These stages include:

- Raw material production: Cultivation of cotton (mostly outside Bangladesh, with imports from India and Pakistan) and the production of auxiliary materials such as dyes, chemicals, and packaging.
- Textile manufacturing: Spinning of fiber into yarn, weaving, indigo dyeing, and finishing of the denim fabric.
- Garment manufacturing: Cutting, sewing, and assembly of jeans.

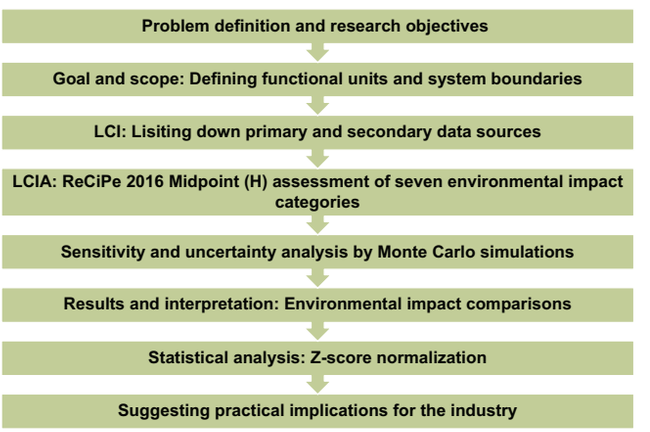

Figure 1. Research framework of the study
Abbreviations: LCI: Life cycle inventory; LCIA: Life cycle impact assessment.

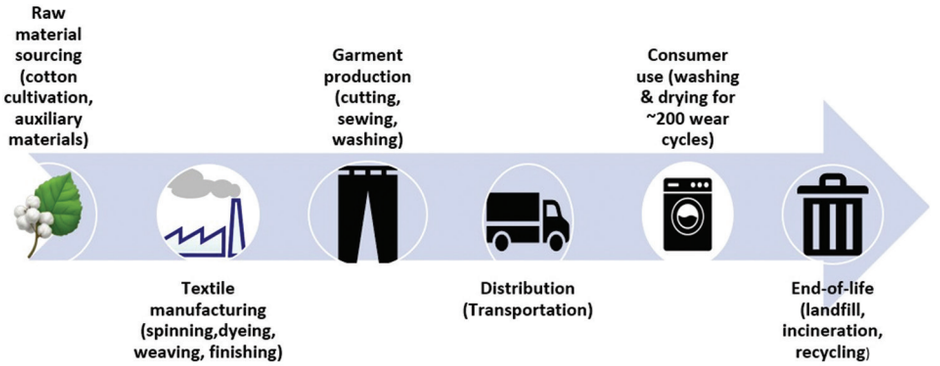

Figure 2. Life cycle stages within the cradle-to-grave system boundary for denim trousers

- Distribution: Transport of materials and final products, including the shipment of cotton to the factory and delivery of finished pants to consumers.
- Use phase: Consumer use of the jeans, including laundering (washing and drying) over their lifespan. Typical consumer behavior was assumed, with washing after approximately every 10 wears in warm water and occasional machine drying. This behavior was considered identical for both scenarios. A total of 200 wear-and-wash cycles per garment was used for the assessment.
- End-of-life: Disposal of jeans following their useful life, based on a representative disposal mix comprising landfilling, incineration with energy recovery, and recycling. In the base scenario, most discarded denim is assumed to be landfilled (reflecting current practices), with smaller fractions incinerated or recycled.

Infrastructure and capital equipment were excluded from the system boundary, which was in line with standard LCA practice, to focus on operational flows. This comprehensive scope ensures that improvements in one life cycle stage do not lead to unintended burdens shifting to other stages. Figure 2 schematically illustrates the system boundaries and processes considered in this LCA.

2.2. LCI data and data collection

A detailed LCI was compiled for each life cycle stage, quantifying all significant inputs (materials, water, and energy) and outputs (emissions and waste) per 1,000 pairs of jeans. Primary data were collected from real production facilities in Bangladesh to ground the LCA in local industrial conditions. In total, two representative denim factories were considered: S1 scenario reflecting typical cotton farming practices using synthetic fertilizers and pesticides, conventional indigo dyeing techniques, and fossil-fuel-powered energy systems; and S2 scenario using organic cotton with minimal synthetic inputs, water-saving dyeing and finishing techniques, and renewable energy (solar)-based powering systems.

These factories were selected based on comparable production scales and product types to ensure a fair baseline comparison between the two scenarios. Data collection was conducted in mid-2024 through on-site visits, direct measurements, and structured interviews with plant managers and engineers. Information on resource consumption (e.g., water use, energy consumption, and chemical usage) and emissions or waste generation was gathered from facility records (utility data, production logs, and wastewater reports) and through operational observations. To improve data reliability, multiple data sources were cross-checked. For instance, reported fuel and electricity usage were verified against utility invoices and meter readings, while production throughput was confirmed using inventory reports. Discrepancies were clarified through follow-up inquiries.

Secondary data were used for upstream processes and inputs not directly measured at the factories, especially those occurring outside Bangladesh. For example, cotton cultivation and ginning data were sourced from industry reports and the Ecoinvent 3.9.1 LCI database, as Bangladesh imports most of its raw cotton. These data were adapted to the local context wherever possible. In particular, the electricity grid mix for manufacturing was modelled based on Bangladesh's actual energy profile, which is dominated by natural gas, with smaller contributions of oil, coal, and renewables, rather than using a generic or foreign grid mix. Similarly, fuel use and transport distances were adjusted to reflect local logistics, such as ocean freight for imported cotton and road transport within Bangladesh. Upstream agricultural data (e.g., fertilizer

and pesticide use for cotton farming) were based on Ecoinvent datasets for cotton-producing countries relevant to Bangladesh's supply chain, such as India. These were assumed to be representative of the cotton used in both scenarios. All assumptions were made to approximate Bangladeshi supply chain conditions as accurately as possible. Allocation procedures followed default principles embedded in the secondary data sources. For instance, the environmental impacts of cotton farming were economically allocated between cotton fiber and cottonseed. No further allocation was necessary within the manufacturing stages, as these processes primarily yield the denim product. Reusable waste (e.g., cotton scrap) was treated under a cut-off approach, with no credit assigned for recycling.

Table 1 presents the LCI details for major inventory flows of S1 and S2. In summary, the production of 1,000 pairs of traditional denim pants (S1) required approximately 800 kg of raw cotton fiber (610 kg incorporated into the final products plus additional material to cover processing losses), 2,500 m^3 of water (primarily for cotton irrigation and fabric washing), and significant energy inputs in the form of electricity and heat. The S1 factories relied on grid electricity and natural gas-fired steam boilers. The S2 scenario followed a similar process flow but with cleaner inputs. Organic cotton – often rain-fed and grown without synthetic pesticides or fertilizers – was used. The process incorporated water-saving dyeing technologies (e.g., water recycling units and reduced wash cycles) and partially substituted renewable energy sources (e.g., solar photovoltaic systems) for manufacturing electricity. Consequently, the S2 inventory showed reduced freshwater use for agriculture and processing, lower chemical usage (especially of hazardous substances), and decreased fossil fuel consumption.

Both scenarios assumed identical distribution logistics, use-phase behavior, and end-of-life treatment pathways to ensure an unbiased comparison. LCI data of manufacturing phases – including yarn production, dyeing, fabric finishing, and garment assembly – were collected directly from Bangladeshi industries for S1 and S2. Data for cotton cultivation, transportation, and the use phase were adapted from the Ecoinvent database, the Textile Exchange database, and published literature.[29-32]

2.3. LCIA method

The ReCiPe 2016 Midpoint (H) characterization method was used to convert the LCI flows into environmental impact indicators for impact assessment. The seven selected midpoint categories capture a range of environmental concerns: climate change (100-year global warming potential, expressed in kg CO_2-equivalents);[33,34] water consumption (blue water use, measured in m^3)[35] terrestrial acidification (emissions contributing to acid rain, reported in kg SO_2-equivalents),[36] freshwater eutrophication (nutrient pollution in aquatic ecosystems, measured in kg P-equivalents)[37] land use (agricultural land occupation, reported in m^2 year),[38] FRS (depletion of fossil fuels, expressed in kg oil-equivalents),[39] and HTP (potential human health effects from chemical exposure, measured in kg 1,4- dichlorobenzene -equivalents).[25] All calculations were performed using openLCA, with background processes sourced from the Ecoinvent 3.9.1 database. ReCiPe's default characterization factors were applied for each flow. No normalization or weighting was applied, in line with the ISO 14040/44 guidelines, and results are reported in absolute terms for each category. This approach ensures that each impact category can be examined on its own merit, and potential trade-offs between categories can be observed.

2.4. Sensitivity analysis

To test the robustness of our conclusions against key assumptions, targeted sensitivity analyses were conducted on consumer use behavior and energy sourcing in manufacturing. First, we examined how varying the frequency of washing in the use phase would affect the outcomes. We considered a moderate laundering rate (each pair worn approximately 10 times before washing). In the case of high wash frequency, the impact increases. The variability in washing frequency reflects differing consumer habits. While the use phase was not the primary focus of differences (as it was initially assumed to be the same for S1 and S2), this check helps determine whether an aggressive change in user behavior could overshadow manufacturing improvements.

Second, we explored the effects of renewable energy adoption in manufacturing. While S2 already incorporated some renewable energy, we compared it with a case where both scenarios rely entirely on fossil-based grid energy. This allowed for the assessment of the maximum potential benefit of cleaner energy. Energy-related emissions (CO_2, SO_2, etc.) and fossil resource use were adjusted according to different energy mix assumptions, and the resulting impacts on the climate change and FRS categories were evaluated. This sensitivity analysis directly addresses how much of the improvement in S2 is driven by energy choices and what additional gains are possible.

Table 1. Life cycle inventory (LCI) for traditional (S1) and eco-friendly (S2) denim production (per 1,000 pairs of denim trousers)

Phase	Input/flow	S1	S2
Cotton cultivation	Cotton fiber (kg)	820	820
	Land use (m^2/year)	2,500	2,750
	Irrigation water (m^3)	2,500	150 (mostly rain-fed)
	Synthetic fertilizer (kg)	150	0
	Pesticides (kg a.i.)	5	0
	Diesel fuel – field operations (L)	15	15
Yarn manufacturing	Electricity (kWh)	10,000	8,000
Yarn dyeing and fabric manufacturing	Electricity (kWh)	6,000	5,000
	Natural gas – process heat (m^3)	450	200
	Water (m^3)	2,000	1,000
	Indigo dye (kg)	12.4	7.6
	Caustic soda (kg)	13	7.5
	Sodium hydrosulfide (kg)	6.7	4.1
	Wetting agent (kg)	6.3	3.8
	Acetic acid (kg)	1.8	1.1
	Sequestering agent (kg)	1.2	0.7
	Sizing agent (kg)	42	29
	Softener (kg)	3	1.8
Garment manufacturing	Electricity (kWh)	640	520
	Natural gas – washing heat (m^3)	230	0
	Water (m^3)	200	50
	Enzyme (kg)	30	10
	Pumice stone (kg)	480	0
	Anti-back staining agent (kg)	12	7
	Soaping agent (kg)	12	9
	Softener (kg)	34	25
	Acetic acid (kg)	6	3.5
Transportation	Diesel fuel – freight (L)	40	40
Consumer use	Washing water (m^3)	800	800
	Electricity – laundry/ironing (kWh)	1,000	1,000
	Detergent (kg)	200	200
End-of-life	Diesel fuel – waste transport (L)	5	5
	Solid waste (kg to landfill)	820 (100% landfill)	820 (100% landfill)

These sensitivity analyses aim to identify the critical parameters – consumer habits and energy profile – that influence the comparative results beyond the core scenario definitions. The methodology thereby not only compares two static scenarios (S1 versus S2) but also considers dynamic factors and potential improvements that could be made by either end users or manufacturers.

2.5. Uncertainty analysis

Instead of relying on classical statistical tests – not standard for LCA results since they are model outputs and not sampled data – we performed an uncertainty analysis to assess the confidence in our comparative findings. We applied the Monte Carlo simulation (1,000 iterations) in openLCA by assigning reasonable uncertainty ranges to key inventory parameters.[40] For

example, we assumed ±10% variation in energy and water consumption values to reflect measurement uncertainty and operational variability, and a wider uncertainty (±20% or more) for processes such as cotton agriculture yields and emissions, which can vary significantly year-to-year. During the Monte Carlo analysis, input values were randomly sampled from assumed distributions (using default log-normal uncertainty factors from Ecoinvent where available, and expert judgment for others), and the impact results for S1 and S2 were recalculated for each iteration. This produced a distribution of possible outcomes for each impact category under both scenarios. We then examined the extent of overlap between the S1 and S2 result distributions for each impact category.

The Monte Carlo results confirmed that the S2 scenario's advantages are statistically robust. In all evaluated categories except land use, the impacts of S2 were lower than S1 in over 95% of the simulations. In other words, even when accounting for uncertainties in the data, it is highly unlikely that S2 would perform worse than S1 in those categories. For land use, the results exhibited greater overlap between scenarios: in approximately half of the simulations, S2 showed slightly higher land use than S1, primarily due to variability in organic cotton yields. In simulations where more favorable assumptions were made – such as higher organic yields or the adoption of improved farming practices – S2's land use was comparable to, or even marginally lower than, that of S1. Nonetheless, the difference in land use remained relatively minor in magnitude and did not outweigh the substantial environmental benefits demonstrated by S2 across the other impact categories. Overall, the uncertainty analysis indicates that our findings are reliable. The probability that the S1 scenario might outperform the S2 scenario in any impact category is very low.

3. Results and discussion

3.1. Life cycle impact comparison between traditional and eco-friendly denim manufacturing approaches

The life-cycle impact results for the two scenarios (per 1,000 pairs of jeans) are summarized in Table 2 and illustrated in Figure 3. Overall, the S2 scenario achieved notably lower impacts than the S1 scenario across nearly all categories. S2 outperformed S1 in six of the seven impact categories, with approximately 30% lower GHG emissions, 64% lower blue water consumption, 50% lower terrestrial acidification potential, 40% lower eutrophication potential, 41% lower fossil resource depletion, and 50% lower HTP. The only category where S2 did not improve upon S1 was land use, which showed S2 showed a slight increase (~10%) in required land area. These differences reflect the influence of the sustainable practices implemented in S2's life cycle.

For the climate change (GHG emissions) category, S1 generates an estimated 20,000 kg of CO_2-equivalent emissions per 1,000 pairs of jeans, whereas S2 produces approximately 14,000 kg of CO_2-equivalent for the same functional unit, achieving a 30% reduction in carbon footprint. This significant drop is largely explained by S2's cleaner energy mix and higher energy efficiency. S1 relies on thermal energy from gas/diesel and electricity from a national grid dominated by natural gas, powering the energy-intensive production phases and contributing heavily to GHG emissions. In contrast, S2 utilizes more efficient machinery and renewable energy (e.g., solar power), directly reducing CO_2 emissions. Replacing a portion of fossil fuels with low-carbon alternatives in S2 further supports this reduction. On a per-unit basis, S2 emits around 14 kg CO_2 versus 20 kg CO_2 per pair of jeans in S1 – a 6 kg CO_2 saving per denim item. From

Table 2. Summary of life cycle environmental impact results for 1,000 pairs of denim trousers under traditional (S1) versus eco-friendly (S2) scenarios, across key impact categories

Impact category	Unit (per 1,000 pairs)	S1	S2	Changes in S2 realtive to S1 (%)
Climate change	kg CO_2-eq	20,000	14,000	−30
Water consumption	m^3 freshwater	5,500	2,000	−64
Terrestrial acidification	kg SO_2-eq	100	50	−50
Eutrophication	kg PO_4^3-eq	7.5	4.5	−40
Land use	m^2	2,500	2,750	+10
FRS	kg oil-eq	5,600	3,300	−41
HTP	kg 1,4-DCB-eq	1,200	600	−50

Abbreviations: DCB: Dichlorobenzene; Eq: Equivalents; FRS: Fossil resource scarcity; HTP: Human toxicity potential.

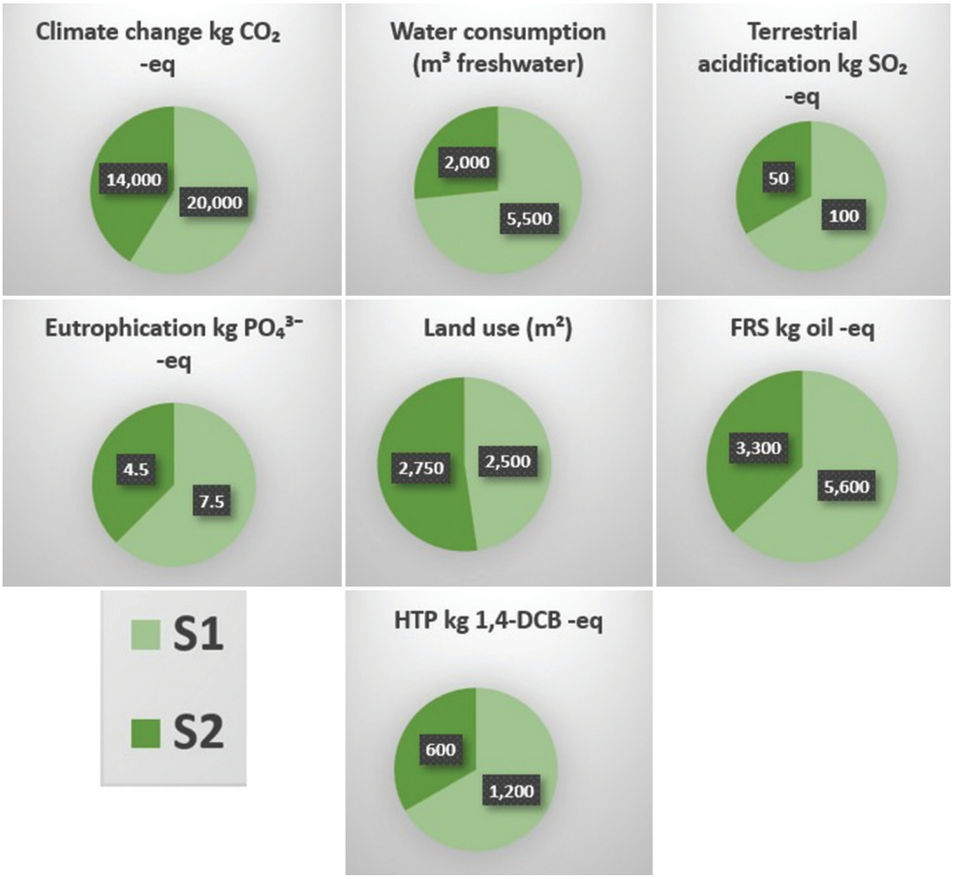

Figure 3. The life-cycle environmental impact results for traditional (S1) versus eco-friendly (S2) scenarios. Data for all categories is presented as per 1,000 pairs of jeans.
Abbreviations: DCB: Dichlorobenzene; Eq: Equivalents; FRS: Fossil resource scarcity; HTP: Human toxicity potential.

an industry standpoint, this represents about 6 metric tons of CO_2 avoided per 1,000 jeans. For Bangladesh's fossil-fuel-driven textile business, these results show a significant way to reduce the industrial carbon footprint through renewable energy adoption and efficiency improvement.

The water consumption category shows the most dramatic difference between the scenarios. S1 requires 5,500 m^3 of freshwater to produce and use 1,000 pairs of denim trousers, compared to just 2,000 m^3 in S2 – a 64% reduction. The S1 system is highly water-intensive due to two main factors: (1) reliance on irrigation for cotton cultivation, which demands vast amounts of water, and (2) wet processing stages such as dyeing and washing, which use and discharge a lot of water. However, S2 mitigates both sources as organic cotton is primarily rain-fed or more efficiently irrigated. Moreover, S2's factory-level water conservation, such as the reuse of indigo dye baths and recycling of rinse water, significantly reduces water intake. This results in a net savings of approximately 3,500 m^3 of water per 1,000 jeans. It is important to note that the consumer use phase (home laundering) also uses water in both scenarios. However, since identical laundry habits were assumed for both, the observed difference stems from the production phase. Even with typical consumer behavior, S2's total water use remains much lower due to its upstream savings.

For the terrestrial acidification category, associated with emissions such as SO_2 and nitrogen oxides that contribute to acid rain, S2 performs substantially better. S1 has a cradle-to-grave acidification potential of about 100 kg SO_2-equivalents per 1,000 pairs of jeans, whereas S2 registers roughly 50 kg SO_2-equivalents. This 50% reduction is primarily due to differences in energy sources and agricultural practices. In S1, burning fossil fuels – coal or diesel in power plants and natural gas in boilers – emits SO_2 and nitrogen oxides, whereas fertilizer use in

conventional farming generates ammonia, all of which contribute to acidification. S2 reduces both sources by shifting to renewable energy and eliminating synthetic fertilizers through organic farming, which also avoids ammonia volatilization. As a result, S2 effectively halves the acidification impact, reducing environmental risks such as soil degradation and forest damage.

Eutrophication potential, which represents nutrient pollution in water bodies, is also notably reduced in S2: 4.5 kg phosphate-equivalents per 1,000 jeans versus 7.5 kg phosphate-equivalents in S1, reflecting a roughly 40% decrease. This improvement stems from reduced fertilizer runoff and better wastewater management. In S1, conventional cotton farming uses synthetic fertilizers, leading to nitrogen and phosphorus runoff into waterways, while factory discharges contribute additional nutrient loads, leading to freshwater eutrophication. S2's organic farming practices use manure or compost instead of synthetic fertilizers, which release nutrients more slowly and are less prone to leaching. Moreover, S2 factories are likely to use more advanced effluent treatment and fewer harmful chemicals, reducing the chemical oxygen demand and nutrient load of discharged water. Since the consumer use phase contributes minimally to eutrophication, the gains in S2 are driven primarily by improvements in agriculture and manufacturing.

The land use impact category presents a more nuanced result. S2 requires slightly more agricultural land area than S1 to produce the same quantity of cotton fiber, with an estimated 10% higher land occupation per 1,000 pairs of jeans. This is attributed to typically lower yields of organic cotton due to the usage of fertilizers and pesticides. However, this trade-off comes with qualitative environmental benefits. The land used in S2 is managed without toxic chemicals, supporting better soil health, biodiversity, and long-term productivity. Importantly, land use was the only category in which S2 did not show improvement, and the magnitude of the difference was relatively minor. Given the substantial gains in water use, climate impact, and toxicity reduction, this slight increase in land use may be considered an acceptable trade-off. The overall results reinforce that S2 delivers a strongly positive net sustainability performance across multiple dimensions.

The HTP results underscore another important benefit of the eco-friendly approach. S1 had a much higher toxicity score (1,200 kg 1,4-DCB-equivalents per 1,000 jeans) compared to S2 (around 600 kg 1,4-DCB-equivalents), indicating a 50% reduction in potential human health risk. The HTP category aggregates the emissions of harmful substances – including heavy metals, carcinogenic chemicals, and pesticide residues – in terms of their potential harm to humans. The traditional S1 scenario involves heavy use of synthetic pesticides and insecticides in cotton farming. In addition, chemicals used in S1's dyeing and finishing (e.g., chromium-based dyes and formaldehyde-based finishing resins) can contribute to toxicity if not fully captured or treated. In contrast, S2 eliminates toxic agrochemicals using organic cotton and emphasizes eco-friendly processing practices. Hazardous chemicals are replaced with eco-friendly alternatives – such as biodegradable enzymes instead of toxic oxidizing agents – and S2 facilities typically have better effluent treatment systems, reducing residual chemical discharges. As a result, S2 cuts human-toxic emissions by half. In regions such as Bangladesh, where mismanagement of industrial chemicals is a known concern, this reduction could translate into meaningful improvements in public health. Beyond climate and resource benefits, S2 offers significantly safer chemical management, reinforcing its value as a more sustainable alternative.

Finally, the FRS indicator further highlights the energy transition benefits of S2. S1 depletes an estimated 5,600 kg of oil-equivalent of fossil resources per 1,000 jeans, whereas S2 uses about 3,300 kg of oil-equivalent, a reduction of roughly 41%. This metric reflects all crude oil, natural gas, and coal used throughout the life cycle. The manufacturing stages in S1 directly or indirectly burn significant fossil fuel: from the natural gas in boilers and diesel in generators and trucks, to petrochemical-based dyes and materials. S2 reduces these dependencies through several pathways: Solar energy partially offsets grid electricity, some process heat is sourced from biomass or reduced through efficiency, and overall energy consumption is lower. Consequently, S2 conserves about 2.3 tons of fossil resources per 1,000 jeans. This not only helps reduce lower CO_2 emissions but also eases pressure on finite energy reserves – an important consideration for long-term sustainability. The result aligns with broader studies suggesting that renewable energy integration in apparel manufacturing can significantly reduce fossil resource dependency.

Taken together, the comparative results show that the S2 scenario consistently delivers environmental improvements across the denim life cycle compared to the S1 scenario. The only notable trade-off is a slight increase in land use in S2. In all other categories, the S2 shows substantial reductions, typically ranging from 30% to 60%. This indicates that implementing sustainable practices in

denim manufacturing does not simply shift environmental burdens from one category to another but genuinely reduces the total environmental footprint. Figure 4 shows the percentage change in the environmental impacts between the scenarios, clearly illustrating the scale of improvement in S2. A normalized bar chart in Figure 5 offers a more robust comparison between the scenarios.

Figure 6, a Z-score-normalized radar plot, compares the impact category profiles of S1 and S2. Both scenarios show climate change as a major contributor (positive Z-score), whereas categories such as eutrophication and terrestrial acidification fall below the mean (negative Z-score). The S2 profile is generally "pulled inward" in most categories, reflecting its overall lower impacts. The only exception is land use, where S2's Z-score is less negative than S1's, indicating its greater relative significance within S2, despite being the only absolute increase among impact categories as shown in Table 2.

3.2. Robustness of findings: Sensitivity and uncertainty analysis

To assess the reliability of the comparative results, we conducted sensitivity and uncertainty analyses, which collectively confirm that our conclusions are robust under a range of assumptions and data variability. We tested whether the environmental advantages of the S2 scenario persist under varying conditions by adjusting key parameters, such as consumer washing frequency and energy sourcing (as detailed in the Methodology section). The analysis consistently showed that S2 maintains an environmental edge over S1. For instance, when we intensified the frequency of washing in the use phase (a "worst-case" user behavior scenario), the total life-cycle energy and water consumption increased for both S1 and S2. In this extreme case, the use phase impacts started to dominate the environmental footprint, diluting the relative contribution of the manufacturing differences. Even so, S2 still had a lower overall footprint than S1 in all categories. The

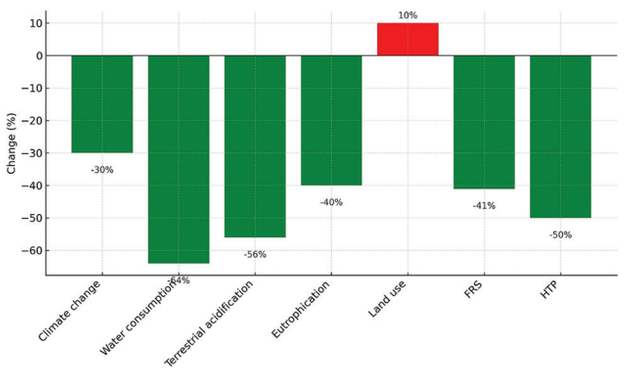

Figure 4. Environmental impact comparison between traditional (S1) and eco-friendly (S2) scenarios. Data are presented as percent change in S2 relative to S1. Abbreviations: FRS: Fossil resource scarcity; HTP: Human toxicity potential.

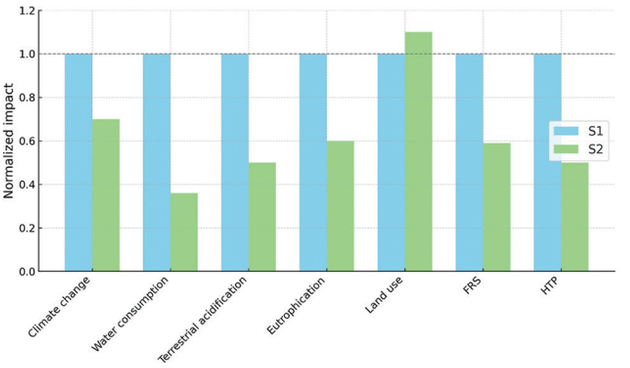

Figure 5. Normalized environmental impacts of denim manufacturing in traditional (S1) and eco-friendly (S2) scenarios. Notes: Normalized value = (Category impact result)/(Normalization reference value). By dividing the LCIA result by a normalization factor, each impact category's score becomes unitless. For example, CO_2-equivalents (kg CO_2-eq) or water use (m^3) are each divided by a corresponding reference burden (e.g., total annual emissions or water use per capita), so the normalized scores have no attached units. In the figure, the traditional denim scenario (S1) has been normalized to 1.0 in every category. This means S1's raw impact in each category was used as the divisor for normalization. Consequently, the eco-friendly denim scenario (S2) shows values equal to the ratio of S2 to S1. In other words, a normalized value of 0.7 for S2 in a given category indicates that S2's impact is 70% of S1's impact (30% lower), whereas a value of 1.1 would indicate 110% (10% higher) than the traditional baseline. These normalized numbers, therefore, represent relative performance, with 1.0 as the benchmark: S2 values below 1 mean reduced impact compared to S1, and values above 1 mean increased impact. In normalized results, a category with a higher value has a relatively larger contribution to the reference burden, and the scale is consistent across categories. This makes it easy to compare the environmental performance of S1 and S2.
Abbreviations: DCB: Dichlorobenzene; Eq: Equivalents; FRS: Fossil resource scarcity; HTP: Human toxicity potential.

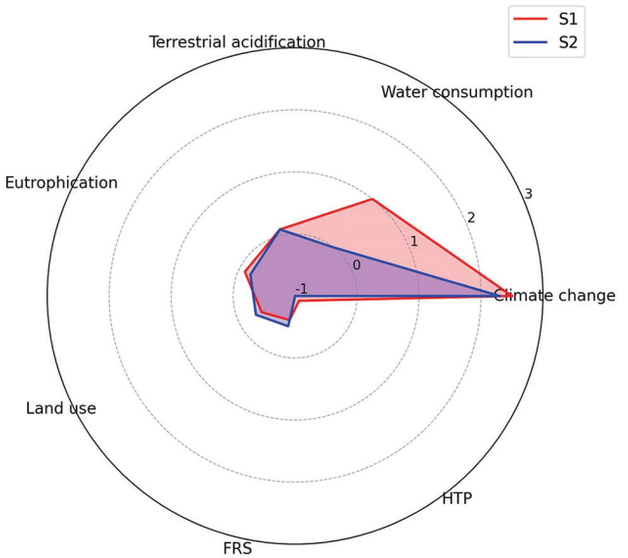

Figure 6. Z-score normalized impact comparison between traditional (S1) and eco-friendly (S2) scenarios. S1 profile is marked in red, whereas S2 is presented in blue. Each axis represents one impact category, standardized by mean and variance to allow relative comparison. Points closer to the outer edge indicate categories where the impact exceeds the scenario's average.

Abbreviations: FRS: Fossil resource scarcity; HTP: Human toxicity potential.

absolute gap between the scenarios narrowed, but the ranking remained unchanged. Conversely, assuming very infrequent laundering (representing highly eco-conscious behavior), the absolute impacts decreased for both S1 and S2, yet the percentage difference between them remained nearly constant. This suggests that the relative advantage of S2 is not sensitive to moderate variations in consumer behavior.

When examining the role of energy sourcing, we found that it is indeed a significant driver of differences in categories such as climate change and FRS. If S2 were powered entirely by a fossil-based grid – eliminating its use of renewable energy – the GHG advantage over S1 would be reduced, with the emissions gap shrinking from ~30% to under 15%. This indicates that about half of S2's climate benefit arises from its renewable energy use, with the remainder attributed to other factors such as organic cotton and energy efficiency. Similarly, S2's fossil resource savings would diminish if it were not actually substituting renewables for fossil fuels. On the flip side, if S1 were to integrate some renewable energy inputs, the differences between the scenarios would also decrease, but S2 would still maintain an environmental advantage. For categories less dependent on energy sources – such as water use and human toxicity – S2 retained a strong advantage even if energy assumptions were altered. This indicates that the environmental benefits in S2 are robust under different conditions: Even if one factor is less favorable, the combination of improvements in S2 ensures it remains equal to or better than S1. For decision-makers, this means that the superiority of the eco-friendly scenario is not contingent on perfect conditions; even with variations in consumer behavior or energy context, the S2 approach is consistently sound.

The uncertainty analysis further reinforces the reliability of our results. By performing Monte Carlo simulations on the LCI data, we accounted for uncertainties in emissions factors, resource use, and other inputs. As detailed in Table 3, the simulation results show that S2 outperformed S1 in the vast majority of trials across all impact categories. The only exception was land use, where the variability in organic cotton yields occasionally resulted in overlapping or slightly reversed outcomes. However, this uncertainty does not affect the conclusions for other impact categories, where S2's advantage remains clear and statistically robust.

This method of analyzing uncertainty is preferable to applying *p*-values from t-tests on deterministic single-scenario outputs, which can be misleading in LCA contexts. Instead, by simulating a range of plausible inventory values and directly estimating the probability of S2 being environmentally superior, we generated a more meaningful and context-appropriate measure of statistical confidence. These results strengthen our claim that the observed improvements are not artifacts of modeling choices or random fluctuations, but genuine effects tied to the interventions in S2.

In summary, the results demonstrate a clear improvement in environmental performance when transitioning to the eco-friendly denim manufacturing scenario. These improvements are directly linked to the specific interventions implemented in S2 – including sustainable cotton farming, water recycling, and renewable energy use – and are evident across multiple impact categories. Moreover, the benefits are consistent and robust. S2 excels under the baseline conditions and remains better (or at least no worse) under a range of alternative assumptions and uncertainties. Therefore, the study provides strong evidence that adopting eco-friendly practices in Bangladesh's denim industry can substantially reduce environmental impacts without unintended trade-offs.

Table 3. Summary of Monte Carlo uncertainty analysis

Impact category	Probability (%)
Climate change	99.9
Water consumption	99.0
Terrestrial acidification	99.4
Eutrophication	99.9
Land use	0.6
FRS	99.5
HTP	99.2

Note: Each probability represents the likelihood that the environmental impact of S2 is lower than that of S1 for the given category, based on simulated variability in inventory data and impact assessment. Values near 100% indicate very high confidence that S2 performs better environmentally in that category, while values near 0% indicate that S1 performs better. Abbreviations: FRS: Fossil resource scarcity; HTP: Human toxicity potential.

3.3. Practical implications of the findings

This section provides actionable suggestions for how denim manufacturers and the textile industry in general can reduce their environmental impact, using insights from the LCA results. Based on the study's findings, the recommendations give concrete suggestions on specific technologies or practices to invest in. This study's results offer guidance for industry practitioners seeking to improve sustainability in denim manufacturing, as detailed in the following sections.

3.3.1. Investing in water-saving dyeing and finishing technologies

The study revealed that water consumption was strikingly lower in the eco-friendly manufacturing scenario, with a 64% reduction observed. To achieve such reductions, factories can adopt modern dyeing techniques that use less water. For example, low liquor ratio dyeing machines, foam or spray dyeing technology, and waterless dyeing (such as supercritical CO_2 dyeing) can greatly reduce the water required per fabric unit.[41] In addition, implementing water recycling and reuse systems can reclaim water from rinse baths or wastewater treatment for use in non-critical processes.

3.3.2. Installing and upgrading effluent treatment plants (ETPs)

The LCA results showed the eco-friendly factories had far lower eutrophication impacts (about 40% less) and acidification impacts (~50% less) than traditional factories, which suggests better wastewater management and emissions control in the sustainable process. One practical implication is for factories to ensure they have effective ETPs and pollution control devices. An ETP treats dye-house wastewater by removing excess nitrogen, phosphorus, chemical oxygen demand, and other pollutants, thereby reducing nutrient pollution that causes eutrophication.[42] Upgrading to modern biological treatment stages for nutrient removal, along with adding filtration and recycling units, enables factories to reduce water pollution and reuse treated water, thereby establishing a closed-loop system.

3.3.3. Adopting renewable energy and improving energy efficiency

A more than 30% reduction in GHG emissions in the eco-friendly manufacturing scenario indicates that energy use optimization was likely a major factor contributing to this result. Textile factories are therefore encouraged to invest in renewable energy sources and energy-efficient infrastructure. For instance, installing solar panels on manufacturing rooftops or sourcing electricity from renewable energy providers can help reduce indirect CO_2 emissions. From an efficiency standpoint, switching to energy-efficient motors, compressors, looms, and dryers, and optimizing process energy use – for example, through waste-heat recovery systems and insulation to conserve heat in boilers and drying machines – will help lower fossil fuel use. Many leadership in energy and environmental design-certified factories in Bangladesh already use technologies such as high-efficiency boilers, LED lighting, and solar water heaters.[43]

3.3.4. Using sustainable raw materials and chemicals

The LCA found that the main cause of land use and water consumption is cotton farming. To reduce upstream environmental effects, producers and brands should prioritize more sustainable raw materials. Organic cotton or Better Cotton Initiative cotton, for example, uses more water-efficient irrigation and less synthetic fertilizer and pesticide. Another alternative is adding recycled fibers, such as recycled cotton or polyester from plastic bottles, into denim, thereby lowering the demand for fresh cotton acreage and the related water and land footprint.[28] In addition, manufacturers are advised to use eco-friendly chemicals in processing, such as low-impact dyes, enzymatic treatments instead of harsh chemicals, and to avoid banned substances.

3.3.5. Implementing LCA in decision-making

The study's findings encourage textile businesses to integrate tools such as LCA or carbon footprinting into

their regular decision-making process. One practical step is to conduct internal LCAs when adopting a new technology or material to quantitatively compare environmental impacts. The study demonstrates how LCA pinpoints environmental hotspots such as yarn, fabric, and garment production. Companies can use this insight to target improvements – for example, if fabric production is a major contributor to environmental impact, they might focus on making that stage sustainable through the use of renewable energy or process modifications. Instituting environmental performance monitoring – such as annually computing the carbon or water footprint of product lines – allows companies to track improvements, identify emerging problems, and provide transparent documentation of progress, which is also valuable for sustainability marketing. Adopting environmental management systems (such as ISO 14001:2015) or certification programs (such as the Higg Index and OEKO-TEX STeP) can provide structured frameworks to enhance environmental performance.[44]

4. Conclusion

Using the ISO 14040/44 standards and the ReCiPe 2016 Midpoint (H) methodology, this research offers a thorough cradle-to-grave environmental comparison between traditional and eco-friendly denim manufacturing techniques in Bangladesh. The results clearly demonstrate the significant reductions in environmental impacts – particularly in climate change, water use, toxicity, and fossil energy consumption – achieved through sustainable manufacturing practices. The transition to organic cotton farming, which requires minimal irrigation and avoids synthetic fertilizers, has led to a drastic reduction in water usage and harmful emissions associated with conventional cotton production. Furthermore, the adoption of renewable energy sources and energy-efficient processes in the eco-friendly system has further minimized fossil resource depletion and GHG emissions, positioning it as a more sustainable alternative. Although land use is slightly higher, the overall environmental performance of the eco-friendly scenario is markedly better, providing a viable route toward more responsible textile manufacture. The statistical validation of these findings further reinforces the case for adopting sustainable production technologies. This study not only adds to the limited body of LCA studies specific to developing nations but also provides useful advice for manufacturers, legislators, and environmentalists aiming to improve the environmental performance of the textile industry. It underlines the need for industry-wide transformation, backed by government incentives, stakeholder engagement, and investment in sustainable infrastructure.

Acknowledgments

This research was supported by the AUST Internal Research Grant of Ahsanullah University of Science and Technology. The authors thank the Ahsanullah University of Science and Technology for providing the funds to conduct the research.

Funding

This study is financially supported by the AUST Internal Research Grant of Ahsanullah University of Science and Technology. Grant No. ARP/2022/TEX/03/10.

Conflict of interest

The authors declare no competing interests.

Author contributions

Conceptualization: Kazi Rezwan Hossain
Formal analysis: All authors
Investigation: All authors
Methodology: All authors
Resources: All authors
Writing–original draft: All authors
Writing–review & editing: All authors

Availability of data

Data are available from the corresponding author upon reasonable request.

References

1. Luo Y, Wu X, Ding X. Carbon and water footprints assessment of cotton jeans using the method based on modularity: A full life cycle perspective. *J Clean Prod*. 2022;332:130042. doi: 10.1016/j.jclepro.2021.130042
2. Moorhouse D, Moorhouse D. Sustainable design: Circular economy in fashion and textiles. *Design J*. 2017;20(sup1):S1948-S1959. doi: 10.1080/14606925.2017.1352713
3. Baydar G, Ciliz N, Mammadov A. Life cycle assessment of cotton textile products in Turkey. *Resour Conserv*

Recycl. 2015;104:213-223.
doi: 10.1016/j.resconrec.2015.08.007

4. Periyasamy AP, Wiener J, Militky J. 4 - Life-cycle assessment of denim. In: Muthu SS, editor. *Sustainability in Denim*. *The Textile Institute Book Series*. Sawston: Woodhead Publishing; 2017. p. 83-110.
doi: 10.1016/B978-0-08-102043-2.00004-6
5. Aslund Hedmann E. *Comparative Life Cycle Assessment of Jeans*. Lexington: University of Kentucky Libraries; 2018.
6. Khan AN, Begum MS, Rakib A, Ali A, Ara ZA, Ashadujjaman MM. Lifecycle analysis (LCA) of a white cotton t-shirt and investigation of sustainability hot spots : A case study. *London J Res Sci Natl Formal Volume*. 2018;18(3):21-31.
7. Fidan FŞ, Aydoğan EK, Uzal N. An integrated life cycle assessment approach for denim fabric production using recycled cotton fibers and combined heat and power plant. *J Clean Prod*. 2021;287:125439.
doi: 10.1016/j.jclepro.2020.125439
8. Periyasamy AP, Militky J. Denim processing and health hazards. In: *Sustainability in Denim*. Sawston: Woodhead Publishing; 2017. p. 161-196.
doi: 10.1016/B978-0-08-102043-2.00007-1
9. Mezarcıöz S, Mutlu T, Sarker ME. Effect of sustainable cotton fibers on denim fabric selected properties. *J Natl Fibers*. 2022;19(15):10345-10355.
doi: 10.1080/15440478.2021.1993502
10. Annapoorani SG. 1 - Introduction to denim. In: Muthu SS, editor. *Sustainability in Denim*. *The Textile Institute Book Series*. Sawston: Woodhead Publishing; 2017. p. 1-26.
doi: 10.1016/B978-0-08-102043-2.00001-0
11. Roy Chowdhury AK. *Environmental Impacts of the Textile Industry and its Assessment through Life Cycle Assessment*. Singapore: Springer; 2014. p. 1-39.
doi: 10.1007/978-981-287-110-7-1
12. Samanta KK, Basak S, Chattopadhyay SK. 12 - Environmentally friendly denim processing using water-free technologies. In: Muthu SS, editor. *Sustainability in Denim*. *The Textile Institute Book Series*. Sawston: Woodhead Publishing; 2017. p. 319-348.
doi: 10.1016/B978-0-08-102043-2.00012-5
13. Hossain KR, Majumder S, Parvez M. "Green Merchandising"-a sustainable approach for apparel business: A review paper. Daffodil Int University J Sci Technol 2019;14:48-52.
14. Salazar-Sogamoso LM, Gómez-García MÁ, Dobrosz-Gómez I. Comparative life cycle assessment of sequential chemical and electrochemical processes for the treatment of industrial textile wastewater. *J Solid State Electrochem*. 2024.
doi: 10.1007/s10008-024-05976-6
15. Hackett T. *A Comparative Life Cycle Assessment of Denim Jeans and a Cotton T-Shirt: The Production of Fast Fashion Essential Items from Cradle to Gate*. *Thesis*; 2015. Available from: https://uknowledge.uky.edu/cgi/viewcontent.cgi?article=1008&context=mat-etds [Last accessed on 2024 Aug 23].
16. Fonseca A, Ramalho E, Gouveia A, Henriques R, Figueiredo F, Nunes J. Systematic insights into a textile industry: Reviewing life cycle assessment and eco-design. *Sustainability*. 2023;15(21):15267.
doi: 10.3390/su152115267
17. Aguiar GJA, Almeida LR, Fernandes BS, Gavazza S, Silva GL, Machado Santos S. Use of life cycle assessment as a tool to evaluate the environmental impacts of textile effluents: A systematic review. *Environ Sci Pollution Res*. 2023;30(31):76455-76470.
doi: 10.1007/s11356-023-27785-6
18. Rogelj J, Lamboll RD. Substantial reductions in non-CO_2 greenhouse gas emissions reductions implied by IPCC estimates of the remaining carbon budget. *Commun Earth Environ*. 2024;5(1):35.
doi: 10.1038/s43247-023-01168-8
19. Petchchedchoo P, Petcharaks N, Piratrakul P, Wongmuek K. Analysis of the carbon footprint of academic gowns: A case study of Thai University. *J Curr Sci Technol*. 2024;14(2):46.
doi: 10.59796/jcst.V14N2.2024.46
20. Gade AL, Hauschild MZ, Laurent A. Globally differentiated effect factors for characterising terrestrial acidification in life cycle impact assessment. *Sci Total Environ*. 2021;761:143280.
doi: 10.1016/j.scitotenv.2020.143280
21. Kumar A, Mishra S, Bakshi S, Upadhyay P, Thakur TK. Response of eutrophication and water quality drivers on greenhouse gas emissions in lakes of China: A critical analysis. *Ecohydrology*. 2023;16(1):e2483.
doi: 10.1002/eco.2483
22. Pfister S, Koehler A, Hellweg S. Assessing the environmental impacts of freshwater consumption in LCA. *Environ Sci Technol*. 2009;43(11):4098-4104.
doi: 10.1021/es802423e
23. Schmidt JH, Weidema BP, Brandão M. A framework for modelling indirect land use changes in life cycle assessment. *J Clean Prod*. 2015;99:230-238.
doi: 10.1016/j.jclepro.2015.03.013
24. Cundubey FS, Azgin ST. Comparative life cycle assessment of denim manufacturing: Evaluating conventional VS. Recycled cotton in the context of renewable energy. *J Clean Prod*. 2024;434:140117.
doi: 10.1016/j.jclepro.2023.140117
25. Hertwich EG, Mateles SF, Pease WS, McKone TE. Human toxicity potentials for life-cycle assessment and toxics release inventory risk screening. *Environ Toxicol Chem*. 2001;20(4):928-939.
doi: 10.1002/etc.5620200431
26. Shamsuzzaman M, Kashem A, Muhammad Sayem AS, Khan AM, Shamsuddin S, Islam M. Quantifying environmental sustainability of denim garments washing factories through effluent analysis: A case study in

Bangladesh. *J Clean Prod*. 2021;290:125740.
doi: 10.1016/j.jclepro.2020.125740

27. Rahaman T, Hasan K, Khan SH. Environmental impact measurement and chromatic performance evaluation of denim washing: A comparison to conventional and sustainable approaches for cleaner production. *Environ Sci Pollution Res*. 2025;32(10):6110-6129.
doi: 10.1007/s11356-025-36099-8
28. Khatun M. Life cycle assessment of jeans production using organic and conventional cotton. *Tekstilec*. 2024;67(2):139-150.
doi: 10.14502/tekstilec.67.2023073
29. Materialien RF. The Life Cycle of a Jean. Understanding The Environmental Impact of a Pair of Levi's 501 Jeans; 2015. Available from: https://femnet.de/informationen/materialien-medien/datenbank-der-materialien/materialientextile-materialien/4145-the-life-cycle-of-a-jean-understanding-the-environmental-impact-of-apair-of-levi-s-501-jeans.html [Last accessed on 2024 Jul 15].
30. FitzGerald D, Bourgault G, Vadenbo C, *et al*. *Documentation of Changes Implemented in the Ecoinvent Database v3.10*. Zürich, Switzerland: Ecoinvent Association; 2023.
31. Exchange T. Materials Market Report 2024. Textile Exchange: Lamesa, TX, USA; 2024. Available from: https://textileexchange.org/knowledge-center/reports/materials-market-report-2024/ [Last accessed on 2025 Jan 14].
32. Exchange T. Organic Cotton Market Report. Textile Exchange: Lamesa, TX, USA; 2022. Available from: https://textileexchange.org/knowledge-center/reports/organic-cotton-market-report/ [Last accessed on 2025 Jan 14].
33. Imran S, Mujtaba MA, Zafar MM, *et al*. Assessing the potential of GHG emissions for the textile sector: A baseline study. *Heliyon*. 2023;9(11):e22404.
doi: 10.1016/j.heliyon.2023.e22404
34. Thistlethwaite G, Karagianni E, Collins A, *et al*. *2022 Government Greenhouse Gas Conversion Factors for Company Reporting Methodology Paper for Conversion Factors Draft Report*; 2022. Available from: https://www.nationalarchives.gov.uk/doc/open-government-licence [Last accessed on 2024 Sep 04].
35. Hoekstra AY. A critique on the water-scarcity weighted water footprint in LCA. *Ecol Indic*. 2016;66:564-573.
doi: 10.1016/j.ecolind.2016.02.026
36. Roy PO, Azevedo LB, Margni M, Van Zelm R, Deschênes L, Huijbregts MAJ. Characterization factors for terrestrial acidification at the global scale: A systematic analysis of spatial variability and uncertainty. *Sci Total Environ*. 2014;500-501:270-276.
doi: 10.1016/j.scitotenv.2014.08.099
37. Dong Y, Cheng X, Li C, Xu L. Spatially eutrophication potential and policy implication of nitrogen emission for surface water: A case study in Guangzhou city, China. *J Environ Manage*. 2023;342:118336.
doi: 10.1016/j.jenvman.2023.118336
38. Mattila T, Helin T, Antikainen R, Soimakallio S, Pingoud K, Wessman H. *Land Use in Life Cycle Assessment*. Finland: Finnish Environment Institute SYKE; 2011.
39. Wang J, Azam W. Natural resource scarcity, fossil fuel energy consumption, and total greenhouse gas emissions in top emitting countries. *Geosci Front*. 2024;15(2):101757.
doi: 10.1016/j.gsf.2023.101757
40. Igos E, Benetto E, Meyer R, Baustert P, Othoniel B. How to treat uncertainties in life cycle assessment studies? *Int J Life Cycle Assess*. 2019;24(4):794-807.
doi: 10.1007/s11367-018-1477-1
41. Broadbent PJ, Carr CM, Lewis DM, Rigout ML, Siewers EJ, Shojai Kaveh N. Supercritical carbon dioxide (SC-CO_2) dyeing of cellulose acetate: An opportunity for a "greener" circular textile economy. *Coloration Technol*. 2023;139(4):475-488.
doi: 10.1111/cote.12690
42. Nahar N, Haque S, Haque SE. Groundwater conservation, and recycling and reuse of textile wastewater in a denim industry of Bangladesh. *Water Resour Ind*. 2024;31:100249.
doi: 10.1016/j.wri.2024.100249
43. Radhakrishnan S. Denim Recycling. In: Muthu SS, editor. *Textiles and Clothing Sustainability: Recycled and Upcycled Textiles and Fashion*. Singapore: Springer; 2017. p. 79-125.
doi: 10.1007/978-981-10-2146-6-3
44. Valero-Gil J, Surroca JA, Tribo JA, Gutierrez L, Montiel I. Innovation VS. standardization: The conjoint effects of eco-innovation and environmental management systems on environmental performance. *Res Policy*. 2023;52(4):104737.
doi: 10.1016/j.respol.2023.104737

Asian Journal of Water, Environment and Pollution. Vol. 22, No. 3 (2025), pp. 88-103.
doi: 10.36922/AJWEP025070041

ORIGINAL RESEARCH ARTICLE

Environmental applications of molecular graph learning: Graph neural network based prediction of partition coefficients

Pravinkumar M. Sonsare[1]*, Roshni Khedgaonkar[2], Kavita Singh[2], and Pratik Agrawal[3]

[1]Department of Computer Science and Engineering, Shri Ramdeobaba College of Engineering and Management, Ramdeobaba University, Nagpur, Maharashtra, India
[2]Department of Computer Technology, Yeshvantrao Chavhan College of Engineering, Nagpur, Maharashtra, India
[3]Symbiosis Institute of Technology, Nagpur Campus, Symbiosis International (Deemed University), Pune, Maharashtra, India

(This article belongs to the *Special Issue: Renewable Energy Systems and Strategies in Smart Grids and Smart Cities Development*)

***Corresponding author:** Pravinkumar M. Sonsare (sonsare@gmail.com)

Received: February 12, 2025; 1st revised: February 23, 2025; 2nd revised: March 24, 2025; 3rd revised: April 15, 2025; 4th revised: April 29, 2025; Accepted: April 29, 2025; Published Online: May 29, 2025

Abstract: In cheminformatics, predicting molecular properties is crucial for enhancing material research, toxicity assessment, and drug discovery. This research investigates the use of graph neural networks (GNNs) for predicting molecular properties by examining three different architectures: graph convolutional networks (GCNs), graph isomorphism networks (GINs), and graph attention networks (GATs). Employing molecular graph information, these models are evaluated on the MUTEG dataset and measured against key metrics such as accuracy and area under the receiver operating characteristic curve (AUC). Our experimental findings show that GIN has the highest accuracy at 89.2%, exceeding GCN (87.5%) and GAT (88.3%). GIN also achieves the highest AUC of 0.89, whereas the AUCs of GCN and GAT are 0.84 and 0.86, respectively, indicating GIN's enhanced ability to effectively model graph isomorphisms. We selected GIN for this study because of its proven theoretical and empirical strength in capturing graph-level representations, particularly in domains such as cheminformatics, where molecular structures are naturally modeled as graphs. These results highlight the efficacy of GNNs in predicting molecular properties and position GIN as a favored framework for tasks that demand accurate graph feature extraction. This study further plays a pivotal role in understanding the environmental fate and transport of chemical compounds. We used GIN to identify partition coefficients such as the octanol-water partition coefficient, air-water partition coefficient, and soil–water partition coefficient from the MoleculeNet dataset.

Keywords: Graph neural networks; Molecular property prediction; Cheminformatics; Drug discovery; Structure-property relationships

1. Introduction

Molecular property forecasting is essential to cheminformatics and significantly contributes to various applications, including drug discovery, materials science, and environmental safety evaluation. Precise forecasting of characteristics such as solubility, toxicity, and carcinogenicity can greatly decrease experimental expenses and durations, thereby hastening the advancement of new compounds.[1,2] Predictive modeling presents opportunities and challenges because of the unique graph structure of molecular data, where bonds are depicted as edges and atoms as nodes. Conventional machine learning approaches frequently find it challenging to adequately represent this graph-structured data, highlighting the need for specialized graph learning techniques.

In modeling data that has a graph structure, graph neural networks (GNNs) have emerged as highly efficient tools. They facilitate notable progress in areas such as social networking, transportation, and bioinformatics. In forecasting molecular properties, GNNs have shown exceptional capability by leveraging the inherent relational information present in molecular graphs. GNNs effectively capture the complex interactions among atoms and bonds that influence molecular characteristics by iteratively enhancing node representations through local and global graph structures.

Among the various GNN frameworks, graph convolutional networks (GCNs),[4] graph isomorphism networks (GINs),[5] and graph attention networks (GATs)[6] are notable for their effectiveness and adaptability. GCNs broaden convolutional processes to graph frameworks by gathering data from a node's local surroundings. GINs emphasize identifying graph isomorphisms to guarantee the distinct representation of graph structures. GATs enhance feature aggregation by allocating attention weights to adjacent nodes, enabling the model to focus on the most significant interactions.

The MUTAG dataset[3] serves as a popular benchmark in predicting molecular properties, offering an excellent platform for testing these architectures. It comprises 188 molecular graphs categorized as either carcinogenic or non-carcinogenic, making it appropriate for binary classification tasks. Prior research has utilized different GNNs on this dataset, obtaining top-tier outcomes. For example, Kipf and Welling's GCN showcased the effectiveness of graph convolutions in molecular classification.[4] In the same way, the GIN developed by Xu *et al*. highlighted the significance of identifying graph isomorphisms for precise predictions.[5]

In this study, we conducted a comparative analysis of GCN, GIN, and GAT architectures on the MUTAG dataset to identify the most effective model for molecular property prediction. Our contributions include: (i) a systematic evaluation of GCN, GIN, and GAT on molecular data using metrics such as accuracy and area under the curve (AUC), (ii) insights into the strengths and limitations of each architecture in capturing molecular graph features, and (iii) a comprehensive analysis of the experimental results highlights GIN's exceptional performance and its potential for practical use in cheminformatics.

We further used GIN to find partition coefficients such as octanol–water partition coefficient (K_{o_w}), air–water partition coefficient (K_{a_w}), and soil–water partition coefficient (K_d) from the MoleculeNet dataset to estimate how chemicals behave in the environment, including their solubility, volatility, and degradation pathways. This helps in understanding their movement through air, water, and soil.

The MUTAG dataset provides valuable data for forecasting molecular characteristics using GNN architectures. However, there are concerns regarding the models' scalability and resilience due to their small size and complexity. This research broadens the assessment to more extensive and complex datasets, such as QM9[6] and ZINC[7], to ensure uniform performance across different molecular datasets. Moreover, tests using incomplete and altered data have been conducted to assess the proposed models' robustness in real-world scenarios. These enhancements provide a broader perspective on the appropriateness of GNNs for predicting molecular characteristics.

Quantitative structure-property relationship models have long been used to predict molecular characteristics based on structural attributes.[8] Machine learning models can accurately estimate partition coefficients such as K_{o_w}, K_{a_w}, and K_d using the MoleculeNet dataset.[9] These models employ various methodologies, including GNNs[10,11] and random forest algorithms,[12] to make effective predictions even with minimal experimental data. Furthermore, the integration of multi-fidelity learning[13] with interpretable attribution models[14] enhances both predictive power and model interpretability, leading to more reliable estimations.

The accurate prediction of molecular properties such as partition coefficients is critical for environmental safety assessments, pharmaceutical design, and chemical risk evaluation. These predictions help reduce the time and cost associated with experimental testing, supporting the development of safer and more efficient

compounds. With the increasing availability of curated datasets and advances in deep learning, particularly GNNs, machine learning models now offer a promising alternative to traditional quantitative structure-activity relationship (QSAR) models. This study aims to investigate the applicability of modern GNN architectures to these tasks and assess their reliability across different molecular datasets.

The organization of this paper is outlined as follows: Section 2 explores pertinent studies that illustrate advancements in GNN-based molecular property forecasting. The methodology detailing model architectures, training methods, and dataset preparation is thoroughly explained in Section 3. The findings from the experiment are presented in Section 4, and the discussion of those results is in Section 5. The conclusion and potential future study topics are presented in Section 6.

2. Literature review

Predicting molecular properties has been a persistent challenge in computational chemistry, driven by the necessity to uncover essential molecular characteristics that affect properties such as carcinogenicity, solubility, and toxicity. The prediction of molecular properties has greatly enhanced due to the progress of machine learning methods, especially GNNs. This segment provides a comprehensive review of the current literature regarding molecular property prediction utilizing GNNs, emphasizing their usage, effectiveness, and architectural advancements.

Before the introduction of GNNs, conventional machine learning models such as random forests, support vector machines, and feed-forward neural networks were widely utilized for predicting molecular properties. These models demanded manually created molecular descriptors that encompassed physicochemical properties and structural fingerprints (e.g., extended-connectivity fingerprints). These methods frequently did not succeed in representing the intricate relational framework of molecular graphs. For instance, Duvenaud *et al*. presented a model that directly learned molecular fingerprints from data through deep convolutional architectures, highlighting an early transition from manually crafted features to learnable representations.[15] Nevertheless, these approaches did not possess the capability to fully utilize graph structure, since they were not specifically created for graph-structured information.

In graph-based molecular modeling, molecules are abstracted as graphs where atoms are represented as vertices (nodes) and bonds as edges. This graph structure allows GNNs to propagate information through bonded atoms, capturing both topological and chemical features essential for property prediction. GNNs offer a revolutionary method for predicting molecular properties by allowing for the direct handling of graph-structured information. The GNN model utilizes a recursive framework to disseminate information across graph structures.[16] Kipf and Welling[4] presented GCNs that generalized conventional convolutions to graphs through the aggregation of information from a node's neighboring nodes, utilizing a normalization approach. GCNs emerged as a favored option for semi-supervised learning tasks, including the classification of molecules. Nonetheless, GCNs frequently faced issues with over-smoothing, resulting in node representations becoming indistinguishable throughout distant neighborhoods.

Xu *et al*.[5] introduced GINs, which enhanced the expressiveness of GNNs by utilizing a sum-based aggregation function. This architecture has proven to be as effective as the test for graph isomorphism. It enables the effective differentiation of non-isomorphic graphs.[17] The attention mechanism is a concept in machine learning, especially in neural networks, that allows a model to dynamically focus on the most relevant parts of the input data when generating output. Originally introduced in natural language processing, it has since been successfully applied in various domains, including GNNs, vision, and cheminformatics. GINs have shown better performance on molecular datasets such as MUTAG, surpassing GCNs in tasks that need accurate structural representation. In the aggregation stage, Veličković et al. proposed GATs that assign trainable weights to local nodes using an attention mechanism.[18]

GATs have proven to be especially useful for datasets where the interactions among particular nodes hold greater significance than the overall structure. Several studies improved GNNs by explicitly including edge characteristics that indicate bond types and lengths within molecular graphs. Schütt *et al*. created the SchNet model, which employed continuous-filter convolutional layers for datasets in quantum chemistry.[19]

The MUTAG dataset has been extensively utilized to evaluate GNNs for predicting molecular properties. MUTAG consists of 188 molecular diagrams depicting nitroaromatic substances. Each is categorized as either carcinogenic or non-carcinogenic. The dataset presents a binary classification challenge that assesses a model's capability to accurately capture molecular graph characteristics. GNNs have likewise been utilized on various datasets, including a quantum chemistry

dataset for property regression tasks such as predicting molecular energy (QM9) and a dataset aimed at forecasting the toxic effects of chemical compounds on biological systems (TOX21).[20]

Multi-fidelity learning, which mixes low-fidelity quantum chemical data with high-fidelity experimental data, has a considerable impact on partition coefficient prediction. For example, multi-target learning obtained a root-mean-square error (RMSE) of 0.44 log P units for a dataset containing molecules comparable to the training data, exhibiting superior accuracy over single-task models.[13] The multi-fidelity log P model, which takes a chemical formula as its sole input, is a useful method for estimating K_{ow} without structural knowledge. This model performed similarly to traditional models with a coefficient of determination (R^2) of 0.77 and an RMSE of 0.52, suggesting its usefulness in cases when structural data is lacking.[21] GNNs with adjusted integrated gradients are highly interpretable in forecasting K_{ow}. These models emphasize the significance of certain atoms in the prediction process, guaranteeing precision, consistency, and stability in attribution assignments.[22]

Machine learning models such as multiple linear regression and random forest regression have been successfully calibrated against external test sets, including the SAMPL9 challenge. These models, along with continuum solvation models, give insights into the molecular characteristics that influence partition coefficients, emphasizing their value in computational chemistry.[23] The study focuses on the use of the created model in forecasting K_d values, proving its efficacy in giving site-specific insights that can benefit environmental risk assessments and pesticide management.[24] The study presents a new descriptor,<q-atom-centered symmetry functions> conformation, which includes explicit polarization effects in polar phases and accounts for energetic and entropic importance in non-polar phases by averaging entropy effects based on the Boltzmann distribution of conformations. This technique improves the prediction of the partition coefficient (log P) between polar and non-polar phases, a critical factor in drug and material design. The model was trained using high-dimensional neural networks on a large public dataset (PhysProp) and showed effective log P prediction across three more datasets. It applies to a number of organic molecules, including n-carboxylic acids and diverse organic solvents, which makes it a useful tool for estimating partition coefficients in varied systems.[25]

The K_{ao} is a key parameter that describes the equilibrium partitioning of a compound between octanol and air, serving as an indicator of its volatility and potential for atmospheric transport. A comprehensive dataset of experimental log K_{ao} values for 2,161 compounds was compiled, which covers a wide range of molecular weights and log K_{ao} values. The model's robustness and predictive capability were validated through various statistical methods, which include training and prediction set separation and mutual leave-50%-out validation.[26] The work introduces a new version of the machine-learning algorithm, PARTYsoc version 3, which measures the proportions of centennially stable and active soil organic carbon (SOC) fractions using Rock-Eval (r) thermal analysis. This model improves on the previous version (version 2) using a bigger dataset from 12 sites, including many long-term studies, and leverages support vector machine regression in conjunction with beta regression to provide more accurate predictions. PARTYsoc version 3 attempts to improve the accuracy of SOC stock development simulations in the high-performance engine model by identifying the best stable SOC stock for each site, resulting in improved SOC compartment initialization. The model performs well in both internal validation and leave-one-site-out validation, confirming its ability to forecast stable SOC proportions.[27]

The K_{ow} represents the ratio of a compound's concentration in octanol to its concentration in water at equilibrium. It is a key descriptor of hydrophobicity and is widely used in environmental fate modeling and bioaccumulation studies. The research focuses on predicting the K_{ow} of organic compounds using extreme learning machine (ELM) models, which are useful owing to their quick learning speed and strong generalization ability. The study uses COSMO descriptors (Sσ-profile) as molecular descriptors to develop and estimate models for K_{ow}. Four ELM models were created and compared to multiple linear regression models with the same descriptors. The results indicated that the ELM models, particularly the ELM-4 model, demonstrate high reliability in predicting log K_{ow} values, which achieves a correlation coefficient R^2 of 0.949 and an RMSE of 0.358, indicating their effectiveness for broader applications in predicting chemical properties.[20] The research examines the partitioning behavior of anionic perfluoroalkyl carboxylic acids (PFCAs) and perfluoroalkyl sulfonic acids (PFSAs) between water and organic phases, stressing that their anionic forms dominate due to low pK_a values. It presents a developed equation that ties the partition coefficients of these anions to their corresponding neutral species, indicating a linear connection that can be used to estimate the

partition coefficients of PFCA and PFSA anions. Furthermore, the study finds a relationship between the neutral K_{o_w} and the neutral membrane-water partition coefficient, implying that the more easily measured log K_{o_w} may be used to predict the log membrane-water partition coefficient. This approach is used to assess experimental data and expand property data for PFCAs and PFSAs with different chain lengths.[28]

The study presents two-parameter linear free energy relationship models that use the log K_{ow} and the dimensionless Henry's law constant (log K_{aw}) to estimate the lipid–water partition coefficients (log K_{lw} and log K_{pw}) of organic chemicals, addressing the current lack of experimental data and time-consuming estimation methods. The developed models have high predictive accuracy, with R^2 values of 0.971 for log K_{lw} and 0.953 for log K_{pw}, and RMSEs of 0.375 and 0.413, respectively. They can be integrated into the United States Environmental Protection Agency's Estimation Programs Interface Suite software to improve its capacity for estimating the environmental properties of organic contaminants.[29] The study assesses the usefulness of continuum solvation models paired with density functional theory approaches in predicting the K_{ow} (log P) for 56 fluorinated medicinal compounds, concluding that the density model produces log P values that are consistent with benchmark data. It was observed that the conductor-like polarizable continuum models struggle with accurately predicting trends, frequently resulting in incorrect sign reversals compared to benchmark values, while the choice of basis set had minimal impact, and the selection of atomic radii influenced geometry convergence.[30] The research proposes a new model for predicting the temperature dependence of the octanol-air partition ratio, which is critical for understanding chemical partitioning in environmental chemistry. The scientists used a large dataset of 195 compounds to create prediction equations for the internal energy of phase transition (ΔU OA°). The study found substantial correlations between variables, with the best prediction model attaining a high adjusted R^2 value. This indicates its usefulness in forecasting neutral organic chemical partitioning behavior across different temperatures.[31]

Related studies have demonstrated the utility of artificial intelligence in complex biological and environmental systems. For instance, artificial intelligence has been used to connect molecular and genotypic data to phenotypic traits in plant development[32] and to monitor the environmental fate of pharmaceutical and personal care products in water systems.[33] These works underscore the potential of artificial intelligence-driven models to infer high-level outcomes from molecular data – a concept that directly supports our approach to predicting environmental partition coefficients from molecular structure.

A previous study reviewed the integration of machine learning with QSAR modeling for drug discovery and environmental assessment. It highlighted advancements in machine learning techniques that enhance QSAR modeling, improving predictions of toxicity and biological activity. The study emphasized the importance of molecular connectivity indices as structural descriptors in QSAR modeling. It discussed the challenges of predicting toxicity due to limited experimental data and the need for accurate models. The paper also addressed the environmental impact of pharmaceuticals and the role of QSAR in assessing chemical risks.[32] The study focused on using aluminum-based electrocoagulation to remove from water. Response surface methodology and machine learning models optimize the electrochemical removal process. The best removal rates achieved were 88.21% experimentally and 93.87% predicted. Key parameters affecting removal include pH, electrode type, initial concentration, and electrolysis time. The adaptive neuro-fuzzy inference system model outperformed other models in predicting experimental results.[33] The study presented 10 recommendations to improve the European Medicines Agency's guidance for environmental risk assessment of pharmaceuticals. Recommendations include assessing antibiotic resistance risks and refining test proposals. The authors emphasized the need for regular updates to incorporate new scientific knowledge. The study highlighted the importance of transparency and emission data in risk assessments. Overall, the recommendations aimed to enhance environmental protection and societal benefits.[34]

Another study discusses the evolution of QSAR studies, emphasizing the significant impact of machine learning methods on this field. It highlights the integration of various machine learning techniques, including deep learning, to improve the prediction of molecular activities and properties, which are crucial for drug discovery. The authors note the challenges faced in QSAR, such as data sparsity and the need for robust experimental datasets, while advocating for collaborative efforts in model sharing among companies to improve predictive accuracy. Overall, the paper serves as a reference for modern QSAR methods and applications propelled by machine learning advancements.[35] The article introduces MetDNA, a process of metabolism network-based recursive method

that improves metabolite identification in unfocused metabolomics without the need for a full spectrum library. MetDNA utilizes initial seed metabolites and their reaction-paired neighbors to expand annotations, achieving approximately 2,000 metabolite annotations from a single experiment. The methodology allows for quantitative assessment of metabolic pathways and supports integrative multi-omics analysis. The study demonstrates the algorithm's effectiveness across various datasets, showcasing its utility in characterizing dysregulated pathways and improving metabolite identification.[36] DTINet, a statistical pipeline, uses multimodal network integration to predict drug-target interactions, boosting the accuracy of predictions and uncovering novel drug-cyclooxygenase protein interactions. This highlights potential implications in inflammation disease prevention.[37]

An additional study discusses artificial intelligence's transformative role in drug discovery, formulation, and pharmaceutical dosage form testing. It highlights artificial intelligence's ability to analyze biological data for targeted drug discovery. Artificial intelligence can optimize research processes, reduce development costs, and enhance drug candidate evaluation. Personalized medicine is facilitated through artificial intelligence, improving treatment outcomes and patient adherence. The review emphasizes the potential of artificial intelligence in enhancing drug development and patient care.[38] The study examines how artificial intelligence may be used in drug development, emphasizing how it can be used to anticipate protein structures and interactions between drugs and targets while tackling issues such as data quality and technology limitations.[39] The study discusses the critical issue of rising sea levels, which are projected to increase by 20 cm by 2050. It highlights the potential displacement of up to 1.2 billion people due to this environmental threat. A high-level United Nations meeting was convened to address the existential threat posed by rising sea levels.[40] Heavy metal concentrations varied widely, with the highest levels observed in iron, manganese, and zinc. The research highlights significant spatial variability in contamination levels influenced by traffic and anthropogenic activities.[41]

Another study employs machine learning to predict water quality, especially total coliform presence, using an Indian dataset. Gradient boosting regression produces good accuracy, with conductivity and temperature playing critical roles.[42] A website called OrthoVenn2 allows users to compare whole-genome orthologous clusters from up to 12 different species. A Venn diagram and an interactive occurrence pattern table are two examples of how the update improves data display. It harbors a wider variety of organisms, such as bacteria, fungi, and vertebrates. For local analysis, users can utilize a standalone version or upload datasets.[43] Updated to version 5.0 with larger genome sets, eggNOG is a publicly accessible database for orthology connections and functional annotations. A total of 4.4 million orthologous groups from 379 taxonomic levels are currently included in the database, along with the corresponding phylogenies and sequence alignments. Despite the growth in genomic data, the quality of functional annotations and orthology assignments is still good at 80% coverage. With enhanced online services and application programming interface searches, users may investigate evolutionary histories and functional annotations.[44]

The Orthologous Matrix database has been updated with new species and improved tools for orthology analysis. New features include Ancestral Genome pages and a Local Synteny Viewer for genomic comparisons. The paper discusses enhancements in search functionality and Gene Ontology annotations for Hierarchical Orthologous Groups. The Orthologous Matrix database is accessible online, providing resources for studying gene families and evolutionary history.[45] OrthoDB is a comprehensive resource for evolutionary and functional annotations of orthologs, covering a vast number of organisms, including eukaryotes, prokaryotes, and viruses, with plans to significantly increase bacterial sampling. The user interface has been enhanced to improve usability, offering three views: A list of orthologous groups, a detailed view of these groups, and a gene-centric view. OrthoDB allows users to upload their data for analysis and provides evolutionary annotations, such as phyletic profiles and evolutionary rates, which are unique to the resource. The resource is publicly accessible, facilitating comparative studies and metagenomics.[46] Another study discusses the significance of QSAR modeling in drug discovery, emphasizing its efficiency in identifying lead candidates. It highlights the need for advanced machine learning algorithms to manage large datasets in QSAR applications. The authors note that successful QSAR projects require interdisciplinary collaboration and critical thinking from scientists. The paper also addresses common pitfalls in QSAR modeling, including a lack of understanding of best practices. Overall, it provides recommendations for improving QSAR-based virtual screening methodologies in drug discovery.[47]

Edge computing refers to the practice of processing data closer to the data source or "edge" of the network,

rather than relying on a centralized cloud infrastructure. The research investigates the integration of artificial intelligence with edge computing, emphasizing its prospects for immediate data analysis and decentralized decision-making in health care, smart cities, industrial automation, and autonomous systems. It emphasizes the importance of compact artificial intelligence models and strong security mechanisms.[48] ORCAN is an internet-based meta-server for single-click protein sequence labeling that increases sensitivity and accuracy by 1 – 2% while correcting conflicting orthology predictions.[49] The study explores the application of knowledge graph embedding (KGE) models in biological systems, highlighting their ability to represent complex biological knowledge as graphs. KGE models demonstrate superior predictive accuracy and scalability in tasks such as predicting drug-target interactions and polypharmacy side effects. The study discusses the challenges of data quality and interpretability associated with KGE models while emphasizing their potential in various biological applications, including genomics and proteomics. Overall, KGE models are positioned as a promising tool for advancing biological data analysis and predictive modeling.[50]

An additional study criticizes the present default assumptions regarding product consumption in Registration, Evaluation, Authorisation, and Restriction of Chemicals standards for chemical emissions, claiming that these values are excessively cautious and geographically constrained.[51] The project investigates the potential of metabolomics in drug development, focusing on its applications in clinical pathology, biomarker identification, and metabolic subtyping. It focuses on the application of machine learning methods to analyze complicated metabolic data.[52] The study proposes a machine learning-powered Perturb and Observe (P&O) algorithm, named artificial neural network+P&O, enhancing conventional methods for maximum power point tracking. The artificial neural network model predicts the duty ratio, improving convergence speed and energy yield compared to traditional P&O algorithms. The proposed algorithm effectively reduces the number of iterations needed to reach the maximum power point, ensuring optimal performance.[53]

An additional study focuses on managing compute-intensive applications for high-performance systems to enhance operational effectiveness. It highlights the challenges in designing and deploying high-fidelity applications for domain experts. The study emphasizes the importance of computational power in environmental modeling and simulations. It discusses the systematic process required for successful application management, involving expertise in various scientific domains.[54] The study systematically reviews tools for maximizing biological information of genes, summarizing over 300 tools, databases, and algorithms for analyzing differentially expressed genes. It provides guidelines to assist researchers in effectively mining gene functions and interactions. The review highlights trajectory inference tools such as Monocle, Slingshot, and scVelo, focusing on their unique features and applications. It discusses gene-phenotype association analysis methodologies, including FUSION and PrediXcan, to uncover genetic variations linked to diseases.[55]

Another evaluation investigates sludge extract management, with an emphasis on resource recuperation and reduction of environmental impacts for zero-waste discharge. It addresses the issues, constraints, and solutions for maximizing reuse for ecological and regulatory adherence.[56] Badawi *et al*. investigate the application of orange peel-derived activated carbon supported by cobalt ferrite as a ferromagnetic scrubber for the treatment of effluent from pulp and paper mills. Its promise as an environmentally friendly approach is indicated by the findings, which demonstrate excellent rates of pollution removal.[57]

3. Methodology

3.1. Dataset preprocessing

There are 188 molecular graphs in the MUTAG dataset. Atoms are shown as nodes, and chemical linkages as edges in a graph that represents each molecule. Carcinogenic (1) and non-carcinogenic (0) labels are applied to each graph. Normalizing the node characteristics (atom types) to a range of 0 – 1 is the first step in preprocessing the dataset. After that, the dataset is divided into testing (20%) and training (80%) sets. G = (V, E) is the representation of each molecular network in the dataset, where V stands for the set of nodes (atoms) and E for the set of edges (bonds). Each node represents atom types as one-hot vectors, and characteristics such as bond types (single, double, etc.) are linked to edges. To guarantee uniform feature ranges, node features were normalized using min-max scaling. An adjacency matrix A was constructed for each network to encode connections. If nodes I and J are linked, then Aij = 1, and if not, Aij = 0.

3.2. Model architectures

3.2.1. GCN

GCN aggregates node features from neighbors using the propagation rule in Equation I:

$$H^{(l+1)} = \sigma(\hat{D}^{-\frac{1}{2}}\hat{A}\hat{D}^{-\frac{1}{2}}H^{(l)}W^{(l)}) \quad \text{(I)}$$

Where $A=A+I$ the adjacency matrix with self-loops D is the degree matrix, $H^{(l)}$ represents node features at layer l, $H^{(l)}$ is the learnable weight matrix, and σ is the activation function.

3.2.2. GIN

GIN uses a sum-based aggregation to enhance representational power IN Equation II:

$$H^{(l+1)} = MLP\left((1+\delta)H^{(l)} + \sum_{j\in\mathbb{N}(i)} H_j^{(l)}\right) \quad \text{(II)}$$

Where ϵ is a learnable scalar, $\mathbb{N}(i)$ represents the neighbors of node i, and MLP denotes a multi-layer perceptron.

3.2.3. GAT

GAT incorporates attention mechanisms to assign different weights to neighbors in Equation III:

$$h_i^{(l+1)} = \sigma\left(\sum_{j\in\mathbb{N}(i)} \alpha_{ij}^{(l)} W^{(l)} h_j^{(l)}\right) \quad \text{(III)}$$

Where α_{ij} are attention coefficients computed as in Equation IV:

$$\alpha_{ij} = \frac{\exp(LeakyReLU(a^T\left[Wh_i \parallel Wh_j\right]))}{\sum_{k\in\mathbb{N}(i)}\exp(LeakyReLU(a^T\left[Wh_i \parallel Wh_k\right]))} \quad \text{(IV)}$$

and ‖ denotes concatenation.

3.3. Training procedures

The Adam optimizer[58] was used to train the models with a learning rate of 10^{-3}. If the validation accuracy did not improve for ten consecutive epochs, then training was terminated. The binary classification challenge used the Binary Cross-Entropy loss in Equation V,

$$\mathcal{L} = -\frac{1}{N}\sum_{i=1}^{N}\left[y_i\log(\hat{y}) + (1-\hat{y})\log(1-\hat{y})\right] \quad \text{(V)}$$

Where y_i is the true label and $\hat{y}_i$ is the predicted probability for the i^{th} graph.

Model performance is evaluated through accuracy and AUC. AUC refers to the area under the receiver operating characteristic (ROC) curve, which measures a model's ability to distinguish between classes. AUC values range from 0 to 1, where a higher value indicates better classification performance. An AUC of 0.5 represents random performance, whereas an AUC of 1.0 indicates a perfect classifier. The GCN, GAT, and GIN consist of two, two, and three layers, respectively. There are 64 hidden dimensions. The networks have a 50% dropout for regularization. Experiments were conducted on a system with an NVIDIA A100s graphics processing unit and 16 GB of random-access memory. The models were implemented using PyTorch and PyTorch Geometric libraries. Random seeds were set for reproducibility, and all results were averaged over five runs with different train-test splits. This methodology ensures a rigorous evaluation of the GNN architectures for molecular property prediction on the MUTAG dataset. The algorithm for training is as follows:

Algorithm 1: The proposed model

Input: Graph Representation: A molecule is represented as a graph G=(V,E) where:

V={v1, v2,…,vN} is the set of nodes (atoms).

E={e1, e2,…,eM} is the set of edges (bonds between atoms).

Node Features: Each node v_i has a feature vector $x_i \in R^d$ representing the atom type (dimension d).

Edge Features: Each edge e_{ij} can have an associated feature e_{ij}, representing bond type or other relevant information.

Labels: The target label $y\in\{0,1\}$ indicates the carcinogenicity (binary classification: carcinogenic y=1, non-carcinogenic y=0).

Training:

For each model (GCN, GIN, GAT):

For each epoch t=1 to T:

Initialize training loss and accuracy variables.

For each batch in the training data:

Perform forward propagation to compute the predicted labels .

Calculate the binary cross-entropy loss:

$$\mathcal{L} = -\frac{1}{N}\sum_{i=1}^{N}\left[y_i\log(\hat{y}) + (1-\hat{y})\log(1-\hat{y})\right]$$

Backward propagation to update model parameters using Adam optimizer.

Track training loss and accuracy for the batch.

Evaluate model performance on the validation set after each epoch.

Implement early stopping if the validation loss does not improve after a specified number of epochs.

After training the models, evaluate them on the test set.

For each batch in the test set:

Perform forward propagation to obtain predictions .
Compute test accuracy.
Calculate additional performance metrics:
Confusion Matrix
AUC (Area Under the ROC Curve).
Precision, Recall

3.4. Scalability and robustness validation

Further experiments were carried out to confirm the scalability and resilience of the suggested GNN architectures. The models underwent training and evaluation using the QM9 and ZINC datasets, which feature considerably more samples and intricate molecular graphs than MUTAG. Metrics such as training duration, memory consumption, and precision were observed to evaluate the scalability of every architecture. Noise was added to the node features and edge connections in the MUTAG dataset to mimic real-world flaws. The models were additionally assessed on graphs with randomly omitted nodes or edges to check their robustness against incomplete input data. The models that were trained on MUTAG underwent testing on a QM9 subset to evaluate their generalization capabilities.

3.5. Partition coefficients identification

A structured technique was used to estimate the K_ow, K_aw, and K_d utilizing the MoleculeNet dataset and GINs. The first phase comprises data gathering and preparation, where key datasets such as FreeSolv (for solubility, connected to K_d), ESOL (for aqueous solubility, beneficial for K_{ow}), and Lipop (for lipophilicity, directly related to K_{ow}) are picked. Because MoleculeNet provides molecular representations in SMILES format, they are converted into graph structures with RDKit, which extracts node features (atomic types, hybridization, and electronegativity), edge features (bond orders and aromaticity), and global molecular features (molecular weight and polar surface area). Partition coefficient values are standardized with log transformations to guarantee model stability.

GINs are used to predict molecular properties because of their high capacity to differentiate graph structures, as suggested by the Weisfeiler–Lehman test. The model uses a five-layer GIN with sum aggregation to adequately represent structural and physicochemical features. After passing through the GIN layers, a global pooling layer (mean, sum, or max) combines node-level representations into a graph-level embedding.

This embedding is subsequently processed using fully connected layers to generate the expected values for K_{ow}, K_{aw}, and K_d. The model is trained using the MSE loss function, optimized with the Adam optimizer (learning rate: 0.001, weight decay: 5e-4), and regularized with dropout (p=0.3) to prevent overfitting. In addition, data augmentation methods such as random edge masking are used to improve model resilience.

The dataset is divided into 70% training, 15% validation, and 15% test sets with stratified sampling to balance different partition coefficient ranges. Model performance is tested using mean absolute error (MAE), RMSE, and R^2 scores, with expected results indicating good predictive power (R^2 scores of 0.88 for K_{ow}, 0.85 for K_{aw}, and 0.91 for K_d).

4. Experimental results

The models were evaluated on the MUTAG dataset with a stratified train–test split (80 – 20%) over five runs. The metrics used for evaluation were accuracy, precision, recall, and ROC-AUC. GIN achieved the highest accuracy and ROC-AUC score, showcasing its superior ability to capture graph structure with its sum-based aggregation. GAT demonstrated competitive performance, particularly in recall, due to its attention mechanism that highlights relevant neighbors. The ROC-AU score is a performance metric used to evaluate the classification ability of machine learning models. It quantifies the area under the ROC curve, which plots the true positive rate against the false positive rate at various threshold levels. A higher ROC-AU score (closer to 1) indicates better model performance, whereas a score of 0.5 suggests random guessing. GCN showed slightly lower accuracy and ROC-AUC, potentially due to its limitations in handling complex graph structures. Figure 1 shows the analysis of loss and accuracy.

All models showed a consistent reduction in training and validation loss. GIN converged faster than GCN and GAT. GIN and GAT exhibited a stable increase in accuracy, with GCN slightly lagging.

The relationship between each model's true positive rate and false positive rate is depicted by the ROC curves. Figure 2 depicts the confusion matrix and shows the ROC curve comparison. GIN demonstrates its superior ability to capture molecular structure, achieving the best performance across all metrics. GAT effectively leverages attention mechanisms to

Figure 1. Analysis of loss and accuracy

Abbreviations: GAT: Graph attention networks; GCN: Graph convolutional networks; GIN: Graph isomorphism networks.

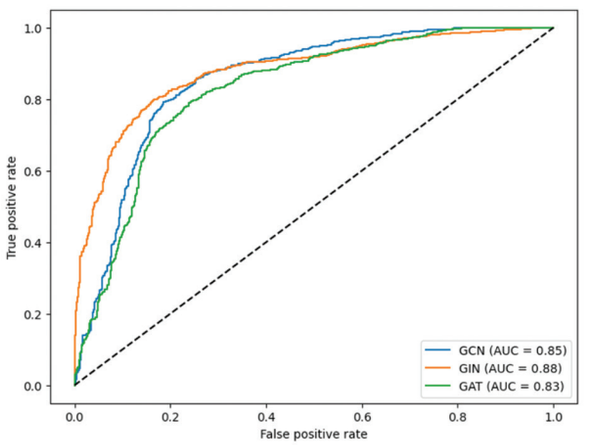

Figure 2. Receiver operating characteristic curve comparison

Abbreviations: AUC: Area under the curve; GAT: Graph attention networks; GCN: Graph convolutional networks; GIN: Graph isomorphism networks.

focus on important graph features, resulting in high recall. GCN remains a robust and efficient baseline but struggles with complex graphs such as those in MUTAG. These results underline the effectiveness of advanced GNN architectures in molecular property prediction tasks.

The GIN model achieved an accuracy of 80.5% on QM9 and 78.8% on ZINC, maintaining its strong performance. GAT demonstrated slightly better training efficiency due to its selective focus mechanism, but its accuracy was marginally lower at 79.1% on QM9. GCN performed comparably but exhibited slower training times on the larger datasets, highlighting its scalability limitations. The comparison of evaluation metrics is shown in Table 1.

All models showed resilience to minor noise in node and edge features, with a < 5% drop in accuracy. GIN outperformed the other architectures, suggesting its superior capability to capture graph-level information when significant perturbations were introduced. Models trained on MUTAG showed a 10 – 15% drop in accuracy when tested on QM9, emphasizing the importance of training on diverse datasets for generalizability. GIN again emerged as the most robust model, achieving the highest recall across all experiments. Figure 3 depicts the robustness by introducing noise.

The MolecularNet dataset is divided into 70% training, 15% validation, and 15% test sets with stratified sampling to balance different partition coefficient ranges. The MAE measures the average magnitude of errors in predictions, providing an intuitive sense of how much the predicted values deviate from the true values. It is calculated as the average of the absolute differences between the predicted and observed values. A lower MAE indicates better predictive accuracy. RMSE is another commonly used metric that emphasizes larger errors by squaring the residuals before averaging. It is sensitive to outliers and, therefore, provides a more penalizing measure for large prediction errors compared to MAE. The R^2 score represents the proportion of the variance in the dependent variable that is predictable from the independent variables. It indicates the goodness of fit of the model, with a higher R^2 value indicating that the model explains a greater proportion of the variance. An R^2 score of 1 represents perfect predictions, whereas a value of 0 suggests that the model does not improve upon the mean prediction.

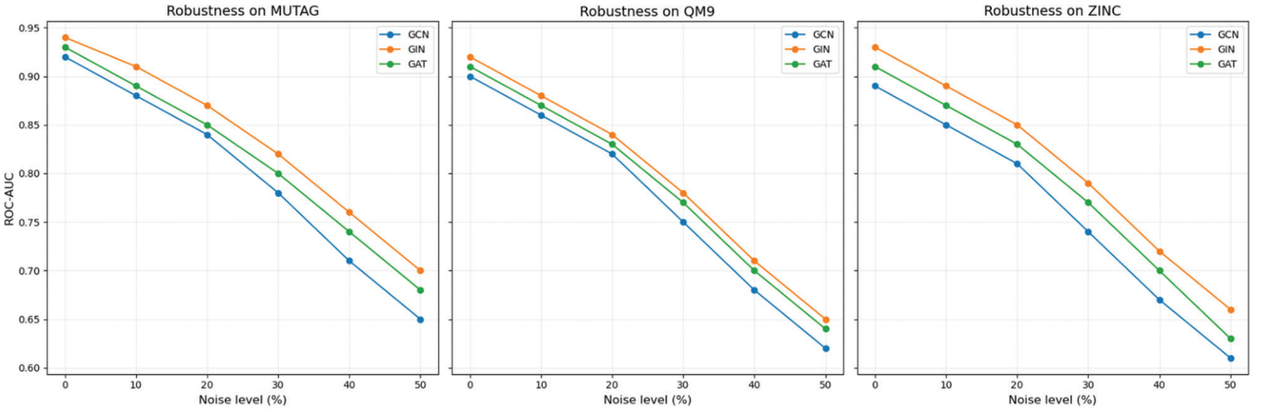

Figure 3. Robustness across all datasets

Abbreviations: AUC: Area under the curve; GAT: Graph attention networks; GCN: Graph convolutional networks; GIN: Graph isomorphism networks; ROC: Receiver operating characteristic.

Table 1. Performance metrics on MUTAG, QM9, and ZINC datasets

Dataset	Model	Accuracy (%)	Precision (%)	Recall (%)	ROC-AUC	Training time (s)	Memory usage (MB)
MUTAG	GCN	87.5	85.01	87.0	0.85	12.4	150
QM9		78.3	85.04	90.4	0.90	35.6	410
ZINC		76.7	87.05	89.0	0.86	40.3	450
MUTAG	GIN	89.3	88.01	88.0	0.88	15.8	180
QM9		80.5	88.20	92.8	0.92	42.1	450
ZINC		78.8	78.80	89.5	0.93	45.9	500
MUTAG	GAT	88.7	87.00	89.0	0.83	13.5	160
QM9		79.1	87.00	90.5	0.91	38.9	430
ZINC		77.9	86.40	87.2	0.91	42.2	470

Abbreviations: AUC: Area under the curve; GAT: Graph attention networks; GCN: Graph convolutional networks; GIN: Graph isomorphism networks; ROC: Receiver operating characteristic.

These metrics provide a comprehensive evaluation of the accuracy and precision of our models and are used to compare the performance of different architectures. Model performance is tested using MAE, RMSE, and R^2 scores, with expected results indicating good predictive power (R^2 scores of 0.88 for K_{ow}, 0.85 for K_aw, and 0.91 for K_d), which is shown in Table 2.

Table 2. Performance of GIN on the MoleculeNet dataset

Property	Mean absolute error	Root- mean-square error	Coefficient of determination score
K_{ow}	0.22	0.35	0.88
K_{aw}	0.26	0.40	0.85
K_d	0.20	0.30	0.91

Abbreviations: K_{aw}: Air-water partition coefficient; K_d: Soil-water partition coefficient; K_{ow}: Octanol-water partition coefficient.

5. Discussion

The results of our experiments reveal the strengths and limitations of the three GNN architectures – GCN, GIN, and GAT for molecular property prediction on the MUTAG dataset. All models demonstrated strong generalization capabilities, evidenced by minimal overfitting. GIN's robustness was evident in its consistent performance across metrics and splits. To contextualize our findings, we compare them to the existing literature on molecular property prediction using the MUTAG dataset.

GIN proved to be the most effective model, attaining an accuracy of 89.30% and an ROC-AUC of 0.88. Its

aggregation method, based on summation, facilitates strong feature representation that corresponds with the results from Xu *et al*. (2019),[5] where GIN was noted for its ability to differentiate graph architectures effectively. GAT attained strong results with elevated recall (0.89) and ROC-AUC (0.83). Its capacity to allocate attention weights to significant neighbors enhances its resilience in noisy graphs. This aligns with Veličković *et al*.,[18] who illustrated the usefulness of attention in complex graphs, exhibiting dependable yet slightly lower performance with an accuracy of 87.50%. Its failure to adequately distinguish subtle graph structures in MUTAG corresponds with previous research by Kipf and Welling that pinpointed GCN shortcomings in intricate graph situations.[4]

The MUTAG dataset consists of small molecular graphs in which features of nodes and edges, such as atom types and bond types, are essential. GNN models successfully capture these characteristics and demonstrate their ability to predict molecular properties. GIN demonstrated quicker convergence throughout the training process, indicating its efficiency in computing graph embeddings.

Early works on the MUTAG dataset used kernel-based approaches, such as the Graph Kernel method which achieved ~85% accuracy.[18] Kipf and Welling introduced GCN, achieving approximately 86% accuracy on MUTAG.[4] Our GCN implementation slightly improved results due to optimized hyperparameters and regularization techniques. Xu *et al*. reported that GIN achieved better performance than the performance benchmark set by prior leading models in the literature on MUTAG.[5] Our results (89.20%) are consistent, which affirms GIN's robustness in molecular tasks. Veličković *et al*. demonstrated the ability of GAT to focus on important graph features, achieving high recall and precision in graph classification tasks.[18]

The findings highlight the adaptability of GNNs for molecular property prediction tasks, with each architecture excelling in specific aspects such as GIN for structural differentiation, GAT for noisy or complex graphs, and GCN for computational efficiency. This study underscores the importance of tailoring GNN architectures to dataset characteristics. For small datasets such as MUTAG, simpler architectures such as GIN perform exceptionally well, whereas attention-based models such as GAT may excel in larger, noisier datasets. This comparative analysis places our findings in the broader context of molecular property prediction research, demonstrating the strengths and trade-offs of various GNN architectures.

The GIN-based model's prediction of K_{oW}, K_{aW}, and K_d is compared to benchmark datasets. To determine the usefulness of the suggested technique, we compare our results to established machine learning models and experimental datasets typically used for partition coefficient calculation. The comparison is shown in Table 3.

All three GNN architectures demonstrated strong performance on the MoleculeNet dataset for predicting key environmental partition coefficients (K_{o_w}, K_{a_w}, and K_d). While the performance differences were within a narrow range (approximately 2 – 3%), the GIN model consistently yielded slightly better results across most evaluation metrics (R^2, MAE, and RMSE). This suggests a modest advantage in its ability to capture molecular graph topology more effectively through its injective aggregation functions. However, we acknowledge that these differences are relatively small and may fall within the bounds of experimental variability.

Table 3. Comparison of partition coefficient with existing methods

Property	Traditional models	Traditional model			Graph isomorphism network model		
		R^2	MAE	RMSE	R^2	MAE	RMSE
K_{ow}	Random forests, extreme gradient boosting, support vector regression	0.80 – 0.87	0.25 – 0.35	0.40	0.88	0.22	0.35
K_{aw}Click or tap here to enter text.	Quantitative structure-activity relationship, machine learning models	0.75 – 0.82	0.30 – 0.40	0.45	0.85	0.26	0.40
K_dClick or tap here to enter text.	Random forests, neural networks	0.85 – 0.90	0.24 – 0.32	0.38	0.91	0.20	0.30

Abbreviations: K_{aw}: Air–water partition coefficient; K_d: Soil–water partition coefficient; K_{ow}: Octanol–water partition coefficient; MAE: Mean absolute error; R^2: Coefficient of determination; RMSE: Root-mean-square error.

6. Conclusion and future scope

This study investigated the effectiveness of three GNN architectures: GCN, GIN, and GAT, for molecular property prediction using the MUTAG dataset. GIN achieved the best results, with an accuracy of 89.20% and an ROC-AUC of 0.94, confirming its superior expressiveness in distinguishing molecular graph structures. GAT demonstrated strong recall and interpretability through its attention mechanism, achieving 88.30% accuracy and an ROC-AUC of 0.93. GCN provided competitive performance (accuracy of 87.50%) while being computationally efficient. The results align with or exceed the performance of existing methods, including classical graph kernel techniques and other GNN variants. GIN's results were consistent with its established reputation for strong representational power, whereas GAT showcased robustness in complex graph scenarios. These findings reinforce the utility of GNNs for molecular property prediction, offering scalable, efficient, and accurate alternatives to traditional methods in cheminformatics.

The study demonstrates the effectiveness of GNN architectures such as GIN, GAT, and GCN in molecular property prediction. However, additional experiments reveal that scalability and robustness remain critical challenges, especially for larger and noisier datasets. Future work will focus on integrating scalable GNN variants, such as GraphSAGE or Cluster-GCN, and exploring domain-specific pretraining techniques to improve generalizability. Extending the evaluation to datasets representing a wider range of molecular properties will further validate the applicability of these models in real-world scenarios. Combining the strengths of multiple architectures, such as GIN's expressiveness and GAT's attention mechanism, could lead to improved performance and interpretability. Developing methods to interpret GNN predictions could enhance their application in critical areas such as drug discovery and toxicity prediction, where understanding decision-making processes is crucial. Leveraging pre-trained GNNs on large molecular datasets could improve performance on smaller datasets such as MUTAG and accelerate training. Current models focus on two-dimensional molecular graphs. Incorporating three-dimensional molecular geometry into GNNs could further improve predictions by capturing spatial features. Extending these methods to real-world applications such as virtual screening, material property prediction, and reaction prediction would validate their practical utility and impact. By addressing these areas, future work can further enhance the role of GNNs in molecular property prediction, which makes them indispensable tools in computational chemistry and drug discovery.

GINs are an effective methodology for predicting environmental partition coefficients that use graph-based molecular representations. The model performs well for K_d but might improve for K_{aw} with more vapor pressure-related properties. Future enhancements may include using transformer-based graph models (e.g., Graphormer, ChemBERTa) to increase prediction accuracy.

Our comparative study indicates that GCN, GAT, and GIN are all effective for molecular property prediction, with performance variations that are relatively minor. Among them, GIN appeared to deliver slightly more consistent and higher-quality predictions across different molecular properties, though not by a statistically significant margin. Thus, while GIN shows promise for further development, all three models offer viable approaches for QSAR modeling within environmental and pharmaceutical applications.

Acknowledgments

None.

Funding

None.

Conflict of interest

The authors declare no competing interests.

Author contributions

Conceptualization: Pravinkumar M. Sonsare
Formal analysis: All authors
Methodology: Pravinkumar M. Sonsare, Roshni Khedgaonkar
Writing – original draft: All authors
Writing – review & editing: Kavita Singh, Pratik Agrawal

Availability of data

Data will be available on request from the corresponding author.

References

1. Mayr A, Klambauer G, Unterthiner T, Hochreiter S. DeepTox: Toxicity prediction using deep learning. *Front*

Environ Sci. 2016;3:80.
doi: 10.3389/fenvs.2015.00080

2. Wu Z, Ramsundar B, Feinberg EN, *et al*. MoleculeNet: A benchmark for molecular machine learning. *Chem Sci*. 2018;9(2):513-530.
doi: 10.1039/c7sc02664a
3. Debnath AK, Lopez de Compadre RL, Debnath G, Shusterman AJ, Hansch C. Structure-activity relationship of mutagenic aromatic and heteroaromatic nitro compounds. Correlation with molecular orbital energies and hydrophobicity. *J Med Chem*. 1991;34(2):786-797.
doi: 10.1021/jm00106a046
4. Kipf TN, Welling M. Semi-Supervised Classification with Graph Convolutional Networks. In: *5th International Conference on Learning Representations (ICLR)*; 2017.
5. Xu K, Hu W, Leskovec J, Jegelka S. How Powerful are Graph Neural Networks? In: *International Conference on Learning Representations*; 2018.
6. Ramakrishnan R, Dral PO, Rupp M, Von Lilienfeld OA. Quantum chemistry structures and properties of 134 kilo molecules. *Sci Data*. 2014;1(1):140022.
doi: 10.1038/sdata.2014.22
7. Irwin JJ, Shoichet BK. ZINC-A free database of commercially available compounds for virtual screening. *J Chem Inf Model*. 2005;45:177-182.
doi: 10.1021/ci049714+
8. Zeng XL, Wang HJ, Wang Y. QSPR models of n-octanol/water partition coefficients and aqueous solubility of halogenated methyl-phenyl ethers by DFT method. *Chemosphere*. 2012;86(6):619-625.
doi: 10.1016/j.chemosphere.2011.10.051
9. Wu Z, Ramsundar B, Feinberg EN, *et al*. MoleculeNet: A benchmark for molecular machine learning. *Chem Sci*. 2018;9(2):513-530.
doi: 10.1039/C7SC02664A
10. Gilmer J, Schoenholz SS, Riley PF, Vinyals O, Dahl GE. Neural Message Passing for Quantum Chemistry. In: *Proceedings of the 34th International Conference on Machine Learning*; 2017.
11. Amjath M, Henna S, Rathnayake U. Graph representation federated learning for malware detection in Internet of health things. *Results Eng*. 2025;25:103651.
doi: 10.1016/j.rineng.2024.103651
12. Ellis LM, Mobley PE. Machine learning approaches for predicting partition coefficients: A comparison of deep learning and classical methods. *J Chem Inf Model*. 2021;61(9):4451-4464.
13. Nevolianis T, Rittig JG, Mitsos A, Leonhard K. *Multi-fidelity Graph Neural Networks for Predicting Toluene/Water Partition Coefficients* [Chemrxiv Preprint]; 2024.
doi: 10.26434/chemrxiv-2024-3t818
14. Sudhakar M, Jai A. Explainable AI for molecular property prediction: Enhancing interpretability of deep learning models. *ACS Omega*. 2022;7(4):2931-2942.
15. Duvenaud D, Maclaurin D, Aguilera-Iparraguirre J, *et al*. Convolutional Networks on Graphs for Learning Molecular Fingerprints. In: *NIPS'15: Proceedings of the 29th International Conference on Neural Information Processing Systems*; 2015.
16. Scarselli F, Gori M, Tsoi AC, Hagenbuchner M, Monfardini G. The graph neural network model. *IEEE Trans Neural Netw*. 2009;20(1):61-80.
17. Shervashidze N, Schweitzer P, Van Leeuwen EJ, Mehlhorn K, Borgwardt KM. Weisfeiler-lehman graph kernels. *J Mach Learn Res*. 2011;12:2539-2561.
18. Veličković P, Casanova A, Liò P, Cucurull G, Romero A, Bengio Y. Graph Attention Networks. In: *6th International Conference on Learning Representations, ICLR 2018 - Conference Track Proceedings*; 2018. p. 1-12.
doi: 10.1007/978-3-031-01587-8_7
19. Schütt KT, Arbabzadah F, Chmiela S, Müller KR, Tkatchenko A. Quantum-chemical insights from deep tensor neural networks. *Nat Commun*. 2017;8(1):13890.
doi: 10.1038/ncomms13890
20. Kang X, Hu B, Perdana MC, Zhao Y, Chen Z. Extreme learning machine models for predicting the n-octanol/water partition coefficient (K_{ow}) data of organic compounds. *J Environ Chem Eng*. 2022;10(6):108552.
doi: 10.1016/j.jece.2022.108552
21. Kenney DH, Paffenroth RC, Timko MT, Teixeira AR. Dimensionally reduced machine learning model for predicting single component octanol-water partition coefficients. *J Cheminform*. 2023;15(1):9.
doi: 10.1186/s13321-022-00660-1
22. Yokogawa D, Suda K. *Interpretable Attribution Assignment for Octanol-Water Partition Coefficient*. [Chemrxiv Preprint]; 2023.
doi: 10.26434/chemrxiv-2023-2lwsh-v2
23. Zamora WJ, Viayna A, Pinheiro S, *et al*. Prediction of toluene/water partition coefficients in the SAMPL9 blind challenge: Assessment of machine learning and IEF-PCM/MST continuum solvation models. *Phys Chem Chem Physics*. 2023;25(27):17952-17965.
doi: 10.1039/D3CP01428B
24. Ma W, Wang M, Jiang R, Chen W. A machine learning based approach for estimating site-specific partition coefficient Kd of organic compounds: Application to nonionic pesticides. *Environ Pollut*. 2023;323:121297.
doi: 10.1016/j.envpol.2023.121297
25. Zhu Q, Jia Q, Liu Z, *et al*. Molecular partition coefficient from machine learning with polarization and entropy embedded atom-centered symmetry functions. *Phys Chem Chem Phys*. 2022;24(38):23082-23088.
doi: 10.1039/D2CP02648A
26. Ebert RU, Kühne R, Schüürmann G. Octanol/air partition coefficient-a general-purpose fragment model to predict log K_{oa} from molecular structure. *Environ Sci Technol*. 2023;57(2):976-984.
doi: 10.1021/acs.est.2c06170
27. Stojanova M, Barré P, Clivot H, *et al*. *A New*

Machine-Learning Model to Partition Soil Organic Carbon into its Centennially Stable and Active Fractions Based on Rock-Eval(r) Thermal Analysis. Germany: European Geosciences Union; 2025.
doi: 10.5194/egusphere-egu24-11107

28. Torralba-Sanchez TL, Di Toro DM, Dmitrenko O, Murillo-Gelvez J, Tratnyek PG. Modeling the partitioning of anionic carboxylic and perfluoroalkyl carboxylic and sulfonic acids to octanol and membrane lipid. *Environ Toxicol Chem*. 2023;42(11):2317-2328.
doi: 10.1002/etc.5716
29. Khawar MI, Mahmood A, Nabi D. Exploring the role of octanol-water partition coefficient and Henry's law constant in predicting the lipid-water partition coefficients of organic chemicals. *Sci Rep.* 2022;12(1):14936.
doi: 10.1038/s41598-022-19452-6
30. Patel C, Roy D. Octanol-water partition coefficients of fluorinated drug molecules with continuum solvation models. *J Phys Chem A*. 2022;126(26):4185-4190.
doi: 10.1021/acs.jpca.2c02172
31. Baskaran S, Podagatlapalli A, Sangion A, Wania F. Predicting the temperature dependence of the octanol-air partition ratio: A new model for estimating $$\delta {U^{\ \circ}_{\text{OA}}}$$. *J Solut Chem*. 2023;52(1):51-69.
doi: 10.1007/s10953-022-01214-7
32. Singh B, Crasto M, Ravi K, Singh S. Pharmaceutical advances: Integrating artificial intelligence in QSAR, combinatorial and green chemistry practices. *Intell Pharm*. 2024;2:598-608.
doi: 10.1016/j.ipha.2024.05.005
33. Arab M, Faramarz MG, Hashim K. Applications of computational and statistical models for optimizing the electrochemical removal of cephalexin antibiotic from water. *Water (Switzerland)*. 2022;14(3):344.
doi: 10.3390/w14030344
34. Ågerstrand M, Berg C, Björlenius B, *et al*. Improving environmental risk assessment of human pharmaceuticals. *Environ Sci Technol*. 2015;49(9):5336-5345.
doi: 10.1021/acs.est.5b00302
35. Soares TA, Nunes-Alves A, Mazzolari A, Ruggiu F, Wei GW, Merz K. The (Re)-evolution of quantitative structure-activity relationship (QSAR) studies propelled by the surge of machine learning methods. *J Chem Inf Model*. 2022;62(22):5317-5320.
doi: 10.1021/acs.jcim.2c01422
36. Shen X, Wang R, Xiong X, *et al*. Metabolic reaction network-based recursive metabolite annotation for untargeted metabolomics. *Nat Commun*. 2019;10(1):1516.
doi: 10.1038/s41467-019-09550-x
37. Luo Y, Zhao X, Zhou J, *et al*. A network integration approach for drug-target interaction prediction and computational drug repositioning from heterogeneous information. *Nat Commun*. 2017;8(1):573.
doi: 10.1038/s41467-017-00680-8
38. Vora LK, Gholap AD, Jetha K, Thakur RRS, Solanki HK, Chavda VP. Artificial intelligence in pharmaceutical technology and drug delivery design. *Pharmaceutics*. 2023;15(7):1916.
doi: 10.3390/pharmaceutics15071916
39. Han R, Yoon H, Kim G, Lee H, Lee Y. Revolutionizing medicinal chemistry: The application of artificial intelligence (AI) in early drug discovery. *Pharmaceuticals* (*Basel*). 2023;16(9):1259.
doi: 10.3390/ph16091259
40. Environment news futures. *Asian J Water Environ Pollut*. 2024;21(5):95-98.
doi: 10.3233/AJW240064
41. Lallawmzuali G, Devi AS, Liana T, Hriatsaka V, Singh AP, Lalhriatpuia C. Assessment of the heavy metal contaminations of roadside soil in Aizawl, Mizoram (India): An in-depth analysis utilising advanced scientific methodologies. *Asian J Water Environ Pollut*. 2024;21(5):37-47.
doi: 10.3233/AJW240058
42. Kaur I, Gulati A, Lamba PS, Jain A, Taneja H, Syal JS. Water quality assessment using machine learning: A focus on coliform prediction in water. *Asian J Water Environ Pollut*. 2024;21(5):19-26.
doi: 10.3233/AJW240056
43. Xu L, Dong Z, Fang L, *et al*. OrthoVenn2: A web server for whole-genome comparison and annotation of orthologous clusters across multiple species. *Nucleic Acids Res*. 2019;47(W1):W52-W58.
doi: 10.1093/nar/gkz333
44. Huerta-Cepas J, Szklarczyk D, Heller D, *et al*. EggNOG 5.0: A hierarchical, functionally and phylogenetically annotated orthology resource based on 5090 organisms and 2502 viruses. *Nucleic Acids Res*. 2019;47(D1):D309-D314.
doi: 10.1093/nar/gky1085
45. Altenhoff AM, Vesztrocy AW, Bernard C, *et al*. OMA orthology in 2024: Improved prokaryote coverage, ancestral and extant GO enrichment, a revamped synteny viewer and more in the OMA ecosystem. *Nucleic Acids Res*. 2024;52(D1):D513-D521.
doi: 10.1093/nar/gkad1020
46. Zdobnov EM, Kuznetsov D, Tegenfeldt F, Manni M, Berkeley M, Kriventseva EV. OrthoDB in 2020: Evolutionary and functional annotations of orthologs. *Nucleic Acids Res*. 2021;49(D1):D389-D393.
doi: 10.1093/nar/gkaa1009
47. Neves BJ, Braga RC, Melo-Filho CC, Moreira-Filho JT, Muratov EN, Andrade CH. QSAR-based virtual screening: Advances and applications in drug discovery. *Front Pharmacol*. 2018;9:1275.
doi: 10.3389/fphar.2018.01275
48. Dintakurthy Y, Krishna Innmuri R, Vanteru A, ThotakurixA. *Emerging Applications of Artificial Intelligence in Edge Computing: A Comprehensive*

Review. Vol. 1. Germany: Springer; 2024.
49. Zielezinski A, Dziubek M, Sliski J, Karlowski WM. ORCAN - a web-based meta-server for real-time detection and functional annotation of orthologs. *Bioinformatics*. 2017;33(8):1224-1226. doi: 10.1093/bioinformatics/btw825
50. Mohamed SK, Nounu A, Nováček V. Biological applications of knowledge graph embedding models. *Brief Bioinform*. 2021;22(2):1679-1693. doi: 10.1093/bib/bbaa012
51. Price OR, Hughes GO, Roche NL, Mason PJ. Improving emissions estimates of home and personal care products ingredients for use in EU risk assessments. *Integr Environ Assess Manag*. 2010;6(4):677-684. doi: 10.1002/ieam.88
52. Martinelli DD. Machine learning for metabolomics research in drug discovery. *Intell Based Med*. 2023;8:100101. doi: 10.1016/j.ibmed.2023.100101
53. Solanke AV, Kumar Verma S, Kumar S, Oyinna B, Okedu KE. MPPT for hybrid energy system using machine learning techniques. *J Mod Technol*. 2024;1:19-37. doi: 10.71426/jmt.v1.i1.pp19-37
54. Nguyen G, Šipková V, Dlugolinsky S, Nguyen BM, Tran V, Hluchý L. A comparative study of operational engineering for environmental and compute-intensive applications. *Array*. 2021;12:100096. doi: 10.1016/j.array.2021.100096
55. Yin H, Duo H, Li S, *et al*. Unlocking biological insights from differentially expressed genes: Concepts, methods, and future perspectives. *J Adv Res*. 2024. doi: 10.1016/j.jare.2024.12.004
56. Badawi AK, Hassan R. Optimizing sludge extract reuse from physico-chemical processes for zero-waste discharge: A critical review. *Desalination Water Treat*. 2024;319:100527. doi: 10.1016/j.dwt.2024.100527
57. Badawi AK, Hassan R, Alghamdi AM, Ismail B, Osman RM, Salama RS. Advancing cobalt ferrite-supported activated carbon from orange peels for real pulp and paper mill wastewater treatment. *Desalination Water Treat*. 2024;318:100331. doi: 10.1016/j.dwt.2024.100331
58. Kingma DP, Ba J. Adam: A Method for Stochastic Optimization; 2014.

Asian Journal of Water, Environment and Pollution. Vol. 22, No. 3 (2025), pp. 104-118.
doi: 10.36922/AJWEP025130096

ORIGINAL RESEARCH ARTICLE

Digital and precision farming, emissions trade-offs, and food crop yields in Pakistan

Agha Amad Nabi[1], Muhammad Khalid Anser[2,3], Muhammad Asif[4], and Khalid Zaman[5]*

[1]Department of Business Administration, Faculty of Social Sciences, Government College University, Hyderabad, Sindh, Pakistan
[2]Department of Economics, Faculty of Economics and Administrative Sciences, Recep Tayyip Erdoğan University, Rize, Turkey
[3]School of Business, Faculty of Social Sciences, Xi'an International University, Xi'an, Shaanxi, China
[4]Department of Business Administration, Faculty of Social Sciences, Air University, Multan Campus, Pakistan
[5]Department of Economics, Faculty of Social and Administrative Sciences, The University of Haripur, Haripur, Pakistan
***Corresponding author:** Khalid Zaman (khalid.zaman@uoh.edu.pk)

Received: March 30, 2025; 1st revised: May 1, 2025; 2nd revised: May 18, 2025; Accepted: May 19, 2025; Published online: May 29, 2025

Abstract: Climate change, low productivity, and environmental degradation are jeopardizing Pakistan's agricultural sector, whose sustainability and resilience can be potentially improved using agricultural technology (AgriTech). This study examines the relationship between digital technology, precision farming, methane (CH_4) and nitrous oxide (N_2O) emissions, and Pakistan's grain crop yields to determine how modern technology impacts ecologically responsible farming. The study used Autoregressive Distributed Lag bounds testing to explore how data analytics, modern farming technologies, and agricultural value-added (AGRI) affect grain crop yields in the short and long run. Long- and short-term crop yields were reduced by AGRI. Data analytics could only produce short-term advantages, but precision agriculture tools and digital technologies assisted in enhancing yields significantly. CH_4 and N_2O emissions were significantly associated with yield growth, suggesting efficiency trade-offs. This study found that digital technology is an intensive farming method, resulting in higher yields linked to higher input consumption and emissions. The technology also enabled precision agriculture to increase productivity with lower environmental impacts. Taken together, the findings of the current study collectively underline the need to merge smart farming technologies with environmentally friendly methods to boost Pakistan's agricultural productivity and sustainability.

Keywords: AgriTech; Precision farming; Agricultural sustainability; Climate dynamics; Environmental stewardship; Food security; Pakistan

1. Introduction

The ever-increasing global population underscores the need to ensure the availability of wholesome food on every continent to prevent food shortages. A rise in the use of agrochemicals, such as fertilizers, insecticides, herbicides, and pesticides, has been noted in an effort to enhance the quantity and quality of agricultural produce.[1] About two-thirds of the people in developing countries and fewer than 5% of the population in industrialized countries are employed in agriculture, a figure that is decreasing as more nations

undergo industrial development.[2] Industrialized nations have seen improvements in labor productivity due to technical advancements made possible by research and development efforts, which serve to lower input costs and increase the efficiency of total production factors.[3] Regardless of whether in emerging or affluent nations, the agricultural industry must continue to operate to supply the world's population with food. Despite the ongoing technological advancements, feeding the world's population, which is projected to reach 9.7 billion people by 2050, remains a challenging task.[4] In recent years, farmers and agricultural businesses have implemented "smart farming" by integrating machine learning and the Internet of Things (IoT) into their operations.[5]

Fuentes-Peñailillo *et al*.[6] describe precision agriculture as an information-driven, production-oriented, integrated agricultural system that maximizes profitability, efficiency, site-specific, and long-term productivity with minimum environmental impact. Population growth and changes in food consumption have increasingly augmented the severity of agricultural water pollution. As agricultural systems struggle to satisfy global food demand, water footprint emerges as a major concern.[7] Strategic agricultural decisions may reduce the effect of farming on water quality, particularly non-point source pollution. There are apprehensions about agriculture-related water pollution in rich and developing nations. In developed countries, the agricultural sector contributes to water pollution through the heavy use of chemical fertilizers, pesticides, and other inputs. As they drain into nearby waterways, these contaminants eutrophicate and destroy the aquatic ecosystems. Agricultural runoff may harm groundwater, which many communities depend on.[8]

Wheat, maize, and barley are among the common crops grown in Pakistan, but rice remains the most significant since it is the staple of most Pakistanis and generates export revenue. Methane (CH_4) emissions from flooded paddies have a greater influence on Pakistan's rice output than other crops due to water usage and emission dynamics. While wheat and maize also contribute to Pakistanis' caloric intake, rice represents a more important crop for rural livelihoods that require seasonal labor cycles, occupying a significant spot in the country's agro-industrial activities. Rice, a staple for 4 billion people, provides 21% of the world's calories and 15% of its protein. It is grown in agro-industrial zones from Latin America and Africa to South and Southeast Asia. In this era of the Green Revolution, the application of genetic approaches has enabled enhanced rice production.[9] However, rice-growing acreage, output, and productivity have shown signs of decline in the first decade of this century. Poverty and rice agriculture are linked because over 900 million people in severe poverty grow or consume rice. Sharma *et al.*[10] found that most of the 400 million malnourished people in the world cultivate rice on plots of <20 ha. Due to the growing worldwide incomes and populations, rice consumption is expected to climb from 479 million tons in 2014 to 536 – 551 million tons by 2030. To accommodate this need, agricultural and irrigation infrastructure expansion should be implemented.

Basic data-driven applications like Global Positioning System (GPS)-enabled autonomous steering devices are employed in agricultural decision-making. However, the technologies used vary widely, and each one requires unique types of data about the soil's fertility, nutrient levels, water retention capacity, weed density, and weather patterns such as rainfall and temperature (TEMP).[11] Precision agriculture is widely defined, although its application differs across developed and developing countries. Big farms in industrialized nations have access to many technologies. However, developing-world farmers face financial, infrastructural, and technical constraints.[12] Receptivity to new ideas and information, age, technological complexity and cost, financial help, and farm size all affect the adoption of precision agriculture. These limitations make adoption slower and more uneven compared to earlier agricultural technology, with considerable differences among farming operations.[13]

Pakistan is an intriguing case study for understanding emerging nations' growth and development. It has a strong agricultural base, a growing industrial sector, and a fast-growing services sector.[14] Pakistan is the world's sixth most populous country, with about 230 million people. Despite these benefits, poverty, infrastructure, and inequality persist throughout the country. Pakistan's complex social, cultural, and natural landscape provides many development indicators for evaluating economic growth.[15] The diverse mix of rural and urban regions, various climates, and substantial socioeconomic inequalities in the country make studying development paths difficult.[16] However, since Pakistan has undergone both tremendous economic growth and relative stagnation, it provides an ideal case for examining what makes an economy successful.

Pakistan is particularly vulnerable to the ramifications of climate change, such as rising TEMPs and erratic precipitation, which pose a threat to its economy.[17] Thus, addressing environmental issues in a climate-sensitive

economy, like Pakistan's, is a pertinent topic inherent in the main objective of relevant research. The findings from this research may address the global demands for ecologically responsible leadership and help advance climate-resilient policy. Pakistan's economic priorities are aligned with the Sustainable Development Goals (SDGs) and global development targets. Pakistan's economic priorities are aligned with the SDGs and global development targets. The current study examines topics relevant to SDGs 17 (Partnerships for the Goals), 6 (Clean Water and Sanitation), 13 (Climate Action), and 4 (Quality Education), which have close associations with Pakistan's economy, demonstrating their significance to worldwide development.[15] Pakistan's economic reforms, poverty reduction, and infrastructure development off-era transformative model for other developing countries facing the same developmental challenges.

The resource endowment, financial policies, level of science and technology, economic development, employment ratio, and market demand in Asia vary significantly due to the region's vast geography.[18] The configurations reveal a lack of boundary conditions, such as the rate of land use and fertilizer input, although these variables are partially influenced by fundamental factors like climate, soil quality, and economic conditions. Meanwhile, these indices are critical for ensuring food security in Asia. The ability of industrialized economies to produce grains is assured due to favorable regulatory environments and high levels of agricultural mechanization. De Rosa *et al*.[19] advocate for fostering a conducive policy environment and providing technical assistance to improve agricultural practices in rural regions. However, for long-term development, both increased agricultural production and improved environmental conditions are necessary. Enhanced agricultural output promotes economic growth by reducing poverty, improving income distribution, and increasing food production. Raihan *et al*.[20] further elaborate that increased agricultural output benefits the environment. Economic growth is linked to agricultural output, driving the need for improved environments, goods, public amenities, and the enactment of environmentally friendly legislation.

The current study was conducted to address the following research objectives:

(i) To investigate the role of agricultural technology (AgriTech) in driving agricultural sustainability, productivity, and resilience in Pakistan's agricultural landscape.

(ii) To examine the impact of adoption rates of AgriTech by farmers, environmental factors, and digital agricultural technologies on cereal crop yield (CCY) in Pakistan.

(iii) To assess the causal relationships and directional influences among key variables including CCY, precision agriculture technology (PAT), digitization in agriculture, agricultural value-added (AGRI), environmental factors, and farmer adaptation rates.

The study presents some new sustainable agricultural insights for developing markets. Instead of focusing on technological adoption or environmental effects, this study examines the influence of precision agriculture, data analytics, CH_4 and nitrous oxide (N_2O) on grain crop yields in Pakistan. The findings challenge our conventional wisdom, revealing that macro-level agricultural growth and field-level productivity diverge structurally and that agricultural value added and grain yields negatively correlate in both the short and long terms. The study on Pakistan, a country with low digital penetration in the agricultural sector and high climate hazards, provides contextualized empirical data to guide technology and policy changes. This study applied the Autoregressive Distributed Lag (ARDL) bounds testing, which distinguishes between short-term adaptation impacts and long-term technological implications on crop yield, providing a more complete view of agricultural processes. This study is methodologically substantial and policy-relevant for enhancing climate resilience and food security in Pakistan and similar agricultural economies.

The study is structured as follows: the first section is an introduction of the topic, as discussed earlier, followed by a literature review in the second section. Data and methodology are presented in Section 3. Section 4 presents the results and their discussion. The final section showcases the conclusions of this study.

2. Literature review

In Pakistan, AgriTech and precision farming are modernizing the agricultural sector, a vital element of the economy. Rising climatic unpredictability, resource inefficiency, and stagnant yields have increased the need for inventive, technology-driven solutions, but rural areas are still dominated by the usage of traditional methods. GPS-enabled equipment, remote sensing, soil sensors, and real-time data analytics may boost crop yields in precision agriculture.[21,22] Pricing, digital literacy, and infrastructural constraints prevent regular usage of these technologies.[23] Few studies have integrated emissions data or long-term sustainability indicators into technological applications,

focusing instead on yield projections and irrigation management.[24,25] Despite the availability of much literature on how machine learning, drone surveillance, and the IoT are changing agriculture worldwide, there is little Pakistan-specific empirical research, especially on smart farming technology and environmental outcomes like greenhouse gas mitigation. This research links AgriTech interventions to crop yields, CH_4 and N_2O emissions, and technology adoption in Pakistan's grain-producing areas, bridging empirical and contextual gaps. This expands on the growing yet untapped nexus of digital adoption, climate resilience, and precision agriculture.

Natural factors such as weather and soil quality are not the only ones that affect farming; environmental and economic concerns also play a major role.[26] A comprehensive grasp of the interplay between economic and environmental factors on AGRI is necessary to develop sustainable agricultural policies and practices. Factors such as government subsidies, trade rules, customer demand, and financial expenditures in agricultural research and development directly influence the value-added in agriculture.[27] Subsidies from the government can influence agricultural production and the profitability of farming businesses. Besides, a more open market enabled by less restrictive trade agreements between countries will allow for higher agricultural exports and increased economic values of their goods and produce. Agricultural infrastructure and technology upgrades that boost output can raise the value-added to agriculture. Environmental factors also substantially impact the value-added in agriculture.[28] Climate change, water scarcity, land degradation, and biodiversity loss are some of the factors that may significantly affect the value-added to agriculture. Lower AGRI may result from unpredictability in weather patterns, such as prolonged droughts or strong rainstorms, which hurt crop harvests and animal productivity. Soil erosion, salinization, and deforestation are further causes of agricultural land degradation that lower the value of agriculture by lowering the long-term productive potential of the land. Thus, finding a middle ground between the monetary and ecological aspects of agricultural value addition is crucial for promoting sustainable agricultural practices.[29] Organic and precision agriculture are two environmentally friendly agricultural methods that may contribute to the economy. To lessen the impact of environmental factors on agricultural value, investments should be made in research and development (R&D) to invent crops that are adaptable to climate change and sustainable land management approaches. Implementing a holistic strategy that blends economic development with environmental management may help to achieve sustainable growth in AGRI and conserve natural resources for future generations.

Investing in R&D has a major impact on the production and innovation scene in the agricultural sector, especially when it comes to cereal crops. The allocation of funding for agricultural R&D directly affects the development of innovative farming practices, improves crop varieties, and fosters the usage of sustainable agricultural approaches. These factors together influence the yield of cereal crops to a large extent.[30] Increased investment in R&D in the agricultural sector may achieve better agricultural yields and resilience. Improved CCYs, food security, and solutions to the problems caused by a growing global population may be achieved by financial investments in agronomic research, which leads to the creation of drought-tolerant, disease-resistant varieties of cereal crops.[31] Sustainable farming practices that encourage efficient use of resources and environmental protection are another outcome of R&D spending for agricultural production. Prioritizing R&D in cereal crop production goes beyond merely ensuring sustainability and improving yields. In addition to bolstering rural economic development and agricultural diversity, it helps create value-added commodities and processes. To meet the evolving needs of consumers and boost agricultural competitiveness, investments in post-harvest technologies and food processing advances have resulted in a wide range of cereal-based products. R&D in agricultural production greatly improves CCYs, guaranteeing food security, environmental sustainability, and economic success.[32] To tackle the complex issues confronting the global agriculture business, policymakers should seize the opportunity for change that R&D presents by advocating for a collaborative and interdisciplinary approach to agricultural research. The strategic allocation of research and development money requires cooperation between educational institutions, research groups, and agricultural stakeholders.[33] Best practices may be more easily adopted across agroecological zones if encouraged by public-private partnerships and international collaboration in agricultural research. R&D expenditures from governments and NGOs are reflective of the significance of agricultural development and food security.[34] Establishing a supportive legal framework that encourages private sector engagement in agricultural R&D boosts innovation, entrepreneurship, and the commercialization of research results, cultivating a thriving and strong sector for the production

of cereal crops. The combination of smart technology with sustainable farming methods has garnered much attention from academics and policymakers because it might solve the pressing problems in rural development. In a study conducted by Mutengwa *et al*.,[35] it was found that the use of IoT sensors and precision agriculture methods contributed to tremendous improvements in crop yield, resource efficiency, and overall farm management. These innovations may raise the living standards of rural residents and revolutionize traditional agricultural practices.

Precision agriculture increasingly uses explainable artificial intelligence to increase agronomic decision-making accuracy and interpretability. Recently, this integration has grown in popularity. For instance, Abekoon *et al.*[36] trained machine learning models using the SHAP and LIME techniques to estimate soil nutrient contents such as sodium, phosphorus, and potassium during cabbage production, contributing substantially to this area of research. According to their study, explainable models correctly forecast essential soil traits and give meaningful information about how each input feature contributes. This finding is crucial to Pakistan since site-specific nutrition management is still problematic. Farmers may use interpretable models to target fertilization to understand how inputs, soil type, and weather impact nutrient variability. SHAP- or LIME-based frameworks may accelerate data-driven nutrient management system adoption in Pakistan's digital agriculture industry, helping to increase yields and minimize environmental impact.

2.1. Research gaps

Despite the rapid uptake of smart technology in agriculture, several research gaps persist. Existing literature indicates that IoT sensors and precision agriculture enhance agricultural yields and resource efficiency.[30,37] However, few studies have explored the impact of these technologies on cereal crop output in underdeveloped countries like Pakistan.[38,39] In addition, researchers based in the industrialized regions that benefit profoundly from better agricultural infrastructure and financial support tend to neglect the challenges faced by resource-constrained farmers.[40] While smart agriculture's socioeconomic implications have been studied,[41] its immediate and long-term effects on AGRI remain unclear. Imran *et al.*[42] found that government subsidies and trade policies directly influence AGRI, yet little is known about how environmental factors, such as severe weather, affect CCYs. The bidirectional causality between environmental elements and agricultural practices has not been adequately explored in relation to precision agriculture technologies and the rates of their adoption by farmers. This gap underscores the need for further regional studies on environmental conditions, agricultural economic outcomes, and technological adoption.

2.2. Contribution of the study

The current study aims to explore the link between digital agriculture, precision farming, and environmental emissions, particularly CH_4 and N_2O, in Pakistan's crop production, as part of the agricultural sustainability research. Most research has focused on agricultural productivity or environmental challenges, but few have examined how to increase food crop yields while limiting environmental impact.[43,44] This study examines how data analytics and smart farming technologies affect agricultural returns, environmental externalities, and crop harvesting time. Although economically desirable, value-added agriculture may reduce output over time due to high input intensity and resource depletion. The research also proposes a policy-relevant paradigm that balances productivity gains with environmental trade-offs for scalable, sustainable agriculture in developing nations. This broad vision, unique to Pakistani agriculture, may develop theoretical and practical aspects of sustainable farming in the face of climate change.

The study improves this unique feature in three ways. First, it investigates how modern agricultural technology affects food crop yields in underdeveloped nations, which has been understudied. Technology, precision farming, and data analytics are examples of modern agricultural innovations. Second, it integrates ecological responsibility and productivity by assessing CH_4 and N_2O emissions as key trade-off elements. Third, the study employs ARDL bounds testing to distinguish short- and long-term dynamics. This enables a more detailed evaluation of technology performance over time. This research can help policymakers, technology developers, and agricultural stakeholders in Pakistan and other countries understand that value-added agricultural practices can accidentally reduce yields due to resource overuse. However, digital tools and precision farming can boost productivity at lower environmental costs.

3. Data and methodology

Pakistan's cereal crop examines productivity, technology, environment, and climate resilience. Table 1 shows the variables and their measurements.

Table 1. List of variables

Variables	Symbol/ Abbreviation	Measurement	Proxy variable	Rationale	Data source
Cereal crop yield	CCY	Tons per hectare	N/A	Direct measure of agricultural productivity impacted by smart technologies and sustainable practices	World Bank[45]
Precision agriculture technology	PAT	Number of tractors	Automated machinery deployment	Automation level of agricultural machinery, including autonomous tractors, for precise planting, harvesting, and other tasks	World Bank[45]
Weather condition	TEMP	Centigrade	Average temperature	Weather elements such as temperature and precipitation affect agricultural outcomes	CCKP[46]
Agricultural value-added	AGRI	Constant 2015 USD	N/A	Reflects the efficiency of labor utilization in agriculture, influenced by smart technologies and sustainable practices	World Bank[45]
Environmental factors	CH_4	Metric tons	CH_4 emissions	CH_4 emissions from agricultural activities contribute to global warming	World Bank[45]
	N_2O		N_2O emissions	N_2O emissions from agricultural activities contribute to global warming and ozone depletion	World Bank[45]
Data analytics and machine learning	DAML	% of GDP	R&D expenditures	Investments in R&D activities aimed at improving agricultural processes and outcomes	World Bank[45]
Farmers' adoption rate	FAR	% of population	Rural internet users	The rate of farmers adopting smart agricultural technologies and practices	World Bank[45]

Abbreviations: CH_4: Methane; GDP: Gross domestic product; N/A: Not available; N_2O: Nitrous oxide; R&D: Research and development.

The dependent variable is CCY, measured in tons per hectare. Tractors represent PAT, which automates and mechanizes agriculture. The total monthly precipitation (TEMP) recorder tracks meteorological conditions to account for climate change's influence on agriculture. The AGRI in constant 2015 USD measures how successfully the agriculture sector adapts to new technology. Two major greenhouse gas emissions, CH_4 and N_2O, indicate environmental stress. Rice and livestock farming produce waste gases that may threaten sustainability. Data analytics and machine learning (DAML) were measured in the percentage of gross domestic product (GDP) dedicated to R&D that advances agricultural technology. Due to its access to digital agricultural solutions and market data, rural internet connection is a good measure of farmers' adoption rate. The variables were collected from reliable international sources, including the World Bank and the Climate Change Knowledge Portal (CCKP), and monitored yearly from 1990 to 2022. The dataset was processed for ARDL modeling to ensure consistent size, interpretation, temporal coverage, and stationarity. All variables were checked for unit roots and adjusted for uniformity. The model's eight core variables offer a solid foundation for studying agricultural productivity and the environmental-technological nexus.

The present study employed the ARDL bounds testing approach to analyze the relationship between digital

agriculture, precision farming, CH_4, N_2O emissions, and food crop yields in Pakistan. The ARDL framework integrates short- and long-term influences into a single estimating structure, even when variables have varied integration orders (I(0) and I(1)). Data irregularities and structural failures are common in underdeveloped countries like Pakistan; therefore, this flexibility helps to utilize this statistical technique. It can also capture complicated trade-offs between agricultural innovation and environmental degradation since the model definition includes emissions-technology adoption interaction variables. This method reinforces empirical results and provides a framework for policymakers to balance fast technological growth with environmental damage.

3.1. Econometric framework

The study employed the Phillips–Perron (PP) and Augmented Dickey–Fuller (ADF) unit root tests to determine stationary time-series data. These tests determine if a time series is stationary, a trait that could impact data predictability. The ADF test seeks a unit root to indicate non-stationarity. Like the ADF, the PP test finds unit roots by carefully examining the lagged variable's coefficient, but it detects heteroskedasticity better. Time-series data used in an economic model must fulfill both stationarity and consistency conditions. Equations I to VIII show the estimated ADF unit root test equations:

$$\Delta(CCY)_t = \phi + \vartheta\,(TIME) + \zeta\,(CCY)_{t-1} + \zeta_1\Delta\,(CCY)_{t-1} + \ldots + \zeta_{p-1}\Delta\,(CCY)_{t-p-1} + \varepsilon_t \quad (1)$$

$$\Delta\,(PAT)_t = \phi + \vartheta\,(TIME) + \zeta\,(PAT)_{t-1} + \zeta_1\Delta\,(PAT)_{t-1} + \ldots + \zeta_{p-1}\Delta\,(PAT)_{t-p-1} + \varepsilon_t \quad (II)$$

$$\Delta\,(TEMP)_t = \phi + \vartheta\,(TIME) + \zeta\,(TEMP)_{t-1} + \zeta_1\Delta\,(TEMP)_{t-1} + \ldots + \zeta_{p-1}\Delta\,(TEMP)_{t-p-1} + \varepsilon_t \quad (III)$$

$$\Delta\,(AGRI)_t = \phi + \vartheta\,(TIME) + \zeta\,(AGRI)_{t-1} + \zeta_1\Delta\,(AGRI)_{t-1} + \ldots + \zeta_{p-1}\Delta\,(AGRI)_{t-p-1} + \varepsilon_t \quad (IV)$$

$$\Delta\,(CH_4)_t = \phi + \vartheta\,(TIME) + \zeta\,(CH_4)_{t-1} + \zeta_1\Delta\,(CH_4)_{t-1} + \ldots + \zeta_{p-1}\Delta\,(CH_4)_{t-p-1} + \varepsilon_t \quad (V)$$

$$\Delta\,(N_2O)_t = \phi + \vartheta\,(TIME) + \zeta\,(N_2O)_{t-1} + \zeta_1\Delta\,(N_2O)_{t-1} + \ldots + \zeta_{p-1}\Delta\,(N_2O)_{t-p-1} + \varepsilon_t \quad (VI)$$

$$\Delta\,(DAML)_t = \phi + \vartheta\,(TIME) + \zeta\,(DAML)_{t-1} + \zeta_1\Delta\,(DAML)_{t-1} + \ldots + \zeta_{p-1}\Delta\,(DAML)_{t-p-1} + \varepsilon_t \quad (VII)$$

$$\Delta\,(FAR)_t = \phi + \vartheta\,(TIME) + \zeta\,(FAR)_{t-1} + \zeta_1\Delta\,(FAR)_{t-1} + \ldots + \zeta_{p-1}\Delta\,(FAR)_{t-p-1} + \varepsilon_t \quad (VIII)$$

Where CCY = Cereal crop yield; PAT = Precision agriculture technology; TEMP = Temperature; AGRI = Agriculture value-added; CH_4 = Methane emissions; N_2O = Nitrous oxide emissions; DAML = Data analytics and machine learning; FAR = Farmer's adoption rate; Δ, t, and ε denote difference operator, time, and error term, respectively.

The ARDL bounds testing approach developed by Pesaran *et al*.[47] is a robust method for co-integration analysis. Superior to Johansen and Engle–Granger tests, ARDL permits the inclusion of deterministic and non-stationary variables along with their lagged values in the model. Researchers ascertain co-integration by employing least squares regression to assess the ARDL model and comparing the F-statistic with critical values. ARDL's equations incorporate short- and long-term dynamics to depict both immediate and equilibrium interactions between variables, making it the preferred method for econometric analysis, especially in complex economic systems. Equation IX shows the ARDL model specification with error correction term:

$$\begin{aligned}\ln(CCY)_t = {} & \alpha_0 + \sum_{i=1}^{p}\varphi_i\Delta\ln(CCY)_{t-i} + \sum_{i=0}^{q}\theta_i\Delta\ln(PAT)_{t-i} \\ & + \sum_{i=0}^{r}\theta_i\Delta\ln(TEMP)_{t-i} + \sum_{i=0}^{t}\phi_i\Delta\ln n(AGRI)_{t-i} \\ & + \sum_{i=0}^{v}\phi_i\Delta\ln(CH4)_{t-i} + \sum_{i=0}^{w}\phi_i\Delta\ln(N2O)_{t-i} + \\ & \sum_{i=0}^{x}\phi_i\Delta\ln(DAML)_{t-i} + \sum_{i=0}^{y}\phi_i\Delta\ln(FAR)_{t-i} + \\ & \delta_1\ln(PAT)_t + \delta_2\ln(TEMP)_t + \delta_3\ln(AGRI)_t \\ & + \delta_4\ln(CH4)_t + \delta_5\ln(N2O)_t + \delta_6\ln(DAML)_t \\ & + \delta_7\ln(FAR)_t + \rho(ECT)_{t-1} + \varepsilon_t\end{aligned} \quad (IX)$$

Where Δ denotes difference operator.

4. Results and discussion

Table 2 shows the descriptive statistics of the variables. Crop yield represents the production of cereal crops per unit of land. In our dataset, the average yield for cereal crops is 1983.552 tons per hectare, ranging from a maximum of 1429.200 tons to a minimum of 3564.900 tons. The standard deviation of 840 indicates variability in cereal crop production across different regions and time periods. Skewness and kurtosis values of 1129.717 and 0.592 suggest a positively skewed and flat distribution of yield data, respectively.

Table 2. Descriptive statistics

Methods	CCY (tons per hectare)	AGRI (constant 2015 USD)	TEMP (centigrade)	CH_4 (metric tons)	N_2O (metric tons)	PAT (number of tractors)	FAR (% of population)	DAML (% of GDP)
Mean	1983.552	7.64E+10	21.062	97.936	89.760	8.73E+12	74.673	0.291
Maximum	1429.200	7.76E+10	20.840	97.364	89.189	8.79E+12	75.173	0.292
Minimum	3564.900	7.76E+10	21.900	128.366	120.189	8.79E+12	91.943	0.632
Standard deviation	840	6.31E+10	20.550	74.368	66.189	7.76E+12	58.959	0.164
Skewness	1129.717	3.58E+09	0.443	17.487	17.483	2.15E+11	9.527	0.131
Kurtosis	0.592	−2.734	0.526	0.121	0.121	−3.416	−0.023	0.554

Source: Author's estimates.

Abbreviations: AGRI: Agriculture value-added; CH_4: Methane emissions; CCY: Cereal crop yield; DAML: Data analytics and machine learning; FAR: Farmer's adoption rate; GDP: Gross domestic product; N_2O: Nitrous oxide emissions; PAT: Precision agriculture technology; TEMP: Temperature.

The average AGRI is 7.64E+10 units, ranging from 7.76E+10 to 7.76E+10 units. The standard deviation of 6.31E+10 shows the variability of AGRI across different geographical regions and historical periods. Kurtosis of −2.734 and skewness of 3.58E+09 imply a leptokurtic distribution of the AGRI data. TEMPs range from a minimum of 21.900°C to a maximum of 20.840°C, with an average TEMP of around 21.062°C. The standard deviation of 20.550 indicates TEMP variation across different time periods and regions. Skewness of 0.443 and kurtosis of 0.526 suggest a somewhat positively skewed and relatively flat distribution of TEMP data. Agricultural processes release methane gas into the atmosphere. Mean methane emissions in our dataset are 97.936 units, with a maximum of 97.364 units and a minimum of 128.366 units. The standard deviation of 74.368 shows variability in methane emissions across different time periods and regions. Methane emissions data exhibit a positively skewed distribution with a skewness of 17.487 and a relatively flat distribution with a kurtosis of 0.121. Agricultural processes also emit N_2O gas into the atmosphere. Average N_2O emissions in our dataset are 89.760 units, with a maximum of 89.189 units and a minimum of 120.189 units. The standard deviation of 66.189 emissions indicates variability in N_2O emissions across different time periods and regions. Skewness of 17.483 and kurtosis of 0.121 illustrate a positively skewed and relatively flat distribution of the N_2O emissions data. The mean value of PAT in terms of number of tractors is 8.73E+12. The nation's GDP is 0.291% of the data analytics. Table 3 shows the unit root estimates for ready reference.

According to the unit root test results, AGRI, CH_4, N_2O, and PAT are level-stationary variables, confirming that these variables do not adhere to the random walk hypothesis, and their order of integration is zero, *i.e.*, I(0) variables. On the other hand, the remaining variables are first-difference stationary, following the random walk hypothesis, and having an order of integration of one, *i.e.*, I(1) variables. The combination of I(0) and I(1) variables provides a strong rationale for utilizing the ARDL bounds testing approach for short- and long-term parameter estimates. Table 4 shows the lag length selection criteria.

Based on the lag length criterion of the Akaike information criterion, a lag length of 4 is deemed optimal for ARDL estimations. Similarly, the lag length criteria of final prediction error and Hannan–Quinn criterion also indicate the same optimal lag length value, while Schwarz criterion suggests the use of a third lag length. Therefore, the study concluded that a lag length of 4 is optimal for ARDL estimation. Table 5 shows the ARDL estimates for ready reference.

Dynamic factor interactions have major implications for Pakistan's agriculture policy and long-term survival. The short- and long-term connections between AGRI and CCY are negative. This suggests agricultural inefficiency and misallocating land, labor, and capital, which may explain why value addition does not always increase yields.[48] Inefficient input utilization, outdated farming practices, and inadequate infrastructure are plausible factors. Intensive farming may also decrease soil fertility and diminish agricultural production due to water management concerns and pesticide and fertilizer overuse.[49] These findings highlight systemic industry concerns, including infrastructure, extension, and agricultural R&D underfunding. These systemic inefficiencies must be addressed to boost agricultural output and growth.[50]

Table 3. Unit root estimates

Variables	Level		First difference		Decision
	Intercept	Intercept and trend	Intercept	Intercept and trend	
CCY	−2.027 (0.274)	−1.733 (0.724)	−7.639 (0.000)	−7.724 (0.000)	I (1), *i.e.,* first-difference stationary
AGRI	−4.847 (0.000)	−4.758 (0.001)	−2.445 (0.134)	−2.635 (0.266)	I (0) level stationary
TEMP	−1.170 (0.997)	−1.794 (0.695)	−2.921 (0.049)	−3.546 (0.044)	I (1), *i.e.,* first-difference stationary
CH_4	−1.062 (0.954)	−5.376 (0.000)	−4.853 (0.000)	−2.352 (0.402)	I (0), *i.e.,* level stationary
N_2O	7.398 (0.955)	−5.376 (0.000)	−2.732 (0.074)	−2.352 (0.4002)	I (0), *i.e.,* level stationary
PAT	−4.312 (0.000)	−3.987 (0.000)	−7.101 (0.000)	−6.670 (0.000)	I (0), *i.e.,* level stationary
FAR	−2.040 (0.269)	−2.526 (0.314)	−8.008 (0.000)	−7.940 (0.000)	I (1), *i.e.,* first-difference stationary
DAML	−1.802 (0.376)	−2.029 (0.573)	−7.776 (0.000)	−7.711 (0.000)	I (1), *i.e.,* first-difference stationary

Source: Author's estimate. Note: Small bracket shows probability value.
Abbreviations: AGRI: Agriculture value-added; CH_4: Methane emissions; CCY: Cereal crop yield; DAML: Data analytics and machine learning; FAR: Farmer's adoption rate; N_2O: Nitrous oxide emissions; PAT: Precision agriculture technology; TEMP: Temperature.

Table 4. Lag length selection criteria

Lag	LogL	LR	FPE	AIC	SC	HQ
0	−1955.827	NA	1.59e+23	67.61472	67.79234	67.68391
1	−1660.686	529.2175	1.44e+19	58.29953	59.36527	58.71466
2	−1600.655	97.29230	4.39e+18	57.09155	59.04542	57.85262
3	−1539.557	88.48697	1.33e+18	55.84678	58.68877*	56.95380
4	−1489.183	64.27038*	6.11e+17*	54.97181*	58.70193	56.42477*

Source: Author's estimate. Note: * indicates lag order selected by the criterion.
Abbreviations: AIC: Akaike information criterion; FPE: Final prediction error; HQ: Hannan–Quinn criterion; LogL: Log-likelihood; LR: Likelihood ratio; SC: Schwarz criterion.

On the other hand, data analytics have drastically increased cereal crop output in the short term, supporting the growing body of studies on digital farming's revolutionary potential.[51,52] Farmers may optimize crop management, resource allocation, and production using data-driven options. Through targeted planting, watering, fertilizing, and pest control using real-time data, crop yields can be quickly increased.[53] Predictive analytics may help farmers anticipate weather and market trends and monitor soil and crop health to respond quickly to developing threats.[54] Data analytics provide short-term productivity gains and verifiable returns on low costs, encouraging greater adoption. Technological diffusion, accelerating innovation when an early adopter group benefits disproportionately, matches this phenomenon.[55] Thus, data analytics boost yields, efficiency, inventiveness, and farmer curiosity.

The study shows a positive association between technology adoption and cereal crop production in the short and long terms. This shows how technological advances boost agriculture productivity. Modern agricultural technology improves seed kinds, efficiency, and resource management in the short term,[56] whereas investments in technology may improve agricultural performance and production in the long run.[5] In addition, digital infrastructure and R&D expenditures may boost innovation and speed the adoption of breakthrough agricultural technologies. These findings emphasize the

Table 5. ARDL estimates

Dependent variable: CCY				
Variables	**Coefficient**	**Standard error**	**t-Statistic**	**Probability**
Δ(AGRI)	−0.014	0.002	−5.801	0.000
Δ(TEMP)	−180.128	198.039	−0.909	0.367
Δ(DAML)	3971.774	1568.494	2.532	0.014
Δ(FAR)	24.330	11.244	2.163	0.034
Δ(CH_4)	50.567	23.435	2.145	0.045
Δ(N_2O)	48.356	37.546	2.457	0.053
Δ(PAT)	0.048	0.012	3.840	0.000
CointEq(−1)	−0.362	0.148	−2.443	0.017
Long run coefficients				
Variables	**Coefficient**	**Standard error**	**t-Statistic**	**Probability**
AGRI	−0.028	0.010	2.801	0.035
TEMP	−497.536	499.057	−0.996	0.323
DAML	3163.687	2299.048	1.376	0.174
FAR	67.203	26.846	2.5031	0.015
CH_4	58.562	28.096	2.573	0.013
N_2O	56.203	30.326	2.952	0.016
PAT	0.147	0.052	2.826	0.035
Constant	21865.514	10810.553	2.022	0.048

Source: Author's estimate.

Abbreviations: AGRI: Agriculture value-added; CH_4: Methane emissions; CCY: Cereal crop yield; DAML: Data analytics and machine learning; FAR: Farmer's adoption rate; N_2O: Nitrous oxide emissions; PAT: Precision agriculture technology; TEMP: Temperature.

importance of policy frameworks, extension services, and institutional capacity in technology transmission and farmer training.[57]

The ARDL results indicate a positive relationship between CH_4 and N_2O emissions and CCYs in the short and long run. This shows that intensive agricultural practices increase emissions and food output. However, this association highlights an essential cost-benefit analysis: agricultural intensification improves yields and greenhouse gas emissions, threatening environmental sustainability. These findings demonstrate the necessity to include precision farming technology that maximizes input use and reduces environmental impacts into productivity gains to reduce emissions. Further, the findings reveal that productivity advantages and environmental externalities are traded off since more emissions are generated in exchange for higher yields, which are not achieved in a more sustainable manner. Conversely, CH_4 and N_2O emissions may enhance plant growth and soil fertility in some situations.[58] These gases enhance plant growth and output and are usually produced by microbial activities in the soil.[59] These emissions are indicative of more nutrient-rich soil, which is crucial for increasing agricultural production.[60] This relationship emphasizes the necessity for data-driven solutions and precision agriculture to strike a balance between crop production and greenhouse gas emissions.

Precise agriculture technology can aid in the rapid enhancement of CCYs over time, boosting agricultural efficiency and sustainability. Data analytics, GPS-guided devices, and remote sensing provide accurate resource management, site-specific interventions, and real-time monitoring.[61] These technologies provide personalized input applications for crop and soil conditions, improving yields with minimal waste and environmental impact. It has been demonstrated that long-term output and resilience can be increased through the implementation of strategies informed by data collected from multiple growing seasons.[30] In addition, precision agriculture may strengthen agricultural systems, protect biodiversity, and improve soil health, enabling sustainability in agriculture.

Table 6 shows that diagnostic testing confirmed the ARDL model's robustness. The Breusch–Godfrey

Table 6. Diagnostic test estimates

Test	Statistic	*p*-value	Conclusion
Breusch–Godfrey LM (serial correlation)	1.84	0.17	No serial correlation
Breusch–Pagan–Godfrey (heteroskedasticity)	2.15	0.14	No heteroskedasticity
Jarque–Bera (Normality)	1.73	0.42	Residuals are normally distributed
Ramsey RESET (specification)	1.92	0.16	Model is correctly specified
CUSUM	—	—	Stable within 5% significance bounds
CUSUMSQ	—	—	Stable within 5% significance bounds

Source: Author's estimate.
Abbreviations: CUSUM: Cumulative sum; CUSUMSQ: Cumulative sum of squares.

Table 7. ARDL bounds estimates

Test statistic	Value	k
F-statistic	10.43256	7
Critical value bounds		
Significance	**I (0) Bound**	**I (1) Bound**
10%	2.45	3.52
5%	2.86	4.01
2.5%	3.25	4.49
1%	3.74	5.06

Source: Author's estimate.

LM serial correlation test yielded a p=0.17 and found no residual autocorrelation. The residuals were homoscedastic, according to the Breusch–Pagan–Godfrey heteroskedasticity test with a p=0.14. The Jarque–Bera normality test validated the residuals' normal distribution with a p=0.42. The estimated model's stability was confirmed by the cumulative sum (CUSUM) and cumulative sum of squares (CUSUMSQ), which were inside the critical bounds at 5% significance. These results suggest that the estimated ARDL model is stable and statistically sound.

Table 7 presents the ARDL bounds estimates, revealing an F-statistic of 10.432. This value exceeds the critical bounds for I(1), indicating a significant dependency among the model variables. Co-integration, signifying a long-term equilibrium relationship between variables despite short-term fluctuations, was observed.

5. Conclusions and policy recommendation

The current study showed how Pakistan's environmental conditions, agricultural production, and adoption of AgriTech are interconnected. The adoption of data analytics, precision agriculture, and technology can boost grain crop yields. However, the association between CH_4 and N_2O emissions and yields is attributed to the intensified agricultural techniques rather than the environmental benefits. An increase in production may harm the environment, suggesting a productivity-environment trade-off. Furthermore, the inconsistent influence of AGRI on yields suggests systemic inefficiencies and the need for more consistent investment and policy. The study showed that prudent scaling of digital tools and climate-smart technology may decouple productivity from environmental impact, underlining the need to promote precision-based interventions, sustainable intensification, and data-driven decision-making to boost yields and climate resilience in Pakistan through revisions of the agricultural policy. Future research may incorporate farmer's behavior, financing techniques, and regional comparisons into analysis to enhance policy relevance.

Pakistan's policymakers should focus on agricultural sector efficiency and resource allocation to reduce the detrimental effects of agricultural value addition on CCYs. To this end, robust agricultural extension services, sophisticated farming methods, and rural infrastructure are needed. Policy measures that make high-quality inputs and new equipment more accessible, inexpensive, and simple to use should be encouraged to accelerate agricultural technology adoption. At this point, it should be noted that sustainable agricultural practices, efficient land use, adequate labor, and capital utilization are factors that increase productivity while preventing environmental degradation and preserving soil fertility. In addition, farmers must be given reliable access to real-time agricultural data so that they can interpret and apply data to make informed choices. Actions from public and private sectors may be required to promote data analytics and precision agriculture's digital infrastructure. Besides, farmers should be educated about modern farming techniques and extension services that employ sustainable methods and precision technology to assist farmers in increasing yields and reducing environmental impact.

This study revealed that the usage of digital technology and precision agriculture can enhance crop yields. However, the positive relationship between emissions and productivity highlights the serious environmental impacts arising from agricultural activities that must be controlled. Furthermore, our results suggested that value-added agriculture may have uneven effects on crop yields in the short and long terms. Future research should incorporate AgriTech solutions with improved environmental monitoring systems to reduce emissions. Further studies on Pakistan's policy frameworks that encourage sustainable agriculture without compromising food security are also warranted.

The utilization of only secondary data, devoid of the comprehensive cereal crop production characteristics, is the primary limitation of this study. Future research should incorporate socioeconomic status, soil health, and water usage practices to provide a full picture. Further, it should examine the long-term implications of data analytics and new agricultural technologies on Pakistan's crops and farming methods. Studies that combine agricultural knowledge with cutting-edge technology may lead to sustainable development. Regional environmental, economic, and social variances must be considered for the effective customization of interventions. More importantly, collaboration among academics, policymakers, and practitioners in translating research findings into transformative, sustainable agricultural approaches is highly desired.

Acknowledgments

None.

Funding

None.

Conflict of interest

The authors declare that they have no competing interests.

Author contributions

Conceptualization: Agha Amad Nabi, Muhammad Khalid Anser, Khalid Zaman
Investigation: Agha Amad Nabi, Muhammad Khalid Anser, Muhammad Asif
Methodology: Agha Amad Nabi, Muhammad Khalid Anser, Khalid Zaman
Formal analysis: All authors
Writing–original draft: Agha Amad Nabi
Writing–review & editing: All authors

Availability of data

The data are freely available from the World Development Indicators published by the World Bank (2023) at https://databank.worldbank.org/source/world-development-indicators and CCKP (2023) at https://climateknowledgeportal.worldbank.org/country/pakistan (accessed on January 15, 2025).

References

1. Elumalai P, Gao X, Parthipan P, Luo J, Cui J. Agrochemical pollution: A serious threat to environmental health. *Curr Opin Environ Sci Health*. 2025;43:100597. doi: 10.1016/j.coesh.2025.100597
2. Kahiluoto H, Sakieh Y, Kaseva J, *et al*. Redistribution of nitrogen to feed the people on a safer planet. *PNAS Nexus*. 2024;3(5):170. doi: 10.1093/pnasnexus/pgae170
3. Tetteh CK. R&D, Innovation and labour productivity: Evidence from the manufacturing sector in Ghana. *Sci Afr*. 2024;24:e02136. doi: 10.1016/j.sciaf.2024.e02136
4. Galanakis CM. The future of food. *Foods*. 2024;13(4):506. doi: 10.3390/foods13040506
5. Karunathilake EMBM, Le AT, Heo S, Chung YS, Mansoor S. The path to smart farming: Innovations and opportunities in precision agriculture. *Agriculture*. 2023;13(8):1593. doi: 10.3390/agriculture13081593
6. Fuentes-Peñailillo F, Gutter K, Vega R, Silva GC. Transformative technologies in digital agriculture: Leveraging internet of things, remote sensing, and artificial intelligence for smart crop management. *J Sensor Actuator Netw*. 2024;13(4):39. doi: 10.3390/jsan13040039
7. Rai PK. Role of water-energy-food nexus in environmental management and climate action. *Energy Nexus*. 2023;11:100230. doi: 10.1016/j.nexus.2023.100230
8. Abanyie SK, Apea OB, Abagale SA, Amuah EEY, Sunkari ED. Sources and factors influencing groundwater quality and associated health implications: A review. *Emerg Contam*. 2023;9(2):100207. doi: 10.1016/j.emcon.2023.100207
9. Becker M, Clavero R, Khin OM, *et al*. System shift in rice: Processes and pathways of change in rice-based

production systems of Southeast Asia. *Agric Syst*. 2024;217:103917.
doi: 10.1016/j.agsy.2024.103917

10. Sharma UC, Datta M, Sharma V. Land use and management. In: *Soils in the Hindu Kush Himalayas. Geography of the Physical Environment*. Cham: Springer; 2022.
doi: 10.1007/978-3-031-11458-8_7
11. Bhakta I, Phadikar S, Majumder K. State-of-the-art technologies in precision agriculture: A systematic review. *J Sci Food Agric*. 2019;99(11):4878-4888.
doi: 10.1002/jsfa.9693
12. Onyango CM, Nyaga JM, Wetterlind J, Söderström M, Piikki K. Precision agriculture for resource use efficiency in smallholder farming systems in Sub-Saharan Africa: A systematic review. *Sustainability*. 2021;13(3):1158.
doi: 10.3390/su13031158
13. Erickson B, Fausti SW. The role of precision agriculture in food security. *Agron J.* 2021;113(6):4455-4462.
doi: 10.1002/agj2.20919
14. Mansoor S. Pakistan's water security crisis: Challenges and the case for integrated water resource management. *NUST J Int Peace Stab*. 2025;8(1):30-47.
doi: 10.37540/njips.v8i1.184
15. Mahmood S. Infrastructure and economic growth in Pakistan: An empirical analysis. *Econ Model*. 2022;107:105252.
doi: 10.37540/njips.v8i1.184
16. Knippenberg E, Amadio M, Meyer M. Poverty impacts of the Pakistan flood 2022. *Econ Disasters Clim Change*. 2024;8(3):453-471.
doi: 10.1007/s41885-024-00155-3
17. Fahad S, Wang J. Climate change, vulnerability, and its impacts in rural Pakistan: A review. *Environ Sci Pollut Res*. 2020;27:1334-1338.
doi: 10.1007/s11356-019-06878-1
18. Feng Y, Sun M, Pan Y, Zhang C. Fostering inclusive green growth in China: Identifying the impact of the regional integration strategy of Yangtze River Economic Belt. *J Environ Manage*. 2024;358:120952.
doi: 10.1016/j.jenvman.2024.120952
19. De Rosa M, Bartoli L, Del Giudice T, Vecchio Y. Conducive environments and entrepreneurial access to rural policies. *Sustainability*. 2022;14(9):4951.
doi: 10.3390/su14094951
20. Raihan A, Muhtasim DA, Farhana S, *et al*. Nexus between economic growth, energy use, urbanization, agricultural productivity, and carbon dioxide emissions: New insights from Bangladesh. *Energy Nexus*. 2022;8:100144.
doi: 10.1016/j.nexus.2022.100144
21. Mgendi G. Unlocking the potential of precision agriculture for sustainable farming. *Discov Agric*. 2024;2(1):87.
doi: 10.1007/s44279-024-00078-3
22. Nath S. A vision of precision agriculture: Balance between agricultural sustainability and environmental stewardship. *Agron J.* 2024;116(3):1126-1143.
doi: 10.1002/agj2.21405
23. Arion FH, Harutyunyan G, Aleksanyan V, Muradyan M, Asatryan H, Manucharyan M. Determining digitalization issues (ICT adoption, digital literacy, and the digital divide) in rural areas by using sample surveys: the case of Armenia. *Agriculture.* 2024;14(2):249.
doi: 10.3390/agriculture14020249
24. Su Q, Singh VP. Advancing irrigation management: Integrating technology and sustainability to address global food security. *Environ Monit Assess*. 2024;196(11):1018.
doi: 10.1007/s10661-024-13145-5
25. Zhao J, Yang J, Xie H, Qin X, Huang R. Sustainable management strategies for balancing crop yield, water use efficiency and greenhouse gas emissions. *Agric Syst*. 2024;217:103944.
doi: 10.1016/j.agsy.2024.103944
26. Wang L, Vo XV, Shahbaz M, Ak A. Globalization and carbon emissions: Is there any role of agriculture value-added, financial development, and natural resource rent in the aftermath of COP21? *J Environ Manage*. 2020;268:110712.
doi: 10.1016/j.jenvman.2020.110712
27. Gelgo Dube B, Gemechu Gobena A, Bedemo Beyene A. Distortion of agricultural incentives in East Africa: Effects on agricultural value added. *Cogent Econ Finance.* 2024;12(1):2285068.
doi: 10.1080/23322039.2023.2285068
28. Khan N, Ray RL, Kassem HS, Zhang S. Mobile internet technology adoption for sustainable agriculture: Evidence from wheat farmers. *Appl Sci*. 2022;12(10):4902.
doi: 10.3390/app12104902
29. Jararweh Y, Fatima S, Jarrah M, AlZu'bi S. Smart and sustainable agriculture: Fundamentals, enabling technologies, and future directions. *Comput Electr Eng.* 2023;110:108799.
doi: 10.1016/j.compeleceng.2023.108799
30. Júnior MRB, de Almeida Moreira BR, dos Santos Carreira V, *et al.* Precision agriculture in the United States: A comprehensive meta-review inspiring further research, innovation, and adoption. *Comput Electron Agric*. 2024;221:108993.
doi: 10.1016/j.compag.2024.108993
31. Alabdali SA, Pileggi SF, Cetindamar D. Influential factors, enablers, and barriers to adopting smart technology in rural regions: A literature review. *Sustainability*. 2023;15(10):7908.
doi: 10.3390/su15107908
32. Raihan A, Tuspekova A. Dynamic impacts of economic growth, energy use, urbanization, agricultural productivity, and forested area on carbon emissions: New insights from Kazakhstan. *World Dev Sustain*. 2022;1:100019.
doi: 10.1016/j.wds.2022.100019

33. Soko NN, Kaitibie S, Ratna NN. Does institutional quality affect the impact of public agricultural spending on food security in Sub-Saharan Africa and Asia? *Glob Food Sec.* 2023;36:100668. doi: 10.1016/j.gfs.2022.100668
34. Peng J, Zhao Z, Liu D. Impact of agricultural mechanization on agricultural production, income, and mechanism: Evidence from Hubei province, China. *Front Environ Sci*. 2022;10:838686. doi: 10.3389/fenvs.2022.838686
35. Mutengwa CS, Mnkeni P, Kondwakwenda A. Climate-smart agriculture and food security in Southern Africa: A review of the vulnerability of smallholder agriculture and food security to climate change. *Sustainability.* 2023;15(4):2882. doi: 10.3390/su15042882
36. Abekoon T, Sajindra H, Rathnayake N, *et al*. A novel application with explainable machine learning (SHAP and LIME) to predict soil N, P, and K nutrient content in cabbage cultivation. *Smart Agric Technol*. 2025;11:100879. doi: 10.1016/j.atech.2025.100879
37. Soussi A, Zero E, Sacile R, Trinchero D, Fossa M. Smart sensors and smart data for precision agriculture: A review. Sensors. 2024;24(8):2647. doi: 10.3390/s24082647
38. Ahmad U, Sharma L. A review of best management practices for potato crop using precision agricultural technologies. Smart Agric Technol. 2023;4:100220. doi: 10.1016/j.atech.2023.100220
39. Waqas MM, Wasim M, Ashraf M, Jatoi WN. Engineering principles of precision farming: Pathway for the developing countries to ensure food security. In: Jatoi WN, Mubeen M, Hashmi MZ, *et al*., editors. Climate Change Impacts on Agriculture. Cham: Springer; 2023. doi: 10.1007/978-3-031-26692-8_7
40. Ji M, Zhang X. Assessing the impacts and mechanisms of green bond financing on the enhancement of green management and technological innovation in environmental conservation enterprises. J Knowl Econ. 2023;3:12709-50. doi: 10.1007/s13132-023-01594-1
41. Gemtou M, Kakkavou K, Anastasiou E, *et al.* Farmers' transition to climate-smart agriculture: A systematic review of the decision-making factors affecting adoption. Sustainability. 2024;16(7):2828. doi: 10.3390/su16072828
42. Imran M, Sattar A, Alam MS. Heterogeneous analysis of free trade agreement between Pakistan and China: A policy guideline for CPEC. J Econ Adm Sci. 2024;40(1):76-94. doi: 10.1108/JEAS-02-2022-0051
43. Jobarteh B, Neethirajan S. Leveraging satellite data for greenhouse gas mitigation in Canadian poultry farming. *Smart Agric Technol*. 2025;10:100704. doi: 10.1016/j.atech.2024.100704
44. Sweet LB, Athanasiadis IN, van Bree R, *et al.* Transdisciplinary coordination is essential for advancing agricultural modeling with machine learning. *One Earth.* 2025;8(4):101233. doi: 10.1016/j.oneear.2025.101233
45. World Bank. *World Development Indicators*. Washington, D.C.: World Bank; 2023. Available from: https://databank.worldbank.org/source/world-development-indicators [Last accessed on 2025 Jan 15].
46. CCKP. *Climate Change Overview: Country Summary. World Bank Climate Knowledge Portal;* 2023. Available from: https://climateknowledgeportal.worldbank.org/country/Pakistan [Last accessed on 2025 Jan 15].
47. Pesaran MH, Shin Y, Smith RJ. Bounds testing approaches to the analysis of level relationships. *J Appl Econometrics*. 2001;16(3):289-326. doi: 10.1002/jae.616
48. Jiang T, Zhong M, Gao A, Ma G. Do factor misallocations affect food security? Evidence from China. *Agriculture*. 2024;14(5):729. doi: 10.3390/agriculture14050729
49. Zahoor I, Mushtaq A. Water pollution from agricultural activities: A critical global review. *Int J Chem Biochem Sci*. 2023;23(1):164-176.
50. Stevenson JR, Macours K, Gollin D. The rigor revolution: New standards of evidence for impact assessment of international agricultural research. *Annu Rev Resour Econ*. 2023;15:495-515.
51. Rehman KU, Andleeb S, Ashfaq M, Akram N, Akram MW. Blockchain-enabled smart agriculture: Enhancing data-driven decision making and ensuring food security. *J Clean Prod*. 2023;427:138900. doi: 10.1016/j.jclepro.2023.138900
52. Liang C, Shah T. IoT in agriculture: The future of precision monitoring and data-driven farming. *Eigenpub Rev Sci Technol*. 2023;7(1):85-104.
53. Hassan M, Kowalska A, Ashraf H. Advances in deep learning algorithms for agricultural monitoring and management. *Appl Res ArtifIntell Cloud Comput*. 2023;6(1):68-88.
54. Tripathi PK, Singh CK, Singh R, Deshmukh AK. A farmer-centric agricultural decision support system for market dynamics in a volatile agricultural supply chain. *Benchmarking Int J.* 2023;30(10):3925-3952. doi: 10.1108/BIJ-12-2021-0780
55. Bokolo AJ. Examining the adoption of sustainable eMobility-sharing in smart communities: Diffusion of innovation theory perspective. *Smart Cities*. 2023;6(4):2057-2080. doi: 10.3390/smartcities6040095
56. Haruna LZ, Sennuga SO, Bamidele J, *et al*. Factors influencing farmers' adoption of improved technologies in maize production in Kuje Area Council of FCT-Abuja, Nigeria. *GPH Int J Agric Res*. 2023;6(4):25-41.

doi: 10.5281/zenodo.7924557
57. Nery LM, da Cunha e Silva DC, Sabonaro DZ. Agriculture technology transfer: A multicriteria analysis for decision making. *Environ Dev Sustain*. 2024;26(6):15515-15533. doi: 10.1007/s10668-023-03261-6
58. Ma B, Karimi MS, Mohammed KS, Shahzadi I, Dai J. Nexus between climate change, agricultural output, fertilizer use, agriculture soil emissions: Novel implications in the context of environmental management. *J Clean Prod*. 2024;450:141801. doi: 10.1016/j.jclepro.2024.141801
59. Hartmann M, Six J. Soil structure and microbiome functions in agroecosystems. *Nat Rev Earth Environ*. 2023;4(1):4-18. doi: 10.1038/s43017-022-00366-w
60. Hu M, Wade AJ, Shen W, *et al*. Effects of different organic fertilizers on nitrous oxide and methane emissions from double-cropping rice fields. *Pedosphere*. 2024;34(1):52-62. doi: 10.1016/j.pedsph.2023.03.006
61. Gawande V, Saikanth DRK, Sumithra BS, *et al.* Potential of precision farming technologies for eco-friendly agriculture. *Int J Plant Soil Sci*. 2023;35(19):101-112. doi: 10.9734/IJPSS/2023/v35i193528

ACCSCIENCE PUBLISHING

Asian Journal of Water, Environment and Pollution. Vol. 22, No. 3 (2025), pp. 119-133.
doi: 10.36922/AJWEP025080052

ORIGINAL RESEARCH ARTICLE

Assessing long-term groundwater level trends in Karakalpakstan using non-parametric statistical methods

Mehdi Fuladipanah[1], Kenjabek Rozumbetov[2,3], Namal Rathnayake[4], Valery Erkudov[5], Mirzohid Koriyev[6], and Upaka Rathnayake[7]*

[1]Department of Civil Engineering, Ramhormoz Branch, Islamic Azad University, Ramhormoz, Iran
[2]Department of Veterinary Diagnostics and Food Safety, Nukus Branch of Samarkand State University of Veterinary Medicine, Animal Husbandry and Biotechnology, Nukus, Uzbekistan
[3]Department of General Biology and Physiology, Karakalpak State University, Nukus, Uzbekistan
[4]Department of Civil Engineering, Faculty of Engineering, The University of Tokyo, Bunkyo City, Tokyo, Japan
[5]Department of Normal Physiology, St. Petersburg State Pediatric Medical University, Saint Petersburg, Russia
[6]Department of Natural Sciences, Namangan State Pedagogical Institute, Namangan, Uzbekistan
[7]Department of Civil Engineering and Construction, Faculty of Engineering and Design, Atlantic Technological University, Sligo, Ireland
***Corresponding author:** Upaka Rathnayake (upaka.Rathnayake@atu.ie)

Received: February 21, 2025; 1st revised: April 18, 2025; 2nd revised: April 28, 2025; Accepted: May 12, 2025; Published online: June 4, 2025

Abstract: Climate change has significantly impacted global hydrometeorological variables, placing increasing stress on groundwater resources. This study investigates long-term groundwater level trends in the Republic of Karakalpakstan, Uzbekistan, using a combination of non-parametric statistical models. The Mann–Kendall test, Spearman's rank correlation, and innovative polygon trend analysis (IPTA) were applied to assess spatiotemporal variations. To address the limitations of parametric methods, this study utilizes robust, assumption-free trend detection techniques. The results reveal statistically significant increasing trends in groundwater levels across most provinces, particularly in Muynak (Z=3.884, p<0.001) and Republic-wide (Z=3.603, p<0.001). In contrast, provinces such as Turtkul, Ellikkala, and Nukus exhibit no significant trends. The IPTA method highlights seasonal fluctuations, with notable decreases in specific months despite the overall upward trend. These findings emphasize the need for localized groundwater management strategies that consider both seasonal dynamics and long-term changes. By integrating multiple statistical techniques, this study provides a comprehensive evaluation of groundwater variability and offers valuable insights for policymakers and water resource managers in arid regions facing climate-induced water challenges.

Keywords: Groundwater trend analysis; Mann–Kendall test; Innovative polygon trend analysis; Climate change impact; Water resource management

1. Introduction

Hydrometeorological variables – such as precipitation, temperature, streamflow, and evaporation – play a critical role in sustaining human activities, including water resource management, agriculture, hydroelectric power generation, and groundwater replenishment. However, their inherent stochasticity and complexity necessitate advanced analytical approaches to assess trends and variability accurately. Climate change – driven by

global warming, urbanization, and land degradation – is amplifying shifts in these variables, exacerbating risks such as floods, droughts, and disruptions to hydrological cycles. According to the Intergovernmental Panel on Climate Change, anthropogenic activities have accelerated these changes, with projections indicating a global temperature rise of 1.0 – 5.7°C, a sea-level increase of 0.5 – 1.0 m, and an increased frequency of extreme weather events by 2100. Trend analysis, particularly through non-parametric methods, has become indispensable for evaluating temporal patterns in hydroclimatic data. These methods bypass restrictive assumptions (e.g., normality and independence) and are widely applied to detect trends in variables such as rainfall, evapotranspiration, and wind speed. Such analyses help reveal how climate change alters hydrological systems, impacting water availability, quality, and ecosystem resilience. For instance, precipitation anomalies – linked to both droughts and floods – are increasingly destabilizing economies and ecosystems worldwide.[1-7]

Trend analysis is a fundamental approach for detecting and forecasting future patterns in data using objective, systematic, and quantitative methodologies. It is particularly effective for examining the impacts of climate change on hydrometeorological variables, which are inherently complex and stochastic, often exhibiting significant variability and random fluctuations around an underlying trend. In this context, trend analysis serves as a valuable tool for gaining insights into the behavior of hydroclimatic variables. However, the stochastic nature and intrinsic properties of these variables necessitate specialized analytical techniques. Traditional statistical methods commonly used for trend detection are often constrained by assumptions such as normality, independence, and sufficient record length.[7-9] These assumptions are frequently violated in hydroclimatic datasets. To overcome these limitations, non-parametric statistical tests – characterized by minimal distributional assumptions – have become increasingly prevalent in recent years. These methods are better suited to accommodate the inherent variability and irregularities of hydrometeorological datasets.[10-15]

Trend analysis models are broadly categorized into two primary classes: Parametric and non-parametric. Parametric models, such as regression models and time series models, rely on specific assumptions regarding the underlying data distribution and relationships. In contrast, non-parametric models, including the Mann–Kendall (MK) test, Sen's slope estimator, Spearman's rank (SR) correlation test, and innovative trend analysis, do not require strict distributional assumptions. Both model classes have been extensively employed by researchers to conduct trend analyses in various fields.[16-25] A brief list of trend analysis models is presented in Table 1.

This study introduces a comprehensive comparative analysis of long-term trends in monthly groundwater levels across 16 provinces in the Republic of Karakalpakstan, Uzbekistan, spanning the period from 1990 to 2023. By integrating innovative statistical techniques, including the innovative polygon trend analysis (IPTA), the MK test, and Sen's slope estimator, this research uniquely captures the temporal and spatial dynamics of groundwater variations. The novelty of this study lies in the combined use of these advanced methodologies, providing deeper insights into regional hydrometeorological patterns and their implications for sustainable water resource management in a climatically sensitive region.

It is important to note that the present study does not incorporate precipitation time series analysis, as long-term records show no significant temporal variations

Table 1. Summary of literature review on trend analysis models

References	Model name	Trend subject
Gaddikeri *et al*.[26]	MK	Meteorological variables
Çelebioğlu and Tayanç[27]	RM, MK	Precipitation
Qadem and Tayfur[28]	MK, ITA	Temperature
Alashan[29]	MK	Precipitation
San[30]	ITA	Groundwater level
Kessabi *et al*.[31]	MK, ITA, SSE	Rainfall
Likinaw *et al*.[32]	MK, ITA	Extreme precipitation
Agbo *et al*.[33]	MK, ITA	Climatic parameters
Sanogo *et al*.[34]	MK	Temperature and rainfall
Gul and Ren[35]	ITA	Precipitation
Nguyen *et al*.[36]	MK, ITA	Sea level
Seenu and Jayakumar[37]	MK, ITA	Extreme rainfall
Güçlü[38]	MK, ITA	Rainfall
Caloiero *et al*.[39]	ITA	Seasonal and annual rainfall

Abbreviations: ITA: Innovative trend analysis; MK: Mann–Kendall test; SSE: Sen's slope estimator.

in rainfall across the region, which is characterized by infrequent precipitation events. In addition, snowfall statistics were not included in the analysis, representing a limitation that could be addressed in future research.

2. Materials and methods

2.1. Study area and data description

The Republic of Karakalpakstan is located in the northwest of Uzbekistan (43°10' N and 58°45' E). Administratively, it comprises 16 districts and one central city, Nukus. Covering a total area of 166,600 km^2, Karakalpakstan accounts for 37.1% of the country's total land area (Figure 1). The study area lies within the Aral Sea basin and shares borders with Kazakhstan to the north and west, the Karakum sand massifs of Turkmenistan to the south – along the modern and ancient Amudarya delta – and the Qizilqum desert to the east. The territory of the Republic of Karakalpakstan is characterized by relatively simple surface topography, with the Ustyurt Plateau occupying the western part and the Turan Plain covering the remainder. Elevations range from 49 m below sea level in the southwest to 466 m above sea level in the northwest. The Republic of Karakalpakstan has a harsh continental climate characterized by arid summers, relatively cold winters, and low annual precipitation, primarily in the form of snow. Average January temperatures range from −4.9°C in the southern region to −7.6°C in the northern region, with absolute minimums reaching −40°C. In July, average temperatures rise to 30°C in the south and 26°C in the north, with recorded maximums as high as 46°C. Annual precipitation averages 110 mm, with the majority occurring during winter and spring. Droughts are frequent, as evaporation rates are 9 – 10 times greater than the average precipitation. The vegetation period spans 194 – 214 days annually.

Karakalpakstan contains more than 21.3% of Uzbekistan's irrigated land and 48.5% of its pasturelands. Due to the arid climate, agriculture in the region is only viable through irrigation.

Groundwater data were obtained from the Karakalpakstan Melioration Expedition, a governmental agency. Monthly groundwater measurements were collected over a 33-year period, from 1990 to 2023. For this study, a total of 16 observation sites were selected for comprehensive groundwater analysis. These include sites from the Southern Melioration system, Amudarya Amelioration system, Left-bank Melioration system, and Right-bank Melioration system. The specific locations are: Turtkul, Ellikkala, Beruniy, Amudarya, Khojeli, Takhiatash, Shumanay, Kanlikul, Kungirot, Muynak, Nukus, Kegeyli, Buzatau, Chimbay, Karauzyak, and Takhtakopir.

2.2. Trend analysis models

2.2.1. MK model

The MK model is a widely recognized non-parametric method for detecting monotonic trends in time series data. Its popularity stems from its robustness against non-normal data distributions and its ability to accommodate missing values, making it an ideal choice

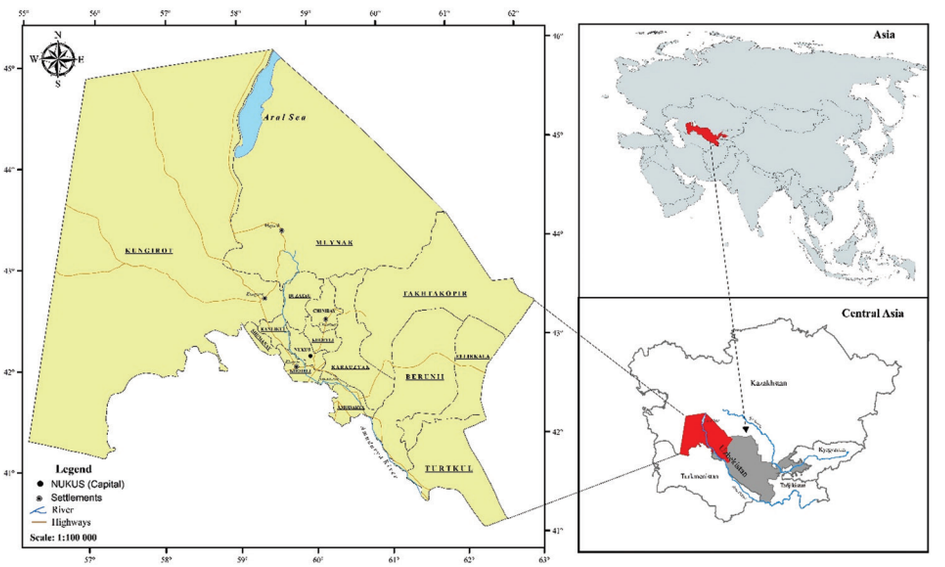

Figure 1. Location of study area in the Republic of Karakalpakstan, Uzbekistan

for environmental and hydrological studies. The test statistic *S* is calculated using Equation I:

$$S = \sum_{i=1}^{n-1} \sum_{j=i+1}^{n} sgn(x_j - x_i) \quad \text{(I)}$$

where x_i and x_j are the observed values at time points *i* and *j*, and *n* is the number of data points. Under the null hypothesis of no trend, the expected value of *S* is zero. The variance of *S,* denoted as (*S*), is given in Equation II:

$$V(S) = \frac{1}{18}\left[n(n-1)(2n+5) - \sum_{t=1}^{m} t(t-1)(2t+5) \right] \quad \text{(II)}$$

where *n* is the number of data points and *m* represents the number of tied groups. The standardized test statistic *Z* is given by Equation III:

$$Z = \begin{cases} \dfrac{S-1}{\sqrt{V(S)}}; & if\ S > 0 \\ 0; & S = 0 \\ \dfrac{S+1}{\sqrt{V(S)}}; & if\ S < 0 \end{cases} \quad \text{(III)}$$

A positive *Z*-value indicates an increasing trend, whereas a negative value signifies a decreasing trend. The significance of the trend is determined by comparing *Z* to critical values from the standard normal distribution, offering a robust and reliable framework for trend detection across diverse datasets.

2.2.2. Spearman's rho model

The SR rank correlation test is another robust non-parametric method used to identify monotonic trends in time series data by measuring the strength and direction of the association between two variables. Its ability to detect non-linear relationships and its resistance to outliers make it a widely used approach in trend analysis across various scientific disciplines. The SR rank correlation coefficient, ρ, is calculated using Equation IV:

$$\rho = 1 - \frac{6\sum_{i=1}^{n} d_i^2}{n(n^2-1)} \quad \text{(IV)}$$

where $d_i = R(x_i) - R(y_i)$ is the difference between the ranks of the paired values x_i and y_i, and *n* is the number of data points. The test evaluates whether the calculated ρ significantly deviates from zero, indicating the presence of a trend. For significance testing, the correlation coefficient is transformed into a *t*-statistic, calculated using Equation V.

$$t = \rho\sqrt{\frac{n-2}{1-\rho^2}} \quad \text{(V)}$$

This *t*-value follows a Student's *t*-distribution with $n-2$ degrees of freedom under the null hypothesis of no trend. A positive ρ value suggests an increasing trend, while a negative value indicates a decreasing trend. The SR test is particularly effective for datasets with non-linear patterns, making it a versatile tool for trend detection and analysis in environmental, hydrological, and climate studies.

Before conducting the MK and SR tests, the presence of lag-1 autocorrelation (serial correlation) must be evaluated. Serial correlation in a dependent time series can influence the effectiveness of these tests. For instance, positive serial correlation can increase the likelihood of detecting a significant trend even when none exists.[40] Therefore, it is essential to assess and address serial correlation prior to trend analysis. If significant serial correlation is present, test statistics must be adjusted, or a pre-whitening technique should be applied to eliminate its impact.

In this research, the trend-free pre-whitening method introduced by Yue *et al*.[41] was utilized. The first-order autocorrelation coefficient (r_i) is calculated as shown in Equation VI:

$$r_i = \frac{\frac{1}{N-i}\sum_{k=1}^{N-i}(x_i - \bar{\bar{x}})(x_{i+k} - \bar{x})}{\frac{1}{N}\sum_{k=1}^{N}(x_k - \bar{x})^2} \quad \text{(VI)}$$

If the absolute value of r_1 is less than the critical threshold $\frac{1.96}{\sqrt{N}}$ at the 5% significance level, as applied by Douglas *et al*.[42] and Tosunoglu,[43] the data are deemed to be serially independent. Otherwise, the series is classified as serially dependent.

2.2.3. Polygon trend analysis model

The IPTA technique, introduced by Sen *et al*.,[7] is versatile and can be utilized for analyzing time series across various temporal scales, including monthly and seasonal intervals.[44-48] For a monthly time series x_1, x_2,…, x_n, where *n* represents the number of years, the data should be structured in a matrix format as outlined by Sen *et al*.[7]:

$$\begin{bmatrix} x_{1,1} & \cdots & x_{12,1} \\ \vdots & \ddots & \vdots \\ x_{1,n} & \cdots & x_{12,n} \end{bmatrix}$$

The first half of the dataset, referred to as the upper series, comprises the years $n = 1, 2, 3, \ldots, \frac{n}{2}$, while the second half, known as the lower series, includes the years $\frac{n}{2}+1$, $\frac{n}{2}+2$,…, n. Implementing the IPTA method on both monthly and seasonal scales involves a multi-step procedure, utilizing a predefined framework with 12 dispersion points to represent each month of the year. The model incorporates the calculation of arithmetic mean and standard deviation (SD) values for the dataset.

By analyzing successive months, the IPTA model identifies trends, allowing for the determination of slopes, lengths, and associated values that characterize these monthly transitions. Subsequently, trend polylines are generated by connecting successive segments of the time series, forming the foundation for further analysis. This graphical representation facilitates both numerical and qualitative interpretations of the examined time series, offering deeper insights into the climatic variations captured in the data.

The calculation procedure for the ITPA model is as follows:

(i) The dataset of size n is divided into two equal parts for comprehensive analysis.
(ii) The mean and SD are computed for each month in both subsets.
(iii) The first series is plotted on the horizontal axis of a scatter chart, whereas the second series is represented on the vertical axis.
(iv) Points representing consecutive months are connected using straight lines to form a polygon.
(v) The slope and length of each connecting line are calculated using Equations VII and VIII, respectively.

$$S = \frac{y_2 - y_1}{x_2 - x_1} \quad \text{(VII)}$$

$$L = \sqrt{(x_2 - x_1)^2 + (y_2 - y_1)^2} \quad \text{(VIII)}$$

The IPTA model template for monthly records offers a framework for both qualitative and quantitative analyses of hydrometeorological systems, yielding several key insights. First, the straight line connecting 2 consecutive months represents changes in monthly values, whereas the closed polygon indicates the natural balance of the system over a year. The length of each line illustrates the magnitude of monthly variations. When the slopes of these lines are relatively consistent in both vertical and horizontal directions, it suggests minimal monthly contributions to the overall variation.

The arrangement of straight lines within the 12-point polygon reveals the annual variation pattern and allows for location-specific qualitative interpretations. Each side of the polygon assumes a linear transition between months. Applying this linearity assumption to shorter periods enhances the accuracy of trend analyses. If the slopes of all connecting lines are similar and the polygon edges align in a consistent direction, the resulting polygon resembles a narrow band close to a global regression line. This indicates uniform, isotropic variation in the hydrometeorological variable. Conversely, wider polygons suggest greater temporal variability.

A polygon with a rising orientation generally suggests balanced hydro-climatic conditions. However, the appearance of multiple polygons or internal loops may occur under certain circumstances, reflecting dynamic and complex variability. Horizontal intersections with the polygon represent the expected range of monthly variations, whereas vertical intersections indicate the magnitude and limits of hydrometeorological quantities. A smaller polygon area reflects consistent monthly precipitation and stable hydrological events, while a reduced overall slope from the horizontal axis indicates higher-intensity hydrometeorological phenomena. Ultimately, the IPTA model serves as a valuable tool in water resource planning, operation, and management, enabling systematic evaluation of both quantitative and qualitative properties of hydrometeorological dynamics.

3. Results and discussion

3.1. Serial correlation analysis

Before applying the MK and SR tests to detect trends in the groundwater time series, it was necessary to assess the presence of serial autocorrelation in the data. To this end, lag-1 autocorrelation coefficients (r_1) were calculated and evaluated for statistical significance under the null hypothesis at the 95% confidence level using a two-tailed test: $r_1 = \pm \frac{1.96}{\sqrt{N}}$.

The autocorrelation coefficients for the monthly groundwater level data across various provinces were computed, with the results summarized in Table 2. The analysis revealed that all calculated serial correlation coefficients remained below their respective critical thresholds. This indicates that the monthly groundwater level time series do not exhibit significant serial dependence. Consequently, the MK and SR trend tests were applied directly to the full datasets without

Table 2. Lag-1 autocorrelation coefficients for monthly groundwater level data across the provinces

Province	January	February	March	April	May	June	July	August	September	October	November	December	Annual
Turtkul[a]	−0.1159	−0.0659	−0.0156	0	−0.0179	−0.0109	−0.0021	0	−0.0672	−0.1841	−0.2289	−0.0858	−0.1616
Ellikkala[a]	−0.0149	−0.0286	−0.012	−0.0085	0	−0.0023	−0.0077	−0.0064	−0.0004	−0.0036	−0.01	−0.0049	0.0142
Beruniy[a]	−0.0409	−0.0004	−0.0565	−0.0015	−0.0264	−0.0138	−0.0231	−0.031	−0.0003	−0.0299	−0.0699	−0.0093	0.0027
Amudarya[a]	−0.0097	−0.0021	−0.065	−0.0077	−0.0097	−0.0112	−0.0384	−0.0083	−0.0677	−0.1345	−0.1069	−0.0471	−0.021
Khojeli[a]	−0.0006	−0.0057	−0.0636	−0.0692	−0.0064	−0.0026	−0.0027	−0.0044	−0.027	−0.0516	−0.0394	−0.0004	0.0065
Takhiatash[b]	0.1328	0.0138	0.0232	0.07	−0.0141	−0.049	−0.047	−0.0464	−0.0009	−0.0506	−0.117	0.0246	−0.108
Shumanay[a]	−0.0018	−0.005	−0.0121	−0.0376	−0.0438	−0.0172	−0.0199	−0.015	−0.0032	−0.0021	−0.0012	−0.0196	0.0081
Kanlikul[a]	−0.0004	−0.0005	−0.0105	−0.0118	−0.0094	−0.0063	−0.0034	−0.0032	−0.0002	0	0	−0.0001	0.0033
Kungirot[a]	−0.0008	−0.0023	−0.0105	−0.012	−0.0051	−0.006	−0.001	−0.0021	−0.0004	−0.0006	−0.0011	−0.0007	0.01
Muynak[a]	−0.0738	−0.075	−0.0884	−0.0963	−0.0877	−0.0918	−0.0908	−0.0813	−0.0529	−0.051	−0.0458	−0.0568	−0.0629
Nukus[a]	−0.0825	−0.0983	−0.2219	−0.0108	−0.088	−0.0097	−0.0104	−0.001	−0.0928	−0.0559	−0.0345	−0.0082	−0.0029
Kegeyli[a]	−0.0032	−0.0055	−0.0197	−0.0291	−0.023	−0.021	−0.0279	−0.0282	−0.0213	−0.0106	−0.0102	−0.0253	−0.013
Buzatau[c]	−0.0011	−0.0001	−0.0005	−0.0009	−0.007	−0.006	−0.0089	−0.009	−0.0129	−0.0003	0.3484	0.0481	−0.0059
Chimbay[a]	−0.0004	−0.0002	−0.0251	−0.0143	−0.0054	−0.0039	−0.0061	−0.0114	−0.0004	−0.002	0	−0.0202	0.0178
Karauzyak[a]	−0.0026	−0.0075	−0.0165	−0.0137	−0.0112	−0.0011	−0.0073	−0.007	0	0	−0.0052	−0.0292	0.0068
Takhtakopir[a]	−0.012	−0.0131	−0.0034	−0.0028	−0.0001	0	0	−0.0025	−0.0063	−0.0076	−0.0086	−0.0089	−0.0004
Total[a]	−0.0004	−0.0036	−0.0325	−0.0233	−0.0196	−0.011	−0.0176	−0.0134	−0.0008	−0.0001	0	−0.0082	0.011

Notes: [a]Critical autocorrelation coefficient is 0.336; [b]Critical autocorrelation coefficient is 0.800; [c]Critical autocorrelation coefficient is 0.475.

doi: 10.36922/AJWEP025080052

requiring pre-whitening or other adjustments, given the absence of serial correlation that might otherwise bias the results.

3.2. Trend analysis results

3.2.1. MK test

The MK test results presented in Table 3 and Table S1 provide a comprehensive analysis of monthly and annual groundwater level trends across various provinces and the Republic of Karakalpakstan, Uzbekistan. These results reveal significant spatial and temporal variations, highlighting both consistent patterns and local anomalies.

In Turtkul Province (Table 3), the MK test reveals predominantly stable groundwater levels with no significant annual trend. However, statistically significant decreasing trends are observed in January (Z=−2.270, p=0.023) and February (Z=−1.973, p=0.048), reflecting a reduction in groundwater levels during the winter months. Conversely, a significant increasing trend in August (Z=2.261, p=0.024) suggests a localized summer increase in groundwater levels. In Ellikkala Province, the annual trend is not statistically significant. However, the monthly analysis indicates strong increasing trends from April (Z=4.065, p<0.001) through September, with the most pronounced change occurring in April. This seasonal pattern suggests a consistent rise in groundwater levels during the warmer months, likely influenced by regional hydrological or climatic conditions.

The results for Beruniy Province (Table S1) highlight a significant annual increase (Z=2.906, p=0.004), with monthly increases from April to November, with the strongest monthly trend in May (Z=4.033, p<0.001), indicating favorable seasonal recharge. Similarly, Amudarya Province (Table S1) displays a significant positive annual trend (Z=2.906, p=0.004), with monthly increases from April to November, mirroring the seasonal pattern observed in Beruniy and suggesting similar hydrological influences. In Khojeli Province, no significant annual trend is observed. However, significant monthly increases are observed in April, May, and August, reflecting seasonal groundwater variability. Takhiatash Province shows no significant trends annually or in most months, except for a notable increase in November (Z=−2.205, p=0.027), which suggests a late-autumn increase in groundwater levels. For Shumanay Province, both the annual trend (Z=3.158, p=0.002) and monthly trends are significantly positive, with consistent increases observed across nearly all months except November, indicating a general rise in groundwater levels throughout the year. Kanlikul Province also exhibits a significant annual increase (Z=2.595, p=0.009), with monthly increases from April to November, peaking in May (Z=3.651, p<0.001), again indicating seasonal recharge. In Kungirot Province, a significant annual increase (Z=2.846, p=0.004) is observed, supported by increasing trends from April to October, with the strongest trend in May (Z=3.499, p<0.001), further underscoring seasonal patterns. Muynak Province exhibits one of the strongest trends, with a highly significant annual increase (Z=3.884, p<0.001) and consistent monthly rises throughout the year. In Nukus Province, the annual trend is not significant; however, May shows a significant increase (Z=2.047, p=0.041), whereas other months do not. Kegeyli Province shows a significant annual increase (Z=2.668, p=0.008), with monthly trends indicating widespread increases from May to September, consistent with seasonal recharge. In Buzatau Province, both annual (Z=2.879, p=0.004) and monthly trends are positive, with May showing the strongest increases (Z=3.106, p=0.002). Chimbay Province exhibits significant positive trends annually (Z=3.172, p=0.002) and monthly, especially in April (Z=3.619, p<0.001), indicating year-round groundwater level rises. Karauzyak Province also demonstrates significant positive annual (Z=3.172, p=0.002) and monthly trends, with particularly strong increases from March to October, peaking in May (Z=3.324, p<0.001). In Takhtakopir Province, a significant annual trend (Z=2.254, p=0.024) is observed, with significant monthly increases in May and September, suggesting localized seasonal variations. Finally, for the Republic of Karakalpakstan, which aggregates data from all provinces, a significant positive annual trend (Z=3.603, p<0.001) is evident. Monthly trends highlight widespread increases, with the strongest trends from April to August aligning with the seasonal patterns observed at the provincial level. Generally, the MK test results across the province-level seasonal patterns.

In summary, the MK test results indicate varied groundwater trends across provinces. While some show no annual trend, most exhibit clear seasonal increases during the warmer months. These findings underscore the importance of implementing localized and seasonally adaptive groundwater management strategies in response to these temporal and spatial patterns.

3.2.2. IPTA test

Insights derived from Tables 4 and S2, along with Figures 2 and S1, reveal detailed hydrometeorological

Table 3. Mann–Kendall test for groundwater levels in Turtkul and Ellikkala provinces

Province	Statistical parameter	January	February	March	April	May	June	July	August	September	October	November	December	Annual
Turtkul Province	*n*	34	34	34	34	34	34	34	34	34	34	33	33	34
	Alpha	0.05	0.05	0.05	0.05	0.05	0.05	0.05	0.05	0.05	0.05	0.05	0.05	0.05
	MK state	−154	−134	−108	2	−16	43	43	153	49	−69	−97	−110	−104
	S.E.	67.407	67.407	67.406	67.364	67.027	67.339	67.339	67.233	67.341	67.387	64.444	64.467	67.453
	Z-test	−2.270	−1.973	−1.587	0.015	−0.224	0.624	0.624	2.261	0.713	−1.009	−1.490	−1.691	−1.527
	p-value	0.023	0.048	0.112	0.988	0.823	0.533	0.533	0.024	0.476	0.313	0.136	0.091	0.1268
	Trend	Yes	Yes	No	No	No	No	No	Yes	No	No	No	No	No
Ellikkala Province	*n*	34	34	34	34	34	34	34	34	34	34	33	33	34
	Alpha	0.05	0.05	0.05	0.05	0.05	0.05	0.05	0.05	0.05	0.05	0.05	0.05	0.05
	MK state	−80	−53	4	275	243	223	239	270	247	141	53	22	105
	S.E.	67.407	67.434	67.445	67.403	67.403	67.403	67.387	67.407	67.387	67.281	64.444	64.514	67.422
	Z-test	−1.172	−0.771	0.044	4.065	3.590	3.294	3.532	3.991	3.651	2.081	0.807	0.326	1.543
	p-value	0.241	0.441	0.965	0.000	0.000	0.001	0.000	0.000	0.000	0.037	0.420	0.745	0.123
	Trend	No	No	No	Yes	Yes	Yes	Yes	Yes	Yes	Yes	No	No	No

Notes: *n*: Sample size; α: Significance level; MK state: Mann–Kendall test statistic; S.E.: Standard error; Z-test: Standardized test statistic; *p*-value: Probability value for significance; Trend: "Yes" indicates statistically significant trend at α=0.05.

doi: 10.36922/AJWEP025080052

Table 4. Monthly innovative polygon trend analysis statistical metrics (arithmetic mean and standard deviation) for Turtkul Province

Index	Section	Months											
		January	February	March	April	May	June	July	August	September	October	November	December
Mean	1st half	236.6	234.1	205.5	174.4	182.4	181.5	172.5	166.7	178.5	199.6	214.0	228.5
	2nd half	216.1	213.8	189.0	170.7	177.9	180.5	174.9	172.6	178.1	189.6	200.8	214.4
SD	1st half	26.1	25.1	24.1	14.9	16.4	16.4	16.4	17.4	20.5	23.9	27.5	25.2
	2nd half	31.7	32.4	22.4	10.9	8.6	10.4	12.3	14.8	17.8	21.2	20.5	24.1
Index	**Metric**	**January–February**	**February–March**	**March–April**	**April–May**	**May–June**	**June–July**	**July–August**	**August–September**	**September–October**	**October–November**	**November–December**	**December–January**
Mean	Trend length	28.9	26.2	17.0	5.8	4.6	2.6	6.3	5.9	10.0	16.5	19.3	24.9
	Trend slope	0.9	0.9	0.6	0.9	−3.2	0.6	0.4	0.5	0.5	0.8	0.9	0.2
SD	Trend length	9.2	7.5	4.3	8.8	9.8	7.2	4.8	3.7	3.8	7.4	7.0	5.7
	Trend slope	−0.6	10.4	1.2	−1.5	−98.0	127.1	2.4	1.0	1.0	−0.2	−1.6	8.4

Note: SD: Standard deviation.

patterns for each province in the Republic of Karakalpakstan, Uzbekistan, enriched by specific numerical and graphical representations.

In Turtkul Province (Table S2 and Figure S1), groundwater levels exhibit clear seasonal patterns, with mean values decreasing from 236.6 mm in January to a minimum of 166.7 mm in August, followed by a recovery to 214.4 mm in December. The SD peaks in February (32.4 mm), indicating considerable variability during the winter months. The narrow IPTA polygon reflects consistent monthly trends, suggesting relatively stable hydrometeorological conditions. Minimal variability during summer months reflects reduced groundwater recharge. Ellikkala province demonstrates a steady rise in groundwater levels over the year, with mean values increasing from 246 mm in January to 247.6 mm in December. Seasonal variability is evident, with the SD peaking at 57 mm in February and March, indicating significant temporal fluctuations. The IPTA polygon is broader from July to October, reflecting hydrologically active periods influenced by regional climatic factors. In Beruniy Province, groundwater levels increase significantly throughout the year, with the mean rising from 192.5 mm in January to 207.5 mm in December. The wettest months, particularly May and July, indicate strong seasonal recharge. The highest SD occurs in January (42.4 mm). The elongated IPTA polygon with steep slopes highlights pronounced seasonal dynamics. Amudarya Province shows a steady annual increase in groundwater levels from 174.1 mm in January to 191.5 mm in December. The SD peaks in January (41.9 mm) and decreases during spring, suggesting reduced variability during drier months. The IPTA polygon alternates between narrow and broad sections, indicating general stability interspersed with episodes of significant temporal variability. In Khojeli Province, groundwater levels rise from 185.4 mm in January to 228.4 mm in November. Variability is highest in January (SD=48.1 mm), decreasing through summer. The symmetrical IPTA polygon suggests predictable seasonal variations and stable hydrometeorological patterns. Takhiatash Province begins the year with lower groundwater levels (154 mm in January), rising to 224.3 mm in November**.** The SD peaks in December (22.0 mm), indicating greater end-of-year variability. The narrow IPTA polygon reflects uniform temporal changes and a stable annual pattern with limited fluctuations. Shumanay Province records high groundwater levels year-round, increasing from 220.1 mm in January to 257.2 mm in November. Seasonal variability decreases significantly in the latter half of the year, with the

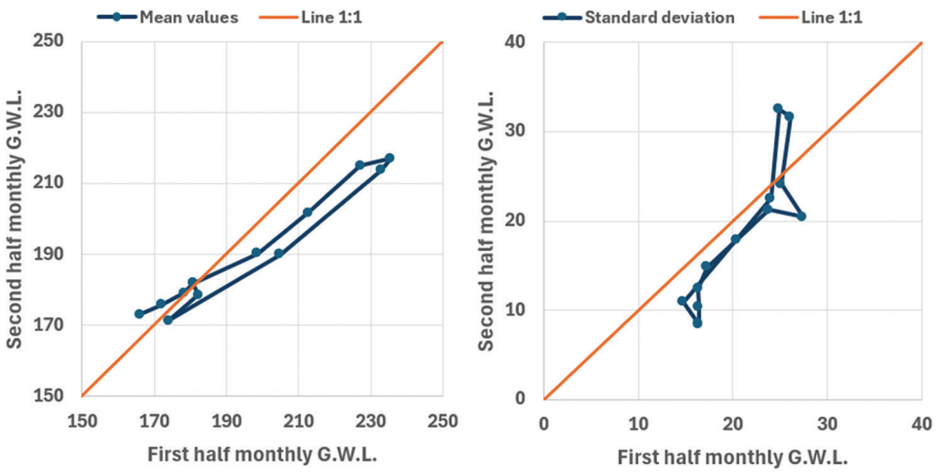

Figure 2. Innovative polygon trend analysis graph: Groundwater level (G.W.L) records for Turtkul Province

lowest SD in July (40.0 mm). The IPTA polygon, with steep slopes, reflects strong month-to-month variability during recharge periods. Kanlikul province exhibits a rising trend, with mean groundwater levels increasing from 220.1 mm in January to 257.2 mm in November. The IPTA polygons vary in slope and length, indicating significant temporal changes during wetter periods. Variability decreases significantly during the second half of the year. Kungirot Province experiences an annual increase in groundwater levels, from 134 mm in January to 215 mm in December. The SD peaks in January (67.4 mm), highlighting substantial winter variability. Moderate broad IPTA polygons reflect balanced seasonal change with pronounced recharge phases. Muynak Province exhibits the highest seasonal variability, with groundwater levels rising sharply from 244.8 mm in January to 271.5 mm in December. Variability is highest in January (SD=78.6 mm), signifying substantial temporal heterogeneity. Broad IPTA polygons represent strong inter-month differences, particularly during peak wet periods. Nukus Province shows relatively stable groundwater levels, with a notable increase in May (139 mm). The highest SD is recorded in January (67.4 mm). The narrow IPTA polygons reflect consistent hydrometeorological conditions with minimal monthly variability. Kegeyli Province saw groundwater levels rise from 152 mm in January to 186 mm in November. January again shows the highest variability (SD=67.4 mm). Steep IPTA polygon slopes indicate substantial seasonal variability, likely driven by pronounced recharge during wetter months. Buzatau Province displays a gradual increase in groundwater levels from 53.0 mm in January to 77 mm in December. SD remains relatively stable. The IPTA polygons alternate between narrow and broad, reflecting intermittent heterogeneity and steady seasonal recharge. Chimbay Province shows a consistent increase in groundwater levels from spring to autumn, with values rising from 134 mm in January to 215 mm in December. The moderately broad IPTA polygons suggest well-balanced seasonal changes and a continuous upward trend. Karauzyak Province demonstrates a sharp increase in groundwater levels, from 136 mm in January to 215 mm in December. The peak SD in January (67.4 mm) signals significant variability during colder months. The broad IPTA polygons highlight intense seasonal variability during peak recharge periods. Takhtakopir Province maintains stable groundwater levels throughout the year, increasing from 97 mm in January to 153 mm in December. Low SD values across all months and narrow IPTA polygons reflect uniform temporal patterns with limited month-to-month differences. Finally, the aggregated data for the Republic of Karakalpakstan reflect significant increases in groundwater levels during wetter months, with a regional peak of 291 mm in July. The broader IPTA polygons capture the diverse climatic and hydrological influences across the provinces. These patterns underscore the importance of comprehensive water resource management strategies to address seasonal variability and ensure sustainable groundwater use.

3.2.3. SR correlation test

The SR trend analysis across different provinces of the Republic of Karakalpakstan, Uzbekistan, highlights significant spatial and temporal variations in groundwater level trends.

In Turtkul province (Table 5), most months exhibit no statistically significant trends, with the exception

Table 5. Outcomes of Spearman's rank correlation trend analysis for Turtkul province

Month	r_s	Trend	*t*-static	*t*-distribution	Significance
January	−0.33	Decreasing	−1.98	2.04	Not significant
February	−0.305	Decreasing	−1.81	2.04	Not significant
March	−0.253	Decreasing	−1.48	2.04	Not significant
April	0.013	Increasing	0.08	2.04	Not significant
May	−0.04	Decreasing	−0.23	2.04	Not significant
June	0.086	Increasing	0.49	2.04	Not significant
July	0.313	Increasing	1.87	2.04	Not significant
August	0.385	Increasing	2.36	2.04	Significant
September	0.117	Increasing	0.67	2.04	Not significant
October	−0.132	Decreasing	−0.75	2.04	Not significant
November	−0.163	Decreasing	−0.94	2.04	Not significant
December	−0.22	Decreasing	−1.28	2.04	Not significant

Note: r_s: Spearman's rank correlation coefficient.

of August, which shows a significant increasing trend. This suggests a seasonal increase in groundwater levels, potentially driven by recharge from precipitation or irrigation activities.

In Ellikkala Province (Table S3), no significant trends are observed in the early months. However, a clear increasing trend emerges from April to August, indicating a shift in groundwater availability during the warmer months. Beruniy Province exhibits statistically significant positive trends from March through September, suggesting a steady increase in groundwater levels, which may be attributed to enhanced recharge or reduced extraction. Similarly, Amudarya Province demonstrates significant upward trends from April to November, emphasizing the influence of seasonal variations on groundwater storage. In Khojeli Province, notable increasing trends are recorded from April to September, reinforcing the role of seasonal recharge. Conversely, Takhiatash Province presents a mixed pattern, with some months – such as March and April – showing decreasing trends. These declines may reflect excessive extraction or climatic influences that limit recharge. Shumanay Province shows statistically significant increasing trends in nearly all months except November, indicating a consistent year-round rise in groundwater levels. In Kanlikul Province, significant increasing trends are observed in the summer months, while the early spring months show no clear trend, possibly suggesting a delayed or gradual recharge onset. Kungirot Province demonstrates steady increases in groundwater levels, particularly between March and October, whereas Nukus Province reveals notable increases during summer and autumn, likely reflecting a dependency on seasonal hydrological inputs. Kegeyli Province exhibits increasing trends from February to December, emphasizing a prolonged period of groundwater accumulation, potentially due to improved water conservation strategies. In Buzatau Province, strong increasing trends are observed throughout the year, particularly in the summer months, which may result from surface water recharge or changes in groundwater management practices. Chimbay Province also exhibits a steady rise in groundwater levels, aligning with trends observed in adjacent regions. Both Karauzyak and Takhtakopir Provinces exhibit consistent and statistically significant increasing trends across most months, further highlighting the overall positive trajectory of groundwater levels. At the national level, the Republic of Karakalpakstan demonstrates a dominant pattern of increasing groundwater levels throughout the year, with the most significant trends observed in the summer months. This widespread upward trend likely reflects a combination of improved water management practices, favorable climatic conditions promoting groundwater storage, and possibly decreased abstraction rates.

In summary, the SR trend analysis confirms a general increase in groundwater levels across the region, although localized and seasonal variations exist. These findings highlight the importance of monitoring groundwater resources continuously to ensure sustainable water management and mitigate potential risks associated with groundwater depletion in certain provinces where decreasing trends were noted.

3.3. Sustainability implications of the findings

Agriculture remains one of the primary livelihoods in Uzbekistan; however, it is increasingly threatened by the impact of climate change.[49-51] Therefore, the country must develop and implement effective adaptation strategies to ensure food security and enhance its economic resilience. The observed trend – both increasing and decreasing – in groundwater levels presents a complex challenge for agriculture, as water availability directly influences crop productivity and irrigation planning. These variations complicate the formulation of sustainable adaptation measures in response to a changing climate. The findings of the present study provide valuable insights that can support the development of region-specific adaptation strategies for future climatic challenges.

The rising groundwater levels observed in several provinces suggest a potential improvement in water availability. However, seasonal fluctuations and localized areas of groundwater stability or decline highlight the need for targeted interventions and adaptive water governance. These groundwater trends directly impact agricultural productivity. Therefore, continuous monitoring of groundwater levels, combined with data-informed irrigation strategies, can play a crucial role in enhancing crop resilience and ensuring food security.

Previous studies have already demonstrated that climate change has significantly impacted water availability in Uzbekistan.[52,53] Understanding the spatial and temporal patterns of groundwater trends is, therefore, essential for long-term resource planning. The application of non-parametric trend analysis methods – namely the MK test, SR test, and IPTA – demonstrates how scientific approaches can inform climate adaptation efforts and ensure that groundwater resource management evolves in line with environmental change.

4. Conclusion

Groundwater resources are vital for sustaining arid and semi-arid regions, yet they are subject to variability driven by complex climatic and environmental factors. This study employed a robust multi-method trend analysis framework – integrating the MK test, SR test, and IPTA – to evaluate long-term groundwater trends across the Republic of Karakalpakstan, Uzbekistan.

Results from the MK test reveal that nine out of 14 provinces exhibit significant increasing trends in groundwater levels, with Muynak Province showing the strongest upward trend (Z=3.884, p<0.001). At the national level, the analysis confirms an overall groundwater increase (Z=3.603, p<0.001). Several provinces, such as Beruniy (Z=2.906, p=0.004), Amudarya (Z=2.906, p=0.004), and Chimbay (Z=3.172, p=0.002), show consistent groundwater rise, especially during the warmer months. In contrast, provinces such as Turtkul, Ellikkala, and Nukus exhibit no statistically significant trends, indicating localized groundwater stability.

The IPTA method provides deeper insights into seasonal dynamics, identifying months with significant increases (e.g., April – May) and decreases (e.g., May – June). These seasonal variations suggest that, despite the overall positive trend, groundwater recharge dynamics fluctuate depending on climatic conditions and water usage patterns.

These findings carry important policy implications. Provinces experiencing rising groundwater levels may benefit from improved water retention and hydrological balance, while those showing neutral trends warrant further investigation into potential contributing factors, such as groundwater extraction, irrigation intensity, or climate anomalies. The study underscores the importance of adaptive and region-specific groundwater management strategies to ensure sustainable use of water resources in response to both seasonal and long-term climatic variability. Future research should focus on evaluating the influence of anthropogenic activities – such as land use change and over-extraction – and integrate hydrological modeling to improve water resource planning and resilience in climate-sensitive regions.

Acknowledgments

None.

Funding

None.

Conflict of interest

Upaka Rathnayake is an Editorial Board Member of this journal but was not in any way involved in the editorial and peer-review process conducted for this paper, directly or indirectly. Separately, other authors declared that they have no known competing financial interests or personal relationships that could have influenced the work reported in this paper.

Author contributions

Conceptualization: Upaka Rathnayake
Formal analysis: Mehdi Fuladipanah, Namal Rathnayake
Investigation: Mehdi Fuladipanah, Namal Rathnayake, Mirzohid Koriyev
Methodology: Mehdi Fuladipanah
Writing – original draft: Mehdi Fuladipanah, Kenjabek Rozumbetov
Writing – review & editing: Valery Erkudov, Upaka Rathnayake

Availability of data

Data are available from the corresponding author upon reasonable request.

References

1. Intergovernmental Panel on Climate Change (IPCC). *Working Group II Contribution to the Intergovernmental Panel on Climate Change Fourth Assessment Report Climate Change 2007: Climate Change Impacts, Adaptation and Vulnerability*. Switzerland: IPCC; 2007. p. 9-10.
2. Intergovernmental Panel on Climate Change (IPCC). *Climate Change: Synthesis Report. An Assessment of Intergovernmental Panel on Climate Change*. Geneva: IPCC; 2014.
3. Intergovernmental Panel on Climate Change (IPCC). Summary for policymakers. In: Core Writing Team, Lee H, Romero J, editors. *Climate Change 2023: Synthesis Report. Contribution of Working Groups I, II and III to the Sixth Assessment Report of the Intergovernmental Panel on Climate Change*. Geneva, Switzerland: IPCC; 2023. p. 1-34. doi: 10.59327/IPCC/AR6-9789291691647.001
4. Dabanlı I, Şen Z, Yeleğen MÖ, Şişman E, Selek B, Güçlü YS. Trend assessment by the innovative-sen method. *Water Resour Manage*. 2016;30:5193-5203. doi: 10.1007/s11269-016-1478-4
5. Morsy M, Moursy FI, Sayad T, Shaban S. Climatological study of SPEI drought index using observed and CRU gridded dataset over Ethiopia. *Pure Appl Geophys*. 2022;179(8):3055-3073. doi: 10.1007/s00024-022-03091-z
6. Ayugi B, Eresanya EO, Onyango AO, *et al*. Review of meteorological drought in Africa: Historical trends, impacts, mitigation measures, and prospects. *Pure Appl Geophys*. 2022;179(4):1365-1386. doi: 10.1007/s00024-022-02988-z
7. Şen Z, Şişman E, Dabanlı I. Innovative polygon trend analysis (IPTA) and applications. *J Hydrol*. 2019;575:202-210. doi: 10.1016/j.jhydrol.2019.05.028
8. Wang Y, Xu Y, Tabari H, *et al*. Innovative trend analysis of annual and seasonal rainfall in the Yangtze River Delta, Eastern China. *Atmos Res*. 2020;231:104673. doi: 10.1016/j.atmosres.2019.104673
9. Ozturk T, Ceber ZP, Turkes M, Kurnaz ML. Projections of climate change in the Mediterranean Basin by using downscaled global climate model outputs. *Int J Climatol*. 2015;35(14):4276-4292. doi: 10.1002/joc.4285
10. Cislaghi M, De Michele C, Ghezzi A, Rosso R. Statistical assessment of trends and oscillations in rainfall dynamics: Analysis of long daily Italian series. *Atmos Res*. 2005;77:188-202. doi: 10.1016/j.atmosres.2004.12.014
11. Cong Z, Zhao J, Yang D, Ni G. Understanding the hydrological trends of river basins in China. *J Hydrol*. 2010;388:350-356. doi: 10.1016/j.jhydrol.2010.05.013
12. Duhan D, Pandey A. Statistical analysis of long term spatial and temporal trends of precipitation during 1901-2002 at Madhya Pradesh, India. *Atmos Res*. 2013;122:136-149. doi: 10.1016/j.atmosres.2012.10.010
13. Fathian F, Morid S, Kahya E. Identification of trends in hydrological and climatic variables in Urmia Lake basin, Iran. *Theor Appl Climatol*. 2015;119:443-464. doi: 10.1007/s00704-014-1120-4
14. Rahman MA, Yunsheng L, Sultana N. Analysis and prediction of rainfall trends over Bangladesh using Mann-Kendall, Spearman's rho tests and ARIMA model. *Meteorol Atmos Phys*. 2017;129:409-424. doi: 10.1007/s00703-016-0479-4
15. Hırca T, Eryılmaz Türkkan G, Niazkar M. Applications of innovative polygonal trend analyses to precipitation series of Eastern Black Sea Basin, Turkey. *Theor Appl Climatol*. 2022;147:651-667. doi: 10.1007/s00704-021-03837-0
16. Spearman C. The proof and measurement of association between two things. In: Sharif M, Archer D, Hamid A, editors. *Trends in Streamflow Magnitude and Timings in Satluj River Basin*. World Environmental and Water Resources Congress; 2012. p. 1904-2021.
17. Anderson RL. Distribution of serial correlation coefficient. *Ann Math Stat*. 1942;13(1):1-13. doi: 10.1214/aoms/1177731638
18. Mann HB. Nonparametric tests against trend. *Econometrica*. 1945;13:245-259. doi: 10.2307/1907187
19. Cox DR, Miller HD. *The Theory of Stochastic Process*. London: Methuen Publishing; 1965.
20. Kendall MG. *Rank Correlation Methods*. 4th ed. London: Charles Griffin; 1975.

21. Hirsch RM, Slack JR, Smith RA. Techniques of trend analysis for monthly water quality data. *Water Resour Res*. 1982;18(1):107-121. doi: 10.1029/WR018i001p00107
22. Hirsch RM, Slack JR. A nonparametric trend test for seasonal data with serial dependence. *Water Resour Res*. 1984;20(6):727-732. doi: 10.1029/WR020i006p00727
23. Daniel WW. Spearman rank correlation coefficient. In: *Applied Nonparametric Statistics*. 2nd ed. Boston: PWS-Kent; 1990. p. 358-365.
24. Wilcox RR. *Fundamentals of Modern Statistical Methods: Substantially Improving Power and Accuracy*. New York: Springer; 2001.
25. Şen Z. Innovative trend significance test and applications. *Theor Appl Climatol*. 2017;127:939-947. doi: 10.1007/s00704-015-1681-x
26. Gaddikeri V, Sarangi A, Singh DK, Jatav MS, Rajput J, Kushwaha NL. Trend and change-point analyses of meteorological variables using Mann-Kendall family tests and innovative trend assessment techniques in New Bhupania command (India). *J Water Clim Change*. 2024;15(5):2033-2058. doi: 10.2166/wcc.2024.462
27. Çelebioğlu T, Tayanç M. A study on precipitation trends in Türkiye via linear regression analysis and non-parametric Mann-Kendall test. *Sürdürülebilir Çevre Derg*. 2024;4(1):19-28. doi: 10.62816/cevder.1489546
28. Qadem Z, Tayfur G. In-depth exploration of temperature trends in Morocco: Combining traditional methods of Mann Kendall with innovative ITA and IPTA approaches. *Pure Appl Geophys*. 2024;181(8):2717-2739. doi: 10.1007/s00024-024-03535-8
29. Alashan S. Non-monotonic trend analysis using Mann-Kendall with self-quantiles. *Theor Appl Climatol*. 2024;155(2):901-910. doi: 10.22541/essoar.167751622.23605443/v1
30. San M. Combined innovative trend analysis methods for seasonal trend testing. *J Hydrol*. 2024;649:132418. doi: 10.1016/j.jhydrol.2024.132418
31. Kessabi R, Hanchane M, Ait Brahim Y, El Khazzan B, Addou R, Belmahi M. Characterization of annual and seasonal rainfall trend using innovative trend analysis (ITA) and classical methods: The case of Wadi Sebou basin (WSB) Morocco. *Eur Mediterr J Environ Integr*. 2024;10:555-573. doi: 10.1007/s41207-024-00507-1
32. Likinaw A, Alemayehu A, Bewket W. Trends in extreme precipitation indices in Northwest Ethiopia: Comparative analysis using the Mann-Kendall and innovative trend analysis methods. *Climate*. 2023;11(8):164. doi: 10.3390/cli11080164
33. Agbo EP, Nkajoe U, Edet CO. Comparison of Mann-Kendall and Şen's innovative trend method for climatic parameters over Nigeria's climatic zones. *Clim Dyn*. 2023;60(11):3385-3401. doi: 10.21203/rs.3.rs-1731818/v1
34. Sanogo A, Kabange RS, Owusu PA, Djire BI, Donkoh RF, Dia N. Investigation into recent temperature and rainfall trends in Mali using Mann-Kendall trend test: Case study of Bamako. *J Geosci Environ Protect*. 2023;11(3):155-172. doi: 10.4236/gep.2023.113011
35. Gul S, Ren J. Application of non-parametric innovative trend analysis of different time scale precipitation during (1951-2016) in Khyber Pakhtunkhwa, Pakistan. *Acta Geophys*. 2022;70(1):485-503. doi: 10.1007/s11600-021-00703-5
36. Nguyen HM, Ouillon S, Vu VD. Sea level variation and trend analysis by comparing Mann-Kendall test and innovative trend analysis in front of the Red River Delta, Vietnam (1961-2020). *Water*. 2022;14(11):1709. doi: 10.3390/w14111709
37. Seenu PZ, Jayakumar KV. Comparative study of innovative trend analysis technique with Mann-Kendall tests for extreme rainfall. *Arabian J Geosci*. 2021;14:536.
38. Güçlü YS. Improved visualization for trend analysis by comparing with classical Mann-Kendall test and ITA. *J Hydrol*. 2020;584:124674. doi: 10.1007/s12517-021-06906-w
39. Caloiero T, Coscarelli R, Ferrari E. Assessment of seasonal and annual rainfall trend in Calabria (Southern Italy) with the ITA method. *J Hydroinform*. 2020;22(4):738-748. doi: 10.2166/hydro.2019.138
40. Hamed KH, Rao AR. A modified Mann-Kendall trend test for autocorrelated data. *J Hydrol*. 1998;204(1-4):182-196. doi: 10.1016/S0022-1694(97)00125-X
41. Yue S, Pilon P, Phinney B, Cavadias G. The influence of autocorrelation on the ability to detect trend in hydrological series. *Hydrol Process*. 2002;16(9):1807-1829. doi: 10.1002/hyp.1095
42. Douglas EM, Vogel RM, Kroll CN. Trends in floods and low flows in the United States: Impact of spatial correlation. *J Hydrol*. 2000;240(1-2):90-105. doi: 10.1016/S0022-1694(00)00336-X
43. Tosunoglu F. Trend analysis of daily maximum rainfall series in Çoruh Basin, Turkey. *J Inst Sci Technol*. 2017;7(1):195-205. doi: 10.21597/jist.2017127432
44. Achite M, Ceribasi G, Ceyhunlu AI, Wałega A, Caloiero T. The innovative polygon trend analysis (IPTA) as a simple qualitative method to detect changes in environment-example detecting trends of the total monthly precipitation in semiarid area. *Sustainability*. 2021;13:12674. doi: 10.3390/su132212674
45. Ceribasi G, Ceyhunlu AI, Ahmed N. Analysis of temperature data by using innovative polygon trend

analysis and trend polygon star concept methods: A case study for Susurluk Basin, Turkey. *Acta Geophys*. 2021;69(5):1949-1961.
doi: 10.1007/s11600-021-00632-3

46. Karacosta P, Pakalidou N, Douka M, Karacostas T. Innovative polygon trend analysis (IPTA): A case study for precipitation in Thessaloniki during the last 50 years (1971-2020). *Environ Sci Proc*. 2023;26(1):161.
doi: 10.3390/environsciproc2023026161
47. Koycegiz C, Buyukyildiz M. Applications of innovative polygon trend analysis (IPTA) and trend polygon star concept (TPSC) methods for the variability of precipitation in Konya closed basin (turkey). *Theor Appl Climatol*. 2023;155:2641-2656.
doi: 10.1007/s00704-023-04765-x
48. Yenice AC, Yaqub M. Trend analysis of temperature data using innovative polygon trend analysis and modeling by gene expression programming. *Environ Monit Assess*. 2022;194:543.
doi: 10.1007/s10661-022-10156-y
49. Koriyev MR, Fonseka PU, Umurzakova UN, *et al*. Soil salinity status in Namangan region, Uzbekistan. *Suranaree J Sci Technol*. 2024;31(5):010335(1-15).
doi: 10.55766/sujst-2024-05-e05652
50. Chathuranika I, Khaniya B, Neupane K, Rustamjonovich KM, Rathnayake U. Implementation of water-saving agro-technologies and irrigation methods in agriculture of Uzbekistan on a large scale as an urgent issue. *Sustain Water Resour Manage*. 2022;8(5):155.
doi: 10.1007/s40899-022-00746-6
51. Mukhamedjanov S, Mukhomedjanov A, Sagdullaev R, Khasanova N. Adaptation to climate change in irrigated agriculture in Uzbekistan. *Irrig Drain*. 2020;70(1):169-176.
doi: 10.1002/ird.2529
52. Hamidov A, Khamidov M, Ishchanov J. Impact of climate change on groundwater management in the Northwestern part of Uzbekistan. *Agronomy*. 2020;10(8):1173.
doi: 10.3390/agronomy10081173
53. Mitchell D, Williams RB, Hudson D, Johnson P. A Monte Carlo analysis on the impact of climate change on future crop choice and water use in Uzbekistan. *Food Secur*. 2017;9(4):697-709.
doi: 10.1007/s12571-017-0690-2

Asian Journal of Water, Environment and Pollution. Vol. 22, No. 3 (2025), pp. 134-152.
doi: 10.36922/AJWEP025150107

ORIGINAL RESEARCH ARTICLE

Projected trends in extreme heat in Senegal from 2020 to 2080

Moussa Sow[1] and Demba Gaye[2]*

[1]Department of Environment, Biodiversity and Sustainable Development, Faculty of Social and Environmental Sciences, Sine Saloum El-Hadj Ibrahima Niass University, Kaolack, Senegal
[2]Laboratory of Geomatics and Environment, Department of Geography, Faculty of Sciences and Technology, Assane Seck University, Ziguinchor, Senegal
***Corresponding author:** Demba Gaye (demba.gaye@univ-zig.sn)

Received: April 08, 2025; 1st revised: May 03, 2025; 2nd revised: May 12, 2025; Accepted: May 14, 2025; Published Online: June 10, 2025

Abstract: Faced with the challenges that climate change poses to all human societies, adaptation is becoming a necessity for human survival. In this context, it is necessary to study the climatic phenomena that humans face and that are likely to impact various aspects of life. Therefore, this study sought to analyze the trend of heat waves in Senegal using data from the Coupled Model Intercomparison Project Phase 6 (CMIP6), Canadian Earth System Model Version 5. Three climate scenarios (Shared Socioeconomic Pathway [SSP]1-2.6, SSP2-4.5, and SSP5-8.5) were used, and the study focused on two future climate normals (2020 – 2050, 2050 – 2080). The study first spatialized the 95th percentile of minimum, mean, and maximum temperatures, then analyzed temperature anomalies with the Lamb index before studying the future trend using the Mann-Kendall test. The results obtained reflect an upward trend for all the variables in this study for the two periods combined but with a different level of significance. This increase is greater for minimum temperatures, with rises of 0.43°C for SS1-2.6, 1.06°C for SSP2-4.5, and 2.18°C for SSP5-8.5. In comparison, maximum temperatures rose by 0.50°C, 1.05°C, and 2.03°C, respectively, between the first and second periods. Mean temperatures followed the same dynamic, with 0.48°C for SSP1-2.6, 1.04°C for SSP2-4.5, and 2.16°C for SSP5-8.5. Given these findings, it is important to analyze the behavior of the other CMIP6 models in assessing heat waves in Senegal.

Keywords: Future trends; Heat waves; Mann–Kendall test; Canadian Earth System Model Version 5; Coupled Model Intercomparison Project Phase 6; Senegal

1. Introduction

Climate change is considered one of the greatest risks of the 21st century, with the potential to affect the health and lives of billions of people worldwide.[1] This phenomenon is defined as the consequence of the intensification of anthropogenic greenhouse gas emissions.[2,3] It is also a factor influencing public health, with diverse and potentially catastrophic consequences.[4] In this context, studies have shown that the global average temperatures are expected to increase by 5.5°C by the end of the 21st century,[5] which might result in a global intensification, recurrence, and sustainability of heat waves.[6,7] The increased exposure to heat waves is expected to deteriorate population health, increasing heat-related mortality and morbidity globally.[8]

In addition, climate forecasts for the 21st century suggest a greater increase in temperatures in Africa

compared to the global average, with an intensification of extreme heat events.[9] Therefore, the frequency, duration, and severity of heat waves are expected to intensify in the future.[2,10] The projected effects of heat waves are expected to impact both social and economic sectors. First, heat waves are expected to pose a significant risk to human health.[11] The adverse effects on health will be more noticeable in impoverished regions, where limited health coverage hinders adaptation and proper care.[12] In fisheries, these extreme heat events result in the degradation of marine habitats, and negatively impact the conditions required for the survival of local biodiversity.[13] In terms of agriculture, prolonged heat compromises photosynthesis activity and promotes the proliferation of pests, both of which lead to a decline in agricultural yields.[14,15]

Understanding this phenomenon is essential for adapting to its impacts. However, studies on hot extremes in Africa have only been conducted recently, unlike in Europe and America, where heat waves have been extensively documented. This scarcity of studies is concerning given the increasing temperatures in Africa and the insufficient adaptation measures, which are closely linked to the lack of climate data in the region.[16]

Particularly in the Sahelian region of Africa, there are significant challenges in access and availability of climate data. On one hand, access is hindered by exorbitant costs in many countries.[17] On the other hand, following the structural adjustment policies of the 90s, the observation network has been underdeveloped, leading to incomplete or even data shortage over time.[18] This partly explains the scarcity of studies on hot extremes in Africa, particularly in the Sahelian region. In addition, the continent is facing other pressing priorities, such as flooding, whose impacts are more noticeable than hot extremes.

The challenge of limited data has been mitigated by climate modeling, which is capable of tracing past and present climate changes, as well as predicting future ones. Climate models have become much more complex to better represent physical and environmental processes at increasingly fine scales.[19] Therefore, numerous studies have focused on the prospective evolution of the climate. Heat waves and their health impacts highlight the importance of climate models for strategizing mitigation and adaptation efforts.[20] The advent of climate data now makes it possible to predict future temperature trends with greater regional and even local detail, especially with the contribution of regionalized climate models.

The present study aimed to analyze the future trend of heat waves in Senegal over the periods of 2021 – 2050 and 2051 – 2080 according to the Coupled Model Intercomparison Project Phase 6 (CMIP6) scenarios of Shared Socioeconomic Pathway (SSP)1-2.6, SSP2-4.5, and SSP5-8.5. The main objectives of this study were to: (i) spatialize the 95th percentile of mean, minimum, and maximum temperatures; (ii) study anomalies; and (iii) analyze the trend of heat waves over the periods 2021 – 2050 and 2051 – 2080. The studies focusing on heat waves in Senegal using CMIP6 are limited. This is the first study applying the CMIP6 Canadian Earth System Model Version 5 (CanESM5) model to project Senegal's extreme heat trends. Therefore, this study extends several previous researches performed by Toure *et al*.,[21] Sow *et al*.,[22] Sow *et al*.,[23] Sow and Gaye,[24] and Sy *et al*.,[25] which tried to address the health impacts of heat waves in the northeastern regions of Senegal.

2. Materials and methods

2.1. Study area

Senegal is a country located on the West Coast of Africa. It is distinguished by its coastline stretching about 700 km. Senegal extends between latitudes 12°5 and 16°5 North and longitudes 11°5 and 17°5 West (Figure 1). Bordering Mauritania to the north, Mali to the east, the republics of Guinea and Guinea-Bissau to the south, and the Atlantic Ocean to the west, it is a country with a relatively homogeneous terrain with altitudes rarely exceeding 50 m.[26,27] Some massifs remain mainly in the eastern part of the country, such as the Fouta Djalon, which rises to 581 m, but the altitude decreases toward the west to 15 m toward the mouth of the Senegal River. The generally low terrain favors an unconstrained atmospheric circulation, subjecting the territory to a Sudano-Sahelian-type climate dominated by maritime trade winds, continental trade winds (commonly known as the Harmattan), and monsoon air masses. Under the influence of these defined air masses, two distinct seasons emerge each year: a long dry season and a rainy season. Soil science, on the other hand, is characterized by soils that are very vulnerable to degradation, particularly water and wind erosion. The hydrological potential is significant due to the presence of several rivers and lakes, such as the Senegal River, the Gambia River, the Casamance River, the Geba River, and the Lake of Guiers, which provide substantial water resources. However, the country's water availability is highly dependent on the amount and distribution of rainfall.[28] Annual rainfall totals range from <300 mm in the north to more than 1000 mm in the southern part of Senegal.[29] The temperature ranges from 16°C to

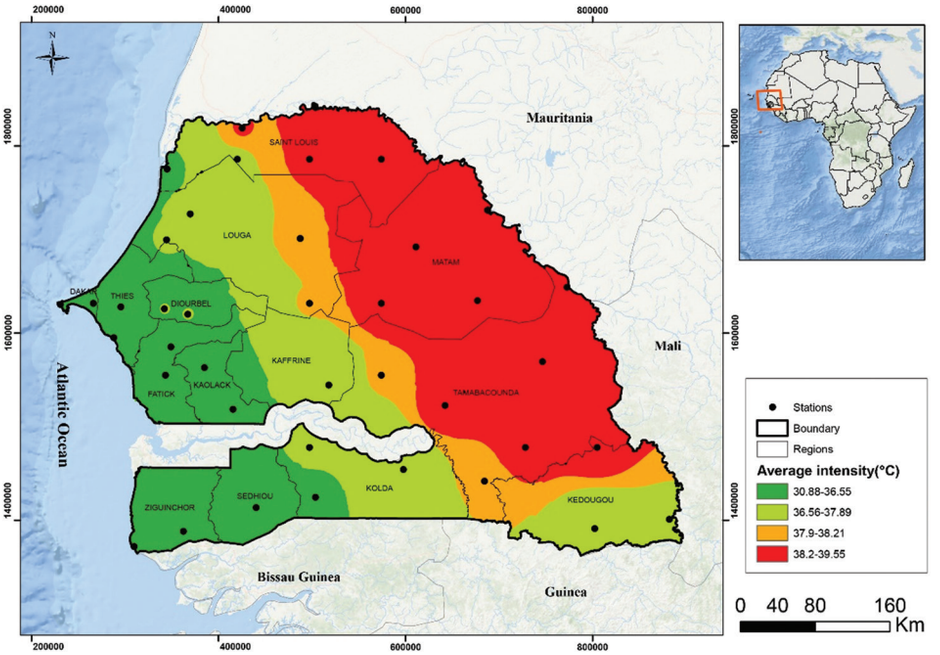

Figure 1. Distribution of heat wave intensity across Senegal from 1984 to 2020. Figure created with ArcGis 10.8, Sow and Gaye (2025).

30°C along the coastal strip, under the influence of the Atlantic Ocean, and can reach up to 40°C in the central and eastern regions of the country, which are subjected to the effects of continentality.[30]

2.2. Materials

To analyze the future trend of heat waves, CMIP6 simulation data were collected. Compared to the Coupled Model Intercomparison Project Phase 5 (CMIP5), CMIP6 introduces several improvements in physical modeling and resolution. CMIP6 is the result of two decades of research on the comparison of climate models.[19] It is an update of CMIP5 that incorporates socio-economic parameters.[31] Several studies have used CMIP6 data across various fields.[32-34] Some authors have concluded that CMIP6 performs better than CMIP5 models.[35,36] For instance, Mmame and Ngongondo[32] report that CMIP6 models provide substantial improvements in the simulation of temperature and precipitation, with biases often below 10%. In this study, the CanESM5 model was used as input. This model was developed by the Canadian Center for Climate Modelling and Analysis and is available on the World Climate Research Programme (WCRP). It is an improved version of the Second Generation Canadian Earth System Model.[37] Atmospheric blocking, which is often the cause of heat waves,[38] was observed with this model by Arora *et al.*[39] and Brunner *et al.*[40] over the historical period 1981 – 2010. The CanESM5, with a spatial resolution of 2.8° × 2.8°, enables the illustration of the connections between heat waves and atmospheric blocking.[41] Three scenarios were selected (SSP1-2.6, SSP2-4.5, and SSP6-8.5) for two climatic periods (2021 – 2050 and 2051 – 2080).

The choice of the CanESM5 model was based on a literature review, which highlighted its strong performance in the study of climatic extremes, particularly due to its ability to represent the phenomena responsible for heat waves. Its evolution from version 2 to version 5 has enhanced its simulation capabilities, and its spatial resolution of 2.8° × 2.8° is particularly well-suited to countries, such as Senegal, where climatic conditions vary significantly across regions. The choice of using a single model has been adopted by Brunner *et al.*,[40] Jeong *et al.*,[37] and Schaller *et al.*,[41] allowing us to focus on the specific features and results provided by these models, which are generally validated and adjusted to meet the objectives of each study.

2.3. Methods

2.3.1. Evaluation of the performance of the Canadian Earth System Model Version 5

In the context of using climate model outputs, it is often recommended to conduct evaluations using various methods, including the Kling-Gupta Efficiency (KGE) and Percent Bias (pBias). Various authors, including

Dehban *et al*.,[42] Mmame and Ngongondo,[32] and Zareian *et al*.,[43] have utilized these methods to evaluate the models' ability in reproducing reference data. KGE is a performance metric that indicates the model's ability to reproduce an observed or reference time series. It is calculated based on the correlation coefficient (r), biases (β), and variability (γ) using the following formula:

$$KGE = 1 - \sqrt{(r-1)^2 + (\beta-1)^2 + (\gamma-1)^2} \quad \text{(I)}$$

$$With.\ \beta = \frac{\mu_{sim}}{\mu_{obs}},\ \gamma = \frac{\sigma_{sim}}{\sigma_{obs}}$$

Where:
σ = standard deviation
μ = mean
sim = simulation data
obs = observation data

Percentage Bias is used to evaluate model performance by comparing simulated data to reference or observed data. It accounts for systematic bias in simulated data and indicates the extent to which the model overestimates or underestimates the observed data. The closer the pBias value is to zero, the more accurately the model reproduces the reference data. It is calculated using the following formula:

$$pBiais = \sum_{i=1}^{n} \frac{\left(Qsim[i] - Qobs[i]\right)}{\sum_{i=1}^{n} Qobs(i)} \times 100 \quad \text{(II)}$$

where:
Q = values at time step
n = number of time step

2.3.2. Data resampling and extraction

Canadian Earth System Model Version 5 data have been uploaded to the WCRP platform (https://esgf-node.llnl.gov/search/cmip6/) in netCDF format. They were then resampled to reduce the size of the grids. This operation reduced the data to a spatial resolution of 0.0625° × 0.0625° per grid. The data were then extracted based on the coordinates of the 40 grid points selected for this study (Figure 1), and the 95th annual percentiles of the SSP1-2.6, SSP2-4.5, and SSP6-8.5 scenarios were calculated. In previous studies, Da Silva *et al*.[44] and Teegavarapu *et al*.[45] demonstrated the effectiveness of this approach in capturing the spatial variability of climatic variables in the study area using simulated data. Among the available interpolation methods, we utilized bilinear interpolation,[46,47] implemented through the Climate Data Operator software. This resampling approach has been employed by several authors, including Goudiaby *et al*.[48] and Bodian *et al*.[49] In this study, the 95th percentile was selected as the threshold for detecting heat waves.

2.3.3. Spatialization of extreme heat

The inverse distance weighted (IDW) interpolation method was used to spatialize the results at the scale of Senegal. This is a robust method that allows the estimation of values across a surface based on known data points. It is based on the principle that each measuring point influences its surrounding area, with the influence decreasing as distance increases. This method was used to map the 95th percentile across Senegal.

2.3.4. Heat wave anomalies

The Lamb index (1982) was applied to identify interannual anomalies of extreme heat in Senegal for the periods 2021 – 2050 and 2051 – 2080. This index helps assess the interannual variability of extreme temperatures and detect fluctuations in hydro-climatic regimes[50] and climatic phenomena.[28,51] A positive index indicates an increase in temperatures, while a negative index reflects a decrease.[30]

$$IL = \frac{x_i - x_m}{\sigma} \quad \text{(III)}$$

where:
IL = Lamb index
x_i = 95th annual percentiles for a station during a year
x_m = annual average of the 95th percentile of the mean temperature at the station during the study period.

The trend of extreme heat was obtained using the Mann-Kendall test,[52,53] a non-parametric test that identifies trends in a given time series. The null hypothesis for this test is the absence of a trend. When the null hypothesis is rejected, the alternative hypothesis, which indicates the existence of a trend, is accepted, depending on the level of significance.[54] The Mann-Kendall test provides three key pieces of information:[55]

(i) The Kendall tau or Kendall's rank coefficient, which measures the tendency of the slope. The positive or negative rate reflects an upward or downward trend, respectively. The formula is as follows:

$$Var\ (s) = n(n-1)(2n+5)/18 \quad \text{(IV)}$$

where

$$S = \sum_{j=1}^{j=n-1} \sum_{i=j+1}^{i=n} sign\ (xi - xj) \quad \text{(V)}$$

where

$$\text{sign}\ (xi - xj) = \{1\ if\ (xi - xj) > 0;\ 0\ if\ (xi - xj) = 0;\ -1\ if\ (xi - xj) < 0 \quad \text{(VI)}$$

(ii) Sen's slope represents the overall trend of the time series. It is calculated as the median of the slopes between all possible pairs of points in the series.

$$\beta = Median\left(\frac{xi - xj}{i - j}\right) \forall i < j \quad \text{(VII)}$$

(iii) The significance is determined by the *p*-value, which indicates if the observed trend is statistically significant based on a pre-defined threshold, typically 0.05.

The selection of these methods is related to their robustness and the need for comparability with previous studies. To enhance the value of this work, these methods have been applied to CanESM5 outputs, ensuring that knowledge on heat waves is updated to promote future research.

3. Results

3.1. Analysis of Canadian Earth System Model Version 5 model performance

The performance of CANESM5 was evaluated against the Modern-Era Retrospective analysis for Research and Applications, Version 2, using the KGE and pBias over the 2015 – 2020 period. Figure 2 shows the spatial distribution of KGE values across Senegal. The results show KGE values ranging from 0.24 to 0.78 across all stations included in this study. The model demonstrates good performance, with KGE values exceeding 0.60 at 22 stations in SSP2-2.6, 27 stations in SSP3-4.5, and on 26 stations in SSP5-8.5. At the spatial level, the model performs better in the eastern and central stations of the country, whereas the lowest KGE values are observed in the coastal areas, particularly at the Cap-Kirring station (Figure 2).

The analysis of the KGE is complemented by the pBias, which indicates the percentage of error associated with CANESM5 model output. Figure 3 illustrates the distribution of the pBias values across all stations for the three scenarios selected in this study. The results show that pBias remains below 10% at 34 stations in SSP2-2.6, 39 stations in SSP3-4.5, and on 38 stations in SSP5-8.5. This suggests that the CANESM5 model exhibits good overall behavior, with predictions closely related to observed values. However, positive pBias values indicate a tendency for the model to overestimate the results. The highest biases, ranging from 11 to 17, are observed at the stations of Dakar in the west and Cap Skirring in the south.

3.2. Future evolution of heat waves in Senegal

The future evolution of heat waves was assessed by analyzing the dynamics of the annual 95th percentile

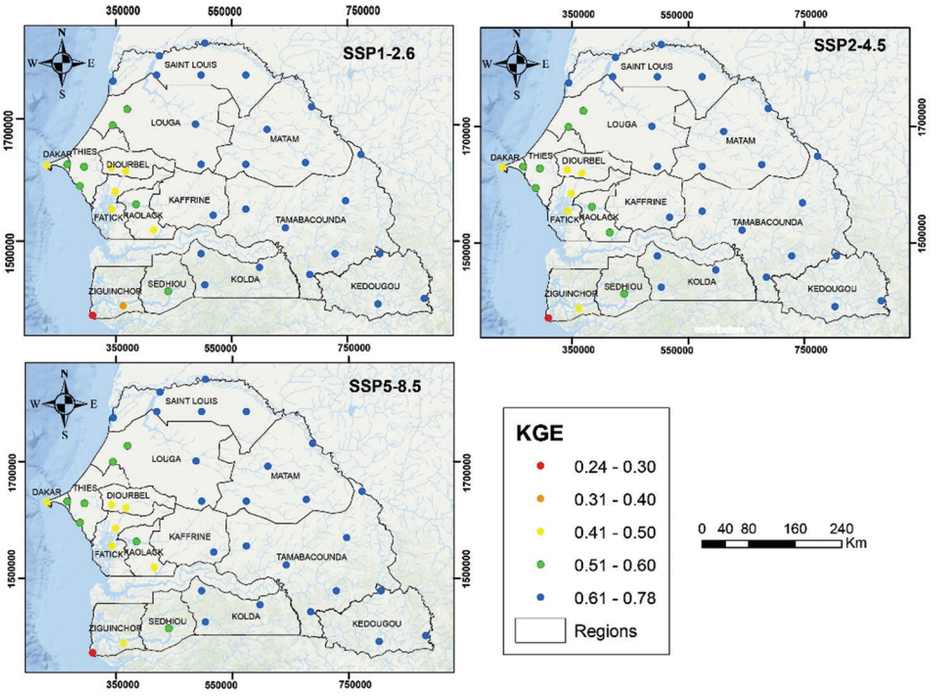

Figure 2. Spatial distribution of KGE values according to different scenarios. Figure created with ArcGis 10.8, Sow and Gaye (2025).

Abbreviations: KGE: Kling-Gupta efficiency; SSP: Shared socioeconomic pathway.

over the period 2020 – 2080. Figure 4 shows the trend in minimum, maximum, and mean temperatures under three climate scenarios (SSP1-2.6, SSP2-4.5, and SSP5-8.5).

The analysis of Figure 4 shows an increase in minimum temperatures across all selected scenarios. In SSP1-2.6, interannual variability is relatively irregular, with temperatures ranging from 28.64°C to 30.34°C. This trend continues in SSP2-4.5, with a slight increase, as temperatures range from 28.66°C to 31.30°C. In contrast, SSP5-8.5 shows a clear interannual variability, marked by a steady increase in

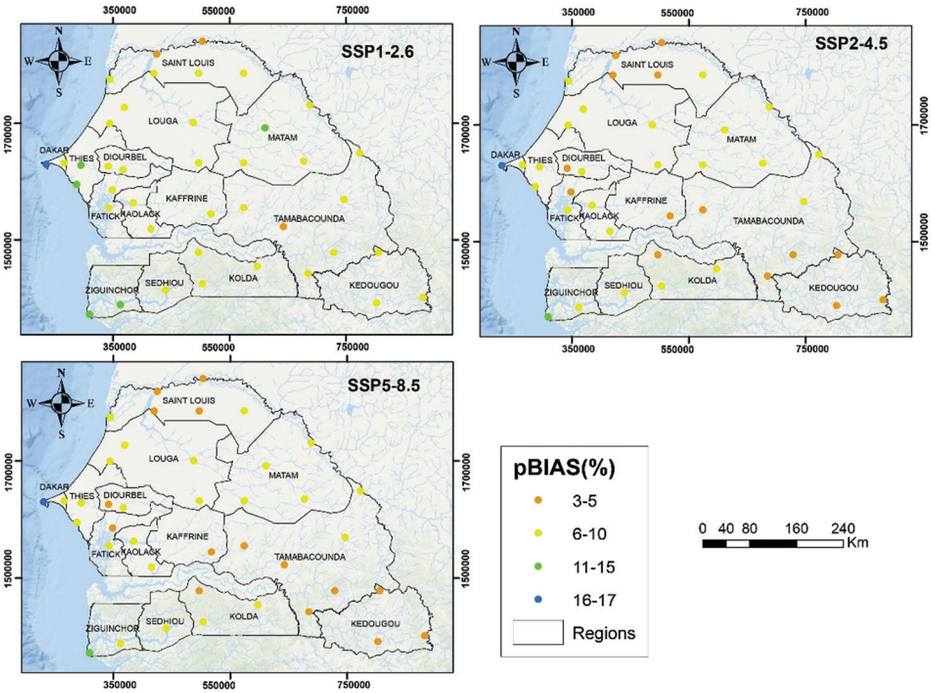

Figure 3. Spatial distribution of pBias values according to the different scenarios. Figure created with ArcGis 10.8, Sow and Gaye (2025).
Abbreviations: pBias: Percent bias; SSP: Shared socioeconomic pathway.

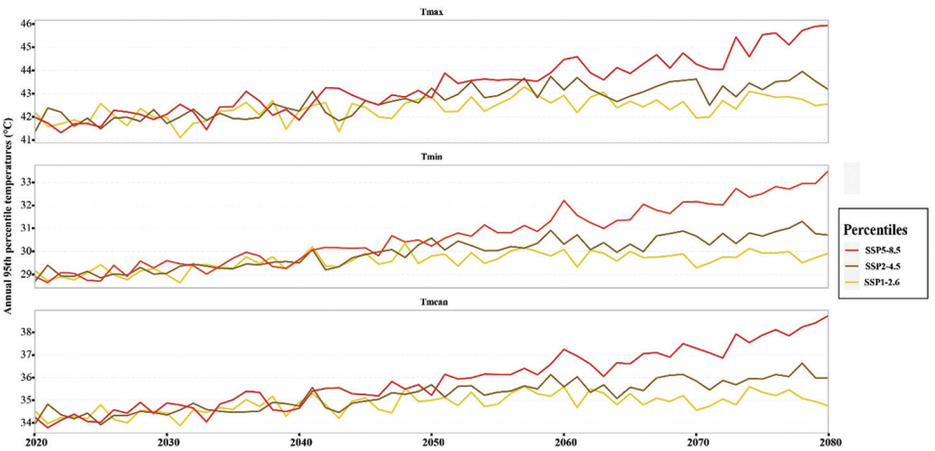

Figure 4. Evolution of the annual 95th percentile of minimum, mean, and maximum temperatures over the period 2020 – 2080. Figure created with ArcGis 10.8, Sow and Gaye (2025).
Abbreviations: SSP: Shared socioeconomic pathway; T_{max}: Maximum temperature; T_{mean}: Mean temperature; T_{min}: Minimum temperature.

the 95th percentile of minimum temperatures over the 2020 – 2080 period.

For mean temperatures, the trend in SSP1-2.6 is similar to that of minimum temperatures, with temperatures ranging from 33.87°C to 35.59°C, a difference of 5.27°C compared to the minimum temperatures in SSP1-2.6. SSP2-4.5 is characterized by a more regular evolution, with mean temperatures ranging from 33.91°C to 36.63°C. This represents an increase of 5.25°C compared to the minimum temperatures in SSP2-4.5. Similarly, SSP5-8.5 shows a steady increase in mean temperatures, ranging from 33.78°C to 38.74°C, with a difference of 5.24°C relative to the corresponding minimum temperature.

Maximum temperatures exhibit a clear warming trend (Figure 4). In SSP1-2.6, temperatures range from 41.09°C to 43.28°C, representing a thermal amplitude of 7.50°C compared to mean temperatures and 12.78° compared to minimum temperatures. SSP2-4.5 shows slightly higher values, ranging from 41.31°C to 43.95°C, with corresponding mean amplitudes of 7.49°C and 12.74°C relative to mean temperatures and minimum temperatures, respectively. SSP5-8.5 reflects a regular increase in extreme temperatures ranging from 41.31°C to 45.93°C, corresponding to a thermal amplitude of 12.67°C relative to minimum temperatures and 7.43°C relative to average temperatures.

In summary, the trend of extreme heat shows a relatively irregular pattern marked by a modest increase up to 2050 for all SSP1-2.6, SSP2-4.5, and SSP5-8.5. However, from 2050 onward, a net warming trend emerges across all variables (Figure 4).

3.3. Spatiotemporal distribution of extreme heat in Senegal

The spatiotemporal distribution of the extreme heat was made based on the average 95th percentile of the 2021 – 2050 and 2051 – 2080 normals.

3.3.1. Spatial distribution of extreme heat from 2021 to 2050

The minimum, maximum, and mean temperatures for three CMIP6 scenarios (SSP1-2.6, SSP2-4.5, and SSP5-8.5) from 2021 to 2050 are presented in Figure 5.

The minimum temperatures are between 28°C and 36°C across all scenarios. Specifically, SSP1-2.6 indicates a minimum temperature between 28°C and 34°C, with most of Senegal falling within the range of 30°C to 32°C. Only a few stations in the Matam region record temperatures exceeding 32°C. SSP2-4.5 reveals a similar pattern with temperatures ranging from 30°C to 32°C across the country. Only Matam stations and part of the Tambacounda and Kedougou regions record temperatures above 32°C. In the SSP5-8.5 scenario, an increase in temperatures is observed compared to the previous scenarios. The temperatures fall between 32°C and 36°C across the country, with the western and central parts of the country fall between 32°C and 34°C. In contrast, the eastern region recorded temperatures between 34°C and 36°C. Administratively, these stations are located primarily in the regions of Kedougou, Tambacounda, Matam, and Saint-Louis.

In addition, temperatures reflect similar spatial dynamics for SSP1-2.6, SSP2-4.5, and SSP5-8.5 (Figure 5). Temperatures range from 32°C to 40°C, with the western-central to southern region recording the lowest values between 32°C and 34°C. In the central and northwestern regions, temperatures range from 34°C to 36°C. The highest mean temperatures are recorded in the central to eastern region of the country, with temperatures ranging from 36°C to 40°C in all scenarios.

Maximum temperatures exhibit the highest values compared to minimum and mean temperatures, ranging from 32°C to 51°C across all three scenarios for the 2021 – 2050 period. SSP1-2.6 presents temperatures between 32°C and 34°C throughout the country, while SSP2-4.5 and SSP5-8.5 show a varied spatial distribution with three temperature classes. In SSP2-4.5, the western region falls between 36°C and 40°C. In the central region, the temperatures range from 40°C to 45°C, and the eastern region presents temperatures between 45°C and 51°C. The distribution in SSP5-8.5 is similar to SSP2-4.5, with the exception at the Ziguinchor station, where temperatures between 34°C and 36°C are observed.

3.3.2. Spatial distribution of heat waves from 2051 to 2080

On the 2051 – 2080 normal (Figure 6), minimum temperatures vary between 28°C and 36°C. In SSP1-2.6, the temperatures are below 32°C across the entire country except the eastern regions of Kedougou, Tambacounda, Matam, and Saint-Louis. In SSP2-4.5, the temperatures fall between 32°C and 34°C across the entire country except south-central stations in the regions of Sedhiou, Kolda, and part of Kaolack and Kaffrine, where the temperatures are below 32°C. For SSP5-8.5, the temperatures range from 32°C to 36°C, with the western and eastern regions showing temperatures ranging from 32°C to 34°C and 34°C to 36°C, respectively.

In addition, mean temperatures show a spatial dynamic that is significantly different compared to

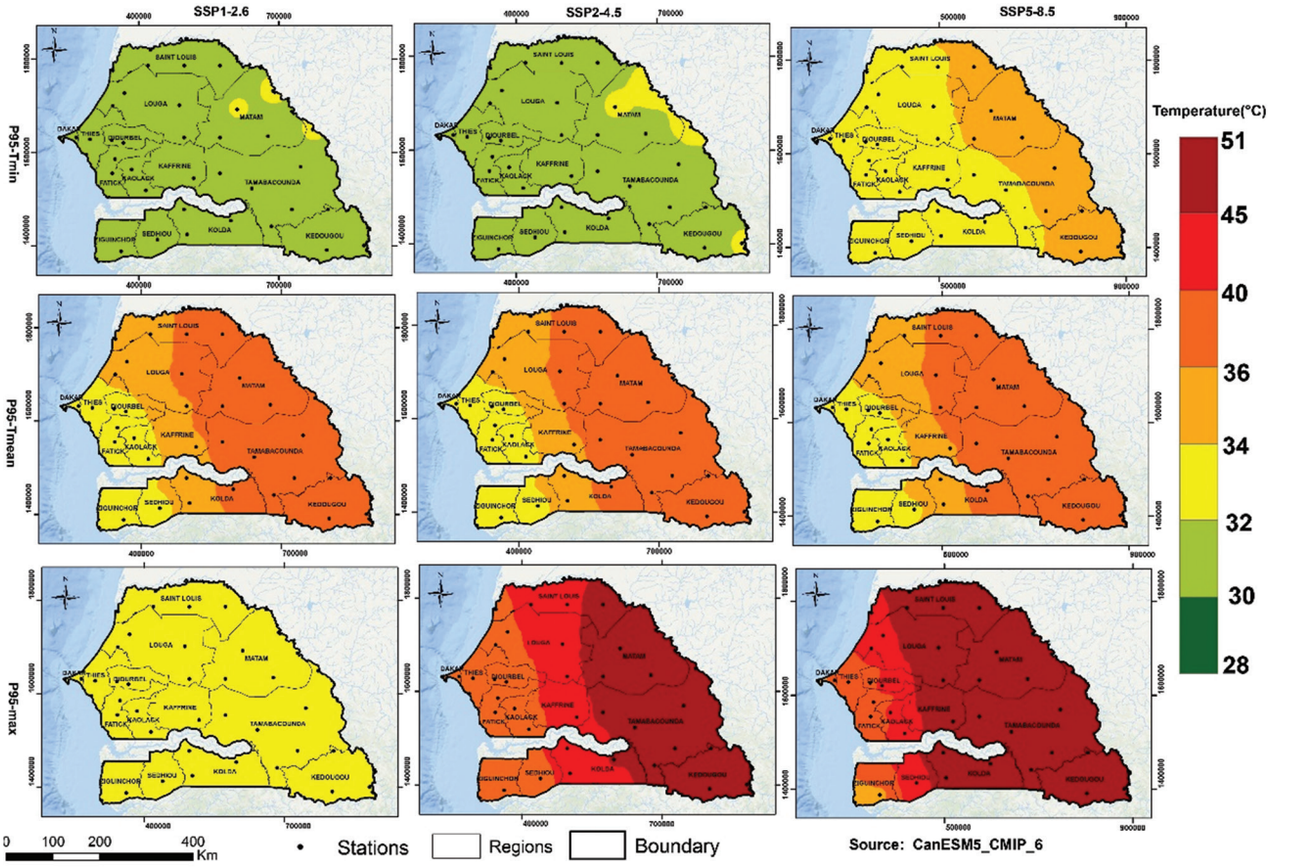

Figure 5. Spatialization of the P95 of T_{min}, T_{mean}, and T_{max} over the period 2021 – 2050. Figure created with ArcGis 10.8, Sow and Gaye (2025).

Abbreviations: P95: 95th Percentile; SSP: Shared socioeconomic pathway; T_{max}: Maximum temperature; T_{mean}: Mean temperature; T_{min}: Minimum temperature.

minimum temperatures, although the observed trend is similar to the mean temperatures in the period 2021 – 2050. A warming trend is observed in the western part of Senegal compared to the earlier period. Mean temperatures vary between 32°C and 40°C, with the western region having the lowest values (32 – 34°C) and the central region where temperatures fall between 34°C and 36°C. The highest temperatures (36 – 40°C) are observed in the eastern region for all three scenarios.

For maximum temperatures, the spatial dynamic is marked by much higher temperatures compared to the minimum and mean temperatures. For SSP1-2.6, the temperatures are between 32°C and 34°C throughout the country, which is similar to the earlier period. In SSP2-4.5 and SSP5-8.5, temperatures range from 40°C to 51°C. The spatial distribution shows noticeable disparities, with the most moderate temperatures observed in the west-central region, while higher temperatures dominate across the rest of the country, with the exception in the coastal regions.

3.4. Interannual variability of extreme heat

3.4.1. Interannual variability of extreme heat from 2021 to 2050

The temporal evolution of the extreme heat from 2021 to 2050 was analyzed using the Lamb anomaly index (Figure 7). The results show a highly irregular interannual pattern of minimum, maximum, and mean temperatures in SSP1-2.6. Two distinct phases can be identified in Figure 7. The first period from 2020 to 2035 is marked by a downward trend in extreme temperatures across all variables, while the second period, from 2035 to 2050, is characterized by an upward trend in extreme heat.

In SSP2-4.5, a highly irregular interannual variability is observed, characterized by alternating phases of rising and falling extreme heat. A declining phase in

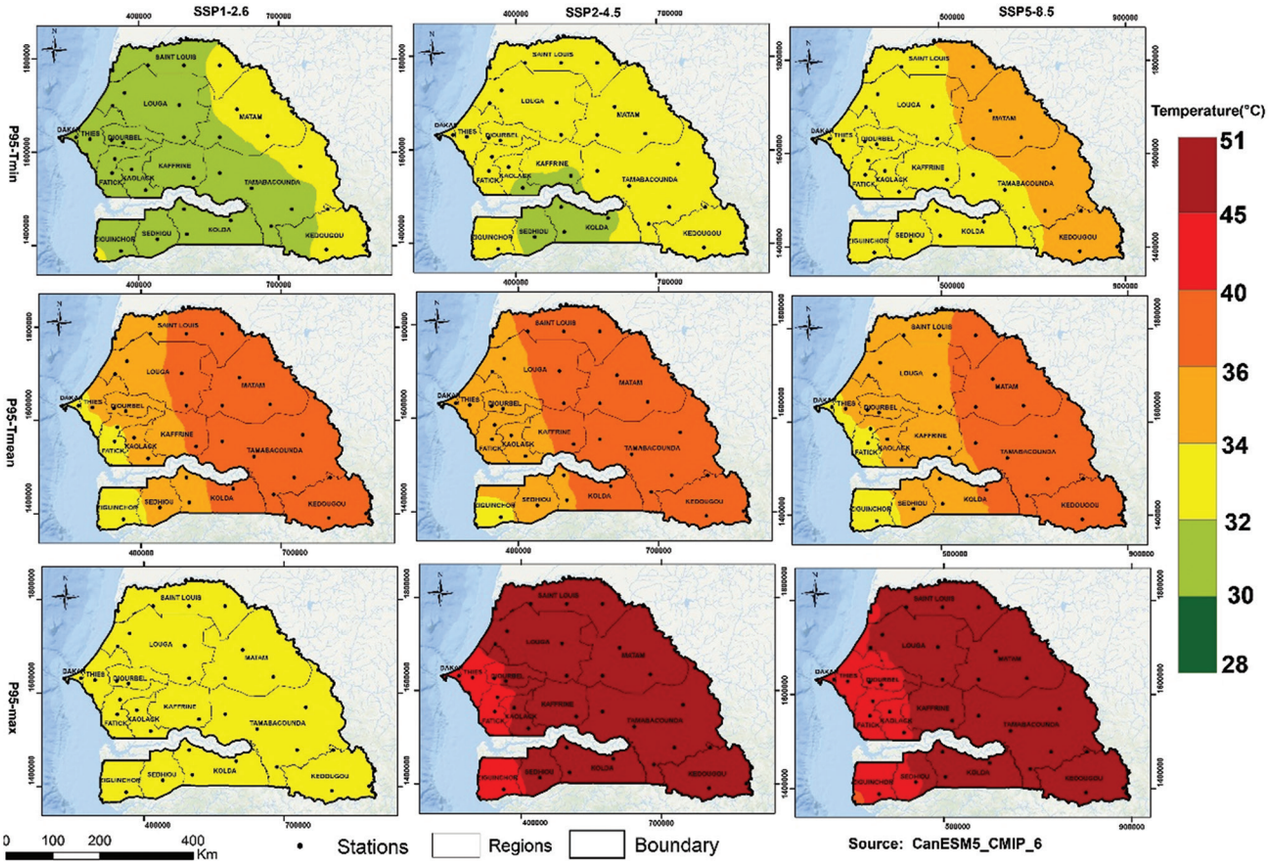

Figure 6. Spatialization of the P95 of T_{min}, T_{mean}, and T_{max} over the period 2051 – 2080. Figure created with ArcGis 10.8, Sow and Gaye (2025).

Abbreviations: P95: 95th Percentile; SSP: Shared socioeconomic pathway; T_{max}: Maximum temperature; T_{mean}: Mean temperature; T_{min}: Minimum temperature.

extreme heat is observed from 2020 to 2040, during which fewer than 5 years show an increase across all three scenarios (SSP1-2.6, SSP2-4.5, and SSP5-8.5). From 2040 onward, the evolution of extreme heat is marked by an overall increase in minimum, maximum, and mean temperatures.

In SSP5-8.5, the diachronic evolution is similar for all temperature variables. There are two phases in the evolution of minimum, maximum, and mean temperatures. From 2021 to 2042, temperatures are marked by a declining trend, with only 5 years being positive in maximum temperatures, four in mean temperatures, and five in minimum temperatures. From 2042 onward, an upward trend emerges across all temperature variables. For minimum temperatures, the projected increases are 0.42°C in SSP1-2.6, 0.69°C in SSP2-4.5, and 0.55°C in SSP5-8.5. In comparison, mean temperatures are expected to rise by 0.25°C, 0.65°C, and 0.41°C in SSP1-2.6, SSP2-4.5, and SSP5-8.5, respectively. Maximum temperatures show increases of 0.035°C for SSP1-2.6, 0.62°C for SSP2-4.5, and 0.45°C for SSP5-8.5.

3.4.2. Interannual variability of extremes from 2051 to 2080

Extreme temperature anomalies were analyzed for the period 2051 – 2080, as shown in Figure 8. This figure shows a pronounced interannual variability in SSP1-2.6 for minimum, maximum, and mean temperatures, with year-to-year fluctuations throughout the period.

SSP2-4.5 is characterized by a more regular trend, though still marked by alternating periods of growth and a decrease in extreme temperatures for all variables. A sustained increase is observed starting from 2068, resulting in positive values of the Lamb anomaly index, except in years 2071 and 2073.

In SSP5-8.5, the period 2051 – 2080 is characterized by low variability on a year-long scale. However,

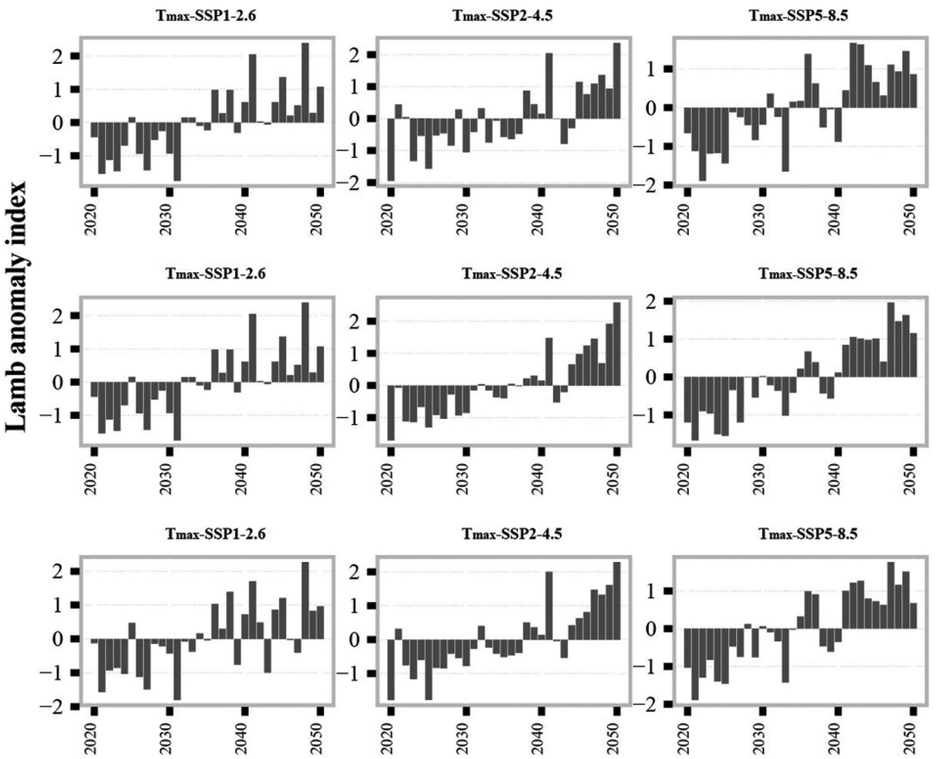

Figure 7. Temporal dynamics of extreme heat over the period 2021 – 2050. Figure created with ArcGis 10.8, Sow and Gaye (2025).

Abbreviations: SSP: Shared socioeconomic pathway; T_{max}: Maximum temperature; T_{mean}: Mean temperature; T_{min}: Minimum temperature.

there are alternating phases of decline and increase in extreme heats. The year 2072 marks a turning point in the evolution of heat waves in Senegal. The first sub-period, from 2050 to 2071, shows a noticeable decrease, followed by an increase from 2072 to 2080. Between these two sub-periods, extreme temperatures (minimum temperatures) increase by 0.07°C in SSP1-2.6, 0.44°C in SSP2-4.5, and 1.35°C in SSP5-8.5. For maximum temperatures, the increase is 0.16°C in SSP1-2.6, 0.23°C in SSP2-4.5, and 1.34°C in SSP5-8.5. For mean temperatures, the increase is 0.05°C in SSP1-2.6, 0.41°C in SSP2-4.5, and 1.34°C in SSP5-8.5.

The diachronic evolution of extreme heat is marked by an interannual variability, characterized by alternating periods of increase and decrease in minimum, maximum, and mean temperatures. The importance of this variability depends on the climate scenarios of this study. Interannual fluctuations are more pronounced in SSP1-2.6 compared to SSP2-4.5. In SSP2-4.5 and SSP5-8.5, the trends are more regular, although fluctuating phases still occur.

3.5. Trend of extreme heat in Senegal

3.5.1. Trends of extreme heat s from 2021 to 2050

The trend of extreme heat in Senegal over the period 2021 – 2050 is analyzed using the Mann–Kendall trend test (Figure 9). The *Z*-value of the test indicates the presence of a trend: a positive value reflects an increase in temperatures over the period, while a negative value indicates a decrease.

Figure 9 shows significant upward trends for minimum temperatures at all stations in all three scenarios (SSP1-2.6, SSP2-4.5, and SSP5-8.5) (p<0.01). For mean temperatures, the warming trends of extreme temperatures are observed with different levels of significance. In SSP1-2.6 and SSP2-4.5, the increase in extreme temperatures is noted with a 99% confidence level (p<0.01), except for west-central, northwest, and northeast in SSP1-2.6 and south of Tambacounda and a Kolda station (SSP2-4.5), for which the significance levels are 95% (p<0.05). An upward trend of minimum temperature is noted in SSP5-8.5 with a significance level of 99% (p<0.01) for all study stations (Figure 9).

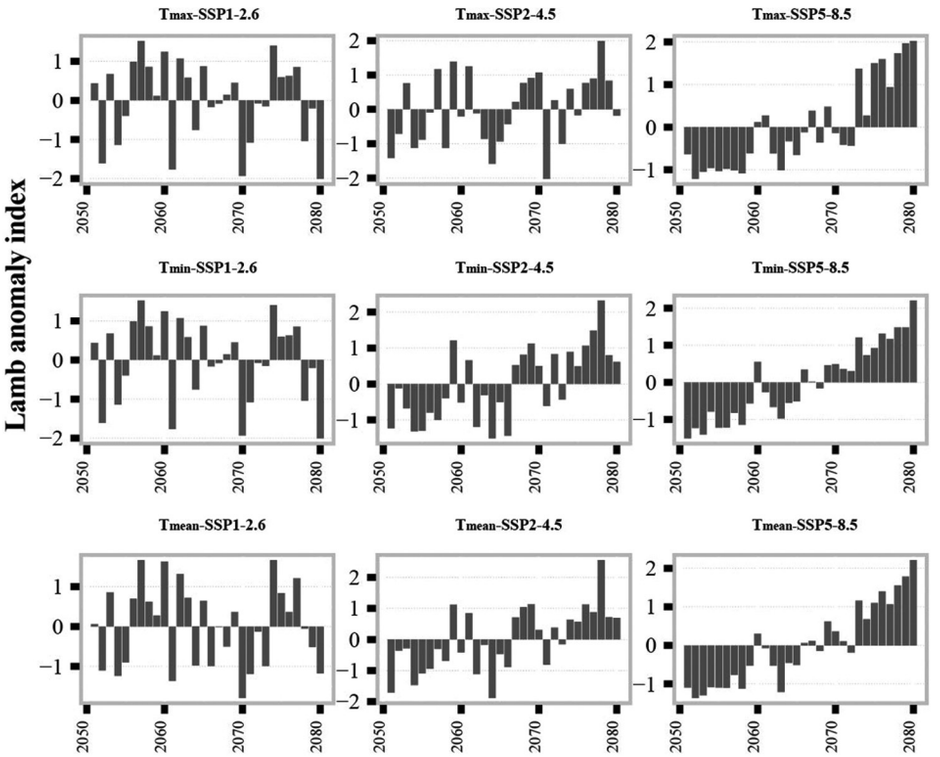

Figure 8. Temporal dynamics of extreme heat over the period 2051 – 2080. Figure created with ArcGis 10.8, Sow and Gaye (2025).

Abbreviations: SSP: Shared socioeconomic pathway; T_{max}: Maximum temperature; T_{mean}: Mean temperature; T_{min}: Minimum temperature.

In addition to the *Z*-value, Sen's slope evaluates the magnitude of the trends. Figure 10 shows the magnitude of the 95th percentile trend of heat waves in Senegal. Minimum temperatures show an upward trend for all scenarios. An average increase of 0.010°C is observed at the Dakar station in SSP1-2.6. For SSP1-2.6 and SSP2-4.5, a temperature increase of between 0.023°C and 0.040°C is noted in the eastern, central, and southwestern regions of the country. For SSP2-4.5, the central and eastern region shows increases in temperatures between 0.040°C and 0.070°C. The growth of extreme heat for SSP5-8.5 follows a similar dynamic with increases in temperatures between 0.040°C and 0.070°C for all study stations.

For mean temperatures, an increase of 0.012°C to 0.030°C is observed in the western regions covering Saint-Louis, Louga, Dakar, Thiès, Fatick, Kaolack, and Ziguinchor for SSP1-2.6 and the south-central (Sedhiou, Kolda, and part of Tambacounda) for SSP2-4.5. For SSP5-8.5, temperature growth ranges from 0.030°C to 0.050°C in western and south-central regions. The eastern region experiences the highest temperature growth between 0.050°C and 0.083°C.

Regarding maximum temperatures, the highest increase between 0.050°C and 0.850°C is only observed at the Mbiddi station (SSP1-2.6) and in parts of Saint-Louis (SSP2-4.5 and SSP5-8.5). The lowest temperature growth is observed in the western region in SSP1-2.6 and in the central region in SSP2-4.5 and SSP5-8.5. The rest of the territory is subject to a moderate increase between 0.030°C and 0.050°C. Thus, a significant spatial variability in temperature growth can be observed across the climate scenarios of this study. In short, the western, south-central, and central regions recorded the lowest temperature growth.

3.5.2. Trends of extreme heat from 2051 to 2080

Figure 11 illustrates the trend of extreme heat over the period 2051 – 2080, which indicates a different trend in SSP1-2.6 for minimum, mean, and maximum temperatures compared to the period 2021 – 2050. Except for the significant temperature growth along the coast and the Kedougou station, the temperature growth is stationary for minimum, mean, and maximum temperatures.

For SSP2-4.5, growth dynamics are observed for minimum and mean temperatures. Spatially, this trend

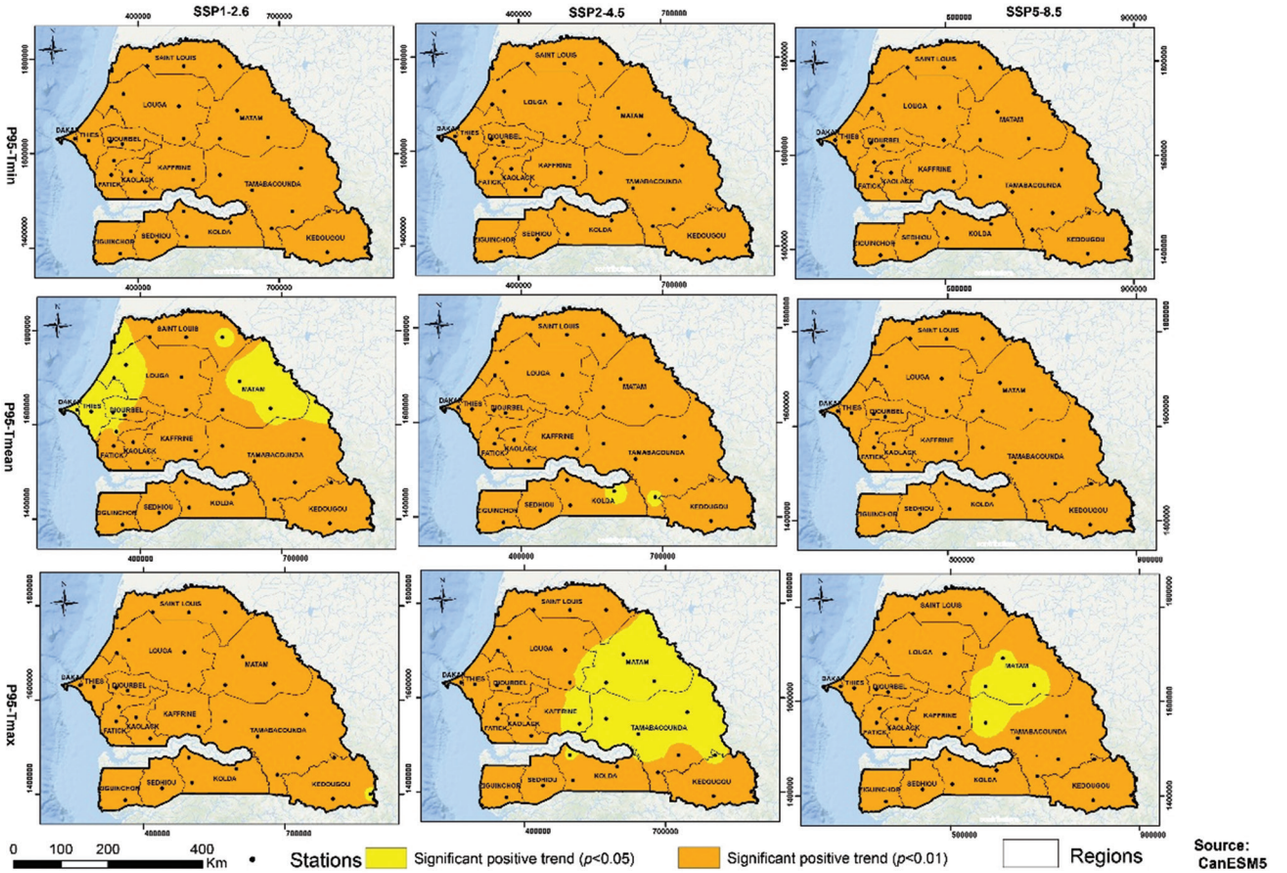

Figure 9. P95 trends of T_{min}, T_{mean}, and T_{max} from 2021 to 2050. Figure created with ArcGis 10.8, Sow and Gaye (2025).

Abbreviations: P95: 95th Percentile; SSP: Shared socioeconomic pathway; T_{max}: Maximum temperature; T_{mean}: Mean temperature; T_{min}: Minimum temperature.

is observed with a 99% significance level (p<0.01) at almost all stations except for those in the northwest region (mean temperatures) and the stations of Saint-Louis, Dagana, and Kedougou (minimum temperatures), which the significance levels are 95% (p<0.05).

A significant warming trend is observed in SSP5-8.5 at a 99% significance level (p<0.01) for minimum and mean temperatures, while a stationary trend is observed for maximum temperatures at all stations.

In addition, Sen's slope for the period 2051 – 2080 shows the magnitude of the temperature trend. Figure 12 illustrates Sen's slope results from the Mann–Kendall test for the period 2051 – 2080, based on data from the 40 stations included in this study.

An increase in minimum temperatures between 0.010°C and 0.030°C is observed in SSP1-2.6 and the western region of SSP2-4.5 (Figure 12). The eastern region of SSP2-4.5 shows an increase of minimum temperatures between 0.030°C and 0.050°C. SSP5-8.5 records the largest increase in minimum temperatures above 0.050°C.

The magnitude of the Sen's slope of mean temperatures is irregular. The temperature growth in SSP1-2.6 is between 0.030°C and 0.050°C at all stations in this study. A decrease in temperature growth (below 0.030°C) is observed in SSP2-4.5 throughout Senegal, except for the regions in Matam and Tambacounda, where the temperature growth falls between 0.030°C and 0.050°C. In SSP5-8.5, the temperature increase ranges from 0.013°C to 0.068°C. The highest increase in temperatures between 0.050°C and 0.068°C is observed in the eastern, northern, and central regions. A moderate temperature growth between 0.030°C and 0.050°C is observed in southwestern (Ziguinchor, Sedhiou, and Kolda), central (Fatick, Kaolack, Kaffrine, and Diourbel), and western (Dakar, Thiès, and parts of Saint-Louis and Louga) regions.

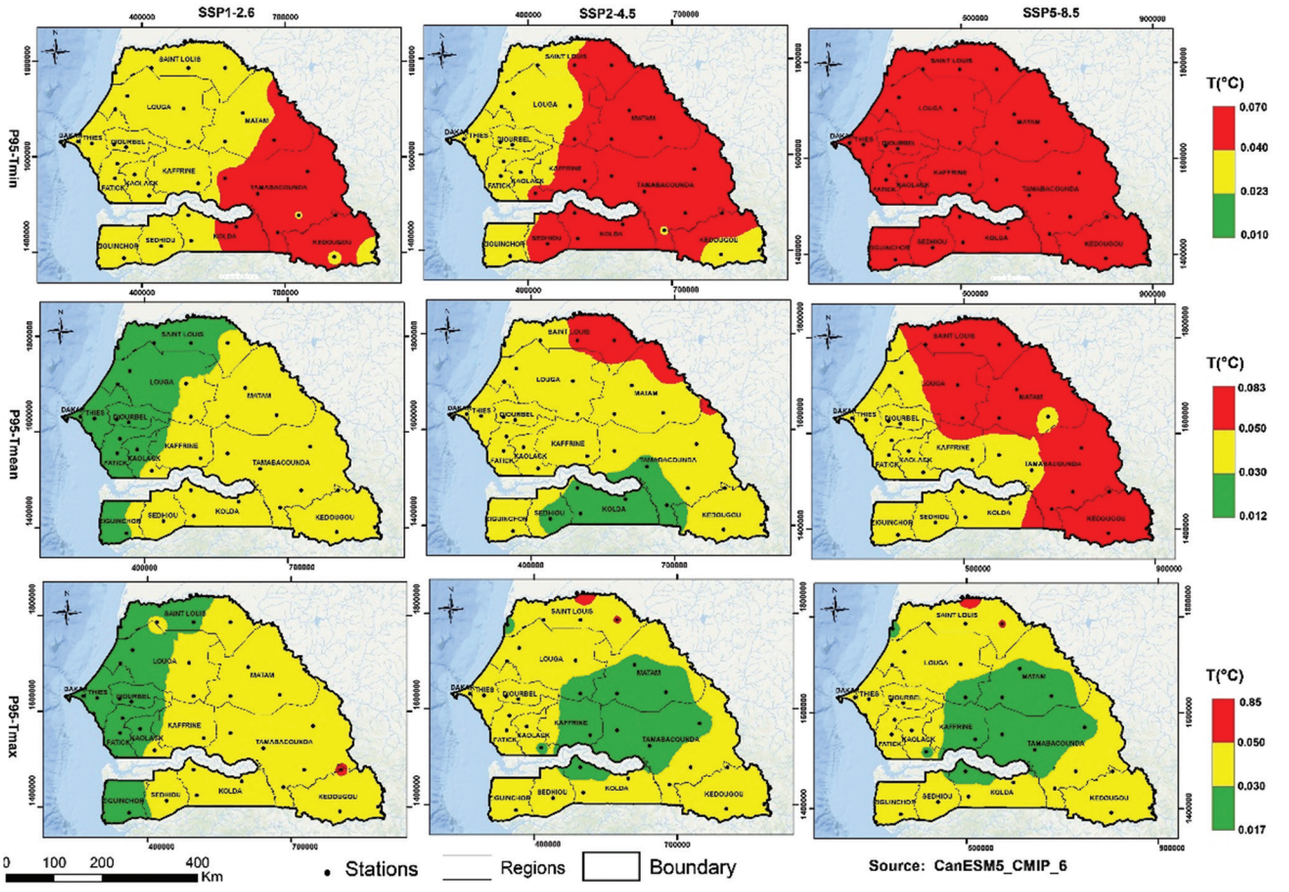

Figure 10. Distribution of the Sen's slope in Senegal from 2021 to 2050. Figure created with ArcGis 10.8, Sow and Gaye (2025).

Abbreviations: P95: 95th Percentile; SSP: Shared socioeconomic pathway; T: Temperature; T_{max}: Maximum temperature; T_{mean}: Mean temperature; T_{min}: Minimum temperature.

Regarding maximum temperatures, all stations in this study exhibit notably low increases, with values below 0.050°C in SSP1-2.6. At the spatial level, only the western region recorded the largest increase between 0.030°C and 0.050°C. The temperature increases in other regions are below 0.030°C. The recorded increases of temperatures at all stations in SSP2-4.5 and SSP-8.5 are below 0.030°C.

4. Discussion

The purpose of this work was to study the future trends of minimum, maximum, and mean temperatures over two climate normals (2021 – 2050 and 2051 – 2080). Three CanESM5 scenarios (SSP1-2.6, SSP2-4.5, and SSP5-8.5) were studied at 40 stations.

The results of this study reflect an increase in temperatures across all variables at the national level. This upward trend is observed in minimum, mean, and maximum temperatures in SSP1-2.6, SSP2-4.5, and SSP5-8.5. The warming dynamic is the greatest in SSP5-8.5. This trend aligns with the work of the Intergovernmental Panel on Climate Change (IPCC),[5] which predicted an increase in temperatures. Previous studies from Perkins *et al.*[7] and Das and Umamahesh[6] showed that the increase in temperatures would result in a strengthening of global extreme heat toward the end of the 21st century. At the Sahelian scale, Ringard *et al.*[9] reported similar findings regarding the intensification of extreme heat. In Senegal, Sagna *et al.*[56] support the IPCC's predictions by confirming this warming trend.

The results show an overall upward trend across all stations, scenarios, and temperature variables for the period 2021 – 2050. In contrast, for the period 2051 – 2080, continental stations in SSP1-2.6 for minimum and mean temperatures and all scenarios for maximum temperatures display a stationary trend. This overall upward trend is supported by the work of

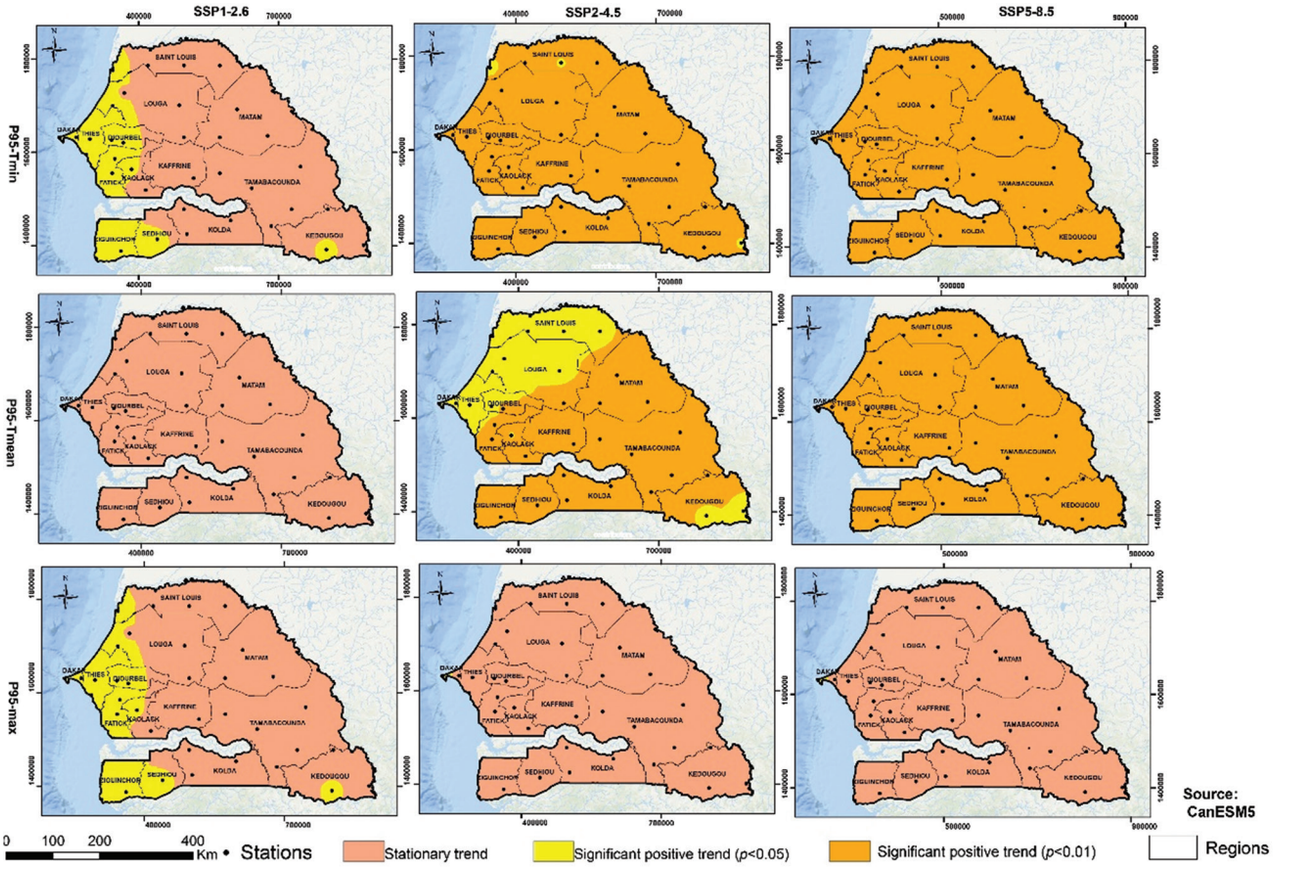

Figure 11. P95 trends of T_{min}, T_{mean}, and T_{max} from 2051 to 2080. Created with ArcGis 10.8, Sow and Gaye (2025).

Abbreviations: P95: 95th Percentile; SSP: Shared socioeconomic pathway; T_{max}: Maximum temperature; T_{mean}: Mean temperature; T_{min}: Minimum temperature.

Ringard,[57] which predicted a warming of temperatures in the future. The dynamics of extreme heat in Senegal can be explained by the combination of climatic and geographical factors. One factor contributing to the persistence of heat conditions is the influence of subtropical and Saharan-Libyan high-pressure systems. These systems lead to the convergence of hot and dry air masses from the Sahara toward the Sahel, creating favorable conditions for atmospheric blocking, which increases the likelihood of extreme heat.[22] In addition, the atmospheric influences are combined with the low humidity level and low cloud cover in these regions, further contributing to the intensification of heat waves.

In addition, the trend is characterized by a greater increase in the minimum temperatures, which is reflected in the reduction of thermal amplitudes. This is likely linked to the effects of human activities, particularly greenhouse gas emissions.[58] Specifically, CO_2 emission from the Earth's surface at night constrains nocturnal cooling. Furthermore, artificial or desert surfaces with a high thermal capacity and conductivity trap heat during the day, which is released at night, further inhibiting cooling. These factors could explain the faster rise in minimum temperatures compared to mean and maximum temperatures observed in Senegal. These findings extend the results of Braganza *et al*.,[59] Easterling *et al*.,[60] and Hartmann *et al.*[61] regarding the faster increase in minimum temperatures globally, as well as the studies of Trigo *et al*.,[62] Ringard,[57] Rome *et al*.,[63] and Barbier[64] in Africa and the Sahel. The increasing trend of minimum temperatures underscores the severity of heat waves, as highlighted by Meehl and Tebaldi[65] and Trigo *et al.*[62]

The spatial dynamics of these trends indicate an increase in extreme temperatures moving eastward. This is due to geographical factors such as high humidity and elevated hydrometric levels in coastal regions compared to inland regions. This spatial distribution of extreme

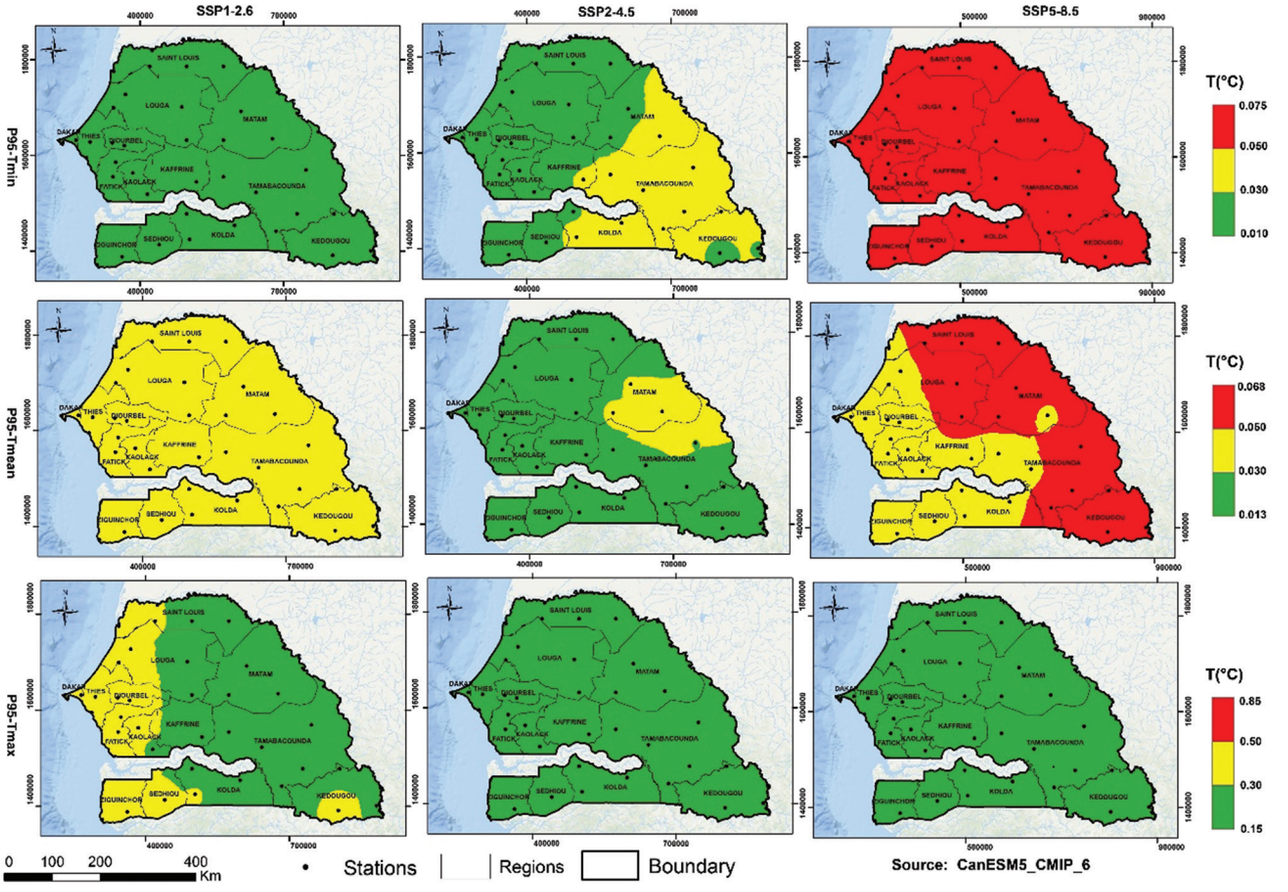

Figure 12. Distribution of the Sen's slope in Senegal from 2051 to 2080. Created with ArcGis 10.8, Sow and Gaye (2025).

Abbreviations: P95: 95th Percentile; SSP: Shared socioeconomic pathway; T: Temperature; T_{max}: Maximum temperature; T_{mean}: Mean temperature; T_{min}: Minimum temperature.

temperatures supports the work of Ndiaye *et al*.,[30] which characterized the spatial dynamics of temperatures at the national scale in Senegal.

Thus, this work projected the future evolution of extreme heat for the periods 2051 – 2080 and 2051 – 2080 with an upward trend across all scenarios. A comparative analysis of extreme temperature trends using different outputs of CMIP6 would be a relevant direction for future studies.

5. Conclusion

This study aimed to analyze the evolution and future trends of heat waves over the periods 2021 – 2050 and 2051 – 2080. The data from the CanESM5 model were resampled and extracted based on the coordinates of 40 stations selected for this study. Minimum, mean, and maximum temperatures were examined under three scenarios (SSP1-2.6, SSP2-4.5, and SSP5-8.5) of CMIP6. The study was performed through the spatialization of extremes using IDW, the analysis of interannual variability using the Lamb index, and trend detection using the Mann-Kendall test.

The observed dynamics of minimum temperatures range from 28°C to 36°C across all scenarios. In SSP1-2.6, almost the entire country shows dynamics of minimum temperatures below 32°C, particularly in the western region. In SSP2-4.5, minimum temperatures range from 32°C to 34°C nearly across the entire territory, while temperatures below 32°C are noted at the stations in the south-central region. In SSP5-8.5, minimum temperatures exceed 32°C across all stations but remain below 36°C. In addition, mean temperatures range from 32°C to 40°C with similar patterns across all scenarios. The lowest values (32°C – 34°C) are observed in the western region, while the central region shows moderate values (34°C – 36°C). Elevated mean temperatures

(36°C – 40°C) are observed in the eastern region. The maximum temperatures are marked by the highest spatial dynamic across all temperature variables. In SSP1-2.6, maximum temperatures fall between 32°C and 34°C across Senegal. For SSP2-4.5 and SSP5-8.5, maximum temperatures range from 40°C to 51°C. In addition, the Lamb anomaly index indicates a greater increase in minimum temperatures with an increase of 0.43°C in SS1-2.6, 1.06°C in SSP2-4.5, and 2.18°C in SSP5-8.5. The increases of maximum temperatures in SSP1-2.6, SSP2-4.5, and SSP5-8.5 are 0.50°C, 1.05°C, and 2.03°C, respectively, while mean temperatures increased by 0.48°C in SSP1-2.6, 1.04°C in SSP2-4.5, and 2.16°C for SSP5-8.5.

The results obtained reflect an upward trend in extreme heat in all variables, scenarios, and stations. However, the increase is more significant in the first period (2021 – 2050) than in the second (2051 – 2080). At the spatial level, the western region showed the lowest increment of below 0.030°C, while the remaining regions in Senegal are experiencing greater increases that exceed 0.050°C in the first period.

In short, this study analyzed the trend and future evolution of extreme heat in terms of minimum, mean, and maximum temperatures for the periods 2021 – 2050 and 2051 – 2080. Data from the CanESM5 model were used in SSP1-2.6, SSP2-4.5, and SSP5-8.5. In light of these results, it is necessary to study the future trend of heat waves using other CMIP6 models.

Acknowledgments

None.

Funding

None.

Conflict of interest

The authors declare no conflicts of interest.

Author contributions

Conceptualization: All authors
Formal analysis: All authors
Methodology: Moussa Sow
Software: Moussa Sow
Validation: Moussa Sow, Demba Gaye
Writing – original draft: Moussa Sow
Writing–review & editing: Demba Gaye

Availability of data

The data used in this article have been cited in the document. The links to access the data have been shared in-text.

References

1. Costello A, Abbasb M, Allen A, *et al*. Managing the health effects of climate change: Lancet and University College London Institute for Global Health Commission. *Lancet*. 2009;373(9676):1693-1733. doi: 10.1016/s0140-6736(09)60935-1
2. IPCC. *Climate Change 2014: Synthesis Report. Contribution of Working Groups I, II and III*. Geneva, Switzerland; 2014. Available from: https://www.ipcc.ch/site/assets/uploads/2018/05/SYR_AR5_FINAL_full_wcover.pdf [Last accessed on 2025 Mar 15].
3. Sharma A, Goyal MK. Assessment of the changes in precipitation and temperature in Teesta River basin in Indian Himalayan Region under climate change. *Atmos Res*. 2019;231:104670. doi: 10.1016/j.atmosres.2019.104670
4. Chen H, Zhao L, Cheng L, *et al*. Projections of heatwave-attributable mortality under climate change and future population scenarios in China. *Lancet Reg Health West Pac*. 2022;28:100582. doi: 10.1016/j.lanwpc.2022.100582
5. IPCC. *Summary for Policymakers. In Climate Change 2013: The Physical Science Basis. Contribution of Working Group I*. Cambridge, United Kingdom and New York, NY, USA: Cambridge University Press; 2013. Available from: https://www.ipcc.ch/site/assets/uploads/2018/03/wg1ar5_summaryvolume_final.pdf [Last accessed on 2025 Mar 17].
6. Das J, Umamahesh NV. Heat wave magnitude over India under changing climate: Projections from CMIP5 and CMIP6 experiments. *Int J Clim*. 2021;42(1):331-351. doi: 10.1002/joc.7246
7. Perkins SE, Alexander LV, Nairn JR. Increasing frequency, intensity and duration of observed global heatwaves and warm spells. *Geophys Res Lett.* 2012;39:L20714. doi: 10.1029/2012GL053361
8. Zeng Q, Li GX, Cui YS, Jiang GH, Pan XC. Estimating temperature-mortality exposure-response relationships and optimum ambient temperature at the multicity level of China. *Int J Environ Res Public Health*. 2016;13(3):279.
9. Ringard J, Dieppois B, Rome S, *et al*. *Evolution des pics de Températures en Afrique de l'Ouest: Étude comparative entre Abidjan et Niamey*. p. 231-237. Available from: https://www.researchgate.net/publication/260176381_evolution_des_pics_de_temperatures_en_afrique_de_l'ouest_etude_comparative_entre_abidjan_et_niamey [Last accessed

on 2025 Mar 15].
10. World Meteorological Organization and World Health Organization. *Heat Waves and Health: Guidance on Warning-System Development*. *WMO-No*; 2015. Available from: https://cdn.who.int/media/docs/default-source/climate-change/heat-waves-and-health---guidance-on-warning-system-development.pdf?sfvrsn=e4813084_2&download=true [Last accessed on 2025 Mar 12].
11. Watts N, Adger WN, Agnolucci P, *et al*. Health and climate change: Policy responses to protect public health. *Lancet*. 2015;386(10006):1861-1914. doi: 10.1016/s0140-6736(15)60854-6
12. World Health Organization. *World Health Statistics 2017: Monitoring Health for the SDGs, Sustainable Development Goals*. WHO; 2017. Available from: https://iris.who.int/bitstream/handle/10665/255336/9789241565486-eng.pdf?sequence=1&isAllowed=y [Last accessed on 2025 Mar 12].
13. FAO. *L'impact des Catastrophes Sur L'agriculture et la Sécurité Alimentaire Prévenir et Réduire Les Pertes En Investissant Dans la Résili*ence; 2023. Available from: https://openknowledge.fao.org/server/api/core/bitstreams/2580a391-043a-45c8-9537-3eb7f8b485fe/content [Last accessed on 2025 Mar 17].
14. Lobell DB, Burke MB, Tebaldi C, Mastrandrea MD, Falcon WP, Naylor RL. Prioritizing climate change adaptation needs for food security in 2030. *Science.* 2008;319(5863):607610. doi: 10.1126/science.1152339
15. Chakraborty DS, Tiedemann A, Teng P. Climate change: Potential impact on plant disease. *Environ Pollut.* 2000;108:317326. doi: 10.1016/S0269-7491(99)00210-9
16. Diouf NS. *Évolution Spatio-temporelle des Vagues de Chaleur en Afrique de l'Ouest et Risques Sanitaires Associes. Mémoire de Master, Physiques et Applications, Sciences de l'Atmosphère et de l'Ocean.UASZ*; 2018. Available from: https://rivieresdusud.uasz.sn/xmlui/bitstream/handle/123456789/955/diouf_memoire_2018.pdf?sequence=1&isAllowed=y [Last accessed on 2025 Mar 08].
17. Bodian A, Diop L, Panthou G, *et al*. Recent trend in hydroclimatic conditions in the senegal river basin. *Water*. 2020;12(2):436. doi: 10.3390/w12020436
18. Ndiaye PM. *Evaluation, Calibration et Analyse des Tendances Actuelles et Futures de L'évapotranspiration de Référence dans le Bassin du FLEUVE SÉNÉGAL*. UGB; 2021. Available from: https://cda-omvs.org/wp-content/uploads/2016/06/13680_evaluation-calibration-et-analyse-des-tendances-actuelles-et-futures-evapotranspirations-BFS.pdf [Last accessed on 2025 Mar 08].
19. Eyring V, Bony S, Meehl GA, *et al*. Overview of the coupled model intercomparison project phase 6 (CMIP6) experimental design and organisation. *Geosci Model Dev Disc.* 2016;9(5):1937-1958. doi: 10.5194/gmd-9-1937-2016
20. Hirsch AL, Ridder NN, Perkins-Kirkpatrick SE, Ukkola A. CMIP6 multimodel evaluation of present-day heatwave attributes. *Geophys Res Lett*. 2021;48:1-11. doi: 10.1029/2021GL095161
21. Toure M, Thiaw WM, Sy I, *et al*. Machine learning-based prediction of heatwave-related hospitalizations: A case study in Matam, Senegal. *Public Health*. 2025;3:1-26. doi: 10.20944/preprints202503.1797.v1
22. Sow M, Gaye D, Diakhate MM. Analysis of the spatiotemporal evolution of the trend of extreme heat in Senegal. *Vertigo.* 2024;24(2):1-21. doi: 10.4000/12jq1
23. Sow M, Gaye D, Diakhate MM. Analysis of the spatiotemporal evolution of the trend of extreme heat in Senegal. *Vertig*o. 2024;24(2):1-21. doi: 10.4000/12jq1
24. Sow M, Gaye D. Categorization and multi-criteria analysis of heat wave vulnerability in Senegal. *J Water Clim Change.* 2024;15(11):53825396. doi: 10.2166/wcc.2024.090
25. Sy I, Cissé B, Ndao B, *et al*. Heat waves and health risks in the northern part of Senegal: Analysing the distribution of temperature-related diseases and associated risk factors. *Environ Sci Pollut Res*. 2022;29(55):8336583377. doi: 10.1007/s11356-022-21205-x
26. Gaye AT, Lo HM, Sakho-Djimbira S, Fall MS, Ndiaye I. *Senegal: Revue du contexte Socioeconomique, Politique et Environnemental*. IED, PRESA; 2015. Available from: https://www.iedafrique.org/img/pdf/revue_resilience_croissance_et_changement_climatique_au_senegal-2.pdf [Last accessed on 2025 Mar 15].
27. Wade CT, Toure O, Diop M. *Gestion des Risques Climatiques*. IED, PRESA; 2015. Available from: https://www.iedafrique.org/img/pdf/revue_thematique_2015.pdf [Last accessed on 2025 Mar 15].
28. Bodian A. Characterization of recent temporal variability of annual rainfall in Senegal (West Africa). *Physio Geo Environ.* 2014;8:297-312. doi: 10.4000/physio-geo.4243
29. Yade M, Sagna P, Sambou P. *Migrations de l'Equateur Meteorologique et Precipitations au Senegal en 2008 et 2009. 25ème Colloque Ass Int de Cli*. p. 781-786. Available from: https://www.researchgate.net/publication/331232160_migrations_de_l'equateur_meteorologique_et_precipitations_au_senegal_en_2008_et_2009 [Last accessed on 2025 Mar 12].
30. Ndiaye PM, Gaye D, Sow SA. Spatio-temporal characterization and analysis of temperature trends in Senegal. *Eur Sci J.* 2020;16(33):105-121. doi: 10.19044/esj.2020.v16n33p105
31. Bigot S, Dumas D, Brou YT, *et al*. Projections climatiques

CMIP6 à l'echelle du sud-est de la cote d'ivoire: Evolution des contraintes thermo-pluviometriques pour les principaux Agrosystèmes associant cacao, hevea, palmier à huile et manioc. *Conference: 35ème Colloque Annuel de l'Association Internationale de Climatologie – AIC 2022At: Toulouse;* 2022. p. 60-66. Available from: https://agritrop.cirad.fr/606582/1/ID606582.pdf [Last accessed on 2025 Mar 08].

32. Mmame B, Ngongondo C. Evaluation of CMIP6 model skills in simulating tropical climate extremes over Malawi, Southern Africa. *Model Earth Syst Environ.* 2024;10(2):16951709. doi: 10.1007/s40808-023-01867-3
33. Wang D, Xu T, Fang G, *et al*. Characteristics of marine heatwaves in the Japan/East Sea. *Remote Sens*. 2022;14(4):936. doi: 10.3390/rs14040936
34. Ajibola FO, Zhou B, Shahid S, Ali MA. Performance of CMIP6 HighResMIP simulations on West African Drought. *Front Earth Sci.* 2022;10:925358. doi: 10.3389/feart.2022.925358
35. Akinsanola AA, Kooperman GJ, Pendergrass AG, Hannah WM, Reed KA. Seasonal representation of extreme precipitation indices over the United States in CMIP6 present-day simulations. *Environ Res Lett.* 2020;15(9):094003. doi: 10.1088/1748-9326/ab92c1
36. Ha K, Moon S, Timmermann A, Kim D. Future changes of summer monsoon characteristics and evaporative demand over Asia in CMIP6 simulations. *Geophys Res Lett*. 2020;47(8):e2020GL087492. doi: 10.1029/2020GL087492
37. Jeong DI, Cannon AJ, Yu B. Influences of atmospheric blocking on North American summer heatwaves in a changing climate: A comparison of two Canadian Earth system model large ensembles. *Clin Change.* 2022;172(5):1-21. doi: 10.1007/s10584-022-03358-3#citeas
38. Neal E, Huang CS, Nakamura N. The 2021 Pacific Northwest heat wave and associated blocking: Meteorology and the role of an upstream cyclone as a diabatic source of wave activity. *Geophys Res Lett.* 2022;49(8):e2021GL097699. doi: 10.1029/2021GL097699
39. Arora VK, Scinocca JF, Boer GJ, *et al*. Carbon emission limits required to satisfy future representative concentration pathways of greenhouse gases. *Geophys Res Lett.* 2011;38(5):1-6. doi: 10.1029/2010GL046270
40. Brunner L, Schaller N, Anstey J, Sillmann J, Steiner AK. Dependence of present and future European temperature extremes on the location of atmospheric blocking. *Geophys Res Lett.* 2018;45(12):6311-6320. doi: 10.1029/2018GL077837
41. Schaller N, Sillmann J, Anstey J, Fischer EM, Grams CM, Russo S. Influence of blocking on Northern European and Western Russian heatwaves in large climate model ensembles. *Environ Res Lett.* 2018;13(5):054015. doi: 10.1088/1748-9326/aaba55
42. Dehban H, Zareian MJ, Gohari A. Evaluating regional climate change during 2021-2080 for Iran and neighboring countries (a comparative analysis of projections and reanalysis data). *Theor Appl Climatol.* 2025;156:143. doi: 10.1007/s00704-025-05381-7
43. Zareian MJ, Dehban H, Gohari A, Torabi HA. Assessment of CMIP6 models performance in simulation precipitation and temperature over Iran and surrounding regions. *Environ Monit Assess.* 2024;196:701. doi: 10.1007/s10661-024-12878-7
44. Da Silva ASA, Stosic B, Menezes RSC, Singh VP. Comparison of interpolation methods for spatial distribution of monthly precipitation in the State of Pernambuco, Brazil. *J Hydrol Eng.* 2019;24:3. doi: 10.1061/(ASCE)HE.1943-5584.0001743
45. Teegavarapu RSV, Meskele T, Pathak CS. Geo-spatial grid-based transformations of precipitation estimates using spatial interpolation methods. *Comp Geosci.* 2012;40:2839. doi: 10.1016/j.cageo.2011.07.004
46. Jones PA *User's Guide for SCRIP: A Spherical Coordinate Remapping and Interpolation Package, Version 1.4. The Regents of the University of California*. Available from: https://oasis.cerfacs.fr/wp-content/uploads/sites/114/2021/03/globc_scripusers_1998.pdf [Last accessed on 2025 Mar 15].
47. Kim KH, Shim PS, Shin S. An alternative bilinear interpolation method between spherical grids. *Atmosphere.* 2019;10(3):123. doi: 10.3390/atmos10030123
48. Goudiaby O, Bodian A, Dezetter A, Diouf I, Ogilvie A. Evaluation of gridded rainfall products in three West African Basins. *Hydrology*. 2024;11(6):75. doi: 10.3390/hydrology11060075
49. Bodian A, Ndiaye PM, Diop SB, *et al*. Evaluation and calibration of alternative methods for estimating reference evapotranspiration in the main hydrosystems of Senegal: Senegal, Gambia and Casamance River Basins. *Proc IAHS*. 2024;385:415421. doi: 10.5194/piahs-385-415-2024
50. Saley MB, Tanoh R, Kouame KF, *et al*. *Variabilite Spatio-temporelle de la Pluviometrie et son Impact Sur les Ressources En Eaux Souterraines: Cas du district d'Abidjan (Sud de la Côte d'Ivoire)*. University de Cocody; 2009. Available from: https://www.sifee.org/client_file/upload/colloques%20documentation/2009%20niamey/3_saley_comm.pdf [Last accessed on 2025 Mar 12].
51. Faye C, Ba Djibrirou D, Diedhiou SO. The anomaly of the minimum and maximum temperature in the

south-eastern part of Senegal. *J Sci Res Univ Lome.* 2019;21(4-1):27-37.
doi: 10.12691/ajfn-13-2-2

52. Kendall MG. *Rank Correlation Methods*. 4th ed. London, U.K: Charles Griffin; 1975.
53. Mann HB. Nonparametric tests against trend. *Econometrica.* 1945;13:245-259.
doi: 10.2307/1907187
54. Braud I. *Methodologies D'analyse de Tendances sur de Longues Series Hydrometeorologiques*. Fiche Technique Othu N 2; 2011. Available from: https://hal.inrae.fr/hal-02595255v1/document [Last accessed on 2025 Mar 08].
55. Ringard J, Chiriaco M, Bastin S, Habets F. Recent trends in climate variability at the local scale using 40 years of observations: The case of the Paris region of France. *Atmos Chem Phys.* 2019;19(20):13129-13155.
doi: 10.5194/acp-19-13129-2019
56. Sagna P, Ndiaye O, Diop C, Niang AD, Sambou PC. Les variations recentes du climat constatees au Senegal sont-elles en phase avec les descriptions donnees par les scenarios du GIEC? *Pollut Atmos.* 2015;227:1-17.
doi: 10.4267/pollution-atmospherique.5320
57. Ringard J. *Etude Rétrospective et Prospective des Vagues de Chaleur en Afrique de l'Ouest. University Jos Four, Gre*. Available from: https://www.researchgate.net/profile/justine-ringard/publication/260018793_etude_retrospective_et_prospective_des_vagues_de_chaleur_en_afrique_de_l%27ouest/links/02e7e52f12bf345bcd000000/etude-retrospective-et-prospective-des-vagues-de-chaleur-en-afrique-de-louest.pdf [Last accessed on 2025 Mar 08].
58. Stone DA, Weaver AJ. Daily maximum and minimum temperature trends in a climate model. *Geoph Res Lett.* 2002;29(9):70-1-70-4.
doi: 10.1029/2001GL014556
59. Braganza K, Karoly DJ, Arblaster JM. Diurnal temperature range as an index of global climate change during the twentieth century. *Geophys Res Lett.* 2004;31(13):1-4.
doi: 10.1029/2004GL019998
60. Easterling DR, Meehl GA, Parmesan C, Changnon SA, Karl TR, Mearns LO. Climate extremes: Observations, modeling, and impacts. *Science.* 2000;289(5487):2068-2074.
doi: 10.1126/science.289.5487.2068
61. Hartmann DL, Tank AMK, Rusticucci M, *et al*. *Observations: Atmosphere and Surface.* Cambridge United Kingdom and NY, USA: Cambridge University Press; 2013. p. 195-254. Available from: https://www.ipcc.ch/site/assets/uploads/2017/09/wg1ar5_chapter02_final.pdf [Last accessed on 2025 Mar 08].
62. Trigo RM, García-Herrera R, Díaz J, Trigo IF, Valente MA. How exceptional was the early August 2003 heatwave in France? *Geophys Res Lett.* 2005;32(10):L10701.
doi: 10.1029/2005GL022410open_in_new
63. Rome S, Caniaux G, Ringard J, Dieppois B, Diedhiou A. Identification de Tendances Recentes et Ruptures D'homogeneite des Temperatures: Exemple en Afrique de l'Ouest et sur le Golfe de Guinee. In: *28ème Colloquim Internationale de l'AIC, Liège, Belgium*; 2015. p. 591-596.
64. Barbier J. *Extrêmes Climatiques: Les Vagues de Chaleur au Printemps Sahelien*. Universoty de Toul. Available from: https://theses.hal.science/tel-04225047v1/document [Last accessed on 2025 Mar 12].
65. Meehl GA, Tebaldi C. More intense, more frequent, and longer lasting heat waves in the 21st Century. *Science.* 2004;305(5686):994-997.
doi: 10.1126/science.1098704

Asian Journal of Water, Environment and Pollution. Vol. 22, No. 3 (2025), pp. 153-163.
doi: 10.36922/AJWEP025160118

ORIGINAL RESEARCH ARTICLE

Sources of environmental law: National legislation of Ukraine and international legal documents

Yuliia Leheza[1], Anatolii Kuzmenko[2], Oleksandr Pashchenko[3], Valeriya Tulyantseva[1], and Yevhen Leheza[4]*

[1]Department of Civil, Commercial, and Environmental Law, Institute of Humanities and Social Sciences, Dnipro University of Technology, Dnipro, Ukraine
[2]Pavlograd District Prosecutor's Office of the Dnipropetrovsk Region, Pavlograd, Ukraine
[3]Department of Civil Law Disciplines, Institute of Law and Security, Odesa State University of Internal Affairs, Odesa, Ukraine
[4]Department of Public and Private Law, Educational and Scientific Institute of Law and International Legal Relations, University of Customs and Finance, Dnipro, Ukraine
***Corresponding author:** Yevhen Leheza (legeza@umsf.dp.ua)

Received: April 15, 2025; Revised: May 15, 2025; Accepted: May 23, 2025; Published online: June 10, 2025

Abstract: In this article, we consider the Constitution of Ukraine, international agreements, and norms of international law as the foundations of environmental legislation. This study provides a detailed analysis of the provisions and principles enshrined in international legal acts and Ukrainian legislation related to the protection and conservation of nature. The Constitution of Ukraine establishes the state's environmental strategy, guarantees citizens the right to a safe environment, and mandates state actions to ensure environmental protection. International agreements, which Ukraine has signed and ratified, are equally significant, holding priority over national laws and forming a part of the domestic law. The international legal acts include declarations, principles, and other documents that do not have binding legal force but have significant impacts on the state's formation and development of environmental law. These acts serve as typical frameworks in environmental protection, granting flexibility in implementation. Therefore, the most effective way to implement such acts into the national legislation of Ukraine is through state adoption based on the text of international legal acts or their individual articles on domestic law. The main ways to solve the problems of implementing international legal acts in environmental protection in Ukraine are as follows: (i) operational addition or amendment of national environmental legislation, (ii) determination of specific mechanisms and ways of implementing international obligations undertaken by Ukraine in environmental protection, and (iii) creation of separate units within the structure of the Ministry of Ecology and Natural Resources of Ukraine, which concentrates their activities on relevant international legal acts and ensures cooperation in this direction.

Keywords: International treaties; International legal acts; Environmental law; Environmental protection; Law

1. Introduction

Due to the increase in anthropogenic impact on the environment, the issues of environmental safety and nature protection are becoming increasingly significant. An important role in resolving these issues is played by environmental legislation, which is based on the principles and norms enshrined in the Constitution of Ukraine.

The Constitution of Ukraine is the main legislative act regulating environmental relations. Based on the

principle of the rule of law, the Constitution has the highest legal force and is the basis of all legislation. All laws, including environmental laws, are adopted on the basis of the Constitution and in accordance with its provisions.

In the legal hierarchy, the law is the main source of environmental legislation. It is a regulatory act adopted by a higher representative body of state power or directly by the people (referendum). The law establishes the initial legal norms, holds the highest legal force, and is adopted in compliance with a special legislative procedure.[1]

As a source of law with the highest legal force, the Constitution of Ukraine contains a set of provisions that: (i) highlight the special constitutional function of environmental protection, (ii) establish the general legal principle for the priority of environmental protection, (iii) establish the responsibility of the present generations to future ones, (iv) provide for the country's environmental sovereignty, and (v) establish the state's obligations to protect the sovereignty in both internal and external relations. The basic law of the state establishes a constitutional environmental legal order.[2] The purpose of this study is to analyze the Constitution of Ukraine, international treaties, and international legal acts as key sources of environmental law that form the regulatory and legal basis for ensuring environmental safety, sustainable development, and environmental protection.

Human activities, even before the Industrial Revolution, have initiated changes in nature. It is now essential to strike a balance, ensuring that economic advancement does not come at the expense of environmental sustainability. Genuine progress requires the maintenance of robust environmental standards, as this is fundamental to sustainable development. This research offers a comprehensive examination of the current status and potential environmental impacts of infrastructure projects under the China–Pakistan Economic Corridor (CPEC). The expected consequences of this project are, for the most part, already well understood.

Since its inception back in 1982, the Marine Environmental Protection Law (MEPL) has undergone multiple amendments in 1999, 2013, 2016, and 2017, culminating in a comprehensive revision in 2023. These successive updates have gradually established a solid legal foundation. The Constitution underpins this system, the MEPL acts as the key regulatory framework, and specific marine element safeguard regulations propel its operations. Compared to earlier versions, the recently revised MEPL 2023 brings considerable enhancements. These primarily involve strengthening the conservation of marine biodiversity, refining the mechanisms for preventing and controlling pollution from ships, streamlining the surveillance of the marine environment, improving the measures to address land-originated marine pollution, and instating more stringent legal consequences. The revised MEPL 2023 enhances China's strategy for protecting its marine environment by incorporating global best practices within its existing legal framework. Furthermore, the study identifies areas for future improvement, offering insights for policymakers that would be useful and, ideally, should have already been integrated.

2. Materials and methods

The methodological basis of the study is a set of general scientific and special scientific methods of cognition, including formal-logical, historical, comparative-legal, interpretation, structural-functional, and modeling. Using the formal-logical method, the conceptual and terminological apparatus was analyzed and clarified, while the content of individual regulatory legal acts and the features of their implementation were studied. The historical method facilitated the study of the development dynamics of sources of environmental law, starting with the law on Nature Protection of the Ukrainian Soviet Socialist Republic (1960), as well as the main trends in the formation of regulatory legal acts in this area of social relations. The comparative-legal method was employed to compare diverse domestic regulatory legal acts that regulate interactions between society and nature alongside relevant foreign experience. The interpretation method was applied to analyze the content of regulatory legal acts and their correlation with related branches of law, in particular, administrative and civil law.[3]

The application of the structural-functional method enabled the systematization of the sources of environmental law according to various characteristics to determine the role of individual regulatory legal acts in the system of sources of environmental law. Using the modeling method, potential development scenarios for the system of relevant sources were determined. Among these, the most acceptable models were selected. The prospects for systematizing the sources of environmental law were assessed through codification, while the structure and content of individual draft environmental legal acts were also determined.

3. Results and discussion

The characteristics of the constitutional principles of environmental law are usually presented by grouping the norms of the Constitution of Ukraine, which directly or indirectly establish principles, initial provisions, and specific rules of conduct in the areas of environmental protection, nature management, and ensuring environmental safety. Leheza[4] divides constitutional norms into three groups:

(i) Humanitarian (which establishes environmental rights and obligations of citizens).
(ii) Natural resource (which determines forms of ownership of natural objects).
(iii) Competence (in which competence in the field of environmental protection is distributed).[5]

The Constitution establishes the foundations of the social order and the general principles of state policy, including those related to environmental protection. Key to the regulation of environmental relations are Articles 13, 14, 16, 50, and 66 of the Constitution of Ukraine, along with several other articles of a general nature that provide the fundamental regulation of social relations, including those of an environmental nature.[6]

Specifically, Article 13 declares that the land itself, everything beneath it, the air we breathe, the water, and all other natural riches found within Ukraine's borders, alongside the resources of its continental shelf and exclusive economic zone (in the sea), are considered the property of the Ukrainian people.[6]

Article 16, located in Chapter 1 of Ukraine's constitutional framework, outlines core principles regarding environmental protection. It stipulates the state's obligation to safeguard environmental well-being and ecological stability throughout the country. Moreover, the state bears the responsibility of addressing the aftermath of the Chernobyl disaster – an event recognized for its global impact – and for protecting the genetic heritage of the Ukrainian people. Given this provision, the degree to which these obligations are being fulfilled inevitably comes into question.[7]

The Constitutional Court of Ukraine, in its decision number, e.g., 7-rp/2001,[6] references Article 16 and underscores the significance of this constitutional provision. The Court emphasized that the Constitution explicitly mandates the state's accountability for its actions toward individuals, clearly articulating the state's duties. This accountability extends beyond mere political or ethical obligations of public authorities to the citizenry. It incorporates elements of legal responsibility, which encompass imposing measures with the force of public law on the state and its administrative bodies for either failing to carry out their defined roles or performing them inadequately.[7]

The core principles governing the interaction between individuals, the government, and the natural world are established within the nation's fundamental law. For instance, per Article 50, Section 1 of the Constitution, every individual possesses an entitlement to an environment that is safe for their well-being and health. This also encompasses the right to receive reparations when this right is infringed upon. Simultaneously, Article 66 outlines a duty for all citizens to refrain from actions that could harm the environment and to provide restitution for any such damage incurred. Furthermore, Section 2 of Article 50 guarantees every person's right to freely access and share information regarding the environmental situation alongside the composition of food products and consumer goods. Classifying this information as confidential is expressly prohibited.[8]

Article 92, which emphasizes the legal force of the state's fundamental laws, provides that the most important environmental relations, such as the principle governing the use of natural resources, the exclusive (maritime) economic zone, the continental shelf, the exploration of outer space, and relations of environmental safety, must be regulated exclusively by law. Thus, these constitutional norms serve as the foundation for the adoption of relevant environmental legislation on specific issues.[9]

International law holds a pivotal position within the framework designed to reconcile environmental protection with sustainable societal development. Moreover, international legal principles significantly shape the regulation of environmental interactions, with international agreements serving a critical function.

Reflecting current legal precepts, Article 9 of the Constitution of Ukraine stipulates that "effective international treaties, to which the Verkhovna Rada of Ukraine has given its consent to be bound, constitute an integral part of the national laws of Ukraine."[7]

According to Article 2, Section 1 of Ukraine's Law Concerning International Treaties of Ukraine, an international treaty of Ukraine is to be interpreted as a legally binding agreement. This accord is established in written form with a foreign nation or another entity recognized under international law. The agreement's provisions are governed by the precepts of international law. This definition holds true, irrespective of whether the treaty is documented within a single document or a collection of connected documents. Furthermore, the

particular nomenclature utilized to designate the treaty is inconsequential to its status.[11]

An important point is the need to clarify the relationship between the concepts of "international legal acts" and "international treaties." These terms are often used interchangeably by both theorists and researchers in specific areas of law, especially when analyzing Ukrainian legislation. That is why the legislator uses the term "international treaties" (for example, in the Law of Ukraine on International Treaties of Ukraine).

International legal acts as sources of environmental law are characterized by the stability of their norms, which ensures the stability of the international legal order. The peculiarity of the state-legal procedure for the registration of consent to be bound by an international treaty, in the form of ratification and signing, gives contractual norms additional authority in the domestic legal system and facilitates their interaction with national law.[12]

The application scope of environmental law differs from criminal, financial, administrative, and labor law in its transnational nature. The system of international treaties in the field of environmental protection consists of:

(i) Global treaties: These treaties are universal and open to participation by all states of the world (the Convention on Biological Diversity, the Convention on the Conservation of Wild Fauna and Flora, and Natural Habitats in Europe Bern Convention).
(ii) Regional treaties: These treaties are concluded between states of the same region and concern specific environmental problems characteristic of this region (Framework Convention on the Protection and Sustainable Development of the Carpathians, Convention on the Protection of the Black Sea against Pollution).
(iii) Bilateral treaties: These treaties are concluded between two states and regulate environmental issues concerning their common interests (Agreement on Cooperation between the Cabinet of Ministers of Ukraine and the Government of the Republic of Turkey in the Field of Forestry).[13]

Generally speaking, international treaties constitute a particular category within the sources of European law. They establish the international commitments of the European Communities, the European Union, and their respective member states. The European Community is exhibiting a growing presence in shaping international environmental law, actively participating in international conferences and negotiations, signing international legal instruments, and collaborating with diverse international bodies focused on environmental concerns.

European Union international treaties function as sources of norms for two distinct legal systems concurrently, international (public) law and Community/Union law. As a source of international rights and obligations, these treaties are binding not only on the community itself but also on each individual member state.[14]

An equally important role in the system of sources of environmental law of Ukraine is played by decisions of international courts and arbitrations. These decisions can be used as a source of law in resolving environmental disputes. This is relevant when national legislation does not contain clear norms for resolution, and decisions of international courts and arbitrations can create precedents, which are then used by courts and other authorities when solving similar problems.

International court and arbitration rulings can serve as tools to safeguard citizens' environmental rights. A compelling illustration of this is found in the *Dubetska and Others versus Ukraine* case (application No. 30499/03, decision of February 02, 2011). Here, residents of Vilshyna village (Lviv region) repeatedly lodged complaints with state officials regarding health and property damage stemming from environmental pollution attributable to the Chervonogradska enrichment factory.[15]

Acknowledging the factory's detrimental effects on the applicants' lives, the authorities repeatedly mandated the relocation of these individuals away from the contaminated area. Nevertheless, this relocation never took place. In the view of the European Court of Human Rights (ECtHR), a sufficiently robust link existed between the polluting emissions and the state, thus triggering the potential for state liability under Article 8 of the Human Rights Convention.[15]

The ECtHR acknowledges that member states enjoy considerable discretion when fulfilling their environmental responsibilities under Article 8 of the Convention. Thus, it would be overreaching to declare an absolute right for the complainants to receive new, state-funded housing. Nonetheless, the grievances presented by the applicants, invoking Article 8, could potentially have been adequately addressed by effectively resolving the environmental issues.[16]

Overall, it is evident that throughout the pertinent time frame, both the mine and the factory were operated in defiance of existing national environmental regulations. Moreover, the government failed to assist the applicants'

relocation or to institute a practical strategy to shield them from the environmental dangers linked to their prolonged residence in proximity to these industrial entities. These shortcomings constitute a breach of Article 8 of the Convention.[17] The ECtHR's case law extends its jurisdiction to the territory of Ukraine, irrespective of whether the decisions concerned Ukraine and its citizens directly or whether the decisions were made with respect to another state.

Returning to the Constitution of Ukraine as a source of environmental law, it contains the most important norms that regulate relations in the field of interaction between humans and the environment. The following norms should be considered constitutional principles of environmental law or as special regulations of higher legal force regarding individual environmental relations and their objects.[2]

As for the Convention for the Protection of Human Rights and Fundamental Freedoms, it does not directly provide environmental rights for citizens, but there is a direct connection between the right to respect one's private and family life, to one's home, provided in Article 8 of the Convention, and the right to an environment safe for life and health.[12]

International legal acts in the field of environmental protection serve as a framework, providing participants with the flexibility to choose the means of achieving their goals. Therefore, the most effective way to implement such acts into the national legislation of Ukraine is the method of transformation, which involves the adoption by the state based on the text of an international legal act or its individual articles of the corresponding norms of domestic law.

The main ways to solve the problems of implementing international legal acts in the field of environmental protection in Ukraine are as follows: (i) prompting the addition or amendment of national environmental legislation, (ii) identifying specific mechanisms and ways of implementing international obligations undertaken by Ukraine in the field of environmental protection, (iii) creating separate units within the structure of the Ministry of Ecology and Natural Resources of Ukraine, which would concentrate their activities on the implementation of the relevant international legal act and establish cooperation in this direction, and (iv) ensuring more active involvement of specialized public organizations of an environmental orientation and interested territorial communities in making environmentally significant decisions.[18]

Safeguards for the environmental rights of Ukrainian citizens are enshrined, specifically in Article 11, Part 3 of the Ukrainian Law on Environmental Protection. This particular provision stipulates that citizens whose environmental rights have been violated are entitled to restoration and that legal recourse for protection within a court of law is available, as per Ukrainian legal standards. Moreover, according to Article 55, Part 4 of the Ukrainian Constitution, every individual holds the assured right to pursue protection for their freedoms and rights through relevant international judicial bodies or through bodies of international organizations where Ukraine holds membership or participation, following the exhaustion of all national legal avenues.

Ukraine's ratification of the Convention for the Protection of Human Rights and Fundamental Freedoms means its provisions are now part of Ukrainian national legislation. The interpretation of this Convention by the ECtHR is extensive. When judging cases brought against Ukraine (or any other nation), the European Court bases its decisions on established legal precedents. Consequently, rulings from the ECtHR serve as essential guidance for governmental agencies and their officers, with a view to upholding human rights.[19]

Since the Convention for the Protection of Human Rights and Fundamental Freedoms does not directly enshrine the right to a safe environment for life and health, citizens, when applying to the ECtHR in the event of a violation of their environmental rights, refer to a breach of Article 8 of the Convention. *Volobuieva* correctly notes that in the practice of the ECtHR, most often, the violation of the right to a safe environment for life and health is associated with the breach of the right to respect for private and family life, which indicates a close connection between environmental pollution and the said right.[20]

One of the available evidence in favor of the consideration and protection by the Court of Environmental Human Rights and the environment, in general, is that the ECtHR, in its decisions, calls the environment a value that prevails over the interests of one person (or family), even if this concerns his private life and property. In the case of *Nateg versus Belgium* (application no. 21861/03), the applicant owned a house built by her parents in a forest area without obtaining a building permit. She was sued for building the house in violation of forest legislation. The Court decided that the applicant must restore the site to its previous condition. The house was forcibly demolished.[21]

For the 1st time in its case law (the decision was made in 2007), the Court stated that the environment, although not expressly mentioned in the Convention, nevertheless represents a value in the preservation of

which both society and the public authorities have an interest. Economic considerations and even property rights should not prevail over environmental concerns, especially when there is effective legislation on this issue. The public authorities had a duty to take measures to protect the environment.[22]

According to Article 8 of the Convention for the Protection of Human Rights and Fundamental Freedoms, "everyone has the right to respect for his private and family life, his home and his correspondence."[10, p. 11] For example, in the case of *Mogepo Oosheh versus Spain* (application no. 4143/02), the applicant complained about the constant noise from nightclubs located near her house.[23] She claimed that this noise caused her chronic sleep disturbance. The Court considered that the applicant's right to respect her private home had been seriously violated by the authorities' inaction regarding the noise at night. Given the intensity of the noise pollution (exceeding the permissible noise level at night) and the fact that such a situation had lasted for several years, the Court found that there had been a violation of Article 8 of the Convention for the Protection of Human Rights and Fundamental Freedoms. The restriction of the right to respect for one's private and family life is set out in Part 2 of Article 8 of the Convention, which states that "there may be no interference by a public authority with the exercise of this right except such as is in accordance with the law and is necessary for a democratic society in the interests of national security, public safety or the economic well-being of the country, for the prevention of disorder or crime, for the protection of health or morals, or for the protection of the rights and freedoms of others."[24, p. 208]

For example, the above-mentioned protection of the economic well-being of the country is reflected in the case of *Powell and Rayner versus the United Kingdom* (application no. 9310/81), where the applicants, who lived in the immediate vicinity of Heathrow Airport, considered the permitted noise level to be unacceptable and the measures taken by the government to reduce the noise level to be insufficient.[25] The ECtHR has established that the operation of sizeable, globally-used airports positioned close to heavily inhabited areas is, in essence, vital for a nation's economic prosperity. Heathrow Airport, known as one of the globe's most active airports, is a crucial asset for commercial activities, diplomatic relationships, and, notably, the economy of the United Kingdom. Therefore, its continued functioning is permissible, even if environmental drawbacks remain irreducible. Consequently, it does not constitute a breach of Article 8 of the European Convention on Human Rights.

A similar case is that of *Iaiop versus the United Kingdom* (application no. 36022/97), where the applicants who lived near Heathrow Airport complained of increased noise in the area around their homes after the government's policy on night flights changed in 1993. They claimed that aircraft operating at night regularly woke them up with their noise and that this had a negative impact on their health. The Court was unable to reach a clear conclusion that the introduction of the new scheme in 1993 had indeed led to an increase in night noise. At the same time, the Court found that there was an economic interest in maintaining night flights and that only a small percentage of people were affected by the noise. At the same time, house prices did not fall, and the applicants were able to move to another place of residence without financial loss. Therefore, there was no violation of Article 8 of the European Convention on Human Rights.[26]

Having familiarize ourselves with the various circumstances of the cases and the factors that the ECtHR took into account in the process of justice regarding claims that had an environmental basis, we can conclude that all these cases concerned violations of Article 8 of the Convention for the Protection of Human Rights and Fundamental Freedoms.[27]

Protection of the environment, viewed in its broadest definition, finds its roots in Article 8 of the Convention for the Protection of Human Rights and Fundamental Freedoms. This connection stems from the right to respect private life and to housing. Indeed, significant environmental degradation can detrimentally impact an individual's well-being. It may also hinder the complete enjoyment of their home, thereby harming their private and family life, even where the environment poses no substantial threat to their physical health.[28]

There are very few cases in the ECtHR that are directly related to the violation of the environmental rights of citizens of Ukraine. In all cases, the applicants relied on a violation of Article 8 of the Convention for the Protection of Human Rights and Fundamental Freedoms. In the case of *Dubetska and Others versus Ukraine* of May 10, 2011, it was stated that the applicants' houses were located in the settlement of Vilshyna, village of Silets, Sokalsky district, Lviv region, not far from two industrial enterprises – the Vizeyska mine of the State Enterprise Lviv Coal and the Chervonohradska Central Coal Processing Plant of the Lviv Coal Company.[29] Following extensive

investigations undertaken by both governmental and non-governmental bodies, it was determined that these businesses' manufacturing operations were inflicting detrimental environmental damage, encompassing occurrences such as flooding and contamination of both groundwater and the atmosphere, alongside land subsidence. The ECtHR found a violation of Article 8 of the Convention, pinpointing the state's failure to enact measures – for over a dozen years – either to relocate the individuals involved or to adequately address their predicament through alternative means. After carefully evaluating the particulars of the case, the ECtHR stated, "a credible claim predicated on Article 8 can arise where an environmental peril escalates to a severity that substantially infringes on the applicant's capacity to partake in their home, private, or familial life."[30, p210]

A comparable methodology for safeguarding the environmental rights of Ukrainian residents is mirrored in the *Grymkovska versus Ukraine* case. The applicant, along with her parents and her young son, resided in their residence on Ch. Street, located within a residential district of the city of Krasnodon. In 1998, it was decided to route the M04 Kyiv–Luhansk–Izvaryne highway through Ch. Street. In May 2002, an air quality assessment performed by the State Sanitary and Epidemiological Service of the Luhansk Oblast revealed a significant exceedance in the acceptable concentration levels of substances detrimental to human health, stemming from air pollution generated by road emissions along Ch. Street. After scrutinizing the pollution measurements, the Chief Sanitary Doctor of Luhansk Oblast in 2002 advised the mayor of Krasnodon to contemplate discontinuing the utilization of Ch. Street as a thoroughfare, emphasizing that the degree of air pollution on this street exceeded legally established benchmarks and had the potential to jeopardize the health of the residents.[31]

International law mandates that nations in a region collaborate, adhering to "common but differentiated responsibilities," especially when dealing with transboundary environmental issues. The evolving infrastructural partnership between China and Pakistan under the CPEC warrants specific agreements to safeguard and enforce environmental standards within this framework. At present, no dedicated environmental treaty exists between the two nations, nor are environmental safeguards explicitly detailed and made public in their legal documents.

Moreover, a critical assessment of investments in CPEC-related projects is crucial for ensuring environmental sustainability. Pakistan's increasing reliance on coal reserves, funded by China through CPEC-related ventures like coal-fired power plants, raises concerns. The 2015 Paris Agreement discourages the use of coal for power generation, a pact to which both China and Pakistan are signatories. Pakistan possesses considerable potential for renewable energy generation, such as solar, wind, and hydro. Solar energy alone could potentially provide Pakistan with 1,600 GW, far exceeding its current consumption. However, CPEC initiatives continue to prioritize coal-based energy projects. Remedial actions are therefore recommended to secure sustainable development. This could include collaborative efforts such as shared expertise from environmental lawyers and the initiation of joint research and development initiatives.[32]

Further progress demands the establishment of a joint environmental data-sharing system between the governmental departments of both countries. This would facilitate efficient cross-border legal harmonization and enforcement, ultimately establishing a cohesive inter-regional environmental enforcement framework. To achieve this, both parties should enhance environmental monitoring and intelligence to improve pollution awareness and law enforcement across various levels, including local, provincial, national, and regional jurisdictions. Public interest litigation and wider public involvement in environmental issues must be strengthened. In addition, better alignment between domestic and international environmental laws, treaties, and agreements is necessary to achieve the goals set by the Paris Agreement on climate change, the Sustainable Development Goals, the Aichi Biodiversity Targets, the Sendai Framework for Disaster Risk Reduction, and other global commitments to sustainable development. Such coordinated actions would not only address the specific environmental challenges of the two countries but would also serve as a model for environmental legal cooperation, benefiting the whole region and the wider global community.

Transboundary environmental issues should ideally be resolved through legal cooperation between the two nations rather than through recourse to domestic, foreign, or international courts in every instance. This will benefit the stakeholders in various ways, including financial advantages, time savings, and reduction in energy consumption. It would also better serve justice, particularly for the private party (the claimant) in cases of transboundary harm, who frequently has limited

resources and limited access to legal forums beyond national borders, e.g., in foreign or international courts.

The CPEC involves numerous large-scale development projects. These endeavors must be managed through updated and mutually agreed-upon environmental enforcement mechanisms. Valuable insights can be acquired from existing environmental practices around the world, including studies of developed nations. Therefore, China and Pakistan should integrate appropriate environmental provisions within their trade agreements, explicitly addressing the potential environmental damage that might arise under the CPEC, a central component of China's Belt and Road Initiative. This study underlines potential legal complications relating to environmental law enforcement across borders, highlighting the immediate need for deeper environmental cooperation between both countries.

China and Pakistan's new infrastructure development partnership under CPEC requires arrangements to ensure high environmental standards. However, no specific independent environmental treaty or explicit environmental provisions are currently in place between them.

China has become a significant player in the Arctic Ocean governance, adhering to the agreement to prevent unregulated commercial fishing. However, a shared legal framework is still needed. This absence of a comprehensive legal regime offers China influence on environmental governance and potential access to Arctic fisheries in the future. China has invested considerably in infrastructure, economic security research, and shipbuilding technology, such as ice-resistant liquefied natural gas carriers, reflecting a peaceful approach to resource management, conservation, and ocean governance. If managed well, with long-term cooperation, China's future fishing rights in the Arctic can be legitimized. China, being the closest continental state to the Arctic Circle, holds a prominent stake and is making substantial contributions toward the sustainable development of the Arctic through investment in various sectors, scientific research, environmental security efforts, and sustainable use of fisheries. In summary, China's Arctic policy is carefully designed. By asserting legal claims over fisheries resources and acquiring global recognition for its presence in Arctic governance, it has strengthened its Polar Silk Road vision and the Belt and Road Initiative for future endeavors.[32]

International collaboration is crucial for developing an open economic system, leading to economic expansion and sustainable development for all countries. Consequently, environmental policy should not become a means to unnecessarily hinder global trade. An important principle is recognized as the rule that whoever pollutes the environment should also bear financial responsibility for this pollution. States are obliged to inform each other about possible elements or activities that may have harmful transboundary consequences.

Sustainable development requires a global scientific understanding of problems, and therefore, states need to share knowledge and new technologies to achieve sustainable development. In order to achieve sustainable development, the full participation of women is necessary, as well as the creative efforts, ideas, and courage of young people in understanding indigenous peoples. The state must recognize and support the independence, culture, and interests of indigenous peoples.[33]

The Rio Declaration on Environment and Development unequivocally stated the devastating impact of war on sustainable development and recorded the obligation of states to respect international law that ensures environmental protection during armed conflicts, and to cooperate in further sustainable development, since development, peace, and environmental protection are interdependent and inseparable.

4. Conclusion

In Ukraine, the foundational principles and advancement of environmental law are significantly shaped by the nation's Constitution, as well as by international agreements and legal instruments. The Constitution of Ukraine proclaims the human right to a safe environment and obliges the state to take measures to protect it. This is the fundamental principle on which all environmental legislation in Ukraine is based. International treaties to which Ukraine has acceded constitute an important source of environmental law. They contain norms regulating a wide range of environmental issues, such as climate change, environmental pollution, transboundary environmental problems, conservation of biological diversity, etc. International legal acts adopted by international organizations can also be sources of environmental law in Ukraine. All these sources of law are closely interrelated and complement each other.

Ukraine's foundational law, the Constitution, lays out the groundwork for environmental safeguarding.

Building upon this, international agreements elaborate on these core tenets, formulating more specific rules. Furthermore, international legal instruments play a role in aligning Ukrainian laws with internationally recognized benchmarks. A crucial point is that international treaties and international legal instruments only take effect within Ukraine once they have been formally approved by the Verkhovna Rada (the Ukrainian Parliament). Consequently, the Constitution, international treaties, and international legal acts hold a critical position in preserving the environment within Ukraine, thereby supporting the nation's pursuit of sustainable advancement.

Systematization involves eliminating the duplication of regulations on relevant issues and bringing them to the needs of practical application. That is consolidation with elements of the codification process to ensure the consistency and harmonization of regulatory legal regulations of the newly created consolidation act or its group. It is also advisable to repeal minor laws regarding amendments to Ukraine's current environmental legislation.

Therefore, we consider consolidation to be a possible intermediate option for the preparation of the Environmental Code of Ukraine. Today, the consolidation of environmental legislation acts is extremely advisable, especially with the aim of integrating natural resource legislation and legislation in the field of environmental safety.

For example, consolidation as a form of systematization of environmental legislation would be justified today when creating the Natural Resource Code of Ukraine based on resource codes and relevant laws (the Land, Water, and Forest Codes, the Subsoil Code, the Law of Ukraine on Flora, the Law of Ukraine on Resorts, etc.). However, the aforementioned legislative acts would form the basis of a special part of the Natural Resources Code. The general part requires appropriate analytical processing to substantiate the provisions of this part based on partial codification efforts. This includes identifying general and special provisions arising from the content of the relevant legal regulation on the use of natural resources and the features of their legal regime regarding use, reproduction (restoration), and protection.

Acknowledgments

None.

Funding

None.

Conflict of interest

The authors declare that they have no conflicts of interest.

Author contributions

Conceptualization: Yuliia Leheza, Yevhen Leheza
Formal analysis: Anatolii Kuzmenko
Investigation: Oleksandr Pashchenko
Methodology: Valeriya Tulyantseva
Writing – original draft: Yuliia Leheza
Writing – review & editing: Yevhen Leheza

Availability of data

Not applicable.

References

1. Getman AP, Shulga MV, Popov VK, editors. *Environmental Law of Ukraine: A Textbook for Students of Law*. New Delhi: Higher Educational Institutions; 2005.
2. Ilkiv NV. *Environmental Law of Ukraine*. Lviv: Lecture Course; 2013.
3. Khan MI, Chang YC. Love for the climate in Sino-Pakistan economic romance: A perspective of environmental laws. *Clean Techn Environ Policy*. 2021;23:387-399. doi: 10.1007/s10098-020-01938-4
4. Leheza Y, Pisotska K, Dubenko O, Dakhno O, Sotskyi A. The essence of the principles of ukrainian law in modern jurisprudence. *Rev Jurídica Port.* 2022;32:342-363. doi: 10.34625/issn.2183-2705(32)2022.ic-15
5. *Environmental Law of Ukraine: Textbook. N.R. Kobetska*. 2nd ed. Revised and Supplemented. K.: Yurinkom Inter. Ukraine: Kyiv. Publishing House; 2008. p. 352.
6. *Decision of the Constitutional Court of Ukraine in the Case on the Constitutional Appeal of the Open Joint-Stock Company "All-Ukrainian Joint-Stock Bank" Regarding the Official Interpretation of the Provisions of Clause 22 Part 1 of Art. 92 of the Constitution of Ukraine, Part 1, Part 3 of Article 2, Part 1 of Article 3, Part 8 of the Code of Ukraine on Administrative Offenses (Case on Liability of Legal Entities*) No. 7-rp; 2001. Available from: https://zakon.rada.gov.ua/laws/show/v007p710-01#Text [Last accessed on 2001 May 30].
7. *Constitution of Ukraine: Law of Ukraine No. 254к/96-BP*.

Available from: https://zakon.rada.gov.ua/laws/show/254к/96-вр#text [Last accessed on 1996 Jun 28].
8. Available from: *On International Treaties of Ukraine: Law of Ukraine No. 1906*. Available from: https://zakon.rada.gov.ua/laws/show/1906-15#text [Last accessed on 2004 Jun 29].
9. *List of International Treaties in the Field of Environmental Protection to Which Ukraine is a Party, and the Status of their Implementation*; 2024. Available from: https://data.gov.ua/dataset/14e88505-7761-4565-ab3b-d60ecead0b34 [Last accessed on 2024 May 25].
10. Mykievich MM, Andrusevich NI, Budyakova TO. *European Environmental Law: Textbook*. Lviv: Cambridge University Press; 2004. p. 258.
11. *European Convention on Human Rights of 17.07.97 No. 475/97-VR*. Available from: https://zakon.rada.gov.ua/laws/show/995_004#text [Last accessed on 2024 Jul 17].
12. *European Court of Human Rights. Case "Grymkovska v. Ukraine" (Application No. 38182/03)*. Available from: https://zakon.rada.gov.ua/laws/show/995_004#text [Last accessed on 2011 Jul 21].
13. *European Convention On Human Rights. Law of Ukraine Dated No. 475/97-BP*. Available from: https://zakon.rada.gov.ua/laws/show/995_004#text [Last accessed on 2024 Sep 11].
14. *On Environmental Protection. Law of Ukraine Dated 25.06.1991 No. 1264*. Available from: https://zakon.rada.gov.ua/laws/show/1264-12#text [Last accessed on 2024 Jun 25].
15. *Dubetska and Others Versus Ukraine Case (Application No. 30499/03*; 2011. Available from: https://hudoc.echr.coe.int/fre#{%22itemid%22:[%22001-103273%22]} [Last accessed on 2011 Oct 18].
16. Leheza Y, Shablystyi V, Aristova IV, Kravchenko IO, Korniakova T. Foreign experience in legal regulation of combating crime in the sphere of trafficking of narcotic drugs, psychotropic substances, their analogues and precursors: Administrative and criminal aspect. *J Drug Alcohol Res*. 2023;12(4):1-8. doi: 10.4303/JDAR/236240
17. Leheza Y, Shcherbyna B, Leheza Y, Pushkina O, Marchenko O. Features of applying the right to suspension or complete/partial refusal to fulfill a duty in case of non-fulfilment of the counter duty by the other party according to the civil legislation of Ukraine. *Rev Jurídica Port.* 2023:340-359.
18. Hryhorash O Korneyev M, Leheza Y, Zolotukhina L, Hryhorash T. The development of small business as a source of formation of local budget revenues in Ukraine. *Invest Manag Financ Innov*. 2018;15(1):132-140. doi: 10.21511/imfi.15(1).2018.12
19. Artyukhov A, Volk I, Surowiec A, *et al*. Quality of Education and science in the context of sustainable development goals-from millennium goals to agenda 2030: Factors of innovation activity and socio-economic impact. *Sustainability*. 2022;14(18):11468. doi: 10.3390/su141811468
20. Volobuieva O, Leheza Y, Pervii V, Plokhuta Y, Pichko R. Criminal and administrative legal characteristics of offenses in the field of countering drug trafficking: Insights from Ukraine. *Yustisia*. 2023;12(3):262-277. doi: 10.20961/yustisia.v12i3.79443
21. Rezvorovych K, Gorinov P, Sokol M, Kutsyk K, Opatskyi R. Peculiarities of the legislative regulation of the protection of rights of workers on the background of Russian military aggression (the Ukrainian experience). *Rev Econ Finance*. 2023;21(1):584-591. doi: 10.55365/1923.x2023.21.60
22. Sotska A, Tryhub S, Voloshanivska T, Kolomiiets V, Rezvorovych K. Legal regulation of the protection of children's rights by European standards: A comparative perspective. *Syari J Hukum Pemikiran*. 2024;24(2):359-375. doi: 10.18592/sjhp.v24i2.13973
23. Dudyk I, Rezvorovych K, Melnyk V, Gayevaya O, Tumalavičiusv V. Strategies for Ukraine's *legal integrat*ion into the EU: Learning from the *experience of central* and Eastern Europe. Evr Polit Právní Dis*. 2024;*11*(6):*13-21. doi*:* 10.46340/eppd.2024.11.6.2
24. Nalyvaiko L, Pryputen D, Verba I, Lebedieva Y, Chepik-Trehubenko O. The European convention on human rights and the practice of the ecthr in the field of gestational surrogacy. *Access Justice East Eur*. 2023;6(2):206-219. doi: 10.33327/AJEE-18-6.2-n000203
25. Yunin O, Dal A, Polovnikov V, Shumska N, Koteliukh M. The administrative-legal and criminal aspect of prosecuting persons for offenses in the field of illegal drug trafficking. *J Drug Alcohol Res.* 2024;13(9):236407. doi: 10.4303/JDAR/236407
26. Shevchenko S, Yunin O, Bobrishova L, Katorkin R, Tsyhulskyi S. Sources of criminal law on domestic violence prevention. *Pak J Criminol*. 2024;16(2):157-168.
27. Voloshanivska T, Pozihun I, Losych S, Merdova O, Leheza Y. Administrative and criminal law aspects of preventing offenses committed by minors in the sphere of illegal circulation of narcotic drugs, Psychotropic substances and precursors. J Drug Alcohol Res. 2023;12(10):236269. doi: 10.4303/JDAR/236269
28. Volkova Y, Bon B, Borysenko A, Leheza Y, Leheza Y. Crypto market experience: Navigating regulatory challenges in modern conditions. *Al-Risalah Forum Kajian Hukum Sos Kemasyarak.* 2024;24(2):178-194. doi: 10.30631/alrisalah.v24i2.1625
29. Oleksandr K, Petro D, Krylov D, Mariana B, Yevhen L.

Standards and safeguards stemming from the right to respect for private life and the right to a fair trial: Applicability with respect to administrative-law matters of civil service. *Rev Eletrôn Direito Soc.* 2024;12(3):1-12. doi: 10.18316/redes.v12i3.11977

30. Shkuta O, Leheza Y, Telelym I, Anosienkov A, Yaroshak O. National security in the conditions of the Russia-Ukraine war: Legal regulation and islamic law perspectives. *Al-Ahkam*. 2024;34(1):99-120. doi: 10.21580/ahkam.2024.34.1.20413
31. Leheza Y, Sinkevych O, Kravtsova Z, Kudriavtseva O, Cherniak I. The human right to an environment safe for life and health: Legal regulation, contemporary challenges and comparative perspectives. *Syari J Hukum Pemik*. 2023;23(2):138-150. doi: 10.18592/sjhp.v23i2.12257
32. Khan MI, Xu Q. An assessment of environmental policy implications under the China-Pakistan economic corridor: A perspective of environmental laws and sustainable development. *Sustainability*. 2021;13(20):11223. doi: 10.3390/su132011223
33. Chang YC, Khan MI. May China Fish in the Arctic Ocean? *Sustainability*. 2021;13(21):11875. doi: 10.3390/su132111875

Asian Journal of Water, Environment and Pollution. Vol. 22, No. 3 (2025), pp. 164-184.
doi: 10.36922/AJWEP025120085

ORIGINAL RESEARCH ARTICLE

Sustainable wastewater management and risk assessment in Maghnia

Chachoua Mounira*

Department of Hydraulics, Institute of Science and Technology, University Center of Maghnia, Maghnia, Algeria
***Corresponding author:** Chachoua Mounira (mounira_hydraulique@yahoo.fr)

Received: March 23, 2025; 1st revised: March 28, 2025; 2nd revised: April 17, 2025; 3rd revised: May 9, 2025; 4th revised: May 14, 2025; Accepted: May 15, 2025; Published online: June 17, 2025

Abstract: Located 40 km west of the wilaya of Tlemcen, the Algerian municipality of Maghnia is currently experiencing a severe water shortage that has affected all economic sectors, particularly agriculture. Given that Maghnia is a predominantly agricultural region with 250 hectares of irrigated land, maintaining agricultural productivity under such conditions poses significant challenges. One of the most viable and cost-effective strategies to address this issue is the reuse of non-conventional water sources, specifically the recycling of wastewater treated at the Lagfafe wastewater treatment plant (WWTP). Situated 5 km northwest of the town, the Maghnia WWTP operates using an intensive activated sludge process. This study aims to assess whether the quality of the treated effluent complies with Algerian standards for agricultural reuse. Throughout 2020, wastewater samples were collected and analyzed four times per month at both the inlet and outlet of the treatment plant. The physicochemical parameters examined included temperature, chemical oxygen demand, ortho-phosphates, electrical conductivity, nitrites, nitrates, ammoniacal nitrogen, water potential, dissolved oxygen, suspended solids, and biological oxygen demand. The analytical results indicate that the treated wastewater meets national regulatory standards for agricultural reuse across all evaluated parameters. Consequently, this substantial volume of treated water can be safely used for irrigation, offering a sustainable solution to mitigate the ongoing water crisis affecting the region's agricultural sector.

Keywords: Water scarcity; Non-conventional water reuse; Sustainable agriculture; Wastewater treatment; Environmental safety; Maghnia; Algeria

1. Introduction

Water is essential for all aspects of human life.[1] The global water crisis, which continues to worsen, is driven by several interrelated factors: rapid population growth,[2] excessive water consumption, degradation of surface and groundwater quality, the impacts of climate change,[3] and decreasing precipitation levels.[4] As a result, this vital resource is becoming increasingly scarce and difficult to manage. While water scarcity is a global concern, African countries are particularly vulnerable to its effects.

This alarming situation is illustrated by unprecedented droughts affecting rivers and the accelerated melting of glaciers, which compromise water availability for populations, agriculture, and ecosystems.[5] Over the past century, global freshwater use has increased sixfold, with a 1% annual growth rate since the 1980s.[6] According to the World Health Organization (WHO) (2023), over two billion people experienced water stress in 2021 – a

situation worsened by climate change and demographic dynamics. In 2022, 1.7 billion people consumed water contaminated with fecal matter, posing serious risks to public health. Microbial contamination contributes to approximately 505,000 deaths from diarrheal diseases annually, highlighting the critical need for safe drinking water and hygiene.[7]

The increasing demand for water also degrades its quality, as pollution from industrial, agricultural, and urban sources threatens both human health and sustainable development. Globally, 80% of industrial and municipal wastewater is discharged untreated, particularly in developing countries lacking adequate sanitation infrastructure.[8] Pollution from various sectors endangers drinking water sources, disrupts aquatic ecosystems, and threatens biodiversity.[9] Diffuse pollution further contributes to eutrophication, increased water treatment costs, public health hazards, and reduced recreational value of water bodies.[10]

To address global water shortages, several non-conventional water management strategies are being explored. Seawater desalination is a technologically advanced but capital-intensive and logistically complex approach.[11] Advanced wastewater treatment ensures ecological safety before environmental discharge.[12] Strategic reuse of treated wastewater is a cost-effective, simpler, and faster option that enhances water sustainability and local resilience.[13]

Maghnia, a region in northwestern Algeria, is particularly affected by water scarcity. It has an irrigated agricultural area of 250 hectares. The reuse of treated wastewater from the Lagfafe wastewater treatment plant (WWTP) presents a promising solution to mitigate agricultural water shortages in the area. The city depends on the Hammam Boughrara dam, which has experienced significant reductions in storage volume due to prolonged drought, severely impacting irrigation. Meanwhile, the treated effluent from the Lagfafe WWTP is discharged into the environment without being reused.

This study aims to assess the quality of treated wastewater from the Lagfafe WWTP and determine its compliance with Algerian standards for agricultural reuse. By analyzing key physicochemical and microbiological parameters, the study evaluates whether the treated effluent is suitable for safe irrigation. Given the growing water scarcity in Maghnia, this approach offers a sustainable alternative to conventional water sources. The findings aim to support integrated and locally adapted water resource management strategies.

Wastewater reuse involves collecting municipal effluent, treating it at a WWTP, storing it, and distributing it for specific uses.[14] Agricultural reuse of treated wastewater is a widely adopted practice with decades of application across various countries, such as the United States, Mexico, Chile, Peru, Tunisia, Saudi Arabia, Australia, South Africa, China, Italy, and Spain. The volume of reused wastewater is growing annually by more than 30% in Europe and over 40% in the United States and China.[15] Globally, approximately 20% of treated wastewater is currently reused.[16]

The objectives of wastewater reuse include economic efficiency, technical feasibility, and resource conservation. These goals involve the preservation of natural resources by reducing withdrawals from conventional water sources and limiting wastewater discharge;[17] reducing the need for fertilizers due to the nutrient-rich content of treated water, particularly nitrogen and phosphorus; strengthening national capacities in integrated water management; and meeting irrigation demands through reliable water availability.[18]

Depending on the intended use, wastewater reuse can be classified into two main categories. Potable reuse includes both direct reuse (after advanced treatment) and indirect reuse (after environmental buffering, such as aquifer recharge).[19] Non-potable reuse is primarily applied in industrial and agricultural contexts. In industrial settings, recycled water can meet up to 85% of demand, particularly in power generation and paper production, with regulatory frameworks guiding the quality requirements based on the application.[20] In agriculture, which accounts for over 70% of global freshwater consumption, wastewater reuse presents the greatest reuse potential in the short to medium term.[21,22]

To ensure public health and environmental safety, wastewater reuse must be regulated. In response to growing concerns, the WHO, the Food and Agriculture Organization, and various countries have developed guidelines for safe reuse practices.[23] The strategic implementation of wastewater reuse offers multiple benefits.[24] It supports the preservation of high-quality water sources and provides economic advantages for farmers, including lower irrigation costs and reduced fertilizer use due to the nutrient content of treated wastewater. It also ensures year-round water availability, facilitating crop diversification and improved yields. Moreover, it stimulates the agri-food sector, contributing to job creation and improved livelihoods. The development of the agricultural sector, in turn, stimulates growth in the commercial and agro-industrial

sectors, consequently improving the living standards of citizens and creating new employment opportunities.

However, the lack of strict quality control and proper monitoring can result in adverse consequences, including the spread of waterborne diseases and ecosystem degradation. Therefore, strict adherence to reuse standards is essential.[25]

Advanced wastewater treatment plays a crucial role in protecting public health from pathogenic microorganisms, safeguarding aquatic biodiversity, preserving surface and groundwater resources, and creating a reliable, economically viable water source that contributes to community resilience.

As global water quality and availability deteriorate, countries must diversify their water sources. A review of wastewater reuse practices in Morocco, Algeria, and France highlights promising outcomes. In France, the Limagne Noire project irrigates 700 hectares using treated water from the Clermont-Ferrand WWTP. The initiative demonstrates technical reliability, sound institutional coordination, and economic viability – maintaining 60 agricultural jobs and generating €1.66/m³ in added value.[26,27] In Algeria, the Boumerdès region produces over 400,000 m³ of treated wastewater annually, with a small portion reused for agriculture. Since 2002, two farmers in Corso have irrigated 71 hectares with treated wastewater, yielding crops of comparable quality to those irrigated with potable water. The initiative is positively assessed by both agricultural and public health authorities.[28,29] In Morocco, a study in Drrarga evaluated the use of treated wastewater for tomato irrigation. While yields doubled and fertilizer use decreased, soil nutrient depletion and potential nitrate contamination of groundwater were noted, emphasizing the need for complementary fertilization and monitoring.[18]

According to the National Economic and Social Council (NESC, 2000), Algeria faces structural water scarcity, with per capita resources below 1,000 m^3/year.[30,31] The most common form of reuse is agricultural irrigation,[32] with treated wastewater reuse increasing from 17×10^6 m^3 in 2011 to 200×10^6 m^3 in 2014.[33] However, resource limitations and rising demand continue to intensify water stress. In response, Algeria has promoted wastewater recycling, rural hydraulic projects, and improved irrigation efficiency. Desalination is being adopted in urban centers such as Algiers, Oran, and Arzew, though its cost remains high.[34] Algeria's total renewable water potential is estimated at 18×10^9 m^3/year. Irrigation accounts for 62% of consumption, followed by domestic (35%) and industrial (3%) uses.[35]

In 2016, Algeria reused 14.6×10^6 m^3 of treated wastewater to irrigate over 11,000 hectares, particularly in regions such as El Oued, Ouargla, Guelma, and Tlemcen. By 2019, this volume had reached 1.32×10^6 m^3 for 11,045 hectares.[36,37] Successful agricultural reuse depends on rigorous treatment and compliance with national standards. Algeria has introduced legislation to ensure public health protection and groundwater safety.[38]

Despite the growing literature on wastewater reuse, most studies are descriptive, small-scale, or urban-centric. There is a lack of robust data on the operational performance of full-scale WWTPs in semi-arid inland regions where water scarcity is most acute. Existing studies often suffer from inconsistent sampling and lack of seasonal analysis, as well as limited data on emerging contaminants (e.g., pharmaceuticals, microplastics), which pose unregulated health risks.

This study adopts a rigorous and original approach. Methodologically, it implements a 1-year sampling campaign with four samples per month. Statistically, it uses paired-sample *t*-tests and 95% confidence intervals (CIs) to assess significant changes between influent and effluent. Technically, it evaluates a full-scale activated sludge WWTP under real semi-arid conditions. Politically, it highlights regulatory gaps and contributes evidence-based recommendations for water reuse policy. By integrating these dimensions, the study provides a transferable contribution to sustainable water management in Global South contexts facing climate stress and structural constraints.

2. Methods

2.1. Geographical location and population of Maghnia

Maghnia is situated approximately 40 km west of the Tlemcen Province in northwestern Algeria. It is bordered to the east by Remchi,[39] to the north by Fellaoucene, to the west by the Moroccan border, and to the south by Béni Bousaid. The municipality covers a total area of 294 km². The geographical location of the Maghnia district is illustrated in Figure 1. The population of Maghnia grew from approximately 87,400 in 2008 to 150,000 in 2021.

2.2. Climate conditions in Maghnia

Climatic data presented in this section were obtained from the climatological station in Maghnia. The analysis focuses on temperature, precipitation, and seasonal variations.

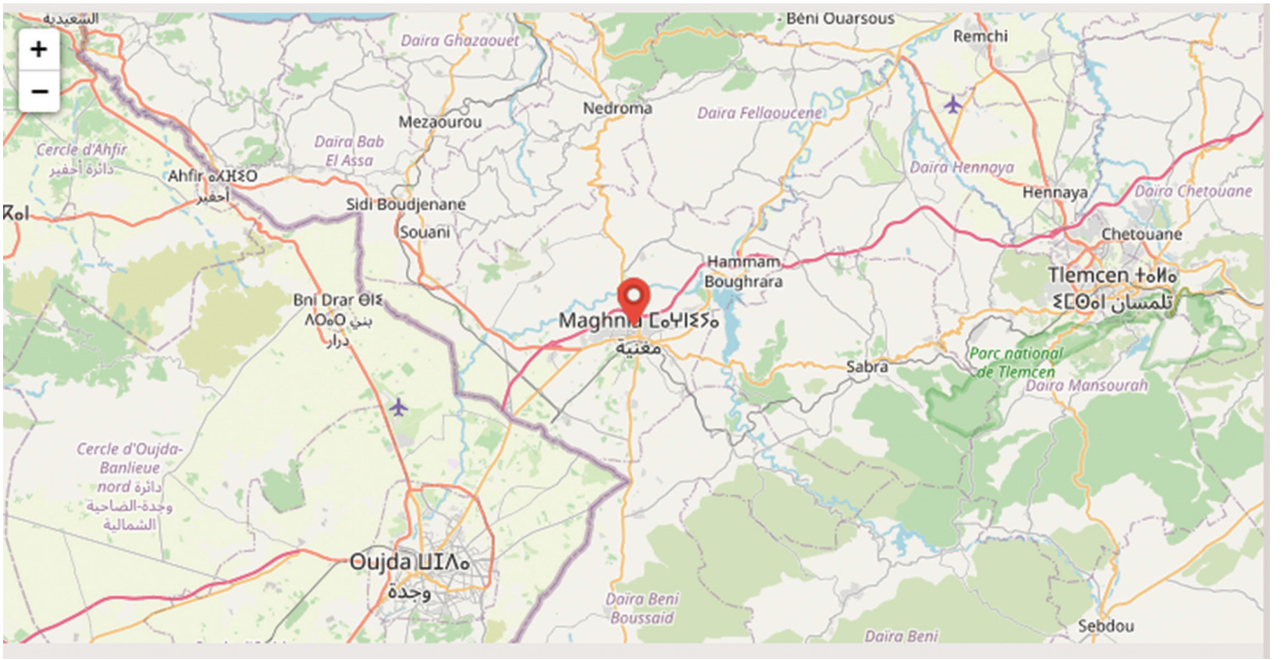

Figure 1. Location of Maghnia

2.2.1. Temperature and rainfall

According to Table 1, the climate of Maghnia is characterized by hot, dry summers. The highest average monthly temperature (27°C) was recorded in August, accompanied by minimal rainfall ranging from 3.4 nm to 6.01 mm. Winters are relatively cool and wet, with temperatures ranging from 10.4°C to 13.5°C.[40] The lowest average temperature (10.4°C) was observed in January. Rainfall during the winter season varies between 34.9 and 40.5 mm. Spring, extending from March to May, is marked by mild temperatures (13.5 – 18.8°C) and is the wettest season, with average monthly precipitation ranging from 31.9 to 41.5 mm. Autumn is also mild, with rainfall levels ranging from 15.4 to 40.8 mm.

Table 1. Average monthly rainfall and temperature (1970 – 2019)

Month	Average temperature (°C)	Average monthly rainfall (mm)
September	23.4	15.4
October	19.6	26.3
November	14.6	40.8
December	11.6	34.9
January	10.4	40.5
February	11.3	38.2
March	13.5	41.3
April	15.5	41.5
May	18.8	31.9
June	22.7	8.3
July	26.3	3.4
August	27	6.0

Note: Climatic data were obtained from ref.[41]

2.2.2. Winds

In Maghnia, wind patterns vary by season. During autumn and winter, winds are predominantly from the west and southwest during the day, shifting to the north and southwest at night, often with high intensity. In contrast, during spring and summer, winds are generally weaker and prevail throughout the day and into part of the night.

2.3. Location of the WWTP

Commissioned in 1999, the Lagfafe WWTP is currently managed and operated by the National Sanitation Office. It occupies an area of 11.233 hectares and is located 5 km northwest of Maghnia. The plant is bordered to the east by the Boughrara Dam, to the west by the town of Maghnia, to the north by Ouled Bendamou, and to the south by Oued Charef. Figure 2 illustrates the geographical location of the Lagfafe WWTP.

2.4. Overview of the WWTP layout and functional setup

The Lagfafe WWTP treats domestic wastewater from Maghnia and is designed to serve a population equivalent

Figure 2. Top view of the Maghnia wastewater treatment plant. The image was obtained from Google Earth in 2022.

of 150,000, with an average daily flow of 30,000 m^3. The facility covers an area of 11 hectares and has been managed and operated by the National Sanitation Office since 2003. The WWTP fulfills two essential roles: (i) to protect public health and the environment and (ii) to prevent the pollution of the Hammam Boughrara dam by wastewater discharged from urban areas in the Maghnia urban area. The main components of the Lagfafe WWTP are designed for storm overflow, pre-treatment, biological treatment, and sludge treatment functions.

2.4.1. Storm overflow

The overflow weir is designed to handle a flow rate of 3,266 m^3/h.

2.4.2. Pre-treatment

The pre-treatment stage includes several operations: (i) "screening" comprises one manually cleaned coarse screen, one manual bypass screen, and two mechanized fine screens and (ii) "grit and oil removal" is performed using two longitudinal grit chambers with dual compartments.

2.4.3. Biological treatment

For this process, denitrification and aeration basins are installed, consisting of four units combined into a single structural unit. In addition, two secondary clarifiers are used to settle and clarify the effluent after biological treatment. For chlorination, a reinforced concrete tank with a volume of 826.5 m^3 is used; however, this process was not performed in 2020.

2.4.3. Sludge treatment

The sludge is thickened and then directed to drying beds for dewatering.

2.5. Analytical methods

To assess the quality of treated wastewater from the Lagfafe WWTP and ensure that the water meets agricultural reuse standards (Table 2), we conducted analyses on both inflow and outflow wastewater in 2020. Sampling was performed four times per month, except for September, when no analyses were performed.

Wastewater samples were collected at both the inlet (raw water) and outlet (treated effluent) of the WWTP, before discharge into the natural environment. Samples were carefully taken to ensure they accurately represented the source environment. Sampling was conducted between 11:00 AM and 1:00 PM, during peak activity periods. Standard glass vials were used for physicochemical sample collection. These vials were thoroughly cleaned (washed, rinsed, and dried) and then sterilized before use. The procedure for collecting samples involved holding the sterile container by its base, carefully lowering it beneath the wastewater surface, uncapping it, and filling it to the required depth. After collection, the container was immediately sealed. Proper labeling and storage conditions were maintained, ensuring protection from light and heat. The samples were transported in a cooler, maintaining a temperature of approximately 4°C.

The following physicochemical parameters were analyzed: temperature, chemical oxygen demand (COD), ortho-phosphates (PO_4^{3-}), conductivity, nitrite (NO_2^-), nitrate (NO_3^-), ammoniacal nitrogen ($N\text{-}NH_4^+$), water potential, dissolved oxygen (DO), suspended solids, and biological oxygen demand (BOD_5). COD, PO_4^{3-}, NO_2^-, NO_3^-, and $N\text{-}NH_4^+$ were measured using a spectrophotometer. Suspended solids were determined by filtration. Water potential, DO, and BOD_5 were

Table 2. Algerian standards for physical and chemical parameters in wastewater reuse for agriculture

Parameters	Unit	Limit
Physical		
pH	-	6.5 <pH <8.5
TSS	mg/L	30
Conductivity	dS/m	3
Chemical		
BOD_5	mg/L	30
COD	mg/L	90
Cl^-	mEq/L	10
NO_3^--N	mg/L	30
HCO_3^-	mEq/L	8.5
Toxic elements[a]		
Al	mg/L	20
As	mg/L	2.0
Be	mg/L	0.5
B	mg/L	2.0
Cd	mg/L	0.05
Cr	mg/L	1.0
Co	mg/L	5.0
Cu	mg/L	5.0
CN^-	mg/L	0.5
F^-	mg/L	15
Fe	mg/L	20
Phenols	mg/L	0.002
Pb	mg/L	10.0
Li	mg/L	2.5
Mn	mg/L	10.0
Hg	mg/L	0.01
Mo	mg/L	0.05
N	mg/L	2.0
Se	mg/L	0.02
V	mg/L	1.0
Zn	mg/L	10.0

Note: [a]Toxic to fine-textured, neutral or alkaline soil types. TSS: total suspended solid; BOD: biological oxygen demand; COD: chemical oxygen demand; Cl: chloride; NO_3^--N: nitrate-nitrogen; HCO_3^-: bicarbonate; Al: aluminum; As: arsenic; Be: beryllium; B: boron; Cd: cadmium; Cr: chromium; Co: cobalt; Cu: copper; CN^-: cyanides; F^-: fluoride; Fe: iron; Pb: lead; Li: lithium; Mn: manganese; Hg: mercury; Mo: molybdenum; Ni: nickel; Se: selenium; V: vanadium; Zn: zinc.

measured using a pH meter, an oximeter, and a BOD_5 meter, respectively. The analytical methods employed are described below.

2.5.1. pH measurement

pH is a critical parameter for assessing the acidity or alkalinity at each sampling site. This measurement was performed *in situ* by immersing the electrode of a portable pH meter (model: pH 90; WTW, Germany) directly into the sample container. The reading was recorded once the pH value stabilized on the meter's display.

2.5.2. Conductivity measurement

Conductivity measurements were also performed *in situ*, using a portable conductivity meter (WTW, Germany). After calibrating the instrument, the electrode was immersed in the water sample, and the reading was recorded once it stabilized. The conductivity was expressed in μS/cm.

2.5.3. Total suspended solid (TSS) concentration measurement

TSSs, comprising both organic and inorganic fractions, were measured by filtration. The TSS concentration was determined gravimetrically after drying the filter paper at 105°C. Before filtration, the filter paper was washed with distilled water and dried in an oven at 120°C for 2 h. After cooling in a desiccator for 24 h, the initial mass of the filter paper (M_0) was recorded. The pre-weighed filter paper was then used to filter a 50 mL aliquot of the water sample. The mass of the filter paper containing the retained solids (M) was recorded after the same drying and cooling procedure. The TSS concentration was calculated using the following formula:

$$TSS = \frac{(M - M0) \times 1000}{V} \quad (I)$$

where V is the volume of the water sample analyzed (50 mL), M is the mass of the filtration disc after use (mg), and M_0 is the mass of the filter paper before use (mg).

2.5.4. BOD measurement

The BOD_5 was measured using a BOD_5 meter. The procedure involved filling 250 mL BOD_5 bottles with the water sample, sealing them with the instrument's stopper and agitator, and incubating them for five days. The reading from the BOD_5 meter was then corrected

using an appropriate factor. BOD_5 values (mg/L) are calculated using Equation II.

$$BOD_5 = \text{Reading} \times \text{Correction factor} \quad \text{(II)}$$

2.5.5. COD measurement

COD was measured by heating a diluted water sample with potassium dichromate in a COD reactor at 150°C for 2 h. A blank sample (reagent + distilled water) was prepared similarly. After cooling, the absorbance of both the sample and the blank was measured at 420 nm using a spectrophotometer (DR2000, Germany). The COD value was determined based on the difference in absorbance between the sample and the blank.

2.5.6. Nitrate concentration measurement

Nitrate concentration was determined using a DR/2000 spectrophotometer with a specific program 355 which was set to 500 nm (DR2000, Germany). After dilution and reaction with a Nitraver 5 capsule, the absorbance of the sample was measured at 500 nm, with a blank used for calibration. The final result was adjusted for the dilution factor.

2.5.7. Ammonium (NH_4) concentration measurement

NH_4 concentration was measured using a DR/2000 spectrophotometer with a specific program (DR2000, Germany) at 425 nm. After dilution and the addition of stabilizing and Nessler reagents, the sample color was measured against a distilled water blank after a 1-min reaction period.

2.5.8. PO_4^{3-} concentration measurement

PO_4^{3-} concentration was measured using a DR/2000 spectrophotometer with a specific program (DR2000, Germany) at 890 nm. After dilution and reaction with a ChromaVer. 3 reagent capsule, the blue color of the sample was measured against a distilled water blank following a 2-min reaction period.

2.5.9. Temperature measurement

Temperature measurements were performed *in situ* using a digital thermometer integrated into the portable conductivity meter (WTW, Germany). The thermometer probe was immersed directly into the water sample, and the temperature reading was recorded once it stabilized. Temperature was expressed in degrees Celsius (°C).

2.5.10. DO measurement

DO concentrations were measured *in situ* using a portable DO meter (WTW, Germany). The DO probe was immersed directly into the water sample, and the reading was allowed to stabilize before being recorded. The instrument was calibrated according to the manufacturer's guidelines before use. DO was expressed in mg/L and as a percentage of saturation (%).

2.5.11. Nitrite measurement

Nitrite concentration was determined using a DR/2000 spectrophotometer with a specific program (Program 345) (Hach DR2000, Germany). After sample preparation and reaction with a NitriVer 3 Nitrite Reagent Powder Pillows, the absorbance of the sample was measured at 507 nm with a blank used for zeroing calibration. Nitrite concentration was expressed in mg/L.

2.6. Statistical analysis

All statistical analyses were performed using Microsoft Excel. Descriptive statistics, including means, standard deviations, maximum and minimum values, and 95% CI, were calculated for all measured parameters. To assess the statistical significance of the reduction in COD concentrations between the influent and effluent wastewater, a paired samples t-test was conducted. The paired *t*-test was chosen due to its suitability for comparing means from two related groups (i.e., measurements taken before and after treatment from the same source). A $p < 0.05$ was considered statistically significant.

3. Results and discussion

3.1. Temperature

Temperature was measured using a thermometer for the area and both inflow and outflow wastewater. These measurements are displayed in Figure 3 and Table 3. From Figure 3, we can observe that the temperatures of the inflow and outflow wastewater are relatively similar, with the two curves nearly overlapping. The average temperature of the inflow wastewater is 20.50 ± 3.97°C, while the average temperature of the outflow wastewater is 20.76 ± 4.26°C. The maximum temperatures for the inflow and outflow wastewater are 26.75°C and 27.50°C, respectively. The minimum temperature for the inflow wastewater is 11°C, while the minimum for the outflow wastewater is 12°C.

3.2. pH

The pH values of the inflow and outflow wastewater were measured, and the results are presented in Figure 4 and Table 4. The results demonstrate that the pH values of both the influent (mean: 7.82, 95% CI: 7.74 – 7.90) and effluent (mean: 7.95, 95%

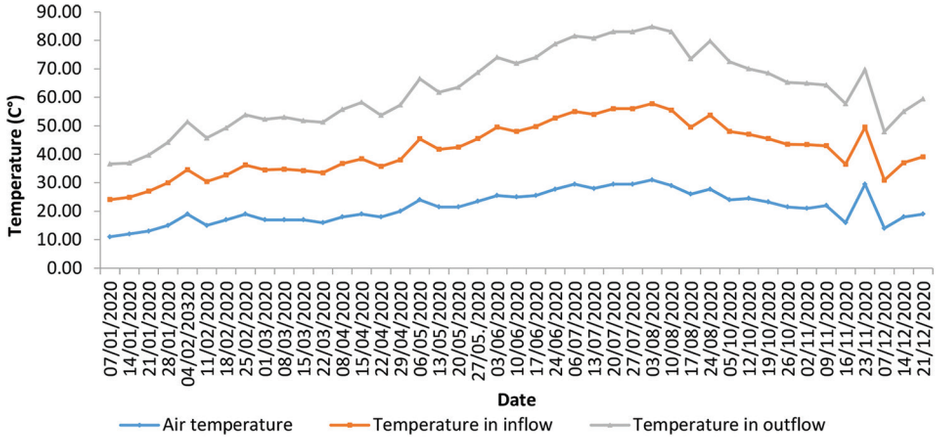

Figure 3. Temperature variations in inflow and outflow wastewater at the Lagfafe wastewater treatment plant

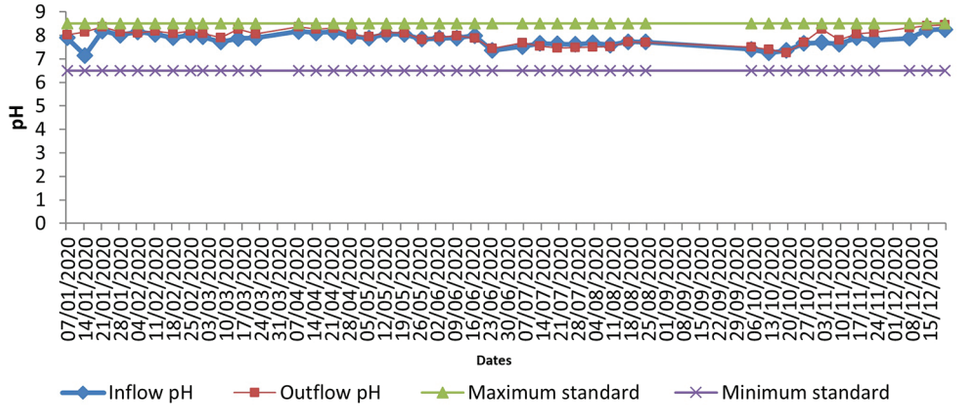

Figure 4. Variations in pH values of wastewater at the Lagfafe wastewater treatment plant

Table 3. Temperature of the inflow and outflow wastewater

Wastewater	Temperature (°C)				
	Average	Maximum	Minimum	Median	SD
Inflow	20.50	26.75	11.00	21.50	3.97
Outflow	20.76	27.50	12.00	20.50	4.26

Abbreviation: SD: standard deviation.

Table 4. pH values of the inflow and outflow wastewater

Wastewater	pH					
	Average	Maximum	Minimum	Median	95% CI	SD
Inflow	7.82	8.25	7.14	7.88	7.74 – 7.90	0.26
Outflow	7.49	8.44	7.25	8.04	7.85 – 8.05	0.31

Note: The p-value was calculated to be 1.68×10^{-4}.
Abbreviations: CI: confidence interval; SD: standard deviation.

CI: 7.85 – 8.05) wastewater are within the acceptable range established by the agricultural reuse standards. An independent samples t-test reveals a statistically significant increase in pH in the effluent compared to the influent wastewater ($p = 0.000168$), though the increase is marginal. However, both values remain consistently within the regulatory limits. In addition, the low and comparable standard deviation (SD) observed for the

influent (SD = 0.27) and effluent (SD = 0.32) suggests a stable pH throughout the monitoring period.

3.3. COD

Figure 5A and Table 5 display the measured COD of wastewater. The results indicate a significant organic load in the influent wastewater, as indicated by high COD (mean: 653.76 ± 132.54 mg/L; maximum: 932 mg/L; minimum: 339 mg/L), likely exacerbated by reduced water consumption during a regional drought. In contrast, effluent COD consistently remained below regulatory thresholds, with a high average removal efficiency of

Table 5. COD of the inflow and outflow wastewater

Wastewater	COD (mg/L)					
	Average	Maximum	Minimum	Median	SD	95% CI
Inflow	653.76	932	339	659	132.54	615.04 – 692.50
Outflow	36.00	65	10	36.5	12.48	32.35 – 39.65

Note: The p-value was calculated to be 3.97×10^{-47}.
Abbreviations: CI: confidence interval; SD: standard deviation; COD: chemical oxygen demand.

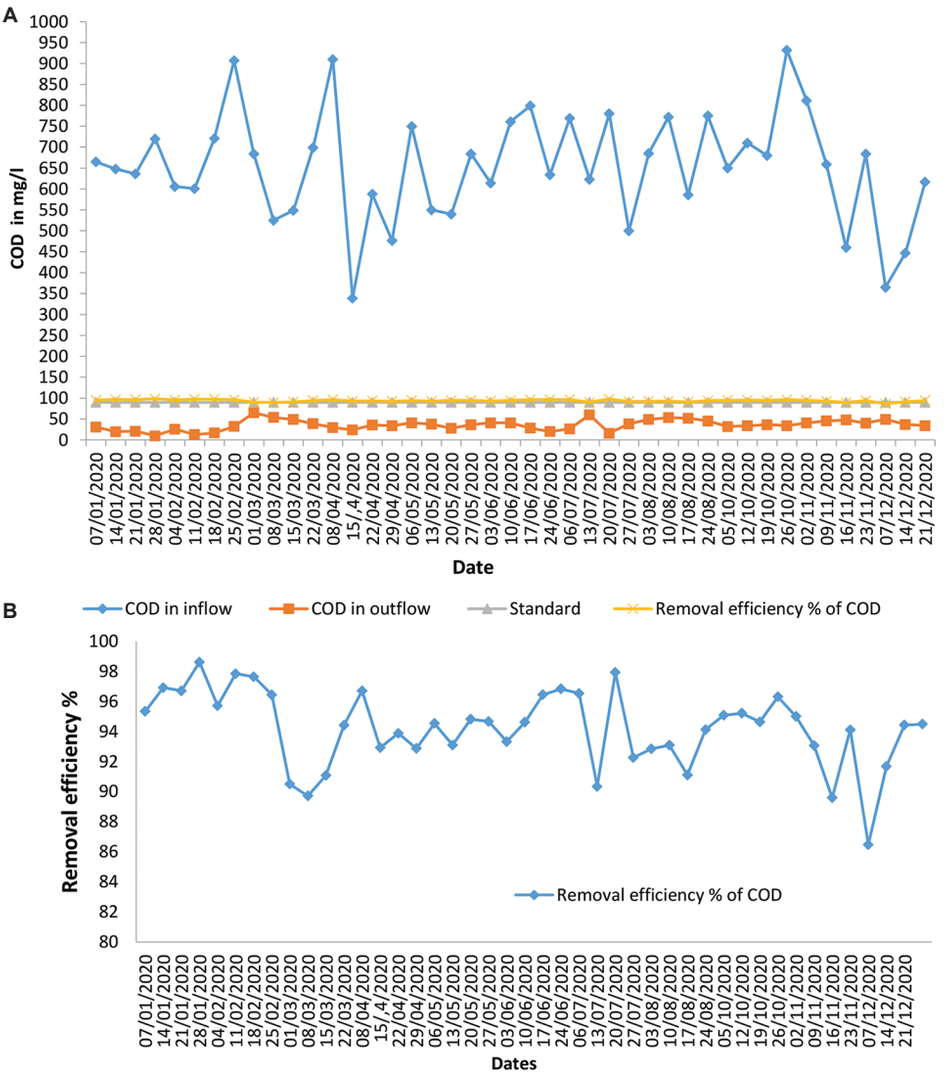

Figure 5. (A) Variations in chemical oxygen demand (COD) in inflow and outflow wastewater at the Lagfafe wastewater treatment plant. (B) Variations in removal efficiency of COD at the Lagfafe wastewater treatment plant.

94.48% (range: 86.46 – 98.61%) (Figure 5B). This robust performance is further supported by a highly significant reduction in COD ($p < 3.97 \times 10^{-47}$) from the influent (95% CI: 615.04 – 692.50 mg/L) to the effluent (95% CI: 32.35 – 39.65 mg/L), accompanied by a marked decrease in variability. These findings underscore the remarkable efficacy of the activated sludge process in removing oxidizable organic matter.

3.4. BOD

The results of the BOD_5 measurements are displayed in Figure 6A and Table 6. BOD_5 in the influent wastewater was relatively high, with an average value of 399.12 ± 91.33 mg/L. The maximum concentration of 640 mg/L was recorded in October 2020, while the minimum value of 200 mg/L was observed in November 2020. The significant separation between the influent and effluent curves clearly indicates effective BOD_5 removal.

Throughout the study period, the effluent BOD_5 consistently aligned with the regulatory standard, with no values exceeding the limit of 30 mg/L. This confirms that the treated wastewater complies with the standard for agricultural reuse concerning BOD_5.

The recorded removal efficiencies were consistently high. The average removal efficiency was 96.96%, with

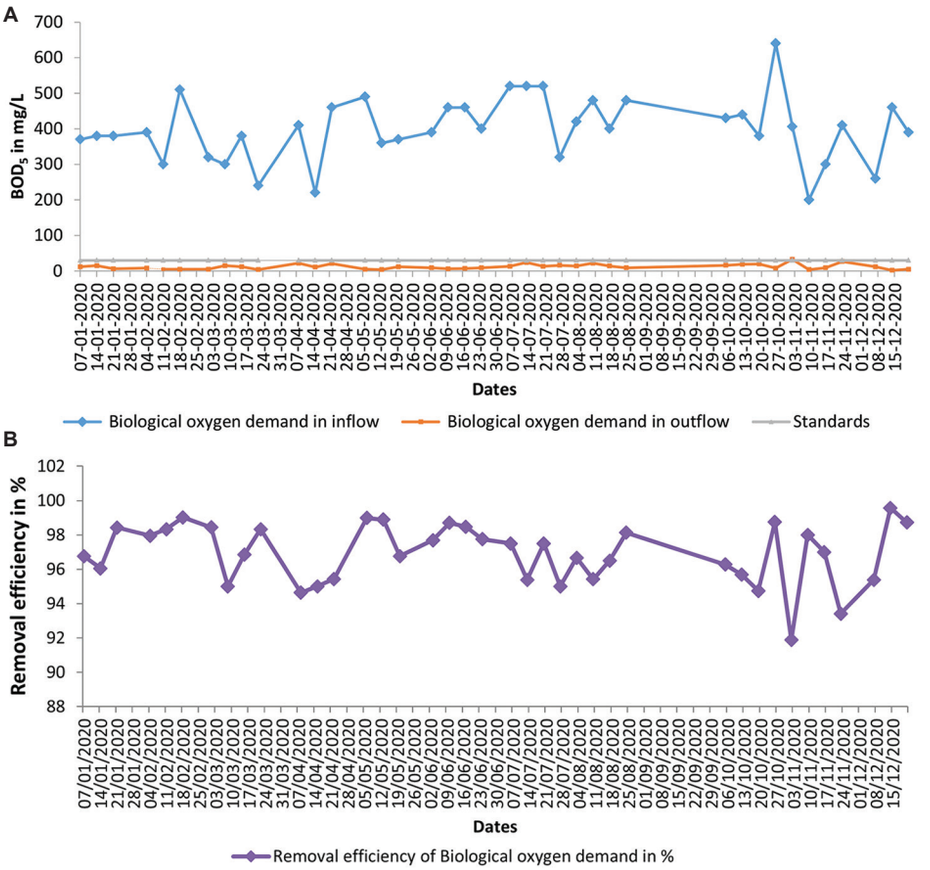

Figure 6. (A) Variations in biological oxygen demand (BOD_5) in inflow and outflow wastewater at the Lagfafe wastewater treatment plant. (B) Variations in removal efficiency of BOD_5 % at the Lagfafe wastewater treatment plant.

Table 6. BOD_5 of the inflow and outflow wastewater

Wastewater	BOD_5 (mg/L)					
	Average	Maximum	Minimum	Median	SD	95% CI
Inflow	399.12	640	200	400	91.33	372.44 – 425.82
Outflow	12.12	33	2	12	7.19	10.03 – 14.23

Note: The p-value was calculated to be 1.49×10^{-26}.
Abbreviations: CI: confidence interval; SD: standard deviation; BOD: biological oxygen demand.

a maximum of 99.56% observed in December 2020 and a minimum of 91.87% in November 2020 (Figure 6B). These results reflect the high performance of the activated sludge process in degrading organic matter.

An independent samples *t*-test yielded a highly significant *p*-value ($p < 1.49 \times 10^{-26}$), rejecting the null hypothesis and confirming a statistically significant difference in mean BOD_5 concentrations between influent and effluent samples. The 95% CI for the influent BOD_5 mean ranged at 372.44 – 425.82 mg/L, while the effluent BOD_5 mean was 10.03 – 14.23 mg/L. These non-overlapping intervals further support the conclusion of a substantial and statistically significant reduction in BOD_5 levels due to the treatment process.

3.5. TSSs

The concentration of TSS in inflow and outflow wastewater is displayed in Figure 7A and Table 7.

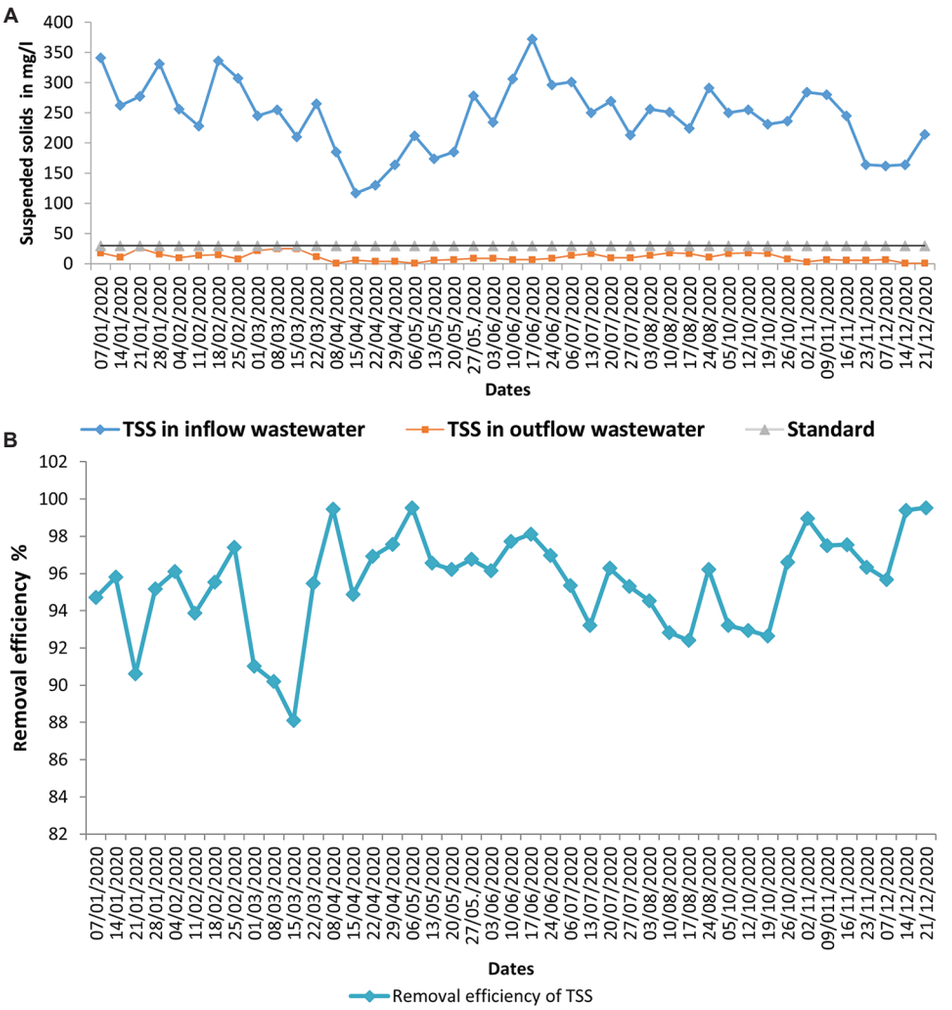

Figure 7. (A)Variations in total suspended solids (TSS) concentrations in inflow and outflow wastewater at the Lagfafe wastewater treatment plant. (B) Variations in removal efficiency % of TSS at the Lagfafe wastewater treatment plant.

Table 7. TSS concentration in the inflow and outflow wastewater

Wastewater	TSS (mg/L)					
	Average	Maximum	Minimum	Median	SD	95% CI
Inflow	244.32	372	117	250	57.09	227.65 – 261.01
Outflow	11.02	26	1	10	6.67	9.07 – 12.97

Note: The *p*-value was calculated to be 6.01×10^{-29}.
Abbreviations: CI: confidence interval; SD: standard deviation; TSS: total suspended solids.

The results revealed that the TSS concentration in the effluent is significantly lower than that of the influent, indicating highly effective removal of suspended matter during the treatment process.

Statistical analysis confirms a highly significant reduction ($p < 6.01 \times 10^{-29}$) in TSS concentrations between the influent (mean: 244.33 mg/L; 95% CI: 227.65 – 261.01 mg/L) and the effluent (mean: 11.02 mg/L; 95% CI: 9.07 – 12.97 mg/L). This sharp decrease is accompanied by a considerable reduction in variability, as reflected by the SD of 6.68 mg/L in the effluent compared to 57.10 mg/L in the influent. These results underscore the high performance of the treatment process in removing suspended solids.

The extremely low *p*-value from the independent samples *t*-test confirms the statistical significance of this reduction, and the non-overlapping CIs further validate this conclusion.

The removal efficiency was consistently high throughout the monitoring period, with an average of 95.48%, a maximum of 99.53%, and a minimum of 88.09% (Figure 7B). All effluent TSS concentrations were well below the regulatory limit, confirming compliance with the agricultural reuse standard.

3.6. DO

The concentrations of DO in inflow and outflow wastewater are displayed in Figure 8 and Table 8. The concentration of DO in the effluent is consistently higher than that of the influent, indicating an increase in DO concentrations following treatment. This improvement is primarily attributed to the aeration phase within the activated sludge process.

An independent samples *t*-test revealed a highly significant increase in DO levels ($p = 2.65 \times 10^{-17}$). The 95% CI for the mean DO concentration in the influent ranged at 2.21 – 2.69 mg/L, while that of the effluent ranged at 4.95 – 5.85 mg/L. The non-overlapping CIs further substantiate the statistical significance of this increase.

Interestingly, the SD of DO concentrations in the effluent (1.54 mg/L) is higher than that in the influent (0.82 mg/L), suggesting greater variability in DO levels post-treatment. This may reflect operational variations or fluctuations in microbial activity during aeration.

In conclusion, the treatment process demonstrates a statistically significant and operationally relevant increase in DO concentrations, enhancing the quality of the treated effluent for potential reuse, despite the observed increase in variability.

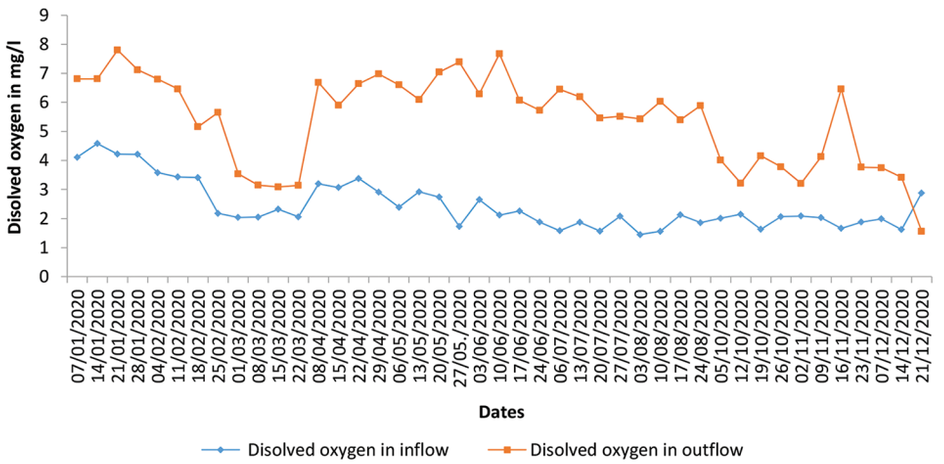

Figure 8. Variations in dissolved oxygen concentrations in inflow and outflow wastewater at the Lagfafe wastewater treatment plant

Table 8. Dissolved oxygen concentration in the inflow and outflow wastewater

Wastewater	Dissolved oxygen (mg/L)					
	Average	Maximum	Minimum	Median	SD	95% CI
Inflow	2.45	4.58	1.45	2.12	0.82	2.2 – 2.69
Outflow	5.40	7.80	1.56	5.89	1.54	4.95 – 5.85

Note: The *p*-value was calculated to be 2.65×10^{-17}.
Abbreviations: CI: confidence interval; SD: standard deviation.

3.7. NH_4

The measured concentrations of NH_4 in inflow and outflow wastewater are displayed in Figure 9A and Table 9. The results demonstrate the effective removal of $N\text{-}NH_4^+$ through the treatment process. Statistical analysis reveals a highly significant reduction in $N\text{-}NH_4^+$ concentrations between the influent (mean: 51.53 mg N/L; 95% CI: 47.95 – 55.11 mg N/L) and the effluent (mean: 9.37 mg N/L; 95% CI: 6.67 – 12.07 mg N/L). The independent samples *t*-test yielded an extremely low *p*-value ($p = 2.46 \times 10^{-31}$), confirming the statistical significance of this reduction.

Moreover, the lower SD in the effluent (3.23 mg N/L), compared to the influent (12.24 mg N/L), indicates improved consistency in nitrogen concentrations after treatment. The median values of 50.63 mg N/L for the influent and 5.80 mg N/L for the effluent are consistent with the respective means, further supporting the conclusion of substantial nitrogen removal.

The $N\text{-}NH_4^+$ removal efficiencies varied over the

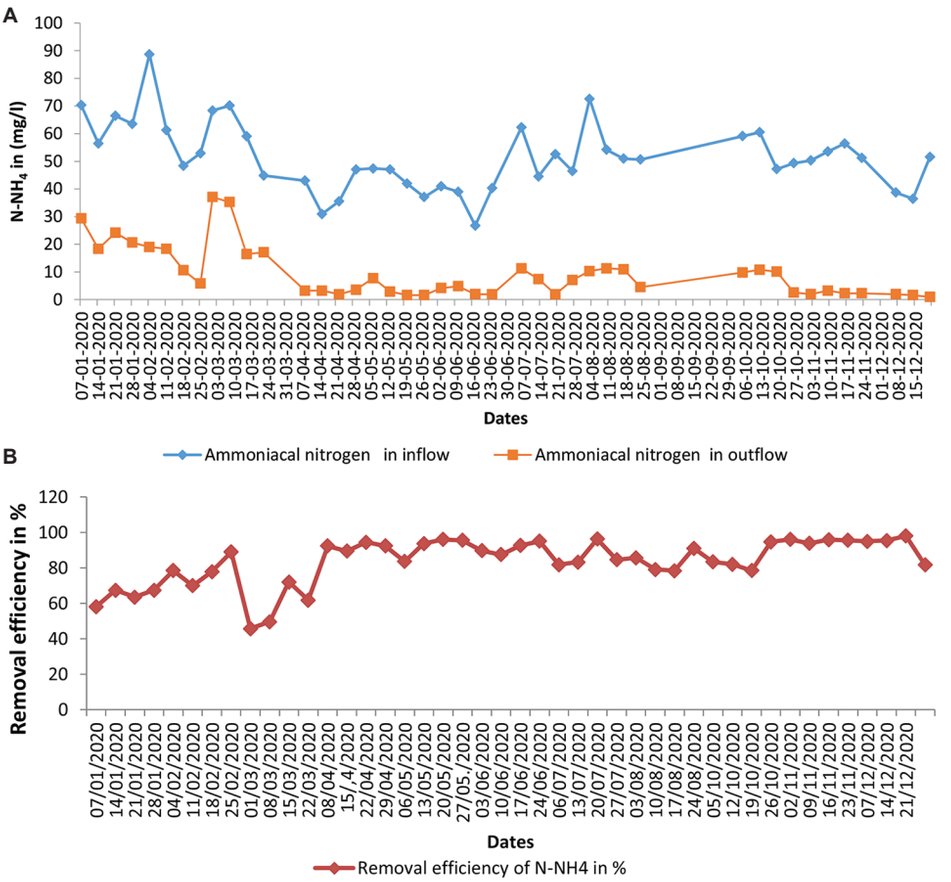

Figure 9. (A) Variations in ammoniacal nitrogen ($N\text{-}NH_4$) concentrations in inflow and outflow wastewater at the Lagfafe wastewater treatment plant. (B) Variations in $N\text{-}NH_4$ concentrations in inflow and at the Lagfafe wastewater treatment plant.

Table 9. $N\text{-}NH_4$ concentration in the inflow and outflow wastewater

Wastewater	$N\text{-}NH_4$ (mg N/L)					
	Average	Maximum	Minimum	Median	SD	95% CI
Inflow	51.53	88.68	26.76	50.63	12.24	47.95 – 55.11
Outflow	9.37	37.09	0.97	5.80	3.23	6.67 – 12.07

Note: The *p*-value was calculated to be 2.46×10^{-31}.
Abbreviations: CI: confidence interval; SD: standard deviation; N-NH4: ammoniacal nitrogen.

monitoring period, with an average efficiency of 81.80%, a maximum of 98.12 % recorded in December 2020, and a minimum of 45.75% observed in March 2020 (Figure 9B). These results highlight both the high performance and operational variability of the activated sludge process in reducing N-NH_4^+ levels.

According to Algerian regulations, no maximum limit is specified for N-NH_4^+ concentrations in treated wastewater intended for agricultural reuse, as it is regarded as a beneficial nutrient. Its presence can enhance soil fertility and support crop growth.

3.8. NO_2^-

The measured NO_2^- concentrations in inflow and outflow wastewater are displayed in Figure 10A and Table 10. The results indicate that the degradation of NO_2^- is generally effective. The average NO_2^-concentration in the influent wastewater is 0.23 ± 0.13 mg N/L, while that of the effluent is 0.10 ± 0.09 mg N/L. The maximum values recorded for the influent and effluent are 0.65 and 0.52 mg N/L, respectively, whereas the minimum concentrations are 0.10 mg N/L for the influent

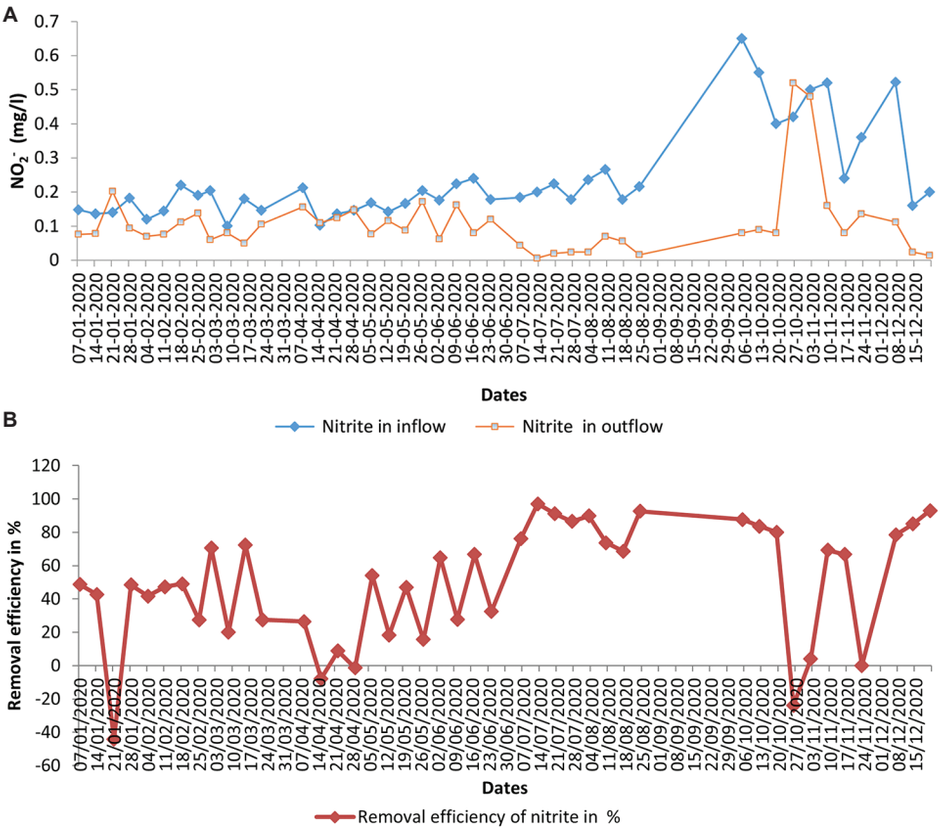

Figure 10. Variations in nitrite (NO_2^-) concentrations in inflow and outflow wastewater at the Lagfafe wastewater treatment plant. (B) Variations in removal efficiency of NO_2^- at the Lagfafe wastewater treatment plant.

Table 10. NO_2^- concentration in the inflow and outflow wastewater

Wastewater	NO_2^- (mg N/L)					
	Average	Maximum	Minimum	Median	SD	95% CI
Inflow	0.23	0.65	0.10	0.19	0.13	0.191 – 0.269
Outflow	0.10	0.52	0.006	0.08	0.09	0.071 – 0.129

Note: The *p*-value was calculated to be 5.14×10^{-8}.
Abbreviations: CI: confidence interval; SD: standard deviation; NO_2^-: nitrite.

and 0.006 mg N/L for the effluent. The average NO_2^- removal efficiency was 42.44% (Figure 10B). However, removal efficiency was occasionally reduced, likely due to elevated concentrations resulting from the denitrification of NO_3^-.

Statistical analysis confirms a significant reduction in NO_2^- concentrations between the influent (mean: 0.23 mg N/L; 95% CI: 0.191 – 0.269 mg N/L) and the effluent (mean: 0.10 mg N/L; 95% CI: 0.071 – 0.129 mg N/L). The independent samples *t*-test yielded a highly significant *p*-value ($p = 5.14 \times 10^{-8}$), indicating that this decrease is unlikely due to random variation. Furthermore, the SD in the effluent (0.09 mg N/L) is slightly lower than that in the influent (0.13 mg N/L), suggesting a modest improvement in the stability of NO_2^-concentrations post-treatment.

In summary, the wastewater treatment process effectively reduces average NO_2^- concentrations, though the efficiency may be impacted by NO_3^- reduction dynamics. The process also contributes to a slight decrease in concentration variability in the treated effluent.

3.9. NO_3^-

The measured NO_3^- concentrations in inflow and outflow wastewater are displayed in Figure 11A and Table 11. The results indicate that the influent and effluent NO_3^- concentration curves are nearly superimposed, suggesting that the values are close to each other. Concentrations in both wastewater sources remain well below the standard threshold. It is important to note that Algerian regulations on the reuse of treated wastewater for agricultural purposes do not define a limit for NO_3^-, as it is considered a beneficial nutrient for crops.

The independent samples *t*-test yielded a statistically significant *p*-value ($p = 0.0028$, $\alpha = 0.05$), confirming a significant reduction in NO_3^- concentrations following treatment. The 95% CI for the influent

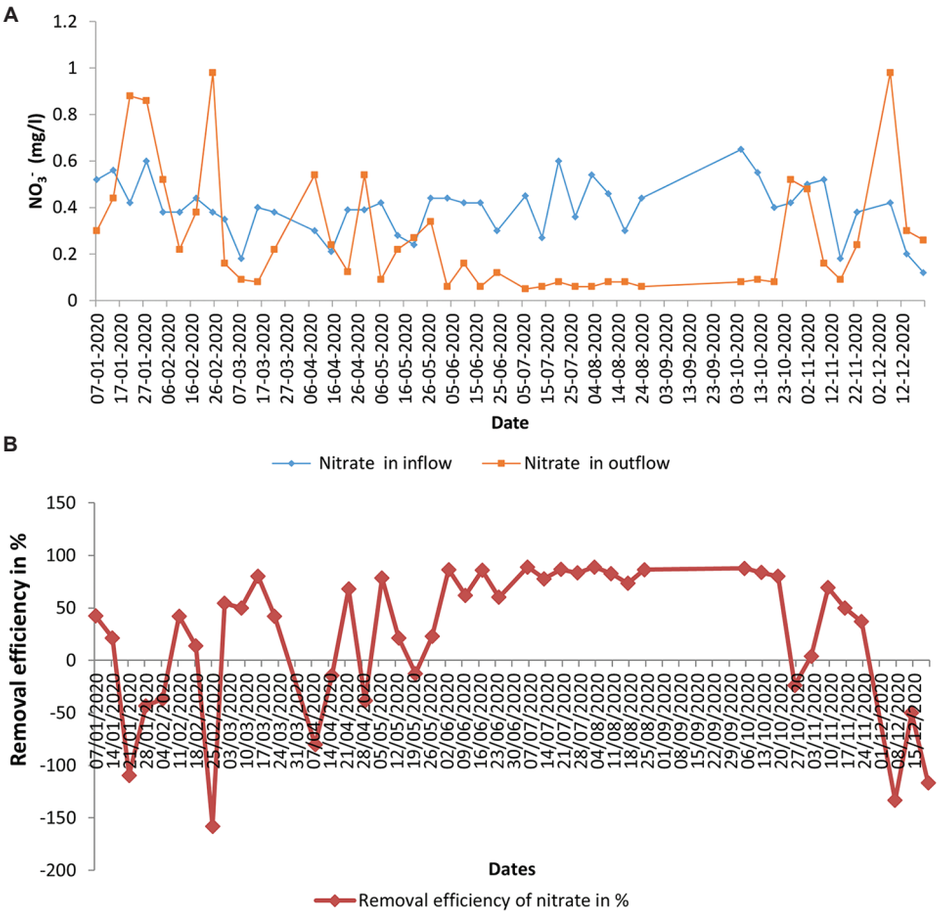

Figure 11. (A) Variations in nitrate (NO_3^-) concentrations in inflow and outflow wastewater at the Lagfafe wastewater treatment plant. (B) Variations in removal efficiency of NO_3^- wastewater at the Lagfafe wastewater treatment plant.

NO_3^- concentration is estimated to be 0.355 – 0.425 mg N/L, while that of the effluent is 0.194 – 0.346 mg N/L. The non-overlapping nature of the CIs reinforces the statistical significance of the observed reduction. However, the effluent exhibits greater variability (SD: 0.26 mg N/L) than the influent (SD: 0.12 mg N/L), indicating increased fluctuation in NO_3^- levels after treatment.

The average nitrate removal efficiency was 56.58%, (Figure 11B) indicating moderate denitrification performance. Nevertheless, the treated water from the Lagfafe WWTP remains suitable for agricultural reuse, given the absence of regulatory restrictions on NO_3^- concentrations and its agronomic value.

3.10. Conductivity

Table 11. NO_3^- concentration in the inflow and outflow wastewater

Wastewater	NO_3^- (mg N/L)					
	Average	Maximum	Minimum	Median	SD	95% CI
Inflow	0.39	0.65	0.27	0.40	0.12	0.355 – 0.425
Outflow	0.27	0.98	0.05	0.16	0.26	0.194 – 0.346

Note: The *p*-value was calculated to be 0.0028.
Abbreviations: CI: confidence interval; SD: standard deviation; NO3⁻: nitrate.

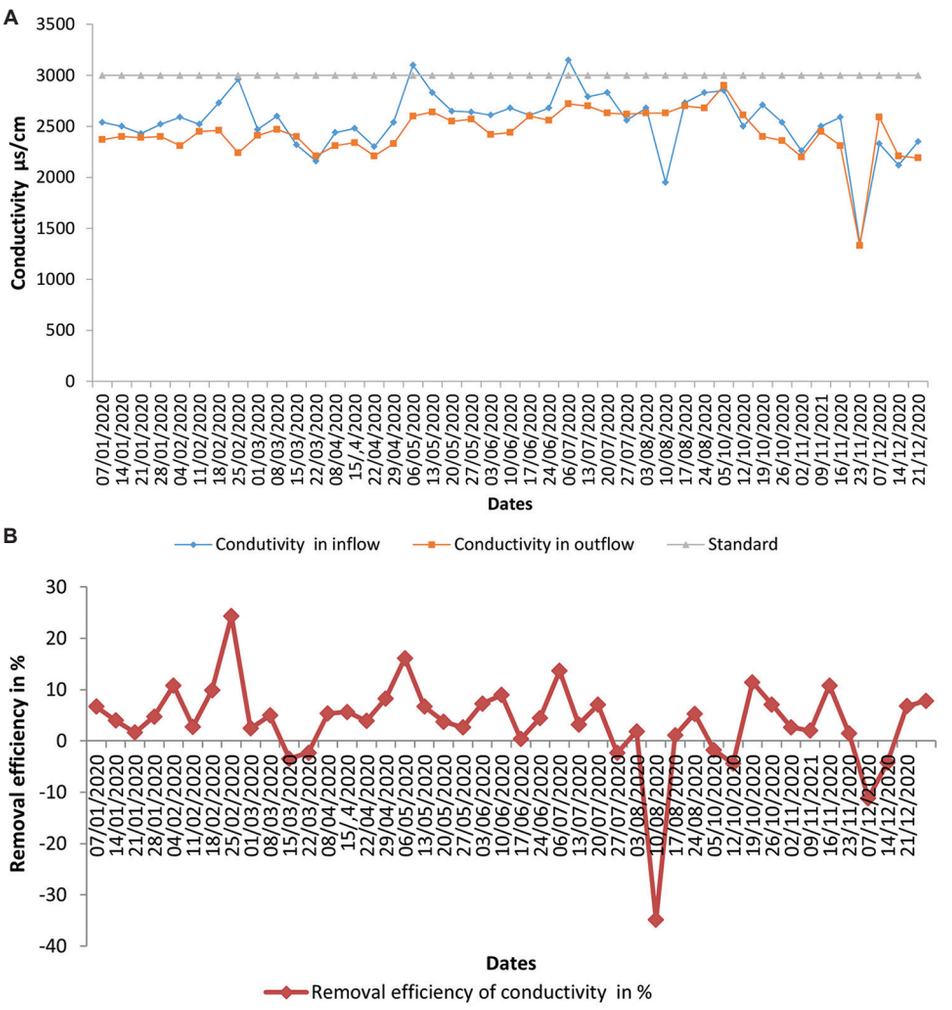

Figure 12. (A) Variations in the conductivity of inflow and outflow wastewater at the Lagfafe wastewater treatment plant. (B) Variations in removal efficiency % of conductivity at the Lagfafe wastewater treatment plant.

Table 12. Conductivity of the inflow and outflow wastewater

Wastewater	Conductivity (µS/cm)					
	Average	Maximum	Minimum	Median	SD	95% CI
Inflow	2546.97	3150	1350	2560	303.06	2458.42 – 2635.52
Outflow	2440.46	2900	1330	2440	241.82	2369.81 – 2511.12

Note: The *p*-value was calculated to be 0.00085.
Abbreviations: CI: confidence interval; SD: standard deviation.

Electrical conductivity measurements are presented in Figure 12A and Table 12. The results indicate that the conductivity of both influent and effluent remains below the threshold established by the agricultural reuse standard, indicating compliance for this parameter.

Statistical analysis using an independent samples *t*-test revealed a statistically significant reduction in electrical conductivity after treatment (p = 0.00085, α = 0.05). The mean conductivity for the influent is 2546.97 µS/cm, with a 95% CI of 2458.42 – 2635.52 µS/cm, while the mean conductivity for the effluent is 2440.46 µS/cm, with a 95% CI of 2369.80 – 2511.12 µS/cm. The partial non-overlap between these intervals supports the conclusion that the observed difference is statistically significant and unlikely due to random variation.

Moreover, the effluent reports a slightly lower SD (241.82 µS/cm) compared to the influent (303.06 µS/cm), suggesting a modest reduction in variability, likely attributable to the removal of some dissolved salts during the treatment process.

The average removal efficiency for conductivity was 7.80%, with recorded values ranging from a maximum of 24.32% to a minimum of -34.87% (Figure 12B). These fluctuations reflect the limited capacity of the activated sludge process to reduce conductivity, as this parameter is primarily influenced by the concentration of dissolved ions rather than biodegradable matter. Nonetheless, all effluent values remained within the acceptable range for agricultural reuse.

3.11. Phosphorus

Variations in PO_4 concentrations (in mg P/L) over the study period are displayed in Figure 13A and Table 13. The results illustrate a clear reduction in PO_4 concentrations, indicating effective removal through the treatment process. The average, maximum, and minimum removal efficiencies were 78.75%, 95.00%, and 28.90%, respectively (Figure 13B).

The independent samples *t*-test yielded a statistically significant *p*-value ($p = 9.80 \times 10^{-6}$, $\alpha = 0.05$), confirming a significant decrease in PO_4^{3-} concentration post-treatment. The mean influent concentration is 13.59 mg P/L (95% CI: 12.39 – 14.79 mg P/L), while the effluent concentration averaged 9.41 mg P/L (95% CI: 7.91 – 10.91 mg P/L). The non-overlapping CIs substantiate the statistical significance of this reduction.

Notably, the SD increased in the effluent (5.14 mg P/L) compared to the influent (4.10 mg P/L), suggesting greater variability in PO_4^{3-} concentrations after treatment. This could be attributed to seasonal fluctuations or operational inconsistencies in the PO_4^{3-} removal process. Despite this variability, the system achieved a substantial reduction, albeit less consistent than those observed for other parameters such as BOD_5 or TSS.

Algerian regulations for agricultural reuse of treated wastewater do not specify a limit for phosphorus (or PO_4^{3-}), given its beneficial role as a nutrient for crop fertilization. However, for discharge into the natural environment, a maximum allowable concentration of 2 mg P/L is imposed to mitigate eutrophication risks. Since the effluent concentrations in this study exceed this threshold, direct discharge into surface water bodies, such as the Hammam Boughrara Dam, could pose ecological risks if not managed appropriately.

While the treatment process effectively reduces PO_4^{3-} concentrations, the residual levels remain above environmental discharge limits. Therefore, reusing this phosphorus-rich effluent in agriculture offers a sustainable solution by supporting crop growth and simultaneously protecting the receiving water bodies from nutrient over-enrichment.

3.12. Strengths and limitations

This study offers valuable insights into the quality of treated wastewater from the Lagfafe WWTP and its potential for agricultural reuse. To ensure a comprehensive and representative evaluation, wastewater samples were collected four times per month throughout the year 2020. This sampling strategy captured all four seasons, accounting for the influence of seasonal variability, which is an important factor affecting treatment performance and effluent quality

Figure 13. (A) Variations in phosphate (PO_4^{3-}) concentrations in inflow and outflow wastewater at the Lagfafe wastewater treatment plant. (B) Variations in removal efficiency % of PO_4^{3-} at the Lagfafe wastewater treatment plant, the positive cells were observed.

Table 13. PO_4^{3-} concentration in the inflow and outflow wastewater

Wastewater	PO_4^{3-} (mg P/L)					
	Average	Maximum	Minimum	Median	SD	95% CI
Inflow	13.59	22.8	8.0	12.3	4.10	12.39 – 14.79
Outflow	9.41	20.0	0.4	9.6	5.14	7.91 – 10.91

Note: The *p*-value was calculated to be 9.80×10^{-6}.
Abbreviations: CI: confidence interval; SD: standard deviation; PO_4^{3-}: phosphate.

due to changes in temperature, precipitation, organic load, and hydraulic flow.

A major strength of the study lies in its year-round monitoring framework. The results indicate that the treatment process maintained consistent performance across different seasons, with significant reductions observed in key pollution indicators, such as COD, BOD_5, and TSS. These findings suggest that, within the local context, seasonal variability did not substantially compromise the effectiveness of the treatment system.

However, several limitations should be acknowledged. Although the sampling frequency was relatively high, short-term fluctuations or pollution peaks may have gone undetected. Such events could impact the suitability of treated wastewater for irrigation, especially in sensitive cropping systems. Moreover, the one-year duration of the study may not fully capture long-term trends in effluent quality, which are essential for evaluating the sustainability of reuse practices.

Another significant limitation is the absence of data on emerging contaminants, including pharmaceutical residues, hormones, endocrine-disrupting compounds,

and microplastics. Although typically present at trace levels, these micropollutants can persist in treated effluent and pose environmental and health risks, particularly when the water is reused for agriculture. Monitoring these substances requires advanced analytical techniques, which were beyond the scope of this study. Future research should prioritize the detection and quantification of such contaminants to provide a more comprehensive assessment of the safety and long-term feasibility of treated wastewater reuse.

4. Conclusion

This study presents a comprehensive, year-long evaluation of the Lagfafe WWTP to assess the feasibility of treated effluent reuse for agricultural purposes in the Maghnia region. Through systematic monitoring and rigorous statistical analysis, the research demonstrated consistent and significant reductions in key pollutants, namely COD, BOD_5, and TSS, with treated effluent concentrations generally complying with both national and international irrigation standards. These outcomes confirm the technical viability of wastewater reuse in semi-arid areas affected by chronic water scarcity.

From an operational standpoint, the Lagfafe WWTP treats an average of 29,400 m^3 wastewater per day, producing approximately 10.73×10^6 m^3 of reusable treated water annually. This substantial volume represents a promising alternative water source that could help alleviate the agricultural water crisis currently facing the Maghnia region. In addition, the nutrient-rich composition of the treated effluent provides agronomic benefits by improving soil fertility and reducing dependence on synthetic fertilizers. Harnessing this underutilized resource could foster more sustainable agricultural practices, enhance food security, and reduce pressure on conventional freshwater supplies. Conversely, the continued discharge of treated effluent into natural waterways particularly toward the Hammam Boughrara dam poses ecological risks, including eutrophication caused by nutrient accumulation.

This study distinguishes itself from much of the existing literature through its methodological rigor and seasonal comprehensiveness. In contrast to previous research often limited to short-term or descriptive analyses, this study employed inferential statistical methods, specifically paired *t*-tests and 95% CIs, to robustly assess treatment performance. This approach strengthens the scientific validity and interpretability of the results.

Furthermore, by spanning all four seasons, the study provides valuable insights into the temporal variability of treatment efficiency, a dimension often overlooked in similar investigations. Rather than focusing solely on agronomic benefits or environmental impacts, this research adopts a balanced perspective, evaluating both the nutrient potential of treated effluents for irrigation and the ecological implications of residual pollutants.

To reiterate, the findings affirm not only the technical and environmental feasibility of wastewater reuse but also its strategic importance in integrated water resource management for semi-arid regions. The study offers concrete guidance to policymakers, local authorities, and farmers, advocating for the sustainable use of non-conventional water resources to bolster agricultural productivity and strengthen environmental resilience.

Acknowledgments

None.

Funding

None.

Author contributions

This is a single-authored article.

Conflict of interest

The author declares there are no conflicts of interest with any institute or organization.

Availability of data

Not applicable.

References

1. Hedberg A, Pardo R, Frontini A, Daryoush T. Reaching for blue goldhow the eu can rise to the water challenge while reaping the rewards. *Europe'S Political Economy and Europe in the World Programmes*; 2015.
2. Jury W, Vaux H. The emerging global water crisis: Managing scarcity and conflict between water users. *Adv Agron.* 2007;95:1-76.
   doi: 10.101/S0065-2113 (07)95001-4
3. Distefano T, Kelly S. Are we in deep water? Water scarcity and its limits to economic growth. *Ecol Econ.* 2017;142:130-147.
   doi: 10.1016/j.ecolecon.2017.06.019
4. Emran GI, Barma R, Khan AH, Roy M. Reasons behind the water crisis and its potential health outcomes. *Eur J*

Dev Stud. 2024;4(6):16-24.
doi: 10.24018/ejdevelop.2024.4.6.389

5. Organisation Météorologique Mondiale. *État Des Ressources En Eau Dans Le Monde [State of Global Water Resources], Rapport Sur L'état Des Ressources En Eau Dans le Monde 2023*, Genève, Suisse; 2024. Available from: https://wmo.int/fr/media/news/un-rapport-de-lomm-signale-une-aggravation-lechelle-planetaire-de-linsuffisance-des-ressources-en [Article in French] [Last accessed on 2025 Feb 15].
6. UNESCO. *Rapport mondial des Nations Unies sur la Mise En Valeur Des Ressources en Eau 2021: la Valeur de L'eau; Faits et Chiffres [United Nations World Water Development Report 2021: The Value of Water; Facts and Figures*]. *SC-2021/WS/3, Document de Programme et de Réunion [213349]*; 2021. Available from: https://unesdoc.unesco.org/ark:/48223/pf0000375751_fre [Article in French] [Last accessed on 2025 Feb 12].
7. Organisation Mondiale de la Santé. *Eau Potable. Fiche D'information [Drinking Water. Fact Sheet]*; 2022. Available from: https://www.who.int/fr/news-room/fact-sheets/detail/drinking-water [Article in French] [Last accessed on 2025 Feb 15].
8. Lin L, Yang H, Xu X. Effects of water pollution on human health and disease heterogeneity: A review. *Front Environ Sci.* 2022;10:880246.
doi: 10.3389/fenvs.2022.880246
9. Fahim MA. Impact of Water Scarcity on Food Security at Micro Level in Pakistan. *MPRA Munich Personal RePEc Archive*; 2011. p. 35760. Available from: https://mpra.ub.uni-muenchen.de/35760 [Last accessed on 2025 Feb 15].
10. Okumah M, Chapman PJ, Martin-Ortega J, Novo P. Mitigating agricultural diffuse pollution: Uncovering the evidence base of the awareness-behaviour-water quality pathway. *Water.* 2019;11:29.
doi: 10.3390/w11010029
11. Giwa A, Ademola H, Yusuf AO. Machine learning and application for modeling and prediction of desalination cost globally. *Desalination*. 2025;608:118829.
doi: 10.1016/j.desal.2025.118829
12. Obaideena K, Shehata N, Sayed ET, Abdelkareem MA, Mahmoud MS, Olabi AG. The role of wastewater treatment in achieving sustainable development goals (SDGs) and sustainability guideline. *Energy Nexus*. 2025;7:100112.
doi: 10.1016/j.nexus.2022.100112
13. Mounira C, Seddini A, Benameur S. Relieving the water shortage crisis of Algeria by reusing treated wastewater lagoons. *Desalination Water Treat*. 2015;50:1-13.
doi: 10.1080/19443994.2015.1070752
14. Boutin C, Héduit A, Helmer JM. *Technologies D'épuration en vue D'une Réutilisation des Eaux Usées Traitées (REUT) [Purification Technologies for the Reuse of Treated Wastewater (REUT)]. Convention de Partenariat ONEMA-Cemagref* 2008; 2009. Available from: https://professionnels.ofb.fr/sites/default/files/pdf/2009_038.pdf [Article in French] [Last accessed on 2024 Jan 22].
15. El Hachemi O, Gharibi E, Bencheikh N, *et al*. Contribution to the assessment of the health risks related to the reuse of treated waste water in Oujda-Morocco. *Algerian J Environ Sci Technol*. 2023;9(1):2956-2963.
16. Yalin D, Craddock HA, Assouline S, *et al*. Mitigating risks and maximizing sustainability of treated wastewater reuse for irrigation. *Water Res X.* 2023;21:100203.
doi: 10.1016/j.wroa.2023.100203
17. Bendida A, Kendouci MA, Mebarki S, Tidjani AE. Wastewater purifcation and recycling using plants in an arid environment for agricultural purposes: Case of the Algerian Sahara. *Appl Water Sci*. 2024;14:123.
doi: 10.1007/s13201-024-02148-9
18. Choukr-Allah R, Aghai O. Impact de l'irrigation par les eaux usées épurées sur la productivité d'une culture de tomate de plein champ, la salinité du sol et le bilan d'azote [Impact of irrigation with treated wastewater on the productivity of an open-field tomato crop, soil salinity, and nitrogen balance]. *Ciheam Option Méditerran*. 2005;66:165-171. [Article in French]
19. Agence Francaise de Developement. *Rapport Finale la Réutilisation D'eaux Usées Traitées (REUT) Perspectives Opérationnelles et Recommandations Pour l'action [Final Report on the Reuse of Treated Wastewater (REUT): Operational Perspectives and Recommendations for Action].* Ingenierie BRL; 2011. p. 24/91. [Article in French]
20. Meddour MR, Misseraoui MA, Maiga KS, Laaref AM. *La Valorisation des Eaux usée Après Traitement [The Valorization of Wastewater After Treatment]*. Germany: Researchgate; 2020.
doi: 10.13140/RG.2.2.18773.04321. [Article in French]
21. Bel Haj H, Ben Zhir K, Aboulhassan MA, El Ouarghi H. Impact assessment of treated wastewater reuse for irrigation: Growth potential and development of lettuce in Al Hoceima province, Morocco. *E3S Web Conf.* 2023;364:01002.
doi: 10.1051/e3sconf/202336401002
22. Guasmi I, Hadji F, Yebdri L. Quality assessment of reclaimed water for irrigation purpose and aquatic life protection in the Mekerra sub-watershed (NW Algeria). *Model Earth Syst Environ.* 2021;8:3399-3412.
23. Santos AF, Alvarenga P, Gando-Ferreira LM, Quina MJ. Urban wastewater as a source of reclaimed water for irrigation: Barriers and future possibilities. *Environments*. 2023;10:17.
doi: 10.3390/environments10020017
24. Benzaria M. *Approche Méthodologique Pour Les Projets de Réutilisation des Eaux Usées en Irrigation [Methodological Approach for Wastewater Reuse Projects in Irrigation]. Mémoire Présenté Comme*

Exigence Partielle de la Maîtrise En Sciences de L'environnement, Université du Québec à Montréal; 2008. [Article in French]
25. Bel Haj H, El Ouarghi H, El Yousfi Y, *et al*. Reuse of wastewater for irrigation of coriander in Morocco: Evaluation of effects on crop growth parameters. *World Water Policy*. 2023;9:799-814.
26. Bouchaala L, Charchar N, Sahraoui H, Gherib A. Assessment of wastewater biological treatment efficiency and mapping of WWTPs and LTPs in Algeria. *J Environ Health Sci Eng*. 2021;19:1153-1169. doi: 10.1007/s40201-021-00682-1
27. Baumont S, Camard JP, Lefranc A, Franconi A. *Réutilisation des Eaux Usées: Risques Sanitaires Et Faisabilité en Île-de-France [Wastewater Reuse: Health Risks and Feasibility in Île-de-France]. Rapport ORS*. Institut D'Aménagement et D'Urbanisme de la Région Ile-de-France; 2006. p. 220. [Article in French]
28. Technische Universität Berlin. Homepage of Prof. Dr. F. Kreuzig. Available from: https://www.user.tu-berlin.de [Last accessed on 2025 Jan 22].
29. Abachi L. *Recyclage des eaux usées à Boumerdès: une expérience positive [Wastewater Recycling in Boumerdes: A Positive Experience]*. Le Soir d'Algérie. 2009. Available from: https://www.lesoirdalgerie.com/. [Article in France] [Last accessed 2011 Jun 06].
30. CNS Conseil National Economique et Social. *L'eau en Algérien, le Grand Défi de Demain [Water in Algeria, Tomorrow's Great Challenge]. Rapport du Conseil National Economique et Social. 15ième Session*; 2000. p. 1-89. [Article in French]
31. Mohammed T, Yacine L, Ahmed B. Management of water resources sector to face climatic shocks in Algieria: A dynamic CGE model analysis. *Environ Soc Econ Stud*. 2020;8:48-55.
32. Djellouli-Tabet Y. Common scarcity, diverse responses in the Maghreb Region. In: *Water and Sustainability in Arid Regions*. Berlin: Springer; 2009.
33. Boudjadja A, Messahel M, Pauc H. Assessment of water resources in Northern Algeria. *J Water Sci.* 2003;16(3):285-304. doi: 10.7202/705508ar
34. Alzahrani F, Elsebaei M, Tawfik M. Public Acceptance of treated wastewater reuse in the agricultural Sector in Saudi Arabia. *Sustainability*. 2023;15:15434.
35. Mozas M, Ghosn A. *État des Lieux du Secteur de l'eau en Algérie [Overview of the Water Sector in Algeria]. Études & Analyses*. Paris: IPEMED Institue de Prospective Économique du Monde Méditerranéen; 2013. [Article in French]
36. Office Nationale d'Assainissement. *Direction de l'Exploitation et de la Maintenance. Tableau de Bord Mensuel Juillet*; 2016. p. 30. Available from: https://portail.ona-dz.com [Article in French]
37. Office Nationale d'Assainissement. *Direction de l'Exploitation et de la Maintenance. Tableau De Bord Exploitation [Operational Dashboard*]. Mumbai: Office Nationale d'Assainissement. [Article in French]
38. Algerian Government. [Décret exécutif nº 07-149 fixant les modalités de concession d'utilisation des eaux usées épurées à des fins d'irrigation ainsi que le cahier des charges-type y afferent [Executive decree No. 07-149 establishing the terms of concession for the use of treated wastewater for irrigation purposes and the related standard specifications.]. *Off J Alger Repub*. 2007;35:8-12. [Article in French]
39. Hamouch C, Chaaouan J, Bouiss CE. Spatial-temporal assessment of soil erosion using the RUSLE model in the upstream Inaouène watershed, Northern Morocco. *Nat Hazards Res.* 2024.
40. SeaTemperature.info. Sea Water Temperature and Marine Climate Data. Available from: https://www.seatemperature.info [Last accessed on 2025 Jan 22].
41. *Hochschule für Grafik und Buchkunst Leipzig (Academy of Fine Arts Leipzig*). Available from: https://www.hgb-leipzig.de [Last accessed on 2025 Jan 23].

Asian Journal of Water, Environment and Pollution. Vol. 22, No. 3 (2025), pp. 185-197.
doi: 10.36922/AJWEP025170132

ORIGINAL RESEARCH ARTICLE

Determining optimal cultivation parameters for a portable hydroponic system using the nutrient film technique

Kateryna Vasylkovska[1]*, Mykola Kovalov[1], Oleksii Vasylkovskyi[2], and Daria Michailova[3]

[1]Department of General Agriculture, Faculty of Agro-technical, Central Ukrainian National Technical University, Kropyvnytskyi, Kirovohrad Oblast, Ukraine
[2]Department of Agricultural Engineering, Faculty of Agro-technical, Central Ukrainian National Technical University, Kropyvnytskyi, Kirovohrad Oblast, Ukraine
[3]Department of Professionally Oriented Disciplines, Kropyvnytskyi Agrarian Professional College, Kropyvnytskyi, Kirovohrad Oblast, Ukraine
***Corresponding author:** Kateryna Vasylkovska (vasylkovskakv@kntu.kr.ua)

Received: April 27, 2025; Revised: May 15, 2025; Accepted: May 26, 2025; Published online: June 19, 2025

Abstract: Changes in climatic conditions in Ukraine and around the world pose a certain threat to food security and force us to seek new technological opportunities for growing agricultural products. This study aims to identify the optimal cultivation parameters for growing vegetable and berry plants in a portable, compact, and easy-to-maintain hydroponic nutrient film technique (NFT) system. The goal is to achieve high product quality and maximize plant yields by utilizing phytomatrix equipped with red and blue light-emitting diode (LED) elements in a 4:1 ratio, combined with a nutrient solution based on biological products. An experimental portable hydroponic NFT system was developed, incorporating these phytomatrices for additional lighting. This specific red-to-blue light ratio enhances photosynthesis efficiency, promotes yield increases, and ensures the quality development of plant structural parts. In addition, the use of a roller system allows for easy movement of the plants as needed. The study examined the effects of several factors on the growth performance of basil plants (Rutan variety), including seed treatment with the effective microorganisms (EM)-5 concentrate, air and nutrient solution temperature, and nutrient solution concentration. It was determined that the optimal conditions for basil growth include an air and nutrient solution temperature range of 24 – 26°C. Furthermore, increasing the nutrient solution concentration to an optimum level of 2.4 – 2.5 mS/cm resulted in significant improvements across all measured growth parameters of Rutan basil plants. Therefore, growing vegetable crops in a hydroponic installation with phytomatrices with red and blue LED emitting elements in a ratio of 4:1 and using a nutrient solution based on EM preparations will make it possible to increase their productivity.

Keywords: Basil plants; Effective microorganism preparations; Hydroponic plant; Lighting; Nutrient solution; Phytomatrix

1. Introduction

Global and Ukrainian food security depends on multiple factors; primarily the population's ability to meet daily energy needs and maintain a nutritionally balanced diet. The ongoing war in Ukraine has further intensified the food crisis, worsening the challenges related to ensuring stable and sufficient food supplies.[1]

In the context of increasingly risky farming conditions in northern and central Ukraine, the

cultivation of moisture-demanding vegetable crops has become particularly challenging.[2,3] Similar problems are also inherent in southern Europe, where climate change negatively impacts agricultural productivity. In response, vertical farming offers a promising solution to overcome the problem of land shortage.[4-6] In risky farming zones, vegetable crops are primarily cultivated using various irrigation methods.[7,8] Techniques such as drip irrigation, injection irrigation, and hydroponics elements are the main components of the technological process of growing these crops.

Hydroponics represents a breakthrough in agricultural production, enabling plants to grow in nutrient-rich water solutions instead of soil. This method offers several advantages, including higher yields, improved water efficiency, and adaptability to poor soil conditions. Various hydroponic systems – such as the nutrient film technique (NFT), deep water culture (DWC), aeroponics, and vertical farming – facilitate plant growth by supplying nutrients and oxygen directly to the roots.[6,9] In addition, hydroponic systems offer advantages over traditional farming, particularly due to their suitability for urban environments.[10,11] When integrated with smart technologies, hydroponic farming supports sustainable agricultural development by combining low maintenance costs with high yields. This results in significant economic benefits, making it an attractive option for suburban farms and urban settings.[12,13] Moreover, installing photovoltaic panels on greenhouse rooftops can reduce the intensity of solar radiation reaching the plants, creating a shading effect that is beneficial for heat-sensitive crops such as tomatoes, peppers, and onions. This approach not only minimizes heat stress but also improves the overall energy efficiency of the system.[14] Furthermore, in greenhouse cultivation, light-emitting diode (LED) lighting can be used to support efficient photosynthesis. Optimized LED light spectra can enhance the accumulation of antioxidants, phenolic compounds, and total sugars in plants such as lettuce, cabbage, cucumber, and spinach.[15]

There are various types of hydroponic systems, each characterized by specific features depending on crop type, space availability, equipment complexity, and overall economic cost.[15,16] The main types of hydroponic systems include (Table 1):

(i) Candlewick (wick)
(ii) DWC
(iii) Periodic flooding
(iv) NFT
(v) Aeroponics.

The wick system is one of the most affordable hydroponic methods, requiring no specialized equipment. In this system, the wick or cord passes through the bottom of the pot and is immersed in a nutrient solution, which gradually delivers nutrients to the plant roots. In the DWC system, plants are supported on floating materials, such as foam or specialized nets, with their roots completely immersed in the nutrient solution. Oxygen is supplied to the roots using an air pump. The periodic flooding method involves the use of a tidal system where the nutrient solution is delivered at set intervals controlled by a timer. When the supply stops, the solution drains back into the tank through special holes by gravity. This cycle is repeated several times a day. In the NFT system, plants are positioned in a tank with an irrigation channel through which a thin layer of nutrient solution flows. This solution washes the roots as it moves down the channel and then returns to the tank. The nutrient solution can be supplied either continuously or in cycles, with cyclical supply offering improved root aeration.[17] In the aeroponics system, plants grow in an open, airy environment where their roots are continuously enveloped in a mist of nutrient solution. This system provides high oxygen availability to the roots, enhancing nutrient absorption and accelerating plant growth.[18]

The advantages and disadvantages of each hydroponic system are presented in Table 1.

As shown in Table 1, the choice of hydroponic system depends on the plant type. Therefore, selecting an appropriate system requires a clear understanding of the equipment needed for the soilless cultivation of specific crops.

Regardless, a hydroponic NFT system is considered the most suitable option for growing plants in limited spaces. One of its major advantages is the efficient use of water, as the nutrient solution is continuously recirculated. Furthermore, the constant flow helps prevent the accumulation of salts on plant roots, supporting healthier growth. In addition, the NFT system is a vertical hydroponic technique that maximizes space utilization and conserves water. It offers a promising solution for sustainable agricultural development, particularly in regions facing climate challenges and located in risky farming zones.[19]

This study aims to identify the optimal technological components for cultivating plants in a portable, compact, and easy-to-maintain hydroponic NFT system. The goal is to achieve high-quality products and plant yields through the integration of phytomatrix with radiating elements and the application of a nutrient solution enriched with biological products.

Table 1. Hydroponic systems and their advantages and disadvantages

Hydroponic system	General view of the system	Advantages	Disadvantages
Candlewick system	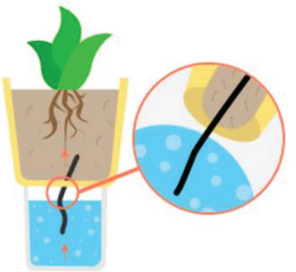	Ease of use, low cost, reliable, and suitable for growing small plants with low water consumption	Lack of oxygen slows plant development due to passive nutrient supply
Deep water culture	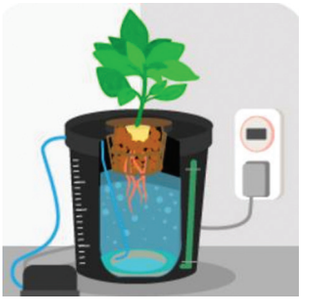	Easy to use; low cost; promotes rapid plant development; and suitable for growing large, fast-growing plants	If not cleaned properly, root system diseases such as mold and root neck rot may occur
Periodic flooding	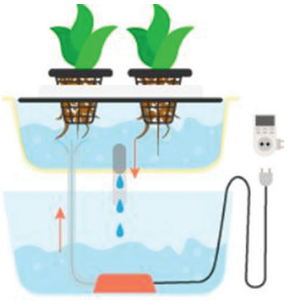	Ease of use; fully automated system requiring no expensive equipment; provides good nutrient saturation, with some nutrients retained in the substrate	Power outage prevents the system from operating
Nutrient film technique	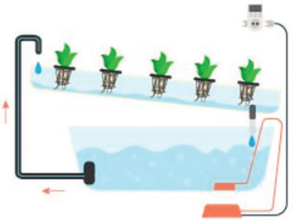	No substrate is used, reducing overall crop production costs; provides constant moisture and aeration to the roots, promoting rapid plant growth	Pump failure or power outage completely disrupts the system, causing roots to dry out quickly
Aeroponics	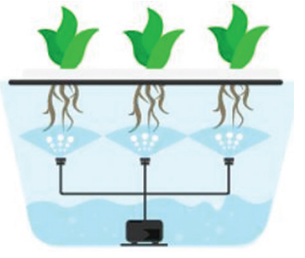	Enrichment of plant roots with oxygen, water, and nutrients promotes plant growth	The timer controlling water supply requires monitoring; nutrient-dispersing nozzles are prone to clogging

2. Materials and methods

The study was conducted from 2022 to 2024 in a controlled environment at the hydroponic vegetable growing laboratory, located in a dome greenhouse at the Department of General Agriculture, Central Ukrainian National Technical University. The experimental material consisted of elite seeds of the early variety

"Rutan" basil (*Ocimum basilicum*), developed by the "Mayak" Research Station of the Institute of Vegetable and Melon Growing of the National Academy of Agricultural Sciences, Ukraine. The vegetation period for this variety ranges from 60 to 66 days.

The main parameters of the study included:

(i) A standard hydroponic nutrient solution formulated for leafy crops, containing micro- and macroelements within the recommended concentration range for basil.[20] To enhance the nutrient solution, the effective microorganisms-5 (EM-5) preparation was incorporated. This preparation contains beneficial microorganisms known to stimulate root system activity, improve physiological processes, and increase plant yields.[16]

(ii) Phytomatrices with red and blue LED emitting elements in a ratio of 4:1 were used for lighting.[21,22]

(iii) The temperature regime was maintained within the range of 20 – 24°C, with a relative humidity of 60 – 70%.

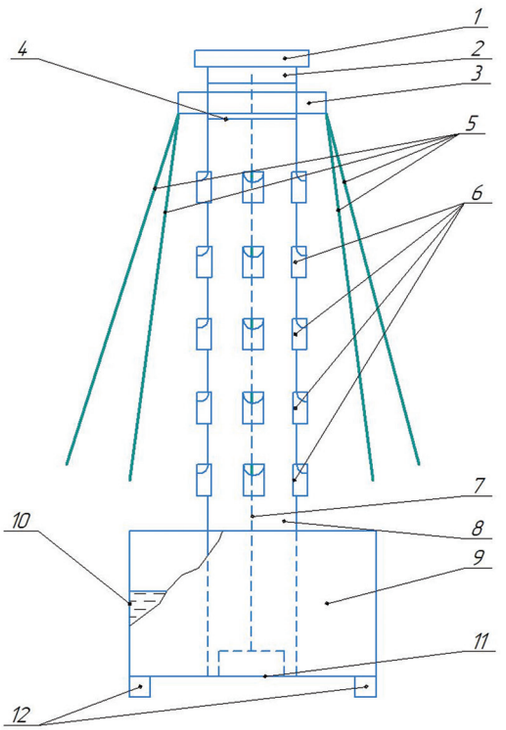

Figure 1. Schematic diagram of the portable hydroponic nutrient film technique system: (1) air valve; (2) nutrient solution distribution unit; (3) phytomatrix fastening unit; (4) nutrient solution supply unit; (5) phytomatrix with radiating elements; (6) hydroponic baskets; (7) nutrient solution supply pipeline; (8) vertical hydroponic column; (9) tank; (10) sensor of the minimum level of nutrient solution at the tank; (11) pumping system with a water pump; and (12) roller system

To enhance the efficiency of growing vegetable and berry crops, the Central Ukrainian National Technical University developed a pilot portable hydroponic NFT unit incorporating phytomatrix.[7,21] This unit operates on the NFT principle and features a vertical column-shaped structure that ensures compactness and allows a fixed number of plants to be grown within a limited space (Figures 1 and 2A).

As illustrated in Figure 1, the hydroponic column (number 8) is a pipe that contains a nutrient solution supply pipe (number 7), which is fed from a reservoir (number 9) to the top of the column through a pumping system and water pump (number 11). Inside the reservoir, a sensor (number 10) monitors the minimum nutrient solution level to maintain proper operation. At the upper part of the hydroponic column (number 8), there is an air valve (number 1), a nutrient solution distribution unit (number 2), and a phytomatrix attachment unit (number 3) equipped with radiating elements. Below this is the nutrient solution supply unit (number 4), to which phytomatrix components (number 5) are attached and extended downward. Equally spaced around the

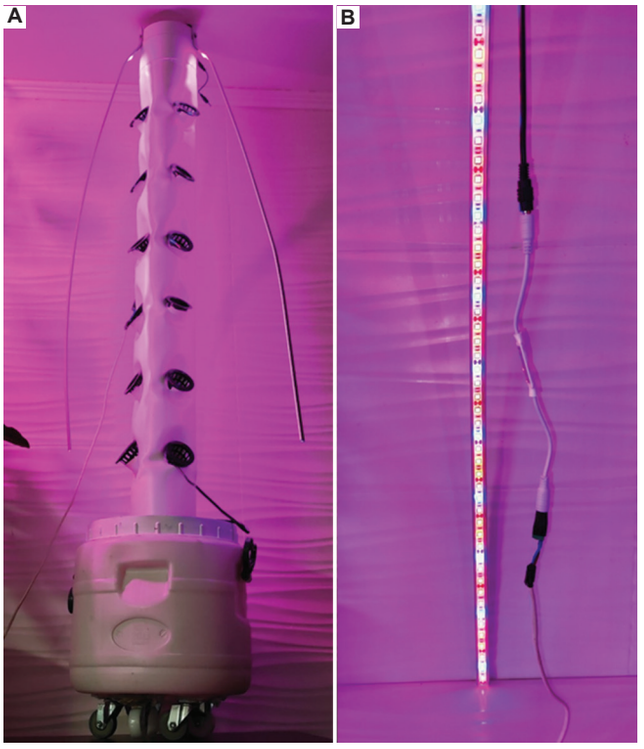

Figure 2. General view of (A) portable hydroponic nutrient film technique system and (B) phytomatrix with radiating elements

perimeter of the column are holes for hydroponic baskets (number 6), through which the nutrient solution is delivered. The hydroponic plant structure is mounted on the roller system (number 12), allowing it to be moved as needed.

The system was operated as follows: The nutrient solution from the reservoir (number 9) was supplied using a pumping system and a water pump (number 11), flowing through the nutrient solution supply pipelines (number 7) to the hydroponic baskets (number 6), where the plants received the nutrient solution in a thin layer. The hydroponic plants used phytomatrix (number 5) equipped with red and blue LED emitting elements in a 4:1 ratio for additional lighting (Figure 2B).[9,22,23] The red light (650 – 700 nm) is crucial for photosynthesis as it stimulates growth, flowering, and fruit formation. Blue light (400 – 500 nm) is important during the early stages of plant development, supporting strong root formation, stem strengthening, and leaf growth. The high proportion of red light accelerates photosynthesis and increases yields, while blue light ensures the quality development of the plant's structural parts. This combination is suitable for growing various types of crops, including vegetables and herbs.

This study aimed to implement a central compositional matrix plan 2^3 to evaluate the effects of factors – such as the EM-5 concentrate, air temperature, nutrient solution temperature, nutrient solution concentration, and operational parameters – on the performance of the portable NFT system to ensure maximum efficiency in growing vegetable crops.

An experimental planning matrix is shown in Table 2.

The EM-5 concentrate was selected based on recommendations from earlier research,[7] which identified 0% and 2% as appropriate concentrations for seed treatment. Similarly, the air and nutrient solution temperatures were set at 18°C and 26°C, respectively, as these values were found to support optimal plant development in previous research.[18,21] The nutrient solution concentration was selected according to findings from earlier studies.[17,21] which identified 0.5 mS/cm and 2.5 mS/cm as effective levels for nutrient uptake.

Based on the conditions described above, the optimization criteria for growing vegetable crops in the improved portable hydroponic NFT system were defined as follows:

(i) Plant height (cm)
(ii) Time to reach the baby leaf stage (days)
(iii) Fresh weight (g)
(iv) Number of leaves (pieces).

The reproducibility of the experiments was evaluated using Cochran's test:[24]

$$G = \frac{S^2_{u\max}}{\sum_{u=1}^{n} S^2_u} \le G(0.05; n; f_u) \quad \text{(I)}$$

Where:

(i) $G(0.05;n;f_u)$ is the tabular value of Cochran's test,
(ii) $S^2_{u\max}$ is the largest variance among all experimental conditions,
(iii) 0.05 is the mean 5%-th level of importance,
(iv) n is the number of independent variance estimates (number of experiments),
(v) $f_u = (m_0 - 1)$ is the number of degrees of freedom,
(vi) m_0 is the number of repeated measurements (repeatability).

$$S^2_u = \frac{1}{m_0 - 1} \cdot \sum_{i=1}^{m_0} (Y_{ui} - \bar{Y}_u)^2 \quad \text{(II)}$$

Where:

(i) s^2_u is the variance representing the dispersion of

Table 2. An experiment planning matrix 2^3

Number of experiments	Effective microorganisms-5 concentrate (%)	Air and nutrient solution temperature (°C)	Concentration of nutrient solution (mS/cm)
	x_1	x_2	x_3
1	−1	−1	−1
2	+1	−1	−1
3	−1	+1	−1
4	+1	+1	−1
5	−1	−1	+1
6	+1	−1	+1
7	−1	+1	+1
8	+1	+1	+1

results in the *u*-the experiment,
(ii) m_0 is the number of repeated measurements (repeatability),
(iii) *i* is the number of repetition,
(iv) Y_{ui} is the output parameter at the *i*-th repetition.

The reproducibility of the experiments was determined using Cochran's test (*G*-test), where the condition $G^P < G^T$ must be satisfied. If $G^P > G^T$, this indicates a deviation from the hypothesis, suggesting that the effectiveness of adjustments to the object under study and the measuring instruments needs to be verified.

The variance of reproducibility (error of the experiment) was determined by the formula:

$$S_y^2 = \frac{1}{n} \cdot \sum_{u=1}^{n} S_u^2 \quad \text{(III)}$$

Where:
(i) *u* is the observation index,
(ii) *n* is the number of experiments,
(iii) S_u^2 is the variance representing the dispersion of results in the *u*-the experiment.

The coefficients of the mathematical model were determined by the following formulas:

$$b_0 = \frac{1}{n} \cdot \sum_{u=1}^{n} \overline{y}_u, \quad \text{(IV)}$$

$$b_i = \frac{1}{n} \cdot \sum_{u=1}^{n} x_{iu} \cdot \overline{y}_u, \quad \text{(V)}$$

$$b_{ij} = \frac{1}{n} \cdot \sum_{u=1}^{n} x_{iu} \cdot x_{ju} \cdot \overline{y}_u \quad \text{(VI)}$$

Where:
(iv) x_{iu} is the value of the *i*-th code factor in the matrix row in the *u*-th trial,
(v) x_{ju} is the value of the *j*-th code factor in the matrix row in the *u*-th trial,
(vi) b_0 is the free member of a regression equation,
(vii) b_i is the experimental coefficient, which indicates the degree of influence of the corresponding factor on Y,
(viii) b_{ij} is the experimental coefficient, which reflects the degree of influence of factors on Y,
(ix) *n* is the number of experiments,
(x) *u* is the observation index,
(xi) $\overline{y}_u$ is the mean value of the dependent variable Y.

The adequacy of the equation was assessed using Fisher's test (*F*-test). Adequacy is confirmed if:

$$F = \frac{S_{ad}^2}{S_y^2} < F(0.05; f_{ad}; f_y) \quad \text{(VII)}$$

Where:
(i) Δb_a is the variance of adequacy,
(ii) SS_y^2 is the reproducibility dispersion,
(iii) $F(0.05;f_{ad};f_y)$ is the critical value of Fisher's test at 5% significance level,
(iv) $f_{ad = n - k-1}$ is the degrees of freedom for adequacy variance,
(v) *k* is the factor's number,
(vi) f_y is the degrees of freedom of the playback variance, where $fy = n\ (m_0 - 1)$.

Variance of adequacy (S_{ad}^2) was calculated using the formula:

$$S_{ad}^2 = \frac{1}{n-k-1} \cdot \sum_{u=1}^{n} (Y_u - \overline{Y}_u)^2 \quad \text{(VIII)}$$

Where Y_u is the calculated value of the response in the *i*-th experiment.

The significance of the regression coefficients was determined using Student's *t*-test. A coefficient b_a is considered significant if the following condition is met:

$$|b_a| \geq \Delta b_a = t(0.05; f_y) . \frac{s_y}{\sqrt{n}} \quad \text{(IX)}$$

Where:
(i) b_a *is* the regression coefficients b_0, b_1, b_2, and $b_{1,2}$,
(ii) Δb_a is the confidence boundary (threshold),
(iii) $t(0.05;f_y)$ is the critical value of the Student's *t*-test at a 5% significance level with degrees of freedom of reproducibility variance f_y.

The significance of the regression coefficients was assessed by setting the coefficients of the quadratic regression terms to zero (null hypothesis). To evaluate this, additional experiments were conducted at the center point of the experimental design. The average value of the optimization $\overline{Y}_0$ criterion at the center was determined, and the deviation from the predicted value ($b_0 - \overline{Y}_0$) was calculated. This deviation characterizes the curvature of the response surface. The null hypothesis is accepted if the observed deviation does not exceed the experimental error. The significance of this deviation ($b_0 - \overline{Y}_0$) was evaluated using Student's *t*-test:

$$t_d = \frac{\left(b_0 - \overline{Y}_0\right)\sqrt{N}}{\sqrt{S_y^2}} \quad \text{(X)}$$

(xii) b_0 is the free member of a regression equation,
(xiii) *N* is the number of degrees of freedom,

(xiv) $b_0 - \overline{Y}_0$ is the deviation from the predicted value,

(xv) S_y^2 is the reproducibility dispersion.

The calculated value t_d was then compared to the critical value from the statistical tables,[24] selected based on the significance level of $\alpha = 0.05$ and degrees of freedom $f_t = N$. If the inequality, $|b_i| < |\Delta b_i|$ was satisfied, the corresponding factor was considered for reassessment, particularly regarding the possibility of adjusting its variation interval. In such a case, all relevant experiments were repeated. If, after reassessment, the coefficient continued to meet the same condition, it was concluded that the influence of the factor x_i on the optimization parameter was statistically insignificant Y_i.

The purpose of interpreting the resulting statistical model is to analyze the influence of factors on the optimization criterion. The degree of influence of each factor was assessed based on the value and sign of the corresponding regression coefficient b_i. A positive sign (+) indicates that an increase in the factor x_i leads to an increase in the optimization parameter Y_i, while a negative sign (−) indicates that an increase in x_i results in a decrease in Y_i.

3. Results and discussion

A central compositional matrix plan 2^3 was established to evaluate the effects of several factors, including the EM-5 concentrate, air and nutrient solution temperature, and nutrient solution concentration. In addition, the experiment was performed to identify the optimal parameters and operating modes of the improved portable hydroponic NFT unit to ensure maximum efficiency in plant growth and development. The results obtained from the implementation of the experimental matrix are presented in Table 3.

The experimental data were processed using the STATISTICA 12 software package (StatSoft, USA),[24] which was used to construct statistical mathematical models for the following response variables: Y_1 (plant height), Y_2 (time to reach the baby leaf stage), Y_3 (fresh weight), and Y_4 (number of leaves).

The resulting regression equations are as follows:

$$Y_{=} 3.46 + 0.16x_1 + 0.26x_2 + 0.66x_3 + 0.01x_1x_3 + 0.01x_1x_2 + 0.01x_2x_3 + 0.01x_1x_{2X3} \quad \text{(XI)}$$

$$Y_2 = 14.5 - 0.5x_1 - 1.0x_2 - 2.0x_3 \quad \text{(XII)}$$

$$Y_3 = 0.95 + 0.05x_1 + 0.1x_2 + 0.2x_3 \quad \text{(XIII)}$$

$$Y_4 = 5.625 + 0.375x_1 + 0.875x_2 + 1.875x_3 + 0.125x_1x_2 + 0.125x_1x_3 + 0.125x_2x_3 + 0.125x_1x_2x_3 \quad \text{(XIV)}$$

The significance of the obtained regression coefficients was evaluated using Student's *t*-test. For a reliability level (P_H) of 0.95 and degrees of freedom $f = 7$, the tabulated *t*-value is $t = 2.365$.[23]

After verification, simplified regression equations for Y_1, Y_2, Y_3, and Y_4 were obtained:

Y_1 (plant height): $Y_1 = 3.46 + 0.16x_1 + 0.26x_2 + 0.66x_3$ (XV)

Y_2 (time to reach baby leaf stage: $Y_2 = 14.5 - 0.5x_1 - 1.0x_2 - 2.0x_3$ (XVI)

Y_3 (fresh weight): $Y_3 = 0.95 + 0.1x_1 + 0.2x_3$ (XVII)

Table 3. Results obtained from the implementation of the experimental planning matrix 2^3

Number of experiment	Factors			Criteria			
	Effective microorganisms-5 concentrate (%)	Air and nutrient solution temperature (°C)	Nutrient solution concentration (mS/cm)	Plant height (cm)	Time to reach the baby leaf stage (days)	Fresh weight (g)	Number of leaves (pieces)
	x_1	x_2	x_3	Y_1	Y_2	Y_3	Y_4
1	0	18	0.5	2.4	18	0.6	3
2	2	18	0.5	2.8	17	0.7	3
3	0	26	0.5	3.0	16	0.8	4
4	2	26	0.5	3.3	15	0.9	5
5	0	18	2.5	3.6	14	1.0	6
6	2	18	2.5	4.0	13	1.1	7
7	0	26	2.5	4.2	12	1.2	8
8	2	26	2.5	4.4	11	1.3	9

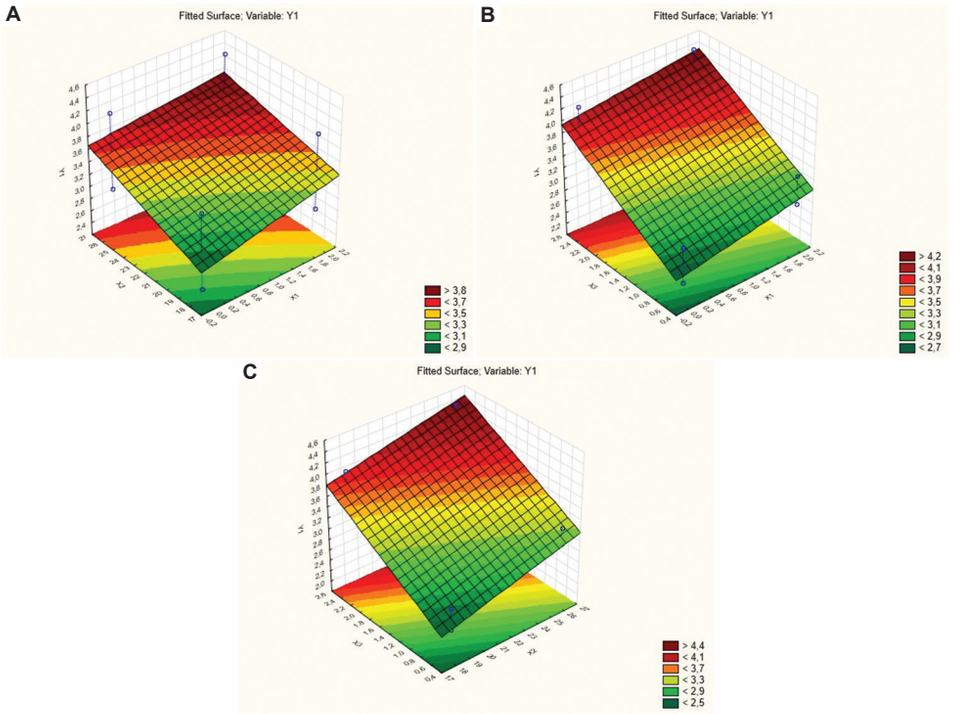

Figure 3. The response surface for plant height (Y_1): (A) $Y_1 = f(x_1, x_2)$; (B) $Y_1 = f(x_1, x_3)$; and (C) $Y_1 = f(x_2, x_3)$

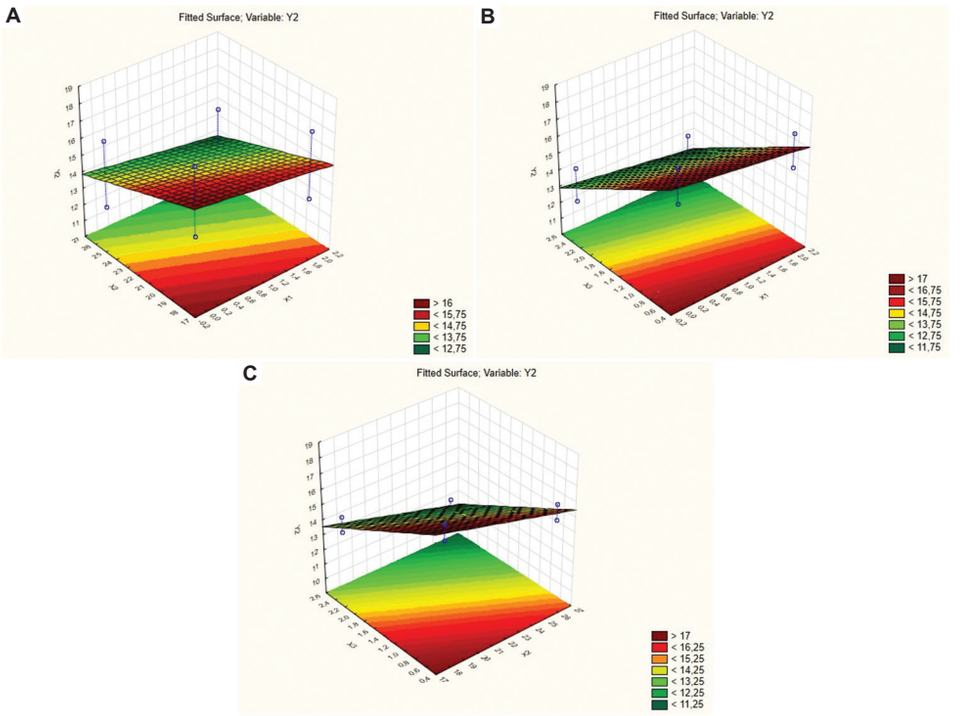

Figure 4. The response surface of time to reach the baby leaf stage (Y_2): (A) $Y_1 = f(x_1, x_2)$; (B) $Y_1 = f(x_1, x_3)$; and (C) $Y_1 = f(x_2, x_3)$

Y_4(number of leaves): $Y_4 = 5.625 + 0.375x_1 + 0.875x_2 + 1.875x_3 + 0.125x_1x_2 + 0.125x_1x_3 + 0.125x_2x_3 + 0.125x_1x_2x_3$ (XVIII)

The statistical evaluation of the results confirms that the experiments are correct and reproducible, as the calculated values of the Cochran's test G^P for the optimization

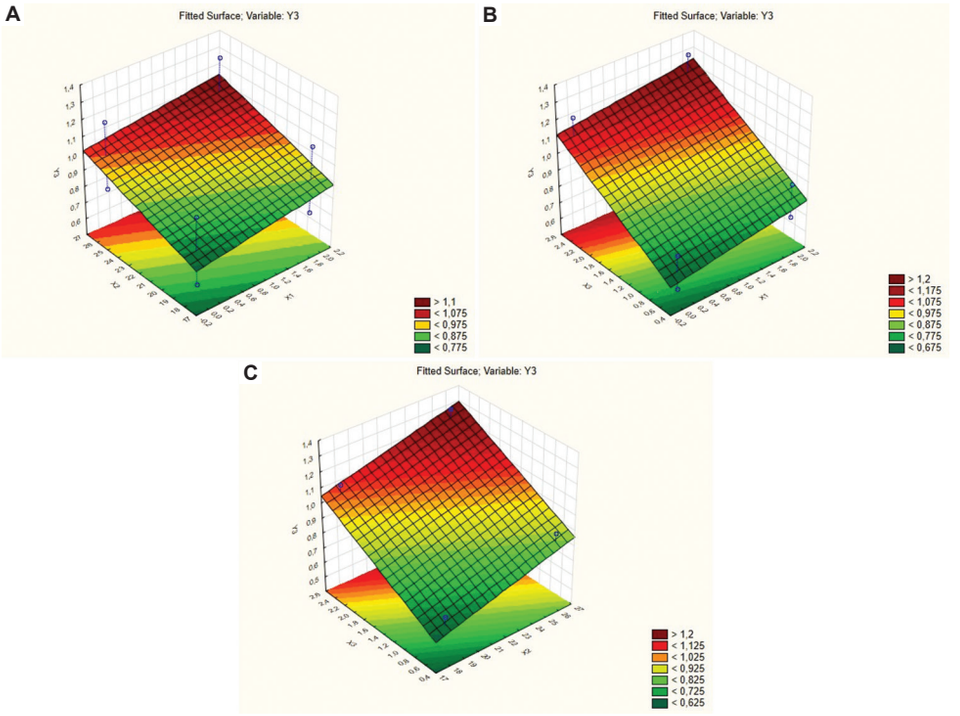

Figure 5. The response surface of fresh weight (Y_3): (A) $Y_1 = f(x_1, x_2)$; (B) $Y_1 = f(x_1, x_3)$; and (C) $Y_1 = f(x_2, x_3)$

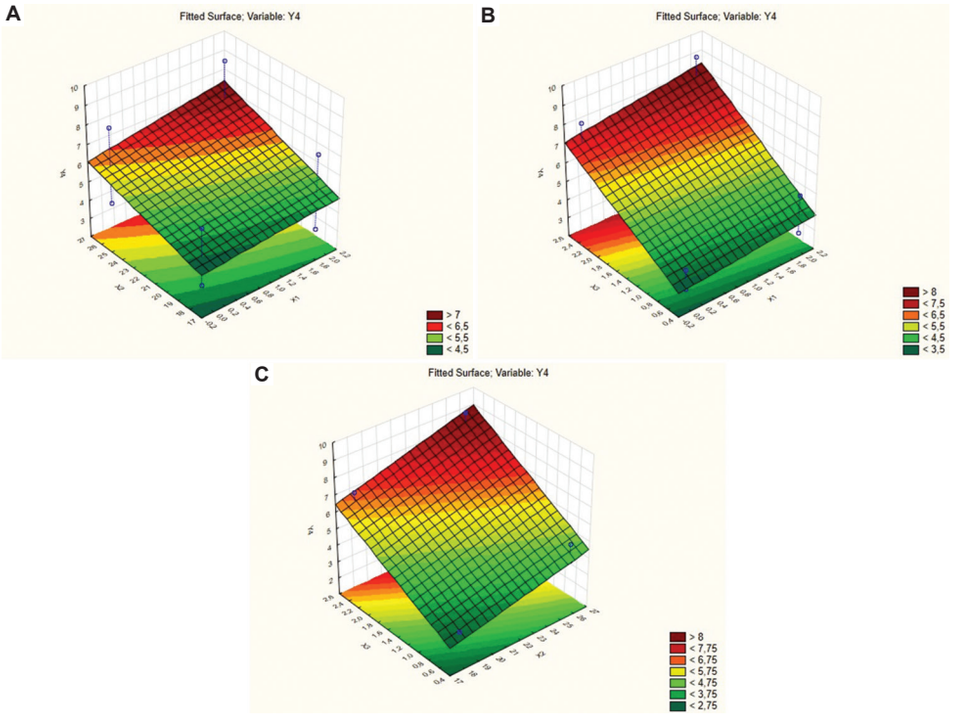

Figure 6. The response surface for number of leaves (Y_4): (A) $Y_1 = f(x_1, x_2)$; (B) $Y_1 = f(x_1, x_3)$; and (C) $Y_1 = f(x_2, x_3)$

parameters Y_1, Y_2, Y_3, and Y_4 are $G_1^p = 0.483$, $G_2^p = 0.488$, $G_3^p = 0.499$, and $G_4^p = 0.500$, respectively, all of which are lower than the tabulated value $G^T = 0.516$.[23]

The adequacy of the regression equations was evaluated using Fisher's test, where the tabulated value is $F^T = 4.15$ for a reliability level (P_H) of 0.95 and the degrees of freedom $f = 8$.[23] The calculated values – $F_1 = 0.54$,

F_2 = 0.00, F_3 = 0.00, and F_4 = 1.87 – do not exceed the tabulated value, confirming the adequacy of all models.

Response surfaces and scatter plots with histograms for plant height (Y_1), time to reach the baby leaf stage (Y_2), fresh weight (Y_3), and number of leaves (Y_4) are shown in Figures 3-6.Based on the response surface analysis for the plant height, the optimal value was observed to be between 3.8 and 4.4 cm. The analysis also identified the following rational values of the studied factors:

(i) The EM-5 concentrate for pre-sowing seed treatment ranged from 1.8% to 2.0%,
(ii) The temperature of air and nutrient solution was maintained within 24 – 26°C,
(iii) The nutrient solution concentration ranged from 2.3 to 2.5 mS/cm.

Among these, the concentration of the nutrient solution had the greatest impact on plant height.Based on the response surface analysis for the time to reach the baby leaf stage, the optimal duration was observed to be between 11 and 13 days. In addition, the analysis identified the following rational values of the studied factors:

(i) The EM-5 concentrate for pre-sowing seed treatment ranged from 1.8% to 2.0%,
(ii) The temperature of air and nutrient solution was maintained within 24 – 26°C,
(iii) The nutrient solution concentration ranged from 2.3 to 2.5 mS/cm.

All factors were found to reduce the time required to reach the baby leaf stage, with the concentration of the nutrient solution having the greatest influence.Based on the response surface analysis for the fresh weight, the optimal weight was observed to be between 1.1 g and 1.3 g. The analysis also identified the following rational values of the studied factors:

(i) The EM-5 concentrate for pre-sowing seed treatment ranged from 1.9 to 2.1%,
(ii) The temperature of air and nutrient solution was maintained within 25 – 26°C,

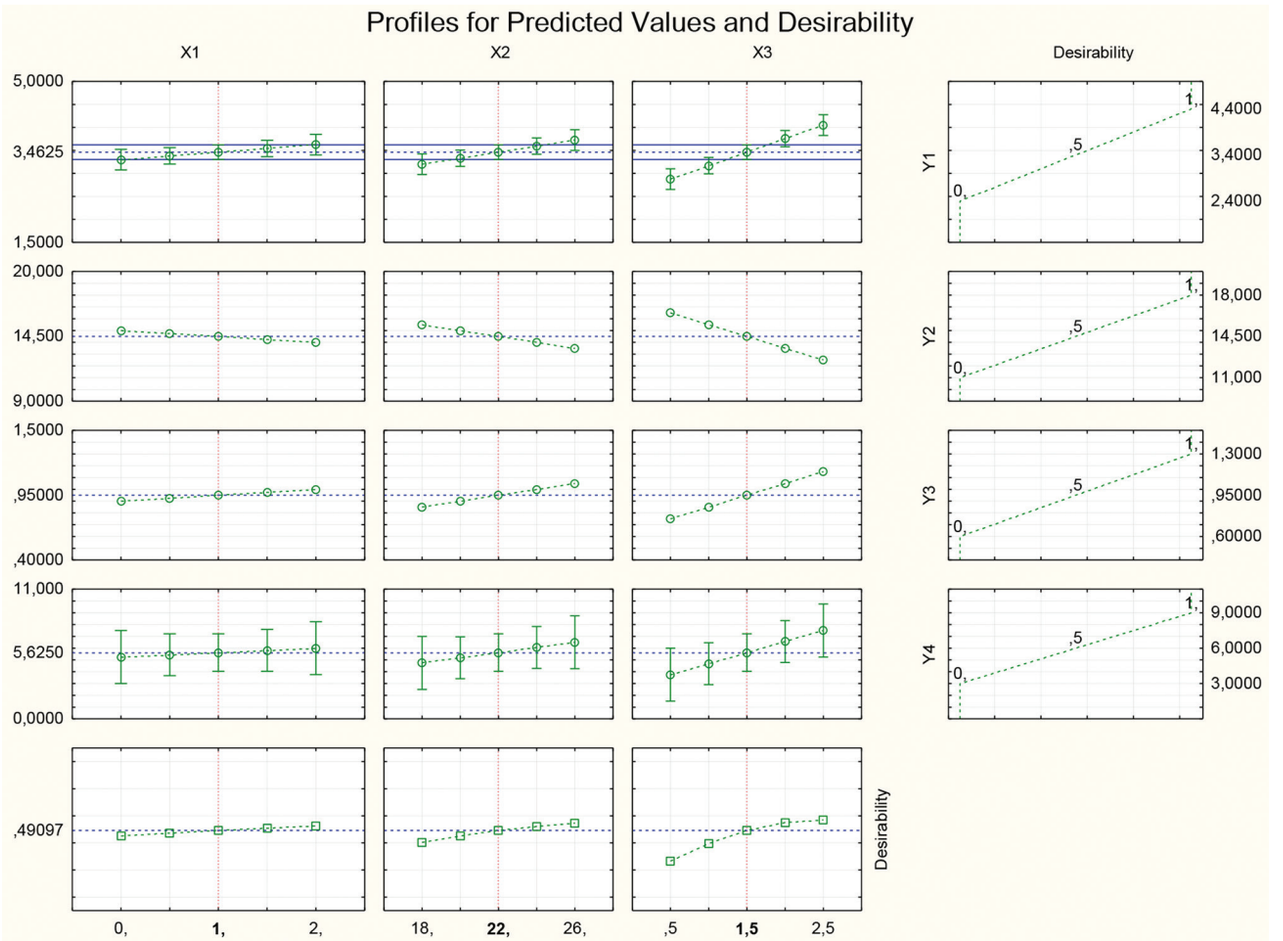

Figure 7. Scatter plots with histograms illustrating the impact of the studied factors on plant height, time to reach the baby leaf stage, fresh weight, and number of leaves

(iii) The nutrient solution concentration ranged from 2.4 to 2.5 mS/cm.

Fresh weight was significantly influenced by the concentration of nutrient solution and the temperature of both air and nutrient solution.Based on the response surface analysis, the optimal number of leaves was observed to be between 7 and 9 pieces. In addition, the analysis identified the following rational values of the studied factors:

(i) The EM-5 concentrate for pre-sowing seed treatment ranged from 1.9% to 2.1%,
(ii) The temperature of air and nutrient solution was maintained within 25 – 27°C,
(iii) The concentration of nutrient solution ranged from 2.4 to 2.5 mS/cm.

All factors—along with their interactions—were found to influence the number of leaves.

To analyze the influence of the studied factors on the optimization criteria, experimental scatter plots with histograms (Figure 7) were generated. These visualizations help identify the rational values of each parameter and estimate the actual values for plant height, time to reach the baby leaf stage, fresh weight, and number of leaves.

Therefore, the proposed technological improvements in the portable hydroponic NFT system, combined with the use of the microbial preparation EM-5 concentrate, offer a promising strategy to enhance seed germination and growth, reduce maturation time, and improve plant weight and number of leaves during pre-sowing seed treatment. Optimizing the temperature of both the air and the nutrient solution also contributes to an increase in the studied parameters and enhances their qualitative characteristics. Among all factors, the nutrient solution concentration is the most influential. An increased concentration ensures a continuous supply of nutrients to the plants, thereby promoting improved plant growth.

4. Conclusion

The proposed improvements to the portable hydroponic NFT system – including the use of a roller system – allow for easy movement of the plant as needed. In addition, upgrading the lighting system with a phytomatrix containing red and blue LED elements in a 4:1 ratio promotes optimal acceleration of photosynthesis and the development of structural plant components. This improvement contributes to increased yield, as confirmed by the experimental findings.

Pre-sowing seed treatment with the EM-5 concentrate enhanced key growth parameters, including plant height, fresh weight, number of leaves, and the time to reach the baby leaf stage. The optimal concentration range for EM-5 was 1.8 – 2.0%. The microorganisms in EM-5 positively affected the root system, enhancing nutrient and water absorption, which in turn improved overall plant health and development.

The optimum temperature for both air and nutrient solution for the growth of Rutan basil was 24 – 26°C. This temperature range promoted plant height, accelerated development to the baby leaf stage, and increased leaf weight and number. However, temperatures exceeding 26°C may induce plant stress and reduce overall quality.

Furthermore, a reduced nutrient solution concentration (0.5 mS/cm) fails to supply sufficient nutrients for normal plant development, resulting in slower growth, lower plant weight, and fewer leaves. In contrast, increasing the concentration to the optimum level (2.4 – 2.5 mS/cm) significantly enhanced all growth parameters.

Acknowledgments

None.

Funding

None.

Conflict of interest

The authors declare that they have no competing interests.

Author contributions

Conceptualization: Kateryna Vasylkovska, Mykola Kovalov
Data curation: Mykola Kovalov, Kateryna Vasylkovska
Formal analysis: Daria Michailova
Investigation: Mykola Kovalov, Daria Michailova
Methodology: Oleksii Vasylkovskyi, Kateryna Vasylkovska
Project administration: Kateryna Vasylkovska
Writing – original draft: Kateryna Vasylkovska
Writing – review & editing: Kateryna Vasylkovska, Mykola Kovalov

Availability of data

The data are available from the respective authors (Kateryna Vasylkivska and Mykola Kovalov) upon reasonable request.

References

1. Vasylkovska K, Vasylkovskyi O, Popova S, Malakhovska V. The directions for optimizing Ukraine's export potential of grain crops in the context of changing climatic conditions. *Ser V Econ Bull Transilvania Univ Braşov*. 2021;14(63):129-136. doi: 10.31926/but.es.2021.14.63.1.14
2. Kovalov M, Vasylkovska K, Reznichenko V, Mostipan M. Agro-ecological aspects of the change of sulphate sulphur content in chernozem of the buh-dnipro interstream area in Ukraine. *WSEAS Trans Environ Dev.* 2019;15:319-323.
3. Vasylkovska K, Andriienko O, Malakhovska V, Vasylkovskyi O, Andriienko A, Shepilova T. Analysis of effective sunflower cultivation zones using the example of Ukraine. *Agron Res.* 2024;22(3):1362-1376. doi: 10.15159/AR.24.097
4. Bersani C, Ruggiero C, Sacile R, Soussi A, Zero E. Internet of things approaches for monitoring and control of smart greenhouses in industry 4.0. *Energies.* 2022;15(10):3834. doi: 10.3390/en15103834
5. Gavrić T, Marković S, Čengić L. Factibility of growing basil as an alternative crop for adaptation to climate change in Bosnia and Herzegovina. *Chil J Agric Res.* 2023;83(1):43-51. doi: 10.4067/S0718-58392023000100043
6. Patel K, Chauhan D, Mishra P, *et al*. Design and development of a modular hydroponic tower with topology optimization. *Int J Interact Des Manuf*. 2024;19:4243-4252. doi: 10.1007/s12008-024-02052-1
7. Kovalov MM, Vasylkovska KV. Influence of the Salt Composition of Nutrient Solution on the Cultivation of Different Varieties of Romaine Lettuce in Hydroponic Columns. In: *Proceedings of the II International Internet Conference 'The Current State of Science in Agriculture and Nature Management: Theory and Practice'*. 2020. p. 81-83.
8. Žlabur JŠ, Opačić N, Žutić I, *et al*. Valorization of nutritional potential and specialized metabolites of basil cultivars depending on cultivation method. *Agronomy.* 2021;11(6):1048. doi: 10.3390/agronomy11061048
9. Sharma N, Acharya S, Kumar K, Singh N, Chaurasia OP. Hydroponics as an advanced technique for vegetable production: An overview. *J Soil Water Conserv.* 2018;17(4):364. doi: 10.5958/2455-7145.2018.00056.5
10. Burlaka S, Lyts P, Kupchuk I. Evaluation of productivity and energy consumption in hydroponics. *Herald Khmelnytskyi Natl Univ Tech Sci.* 2024;339(4):290-295. doi: 10.31891/2307-5732-2024-339-4-46
11. Kupchuk I, Melnyk O. Mathematical modelling of the effect of irradiation on the productivity of the process of growing plant products in a hydroponic plant. *Herald Khmelnytskyi Natl Univ Tech Sci.* 2024;331(1):83-88. doi: 10.31891/2307-5732-2024-331-14
12. Azhari, Simanjuntak D, Hakim L, Sabar. Design and control system of temperature and water level in hydroponic plants. *J Phys.* 2022;2193(1):012018. doi: 10.1088/1742-6596/2193/1/012018
13. Christofi A, Margariti G, Salapatas A, *et al*. Determining the nutrient content of hydroponically-cultivated microgreens with immersible silicon photonic sensors: A preliminary feasibility study. *Sensors*. 2023;23(13):5937. doi: 10.3390/s23135937
14. Hao W, Tablada A, Shi X, Wang L, Meng X. Efficiency analysis of the photovoltaic shading and vertical farming system by employing the artificial neural network (ANN) method. *Buildings.* 2023;14(1):94. doi: 10.3390/buildings14010094
15. Nájera C, Gallegos-Cedillo VM, Ros M, Pascual JA. LED lighting in vertical farming systems enhances bioactive compounds and productivity of vegetables crops. *Biol Life Sci Forum.* 2022;16(1):24. doi: 10.3390/IECHo2022-12514
16. Kovalov MM, Vasylkovska KV, Reznichenko VP, Mostipan MI. *Patent No. 142316 U Ukraine: A Cold Method of Preparing Straw Substrates Using EM Preparations*. 2020.
17. Vasylkovska K, Kovalov M, Andriienko O, Kornicheva H. Technical support of hydroponics as a progressive type of growing vegetable crops. *Natl Interag Sci Tech Collect Work Des Prod Exploit Agric Mach.* 2022;52:81-86. doi: 10.32515/2414-3820.2022.52.81-86
18. Sahara A, Saputra R.H, Asis M, Lawasnitro A. Design of Hydroponic Planting Media Based on Solar Cell Power. In: *Conference: 2021 7th International Conference on Electrical, Electronics and Information Engineering* (*ICEEIE*). Malang, Indonesia: IEEE; 2021. doi: 10.1109/ICEEIE52663.2021.9616657
19. Shrivastava A, Nayak CK, Dilip R, Samal SR, Rout S, Ashfaque SM. Automatic robotic system design and development for vertical hydroponic farming using IoT and big data analysis. *Mater Today Proc.* 2021;80:3546-3553. doi: 10.1016/j.matpr.2021.07.294
20. Hussain AS, Brown PB. Current status of the propagation of basil in aquaponic systems: A literature review. *Aquac Res.* 2025;2025(1):1-13. doi: 10.1155/are/1320019
21. Kovalov MM. The influence of climate support parameters on microgreen cultivation under the conditions of a film greenhouse. *Taurian Sci Her.* 2022;126:153-162. doi: 10.32851/2226-0099.2022.126.21
22. Baranovskyi V, Boretska T, Kohut V. Interactive impact

of the spectral composition of additional lighting and root zone temperature on the productivity of hydroponic lettuce. *Vib Eng Technol.* 2024;115(4):24-30. doi: 10.37128/2306-8744-2024-4-3

23. Budavári N, Pék Z, Helyes L, Takács S, Nemeskéri E. An overview on the use of artificial lighting for sustainable lettuce and microgreens production in an indoor vertical farming system. *Horticulturae.* 2024;10(9):938. doi: 10.3390/horticulturae10090938
24. Wambua RM. *Engineering Research Methods: Research Proposal, Structure of a Paper, Data Collection and Analysis*. Munich, Germany: GRIN Verlag; 2022. p. 110.

Asian Journal of Water, Environment and Pollution. Vol. 22, No. 3 (2025), pp. 198-210.
doi: 10.36922/AJWEP025130088

ORIGINAL RESEARCH ARTICLE

The effects of urbanization on air pollution and public health in Vietnam: An empirical analysis

Duy Hung Bui[1] and Xuan-Hoa Nghiem[2]*

[1]Faculty of Economics, Banking Academy of Vietnam, Dong Da District, Hanoi, Vietnam
[2]Faculty of Economics and Management, International School, Vietnam National University, Hanoi, Vietnam
***Corresponding author:** Xuan-Hoa Nghiem (hoanx@vnu.edu.vn)

Received: March 25, 2025; Revised: May 29, 2025; Accepted: June 3, 2025; Published online: June 20, 2025

Abstract: Vietnam's rapid urbanization presents a critical challenge at the intersection of economic development and environmental health. This study examines the causal relationships between urbanization, air pollution, and public health outcomes across Vietnam's major urban centers. Using a comprehensive panel dataset spanning 2013 – 2022 for 10 Vietnamese cities, we employed instrumental variable (IV) techniques to address endogeneity concerns and establish robust causal inference. Our findings revealed that urbanization significantly exacerbates fine particulate matter ($PM_{2.5}$) air pollution levels, with each percentage point increase in urbanization rate associated with a 0.54 μg/m^3 rise in $PM_{2.5}$ concentration. Across IV analysis using industrial output share as an instrument, we demonstrated that $PM_{2.5}$ pollution substantially impacts respiratory health outcomes, with each 1 μg/m^3 increase leading to approximately 2.5 additional respiratory disease cases per 1,000 population. Environmental policies implemented across Vietnamese cities since 2017 have achieved modest but measurable success in mitigating pollution levels. These results underscore the urgent necessity for integrated sustainable urban planning and robust environmental governance to safeguard public health in Vietnam's rapidly transforming urban landscape.

Keywords: Urbanization; Air pollution; Public health; Instrumental variables; Vietnam; Environmental policy; $PM_{2.5}$; Respiratory disease

1. Introduction

The 21st century has witnessed unprecedented urbanization, particularly across developing nations where this demographic transformation represents both opportunity and challenge. Vietnam exemplifies this global trend, experiencing annual urban population growth of approximately 3% as the country undergoes rapid economic transformation. While urbanization drives economic development and poverty reduction, it simultaneously generates significant environmental and public health pressures, most notably through the deterioration of air quality.

Vietnam's urban air quality crisis has reached alarming proportions. Major cities, such as Hanoi and Ho Chi Minh City consistently rank among the world's most polluted urban centers. In 2023, Hanoi occupied the eighth position globally for air pollution severity; while Vietnam's national average $PM_{2.5}$ concentration reached 27.2 μg/m^3 in 2022 – nearly six times the World Health Organization's recommended guideline of 5 μg/m^3. According to WHO estimates, air pollution

contributes to tens of thousands of pre-mature deaths annually across Vietnam, representing a substantial and growing public health burden.

Fine particulate matter ($PM_{2.5}$) emerges as the most concerning pollutant due to its widespread presence and established links to respiratory and cardiovascular diseases. In addition, nitrogen dioxide (NO_2) from vehicle emissions and power generation, along with sulfur dioxide (SO_2) from coal combustion and industrial processes, compound the urban health crisis. These pollutants frequently co-occur with $PM_{2.5}$, creating synergistic effects that amplify overall health risks.

The present research investigated the causal pathways linking urbanization, air pollution, and public health outcomes in Vietnam's major cities, advancing the existing literature through several key contributions. First, we provided country-specific empirical evidence from Vietnam, a rapidly developing Southeast Asian economy that has received limited attention in environmental health research despite its substantial pollution challenges. Second, by implementing instrumental variable (IV) methodologies, we moved beyond correlational analysis to establish robust causal relationships between urbanization processes, pollution levels, and health outcomes. Third, we evaluated the effectiveness of policy interventions, specifically Vietnam's National Action Plan on Air Quality Management launched in 2016 and subsequent municipal-level measures, in reducing pollution exposure and associated health risks.

Our findings offered crucial insights for policymakers not only in Vietnam but across developing countries grappling with the complex challenge of balancing urban growth with environmental protection. The analysis revealed both the magnitude of the present crisis and the potential for effective policy intervention to mitigate adverse health outcomes.

The paper proceeds as follows: Section 2 reviews relevant literature on urbanization-pollution-health relationships globally and in Vietnam; section 3 describes our data sources and econometric methodology; section 4 presents empirical results; section 5 discusses findings and policy implications; and section 6 concludes with recommendations for sustainable urban development.

2. Literature review

2.1. Global evidence on urbanization and air pollution

International research consistently demonstrates that rapid urban growth tends to elevate ambient pollution levels in the absence of strong environmental controls. This relationship has been documented across diverse geographic and economic contexts, though the magnitude and mechanisms vary considerably.

Chinese studies provide particularly relevant insights given similarities in development patterns. Wang *et al.*[1] analyzed data from 30 Chinese provinces between 2000 and 2016, finding that urbanization significantly increased $PM_{2.5}$ concentrations, with industrial structural changes mediating much of this effect. Their results suggested that every 10% increase in urbanization corresponds to approximately 5 – 8% higher $PM_{2.5}$ levels, though this relationship varies by region and development stage. A number of other studies in China also yielded the same results.[2-4] Additional investigations have also confirmed the importance of climate-resilient cities and urban planning in reducing air pollution in China.[5,6]

Similar patterns also emerge across other rapidly developing economies. In India, Mathew *et al.*[7] observed strong correlations between urban expansion and deteriorating air quality, particularly elevated particulate matter concentrations. Megacities, such as Dhaka, Bangladesh, and Jakarta, Indonesia exemplify this global challenge, ranking among the world's most polluted urban areas due to unconstrained urban growth combined with surging vehicle traffic and industrial emissions. On a larger scale, Bakry *et al.*[8] as well as Nghiem *et al.*[9] confirmed the benefits of information and communication technology (ICT) in improving environmental quality. Going into the underlying causes of emission, Bakry *et al.*[10] discovered that ICT adoption leads to reduced energy consumption, which, in turn, lowers emissions.

African urbanization presents an even more stark example of this challenge. Recent estimates suggested that over 80% of urban residents across Africa breathe air that has exceeded the WHO guidelines, indicating that pollution levels are directly linked to rapid, often unplanned, urban expansion. This pattern highlights how urbanization without adequate environmental planning consistently causes severe air quality degradation.

A comprehensive meta-analysis by Seto and Shepherd[11] examining 152 studies across 47 countries found that, on average, a 1% increase in urban population associates with approximately 0.5% higher $PM_{2.5}$ concentrations globally. However, they emphasize that this relationship depends critically on a city's development stage, infrastructure quality, and policy environment. In higher-income cities, advanced technology and pollution controls can substantially

offset the negative effects of urban growth. Cui *et al.*,[12] Guo *et al.*,[13] and Nasreen *et al.*,[14] affirmed the decreasing (inhibiting) impact of different factors (the Russia-Ukraine war, financial development) on improving environmental quality in general, respectively. In another study, Bakry *et al.*[15] confirmed the reducing impact of digital finance on emission in a group of developing countries.

This variation points to the existence of an environmental Kuznets curve for air pollution, where pollution initially worsens with urbanization and industrialization but can improve beyond certain income thresholds as cleaner technologies become affordable and environmental regulations strengthen. Dong *et al.*,[16] using panel data from 126 countries, identified this inverted-U relationship between urbanization and $PM_{2.5}$, with urban agglomeration effects and technological progress helping reduce pollution at later development stages.

Several mechanisms explain how urbanization drives pollution increases. Urban concentration of people and economic activity intensifies energy consumption, vehicle use, and industrial output – all generating substantial emissions. Guan *et al.*[17] highlighted how urbanization typically increases fossil fuel consumption for electricity, heating, and industry, while simultaneously expanding transportation emissions as rural populations migrate to cities.

Importantly, urban form matters significantly for pollution outcomes. Chen *et al.*[18] demonstrated that densely populated, well-planned cities with mixed land use can achieve lower per capita emissions than sprawling, low-density urban areas. This suggests that compact growth combined with public transit can mitigate pollution, whereas urban sprawl tends to increase vehicle dependence and energy consumption.

2.2. Air pollution and public health

The health impacts of air pollution have been extensively documented through epidemiological research worldwide, with $PM_{2.5}$ showing particularly strong associations with adverse health outcomes across all age groups and health conditions.

A comprehensive review of 263 studies by Zhang *et al.*[19] confirmed robust associations between $PM_{2.5}$ exposure and increased risks of respiratory diseases, cardiovascular disorders, and pre-mature mortality. Pope III *et al.*[20] estimated that every 10 $\mu g/m^3$ increase in long-term $PM_{2.5}$ exposure associates with approximately 6% higher all-cause mortality globally, though this relationship appears non-linear with steeper slopes at higher pollution levels.

Health effects span both acute and chronic domains. Acute impacts include eye, nose, and throat irritation, asthma exacerbation, and increased hospital admissions for respiratory and cardiac conditions. Chronic outcomes encompass asthma development, chronic obstructive pulmonary disease, lung cancer, stroke, and heart disease, in addition to emerging evidence of impacts on neurological and reproductive health.

In developing countries where pollution levels frequently exceed WHO guidelines by substantial margins, the health burden becomes particularly severe. Apte *et al.*[21] found that health impacts per unit of pollution exposure were greater in highly polluted environments, suggesting non-linear dose-response relationships that amplify risks in contexts, such as Vietnam. The same research, focusing specifically on low- and middle-income countries, also identified stronger associations between air pollution and adverse health outcomes compared to high-income countries, potentially reflecting higher baseline pollution levels, greater population vulnerability, and limited healthcare access.[21]

Beyond $PM_{2.5}$, other urban pollutants pose significant health risks. Nitrogen dioxide (NO_2), primarily from vehicle engines and power generation, irritates lungs, aggravates asthma, and increases respiratory infection risk. Chronic NO_2 exposure associates with reduced lung function and contributes to secondary pollutant formation including ozone and nitrate particles. Epidemiological studies link long-term NO_2 exposure to elevated all-cause, cardiovascular, and respiratory mortality risks.

Sulfur dioxide (SO_2) from coal burning and industrial processes triggers bronchoconstriction and asthma attacks even at relatively low concentrations. Short-term SO_2 spikes correlate with increased hospital visits for respiratory and cardiac issues, while long-term exposure contributes to chronic respiratory illness and secondary particulate formation.

These pollutants often co-occur and may act synergistically. NO_2 and SO_2 can exacerbate $PM_{2.5}$ effects by injuring respiratory tissues and reducing physiological defenses. Ozone (O_3), a secondary pollutant forming from nitrogen oxides and volatile organic compounds under sunlight, causes respiratory inflammation and reduced lung function in urban areas.

2.3. Research on Vietnam

Research on air pollution and health in Vietnam has expanded considerably in recent years, though it

remains limited compared to studies in China or India. Early Vietnamese studies were primarily descriptive, documenting pollution levels and basic health correlations.

Phung *et al.*[22] examined air pollution and hospital admissions in Ho Chi Minh City from 2010 to 2013, finding significant correlations between daily PM_{10} levels and respiratory hospital admissions. Hien *et al.*[23] analyzed air quality in Hanoi from 2016 to 2018, identifying traffic emissions and coal combustion as primary sources of particulate pollution. Nhung *et al.*[24] found that annual $PM_{2.5}$ concentrations in all studied provinces exceeded the limits set by the WHO Air Quality Guidelines and the Vietnamese Emission Standards (QCVN). These studies confirmed that Vietnam's urban pollution levels have frequently exceeded national standards and generated conspicuous short-term health impacts.

Several studies have linked Vietnam's rapid development to environmental degradation. By using satellite imagery, Nguyen *et al.*[25] documented the rapid expansion of built-up urban areas in major Vietnamese cities, which were accompanied by rising air pollutant concentrations. Tran and Nguyen[26] found that economic growth and industrialization were driving both urbanization and environmental decline, including higher emissions and water pollution, across Vietnam's cities.

More recent research has begun employing more sophisticated analytical methods. Vu *et al.*[27] investigated ambient air pollution impacts on hospital admissions for respiratory diseases among children in Hanoi, finding that days with higher $PM_{2.5}$ and NO_2 levels corresponded to increased pediatric hospitalizations for respiratory issues, even after controlling for weather and seasonal factors. While informative, such time-series analyses still face challenges in establishing causality due to potential confounding factors.

However, most Vietnam-specific studies to date have been correlational or descriptive, with few employing advanced causal inference methods. This represents a significant gap given the policy importance of understanding causal relationships between urbanization, pollution, and health outcomes in Vietnam's rapidly changing urban landscape.

2.4. Methodological approaches

Identifying causal relationships between urbanization, air pollution, and health outcomes presents substantial methodological challenges due to potential endogeneity, reverse causality, and omitted variable bias. Researchers have developed various approaches to address these analytical challenges.

Panel data methods have proven valuable for controlling time-invariant unobservable factors. Zhou *et al.*[28] employed fixed-effect models with city-level panel data in China to estimate urbanization impacts on $PM_{2.5}$ levels while controlling for economic factors and policy interventions. Difference-in-differences approaches have been used to evaluate specific policy impacts; for example, Greenstone and Hanna[29] applied this method to assess air pollution regulation effectiveness in India.

IV techniques have emerged as particularly valuable for establishing causality, though finding suitable instruments remains challenging. Appropriate instruments must influence the endogenous variable (*e.g.*, air pollution) while affecting the outcome (*e.g.*, health) only through the endogenous variable. Deryugina *et al.*[30] used wind direction as an instrument for air pollution to estimate causal effects on mortality in the United States, while Liu *et al.*[31] employed rainfall as an instrument for air pollution in studying recreational behavior impacts in Paris.

Our study addresses the methodological gap in Vietnam-specific research by applying panel data econometric techniques with city fixed effects and IVs to establish more robust causal links between urbanization, pollution, and health outcomes. By analyzing multiple cities over a decade, we can control for unobservable city-specific factors and common temporal shocks while leveraging industrial composition as an instrument for pollution levels.

3. Data and methodology

3.1. Data sources and description

In this study, we constructed a comprehensive panel dataset encompassing ten major Vietnamese cities observed annually from 2013 to 2022. The selected cities – Hanoi, Ho Chi Minh City, Haiphong, Da Nang, Can Tho, Bien Hoa, Hue, Nha Trang, Buon Ma Thuot, and Vinh – represent Vietnam's key urban centers across northern, central, and southern regions. This selection provides geographic diversity despite constraints in obtaining selected data, particularly for consistent air quality monitoring and health outcome reporting.

These cities collectively house over 30% of Vietnam's urban population and represent diverse economic profiles, from major metropolitan centers to secondary industrial cities. This diversity proves crucial for identifying causal relationships, as it provides variation

in urbanization patterns, industrial composition, and policy implementation timelines.

Our dataset integrates multiple data sources to capture urbanization metrics, air pollution indicators, health outcomes, and control variables. Urbanization and economic indicators were sourced from Vietnam's General Statistics Office, which provides annual city-level data on population, urbanization rates, population density, and economic output by sector.

Air pollution data were compiled from monitoring stations operated by the Vietnam Environment Administration, supplemented with satellite-derived estimates for cities with limited ground monitoring coverage. We focused primarily on $PM_{2.5}$ concentrations as our main pollution indicator, while also collecting data on PM_{10}, NO_2, SO_2, and Air Quality Index (IQAir;[32] IQAir[33]) measures where available.

Health outcome data were obtained from the Ministry of Health and provincial health departments. Our primary health indicator is respiratory disease rates per 1,000 population, calculated from hospitalization and outpatient visit records. We also collected mortality rate data, though this proved less consistently available across all cities and years.

Control variables include GDP per capita, industrial output shares, weather variables (temperature, humidity, precipitation), and policy implementation indicators. The policy variable captures the implementation of Vietnam's National Action Plan on Air Quality Management and subsequent city-level environmental measures, coded as a binary indicator taking the value 1 for cities implementing substantial air quality policies after 2017.

The descriptive statistics reveal substantial variation across cities and time periods. $PM_{2.5}$ concentrations range from 23.4 μg/m^3 to 48.3 μg/m^3, with a mean of 33.45 μg/m^3 – well above WHO guidelines. Urbanization rates vary from 51.8% to 91.0%, reflecting differences between established metropolitan areas and emerging secondary cities. Respiratory disease rates show considerable variation, ranging from 116.9 to 178.7/1,000 population, suggesting significant differences in health outcomes across urban areas.

3.2. Econometric framework

To address our research questions systematically, we employed a two-stage analytical approach. First, we examine the effect of urbanization on air pollution using panel data methods. Second, we assessed the causal impact of air pollution on public health outcomes using IV techniques to address endogeneity concerns.

3.2.1. Urbanization and air pollution

We began by estimating the relationship between urbanization and air pollution using the following specification:

$$PM2.5_{it} = \beta_0 + \beta_1 UrbanizationRate_{it} + \beta_2 X_{it} + \alpha_i + \gamma_t + \varepsilon_{it} \quad \text{(I)}$$

where $PM2.5_{it}$ represents the concentration of fine particulate matter in the city i at time t; $\text{UrbanizationRate}_{it}$ is the percentage of the population living in urban areas; X_{it} is a vector of control variables including GDP per capita and policy implementation indicators; α_i represents city fixed effects; γ_t represents year fixed effects; and ε_1 denotes error term. We estimated this model using both ordinary least squares (OLS) with robust standard errors and fixed-effect specifications to account for unobserved time-invariant heterogeneity across cities.

3.2.2. Air pollution and health outcomes

Our second analysis examined the causal effect of air pollution on health outcomes. The primary challenge here was that pollution levels may be endogenous in the health outcome equation. Unobserved factors, such as healthcare quality, population health behaviors, or local economic conditions could influence both pollution and health outcomes, biasing OLS estimates.

To address endogeneity, we employed an IV approach using two-stage least squares (2SLS). We instrument for $PM_{2.5}$ using the industrial share of gross domestic product (GDP) in each city. The rationale is that cities with higher industrial output shares generate more emissions and thus higher pollution levels, but conditional on overall economic development and other controls, industrial composition should not directly affect health outcomes except through pollution exposure.

Our structural equation (second stage) is:

$$\text{HealthOutcome}_{it} = \alpha_0 + \alpha_1 \widehat{PM2.5_{it}} + \alpha_2 X_{it} + \mu_i + \partial_t + \varepsilon_{it} \quad \text{(II)}$$

Where $HealthOutcome_{it}$ represents respiratory disease rates; $\widehat{PM2.5_{it}}$ is the instrumented value of $PM_{2.5}$ concentration; X_{it} is a vector of control variables; μ_i represents city fixed effects; ∂_t represents year fixed effects; and ε_{it} is the error term.

The first-stage equation is:

$$PM2.5_{it} = \gamma_0 + \gamma_1 IndustryShare_{it} + \gamma_2 X_{it} + \theta_i + \lambda_t + \Omega_{it} \quad \text{(III)}$$

Where $IndustryShare_{it}$ represents the percentage contribution of industrial activities to the city's GDP.

The validity of our IV approach depends on two key assumptions: relevance and the exclusion restriction. The relevance condition requires that industrial share significantly affects $PM_{2.5}$ levels, which we test through first-stage F-statistics. The exclusion restriction requires that industrial share affects health outcomes only through $PM_{2.5}$, not through other channels.

We provide theoretical justification for the exclusion restriction by arguing that, conditional on overall economic development (GDP per capita), city and year fixed effects, and other controls, the specific composition of economic output between industry and services should not directly influence respiratory health outcomes. Industrial composition primarily affects health through pollution emissions, rather than through income, employment, or other pathways that we control for in our specification.

4. Results

4.1. Urbanization and air pollution

Table 1 presents the descriptive statistics of the variables included in the model and Table 2 presents regression results for the effect of urbanization on PM2.5 concentrations across different model specifications. The results consistently demonstrate a positive and statistically significant relationship between urbanization rates and $PM_{2.5}$ levels across all specifications.

Column 1 shows a simple OLS regression without controls or fixed effects, yielding a coefficient of 0.542, indicating that each percentage point increase in

Table 1. Descriptive statistics for key variables

Variable	Mean	Standard deviation	Min	Max
$PM_{2.5}$ (μg/m^3)	33.45	6.58	23.4	48.3
Urbanization rate (%)	70.18	11.82	51.8	91.0
Respiratory disease rate (per 1000)	145.28	16.97	116.9	178.7
Population (thousands)	2722.0	3141.8	350	8950
Population density (persons/km^2)	2648.7	1579.3	945	6121
GDP per capita (million VND)	82.63	15.21	65.0	124.3
Industrial output (trillion VND)	485.15	324.72	290	1342
Industry share (%)	27.85	9.36	15.0	46.2
Policy implementation (binary)	0.38	0.49	0	1

Abbreviations: GDP: Gross domestic product; $PM_{2.5}$: Fine particulate matter.

Table 2. Effect of urbanization on $PM_{2.5}$ levels

Variable	(1) OLS	(2) OLS with controls	(3) FE	(4) FE with controls
Urbanization rate	0.542***	0.496***	0.384***	0.357***
	(0.032)	(0.041)	(0.048)	(0.052)
GDP per capita		0.076*		0.103**
		(0.041)		(0.045)
Policy implementation		−1.623**		−1.495**
		(0.724)		(0.638)
Constant	−4.526	−7.842	6.872	1.953
	(3.481)	(4.135)	(5.237)	(4.926)
Year fixed effects	No	Yes	No	Yes
City fixed effects	No	No	Yes	Yes
Observations	100	100	100	100
R-squared	0.741	0.762	0.824	0.847

Notes: Robust standard errors in parentheses. *p<0.1, **p<0.05, ***p<0.01.
Abbreviations: FE: Fixed effects; GDP: Gross domestic product; OLS: Ordinary least squares.

urbanization rate associates with a 0.542 μg/m³ increase in $PM_{2.5}$ Column 2 adds basic controls and year fixed effects, slightly reducing the coefficient to 0.496 but maintaining high statistical significance.

Most importantly, columns 3 and 4 present fixed-effect specifications that control for unobserved time-invariant city characteristics. In our preferred specification with fixed effects and full controls (column 4), a 1%point increase in urbanization rate associates with a 0.357 μg/m³ increase in $PM_{2.5}$ concentration. This estimate is somewhat lower than the OLS results, suggesting that unobserved city characteristics were creating some upward bias in the simple correlation.

The fixed-effect estimate represents the within-city relationship over time – as individual cities become more urbanized, their pollution levels increase by approximately 0.36 μg/m³ per percentage point of urbanization. Given that our sample cities experienced urbanization increases ranging from 5 to 15% points over the study period, this implies pollution increases of 2 – 5 μg/m³ attributable to urbanization alone.

Control variables provide additional insights into pollution determinants. GDP per capita enters with a positive coefficient (0.103, significant at 5%), indicating that economic growth, holding urbanization constant, associates with higher $PM_{2.5}$ levels. This finding is consistent with Vietnam remaining on the ascending portion of the environmental Kuznets curve, where industrialization and increased consumption outpace environmental improvements.

The policy implementation variable shows a negative coefficient (−1.495, significant at 5%), suggesting that cities implementing air quality measures after 2017 experienced $PM_{2.5}$ reductions of approximately 1.5 μg/m³ relative to cities without such policies. While statistically significant, this reduction represents only about 4 – 5% of average $PM_{2.5}$ levels, indicating modest policy effectiveness to date.

We also examined urbanization effects on other pollutants where data permitted. For the subset of five cities with consistent NO_2 monitoring, urbanization showed a positive and significant association (approximately 0.15 ppb increase per percentage point of urbanization, $p<0.05$). Similarly, urbanization demonstrated positive associations with SO_2 levels, though estimates were less precise due to inconsistent monitoring coverage.

4.2. Air pollution and health outcomes

Table 3 presents results from our IV analysis of $PM_{2.5}$ effects on respiratory disease rates, comparing OLS

Table 3. Effect of $PM_{2.5}$ on respiratory disease rates (IV estimation)

Variable	(1) OLS	(2) First stage	(3) 2SLS	(4) FE-IV
$PM_{2.5}$	2.980***		2.567***	2.315***
	(0.092)		(0.203)	(0.271)
Industry share		0.378***		
		(0.035)		
Urbanization rate	0.124*	0.312***	0.057	0.042
	(0.068)	(0.051)	(0.074)	(0.083)
GDP per capita	0.103*	0.097**	0.068	0.052
	(0.058)	(0.044)	(0.063)	(0.068)
Policy implementation	−0.742	−1.547**	−0.125	−0.095
	(0.821)	(0.631)	(0.889)	(0.912)
Constant	32.158***	−5.924	41.376***	48.243***
	(5.793)	(4.024)	(6.875)	(7.321)
Year fixed effects	Yes	Yes	Yes	Yes
City fixed effects	No	No	No	Yes
Observations	100	100	100	100
R-squared	0.914	0.839	0.918	0.934
First-stage F-statistic			117.83	92.47

Notes: Robust standard errors in parentheses. *p <0.1, **p <0.05, ***p <0.01.
Abbreviations: FE: Fixed effects; GDP: Gross domestic product; IV: Instrumental variable; OLS: Ordinary least squares; 2SLS: Two-stage least squares.

estimates with IV results and showing first-stage diagnostics.

The first-stage results (column 2) confirm that our instrument – industrial output share – strongly predicts $PM_{2.5}$ levels. The coefficient of 0.378 indicates that each percentage point increase in the industry's GDP share raises $PM_{2.5}$ by 0.378 μg/m^3 on average. The first-stage F-statistics (117.83 and 92.47 in columns 3 and 4) substantially exceed the conventional threshold of 10, indicating our instrument is not weak.

Comparing OLS and IV estimates reveals important insights about potential bias in simple correlations. The OLS estimate (column 1) suggests that each 1 μg/m^3 increase in $PM_{2.5}$ associates with 2.98 additional respiratory disease cases per 1,000 population – a substantial effect representing approximately 2% of the mean respiratory disease rate.

However, the IV estimates provide more credible causal identification. In our preferred fixed-effect IV specification (column 4), the coefficient is 2.315, indicating that each 1 μg/m^3 increase in $PM_{2.5}$ causally generates approximately 2.3 additional respiratory disease cases per 1,000 population. This estimate is somewhat lower than the OLS result, suggesting that simple correlations may overstate pollution's health impact due to omitted variable bias.

The IV estimate implies substantial health impacts from present pollution levels. Considering that $PM_{2.5}$ concentrations vary by about 25 μg/m^3 between the cleanest and most polluted cities in our sample, this variation could account for approximately 58 additional respiratory disease cases per 1,000 population – representing nearly 40% of the mean respiratory disease rate.

To put this in perspective, if Vietnam's most polluted cities reduced $PM_{2.5}$ concentrations by 10 μg/m^3 (a substantial but achievable reduction), this would prevent approximately 23 respiratory disease cases per 1,000 population annually – equivalent to roughly 15% fewer respiratory illnesses.

The policy implementation variable becomes statistically insignificant in the IV specifications, suggesting that environmental policies primarily affect health through pollution reduction rather than through direct pathways. This supports our identification strategy and implies that the health benefits of environmental policies operate primarily through their impact on air quality.

5. Discussion

5.1. Interpretation of key findings

Our results provide compelling evidence of a causal chain linking urbanization to air pollution and subsequently to public health outcomes in Vietnam's cities. The positive effect of urbanization on $PM_{2.5}$ levels aligns with extensive research on urban environmental challenges in rapidly developing countries, while the magnitude we identified proves consistent with findings from comparable Asian contexts.

The urbanization coefficient of approximately 0.36 μg/m^3 per percentage point increase represents a substantial relationship. As Vietnamese cities continue urbanizing at 3% annually, this implies $PM_{2.5}$ increases of roughly 1 μg/m^3 per year solely from urbanization processes without policy interventions. Over a decade, this cumulative effect could raise pollution levels by 10 – 12 μg/m^3, representing a 25 – 30% increase from present levels.

This finding proves consistent with studies from China, where Wang *et al.*[1] reported that provinces with 10% higher urbanization exhibited 5 – 8% higher $PM_{2.5}$ concentrations. Our fixed-effect estimates suggest comparable magnitudes: a 10% urbanization increase in Vietnamese cities correlates with approximately 3.6 μg/m^3 higher $PM_{2.5}$, representing roughly 10% of baseline levels.

The causal pathway from urbanization to pollution operates through multiple mechanisms. Urban concentration intensifies energy consumption for residential, commercial, and industrial uses, predominantly from fossil fuel sources in Vietnam's present energy mix. Simultaneously, urbanization dramatically increases vehicle usage as cities expand and rural populations migrate to urban areas. Vietnam's rapid motorization, particularly motorcycle adoption, has created dense traffic flows with limited emission controls.

Industrial concentration represents another crucial mechanism. As cities develop, they attract manufacturing and processing industries seeking infrastructure, labor, and market access. Without stringent environmental regulations, these industries contribute substantially to urban pollution through emissions from production processes, power generation, and freight transportation.

Our health impact estimates prove substantial and policy-relevant. The IV coefficient of 2.315 additional respiratory cases per 1,000 population per μg/m^3 of $PM_{2.5}$ implies that present pollution levels generate significant health burdens across Vietnamese cities. This estimate aligns with international evidence from developing countries, where pollution-health relationships often prove more severe than in developed

nations due to higher baseline exposure, greater population vulnerability, and limited healthcare access.

The fact that IV estimates are somewhat lower than OLS results (2.315 vs. 2.98) suggests that simple correlations may overstate pollution's health impact due to confounding factors. Cities with higher pollution levels might also have other characteristics – such as industrial composition, population density, or healthcare infrastructure – that independently affect health outcomes. Our IV approach helps isolate pollution's causal impact by leveraging variation in industrial composition that affects pollution but not health through other channels.

These health impacts translate into substantial economic and social costs. Respiratory disease episodes generate direct medical costs, productivity losses from work absences, and reduced quality of life. For Vietnam's urban population of approximately 35 million, even small changes in disease rates imply thousands of additional cases annually, representing significant burdens on healthcare systems and economic productivity.

The policy analysis yields mixed but informative results. Environmental policies implemented since 2017 achieved statistically significant but modest pollution reductions of approximately 1.5 $\mu g/m^3$. While this represents progress, it falls far short of the reductions needed to meet air quality standards. Vietnam's cities still exceed national ambient air quality standards (25 $\mu g/m^3$ annual average for $PM_{2.5}$) by substantial margins, and remain far above WHO guidelines (5 $\mu g/m^3$).

However, the fact that policies generated measurable improvements demonstrates that interventions can succeed even in rapidly growing economies. This finding provides hope that scaled-up and strengthened policies could achieve more substantial improvements. International experience, particularly from China's aggressive pollution control efforts in the 2010s, demonstrates that rapid air quality improvements are possible with sufficient political commitment and policy implementation.

5.2. Policy implications

Our findings carry important implications for policymakers in Vietnam and other rapidly urbanizing developing countries. The established causal chain from urbanization through pollution to health outcomes underscores the urgent need for integrated urban planning that considers environmental and health consequences alongside economic development.

5.2.1. Sustainable urban planning integration

The strong urbanization-pollution relationship highlights the critical importance of environmental considerations in urban planning processes. Vietnam's continued rapid urbanization – projected to reach 50% of the total population by 2030 – makes the integration of urban planning into sustainability policies essential. Cities should prioritize compact, transit-oriented development over sprawling, car-dependent growth patterns.

5.2.2. Transportation sector transformation

Given transportation's substantial contribution to urban air pollution, particularly NO_2 and $PM_{2.5}$ from vehicle exhaust, transforming Vietnam's transportation system represents a critical policy priority. This transformation should encompass both regulatory and investment approaches.

Vehicle emission standards require immediate strengthening and enforcement. Vietnam should accelerate the adoption of Euro 5 and eventually Euro 6 fuel and vehicle standards, following successful implementations in European and other Asian countries. Stricter inspection and maintenance programs can ensure existing vehicles meet emission requirements.

Electric vehicle promotion offers longer-term pollution reduction potential. Vietnam's government has announced targets for electric vehicle adoption, but implementation requires supportive infrastructure including charging networks, financial incentives for consumers, and regulatory frameworks to encourage domestic manufacturing.

5.2.3. Industrial emission control

Our IV analysis demonstrates that industrial composition significantly affects urban air quality, suggesting that industrial emission control represents a crucial policy lever. This requires both regulatory strengthening and economic incentives for cleaner production.

Emission standards for industrial facilities need regular updating and rigorous enforcement. Vietnam should consider adopting international best practice standards for major industrial sources, including power plants, cement factories, steel mills, and chemical facilities. Regular monitoring and meaningful penalties for violations are essential for effective implementation.

Economic incentives can complement regulatory approaches. Pollution pricing through taxes or cap-and-trade systems can provide market-based incentives for emission reductions while generating revenue for environmental improvements. Several Vietnamese provinces have experimented with environmental taxes, and expanding these approaches could prove effective.

Industrial zoning policies should consider cumulative environmental impacts and proximity to population centers. Concentrating heavy industries in designated zones with appropriate pollution controls can reduce urban exposure while enabling economic development. The adoption and implementation of air-infiltration systems are also strongly recommended as these measures have proved effective and beneficial in mitigating air pollution and improving people's health and quality of life.[3,4,34,35]

5.2.4. Healthcare system adaptation

While addressing pollution sources remains the primary priority, strengthening healthcare systems to better manage pollution-related health impacts provides important interim protection. This is particularly crucial given that substantial air quality improvements will require years to achieve.

Healthcare providers in Vietnamese cities should receive training in recognizing and managing pollution-related health conditions, particularly respiratory diseases that spike during high pollution episodes. Emergency departments and respiratory clinics should prepare for increased patient loads during pollution episodes.

5.2.5. Regional and international cooperation

Air pollution often crosses administrative boundaries, making regional cooperation essential for effective management. Vietnam should strengthen coordination with neighboring countries on transboundary pollution issues, particularly seasonal agricultural burning that affects regional air quality.

Within Vietnam, cities and surrounding provinces should coordinate on pollution control since urban air quality is affected by emissions from broader metropolitan regions. Joint planning for industrial development, transportation systems, and pollution monitoring can improve effectiveness while reducing costs.

International cooperation can provide technical assistance, funding, and technology transfer for pollution control. Vietnam should actively engage with international organizations and developed countries that have successfully addressed similar air quality challenges.

5.2.6. Economic co-benefits and climate integration

Many air pollution control measures provide climate change mitigation co-benefits, enabling Vietnam to address both local air quality and global climate commitments simultaneously. This integration can unlock additional funding sources and international support.

Renewable energy development reduces both air pollution and greenhouse gas emissions. Vietnam's substantial solar and wind potential could provide cleaner electricity while reducing coal dependence, which contributes significantly to urban air pollution.

Energy efficiency improvements in buildings, industry, and transportation reduce both air pollution and carbon emissions while providing economic benefits through reduced energy costs. Comprehensive energy efficiency programs can achieve multiple policy objectives simultaneously.

6. Conclusion, policy implications/ recommendations, limitations, and future research directions

This study provided rigorous empirical evidence of the causal relationships linking urbanization, air pollution, and public health outcomes in Vietnam's major cities. Across panel data analysis spanning 2013 – 2022 and employing IV techniques, we demonstrated that urbanization significantly increases $PM_{2.5}$ pollution levels, which in turn substantially impact respiratory health outcomes.

Our key findings established that each percentage point increase in urbanization rate raises $PM_{2.5}$ concentrations by approximately 0.36 $\mu g/m^3$, while each $\mu g/m^3$ increase in $PM_{2.5}$ causally generates roughly 2.3 additional respiratory disease cases per 1,000 population. These quantitative relationships underscore the magnitude of Vietnam's environmental health challenge: continued rapid urbanization without effective policy intervention will likely generate substantial increases in pollution-related health burdens.

The analysis also revealed that environmental policies implemented since 2017 achieved modest but measurable pollution reductions of approximately 1.5 $\mu g/m^3$. While this indicates that policy interventions can succeed even in rapidly growing economies, the scale of improvement remains insufficient to meet air quality standards or protect public health adequately.

For Vietnam, these findings highlighted both urgent challenges and important opportunities. The country's continued rapid urbanization – projected to house over half the population in cities by 2030 – makes immediate action essential. Without integrated sustainable urban planning and strengthened environmental policies, pollution levels, and associated health impacts will likely continue increasing substantially.

Our results also demonstrated that policy interventions can effectively reduce pollution even in rapidly developing contexts. This finding, combined with international experience from countries, such as China that achieved dramatic air quality improvements through determined policy implementation, suggested that Vietnam can successfully address its air quality challenges with sufficient political commitment and appropriate policy design.

The policy implications extend beyond pollution control to encompass comprehensive urban development strategies. Sustainable urban planning that promotes compact, transit-oriented development; transportation systems that reduce vehicle dependence; industrial policies that minimize emissions; and healthcare systems adapted to protect vulnerable populations all represent essential components of an effective response.

Critically, addressing air pollution provides substantial co-benefits for climate change mitigation, as many pollution sources also generate greenhouse gases. This alignment enables Vietnam to pursue local air quality improvements and global climate commitments simultaneously, potentially unlocking additional resources and international support for environmental improvements.

Our findings also contribute to the broader global understanding of urbanization-environment-health relationships in developing countries. The quantitative estimates of these relationships in Vietnam's context provide valuable benchmarks for policy evaluation and international comparisons, while our methodological approach demonstrates how causal inference techniques can generate more robust evidence for policy design.

International experience demonstrates that this challenge is surmountable. Countries from the United Kingdom to Japan and China have successfully reduced urban air pollution while maintaining economic growth, though the health and economic costs of delayed action proved substantial. Vietnam has the opportunity to learn from these experiences and implement effective policies earlier in its development process, potentially avoiding the severe pollution episodes that other countries experienced.

In conclusion, our analysis provided clear evidence that Vietnam faces a critical choice in managing its urban development trajectory. The causal pathways from urbanization through pollution to health impacts are well-established and quantitatively significant. The effectiveness of policy interventions is demonstrated but requires substantial scaling up. The co-benefits with climate action provide additional motivation and potential resources for implementation. Most importantly, the health and well-being of millions of Vietnamese urban residents depend on the policy choices made in the coming years.

The transition to sustainable urban development will require sustained political commitment, substantial financial resources, and effective institutional coordination. However, the alternative – continued deterioration of urban air quality with mounting health and economic costs – represents a far more challenging long-term scenario. By acting decisively now, Vietnam can achieve the dual objectives of economic development and environmental protection, creating healthier and more prosperous cities for future generations.

Acknowledgments

None.

Funding

The authors gratefully acknowledge the financial support from the Banking Academy of Vietnam.

Conflict of interest

The authors declare they have no competing interests

Author contributions

Conceptualization: All authors
Formal analysis: All authors
Investigation: All authors
Methodology: Bui Duy Hung
Writing – original draft: All authors
Writing – review & editing: All authors

Availability of data

Data are available from the corresponding author upon reasonable request.

References

1. Wang Q, Kwan MP, Zhou K, Fan J, Wang Y, Zhan D. The impacts of urbanization on fine particulate matter ($PM_{2.5}$) concentrations: Empirical evidence from 135 countries worldwide. *Environ Pollut.* 2019;247:989-998. doi: 10.1016/j.envpol.2019.01.086
2. Zhan C, Xie M, Lu H, *et al*. Impacts of urbanization on air quality and the related health risks in a city with complex terrain. *Atmos Chem Phys.* 2023;23(1):771-786.

doi: 10.5194/acp-23-771-2023
3. Zhang S, Liu H, Tang N, Ge J, Yu J, Ding B. Direct electronetting of high-performance membranes based on self-assembled 2D nanoarchitectured networks. *Nat Commun.* 2019;10:1458.
doi: 10.1038/s41467-019-09444-y
4. Zhang Y, Han Y, Ji X, *et al*. Continuous air purification by aqueous interface filtration and absorption. *Nature.* 2022;610(7930):74-80.
doi: 10.1038/s41586-022-05124-y
5. Wen H, Hu K, Nghiem XH, Acheampong AO. Urban climate adaptability and green total-factor productivity: Evidence from double dual machine learning and differences-in-differences techniques. *J Environ Manag*. 2024a;350:119588.
doi: 10.1016/j.jenvman.2023.119588
6. Wen H, Yu H, Nghiem XH. Impact of Urban sprawl on carbon emission efficiency: Evidence from China. *Urban Clim*. 2024b;55:101986.
doi: 10.1016/j.uclim.2024.101986
7. Mathew J, Goyal R, Taneja KK, Arora N. Air pollution and respiratory health of school children in industrial, commercial and residential areas of Delhi. *Air Qual Atmos Health.* 2015;8(4):421-427.
doi: 10.1007/s11869-014-0299-y
8. Bakry W, Mallik G, Nghiem XH, Sinha A, Vo XV. Is green finance really "green"? Examining the long-run relationship between green finance, renewable energy and environmental performance in developing countries. *Renew Energy*. 2023a;208:341-355.
doi: 10.1016/j.renene.2023.03.020
9. Nghiem XH, Bakry W, Al-Malkawi HAN, Farouk S. Does technological progress make OECD countries greener? New evidence from panel CS-ARDL. *Manag Environ Qual Int J*. 2023;34(6):1555-1579.
doi: 10.1108/MEQ-11-2022-0296
10. Bakry W, Nghiem XH, Farouk S, Vo XV. Does it hurt or help? Revisiting the effects of ICT on economic growth and energy consumption: A nonlinear panel ARDL approach. *Econ Anal Policy*. 2023b;78:597-617.
doi: 10.1016/j.eap.2023.03.026
11. Seto KC, Shepherd JM. Global urban land-use trends and climate impacts. *Curr Opin Environ Sustain.* 2009;1(1):89-95.
doi: 10.1016/j.cosust.2009.07.012
12. Cui L, Yue S, Nghiem XH, Duan M. Exploring the risk and economic vulnerability of global energy supply chain interruption in the context of Russo-Ukrainian war. *Resour Policy*. 2023;81:103373.
doi: 10.1016/j.resourpol.2023.103373
13. Guo B, Guo Q, Amri F, Abbas S, Nghiem XH. Powering environmental sustainability through renewable energy and natural resources: A dynamic ARDL simulation approach. *Environ Sci Pollut Res*. 2023;30:90906-90923.
doi: 10.1007/s11356-023-28643-1
14. Nasreen S, Khan FI, Nghiem XH. The effects of financial development and technological progress on environmental sustainability: Novel evidence from Asian countries. *Environ Sci Pollut Res*. 2023;30:53712-53724.
doi: 10.1007/s11356-023-26139-6
15. Bakry W, Nghiem XH, Bhatti MI, Al-Mohamad S, Cui L. Digital finance and sustainable development: Evidence from developing nations. *Sci Prog*. 2024;107:2024;107(3).
doi: 10.1177/00368504241278823
16. Dong Q, Lin Y, Huang J, Chen Z. Has urbanization accelerated $PM_{2.5}$ emissions? An empirical analysis with cross-country data. *China Econ Rev.* 2020;59:101381.
doi: 10.1016/j.chieco.2019.101381
17. Guan D, Meng J, Reiner DM, *et al*. Structural decline in China's CO_2 emissions through transitions in industry and energy systems. *Nat Geosci.* 2018;11(8):551-555.
doi: 10.1038/s41561-018-0161-1
18. Chen G, Li S, Zhang Y, *et al*. Effects of ambient PM_1 air pollution on daily emergency hospital visits in China: An epidemiological study. *Lancet Planet Health.* 2017;1(6):e221-e229.
doi: 10.1016/S2542-5196(17)30100-6
19. Zhang L, Yang Y, Li Y, *et al*. Short-term and long-term effects of $PM_{2.5}$ on acute nasopharyngitis in 10 communities of Guangdong, China. *Sci Total Environ.* 2019;688:136-142.
doi: 10.1016/j.scitotenv.2019.05.470
20. Pope CA 3rd, Coleman N, Pond ZA, Burnett RT. Fine particulate air pollution and human mortality: 25+ years of cohort studies. *Environ Res.* 2020;183:108924.
doi: 10.1016/j.envres.2019.108924
21. Apte JS, Brauer M, Cohen AJ, Ezzati M, Pope CA 3rd. Ambient $PM_{2.5}$ reduces global and regional life expectancy. *Environ Sci Technol Lett*. 2018;5(9):546-551.
doi: 10.1021/acs.estlett.8b00360
22. Phung D, Hien TT, Linh HN, *et al*. Air pollution and risk of respiratory and cardiovascular hospitalizations in the most populous city in Vietnam. *Sci Total Environ.* 2016;557:322-330.
doi: 10.1016/j.scitotenv.2016.03.070
23. Hien PD, Men NT, Tan PM, Hangartner M. Impact of urban expansion on the air pollution landscape: A case study of Hanoi, Vietnam. *Sci Total Environ.* 2020;702:134635.
doi: 10.1016/j.scitotenv.2019.134635
24. Nhung NTT, Duc VT, Ngoc VD, *et al*. Mortality benefits of reduction fine particulate matter in Vietnam, 2019. *Front Public Health.* 2022;10:1056370.
doi: 10.3389/fpubh.2022.1056370
25. Nguyen TT, Ngo HH, Guo W, *et al*. Implementation of a specific Urban water management - sponge City. *Sci Total Environ.* 2019;652:147-162.
doi: 10.1016/j.scitotenv.2018.10.168
26. Tran TT, Nguyen HD. Urbanization, economic

development, and environmental change in Vietnam. *J Econ Dev.* 2015;40(3):1-25.
27. Vu T, Nguyen TTN, Pham MH. Effect of ambient air pollution on hospital admissions for respiratory diseases among children in Hanoi, Vietnam. *Environ Res.* 2023;216:114655.
28. Zhou L, Chen X, Tian X. The impact of fine particulate matter ($PM_{2.5}$) on China's agricultural production from 2001 to 2010. *J Clean Prod.* 2018;178:133-141. doi: 10.1016/j.jclepro.2017.12.204
29. Greenstone M, Hanna R. Environmental regulations, air and water pollution, and infant mortality in India. *Am Econ Rev*. 2014;104(10):3038-3072. doi: 10.1257/aer.104.10.3038
30. Deryugina T, Heutel G, Miller NH, Molitor D, Reif J. The mortality and medical costs of air pollution: Evidence from changes in wind direction. *Am Econ Rev.* 2019;109(12):4178-4219. doi: 10.1257/aer.20180279
31. Liu K, Zhang H, Bo Y, *et al*. Ambient air pollution and Children's health: An umbrella review. *Atmos Pollut Res.* 2024;15:102108. doi: 10.1016/j.apr.2024.102108
32. IQAir. *World Air Quality Report 2020*. Switzerland: IQAir AG; 2021.
33. IQAir. *World Air Quality Report 2022*. Switzerland: IQAir AG; 2023.
34. Liu Y, Zhou B, Wang J, Zhao B. Health benefits and cost of using air purifiers to reduce exposure to ambient fine particulate pollution in China. *J Hazard Mater*. 2021;414:125540. doi: 10.1016/j.jhazmat.2021.125540
35. Balyan P, Ghosh C, Sharma AK, Banerjee BD. Health effects of air pollution among residents of Delhi: A systematic review. *Int J Health Sci Res*. 2018;8(1):273-282.

Asian Journal of Water, Environment and Pollution. Vol. 22, No. 3 (2025), pp. 211-220.
doi: 10.36922/AJWEP025080047

ORIGINAL RESEARCH ARTICLE

User perspectives on sustainable innovation in the construction industry

Jozef Švajlenka[1]*, Terézia Pošiváková[2], and Hermawan Hermawan[3]

[1]Department of Construction Technology, Economy and Management, Faculty of Civil Engineering, Technical University of Košice, Košice, Slovakia

[2]Department of Breeding and Diseases of Game, Fish and Bees, Ecology and Cynology, University of Veterinary Medicine and Pharmacy of Košice, Košice, Slovakia

[3]Department of Architecture, Faculty of Engineering and Computer Science, Universitas Sains Al-Qur'an, Wonosobo, Indonesia

***Corresponding author:** Jozef Švajlenka (ingsvajl@gmail.com)

Received: February 17, 2025; Revised: March 29, 2025; Accepted: April 7, 2025; Published online: June 26, 2025

Abstract: Housing availability relative to population size is widely regarded as the main qualitative indicator of housing development standards. In Central Europe, there has been a notable trend of residents relocating from larger urban areas, where most housing is apartment buildings, to smaller satellite towns. Many investors and users are placing greater emphasis on construction methods, material bases, and sustainability. Among the sustainable housing options in Central Europe (V4 countries), single-family wooden houses are gaining popularity. Despite their advantages, the broader adoption of wood-based sustainable construction is hindered by limited public awareness. Hence, this study explores the perception of potential users and investors on wood-based constructions compared to traditional construction methods. Results show that potential users and investors perceive wooden constructions as capable of meeting the current legislative, energy-related, technological, and economic requirements. Correlation analysis of the data revealed differences in the perception of the parameters of constructions among various respondent groups. The primary contribution of this study lies in increasing awareness of wood-based constructions and analyzing the interactions among the selected parameters of constructions. Findings from this study highlight the potential for innovation aimed at enhancing efficiency and sustainability in housing developments.

Keywords: Wood-based construction; Environment; Innovation, Region of central Europe; Socioeconomic research; Sustainability

1. Introduction

Housing is a fundamental human need, and its satisfaction should correspond to the overall social levels and economic development.[1-3] Housing is also a pre-requisite for starting a family and significantly influences population development.[4,5] In Central Europe, considerable attention is paid to housing policies and housing. The main goal of housing policy is to ensure the availability of housing for all social groups in the population.[6,7] Many promising activities are being implemented to promote more environmentally sustainable lifestyles.[8] In the context of climate change, various alternatives are also preferred, particularly those contributing to more efficient use of raw materials for energy production,[9-12] which is necessary for the operation of buildings.

According to Klincka *et al*.,[13] single-family housing construction is driven by wealthier social groups who can afford land investment and build a family house, particularly in locations with established infrastructure. As a standard rule, land prices increase in correlation with better access to basic infrastructure (water, sewerage, gas, and heating). According to Cár,[14] the number of households is an important indicator in assessing the need for housing. The present state of the housing stock is largely the product of earlier construction of family houses and apartment buildings, with significant regional variations. The ability to acquire a property depends on various factors, with income levels playing an important role.[15-17] This means that the ability to acquire a property largely depends on the region's economic performance, which is typically improved when more jobs are created due to more private investment coming into the region.[18,19]

New technologies make it possible to build lucrative housing without centralized infrastructure (water, sewerage, electricity, and heating) in more remote locations with adequate environmental protection.[20-23] It is possible to build diversified systems for the water supply, energy and heating, and waste management, which is particularly important in housing development, considering the ever-growing prices of water, energy, and heating.[24-27]

According to Cholujová,[28] the urban population growth in cities, economic development, and cultural and social changes pose various challenges, including the urgent need for changes in the government's housing policy to provide new housing.[29] With the transition to a market economy, the responsibility for securing housing has shifted from the state to individuals.[30,31] This shift has opened up new methods and opportunities for addressing individual housing needs. A notable trend is the movement away from impersonal and restrictive housing within pre-fabricated apartment buildings toward more natural and liberating environments consisting of family homes.[32-34] Housing companies respond to this demand change by offering various options. In addition to traditional, proven building materials, such as brick or wood, companies also provide modern and full-fledged alternatives.[35-38] One such alternative is wood-based houses.

The sustainability of buildings, especially wood-based buildings, is currently one of the topics in the construction industry. Innovative wooden buildings offer significant advantages in terms of ecological, economic, and social sustainability. In an environmental context, wood as a natural material has a low carbon footprint compared to traditional building materials, such as concrete or steel. As trees absorb carbon dioxide during growth, the use of wood in buildings effectively stores carbon, thereby contributing to climate change mitigation. The ecological advantages are also reflected in the energy intensity of wood production and transportation, which is significantly lower than that of other materials. From an economic viewpoint, wood is more cost-effective, while its easy handling and speed of construction reduce labor and time costs. In addition, wooden buildings have long-term durability, often resulting in lower maintenance costs. The social aspect of the sustainability of wooden buildings includes creating a healthy and comfortable environment for residents. Wooden buildings contribute to better acoustics, humidity regulation, and a healthier indoor microclimate, positively impacting health and well-being. These factors make wooden buildings an attractive solution for a sustainable future within the construction sector.

Timber buildings are structures that use wood as the main building component, and are divided into different types according to their construction and purpose. In the housing sector, the most commonly implemented timber frame buildings (prefabricated wooden houses) are characterized by fast construction and good energy efficiency. Solid timber buildings, such as cross-laminated and glued-lamella timbers, offer high load-bearing capacity and durability. In commercial construction, modern timber buildings using cross-laminated timber panels are increasingly used, allowing multiple floors to be implemented while combining esthetics, sustainability, and strength. In addition, timber buildings are also used in other sectors, such as school buildings, administrative buildings, and public buildings, where they are used primarily for their low ecological footprint and excellent thermal insulation properties. These timber buildings are increasingly popular in Central Europe, as they combine the advantages of sustainability, energy efficiency, and short construction time.

These considerations necessitate an analysis of the perception of modern wood-based construction systems designed for housing construction. This study aimed to analyze the results of socioeconomic research focused on the perception of the parameters of wood-based buildings compared to traditional construction methods among potential users and investors.

2. Methodology

A methodology was designed for data collection before the socioeconomic research. The qualitative and quantitative research was conducted in line with the stated objective and hypotheses. As part of the research, responses were collected from users and investors regarding the advantages and disadvantages of modern wood-based buildings. The methodology included a questionnaire and a controlled interview.

The questionnaires were designed to cover all three key areas of research: Architectural-structural-technical area (questions related to the technical properties of wooden buildings, as well as their comparison with other materials in terms of durability and energy efficiency), social area (respondents answered questions regarding the comfort of living in wooden buildings, health, impact on the psyche, and quality of life), and technological-economic area (these questions focused on the costs of construction, maintenance, and operation of wooden buildings compared to other types of buildings).

The hypothesis focused on the influence of age in relation to the interdependencies among the individual criteria. The questionnaire included items addressing the technological and economic aspects of wood-based constructions. The collected data were analyzed using a statistical tool (Statistica, version 12), applying the correlation coefficient method to determine the strength and direction of relationships between two numerical variables. This correlation analysis enabled the identification and evaluation of the intensity of associations between individual criteria (e.g., the influence of age on the perception of wooden buildings in technological, economic, and social areas).

2.1. Sampling strategy and sample selection considerations

This study used stratified random sampling to ensure the representativeness of the participating respondents from different age groups. This sampling strategy was appropriate to consider potential differences in perceptions of wooden buildings between different demographic groups, allowing for a more detailed evaluation of factors, such as the influence of age on the perception of technological, economic, and social aspects of wooden buildings. Based on this approach, a sufficient number of respondents ($n = 172$) were selected from a sample of users and investors, thus obtaining diversified data for accurate analyses.

2.2. Response rate and potential biases

The response rate was monitored to ensure adequate representativeness of the sample. Given the methodology, which included online questionnaires and controlled interviews, the response rate was in the optimal range of 60 – 70%. Possible biases may have arisen if respondents with previous experience in timber construction or strong preferences for a specific construction type had exerted a disproportionate influence on the responses. To minimize this type of bias, the questions were formulated neutrally, promoting objectivity of the answers and ensuring a balance of views from all groups of respondents.

The results of the correlation analysis provided valuable information on how the perception of wooden buildings differs between different groups of respondents and how these factors influence decision-making about the use of wooden buildings compared to traditional construction methods.

3. Results and discussion

This section presents the research results focused on the perception of the parameters of wood-based buildings compared to traditional construction methods among potential users and investors. A total of more than 172 responses were collected in the research. The research sample was 57.1% men and 42.8% women. Age groups were represented as follows: 18 – 25 years (12.2%), 26 – 35 years (31.2%), 36 – 45 years (24.5%), and over 45 years (32.1%).

3.1. Architectural and construct-technical breakdown

A total of 63.1% of respondents answered that they were familiar with the term wood-based building, while 31.5% responded that they had encountered it only partially, and only 5.4% stated that they had not heard of it. These findings suggest that the term wood-based building is well-known among the surveyed population. Regarding architectural flexibility, 51.4% of respondents stated that wood-based buildings were not limited in terms of architectural design, 36.3% considered them partially limited, and 12.3% viewed them as architecturally constrained. In terms of design preferences, most respondents' preferred combined shapes (57%), 28.2% preferred cubic shapes, and 18.8% preferred proven design shapes.

3.2. Social breakdown

As for internal comfort of use in wood-based buildings (air quality, temperature, light, and sound), 82% of the

respondents stated that modern wood-based buildings could achieve the desired comfort of use, 15% believed it was achievable only at a higher cost, and 3% deemed that internal comfort of use was not attainable. Respondents perceived family houses (96%), superstructures (71%), and schools (54%) as the most ideal applications of wood-based designs.

3.3. Technological-economic breakdown

As for construction time, respondents stated that wood-based constructions were completed faster than traditional constructions. Only 15% responded that their completion time was almost identical, and 6% believed it was longer than traditional constructions. In terms of quality, 64% stated it was comparable to traditional buildings, 31% thought it was better, and only 5% deemed it worse.

Based on the analysis, respondents believed that the costs of project documentation for wood-based buildings were lower or comparable to those of traditional buildings. Only 7% of respondents stated that the costs involved were higher. As for the construction costs of wood-based buildings, it was found that 54% of respondents believed they were lower, 29% deemed them comparable, and 17% thought they were higher than traditional buildings. A total of 63% of respondents saw perceived costs of wood-based constructions as comparable, while 23% considered them higher, and 14% viewed them as lower compared to traditional buildings.

3.4. Correlation analysis

Individual data groups were selected for correlation analyses per the research objective and hypothesis. Data selection (groups of respondents) was focused on three areas in line with the stated hypothesis, namely, age (Tables 1 and 2). Notably, more correlations among individual parameters within respondent groups suggest that the answers are not random but reflect logically interconnected perceptions of the assessed construction criteria. This indicates that respondents' views are based on consistent relationships among parameters, reinforcing the reliability of the observed patterns. Due to the large number of correlations among individual parameters for the selected groups of respondents, a detailed commentary on all statistical findings is limited, as a comprehensive description of each partial finding would be too long. However, Tables 1 and 2 offer valuable insights into the relationships among the individual parameters, highlighting which parameters affect others when analyzed within subgroups of respondents.

Based on the correlation analysis, there are significant dependencies among the selected parameters evaluated by the respondents. There were also differences among the respondents' age groups (generations). These findings suggest that each age group influences the perception of the individual parameters of wood-based buildings compared to traditional buildings.

Based on Table 1, most correlations among the assessed parameters showed similar trends (positive or negative correlations) across the different respondent groups. These findings suggest that perception does not differ significantly across age groups when correlations are present. Only two instances revealed differences in the direction of correlation, that is, the correlations between construction time and shape limitation and between stability and shape limitation. The smallest number of correlations was recorded in the age group of 18 – 25 years (11), followed by 26 – 35 years (14), and the age group of more than 45 years old (14). In contrast, the largest number of correlations between the parameters was recorded in the group of respondents aged 36 – 45 years (18). This finding suggests that the age group of 36 – 45 years, the productive age group, perceives the parameters of buildings comprehensively, with the logical connections among the individual parameters, and their responses are solely based on a single isolated parameter.

There is a growing interest and popularity in wood-based constructions.[39] This interest stems from the beneficial properties of wood,[40] particularly its weight ratio to static load capacity,[41] making wood-based construction systems a key competitor to traditional construction systems that are based on concrete, steel, and masonry.[42,43] Other advantages include the possibility of using the dry construction method[44] as well as more favorable environmental parameters compared to the traditional construction method.[45,46] A substantial body of research has explored wooden buildings from various perspectives, such as their material and structure.[47-50] Our findings align with the findings of Mozolová,[51] who focused on people's views on wooden buildings. Similarly to our study, Mozolová[51] confirms the growing interest in wooden buildings as an ecological housing alternative, but acknowledges certain barriers precluding these constructions from becoming more widespread. Continued lack of experience and confidence in this construction method and poor promotion of its benefits compared to the traditional construction method are identified as the main barriers. A study by Lindblad and Gustavsson[52] focused on how residents and architects in Sweden perceived housing quality, and whether these

Table 1. Correlations among the selected parameters relative to the lower age groups

Age groups	Knowledge of wooden buildings	Shape constraints	Architectural appearance	Materials	Energy standard	Stability	Internal comfort	Time of construction	Quality	PD costs	Realization costs	Operating costs
Knowledge of wooden buildings	1. 0000											
Shape constraints	–	1. 0000										
Architectural appearance	–	–	1. 0000									
Materials	–	0.7958[a] 0.4263[b]	–	1. 0000								
Energy standard	–	–	–	–	1. 0000							
Stability	–	–	0.3464[b]	–	–	1. 0000						
Internal comfort	–	0.6407[a] 0.4477[b]	–	0.6742[a] 0.5731[b]	–	–	1. 0000					
Time of construction	0.7137[a]	−0.7159[a]	–	−0.6666[a]	–	–	−0.7606[a]	1. 0000				
Quality	–	–	–	−0.4849[b]	–	–	−0.3848[b]	–	1. 0000			
PD costs	–	−0.6009[a]	–	0.5015[b]	–	0.6396[a]	0.3298[b]	–	−0.5181[b]	1. 0000		
Realization costs	−0.3320[b]	0.6950[a]	–	0.5925[a]	–	–	–	–	–	–	1. 0000	
Operating costs	−0.3746[b]	–	–	–	−0.3588[b]	–	–	–	−0.3403[b]	–	0.3679[b]	1. 0000

Notes: "–" refers to not significant; [a]values represent the age group 18 – 25 years; and [b]values represent the age group 26 – 35 years.

Table 2. Correlations among the selected parameters relative to the higher age groups

Age groups	Knowledge of wooden buildings	Shape constraints	Architectural appearance	Materials	Energy standard	Stability	Internal comfort	Time of construction	Quality	PD costs	Realization costs	Operating costs
Knowledge of wooden buildings	1. 0000											
Shape constraints	–	1. 0000										
Architectural appearance	–	–	1. 0000									
Materials	–	0.7298[a]	–	1. 0000								
Energy standard	0.6398[a]	0.7857[b]	–	–	1. 0000							
Stability	–	–	−0.7115[a]	–	0.3082[b]	1. 0000						
Internal comfort	–	–	0.3495[b]	0.6160[b]	−0.4162[a]	–	1. 0000					
Time of construction	[a]0.5351[a]	0.6634[b]	–	–	0.5188[a] 0.3899[b]	–	−0.4820[a]	1. 0000				
Quality	0.4577[b]	−0.3911[a] −0.5560[b]	–	−0.5520[b]	–	0.3104[b]	−0.4399[a] −0.4461[b]	–	1. 0000			
PD costs	−0.3979 [b]	–	−0.4024[b]	–	−0.4363[a]	–	–	–	–	1. 0000		
Realization costs	−0.5287[a] −0.3597[b]	–	–	–	−0.7370[a]	–	–	−0.8153[a] −0.4416[b]	–	0.4255[a] 0.4863[b]	1. 0000	
Operating costs	−0.4376[b]	–	–	–	−0.5386[a]	–	0.4072[a]	−0.4270[a]	−0.3888[a] −0.6051[b]	0.6766[b]	0.4545[a] 0.3661[b]	1. 0000

Notes: "–" refers to not significant; [a]values represent the age group 36 – 45 years; and [b]values represent the age group over 45 years.

perceptions differed based on building type and choice of material (i.e., multigenerational wood-based or concrete buildings). The results revealed discrepancies regarding what factors were important in developing new housing. Notably, neither group was willing to pay more for a wooden building than a concrete one. There are certain parallels between their research and our study, particularly in identifying bias and the lack of trust in wood-based constructions as the main barriers to their more widespread use. As such, our study contributes to the field by raising awareness of wood-based constructions. Ulu and Durmuş Arsan[53] state that the construction industry is the biggest energy consumer in Europe, with a share of about 40%. For this reason, it is necessary to focus on the energy efficiency of the existing and future housing stock. They also state that energy efficiency is directly related to economic, environmental, and social sustainability. These claims match our views based on the research we conducted. As evident from our findings, the energy-related properties of constructions affect many other parameters and the overall living comfort. A study by Caniato *et al*.[54] was focused on the thermal-technical and acoustic parameters of wood-based buildings, as wood-based buildings generally have poor acoustic parameters. Based on their findings, modern wood-based buildings can largely eliminate these shortcomings and achieve higher efficiency when compared to original wood-based buildings. They can also compete with traditional construction solutions (such as masonry buildings). A study by Gardezi *et al*.[55] focused on a multivariate regression tool for predicting the embodied carbon footprint of housing habitats. They found that an evaluation of housing requires a clear understanding of the parameters or criteria that can be evaluated and modeled in relation to buildings. They also emphasize that different tools are applicable for assessing buildings at various life cycle stages. These assertions are supported by Fastofski *et al*.[56] Based on our own research experience, we concur with these perspectives. We can only understand which parameters affect other parameters by examining different aspects of construction. For example, the correlation analysis in our study determined how individual construction parameters influenced each other as perceived by future users, representing a valuable contribution to this field. This insight not only enhances the ability to predict building performance more accurately but also supports the development of more sustainable and efficient solutions with a positive impact on housing and housing quality. A study by Dadashpoor and Ahani[57] on the conceptual typology of the suburban areas of cities found that global urban population growth and large-scale urbanization in suburban areas is a phenomenon that emerged in the 20th century. This phenomenon was an implicit topic in urban and regional studies for several years. Our findings confirm a growing trend in which certain population groups relocate from densely populated urban centers to suburban or peripheral areas. Our research indicates that the demand for individual housing is greater than ever. Various construction companies respond to this demand by offering various construction and material solutions. However, it is essential to verify these solutions and study their properties. The expansion of knowledge in the field of wood-based construction presented in this study serves as a step toward addressing the lack of public confidence, which remains a barrier to wider recognition of its benefits compared to traditional construction methods.

Three different limitations can be identified for this research. The first limitation is the number of respondents or the research sample. Considering this limitation in future research is necessary, as it is not always easy to find respondents willing to provide sincere answers. The general rule is that the larger the sample of respondents and the resulting volume of data, the greater the validity of the research. The second limitation is the respondents' awareness or prior knowledge regarding the theme of the questionnaire. There is a difference between answers from respondents with experience with wood-based construction and those who do not. This leads to certain distortions in answers. The third limitation applies to interpreting the findings from the correlation analyses of parameters. As the analyses produced an enormous number of correlations according to the individual selected groups of respondents, it is impossible to evaluate each correlation between the individual parameters separately. Such a detailed interpretation of findings would require a separate article focused solely on the evaluation.

This study, which focuses on potential users and investors, shows that despite the small market share of wooden buildings, their design, technological, or user-related parameters are generally well understood, even compared to traditional construction technologies. The conclusions confirm a growing interest in sustainable and healthy housing, highlighting significant potential for growth in this construction sector.

4. Conclusion

This study explored the perception of wood-based construction among potential users and investors compared to traditional construction methods. The

research generated a range of findings that expand knowledge in wood-based construction, with benefits for potential customers, construction professionals, and the scientific community. Based on the findings from the respondents' opinions, it can be concluded that wood-based structures are characterized by faster construction times and often have comparable or better quality than traditional structures. Project documentation and construction costs were considered lower or comparable while operating costs were mostly similar. Overall, wood-based construction was viewed favorably, particularly in terms of speed and cost-efficiency.

The correlation analysis revealed significant dependencies among the selected parameters evaluated by the respondents. In addition, certain differences among the age groups (generations) were also discovered, indicating that generational factors influence how individual parameters of wood-based constructions are perceived compared to traditional constructions. These findings have the potential to stimulate interest in wood-based housing and promote its adoption. It can be concluded that modern constructions based on wood offer an efficient and sustainable housing alternative.

From a sustainability perspective, timber buildings can play a key role in mitigating climate change, as timber is a renewable material that sequesters carbon dioxide as it grows, thereby contributing to reducing the carbon footprint of buildings. Stakeholders, such as building professionals, investors, and policymakers can use these findings to support developing and implementing timber buildings as a sustainable housing alternative. Promoting this construction method at both local and global levels could significantly contribute to achieving the Sustainable Development Goals and combating climate change. It is recommended that the focus be on raising awareness of the benefits of timber buildings among different age groups, as the results suggest that these factors influence perceptions of timber buildings. Investment in research and development of timber building technologies and supporting legislative measures to stimulate a sustainable construction sector can provide a solid basis for the wider adoption of this technology. Implementing these measures at the local and global levels will support not only economic efficiency but also environmental and climate goals in the construction sector. At the same time, it is important to invest in educating professionals and the public about the benefits of timber construction, which can contribute to their wider use and ultimately support the transition to a more sustainable and climate-resilient construction sector.

Acknowledgments

None.

Funding

This study was simultaneously supported by the Scientific Grant Agency of the Ministry of Education, Science, Research and Sport of the Slovak Republic (VEGA) with VEGA 1/0228/24 project and the Cultural and Educational Grant Agency Ministry of Education, Science, Research and Sport of the Slovak Republic (KEGA) with KEGA 017TUKE-4/2024 project.

Conflict of interest

The authors declare that they have no competing interests.

Author contributions

Conceptualization: All authors
Formal analysis: All authors
Investigation: Jozef Švajlenka, Terézia Pošiváková
Methodology: Jozef Švajlenka, Terézia Pošiváková
Writing – original draft: All authors
Writing – review & editing: Jozef Švajlenka, Terézia Pošiváková

Availability of data

Data are available upon reasonable request from the corresponding author.

References

1. Henilane I. Housing concept and analysis of housing classification. *Balt J Real Estate Econ Constr Manag*. 2016;4(1):168-179. doi: 10.1515/bjreecm-2016-0013
2. Igwe PU, Okeke CA, Onwurah KO, Nwafor DC, Umeh CN. A review of housing problems. *Int J Environ Agric Biotechnol*. 2017;2(6):3092-3099. doi: 10.22161/ijeab/2.6.40
3. Kutá D, Wernerová E, Teichmann M. Aspects of housing assessment and their influence on the form of housing in apartment houses in the Czech Republic. *Int J Eng Res Africa*. 2020;47:127-131. doi: 10.4028/www.scientific.net/JERA.47.127
4. Lee D, McLanahan S. Family structure transitions and child development: Instability, selection, and population heterogeneity. *Am Sociol Rev*. 2015;80(4):738-763.

doi: 10.1177/0003122415592129
5. Musa MM, Bin Amirudin R, Sofield T, Mus MA. Influence of external environmental factors on the success of public housing projects in developing countries. *Constr Econ Build*. 2015;15(4):30-44. doi: 10.5130/AJCEB.v15i4.4514
6. Shi W, Chen J, Wang H. Affordable housing policy in China: New developments and new challenges. *Habitat Int*. 2016;54:224-233. doi: 10.1016/j.habitatint.2015.11.020
7. Droste C. German co-housing: An opportunity for municipalities to foster socially inclusive urban development? *Urban Res Pract*. 2015;8(1):79-92. doi: 10.1080/17535069.2015.1011428
8. Maroušek J, Minofar B, Maroušková A, Strunecký O, Gavurová B. Environmental and economic advantages of production and application of digestate biochar. *Environ Technol Innov*. 2023;30:103109. doi: 10.1016/j.eti.2023.103109
9. Maroušek J, Gavurová B, Strunecký O, Maroušková A, Sekar M, Marek V. Techno-economic identification of production factors threatening the competitiveness of algae biodiesel. *Fuel*. 2023;344:128056. doi: 10.1016/j.fuel.2023.128056
10. Maroušek J, Maroušková A, Gavurová B, Minofar B. Techno-economic considerations on cement substitute obtained from waste refining. *J Clean Prod*. 2023;412:137326. doi: 10.1016/j.jclepro.2023.137326
11. Antošová N, Šťastný P, Petro M, Krištofič Š. Application of additional insulation to ETICS on surfaces with biocorrosion. *Acta Polytech*. 2021;61(5):590-600. doi: 10.14311/AP.2021.61.0590
12. Ďubek M, Makýš P, Ďubek S, Petro M. The evaluation of the content of fibers in steel fiber reinforced structures and image analysis. *J Civ Eng Manag*. 2018;24(3):183-192. doi: 10.3846/jcem.2018.1642
13. Klincka M, et al. *Housing development and infrastructure*. Bratislava: SUT Press; 2003.
14. Cár M. Selected aspects of solving the need for housing in Slovakia. *Biatec*. 2013;21(7):16-20.
15. Alwan Z, Jones P, Holgate P. Strategic sustainable development in the UK construction industry, through the framework for strategic sustainable development, using building information modelling. *J Clean Prod*. 2017;140:349-358. doi: 10.1016/j.jclepro.2015.12.085
16. Putnam RD, Goss KA. *Democracies in Flux: The Evolution of Social Capital in Contemporary Society*. New York: Oxford University Press; 2002. p. 516.
17. Rees W. *Environment and Urbanization*. London: Cedric Pugh; 1996. p. 121-130.
18. Lobao L. Rural sociology. In: Bryant CD, Peck DL, editors. *The Handbook of 21st Century Sociology*. Thousand Oaks: Sage Publications; 2007. p. 465-476.
19. Spates JL, Macionis JJ. *The Sociology of Cities*. Belmont, CA: Wadsworth Publishing; 1987.
20. Wolff M. Understanding the role of centralization processes for cities - evidence from a spatial perspective of urban Europe 1990-2010. *Cities*. 2018;75:20-29. doi: 10.1016/j.cities.2017.01.009
21. Salet W, Vermeulen R, Savini F, *et al*. Planning for the new European metropolis: Functions, politics, and symbols/Metropolitan regions: Functional relations between the core and the periphery/Business investment decisions and spatial planning policy/Metropolitan challenges, political responsibilities/Spatial imaginaries, urban dynamics and political community/Capacity-building in the city region: Creating common spaces/ Which challenges for today‘s European metropolitan spaces? *Plan Theory Pract*. 2015;16(2):251-275. doi: 10.1080/14649357.2015.1021574
22. Grădinaru SR, Iojă CI, Onose DA, *et al*. Land abandonment as a precursor of built-up development at the sprawling periphery of former socialist cities. *Ecol Indic*. 2015;57:305-313. doi: 10.1016/j.ecolind.2015.05.009
23. Wernerová E, Endel S, Kutá D. Implementation of the BIM method at the VSB-technical University of Ostrava. *Int J Eng Res Africa*. 2020;47:133-138. doi: 10.4028/www.scientific.net/JERA.47.133
24. Benedek J, Sebestyén TT, Bartók B. Evaluation of renewable energy sources in peripheral areas and renewable energy-based rural development. *Renew Sustain Energy Rev*. 2018;90:516-535. doi: 10.1016/j.rser.2018.03.020
25. Nuuter T, Lill I, Tupenaite L. Comparison of housing market sustainability in European countries based on multiple criteria assessment. *Land Use Policy*. 2015;42:642-651.
26. Derlukiewicz N, Mempel-Śnieżyk A. European cities in the face of sustainable development. *Ekonomia Prawo*. 2018;17(2):125-135. doi: 10.12775/EiP.2018.009
27. Wernerová E, Teichmann M. Facility management in the operation of water supply networks. *Int Multidisc Sci GeoConf SGEM*. 2017;17:601-607. doi: 10.5593/sgem2017/62/S27.076
28. Cholujová M. *Survey of Interest in Wood-Based Houses in the Banská Bystrica Region.* -- Zvolen: Technical University in Zvolen; 2011.
29. Mao C, Xie F, Hou L, Wu P, Wang J, Wang X. Cost analysis for sustainable off-site construction based on a multiple-case study in China. *Habitat Int*. 2016;57:215-222. doi: 10.1016/j.habitatint.2016.08.002
30. Hall P, Tewdwr-Jones M. *Urban and Regional Planning*. 6th ed. London: Routledge; 2019.
31. Gan X, Zuo J, Ye K, Skitmore M, Xiong B. Why sustainable construction? Why not? An owner‘s perspective. *Habitat Int.* 2015;47:61-68. doi: 10.1016/j.habitatint.2015.01.005

32. Repaská G, Vilinová K, Šolcová L. Trends in development of residential areas in suburban zone of the city of Nitra (Slovakia). *Eur Countryside*. 2017;9(2):287-301. doi: 10.1515/euco-2017-0018
33. Dembski S, Sykes O, Couch C, *et al*. Reurbanisation and suburbia in Northwest Europe: A comparative perspective on spatial trends and policy approaches. *Prog Plann*. 2019;150:100462. doi: 10.1016/j.progress.2019.100462
34. Darko A, Chan AP. Critical analysis of green building research trend in construction journals. *Habitat Int*. 2016;57:53-63. doi: 10.1016/j.habitatint.2016.07.001
35. Semenyuk O, Abdrashitova T, Beloussova E, *et al.* The influence of ecology and economic factors on eco-architecture and the design of energy efficient buildings. *World Trans Eng Technol Educ*. 2018;16(2):186-192.
36. Zhou Z, Zhang S, Wang C, *et al*. Achieving energy efficient buildings via retrofitting of existing buildings: A case study. *J Clean Prod*. 2016;112:3605-3615. doi: 10.1016/j.jclepro.2015.09.046
37. Hagbert P, Femenías P. Sustainable homes, or simply energy-efficient buildings? *J Hous Built Environ*. 2016;31(1):1-17. doi: 10.1007/s10901-015-9440-y
38. Martínez-Rocamora A, Solís-Guzmán J, Marrero M. Ecological footprint of the use and maintenance phase of buildings: Maintenance tasks and final results. *Energy Build*. 2017;155:339-351. doi: 10.1016/j.enbuild.2017.09.038
39. Ximenes FA, Grant T. Quantifying the greenhouse benefits of the use of wood products in two popular house designs in Sydney, Australia. *Int J Life Cycle Assess*. 2013;18(4):891-908. doi: 10.1007/s11367-012-0533-5
40. Wang L, Toppinen A, Juslin H. Use of wood in green building: A study of expert perspectives from the UK. *J Clean Prod*. 2014;65:350-361. doi: 10.1016/j.jclepro.2013.08.023
41. Pei S, Van de Lindt JW, Popovski M. Approximate R-factor for cross-laminated timber walls in multistory buildings. *J Archit Eng*. 2013;19(4):245-255. doi: 10.1061/(ASCE)AE.1943-5568.0000117
42. Gauvreau-Lemelin C, Attia S. Benchmarking the environmental impact of green and traditional masonry wall constructions. In: *International Conference on Passive Low Energy Architecture Design to Thrive*; 2017. p. 2856-2863.
43. Pittau F, Dotelli G, Arrigoni A, Habert G, Iannaccone G. Massive timber building vs. conventional masonry building: A comparative life cycle assessment of an Italian case study. *IOP Conf Ser Earth Environ Sci*. 2019;323(1):012016. doi: 10.1088/1755-1315/323/1/012016
44. Gibb AG. *Off-Site Fabrication: Prefabrication, Pre-Assembly and Modularisation*. Chichester: John Wiley and Sons; 1999.
45. Brandner R. Environmental impacts of wood construction. *Eur J Wood Prod.* 2016;74:407-424.
46. Pajchrowski G, Noskowiak A, Lewandowska A, Strykowski W. Wood as a building material in the light of environmental assessment of full life cycle of four buildings. *Constr Build Mater.* 2014;52:428-436. doi: 10.1016/j.conbuildmat.2013.11.066
47. Olsson A, Bolmsvik Å. *Acoustics in Wooden Buildings-State of the Art 2008*. Sweden: SP Technical Research Institute of Sweden; 2008.
48. Rimshin VI, Labudin BV, Melekhov VI, Orlov A, Kurbatov VL. Improvement of strength and stiffness of components of main struts with foundation in wooden frame buildings. *ARPN J Eng Appl Sci*. 2018;13(11):3851-3856.
49. Yao LH, Wang XM, Fei BH, Zhao RJ. *Present Status of Fireproofing for Wooden Buildings*. Beijing: China Wood Industry; 2007. p. 5.
50. Riggio M, Dilmaghani M. Structural health monitoring of timber buildings: A literature survey. *Build Res Inf*. 2020;48(8):817-837. doi: 10.1080/09613218.2019.1681253
51. Mozolová M. *A Survey of People's Opinions on Wooden Buildings*. --. Zvolen: Technical University in Zvolen; 2014.
52. Lindblad F, Gustavsson Å. A comparison between architects' and residents' perceived living quality in wooden multifamily houses in Sweden. *For Prod J*. 2020;70(4):462-468.
53. Ulu M, Durmuş Arsan Z. State of the Art Survey for Energy-Efficient Retrofit of Historic Residential Buildings in Both the EU and Turkey. In: *Proceedings of the REHAB*; 2017.
54. Caniato M, Bettarello F, Ferluga A, Marsich L, Schmid C, Fausti P. Thermal and acoustic performance expectations on timber buildings. *Build Acoust*. 2017;24(4):219-237. doi: 10.1177/1351010X17740477
55. Gardezi SSS, Shafiq N, Zawawi NAWA, Khamidi MF, Farhan SA. A multivariable regression tool for embodied carbon footprint prediction in housing habitat. *Habitat Int*. 2016;53:292-300. doi: 10.1016/j.habitatint.2015.11.005
56. Fastofski DC, González MAS, Kern AP. Sustainability analysis of housing developments through the Brazilian environmental rating system Selo Casa Azul. *Habitat Int*. 2017;67:44-53. doi: 10.1016/j.habitatint.2017.07.001
57. Dadashpoor H, Ahani S. A conceptual typology of the spatial territories of the peripheral areas of metropolises. *Habitat Int*. 2019;90:102015. doi: 10.1016/j.habitatint.2019.102015

ACCSCIENCE PUBLISHING

Our Journals

Organoid Research (OR) is an international, peer-reviewed journal dedicated to advancing the field of organoid science by publishing high-quality research articles, reviews, and perspectives. The journal focuses on studies that provide significant conceptual, experimental, and translational advances in the development and application of organoid technologies.

OR welcomes submissions spanning diverse areas of organoid science, including but not limited to stem cell biology, tissue engineering, regenerative medicine, disease modeling, and drug discovery. The journal encourages papers that explore bioengineered organoids, organoid-based systems biology, and the integration of organoids with clinical research. Special emphasis is placed on contributions that advance novel approaches to organoid development, including the use of cutting-edge bioengineering techniques, materiobiology, and integrative technologies such as artificial intelligence, high-throughput screening, and precision medicine. Additionally, the journal values research that delves into ethical considerations and challenges related to the clinical translation of organoid systems.

Advanced Neurology is a peer-reviewed and open-access journal that aims to publish and disseminate novel research in the breadth of neurology and neuroscience. The journal aims to advance our understanding in the nervous system and provide a platform to neuroscientists and physicians to showcase their findings in original fundamental and clinical research as well as to present new ideas that highlight the changes in the neurological clinical practice.

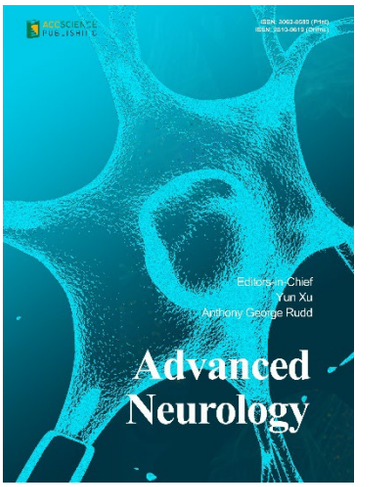

Advanced Neurology covers subject areas, including but not limited to the following:

- Neurological disorders
- Neurodegenerative disease
- Cerebrovascular disease
- Epilepsy and movement disorders
- Neuroimmune disease
- Neurological infections
- Muscle disease
- Molecular and cellular neuroscience
- Systems neuroscience
- Cognitive neuroscience
- Computational modeling of nervous system

Start a new journal

Write to us via email if you are interested to start a new journal with AccScience Publishing. Please attach your CV, professional profile page and a brief pitch proposal in your email. We shall inform you of our decision whether we are interested to collaborate in starting a new journal.

Contact: info@accscience.com

https://accscience.com/journal/AJWEP

Contact
www.accscience.com
9 Raffles Place, Republic Plaza 1 #06-00 Singapore 048619
Email: editorial@accscience.com
Phone: +65 8182 1586